X-650-62-226

405 p.

N63 18601—N63 18622

CODE-1

PROCEEDINGS OF THE NIMBUS PROGRAM REVIEW

OTS PRICE

XEROX $ 22.25 pl

MICROFILM $ 12.35 mf

NOVEMBER 14-16, 1962

PROCEEDINGS

OF THE

NIMBUS PROGRAM REVIEW

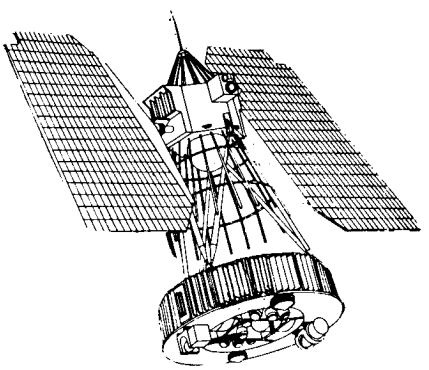

November 14-16, 1962

GODDARD SPACE FLIGHT CENTER

Greenbelt, Md.

NATIONAL AERONAUTICS AND SPACE ADMINISTRATION

GODDARD SPACE FLIGHT CENTER

PROCEEDINGS OF THE NIMBUS PROGRAM REVIEW

FOREWORD

The Nimbus program review was conducted at the George Washington Motor Lodge and at General Electric Missiles and Space Division, Valley Forge, Pennsylvania, on November 14, 15, and 16, 1962. The purpose of the review was twofold: first, to present to top management of the Goddard Space Flight Center (GSFC), National Aeronautics and Space Administration (NASA) Headquarters, other NASA elements, Joint Meteorological Satellite Advisory Committee (JMSAC), Weather Bureau, subsystem contractors, and others, a clear picture of the Nimbus program, its organization, its past accomplishments, current status, and remaining work, emphasizing the continuing need and opportunity for major contributions by the industrial community; second, to bring together project and contractor technical personnel responsible for the planning, execution, and support of the integration and test of the spacecraft to be initiated at General Electric shortly. This book is a compilation of the papers presented during the review and also contains a list of those attending.

Harry Press
Nimbus Project Manager

CONTENTS

FOREWORD

1. INTRODUCTION TO NIMBUS
   by W. G. Stroud, GSFC

2. THE NIMBUS PROJECT– ORGANIZATION, PLAN, AND STATUS
   by H. Press, GSFC

3. METEOROLOGICAL APPLICATIONS OF NIMBUS DATA
   by E.G. Albert, U.S. Weather Bureau

4. NIMBUS SPACECRAFT SYSTEM CONCEPT
   by Dr. R. Stampfl, GSFC

5. NIMBUS SPACECRAFT SYSTEM DEVELOPMENT
   by J.V. Michaels, GSFC

6. STATUS OF THE NIMBUS INTEGRATION AND TEST PROGRAM
   by L. Michelson, GE/Missiles and Space Division

7. NIMBUS GROUND SYSTEM
   by L. Stelter, GSFC

8. STABILIZATION AND CONTROL SUBSYSTEM
   by K. Hoepfner, GSFC; J. Turtil,
   GE/Missiles and Space Division

9. STRUCTURAL CONCEPTS IN NIMBUS SPACECRAFT DESIGN
   by A.F. White, Jr. and M.B. Weinreb, GSFC

10. DEVELOPMENT OF THE NIMBUS STRUCTURE
    by E.O. Stengard, GSFC

11. THERMAL CONTROL OF THE NIMBUS SPACECRAFT
    by P. Crossfield, GSFC; F. Drummond,
    GE/Missiles and Space Division

12. SPECIAL ASPECTS OF NIMBUS SPACECRAFT INTEGRATION
by J. P. Strong, Jr., GSFC; R. DiGirolamo, GE/Missiles and Space Division

13. NIMBUS SOLAR POWER SUPPLY
by M. B. Weinreb and C. MacKenzie, GSFC

14. NIMBUS COMMAND SUBSYSTEM
by J. J. Over, GSFC; D. W. Gade, R. E. Trousdale, and F. Wiley, California Computer Products, Inc.; J. Bunn, RCA/Astro Electronics Division

15. NIMBUS TELEMETRY
by R. Golden, GSFC; F. L. Adkins and C. E. Griffin, Radiation, Inc.

16. NIMBUS RADIOMETRY
by I. L. Goldberg, GSFC

17. NIMBUS ADVANCED VIDICON CAMERA SYSTEM
by G. L. Burdett and R. Shapiro, GSFC; Dr. J. E. Keigler, RCA/Astro Electronics Division

18. NIMBUS AUTOMATIC PICTURE TRANSMISSION SYSTEM
by C. M. Hunter, GSFC; P. H. Werenfels, L. G. Saxton and M. Shepetin, RCA/Astro Electronics Division; T. F. Maher and P. Metzner, Fairchild Stratos Electronic Systems Division

19. ENGINEERING APPLICATIONS OF THE NIMBUS TELEMETRY
by D. Beiber, GSFC; M. Schmitt and R. Cox, GE/Missiles and Space Division

20. NIMBUS COMPUTER SYSTEM DESIGN
by L. H. Byrne, GSFC; H. G. Klose and F. E. Lilley, GE/Missiles and Space Division

21. NIMBUS INTEGRATION AND TEST PROGRAM PLAN
by J. V. Michaels, GSFC; J. F. McGuckin, GE/Missiles and Space Division

ATTENDANCE LIST

1. INTRODUCTION TO NIMBUS

By W. G. Stroud, GSFC

1. INTRODUCTION TO NIMBUS

By W. G. Stroud, GSFC

The Nimbus project is conducting its second annual review of the program, emphasis being placed on the systems approach. Nimbus is for NASA and Goddard Space Flight Center unique in many technical and managerial aspects. The purpose of this review is to bring before the participants and interested managers and observers the status and the immediate plans for the project.

Just what is Nimbus?

Nimbus is a cloud form -
- - intangible but none the less real.

Nimbus is a project -
- - one of a number designed to bring the earth's atmosphere under observation: TIROS, S-6, POGO, and the future synchronous spacecraft. It is of particular importance and interest to the nation because of its capabilities as a meteorological observatory.

Nimbus is a system -
- - from the sensing of physical parameters to the assimilation and understanding of data by the scientist, it includes spacecraft, launch vehicle, data acquisition, and data-utilization facilities, equipments, and operations.

Nimbus is a research and development effort -
- - managed by NASA's GSFC with the objectives of studying the earth's lower atmosphere, and laying the scientific and engineering foundations for a global meteorological satellite system.

Project Nimbus, so christened by Ed Cortright, now Deputy Director of the Office of Space Sciences, NASA Headquarters, was conceived in the summer of 1959, before the first TIROS launch-- even before Goddard Space Flight Center had a completed TIROS spacecraft.

During that summer and fall (1959), Mr. Cortright and the author addressed themselves to what was considered the most serious defect of TIROS: the lack of a controls and stabilization subsystem that would keep the atmospheric sensors pointed toward the earth at all times. Visits were made to the various groups working in this area; discussions were held with the experts, none of whom at that time had flown a three-axis controls system even for a short time; and the ideas and opinions were formed that were later built into this complex subsystem.

During that winter and the spring of 1960, while the Aeronomy and Meteorology Division at GSFC was launching the TIROS I, serious thought was also being given to Nimbus. The first working group meeting occurred that spring, and the first published summary of Nimbus--looking surprisingly like the present system--was dated April 1960.

The first Nimbus contract, for the controls subsystem, was placed in October 1960; the final major contractor, for integration and testing, was selected in February 1961.

During a 6-month period, the GSFC group prepared specifications for some fifteen subsystems, put them out for bid, evaluated the responses, and put the contractors to work. Some of these specifications were good, some were poor; some of our contractors were good, others were poor; some of the GSFC technical management was good, some was poor.

The project has had some real successes as well as some dismal failures. But, if the attendees who were here last year, when GSFC conducted its first systems review of Nimbus, will compare then with now, they will find two things:

- Together with industry, GSFC has undertaken an enormous, technically difficult task; the understanding of this by the various participants is one purpose of this meeting.

- The project is succeeding; the hardware seen in aggregate is intended to demonstrate this.

In conclusion the purpose of the Nimbus program review meeting may be summed up as follows:

It is the intent of the papers presented at the meeting to give the participants in the Nimbus project, that is, the men who are working on the individual parts of the system, an opportunity to see the whole system. In addition, with hardware on hand, this is an opportunity to conduct a "tire-kicking" review of where the effort stands after 2 years of work. And, finally, the latter part of the meeting will be used to brief the individual participant in the integration and test program as to his responsibility and his role in the work conducted at the integration and contractor's plant at Valley Forge.

Although the emphasis in these presentations and in the hardware on display will be on the spacecraft and its ground equipment, a primary objective of the Goddard attack on the Nimbus project has been to produce a system of the highest possible integrity. Many particulars are presented in the following papers, but it is hoped that the emphasis on the spacecraft systems test and performance will be most obvious. Time after time the word systems, whether it be applied to spacecraft, launch vehicle, data acquisition or data utilization, will be used. Each of these is but a subsystem to the whole - the Nimbus project.

2. THE NIMBUS PROJECT — ORGANIZATION, PLAN, AND STATUS

By Harry Press, GSFC

2. THE NIMBUS PROJECT — ORGANIZATION, PLAN, AND STATUS

ILLUSTRATIONS

Figure		Page
1	Nimbus System Complex	9
2	Nimbus Launch Sequence	10
3	Nimbus Spacecraft	11
4	Performance Achievements	12
5	Data-Acquisition System	13
6	Data-Utilization System	14
7	Nimbus Organization Chart	15
8	Nimbus Spacecraft Contractors	16
9	Nimbus Spacecraft Contractors (cont.)	17
10	Other Contractors	18
11	Nimbus Program Plan	19

2. THE NIMBUS PROJECT—

ORGANIZATION, PLAN, AND STATUS

By Harry Press, GSFC

INTRODUCTION

This report on the Nimbus project is intended to provide an overall framework for the reports which follow. It will discuss briefly the following subjects:

(1) Objectives and scope of the Nimbus project
(2) Project organization
(3) Summary of project accomplishments
(4) Present status of and future plans for the project

These four topics will give a broad view of the entire project, and succeeding reports will provide the details necessary to make the Nimbus story more meaningful and complete.

OVERALL OBJECTIVES

The objective of the Nimbus project is to develop an operational meteorological satellite system. This system will provide the regular global observational coverage needed by the weather services for forecasting and, hopefully, will also provide basic data leading to a better understanding of atmospheric phenomena.

The project is concerned not only with the development of a spacecraft, but also with the development of a fully integrated observation and processing system. Figure 1, a diagram of the system, encompasses the following major elements:

- A launch vehicle that will place the spacecraft into the precise orbit required, with a high degree of reliability

- A spacecraft of wide and expanding capability for observation of the atmosphere and for rapid transmission of the collected data

- A ground command and data-acquisition system, to control the spacecraft in orbit, and to receive data

- Finally, a sophisticated ground data-processing and transmission system to provide the users (meteorologists and atmospheric physicists) with the necessary information in a convenient and meaningful form and in the appropriate timescale

As the perishable aspects of weather data make the timeframe particularly vital, it is planned to make the processed satellite measurements available to the forecasting meteorologistics within 1 to 2 hours of the observation time. Each of these elements is discussed briefly below:

LAUNCH VEHICLE

Figure 2 gives the sequence of events for the Nimbus launch. The spacecraft will be launched from the Pacific Missile Range (PMR) into a polar orbit by a Thor-Agena vehicle. The launch will take place at about midnight in order to achieve the desired high-noon orbit. Following Thor burnout, the Agena-Nimbus combination separates and coasts to an altitude of 60 nautical miles. Two Agena burns are used to achieve the desired Nimbus circular orbit (500 nautical miles for initial flights). Spacecraft separation then takes place, the solar paddles are unfolded, and the spacecraft pitchup is initiated. Stabilization in relation to the earth then proceeds.

In order to ensure a successful launch operation, a variety of studies and developments have been required, such as:

- The development of a suitable shroud

- The design and construction of an adapter

- The development of a precision spacecraft-separation system

These activities have proceeded well and are now largely completed.

SPACECRAFT SYSTEM

Figure 3 illustrates the Nimbus spacecraft configuration, consisting of three major elements:

- A large torus-like ring to house the electronic systems and sensors
- An upper housing containing the complete stabilization and control subsystem
- The large solar paddles

Major characteristics of the spacecraft system are also shown on the chart. First, and most important, Nimbus will be the first spacecraft to permit complete earth coverage on a daily basis. It will achieve this goal by combining the polar orbit with the earth-oriented control system; the polar orbit provides the latitudinal coverage, and the rotation of the earth provides the mechanism for longitudinal coverage over successive orbits.

The second major distinctive feature of the Nimbus spacecraft is the complete modular design approach. The separate and independent control system, together with a sensory ring design consisting of 18 separate module bays, allows for separate development, evolution, and improvement of individual subsystems with a minimum of interface problems. This flexibility feature is required to permit the smooth product improvement and evolution which is fundamental to the Nimbus concept.

Other features of the design are the large data-transmission capacity, and the long life needed to make the system a practical one.

The performance chart, Figure 4, compares the initial performance design objectives with the values actually accomplished by the initial spacecraft in the areas of weight, stabilization accuracy, power, and the resolutions of the advanced vidicon camera system (AVCS) and the high-resolution infrared radiometer (HRIR). Comparison of these design objectives with the actual values indicates that, although there are some disparities, agreement is fairly close. The low weight was achieved only by sacrificing much of the redundancy

originally planned. Although the desired control accuracy, and the resolution of the HRIR, could not be perfected in initial designs, it is expected that they will be achieved in later flights. Considering the Nimbus project as a whole, the design objectives may be said to be largely realized.

Accomplishment of these design objectives has posed a real challenge to existing technology and capabilities. That it has taken longer than planned to reach these goals should not surprise anyone, nor cause alarm. A study of the following reports indicates that most major problems have been solved, and successful completion of the spacecraft development is now virtually assured.

DATA ACQUISITION

Figure 5 illustrates the data-acquisition system. This task requires the development and placing in operation of a number of command and data-acquisition (CDA) stations. Two stations are currently planned: one at Fairbanks, Alaska, and a second in Nova Scotia, Canada. These will provide complete orbital coverage. A third station, to be located in Europe for backup and local use, is under consideration for the future. These stations will have 85-foot steerable tracking-antenna systems with full automatic-tracking capability. A sophisticated electronic complex involving over 100 racks of equipment for data processing will also be located in each station. This task is complicated by the requirement for full earth coverage, which forces the stations into remote locations and often into inhospitable climates.

The complex nature of the spacecraft and the ground stations necessitates a centralized overall system control. Development of a central Nimbus Technical Control Center (NTCC) to provide full system control of the spacecraft in orbit and of the ground system complex in operation is in the planning stage. This center will be located at GSFC.

DATA UTILIZATION

Figure 6 illustrates the scope and size of the data-utilization system, which encompasses the ground processing of the data, the transmission of the data in appropriate time scales to the users, and the meteorological applications of the data. This presents a tremendous

data-logistics problem involving assessment, quality control, transmission, interpretation, and analysis of a vast mass of data, totaling almost half a billion bits of information per orbit. The real-time application of this data, in particular, makes this task a real challenge. Extensive processing at the CDA stations, and wideband microwave transmission links from the CDA sites to the NTCC, will help overcome the time restraints.

From the NTCC, the data will be transmitted to cognizant GSFC research personnel and to the National Weather Satellite Center (NWSC) of the U. S. Weather Bureau. At Goddard, the engineering data will be used for spacecraft evaluation, and the sensory data for studies of atmospheric physics. The Weather Bureau will apply the sensory data directly to the weather forecasting problem. Integrating these data with conventional weather data will provide significant improvements in cloud-cover, snow and ice, and storm-track forecasts. The data will also be processed into archival form to make it readily available for future studies by interested research personnel.

The value of immediate and direct application of cloud pictures to weather forecasting is apparent from the TIROS program. The infrared radiation measurements will provide fundamental data on the atmospheric heat balance, and these data may well lead to new and significant understandings of atmospheric processes. The pursuit of such new understandings is vital in the long-range development of satellite meteorology.

NIMBUS ORGANIZATION

Goddard Space Flight Center has been assigned the overall responsibility within NASA for the execution of the Nimbus project. To meet this responsibility, GSFC has organized the Nimbus Project Office as a part of the Aeronomy and Meteorology Division, and has assigned full responsibility for execution of the project to this office. Figure 7 shows the basic organizational structure of the Nimbus Project Office, which consists of the project manager and his immediate technical and administrative staffs, comprising about 20 people, who are responsible for:

- Overall planning
- Task assignments to functional groups
- Procurement management
- Technical, schedule, and fiscal management
- Technical review of progress
- Resolution of system interface problems

Actual development of the various systems is assigned to the following four systems managers:

- The launch vehicle manager - F. Duerr, Marshall Space Flight Center (the center responsible for providing the Thor-Agena vehicle)
- The spacecraft manager - Jack Michaels, GSFC
- The data-acquisition manager - Laverne Stelter, GSFC
- The data-utilization manager - G. Albert, U. S. Weather Bureau (full-time project assignee)

Each of these managers calls on the organizations involved for the support required to accomplish their missions. This support includes the technical officers responsible for the management of individual contracts, as well as various technical and administrative specialists who assist them in directing and managing the individual activities.

In all, about 100 government employees are directly occupied on a full-time basis in developing the Nimbus system. This group, in a sense, constitutes the prime contractor on the Nimbus project, and provides the overall system engineering, the subsystem technical management, and the administrative management for the project.

Developing the actual hardware for the various systems requires the services of many industrial concerns to assist in the design,

fabrication, test, and operation of the various systems. As can be seen in Figures 8 and 9, some 15 major contracts, 11 separate contractors, and numerous subcontractors are involved in the development of the spacecraft system alone; Figure 10 lists some of the contractors involved in other systems, such as launch vehicles, data acquisition, and data utilization. An estimated 3000 to 4000 government and industry people are engaged in the Nimbus program on essentially a full-time basis.

PROGRAM PLAN

The overall program plan, Figure 11, shows in broad terms the planned schedule for the prototype, and for flight spacecraft development, integration, and testing. Estimated completion dates for the ground station are also shown. Each of the spacecraft subsystems is developed independently by each contractor, with appropriate management and coordination by technical officers and the spacecraft manager. The systems are then collected, integrated into the spacecraft at the General Electric Company, and tested as a complete system.

The chart shows the time schedule for initial subsystem development and construction. The spacecraft integration and test program is divided into two sequential elements, the sensory ring activity and the complete spacecraft activity.

As indicated by the dashed line on the chart, the individual prototype subsystems are very close to completion, and the integration and testing of a full prototype spacecraft system will occur in the near future.

Roughly half the major spacecraft subsystems are now available in fully qualified prototype hardware. The spacecraft structure, the PCM telemetry, and the clock command subsystems have been qualified; the power supply, the AVCS subsystem, and the stabilization and control subsystems are not yet qualified, but are all in advanced stages of development.

I initially proposed as a theme for this meeting, "NIMBUS A IN 63." However, Mr. Huston of the Nimbus Project Office offered an addendum: he proposed "NIMBUS A IN 63, FOUR MORE IN 64." I propose this theme now, and suggest that it be accepted as our joint immediate goal.

To realize the long-range goals for full exploitation of Nimbus's potential, the joint attention and technical effort of all concerned will be required for at least a decade.

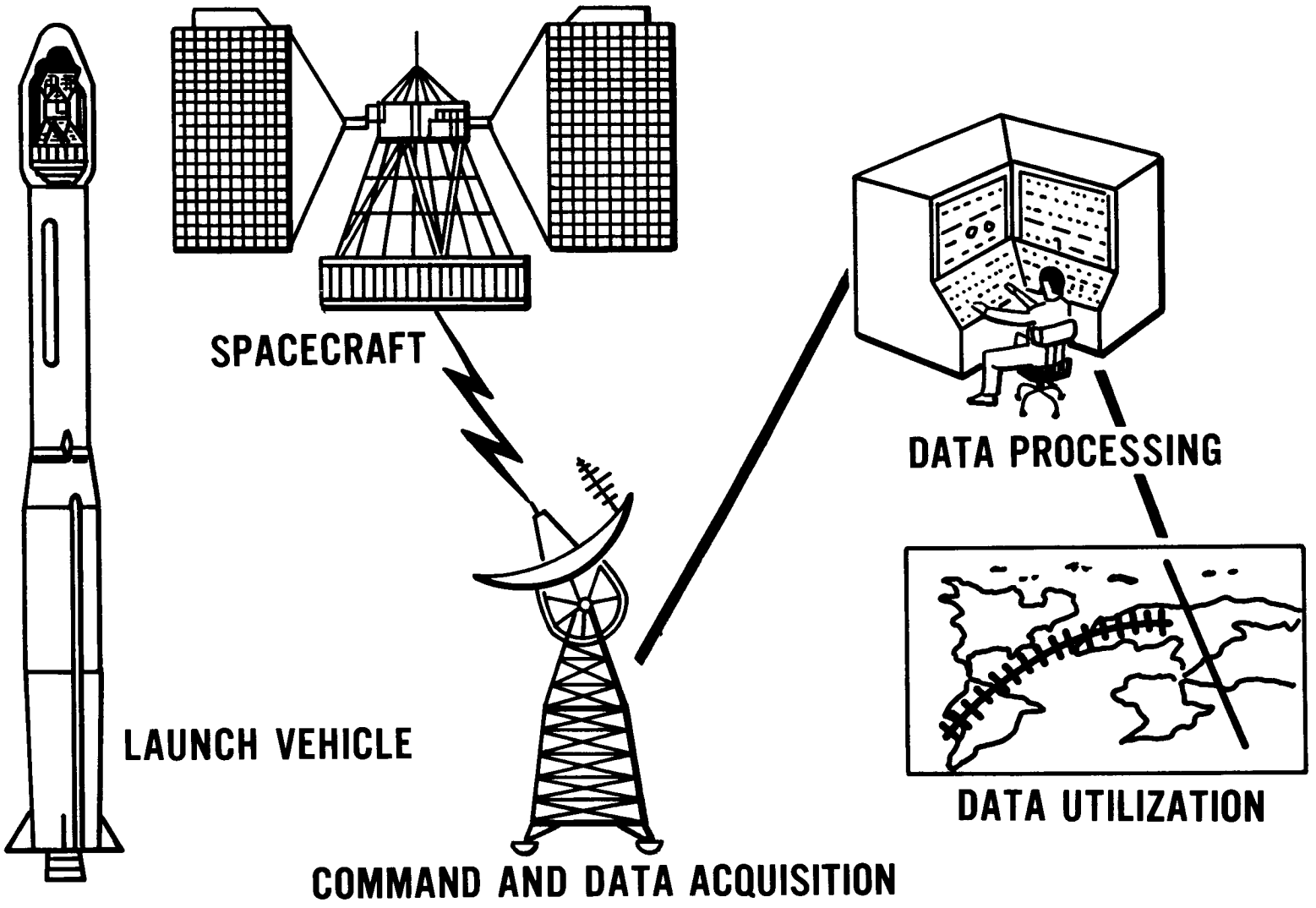

Figure 1 – Nimbus System Complex

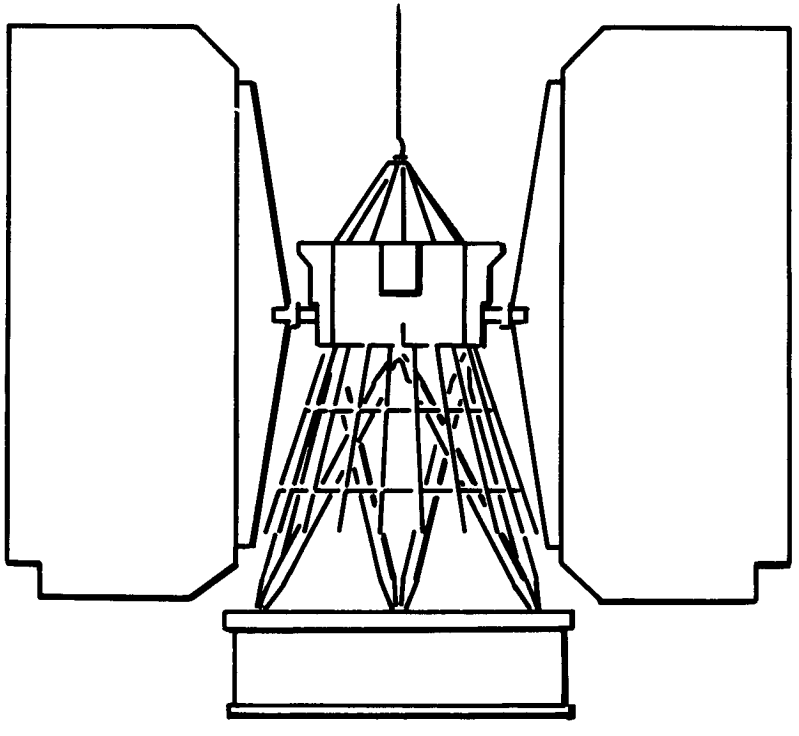

CHARACTERISTICS

- COMPLETE EARTH COVERAGE
- POLAR ORBIT
- EARTH STABILIZED (±1 DEGREE)
- MODULAR DESIGN
- SENSORY GROWTH
- RAPID DATA TRANSMISSION
- LONG LIFE (6 MONTHS)

Figure 2 – Nimbus Launch Sequence

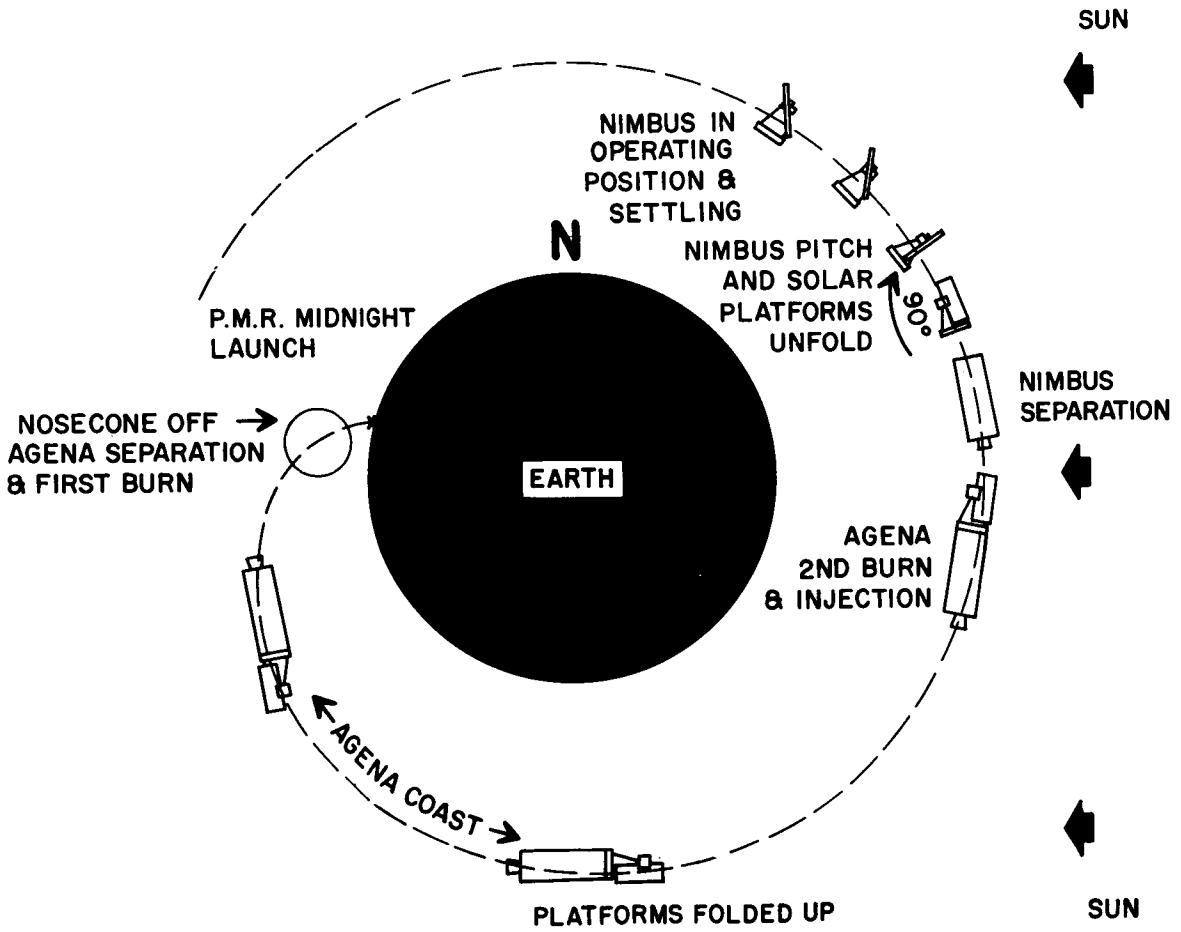

Figure 3 – Nimbus Spacecraft

	DESIGN OBJECTIVE	ACHIEVEMENT
WEIGHT	650 LBS	700 LBS.
STAB. ACCURACY	± 1°	± 2°
POWER (MAX)	450 WATTS	400 WATTS
AVCS (RES.)	½ MILE	½ MILE
PCM TELEMETRY	544 (RECORDED) + 128 (REAL-TIME)	544 (RECORDED) + 128 (REAL-TIME)
HRIR (RES.)	2 MILES	5 MILES
MRIR (RES.)	30 MILES	30 MILES
COMMANDS	128	128

Figure 4 – Performance Achievements

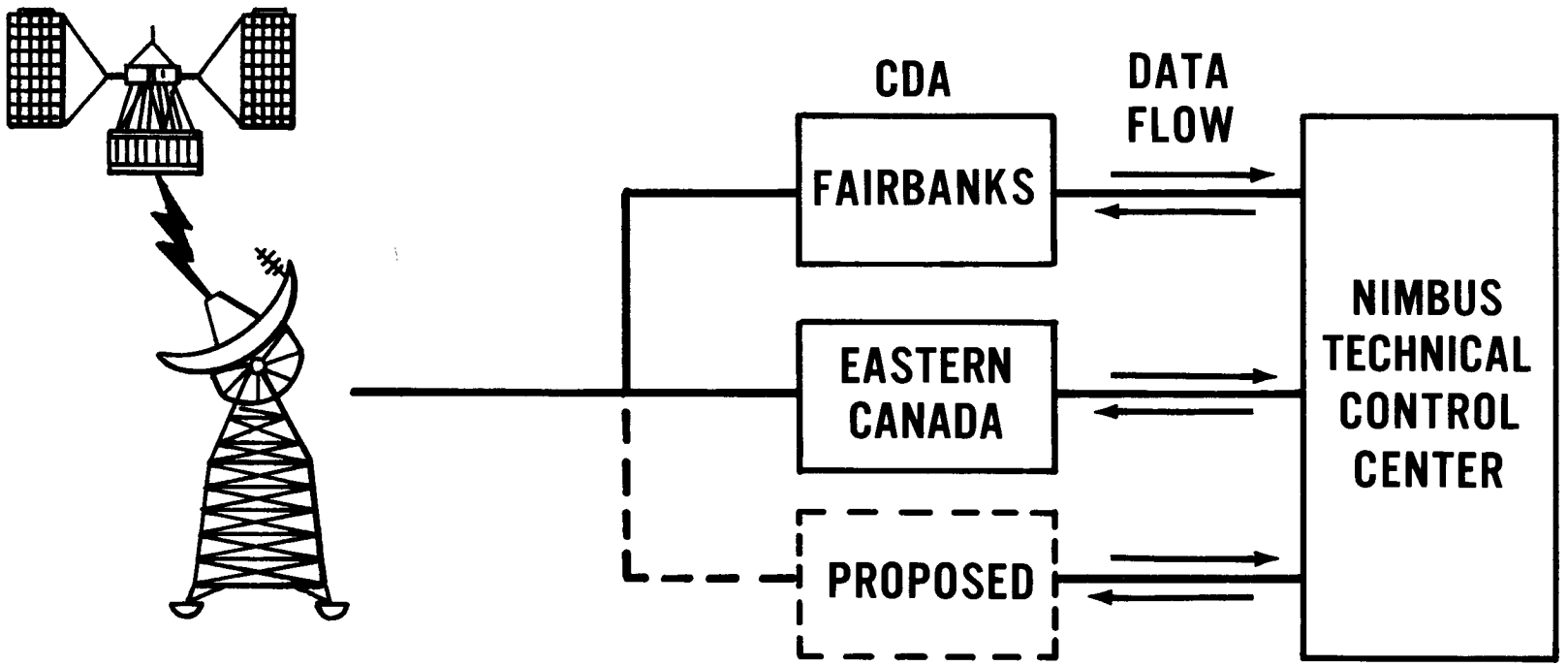

Figure 5 – Data-Acquisition System

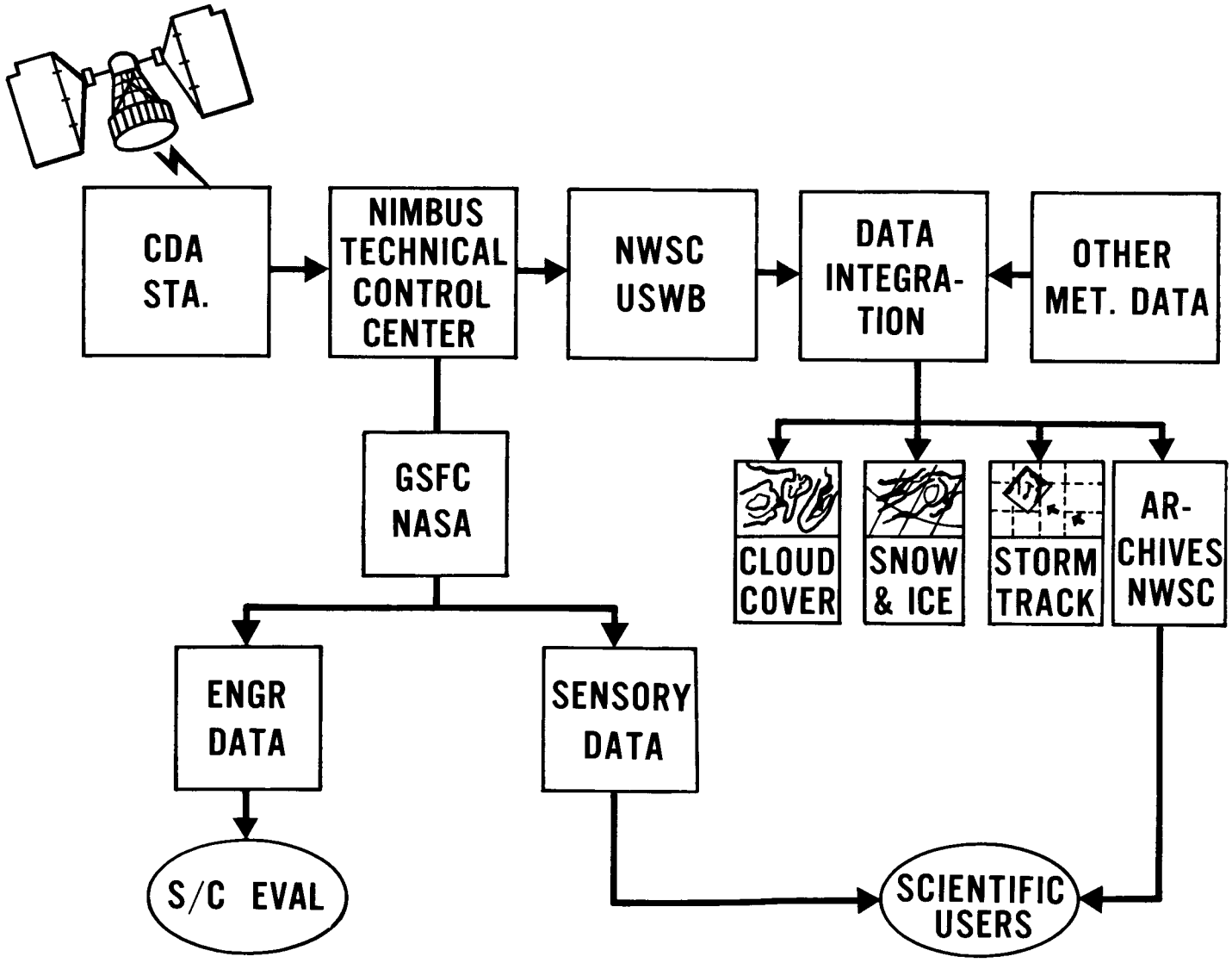

Figure 6 - Data-Utilization System

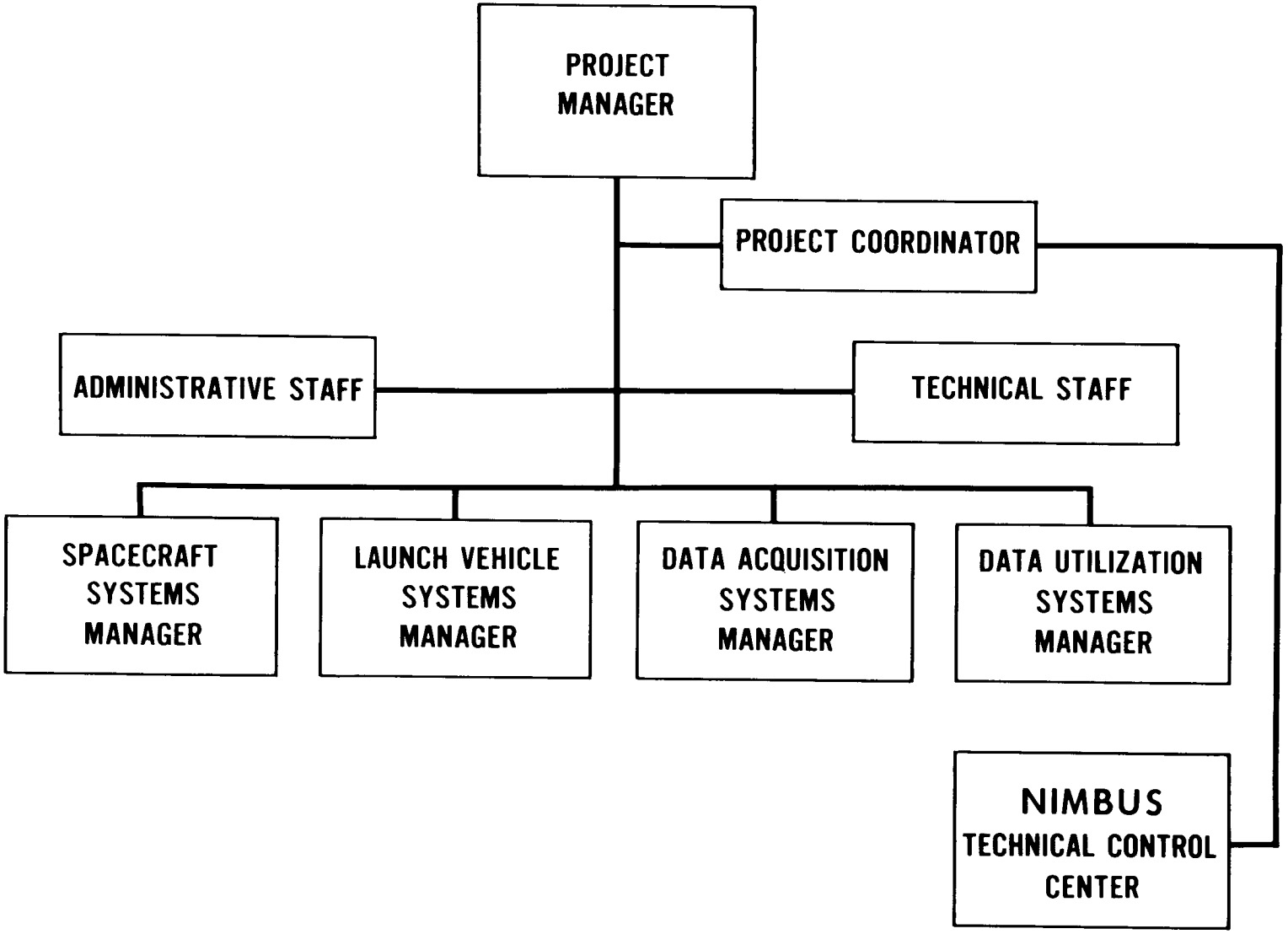

Figure 7 – Nimbus Organization Chart

INTEGRATION AND TEST	G. E. MISSILES AND SPACE DIVISION
CONTROLS AND STABILIZATION	G.E. MISSILES AND SPACE DIVISION
ADVANCED VIDICON CAMERA SYSTEMS	RCA-ASTRO-ELECTRONICS DIVISION
S-BAND XMTR	GENERAL ELECTRONICS LABORATORY
PCM TELEMETRY	RADIATION, INC.
PCM/AM XMTR	HUGHES AIRCRAFT CO.
COMMAND CLOCK	CALIFORNIA COMPUTERS PRODUCTS
CLOCK RECEIVER	RCA-ASTRO-ELECTRONICS DIVISION
SOLAR POWER	RCA-ASTRO-ELECTRONICS DIVISION

Figure 8 – Nimbus Spacecraft Contractors

MEDIUM RESOLUTION INFRARED RADIOMETER	SANTA BARBARA RESEARCH CENTER
MEDIUM RESOLUTION INFRARED RADIOMETER ELECTRONICS	AERO-GEO-ASTRO
MEDIUM RESOLUTION INFRARED RADIOMETER/FM XMTR	TEXAS INSTRUMENTS
PCM AND MEDIUM RESOLUTION INFRARED RADIOMETER TAPE RECORDERS	RAYMOND ENGINEERING
HIGH RESOLUTION INFRARED RADIOMETER	INTERNATIONAL TELEPHONE AND TELEGRAPH
HIGH RESOLUTION INFRARED RADIOMETER TAPE RECORDER	RCA-ASTRO-ELECTRONICS DIVISION

Figure 9 – Nimbus Spacecraft Contractors (cont.)

LAUNCH VEHICLE	LOCKHEED MISSILE AND SPACE CO.
SEPARATION SYSTEM AND SHROUD	DOUGLAS AIRCRAFT CO.
85 FT. ANTENNA	ROHR CORP.
ANTENNA ELECTRONICS	COLLINS RADIO CO.
RELIABILITY	OPERATIONS RESEARCH, INC.
S/C ANTENNA DESIGN	UNIVERSITY OF NEW MEXICO
COMPUTERS	CONTROL DATA CORP.
GROUND STATION	FAIRCHILD STRATOS
REAL-TIME DATA STUDY	STANFORD RESEARCH INST.
DATA UTILIZATION HANDLING SYSTEM	ESS GEE INC.
WIDE BAND TRANSMISSIONS	AMERICAN TELEPHONE AND TELEGRAPH CO.
ATMOSPHERIC RESEARCH	GEOPHYSICAL INST. OF UNIVERSITY OF ALASKA

Figure 10 – Other Contractors

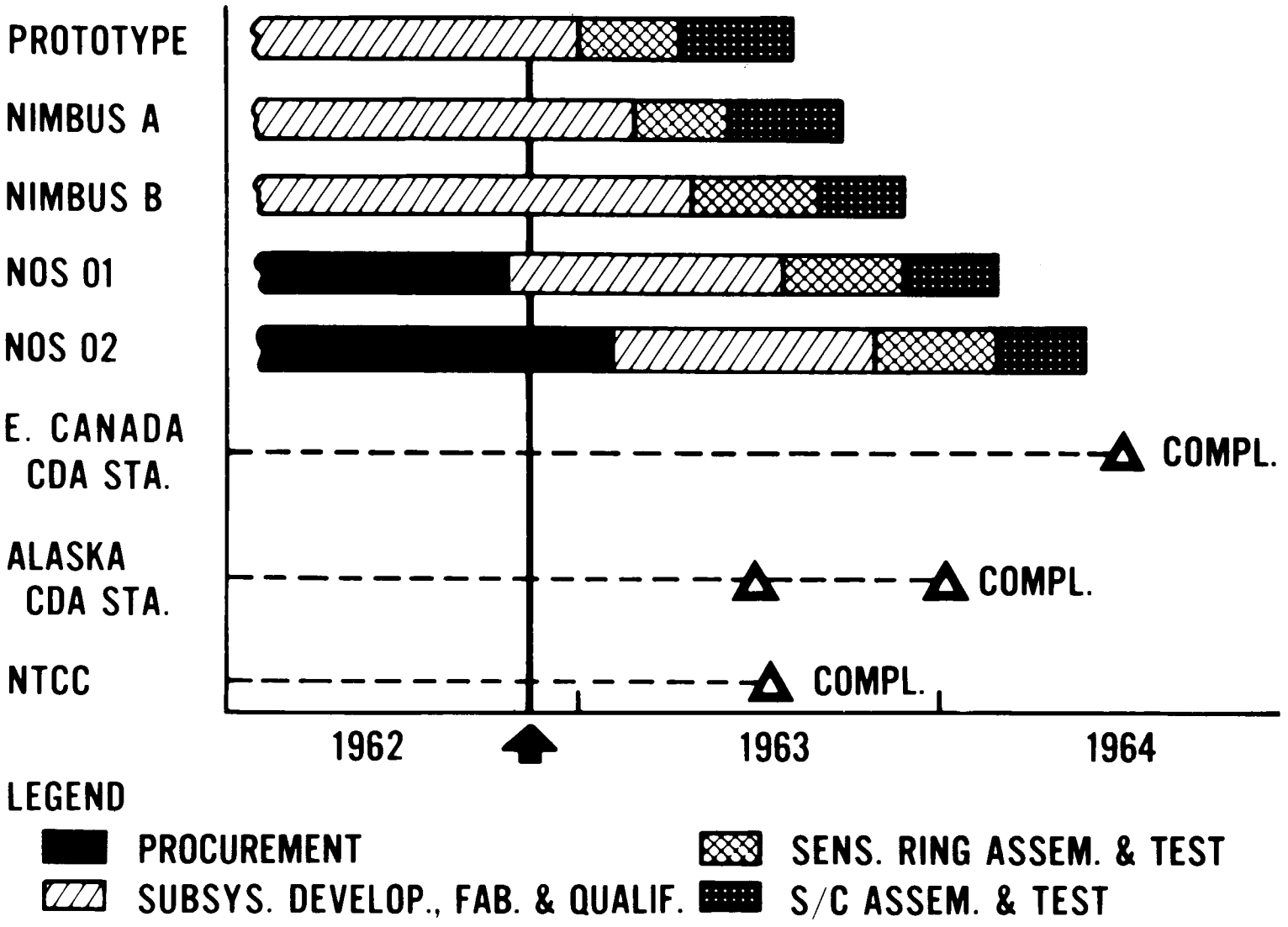

Figure 11 – Nimbus Program Plan

3. METEOROLOGICAL APPLICATIONS OF NIMBUS DATA

By E. G. Albert, U. S. Weather Bureau

3. METEOROLOGICAL APPLICATIONS OF NIMBUS DATA

ILLUSTRATIONS

Figure		Page
1	Primary Weather-Observing Stations in the Northern Hemisphere	12
2	Cloud Depiction Chart Prepared from TIROS Photographs Taken on May 20, 1960	13
3	Comparison of Conventional Cloud Analysis with TIROS II Infrared Measurements	14
4	TIROS I Picture of Thunderstorms over the Central United States	15
5	Rectification of Uncalibrated TIROS III Radiometer Channel 2 Response Superimposed on the Corresponding TIROS III TV Picture	16
6	Six-Day Change in Location of Sea Ice near Anticosta Island in the Gulf of St. Lawrence	17
7	Mountain Snow Fields	18
8	TIROS II Outgoing Longwave Radiation (10^{-2}LY/MIN) 1927 Z, January 1, 1961 to 0654Z, January 2, 1961	19
9	Artist's Composite of TIROS I Pictures, 12 GMT to 12 GMT, May 19-20, 1960	20
10	Geographical Area Covered by One Nimbus AVCS Picture Triplet and the Corresponding Perspective Latitude-Longitude Grids	21
11	Analog and Digital Representations of a Perspective Cloud Picture	22
12	Representation of a Cloud Picture in Digitally Rectified Form on a Mercator Base Map	23

Figure		Page
13	Nimbus Meteorological Data Processing	24
14	Archived Products of the Early Nimbus Data-Processing System	25
15	Hurricane Debbie as Observed by TIROS III, September 13, 1961	26

3. METEOROLOGICAL APPLICATIONS OF NUMBUS DATA

By E. G. Albert, U. S. Weather Bureau

INTRODUCTION

BACKGROUND

Ever since the first realization, a century or so ago, that today's weather here is related to yesterday's weather somewhere else, there has been urgent demand to expand observational capability in both the horizontal and vertical directions. This demand is a reasonable one. It is based on the fact that the ability to predict the future state of the atmosphere depends directly, in both a mathematical and a practical sense, on the completeness of knowledge of the current state of the atmosphere.

Many advances have been made in the past. Hundreds of observation sites interconnected by teletype circuits exchange frequent reports. However, as Figure 1 shows, vast areas of the earth still yield no reports. The black dots in Figure 1 represent the primary weather-reporting stations in the northern hemisphere. Even in the comparatively dense observation areas of North America, western Europe, and eastern Asia, the distance between stations is generally large enough to allow some significant weather features to go undetected. Nimbus will fill these gaps.

ILLUSTRATION OF NUMBUS POTENTIAL

As an illustration of the Nimbus potential, consider the surface area of the earth—approximately 200 million square miles. An observer on the ground can view portions of cloud patterns effectively over no more than a few hundred square miles. On this basis, Nimbus can do the work of several hundred thousand observing stations (Reference 1).

This is, of course, a faulty example. It is unfair to Nimbus, because the interconnection of those hundreds of thousands of stations and the assembly of a coherent cloud pattern from their reports would be extremely complex undertakings. Also, the cost of such a system would be measured in billions, not millions, of dollars.

The comparison is unfair to the observing network, too. Nimbus will provide no measurement of atmospheric pressure, a fundamental parameter in mathematical weather prediction. Measurements from a satellite of wind and temperature in the lower atmosphere are years away, at best.

The point to be made is that the Nimbus meteorological satellite system and the existing conventional observation networks are complementary systems, not duplicate or competitive ones. Working together, the two systems will provide significantly improved knowledge of the existing state of the earth's atmosphere. Better definition of initial conditions should, in turn, lead to better solutions of the differential equations which describe the atmosphere. In other words, the net result should be more precise weather forecasts for longer periods of time.

QUESTIONS TO BE ANSWERED

In the remainder of this paper, an attempt will be made to answer three questions:

(1) What are the specific applications of the Nimbus system in solving meteorological observation problems?

(2) What means will be available for handling enormous quantities of Nimbus data and presenting them to meteorologists in useful forms?

(3) What is the plan for integrating the various data-handling techniques in actual operation, in order to present the data in a timely fashion?

APPLICATIONS

MAJOR STORM SYSTEMS

Figure 2 is probably quite familiar to many readers. The material was first assembled by Oliver from TIROS I pictures and National Meteorological Center analyses for May 20, 1960 (Reference 2). It shows in a striking way the type of meteorological organization observable from a satellite. This is indeed nature's own weather map.

TIROS experience gained over the past two and a half years has proved that weather features of this scale, major storm systems having characteristic spacings of a thousand or more miles, are easily and accurately identified from satellite photographs. Inferences can be drawn concerning each system's intensity and its stage of development (Reference 3).

CLOUD TOPS FROM IR DATA

Figure 3 illustrates the kinds of information which may be derived from the high-resolution infrared radiometer (HRIR) planned for Nimbus A. Winston assembled and analyzed this TIROS II infrared data and all available conventional cloud data over the United States for the corresponding time period.

Close examination of Figure 3 shows that, in addition to the gross agreement in pattern between the radiation and cloud data, there is also agreement on a finer scale. The cloud tops associated with the eastern United States frontal system increase in height rapidly on the western side of the cloud mass. The maximum cloud-top heights, representing the most intense development, appear in the Carolina-Virginia area. A similar pattern can be seen in the infrared data, with the coldest temperatures appearing in the same area. Similar agreements appear over the remainder of the map. This illustrates a use of radiometer data which is different from the possible use of the television data; the radiometer provides measurements which may be interpreted in terms of temperature of cloud tops, and these temperatures in turn may be interpreted in terms of the height of the cloud top. Such quantitative data is much more useful than the mere cloud-area delineation and subjective identification allowed by the television pictures.

Other different and important kinds of information can be derived from radiation data provided by the medium-resolution infrared radiometer (MRIR): for example, earth-surface temperature in cloudfree areas and tropopause temperatures or heights. These measurements may be combined to yield average lapse rate, or average stability of the troposphere (References 4, 5, 6).

MESOSCALE PATTERNS

Figure 4 illustrates a satellite's capability to observe atmospheric organization on a smaller scale. This picture, taken by TIROS I, shows

conditions in the central United States on May 16, 1960. An analysis by Whitney (Reference 7) revealed that cloud mass A was produced by a group of severe thunderstorms along a cold front in northern Missouri, while cloud mass B represents a separate group of pre-frontal thunderstorms south of St. Louis. It is entirely possible for satellite observations to detect important small-scale circulation features such as these, which may be missed by a fairly dense conventional observing network.

Figure 5 is a result of Fujita's study of TIROS infrared radiation data (Reference 8). His precise manual methods of television-and-infrared rectification produce combined analyses which show the direct relationship between radiation measurements and cloud locations on a very small scale. Close examination of this picture shows that the radiation isopleths agree very well with the TV image. If it proves feasible to automate Fujita's procedures, nighttime cloud cover may be mapped by the Nimbus HRIR with a resolution approaching that of TIROS television pictures.

ICE FIELDS

Another important class of observations which can be made from a satellite is illustrated by Figure 6. These TIROS II narrow-angle camera pictures were assembled and studied by Wark and Popham (Reference 9). The 6-day change in the character of the ice fields at the eastern end of Anticosti Island is clearly shown. Between March 23 and 29, a large area of open water developed in the Gulf of St. Lawrence where apparently solid sea ice previously existed. Information of this sort on worldwide ice fields will be of great economic value to shipping interests and to all others affected by the navigability of the world's waterways.

The white patch near the center of Anticosti Island is the deforested area left by an earlier forest fire. It appears as it does in this picture because the snow cover can be seen clearly in the burned area, while in the surrounding forest the snow is partially hidden by overhanging branches. Other pictures were taken in which the smoke from an existing forest fire can be seen. Pictures such as these lead to interesting speculation about the use of Nimbus data in nonmeteorological fields such as forestry or conservation, and even in locating locust swarms and schools of fish.

SNOW FIELDS

Observation of another form of solid water on the earth's surface is illustrated in Figure 7. Mountain snowfields are the water-supply reservoirs for many important civilized areas. Early knowledge of snowfield extent has great economic value for those areas and has been very difficult to obtain with any accuracy. Nimbus pictures will allow precise mapping of the extent of snowfields.

The hook-shaped white area in picture 1 of Figure 7 represents the snow-capped Alps extending to the Mediterranean coast. Picture 2 shows snow on the southern Andes somewhat less distinctly.

Pictures 3 and 3a of Figure 7 are particularly interesting for their comparison of different resolutions. The upper frame, taken by the TIROS I wide-angle camera, is a general view of the Himalayas with a TV raster linewidth of 2 or 3 miles in the foreground mountain area. This is similar to the resolution expected near the edges of the Nimbus side cameras. Picture 3a is a nearly simultaneous narrow-angle picture with about one order-of-magnitude better resolution. This is somewhat better than the resolution expected from the center Nimbus camera. While the high-resolution picture shows terrain features more distinctly, both show the finely detailed boundaries of the white areas which Fritz has found to be characteristic of mountain snowfields, distinguishing them from clouds (Reference 10).

Another means of separating clouds from snowfields and other potentially confusing backgrounds will make use of global background-brightness maps, which will be prepared and updated routinely at the National Weather Satellite Center for several purposes. Snowfields and ice packs will be outlined each time they are seen. Since these features will generally change much less rapidly than clouds, a series of observations over a period of days will lead to continual improvement in the accuracy with which the boundaries are drawn.

When observations of the MRIR become available on later Nimbus satellites, it will be possible in many cases to positively distinguish between clouds and cloud-free snow or ice surfaces.

HEAT BALANCE

Another application of the MRIR data, and one which may well become its most important application, will be the routine measurement of the

entire earth's outgoing longwave radiation. This is illustrated in Figure 8. This map of outgoing longwave radiation was assembled by Winston from TIROS II radiometer data (Reference 11). Information of this sort can be combined with knowledge of the incoming energy from the sun to determine the latitudinal and longitudinal variations in earth's heat balance. These large-scale energy exchange processes play an important, but not yet well understood, part in the production of large-scale weather features.

SUMMARY OF APPLICATIONS

To summarize the applications of Nimbus meteorological data:

(1) There is the application positively established in routine TIROS operations, the identification and positioning of major weather systems. This capability will improve from the somewhat uncertain, variable area coverage achieved with TIROS (as illustrated in Figure 9, which shows the northern hemisphere TIROS I swaths in one 24-hour period) to the complete surveillance of the entire globe on a daily basis with Nimbus.

(2) Smaller scale features which may go unobserved by a conventional observing network will be located and identified.

(3) There is a variety of applications concerning conditions at earth's surface, including the delineation of ice packs and mapping of snowfields.

(4) Radiation data may be used to determine the earth's heat balance and local heat anomalies.

DATA HANDLING

To realize the potential of these applications, data-handling techniques are required which can accept Nimbus data from the spacecraft-ground station complex and reduce them to meteorological data suitable for incorporation into weather forecasts. Several techniques are under development.

GRIDDED PICTURES

A question which needed an early answer was: What format will be most useful to the ultimate user? One obvious answer was analog pictures with superimposed latitude-longitude grids. This format can be produced in a comparatively straightforward manner.

Figure 10 shows the geographical coverage of one possible Nimbus picture triplet. The area viewed by the two obliquely facing side cameras extends about 900 miles to either side of the satellite subpoint track, and assumes this particular shape for obvious geometrical reasons. Computer-prepared grids for these pictures are shown at the bottom. Latitude and longitude lines, coastal outlines for verification of grid fit, and numerical labels are provided.

Development of this output capability is at an advanced stage. Gridded TV and IR pictures will be available for meteorological use during Nimbus A operation.

DISADVANTAGES OF GRIDDED PICTURES

Gridded analog pictures are not the best answer to the original question, however; their major drawback is that a man must look at and interpret them before they can be used.

A man must perform two kinds of operations on gridded pictures. One is the important, in fact indispensable, application of professional knowledge to extract the meteorological information. The other operation—the purely mechanical one of transferring cloud shapes from the oblique-perspective picture to a suitable map base so that comparisons can be made with more conventional types of data—is basically the procedure currently used in TIROS operations. It is time-consuming, and depends heavily on artistic ability and professional experience to produce the map-scale rectification.

DIGITAL TECHNIQUES

From another point of view, since weather forecasting today is based on digital-computer solution of mathematical models of the atmosphere, it would be far better to provide Nimbus data in a format compatible with computer-input requirements. For this reason, hardware and computer techniques are being developed which will digitize the Nimbus

data and operate on them. The output of these routines will be in a format suitable for use by the numerical weather-prediction group of the National Meteorological Center, the comparable Air Force group at Offutt Air Force Base, and all other domestic and foreign meteorological organizations possessing adequate computer capability.

An added benefit of this digital computer data-handling scheme will be automatic rectification into standard map-projection presentations. A simple manipulation of the data in the computer allows it to be presented on a standard facsimile machine, so that the resulting copy has the proper scale and distortion to fit a standard map base. The rectification can be directly annotated by a satellite meteorologist and transmitted to weather stations around the world.

Figures 11 and 12 illustrate this digital procedure. Figure 11 shows an analog and a digital representation of one perspective cloud picture; Figure 12 shows two representations of that picture in a digitally rectified form. Both of these are rectified to a standard Mercator map base. The only difference between the two representations is that, in the upper one, additional picture bits have been filled in by program logic in areas where gaps resulted from the extreme spreading-out effect near the picture horizon.

Mathematically similar mapping techniques can be applied to the radiation data to provide similar rectified presentations.

SUMMARY OF DATA-HANDLING TECHNIQUES

To summarize, the basic television and radiometer meteorological data to be provided by Nimbus will be presented to the ultimate user in three basic formats: (1) gridded analog pictures; (2) digital computer-digested summaries, in a format suitable for use by computational facilities; and (3) a computer-prepared map-scale rectification which will be professionally interpreted and annotated.

OPERATIONAL USE

How do these various applications of Nimbus data and processing techniques fit together into an efficient data-utilization scheme?

Figure 13 broadly outlines the flow of data, and the processing necessary for timely operational use. Nimbus data received at the CDA

station and appropriately processed are transmitted to the National Weather Satellite Center where the meteorologically useful Nimbus data presentations are prepared, compared with conventional data, annotated by professional meteorologists, and presented to the responsible forecasting agencies. Present plans call for this final observational output to be available to forecasters in less than one Nimbus orbital period. Development in this area is sufficiently advanced to make the meeting of this objective reasonably certain.

ARCHIVING SYSTEM

Since Nimbus meteorological data is unique and valuable for research purposes as well as for operational use, a rather sophisticated archiving system is an important part of the data-utilization effort. Figure 14 schematically presents some of the products of the system.

The special archiving system will be implemented to preserve Nimbus data in the best possible form with the least possible degradation. Basic archival material will be prepared from magnetic tapes made at the CDA station. Magnetic tape, however, will not be the final archival form. Television pictures will be preserved on high-quality photographic film, and accurate latitude-longitude grids specially prepared after the fact will be available. Computer-treated radiation data will be stored in microfilm form, as will the more useful operational products.

RESEARCH AND DEVELOPMENT NEEDS

In conclusion, some areas must be briefly mentioned which require urgent study if Nimbus data utilization is to fully realize its potential.

Figure 15 is a very poor TIROS picture. When this picture of Hurricane Debbie was taken on September 13, 1961, the brightness-response capability of TIROS III had degraded to a very poor level. Only the gross presence or absence of clouds can be distinguished, and none of the detail necessary to identify cloud types is present. Nevertheless, no satellite meteorologist could conceivably fail to identify this cloud mass for what it is—a very intense tropical storm, probably a hurricane. But no automatic pattern-recognition technique has yet been demonstrated that will identify tropical cyclones or any other specific cloud patterns in their various appearances and distinguish them from other cloud masses.

Considerable basic research is certainly required in the area of infrared data interpretation. Answers are needed for such questions as: What wavelength intervals are most useful in detecting particular meteorological parameters, and what are the relationships between energy imbalances and weather-system genesis?

Further developments are certainly possible in the data-handling area. In addition to pattern recognition, improved computer capability is needed to manipulate the hundreds of millions of bits of information produced on each Nimbus orbit.

Another area requiring both basic and applied research is the actual incorporation of Nimbus cloud data, in digital form, into numerical weather-prediction routines. Some research is now in progress, but greater effort is needed along these lines.

All these areas, and others discussed, offer exciting and worthwhile research opportunities, and each could benefit greatly from industry participation.

REFERENCES

1. Fritz, S., "On Observing the Atmosphere from Satellites-I, Cloud Observations," Weatherwise, Vol. 12, (August 1959).

2. Oliver, V. J., "TIROS Pictures a Pacific Frontal Storm," Weatherwise, Vol. 13, (October 1960).

3. Bouchet, R. J. and Newcomb, R. J., "Synoptic Interpretation of Some TIROS Vortex Patterns: A Preliminary Cyclone Model," Journal of Applied Meteorology, Vol. 1, (June 1962).

4. Fritz, S. and Winston, J. S., "Synoptic Use of Radiation Measurements from Satellite TIROS II," Monthly Weather Review, (January 1962).

5. Bandeen, W. R., et al, "Infrared and Reflected Solar Radiation Measurements from the TIROS II Meteorological Satellite," Journal of Geophysical Research, (October 1961).

6. Allison, L. J., "Preliminary Synoptic Analysis of TIROS II Radiation Data Over New Zealand at Night," unpublished.

7. Whitney, L. F., "Another View from TIROS I of a Severe Weather Situation—May 16, 1960," Monthly Weather Review, (November 1961).

8. Fujita, T., et al, "Meteorological Interpretation of Convective Neph Systems Appearing in TIROS Cloud Photographs," Research Paper No. 9, Mesometeorology Project, University of Chicago (April 1962).

9. Wark, D. Q. and Popham, R. W., "Ice Photography from the Meteorological Satellites TIROS I and TIROS II," Meteorological Satellite Laboratory Report No. 8.

10. Fritz, S. and Wexler, H., "Planet Earth and Sun from Space," in G. P. Kuiper and B. M. Middlehurst (ed.), Planets and Satellites, Solar System, Vol. 3, University of Chicago Press (1961).

11. Winston, J. S. and Rao, P. Krishna, "Temporal Variations in the Planetary-Scale Outgoing Long-Wave Radiation as Derived from TIROS Measurements," unpublished.

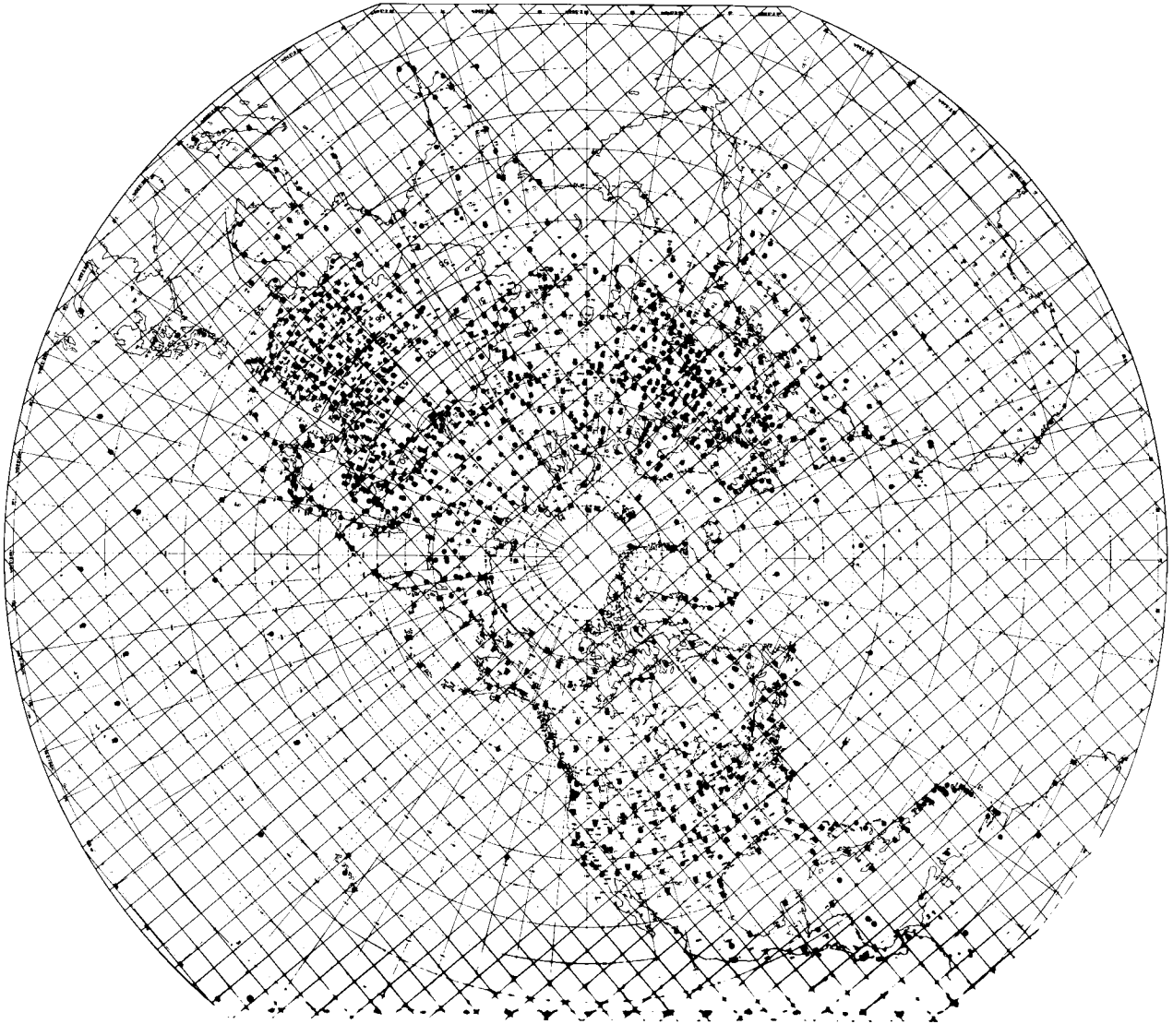

Figure 1 – Primary Weather-Observing Stations in the Northern Hemisphere

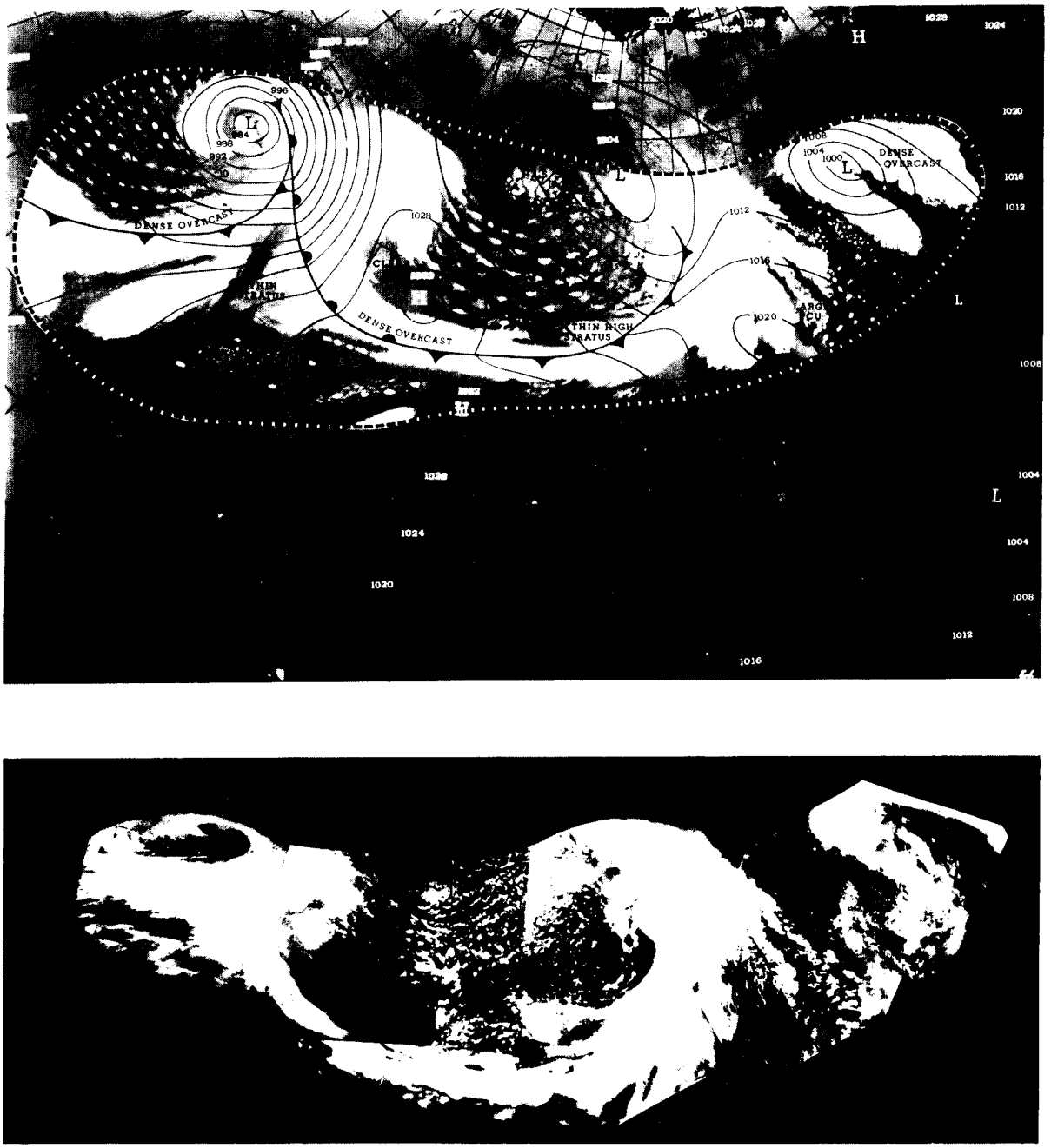

Figure 2 – Cloud Depiction Chart Prepared from TIROS Photographs Taken on May 20, 1960

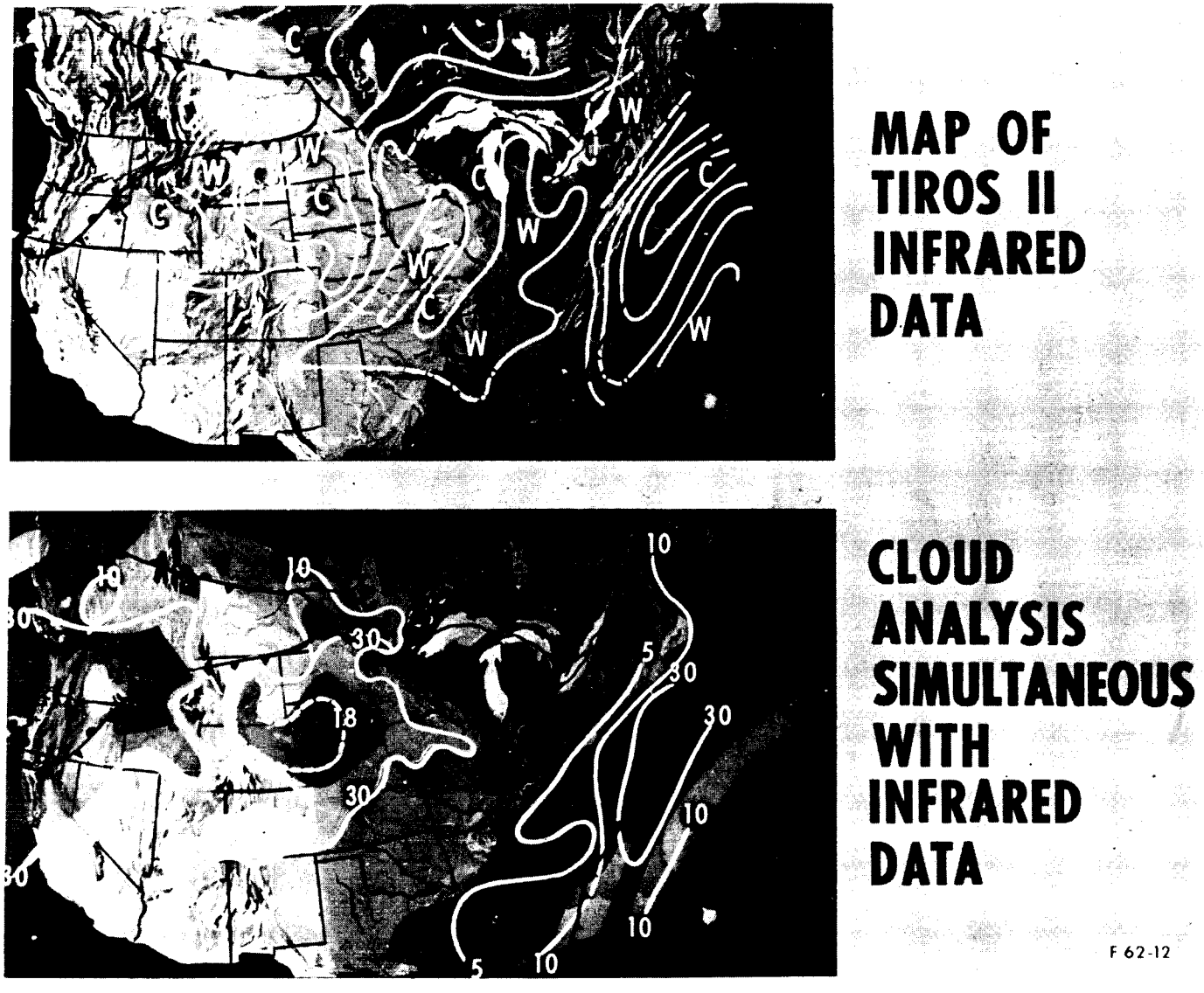

Figure 3 – Comparison of Conventional Cloud Analysis with TIROS II Infrared Measurements

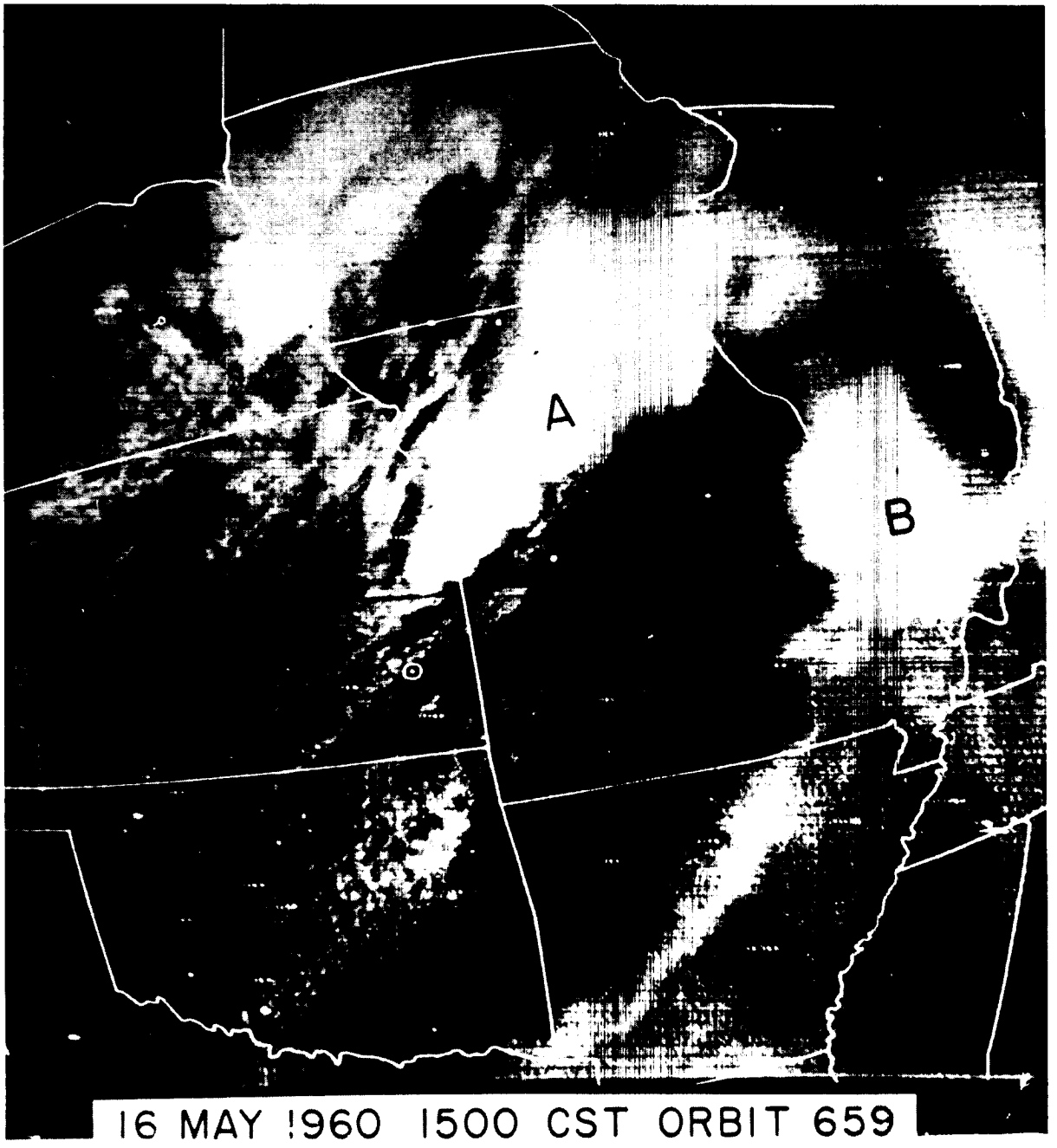

Figure 4 – TIROS I Picture of Thunderstorms over the Central United States

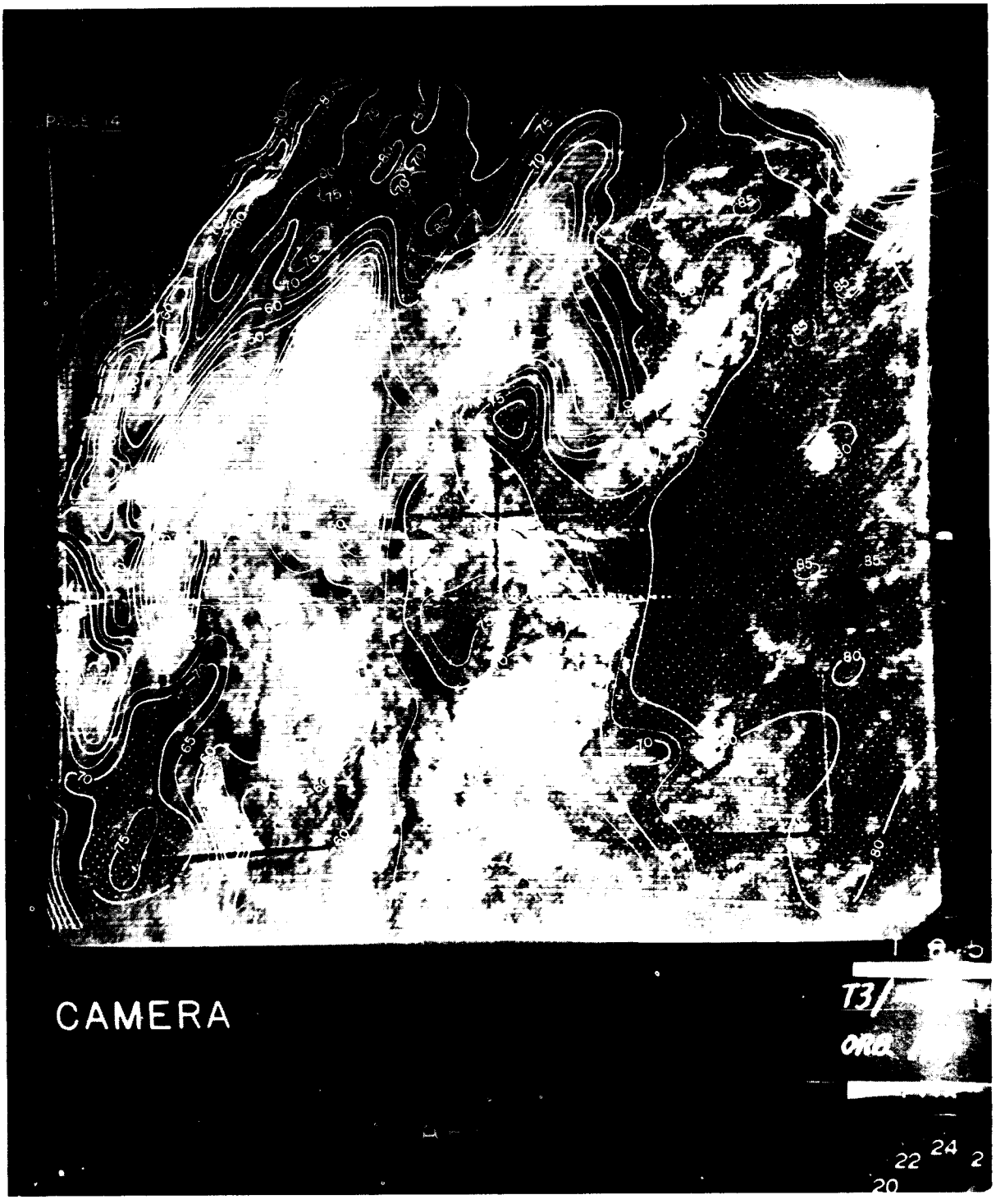

Figure 5 - Rectification of Uncalibrated TIROS III Radiometer Channel 2 Response, Superimposed on the Corresponding TIROS III TV Picture

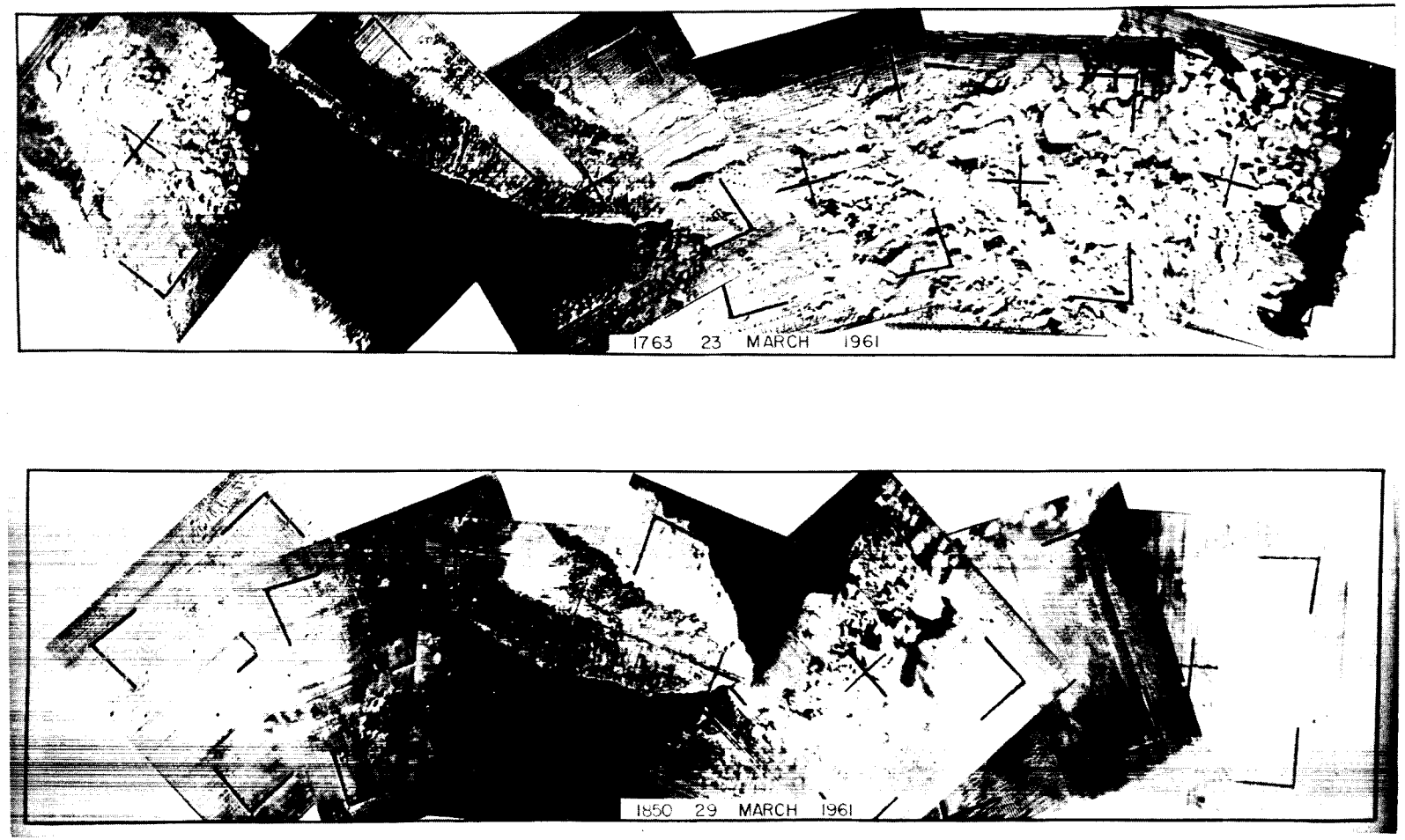

Figure 6 – Six-Day Change in Location of Sea Ice near Anticosta Island in the Gulf of St. Lawrence

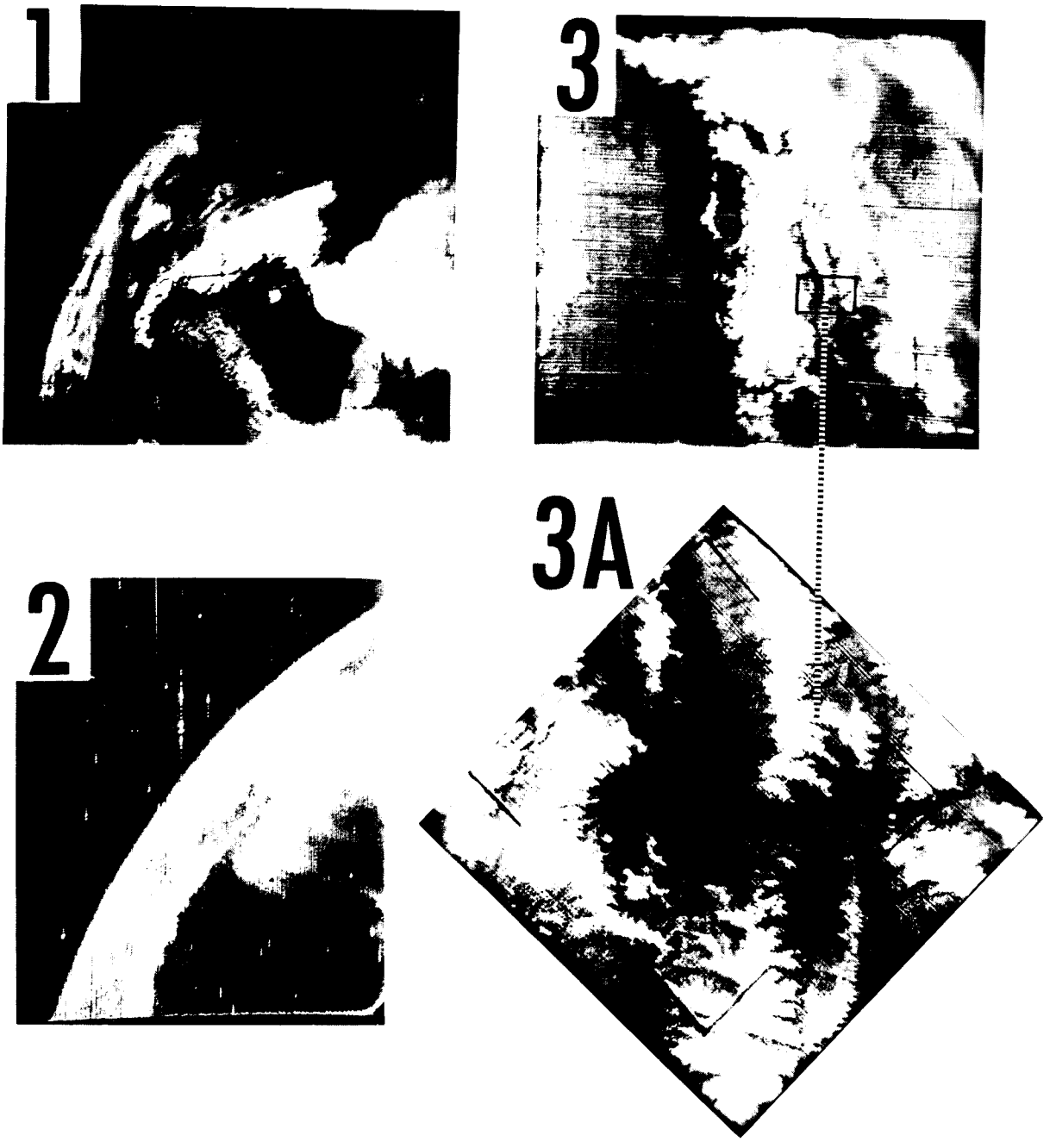

Figure 7 – Mountain Snow Fields

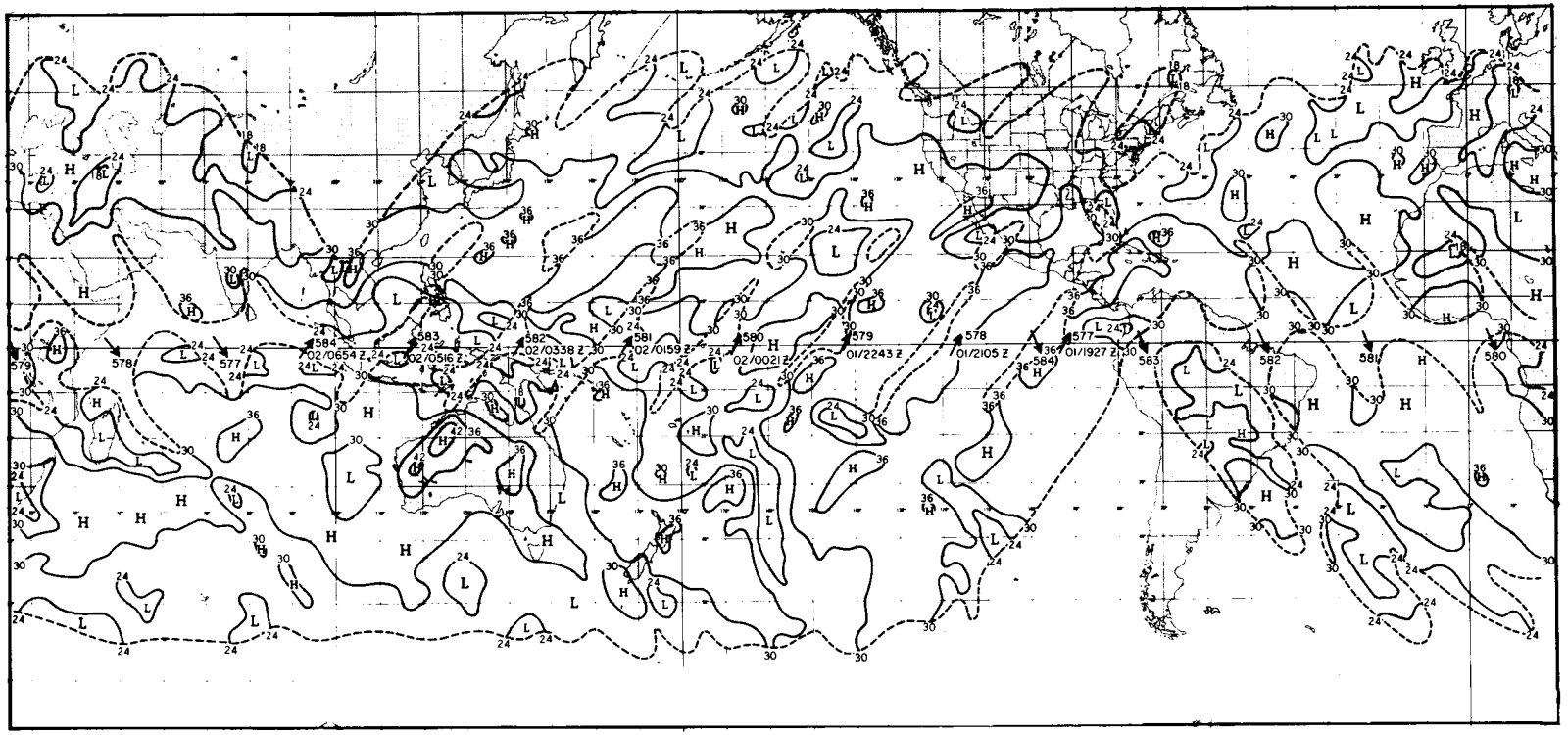

Figure 8 – TIROS II Outgoing Longwave Radiation (10^{-2} LY/MIN)
1927 Z, January 1, 1961 to 0654Z, January 2, 1961

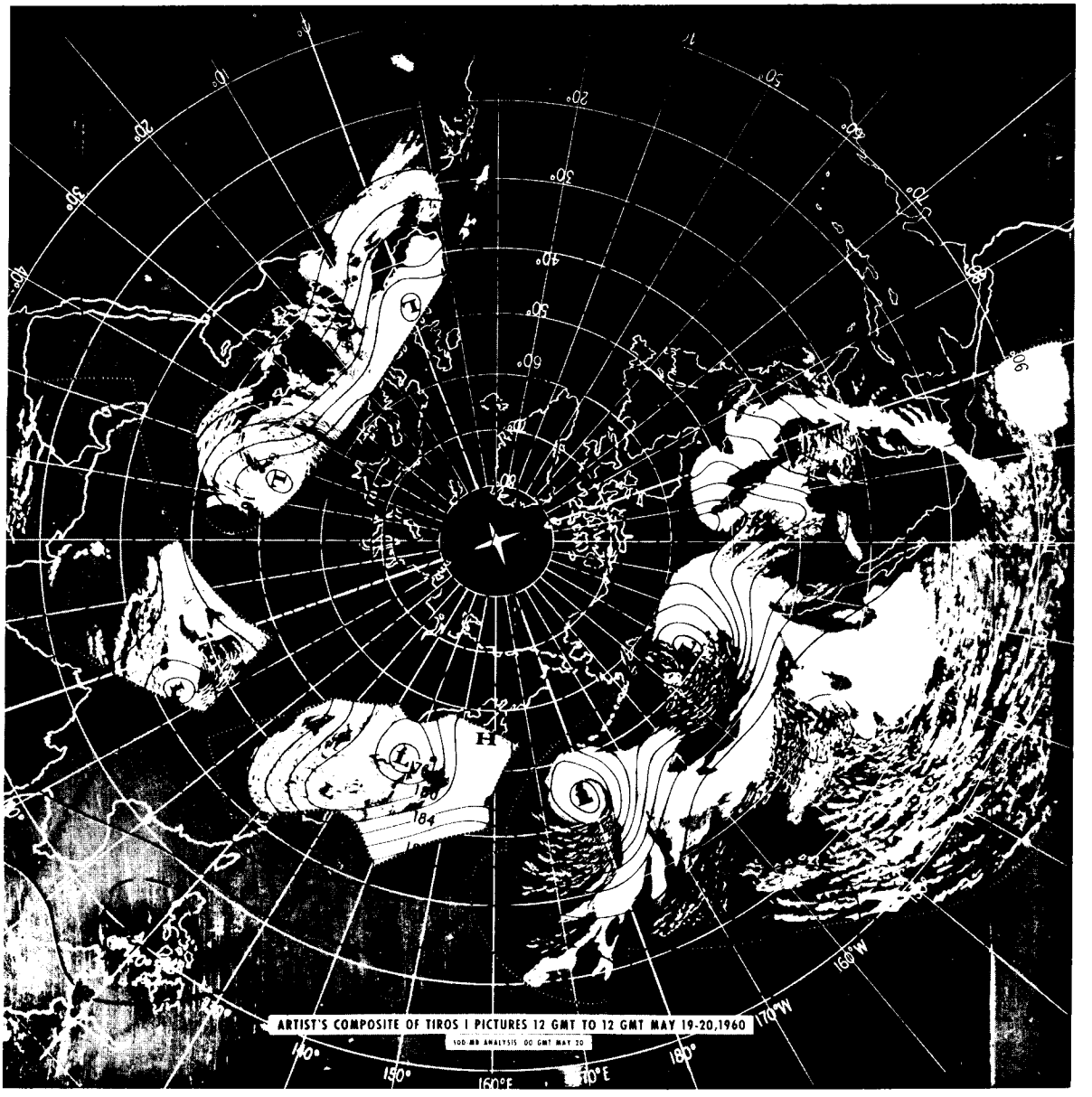

Figure 9 – Artist's Composite of TIROS I Pictures, 12 GMT to 12 GMT, May 19–20, 1960

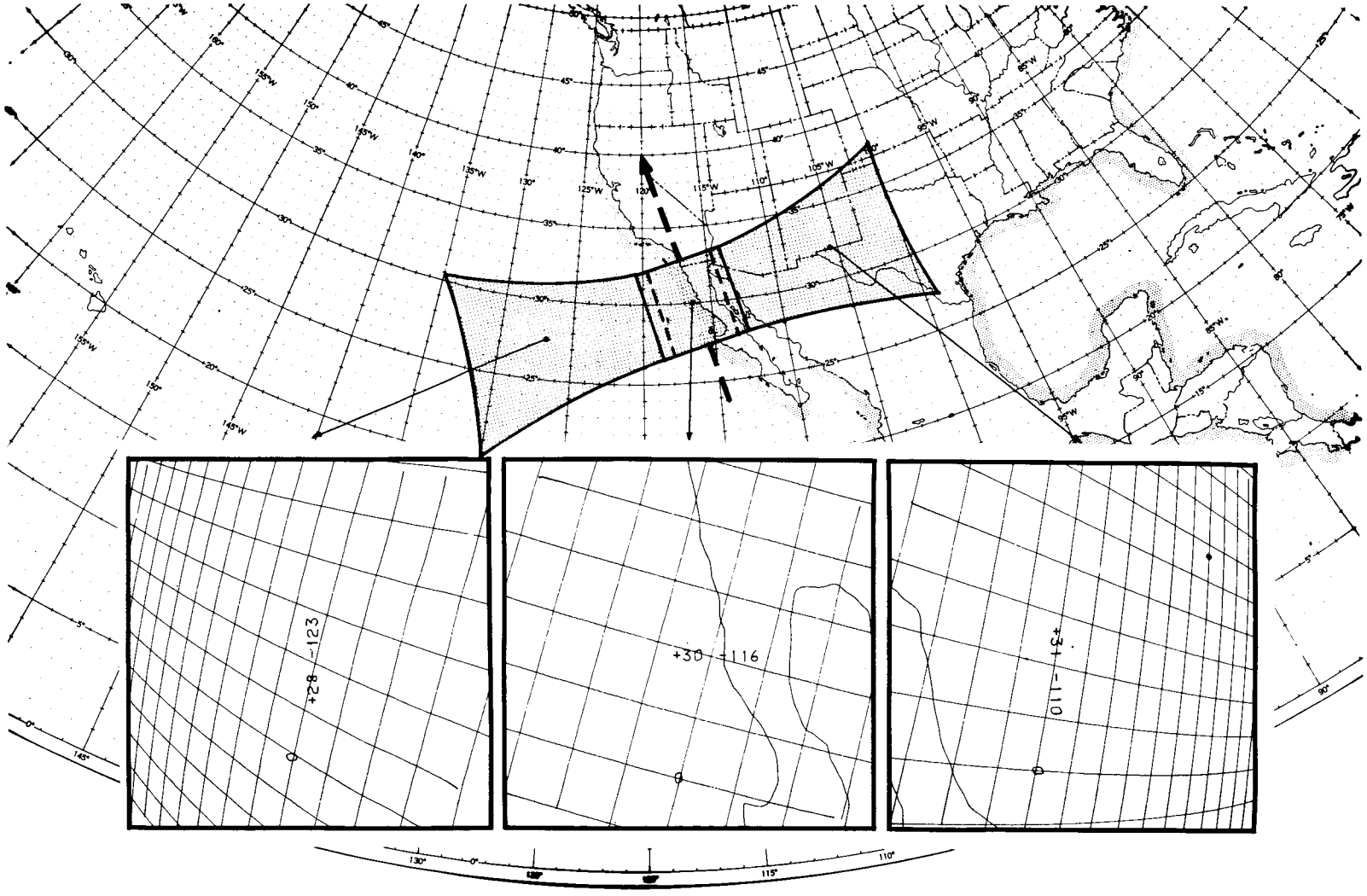

Figure 10 – Geographical Area Covered by One Nimbus AVCS Picture Triplet and the Corresponding Perspective Latitude-Longitude Grids

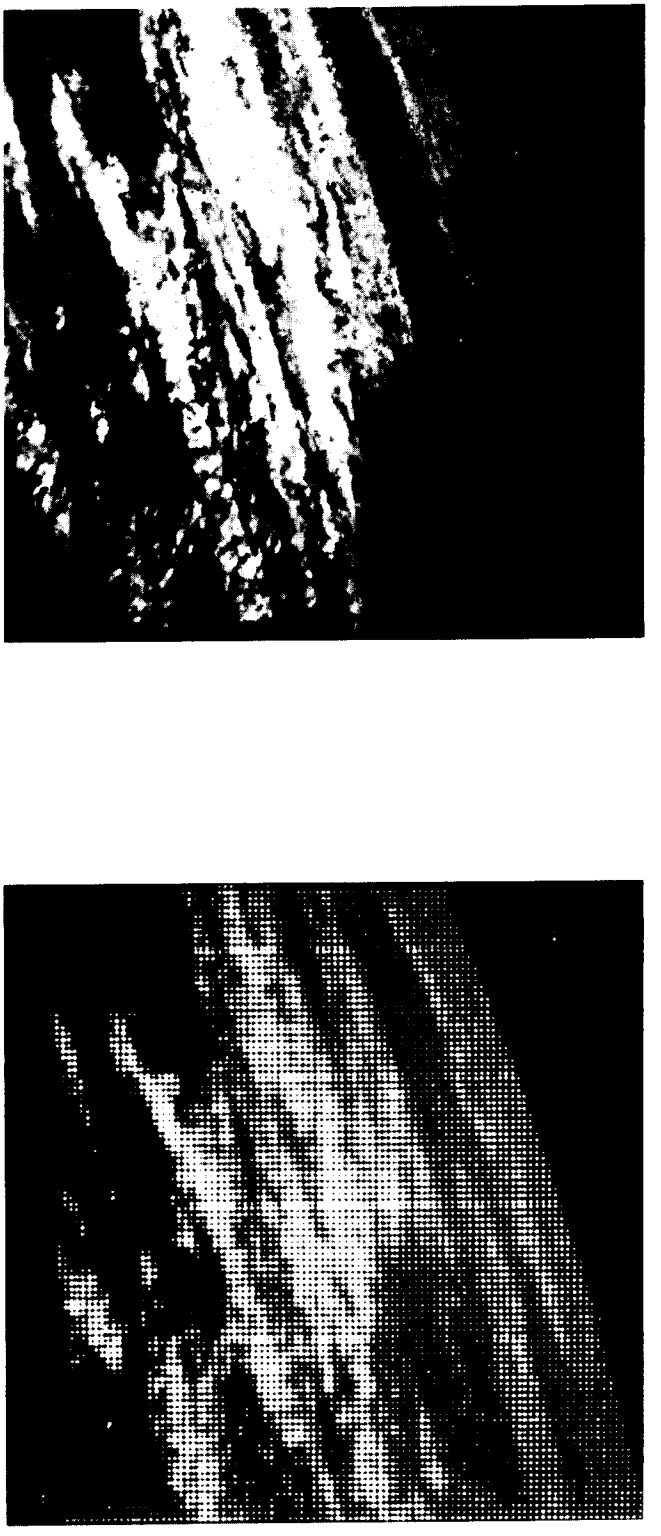

Figure 11 - Analog and Digital Representations of a Perspective Cloud Picture

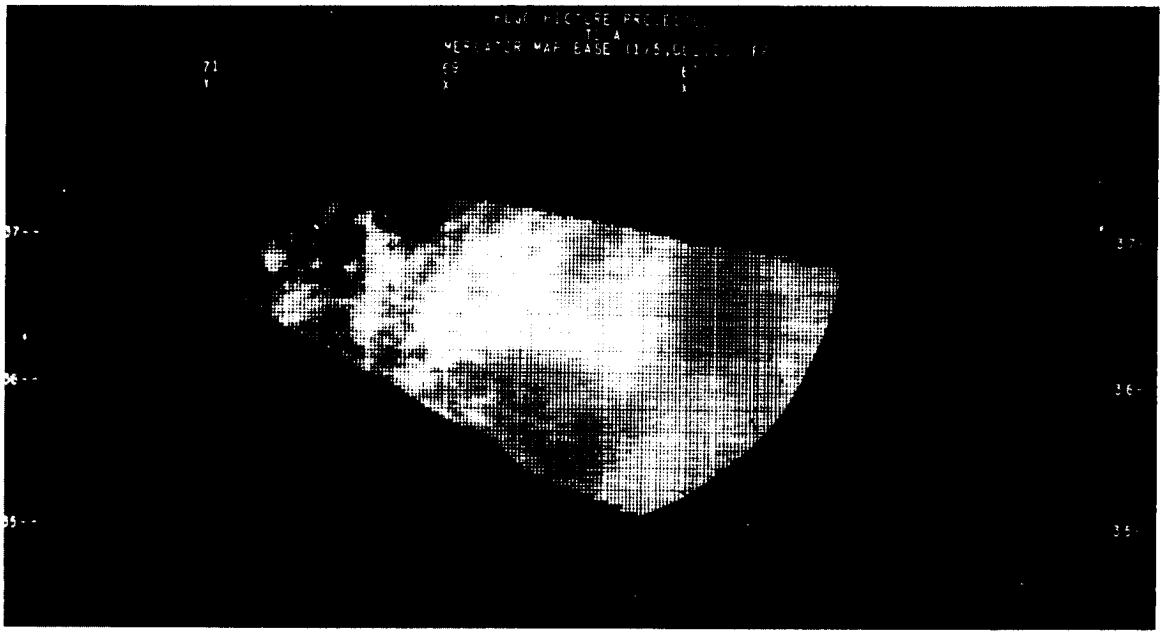

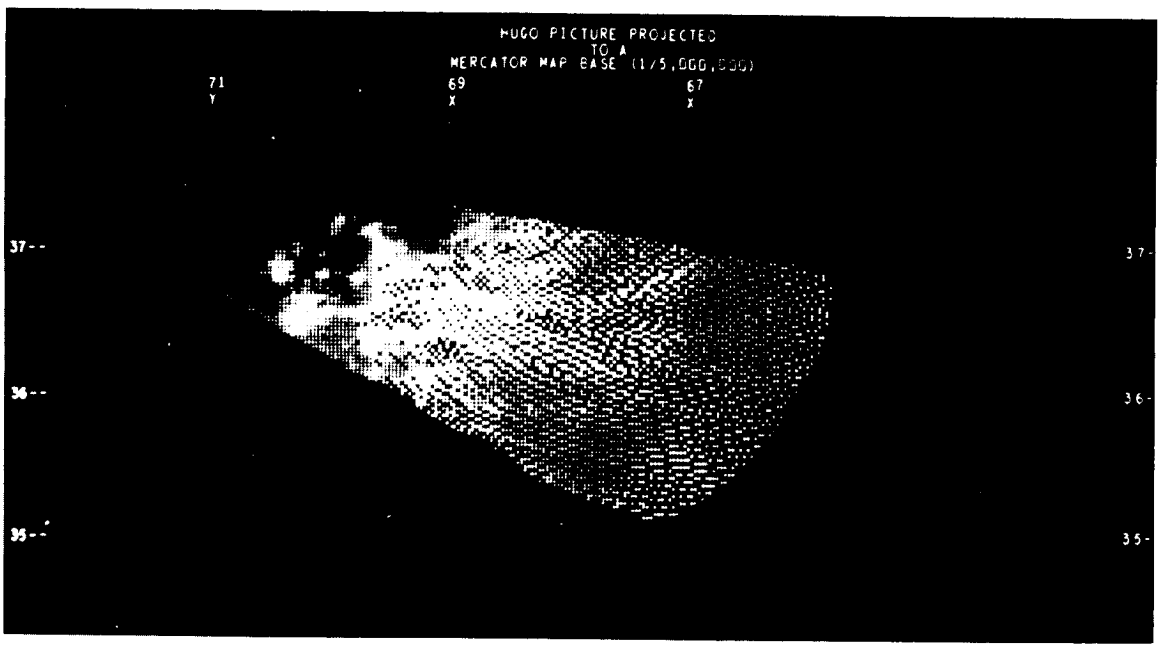

Figure 12 - Representation of a Cloud Picture in a Digitally Rectified Form on a Mercator Base Map

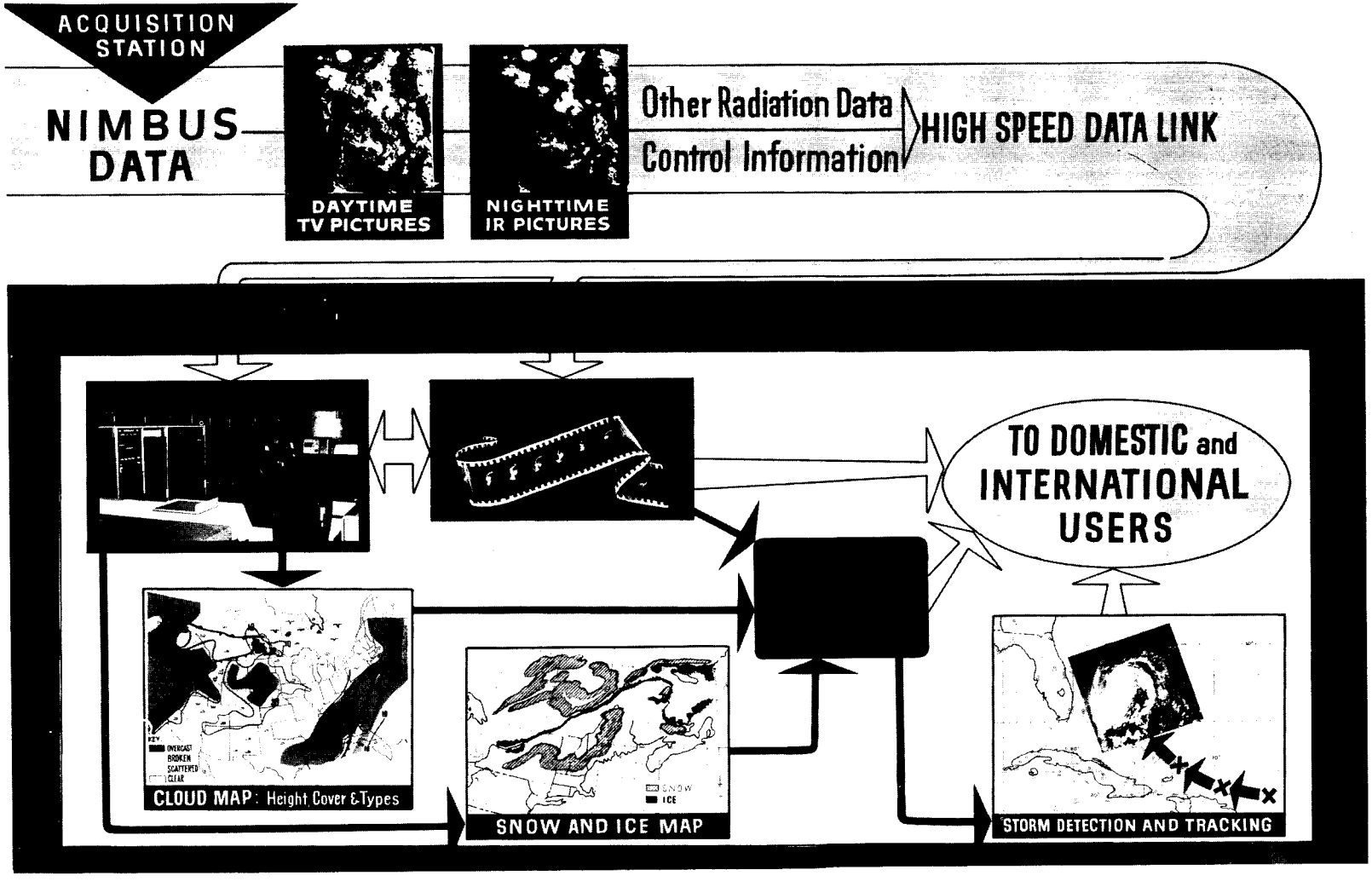

Figure 13 – Nimbus Meteorological Data Processing

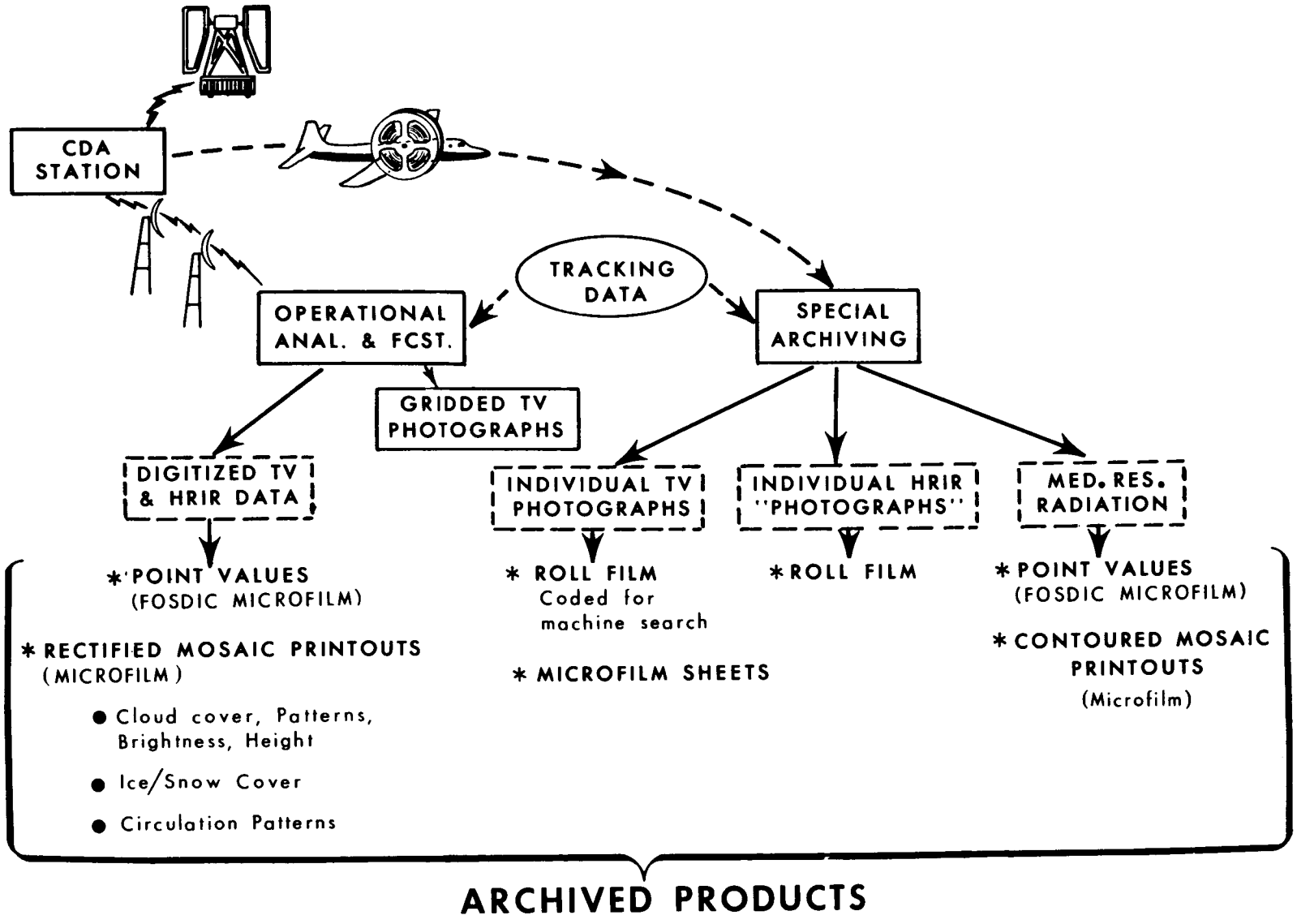

Figure 14 - Archived Products of the Early Nimbus Data-Processing System

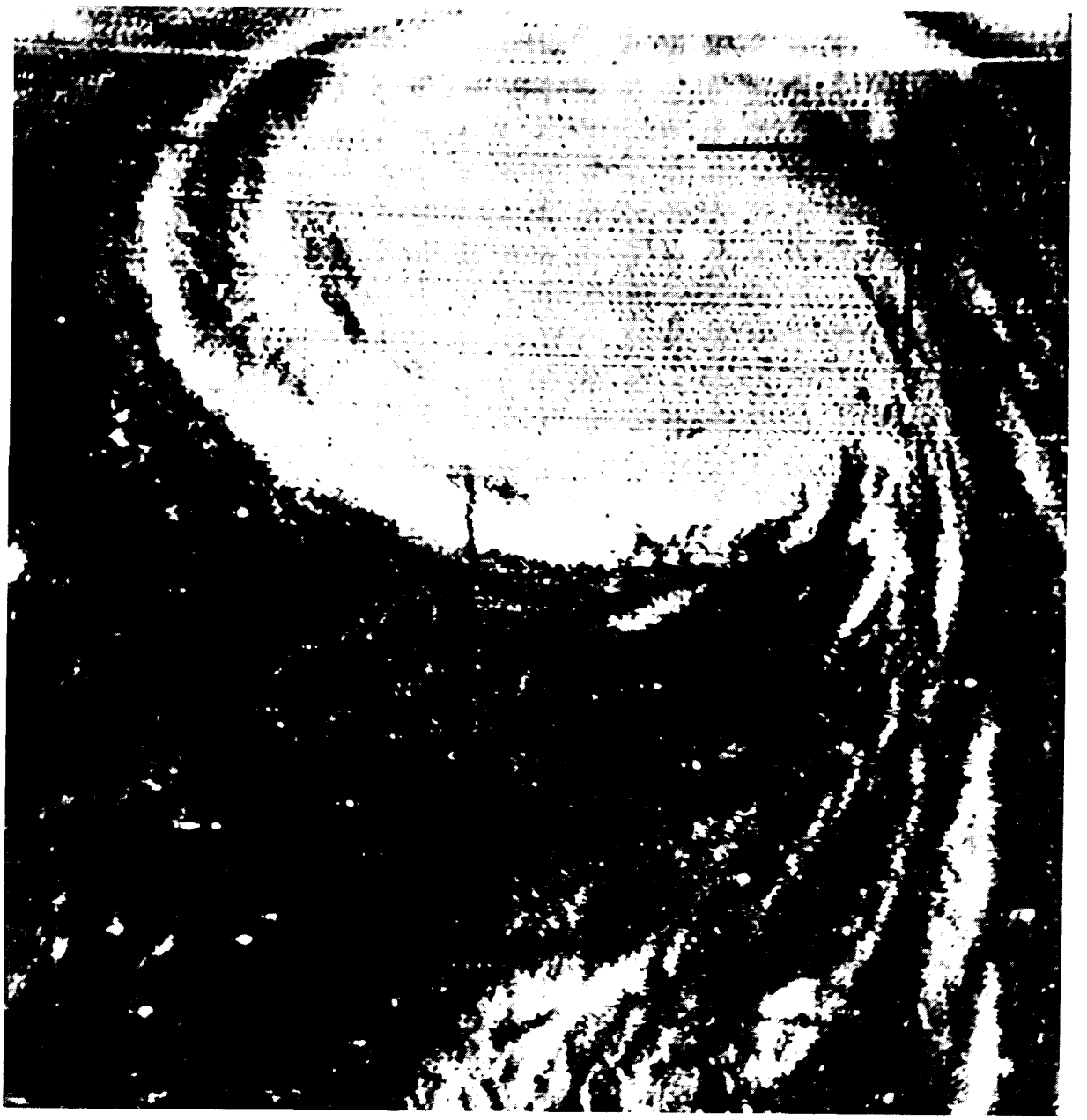

Figure 15 - Hurricane Debbie as Observed by TIROS III, Sept. 13, 1961

4. NIMBUS SPACECRAFT SYSTEM CONCEPT

By Dr. R. Stampfl, GSFC

4. NIMBUS SPACECRAFT SYSTEM CONCEPT

ILLUSTRATIONS

Figure		Page
1	Nimbus Spacecraft	10
2	Nimbus Constraints	11
3	Nimbus Structure	12
4	Nimbus Television Coverage	13
5	Nimbus Design Criteria	14
6	Data-Acquisition Site, Fairbanks, Alaska	15

4. NIMBUS SPACECRAFT SYSTEM CONCEPT

By Dr. R. Stampfl, GSFC

This presentation is an attempt to explain just why Nimbus is designed as it appears in Figure 1. The Nimbus spacecraft was conceived at a time when TIROS I had not yet been launched, although the development experience from the TIROS satellite was available. The design was aimed primarily at support of the basic sensors which would measure atmospheric phenomena; therefore, many of its features were tailored specifically to the requirements for continued television coverage of the earth, and for infrared radiation measurement. It was obvious that a stabilized platform would be most useful for the measurement of terrestrial phenomena, and that consequently a stabilization and control system would be needed; it was also recognized that the design of such a control system would be the most significant advance in the state-of-the-art beyond the TIROS satellite. To minimize the effort of developing the control system, many features of the design were chosen to keep it as simple as possible. Other important design considerations for Nimbus were a high degree of flexibility, making it possible to change sensors and experiments in the future, and to take advantage of advances in technology with the fewest possible modifications to the structure. Constraints (Figure 2) placed on the system design included complying with dimensions and weight requirements of a medium-size booster system, the Thor-Agena B, and the design objective of a 6-month lifetime which dictated the use of state-of-the-art components and techniques. System reliability and early flight capability were thereby assured.

One of the factors that led to the choice of a high-noon retrograde orbit was that of placing the least possible burden on the development of the control system. The orbital plane drifts around the earth when the satellite is launched with an arbitrary inclination; by choosing an 80-degree angle from the equator toward the southwest, the orbital drift is exactly that of earth's rotational movement around the sun, so that the earth-sun line always remains in the orbital plane. As a consequence, the solar-power collectors have to rotate about only one axis.

Other features of the control system resulted from the requirements of the TV cameras; the design objective was to point as accurately as $\pm$ 1 degree in all three axes and at a rate slower than .05 degree per second. The conflicting requirements of a low orbit for best TV camera resolution, and a high orbit for the maximum area of TV coverage, were reconciled by the choice of a 600-nautical-mile altitude orbit. Changing this orbit to 500 nautical miles or to 700 nautical miles makes no significant difference in the system parameters.

Finally, a mechanical design promoting a flexible system was chosen (Figure 3) with the control system connected at only three points to the rest of the spacecraft, and the sensory ring subdivided into modules for easy replacement and serviceability. The spacecraft design had to comply with the testing philosophy of the project, which essentially dictates that an entire orbital flight must be simulated on the earth; this posed the requirement for the spacecraft center of gravity to be accessible. In the present arrangement, the control system is assisted by the mass distribution of the spacecraft structure, balanced and connected like the end sections of a dumbbell. The three main parts of the structure are evident in Figure 1: the toroidal ring houses all the sensory equipment and associated electronics; the hexagonal package houses the complete control system, including horizon scanners; and the two 8- x 3-foot solar paddles forming part of the solar-power supply are connected to the driveshaft of the control system being driven at orbital rates.

Further advantages of the structural design include the large base area available for interference-free installation of optical sensors and scanners. The multiple compartments in the sensory ring make it possible to balance the spacecraft and to maintain this balance even when changes in subsystems occur; the cylindrical volume in the sensory ring offers flexibility for the packaging of bulky equipment, such as tape recorders and cameras. Alignment of the control system is easy, since only three points are affected. Alignment of cameras can also easily be accomplished within the sensory ring. Relatively high packing density in the electronic compartments of the sensory ring helps to maintain an isothermal range in this portion of the spacecraft. Thermal control on individual compartments is provided, in order to maintain as narrow a temperature range as practical under given load conditions, the optimum being 25°C with + 10°C deviations. Many subsystem compartments are regulated to $\pm$ 3°C.

Based on the experience accumulated during the design of the TIROS satellite, a large amount of redundancy was considered desirable. Redundancy can be provided in spacecraft systems in two ways-- either by duplication of entire subsystems, or by making use of identical components among subsystems. The first approach is only a small step towards the final goal of achieving multiple integrated redundancy in spacecraft systems. The present Nimbus system uses only redundant subsystems and not integrated component redundancy; Nimbus A will not include redundancy to the extent originally planned, because of weight restrictions.

The Nimbus television subsystem is a design extension of the cameras flown on the TIROS series. It was clear at the time of design that resolutions higher than 800 lines in standard 1-inch vidicons cannot be achieved and maintained, except in laboratory experiments; consequently, multiple cameras had to be used to obtain coverage as shown in Figure 4. The optical angle of the three cameras is chosen so that the earth's rotational movement during one orbit will be exactly equal to the angular width of a set of three pictures. Time of picture-taking is arranged so the satellite flies one picture-width until the next set of three pictures is taken; thereby, a mosaic of three picture sets is generated with no overlap in the equator region and an increasing amount of overlap from orbit to orbit as the satellite travels further towards the two poles. Originally, two such systems were planned to be flown, with the capability of exchanging any camera against any other or any tape recorder against any other, so that failures in any one of the two complete subsystems would find a replacement part in the other. Choice of frequency-multiplexing and multiple-track tape recording was a direct extension of the experience gained in TIROS. It may be asked why a single transmitter was chosen and frequency-multiplexing applied, rather than a multiplicity of transmitters. Investigating the efficiency of using three transmitters with three cameras leads quickly to the conclusion that a single higher powered transmitter provides a system advantage; secondly, three frequencies would have to be radiated either from three antennas or from a single antenna, requiring RF multiplexing and complex antenna design. The resultant system would be less reliable than the one chosen.

The television and the other Nimbus experiments are supported by other functional systems in the spacecraft. These are an electronic

clock; a pulse-code-modulated (PCM) telemetry subsystem to transmit housekeeping and event information; a power supply to provide power for the entire spacecraft; and the control system for stabilization of the spacecraft. These subsystems were planned to be as independent as possible, so that they might be designed in the most expeditious manner with uniform interfaces and with the possibility of being changed on future missions. The electronic clock derives from an 800-kc oscillator a number of frequencies which it feeds to other points in the spacecraft; it generates the standard NASA and range time code, and, through additional logic, it provides command access to the spacecraft. These functions provided by the clock and command subsystem are distributed throughout the spacecraft and used by individual subsystems. The command system is secure against manmade interference such as broadcast stations, air-to-ground traffic, etc. Transmission rates of the command system and receiver properties were designed around convenient engineering choices without demanding any advance in the state-of-the-art.

The complexity of the Nimbus spacecraft obviously demands telemetry capability for transmitting and receiving engineering information which is needed both during the satellite's test cycle, and later during flight in orbit, for assessment of system functioning and for possible improvement of later flights. The choice and the properties of such a telemetry system puts the system design engineer in the position of reconciling conflicting demands, from the requirement of accuracies of better than 1 percent on the one hand, to the determination of the mere presence of a signal on the other. Sampling rates of the test points vary widely; on the one hand, transient phenomena are telemetered on occurring, and on the other hand, periodic detection and measurement of dc levels at certain tests points is required. Other considerations included the anticipated future demands on the telemetry system when different subsystems and experiments will be flown, and the most convenient arrangement for ground display and data handling. Considering these problems, it was concluded that pulse-code modulation would provide the necessary flexibility for the future. GSFC has adapted PCM as a standard telemetry technique for all major satellites, and the Nimbus system complies fully with the Goddard PCM standard. This may be attributed to the fact that this author drafted the first PCM standard while the Nimbus telemetry was being designed. A tremendous effort in the United States is being applied to logic blocks so that improvements and higher reliability can be anticipated, and the sampling

rate can easily be changed within limits, if the need should arise. For Nimbus, as conceived two years ago, it appeared that the highest sampling rate of 1 per second would be compatible with the data requirements, and that information sampled during the entire orbital period should be recorded on a tape recorder. It was determined further that the tape would be played back upon command at 30 times the record speed, and transmitted to the ground receiving station at one-thirtieth the recording time. The main features of the PCM telemetry system can be summarized by citing the numbers of channels available: 30 channels are sampled once per second, 256 channels are sampled once per 16 seconds; an additional 256 channels are again sampled once per 16 seconds, and the system can expand to twice that number at twice the sampling time, should need arise.

For tracking, Nimbus uses a 350-milliwatt 136-Mc beacon which normally transmits the standard Minitrack time signal, which uses amplitude modulation. When interrogation of telemetry is commanded, the time signal is turned "off," and the PCM signal is played back from the tape recorder and transmitted through the beacon transmitter. When the "B" telemeter is turned on, it cycles 128 data channels once, which transmit through a 5000-cycle subcarrier modulating the beacon. Interrogation of the recorder and the "B" telemeter at the same time is neither possible nor necessary.

The control and stabilization system is reviewed in detail in another report; it is sufficient to say that this is the only subsystem where an initial design objective had to be modified substantially. Although it appeared desirable, initially, to stabilize within a cone of 2 degrees centered at the principal axis of the spacecraft, difficulties encountered later in the error detector of the control system relaxed this requirement to approximately 3 or 4 degrees. At present the control system is under test, and in the very near future the exact accuracy figures which the control system is able to deliver will be determined. Accuracies cannot be improved at this time because of inherent limitations in the error detector; only the use of a more advanced type, such as the one used in the Orbiting Geophysical Observatory (OGO) satellite, can alleviate this situation.

The automatic picture transmission subsystem (APTS) for Nimbus is a storage vidicon system capable of long duration and a very slow

readout rate. A pulse technique was chosen over other techniques for slow readout because of a better signal-to-noise ratio. The system takes wide-angle pictures continuously throughout the daylight portion of each orbit, reading out one picture every 208 seconds. The system has a linearity of 0.5 percent and a resolution of approximately 700 lines. Each picture will cover a ground area of approximately 1150 by 1150 nautical miles, with a north-south overlap of 300 nautical miles.

The vidicon is identical to those used for the AVCS, except for the addition of a layer of polystyrene which provides the image-storage capability. The vidicon is located in the center of the sensory ring for direct earth viewing.

The telemetry-type 5.5-watt FM transmitter transmits real-time information through an antenna mounted on the bottom surface of the spacecraft and facing the earth at all times. The antenna produces a linearly polarized radiation pattern, so that the satellite-to-ground antenna relationship remains constant, independent of their relative positions within line of sight. The APTS system is covered in more detail in another paper.

Resolution of the three-camera TV subsystem flown in Nimbus A has essentially been met, although in the second TV system less resolution had to be accepted; gray scale in the camera itself turned out to be poorer than expected in the three-camera TV system, and substantially poorer in the storage vidicon. The properties of the radiometers have not changed very much except in the high-resolution infrared radiometer (HRIR), where it was recognized very early in the study phase that the objective resolution was unrealistic.

One subsystem should be mentioned which will not be flown on Nimbus "A" but which is available for flight as soon as weight limitations on Nimbus permit its integration. The medium-resolution infrared radiometer (MRIR) described in another report uses the same system components as those flown on TIROS, with the exception of the radiometer itself. The telemetry and data-transmission technique is derived from the experiment on TIROS, represents the state-of-the-art approximately 5 years ago, and is completely outmoded at this time. Higher accuracies can be achieved when more modern techniques for

the data transmission can be applied and hardware can be produced.

A few words are in order on the rationale guiding the design of the Nimbus antenna. Tracking and telemetry are required even if the control system has failed to function. This is necessary so that the failure can be evaluated. Numerous difficulties arose in designing an omnidirectional pattern resembling that of a turnstile with power radiated in all directions; the beacon wave length of 2.2 meters is approximately the length of the spacecraft and, consequently, severe interference patterns resulted. Furthermore, antenna performance is affected by solar paddles; the radiation patterns will obviously change with the position of the solar paddles. Extensive measurements were needed in order to determine how close an isotopic radiator could be approached. The test results showed that it would be almost impossible to achieve a design with no deep fading in the antenna pattern, forcing relaxation of the requirement that reception from a tumbling spacecraft should be of a quality equal to that from a stabilized spacecraft. However, detailed examination of the pattern showed that reasonable reception, with only small loss of data, can be expected if the spacecraft should tumble.

The same situation holds true for the design of the interrogation antenna which is affected by the rotation of the solar paddles. Antennas associated with experiments are mounted on the baseplate and radiate approximately in a 120-degree cone.

How well the planned spacecraft design has been achieved is demonstrated by the preprototype and many prototype subsystems available today. As mentioned already, the control system alignment accuracies have to be degraded. Power supply output was specified to 200 watts continuously, and is now estimated to be 155 watts.

Figure 5 is a table listing two more criteria to judge how well the design objective was met; it lists the specified weight, the weight actually achieved, the specified power, and the power which is now being delivered. Significant weight increase was necessary in the control system, in the batteries, in the structure, and in all camera systems; this situation forced the elimination of redundancy, in order to meet the total weight capabilities of the booster system.

To summarize, the total spacecraft weight was specified to be less than

650 pounds. The present assembly weighs 856, corresponding to an increase of one-third over the design goal. Had Nimbus A been specified originally, only 542 pounds would have been the expected total, and the actual weight reached would have been 702 pounds. Comparison of the specified power levels with the actual levels shows that those have been met in practically all respects.

A few comments are necessary concerning the ground receiving equipment which forms an integral part of the Nimbus system (Figure 6).

Transmitter power for all subsystems of the satellite was chosen sufficiently high so that no serious advance in the ground receiver state-of-the-art was necessary, and no extremely low-noise receivers had to be employed. Conventional parametric amplifiers for VHF and conventional low-noise preamplifiers for the S-band are adequate for good reception. A system design compatible with a 60-foot parabolic antenna was initially assumed, and the additional 3 db available through the choice of an 85-foot reflector was welcomed as an unexpected margin for the system performance.

It is apparent that a certain amount of equipment peculiar to the Nimbus satellites must be available at the receiving sites. In particular, a command console is provided which allows an operator to prepare command sequences and transmit them to the satellite when directed to do so by the Nimbus Technical Control Center (NTCC) located at GSFC. Its features include high flexibility, ranging from an operational program prepared on teletype tape by NTCC to issuance of single commands by an operator.

The large quantity of engineering-type information transmitted from the satellite demands a small data-processing system which can determine, within or without specification, the limits of important equipment data by checking test points automatically at the receiving site. In this way it is not necessary to transmit and evaluate data point by data point at the NTCC. Only information which is necessary and timely will be transmitted to the NTCC. At the same time all information is recorded in analog form on magnetic tape, and digital tapes are prepared concurrently by the data-processing equipment. These tapes can be analyzed later by subsystem engineers and contractors for valuable engineering information. In particular, the attitude of the

spacecraft can be analyzed for each second in orbit.

Information flow and its presentation is a subject which is being carefully studied in large communications and data-processing systems before system decisions are made. The Nimbus data system, like all other information systems, presented to its designer the question of what the final product of the information should be. To illustrate this point, a series of television pictures might be considered the end product. Satellite parameters have to be mated to the pictures to achieve this objective. A nephanalysis also could be considered the end product, rather than a series of television pictures or a mosaic from which a nephanalysis can be produced. Or, one could consider the final weather forecast or the information fed into the world meteorological system as the end product. With respect to data gathered for further research, the decision is easier to make. Infrared radiation data collected by the medium-resolution radiometer need only be converted to a format suitable for analysis by large computers. With regard to television, the many alternatives mentioned indicate that the choice of the final product is a difficult one and will probably undergo changes as the system is being put to use and experience is gained. At the present time, film containing cloud pictures is considered to be the most satisfactory end product.

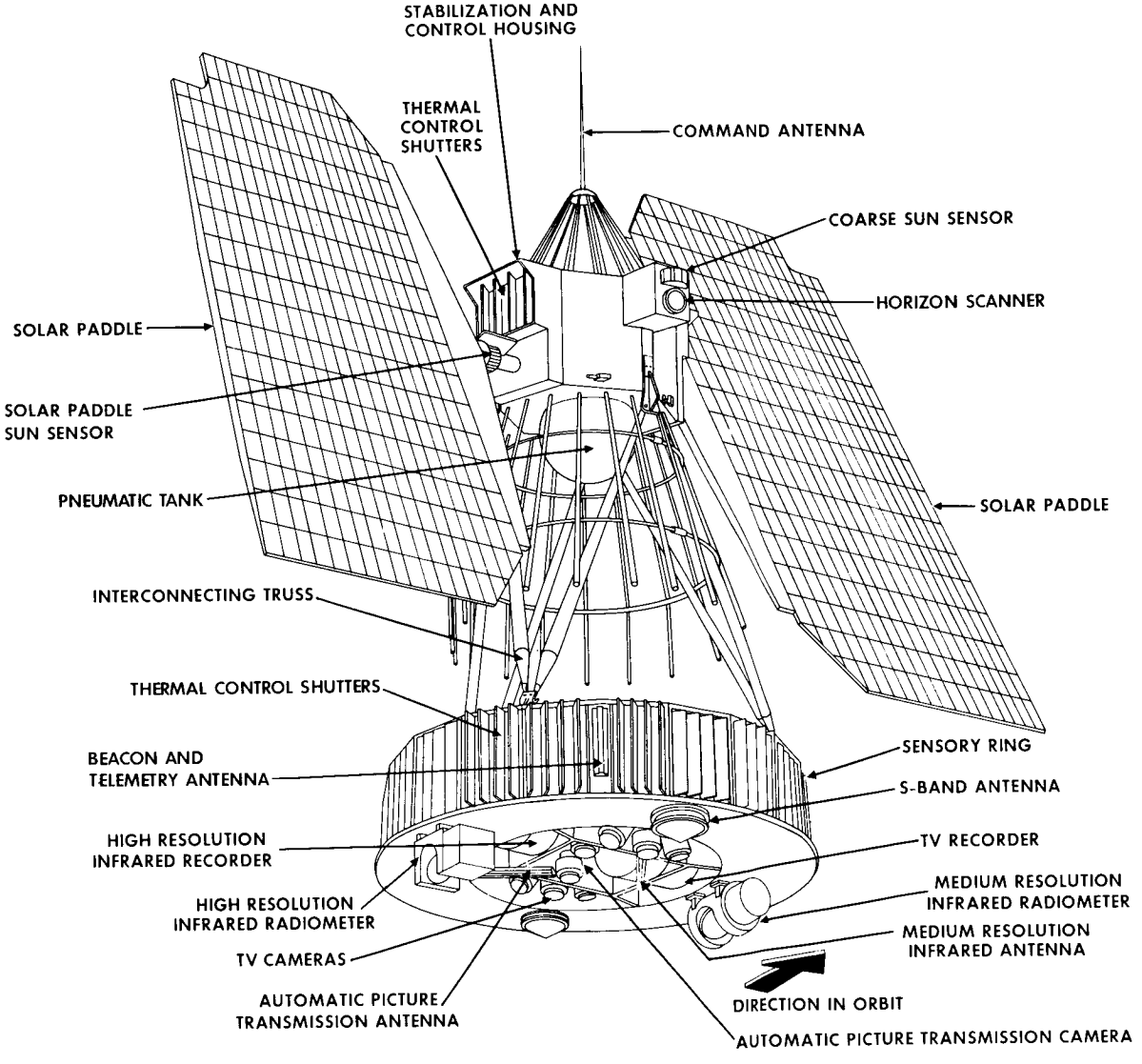

Figure 1 – Nimbus Spacecraft

- WEIGHT COMPATIBLE WITH MEDIUM BOOSTER
- RETROGRADE ORBIT
- MASS DISTRIBUTION TO AID CONTROL SYSTEM
- ALTITUDE 900–1300 km CIRCULAR ORBIT

Figure 2 – Nimbus Constraints

- ▶ CONTROL SYSTEM SEPARATE ENTITY
- ▶ MODULAR CONSTRUCTION OF SENSORY RING
- ▶ BASE AREA FOR INTERFERENCE – FREE INSTALLATION OF OPTICAL SENSORS
- ▶ CENTER OF GRAVITY ACCESSIBLE
- ▶ FLEXIBILITY FOR FUTURE CHANGES
- ▶ ALIGNMENT OF CONTROL SYSTEM AND SENSORS TO BE EASILY ACCOMPLISHED
- ▶ VARIABLE A/E TYPE TEMPERATURE CONTROL

Figure 3 – Nimbus Structure

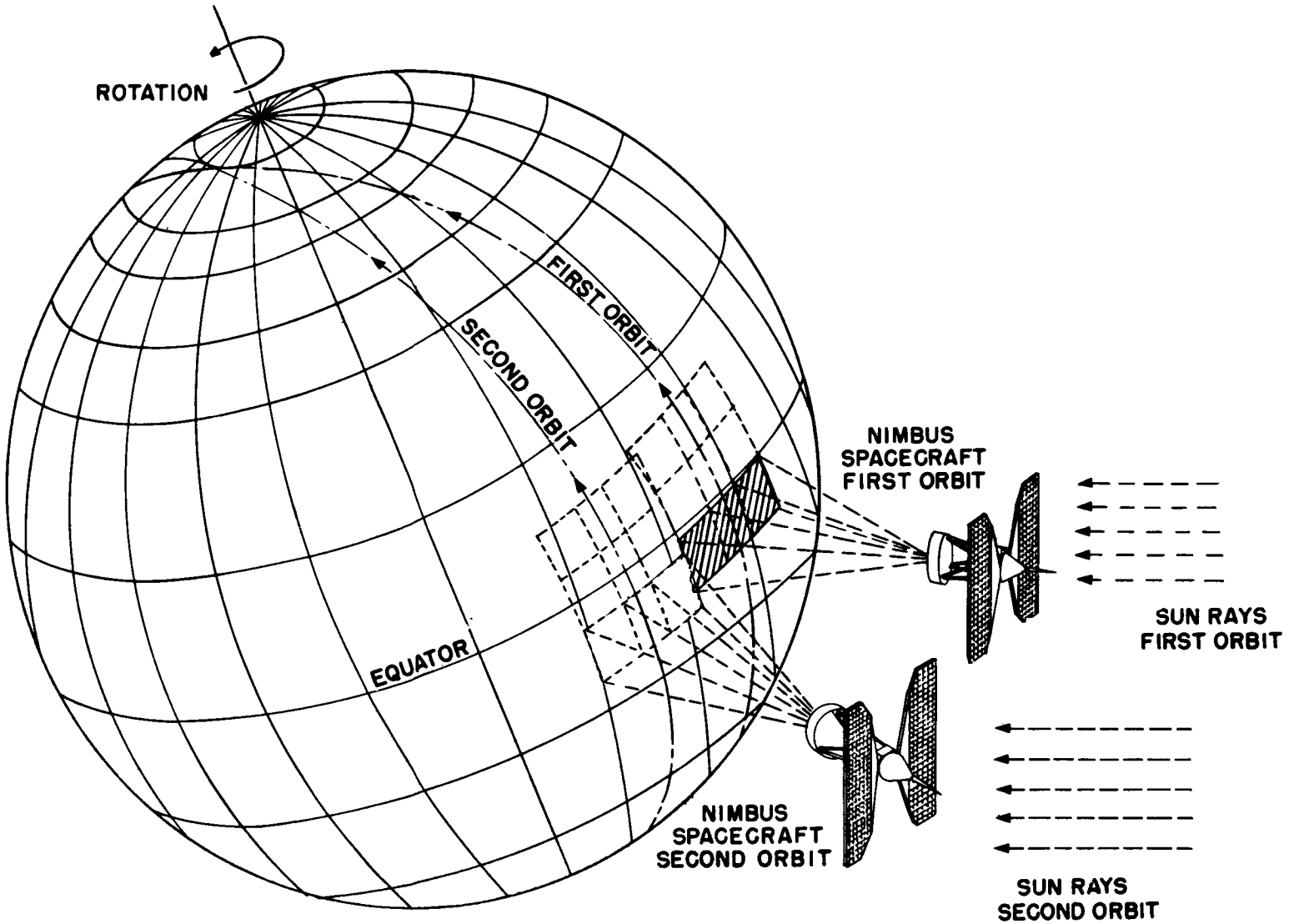

Figure 4 – Nimbus Television Coverage

SUBSYSTEM	SPEC WEIGHT	PRESENT WEIGHT	%	SPEC POWER	PRESENT POWER
CONTROLS	100	138	38	75(d,n)	82(d,n)
POWER SUPPLY					
PADDLES	54	58	7		
BAT & ELEC*	96	128	33		
NIMBUS "A"	86	113	31		
PCM*	55	60	8	5(d,n), 16(1)	6(d,n), 14(i)
NIMBUS "A"	49	53	7		
CLOCK, CMD	22	24	9	9(d,n)	9(d,n)
STRUCTURE	142	173	22		
AVCS, HRIR*	129	190	48	32(d), 10(n), 207(i)	21(d), 13(n), 186(i)
NIMBUS "A"	76	116	53		
TVCS*	23	52	124	34(d)	42(d)
NIMBUS "A"	12	27	126		
MRIR	23	35	51	8(d,n), 24(i)	10 (d,n), 24(i)
TOTAL*	644	855	33	163(d),107(n),365(i)	173(d),123(n),360(i)
NIMBUS "A"	542	702	30	155(d),99(n),341(i)	163(d),113(n),336(i)

*REDUNDANT NIMBUS (d)-DAY (n)-NIGHT (i)-INTERROGATION

Figure 5 – Nimbus Design Criteria

- 85FT. DISH
- AUTOTRACK, PROGRAMMED; S–Bd. & VHF
- LOW NOISE RECEIVERS
- COMMAND CAPABILITY
- TELEMETRY DATA PROCESSING
- TV & HRIR PICTORIAL PRESENTATION
- DATA TRANSMISSION

Figure 6 – Data-Acquisition Site, Fairbanks, Alaska

5. NIMBUS SPACECRAFT SYSTEM DEVELOPMENT

By J. V. Michaels, GSFC

5. NIMBUS SPACECRAFT SYSTEM DEVELOPMENT

ILLUSTRATIONS

Figure		Page
1	Sensory Ring	7
2	Nimbus "A" Spacecraft	8
3	Subsystem Mission Duality	9
4	Spacecraft Development Plan	10
5	Preparatory Spacecraft Development Effort	11
6	Nimbus Full-Scale Antenna Model	12
7	Nimbus Thermal Model	13
8	Vibration Facility with Nimbus Vibration Model	14
9	Nimbus Half-Scale Vibration Model	15
10	Nimbus Preprototype Sensory Ring	16
11	Spacecraft Separation Drop Test	17

5. NIMBUS SPACECRAFT SYSTEM DEVELOPMENT

By J. V. Michaels, GSFC

This report describes how the original concept of Nimbus developed into a realizable spacecraft system. It stresses the special nature of the approach, the government being responsible for system design and management; and it discusses the role of the spacecraft and subsystem contractors in evolving the development plan. Progress is reviewed for the Nimbus system to date, and the effort remaining to assure the Nimbus A flight in 1963 is outlined.

The Nimbus spacecraft system is characterized by the many interfaces between the overall system and the subsystems, and those between the subsystems themselves. Although this report is fundamentally equipment-oriented, it should be noted that these interfaces transcend the hardware domain and also include people and companies.

NIMBUS SPACECRAFT

The Nimbus spacecraft is no longer merely a concept. It is now backed up by a qualified spacecraft structure, by components and hardware, and by several qualified subsystems. Features of the Nimbus spacecraft include:

(1) Active thermal control, or thermostating, with independent systems for the base sensory ring and the control subsystem

(2) A 672-channel telemetry subsystem, using pulse-code modulation (PCM), and capable of being almost doubled in future versions of Nimbus

(3) A large array of sensory subsystems, with a large base area for interference-free sensor installation, and adequate volume in the center of the sensory ring to accommodate recorders and cameras

(4) A fully earth-stabilized platform, its most significant feature, for the operation of the sensory subsystems and efficient generation of electrical power

The spacecraft measures 114 inches from the base of the sensory ring to the tip of the interrogation antenna. The sensory ring, 13 inches high by 57 inches in diameter, houses the operating subsystems. The hexagon-shaped control subsystem, including the equipment for spacecraft stabilization, measures about 17 by 33 inches wide, and is separated about 48 inches from the sensory ring by struts. The solar paddles which furnish the prime electrical power are each 39 by 96 inches long, and their drive system is provided by the controls package.

SENSORY RING CONTENTS

Figure 1 is a top view of the Nimbus sensory ring, containing 18 separate compartments numbered clockwise starting from the front of the picture. These compartments, or module bays, house the following items or subsystems:

Module bay number	Equipment
1	S-band transmitter (General Electronics Labs.)
2	Command clock subsystem (California Computer Products)
3, 6, 8, 11, 12, 13, 15, 17	Solar power supply (RCA)
4	Interrogation receiver (RCA)
5	HRIR (ITT)
7	Spacecraft components
9, 10	Telemetry subsystem (Radiation, Inc.) including beacon transmitters by Hughes Aircraft Co.
16, 18	Vidicon camera subsystem (RCA)

The RCA television cameras and recorders are supported by the ladder section in the sensory ring.

WEIGHTS OF NIMBUS A COMPONENTS

Total weight of the Nimbus A spacecraft is 702 pounds, 20 percent of this representing the sensory subsystems in the AVCS, HRIR, and miscellaneous-weight categories shown in Figure 2. This, in a sense, is the payload efficiency of Nimbus A. The basic structure, including harnesses and antennas, accounts for only 25 percent of the payload weight.

The rest of the Nimbus spacecraft system consists of ground station elements, specialized spacecraft test facilities, and spacecraft handling and transportation equipment. These items, called aerospace ground equipment (AGE), are discussed in other reports in this series.

A notable feature of the Nimbus system is that the subsystem contractors supply complete and compatible flight-to-ground hardware combinations. Figure 3 shows that this requirement goes beyond ground-station demodulators, demultiplexers, and displays, as it includes specialized test equipment and continuous aggressive maintenance and operation. Steps have been taken to strengthen contractual relationships in these areas.

SPACECRAFT DEVELOPMENT PLAN

The modular aspect of the Nimbus concept has enabled the job to be divided into many smaller tasks, so that subsystem development could run concurrent with preparatory spacecraft effort. Figure 4 gives the phased spacecraft development plan in the PERT format; the cross-hatched areas in the figure indicate accomplishments to date. Design and analysis have proceeded simultaneously on the subsystem and system levels. Subsystem breadboard activity was conducted to demonstrate performance, and subsystem preprototypes were used to establish packaging and compatibility with required wiring, signal, command, and telemetry logic. To date, an electrical preprototype for every Nimbus A subsystem has been delivered to the integrator's plant, and has been, or is being, checked for compatibility with the other subsystems; this checking has revealed some wiring, telemetry, and command discrepancies, as well as a few infractions of grounding and shielding rules.

The development of prototype subsystems follows the performance, packaging, and compatibility milestones; the intent here is to demonstrate

a conservative margin of safety with rigorous subsystem qualification. The same margin of safety is demonstrated on the integrated prototype spacecraft by using qualification levels more severe than the actual flight levels. For flight spacecraft, test levels used are the best possible simulations of anticipated flight levels.

Several subsystems have reached the exalted status of "qualified prototypes"; most of the remaining subsystems have reached the prototype qualification stage. The solar paddles and control subsystems are considered critical because they are not yet qualified, and it is impossible to predict the effect of any development difficulties that may arise. However, the control subsystem appears to be essentially on schedule; the preprototype has completed its air-bearing tests, and the prototype is on the air bearing at the present time.

Solar-paddle development has been beset by solar-cell and cell-module difficulties described in the report on the Nimbus power supply; however, despite the recent complication due to radiation damage in space, the program is in a position to move forward.

The phased development permitted a substantial amount of advance analysis (and corroboration of this analysis) by preprototype model testing. Figure 5 lists the six spacecraft models used in conjunction with various studies to establish the ultimate design. Models listed in the figure include a mockup which was used for form fitting, detection of basic mechanical incompatibilities, and layout of wiring harnesses.

Figure 6 shows the full-scale antenna model sent to New Mexico State University for antenna measurements and pattern generation. This test arrangement worked out well because that university developed the original antenna designs; the tests, completed in June 1962, indicated that performance of the antennas was as expected. Incidentally, the mesh paddles seen in Figure 6 appear as a solid ground plane at the spacecraft frequencies.

Figure 7 shows the full-scale sensory-ring thermal model, complete with simulated heat inputs, temperature controllers, and instrumentation. The sensory-ring thermal test completed satisfactorily early this year is described in the report covering thermal control of the Nimbus spacecraft.

Figure 8 shows the vibration model being readied for testing. Vibration-model testing, completed in September, demonstrated that the spacecraft design will withstand the launch environment. This phase of the program is also covered in other reports. An accompanying structural analysis of the Nimbus spacecraft was conducted by Dr. George W. Brooks, head of the vibration and dynamics branch at the NASA Langley Research Center. Figure 9 shows the half-scale model constructed by his group, which is structurally and dynamically similar to the vibration model shown in Figure 8. The ease of making, and proving out, structural modifications to the half-scale model, before incorporating them in the full-scale vibration model, provided a valuable design tool to the project, and helped solve vibration difficulties.

Figure 10 illustrates what is called the "ad hoc" model, consisting of structural hardware from the thermal model, preprototype subsystems, and prototype harness. This is the vehicle used for the subsystem compatibility tests, and it constitutes an extremely important piece of the Nimbus test program.

Figure 11 shows the separation model being used in an adapter drop test, to determine separation characteristics of the spacecraft from the Agena B vehicle. Mission requirements are that the spacecraft separate from the Agena B vehicle with a minimum separation velocity of 4 ft/sec and a maximum tumbling rate of 0.5 deg/sec. It has been concluded from six controlled separation drop tests that the demonstrated separation performance is within the design specifications.

A considerable amount of test planning preceded the tests described above. At present all the required integration test planning has been done and approved in principle; however, accomplishments in this regard are not considered final. The test plans are regarded as evolutionary in nature, and are subject to modification as the spacecraft environment and the understanding of the logic of spacecraft qualification improves.

Closely related to test planning are the engineering evaluation of spacecraft and subsystem performance during qualification and in orbit, and the activity in data-system design. Accomplishments in these areas are covered in other reports; criteria have been established for using Nimbus telemetry, and actual programming is proceeding rapidly.

The flexibility obtained from the Nimbus spacecraft system development plan and from the modular design concept has been described; the price paid for this flexibility was the need for close supervision of subsystem development, and for tight control of interfaces. Directives have been issued for weekly weight and power reports, and seemingly unreasonable requests have been made for interconnection lists, telemetry calibration, and other subsystem data. In general, the response of program participants has been good; this cooperation has brought good results, and continued cooperation is essential.

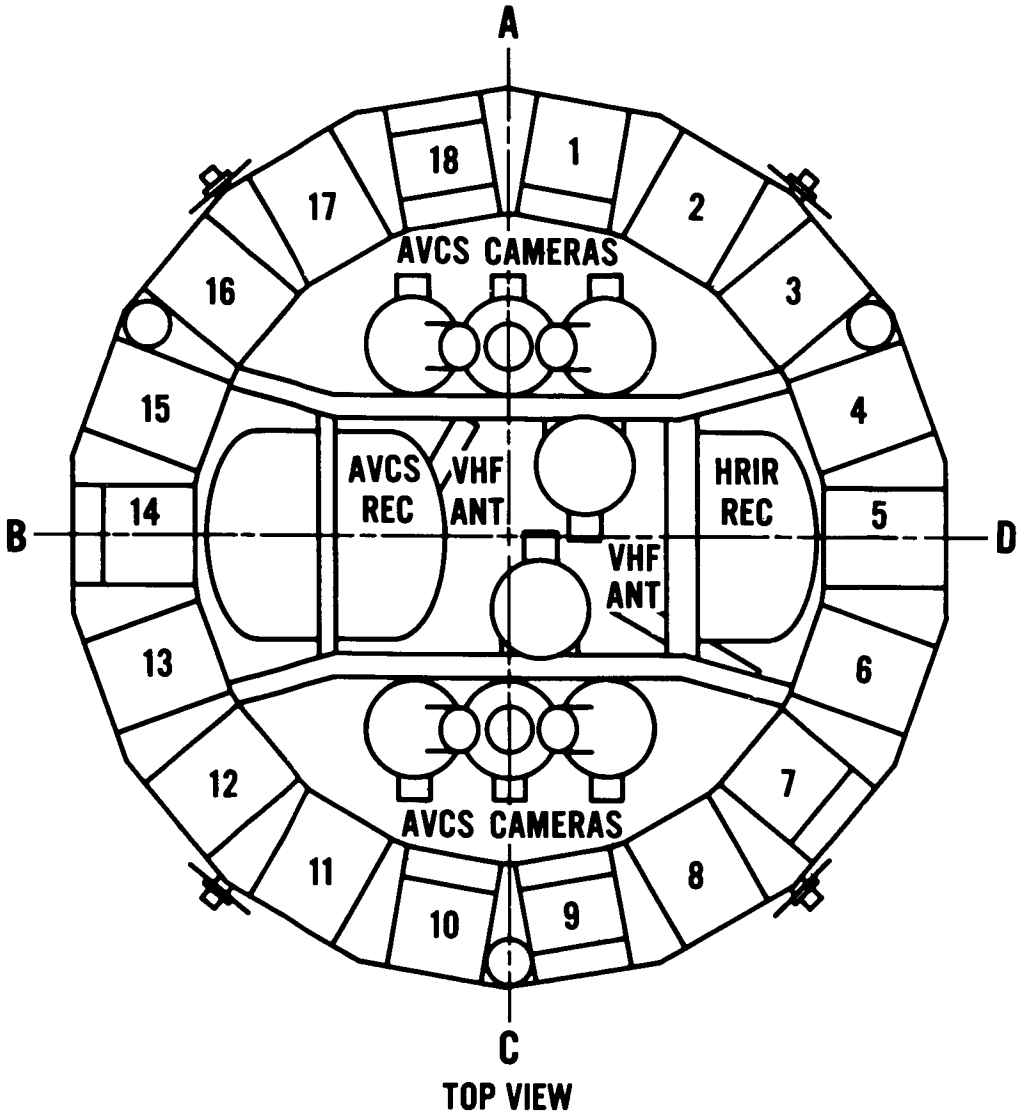

Figure 1 - Sensory Ring

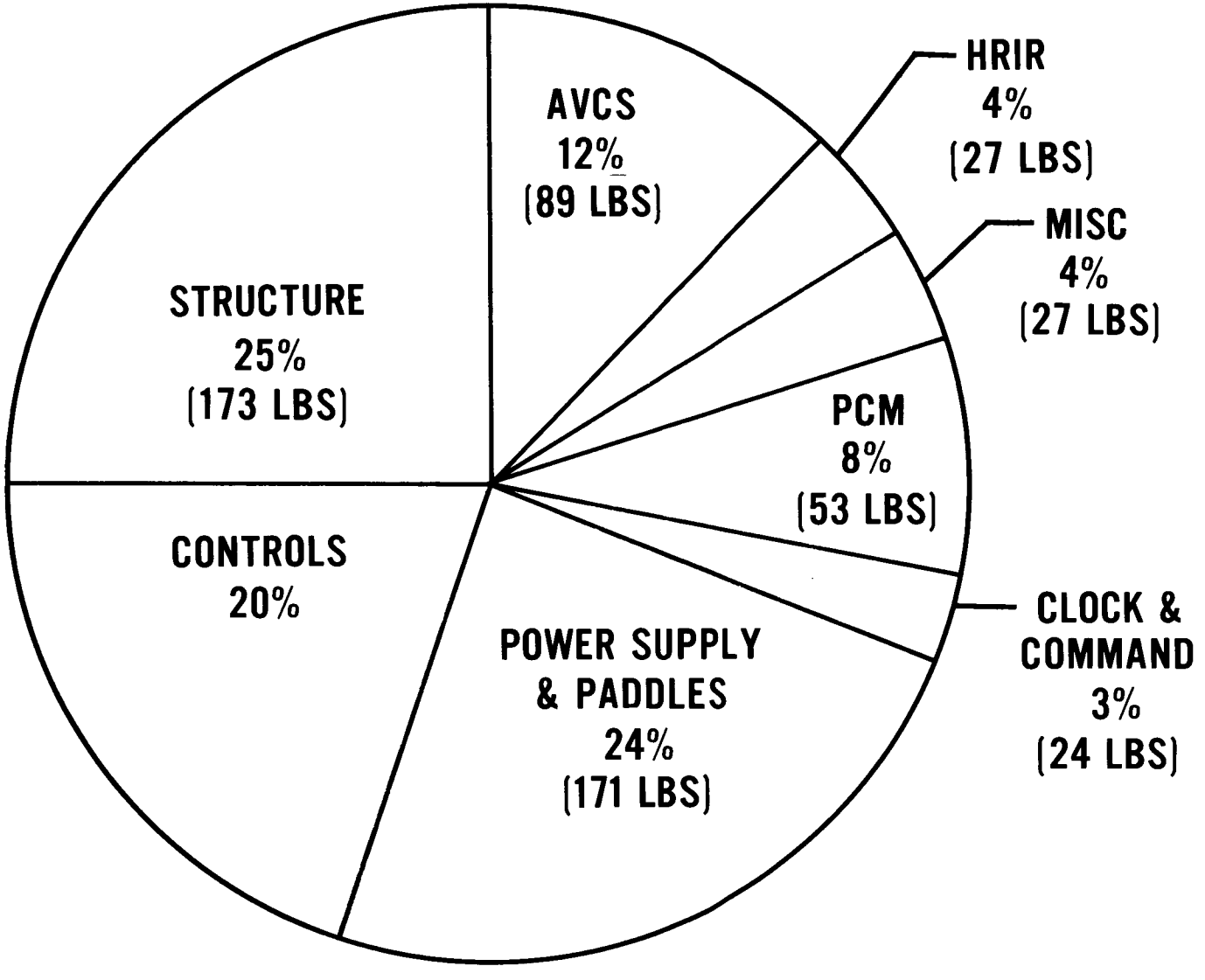

Figure 2 - Nimbus "A" Spacecraft

1. MISSION SUPPORT EQUIPMENT

   A. SPACECRAFT

   B. GROUND

2. MISSION SUPPORT MAINTENANCE & OPERATION

   A. SPACECRAFT QUALIFICATION

   B. LAUNCH SUPPORT

   C. POST LAUNCH OPERATIONS

Figure 3 – Subsystem Mission Duality

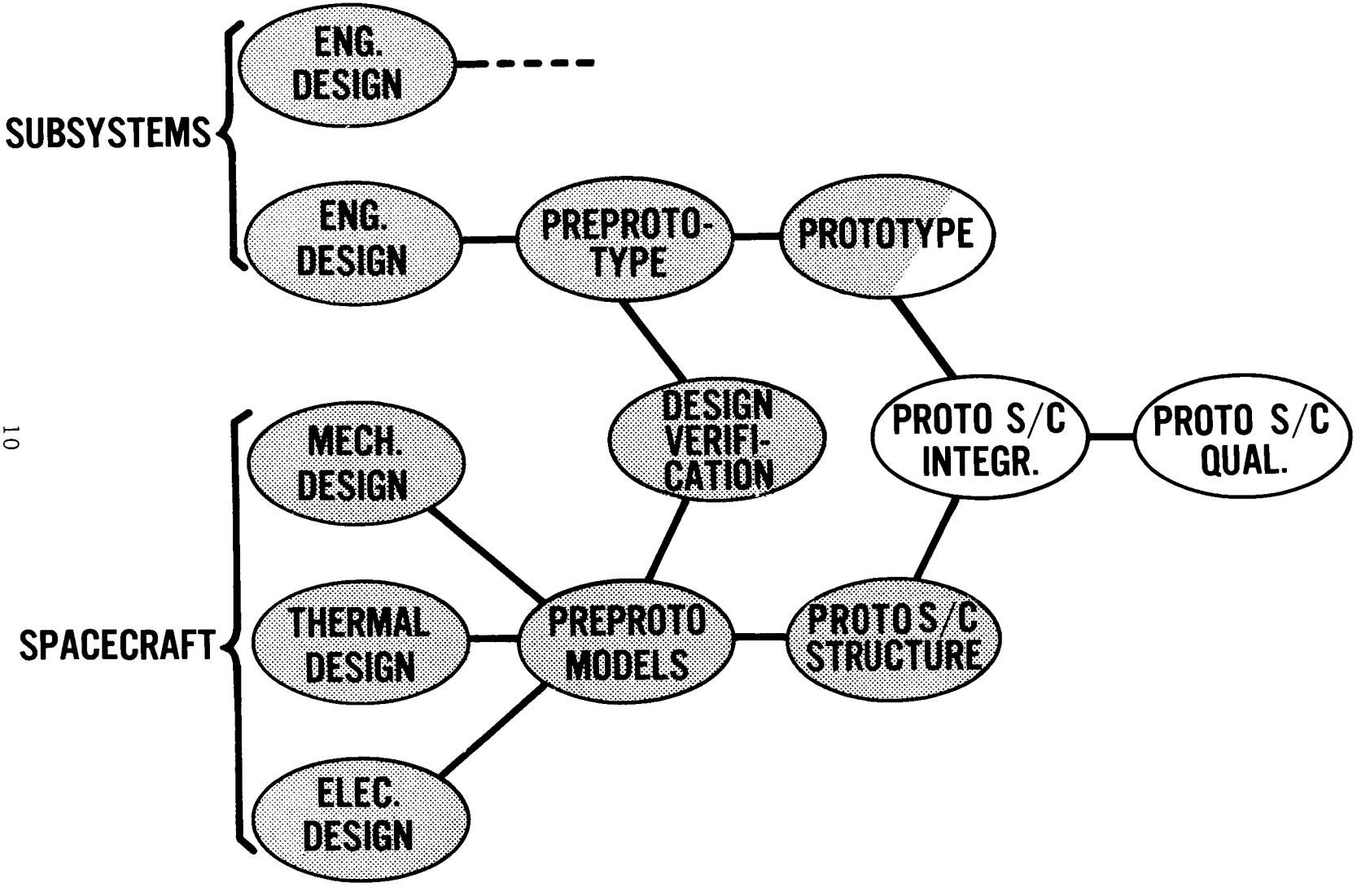

Figure 4 – Spacecraft Development Plan

CONFIGURATION STUDY	S/C MOCKUP MODEL	FORM FITTING
ANTENNA STUDY	S/C ANTENNA MODEL	MEASUREMENTS & TEST
THERMAL STUDY	S/C THERMAL MODEL	MEASUREMENTS & ANALYSIS
MECHANICAL STUDY	S/C VIBRATION MODEL	MEASUREMENTS & ANALYSIS
SUBSYSTEM COMPATIBILITY STUDY	S/C PREPROTOTYPE MODEL	PERFORMANCE TESTS
SEPARATION STUDY	S/C SEPARATION MODEL	ADAPTER DROP TESTING

Figure 5 – Preparatory Spacecraft Development Effort

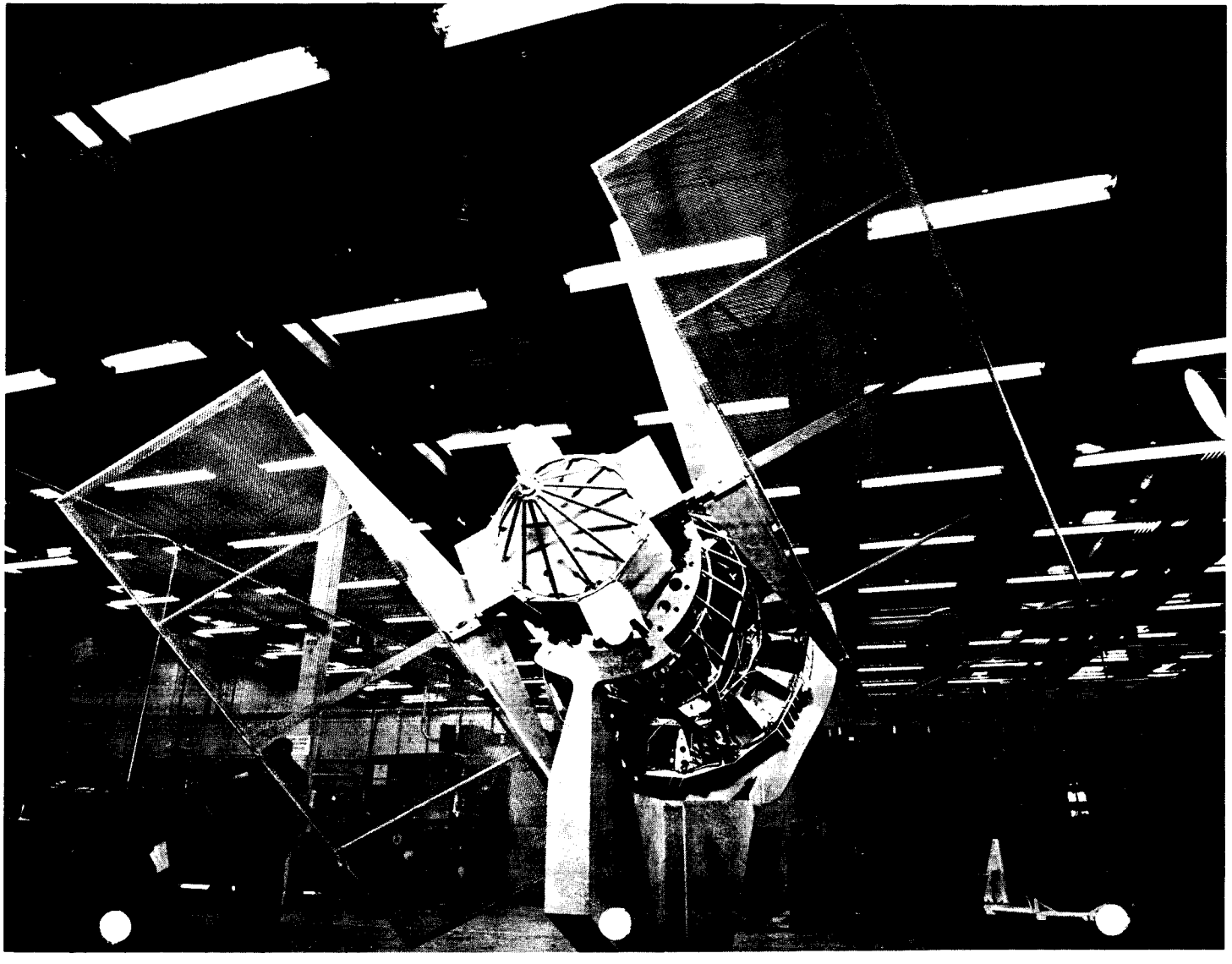

Figure 6 – Nimbus Full-Scale Antenna Model

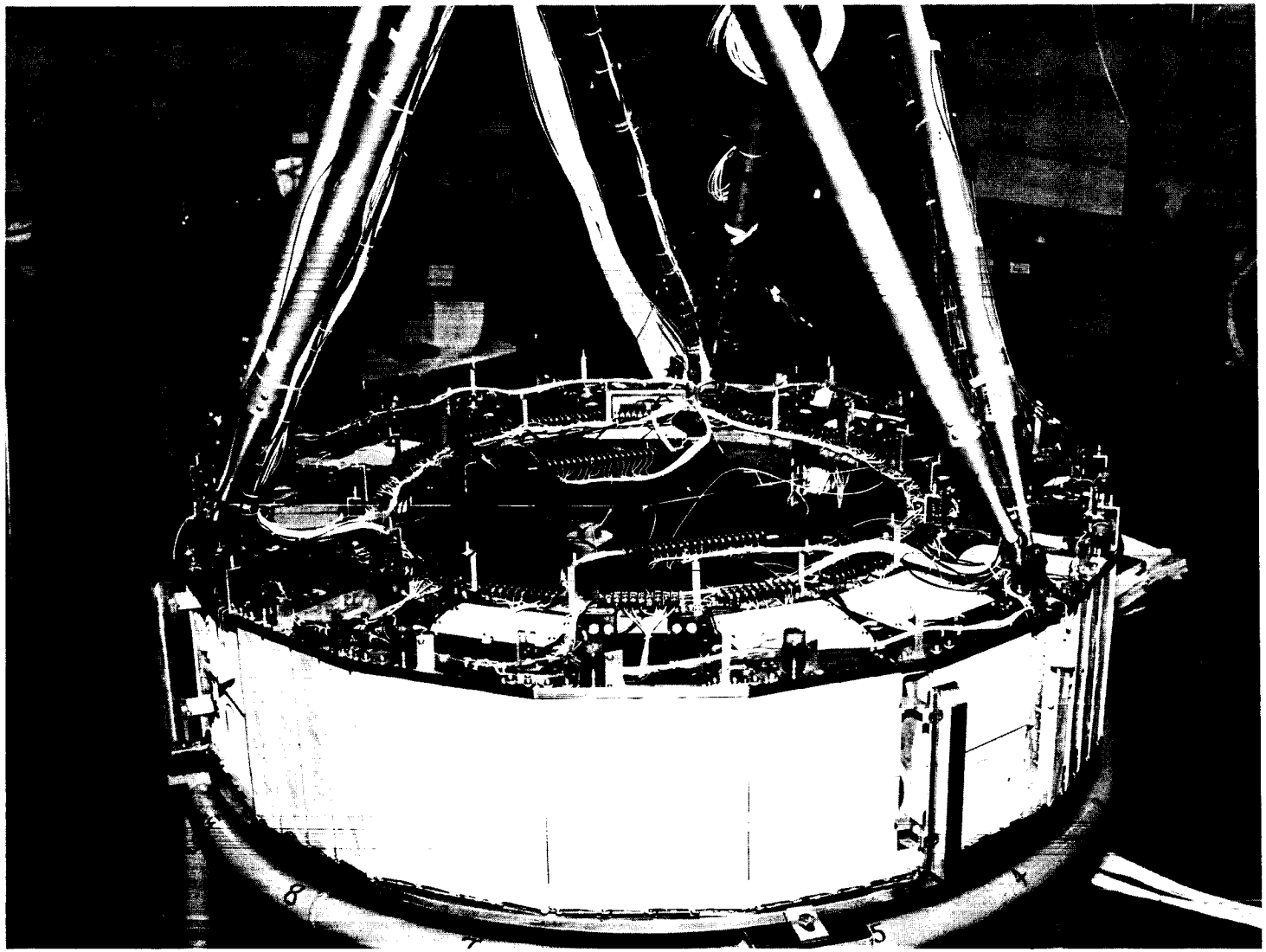

Figure 7 – Nimbus Thermal Model

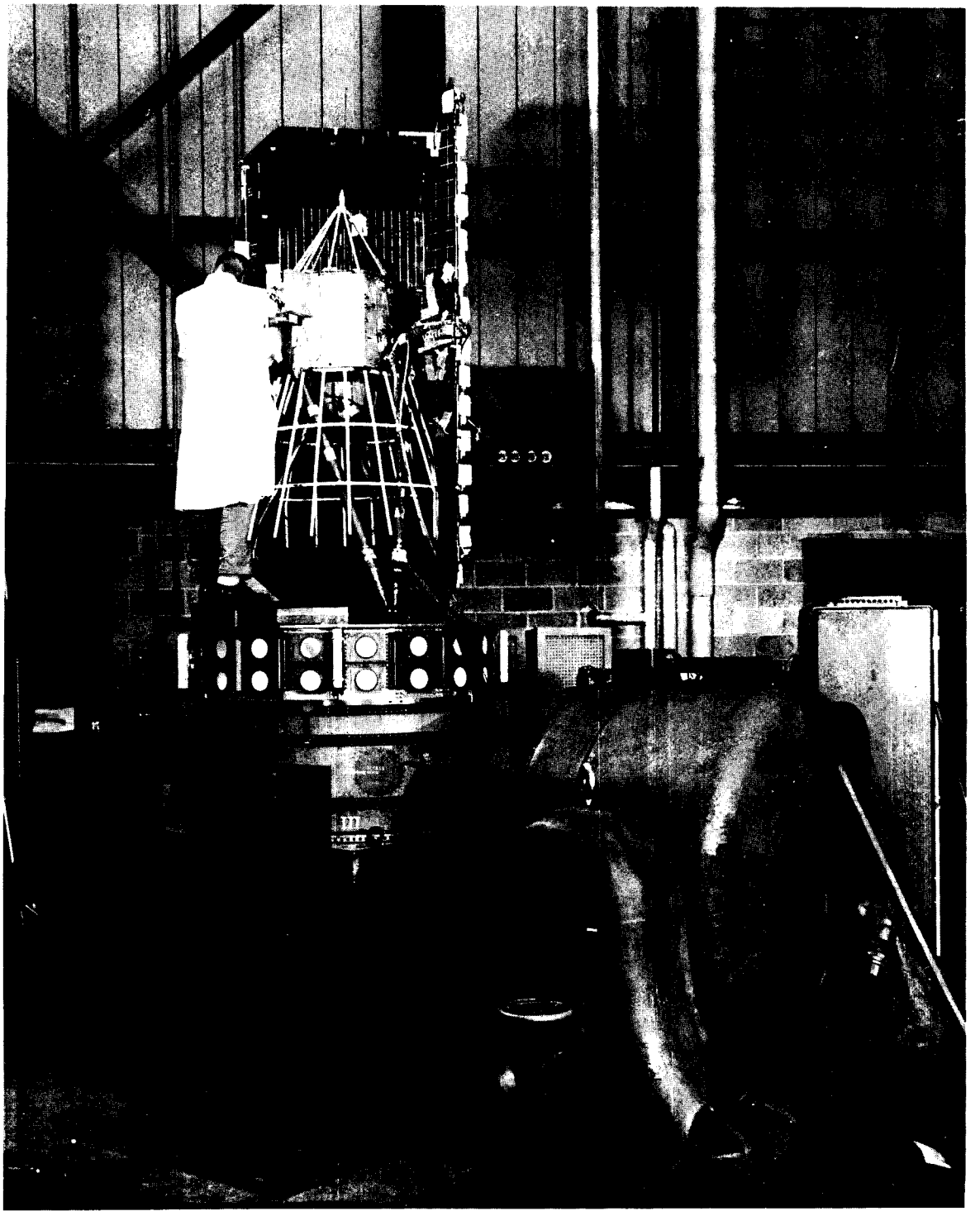

Figure 8 – Vibration Facility with Nimbus Vibration Model

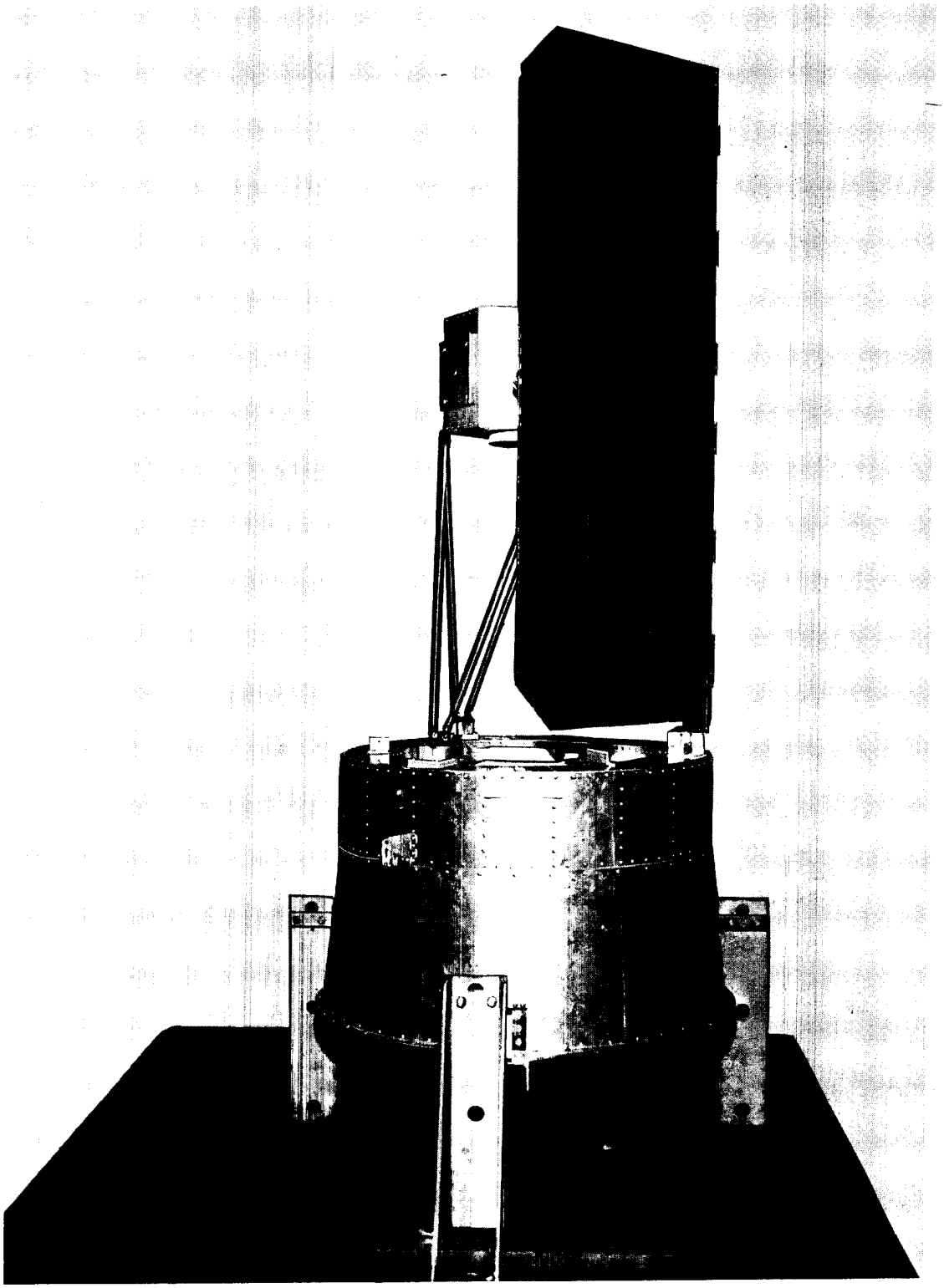

Figure 9 – Nimbus Half-Scale Vibration Model

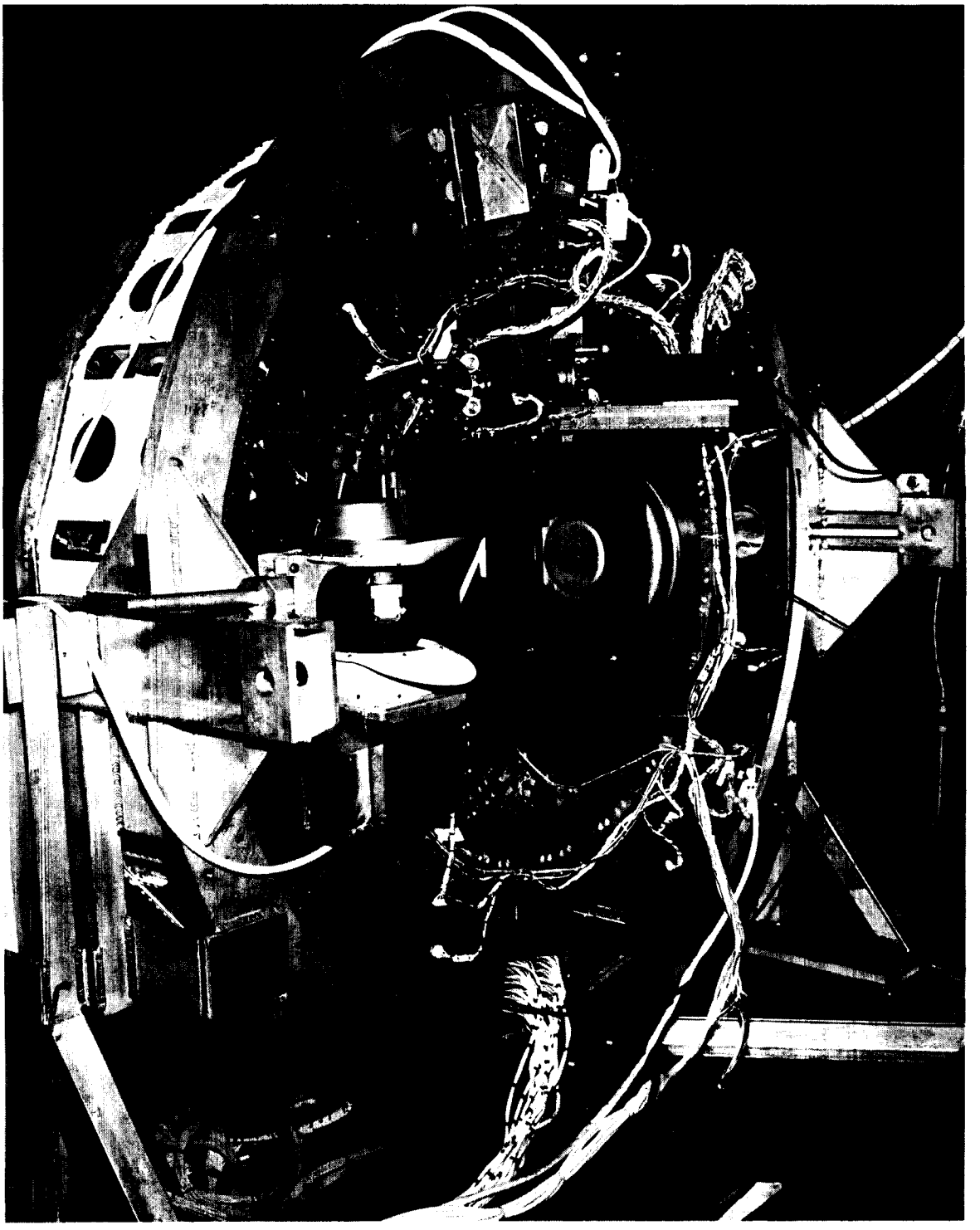

Figure 10 – Nimbus Preprototype Sensory Ring

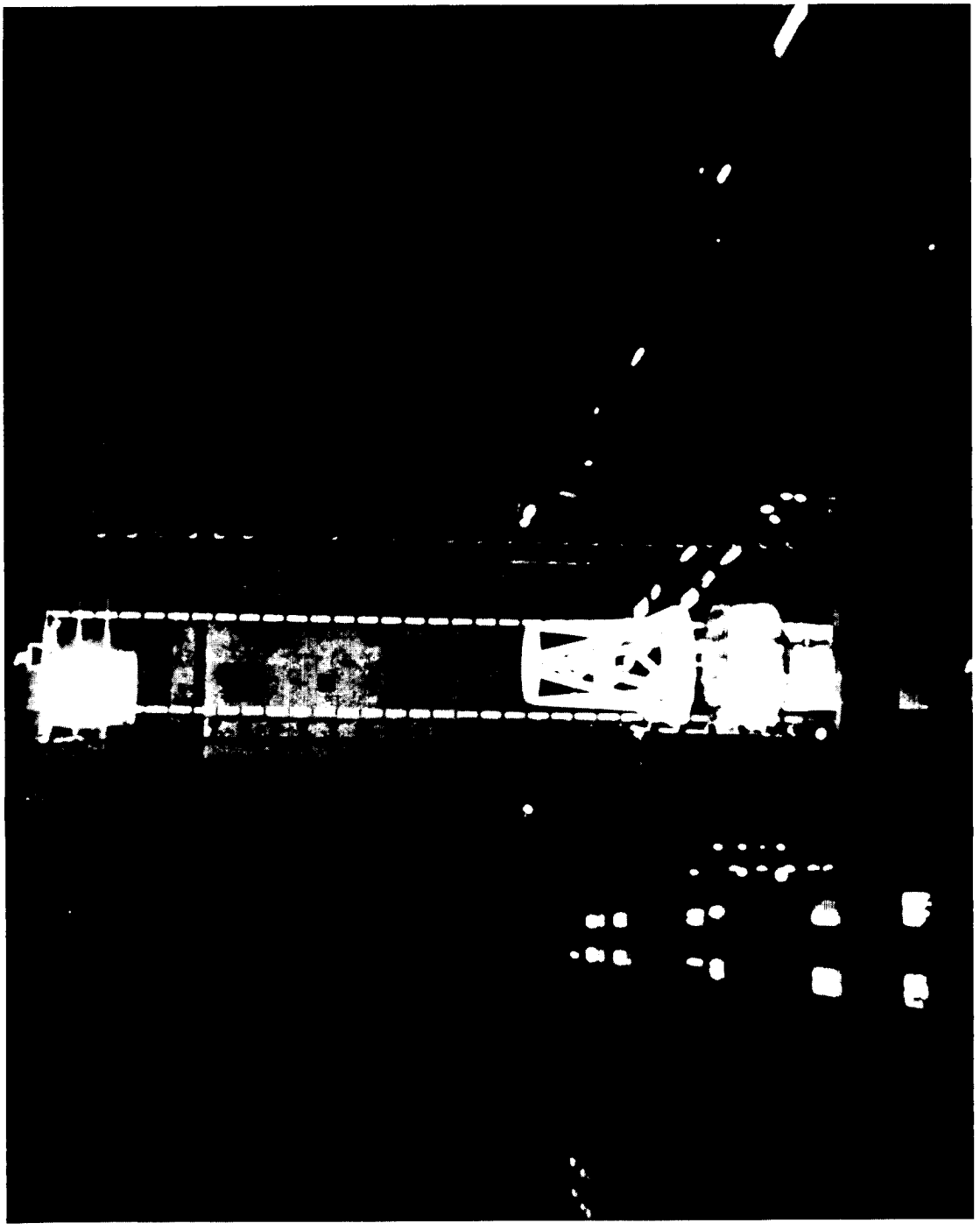

Figure 11 - Spacecraft Separation Drop Test

6. STATUS OF THE NIMBUS INTEGRATION AND TEST PROGRAM

By L. Michelson, GE/Missiles
and Space Division

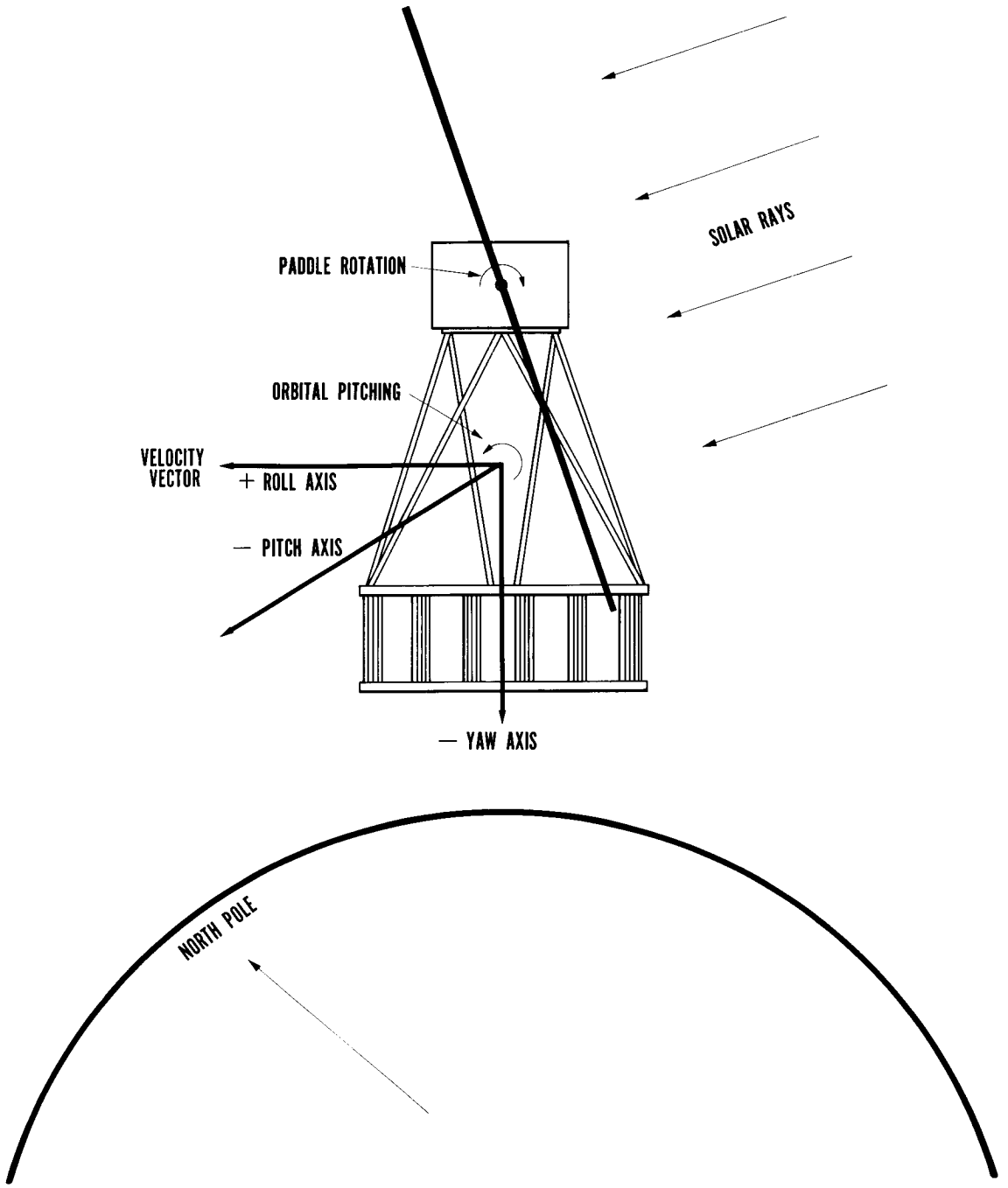

Figure 2 – Nimbus Spacecraft Body Axes

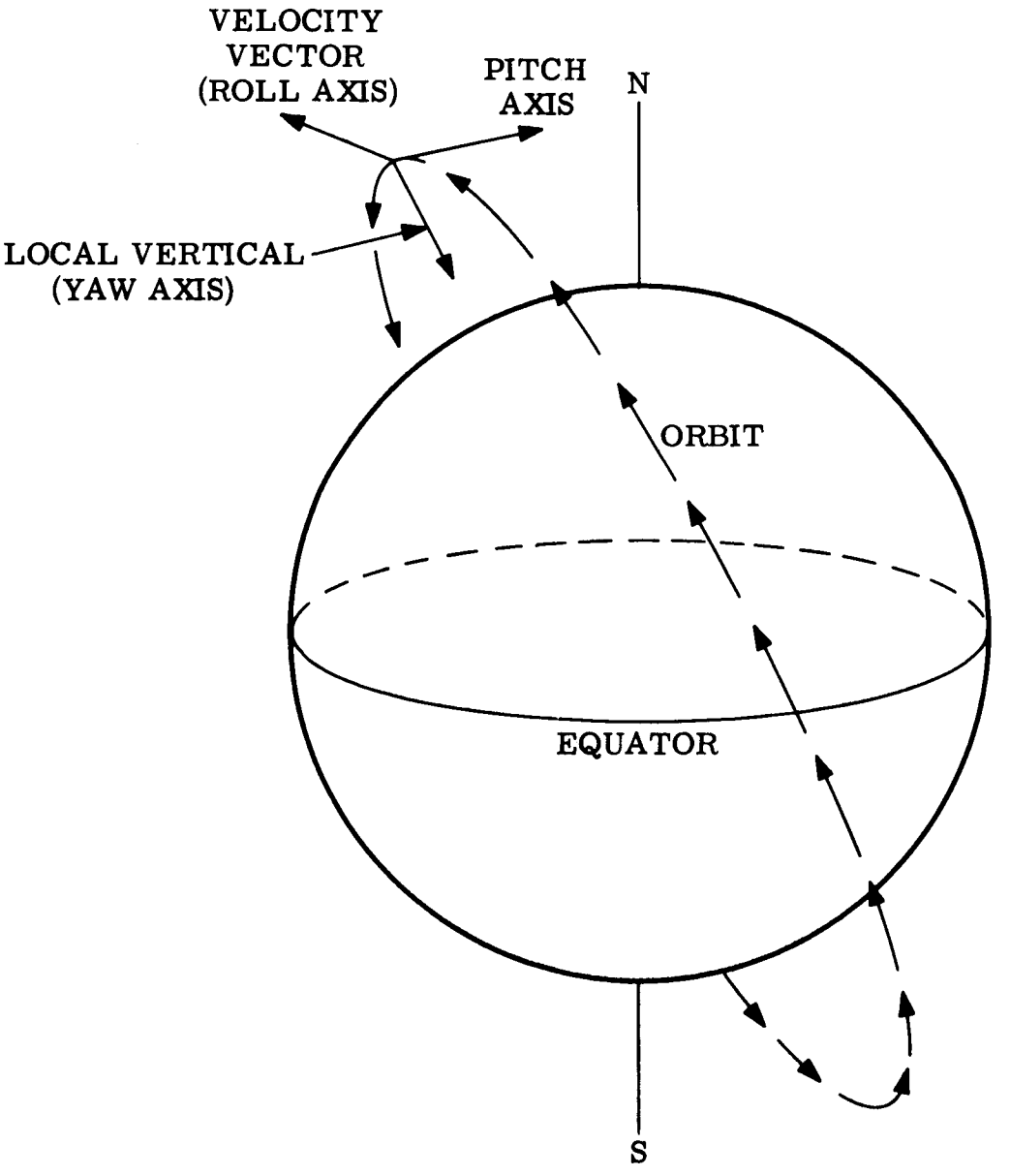

Figure 3. Definition of Orbit Axis

Figure 3 – Definition of Nimbus Orbit Axes

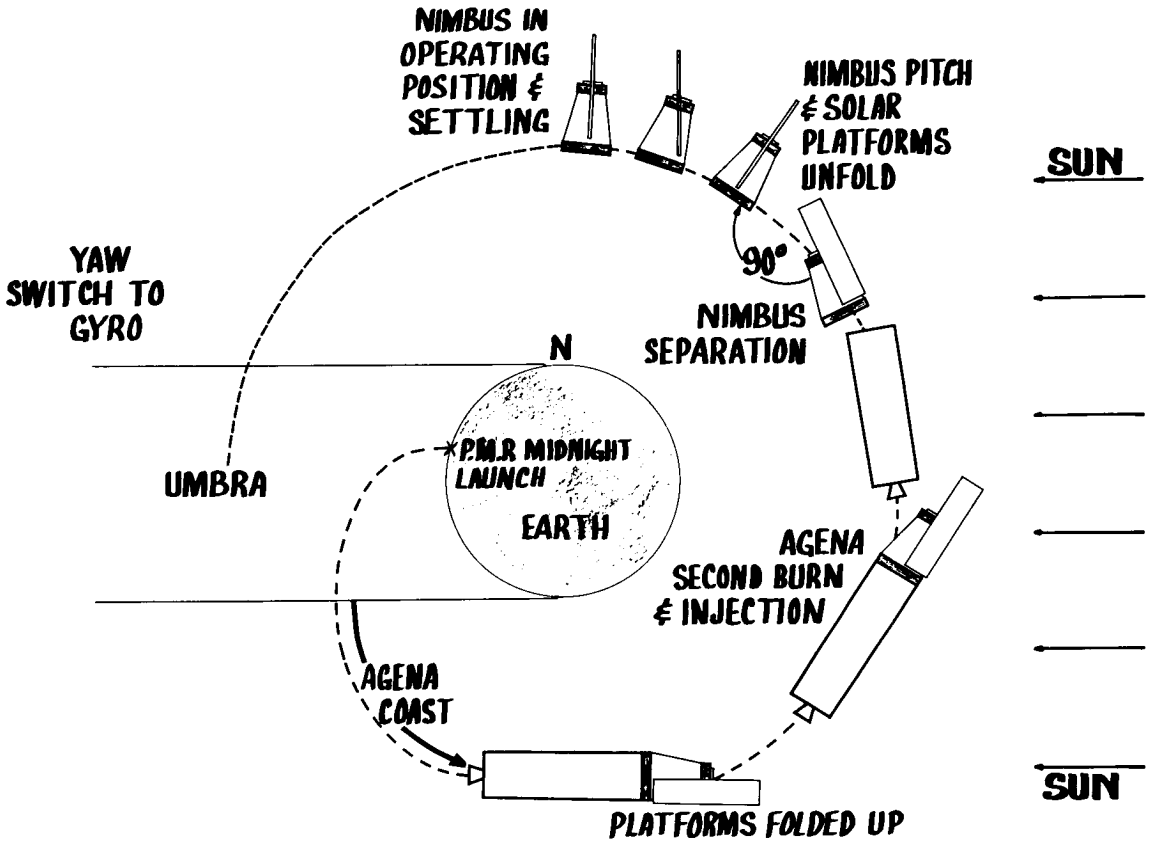

t = 0 SEC SEPARATION
t = 2 SEC PITCHUP & PADDLE UNFOLD
t = 22 SEC ROLL & PITCH
t = 182 SEC YAW - COARSE SUN SENSOR
SOLAR ARRAY DRIVE
ENTERING UMBRA - SWITCH TO GYRO

Figure 4 – Nimbus Stabilization Sequence

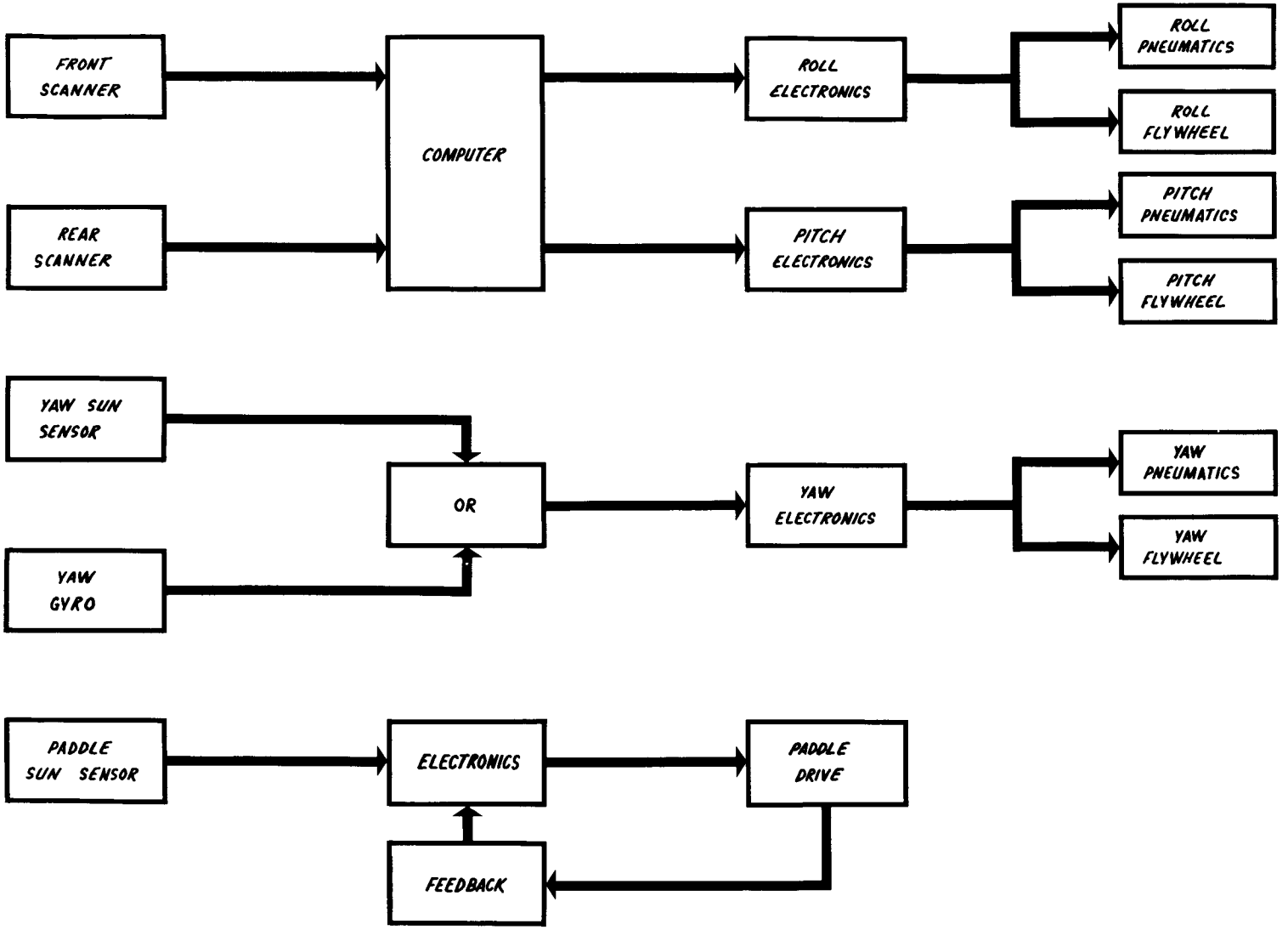

Figure 5 - Nimbus Control Subsystem, Block Diagram

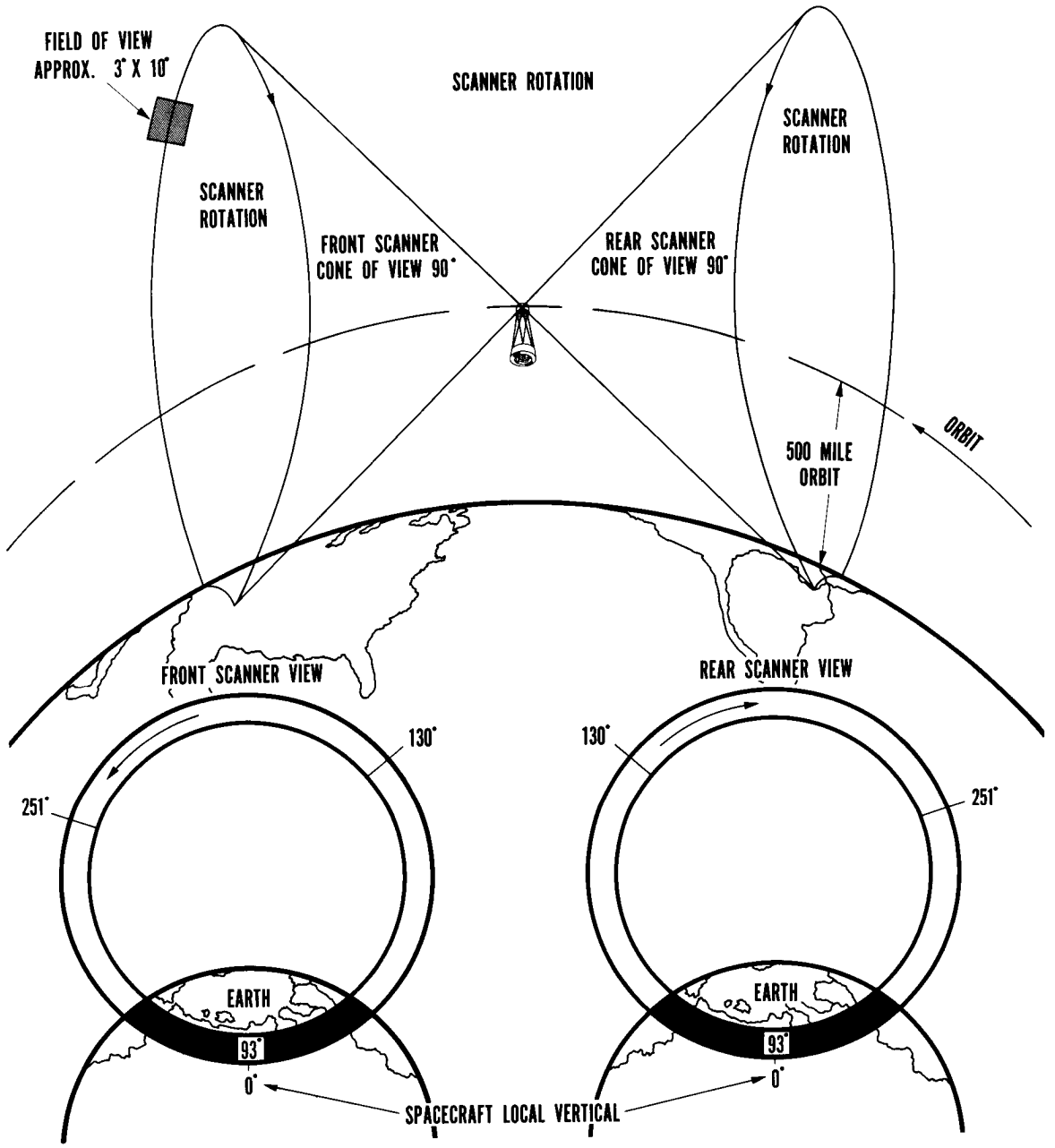

Figure 6 – Earth as Seen by Scanners in Stabilized Nimbus

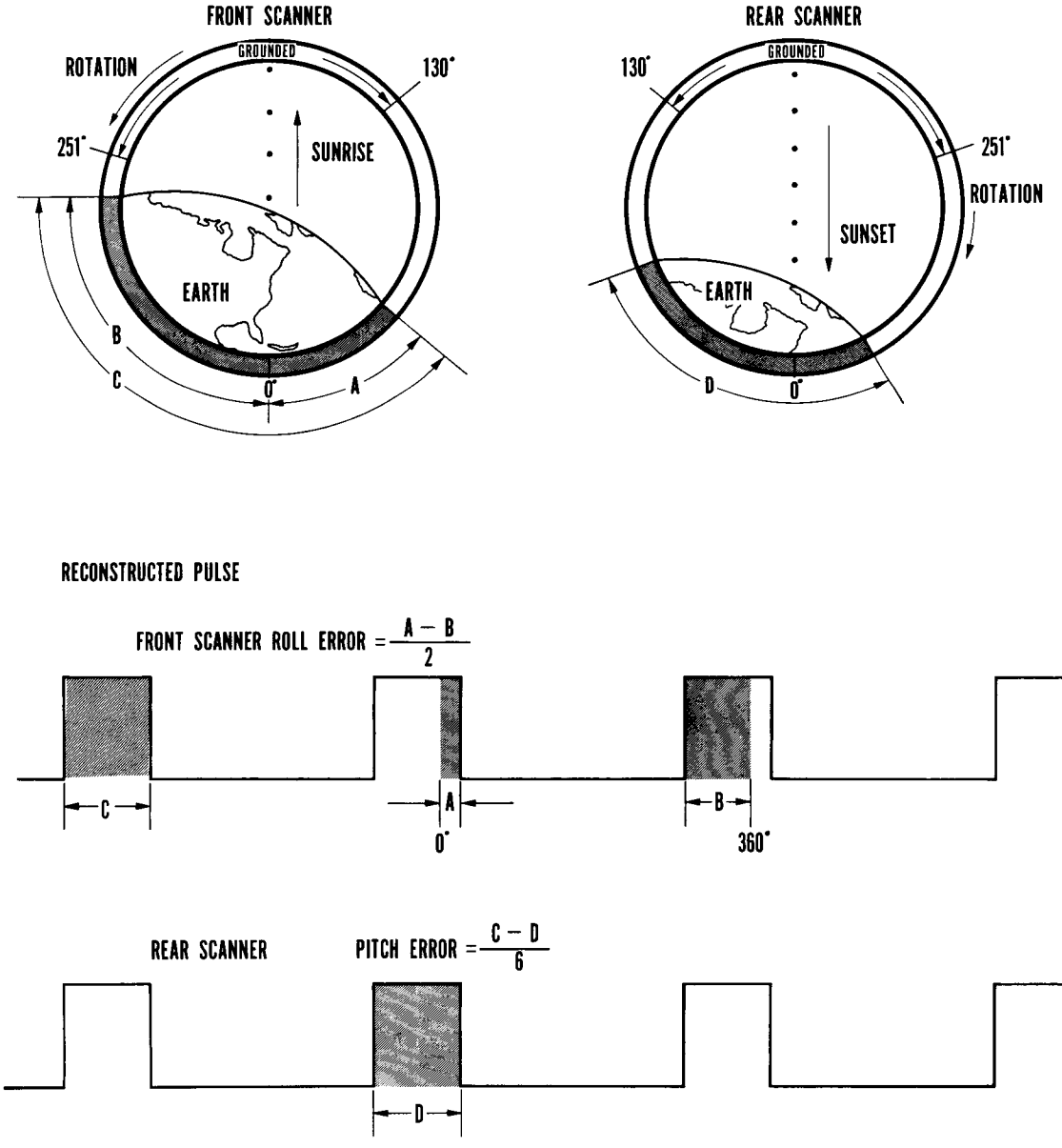

Figure 7 – Roll and Pitch Error Computation from Front and Rear Scanners

CONFIGURATION

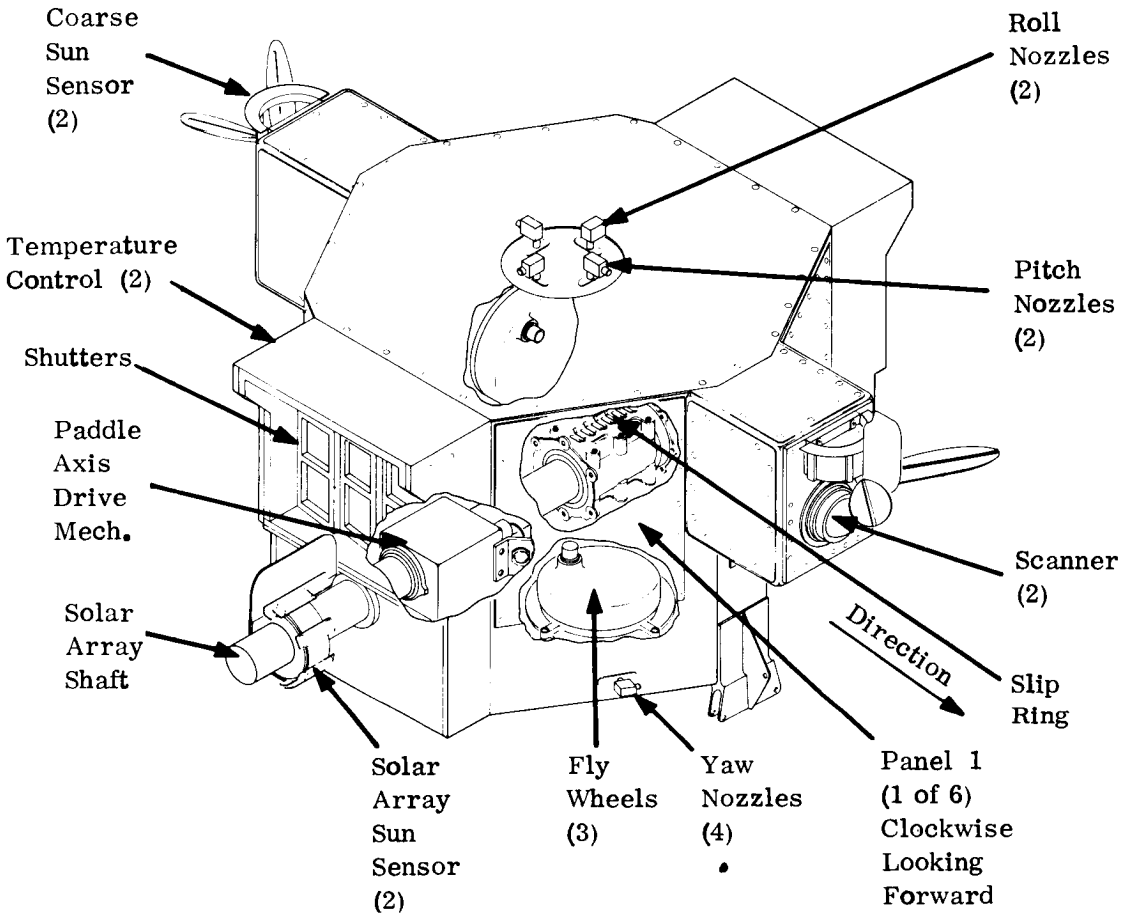

Figure 8 – Nimbus Control Prototype

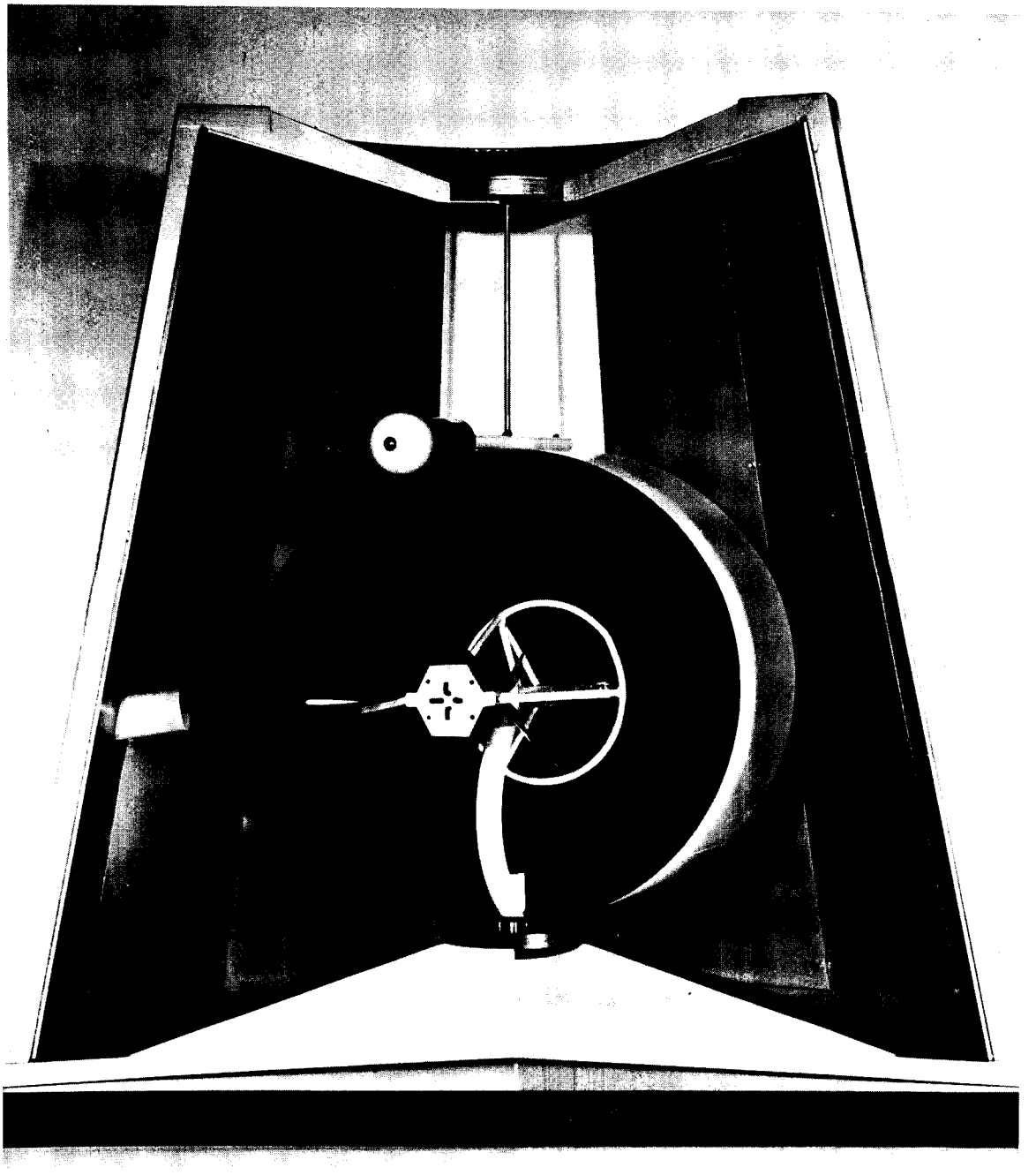

Figure 9 – Model of Three-Axis Test Facility

6. STATUS OF THE NIMBUS INTEGRATION AND TEST PROGRAM

ILLUSTRATIONS

Figure		Page
1	Empty Prototype Sensory Ring	5
2	Nimbus Spacecraft Antennas	6
3	Spacecraft Adapter Interior	7
4	Spacecraft Adapter Exterior	8
5	Interior of 10-by-24-Foot Vacuum Chamber, Showing Check and Calibration Adapter	9
6	Motion-Simulation System for 39-Foot Vacuum Chamber	10
7	Ram Assembly and Check-of-Calibration Adapter	11
8	Pulse-Code-Modulation Ground Station	12
9	Pacific Missile Range Vans	13
10	Nimbus Transportation Equipment	14
11	Prototype and Flight 1 Master Program Schedule	15
12	Nimbus Integration and Test Organization Chart	16

6. STATUS OF THE NIMBUS INTEGRATION AND TEST PROGRAM

By L. Michelson, GE/Missiles

and Space Division

This report will deal briefly with the progress of the integration and test effort, and will discuss the remaining program plans.

General Electric's role in the Nimbus project includes the responsibility for design detailing, fabrication of structure, subsystem integration, and spacecraft qualification, as well as the responsibility for design, fabrication, and qualification of the spacecraft separation system, and the development, construction, and application of a vast array of aerospace ground equipment.

Basic spacecraft structural hardware and operating components are essentially completed; hardware items built by General Electric include thermal controllers, solar-platform lock assembly, sensory cross-beam structure assembly, and struts. The major assembly is the torus structure; Figure 1 shows the empty prototype sensory ring, with part of the protective cover removed for photographing.

Electrical operating components which have been completed include the beacon killer, telemetry conversion circuitry, sequence timers, load simulators, flight targets, harness, and the spacecraft antennas shown in Figure 2. From left to right are the S-band conical spiral antenna, the VHF, the folded ground-plane interrogation antenna and the quadraloop antenna.

As discussed previously, six models of the spacecraft have been built to corroborate various analyses. A physical mockup was built for dimensional checks and harness cabling; this was followed by a vibration model in flight materials which passed all its tests, and a thermal model in flight materials on which exhaustive thermal tests were run. This latter model proved that the shutters could control the temperature in each of the eighteen compartments within the specified limits of ± 10 degrees throughout the duty cycle, regardless of the various solar fluxes experienced in orbit.

As part of GE's responsibility for developing the spacecraft separation system, an adapter for mounting the spacecraft on the Thor Agena B has been developed in conjunction with the Douglas Aircraft Company. Figure 3 shows the interior of the flight adapter before installation of go/no-go targets and sensory devices. Upon separation, explosive bolts are fired, and the four springs arranged in quadrature separate the spacecraft from the launch vehicle with a precise separation velocity and carefully controlled angular rate. Extensive tests of the flight adapter have been successfully completed, with variables introduced such as spacecraft center-of-gravity offset, or out-of-flatness between the spacecraft and the adapter.

Figure 4 is a closeup of the exterior of the flight adapter, showing the Marman-type D clamp that seats around the separation rings, and the explosive-bolt arrangement. Redundancy is provided by a duplicate explosive-bolt arrangement on the other side of the adapter.

The extensive test facilities required for support of the Nimbus program are essentially completed; Figure 5 is a photograph of the 10-by 24-foot vacuum chamber with its check-of-calibration adapter for accepting the sensory ring. This chamber, which has cryogenically cooled walls, is capable of an ultimate vacuum of about 10^{-9} millimeters of mercury.

After tests in the 10-by 24-foot vacuum chamber, the sensory ring is combined with the other spacecraft elements, and tests of the alignment and electrical system follow. The spacecraft is next vibrated in GE's C210 vibration facility. Only after vibration does the prototype spacecraft undergo acceleration and humidity testing.

The culmination of spacecraft qualification is essentially the 39 days of vacuum-thermal testing in the Nimbus 39-foot vacuum chamber. During part of these tests, the spacecraft will be completely free of any ground connection, floating on a film of air, communicating only by radio, and maneuvering as it does in orbit.

Figure 6 shows the motion-simulation system which simulates the perambulations of the spacecraft in orbit; the support arm maintains the spacecraft on a friction-free film of air and permits it to move without impedance. The simulated earth horizon in the background is rotated at the earth rate, providing a tracking target for the spacecraft in

orbit. A photoelectric followup system observes a small mirror on the tip of the interrogation antenna, and tracks it to indicate the position of the spacecraft to an observer outside the 39-foot chamber.

Because the time is limited during which the batteries can power the spacecraft, provision has been made for periodically charging the batteries. The spacecraft will not carry its solar paddles during this test, and the battery must be charged by hardwire connection; to do this, the spacecraft is remated with its adapter by means of the ram assembly shown in Figure 7. During this battery-charging period, the control subsystem nitrogen gas reservoir is replenished and a complete sensory subsystem check is made.

Figure 8 shows the checkout ground station which has been installed in the space environment test facility area. This illustration shows only the PCM ground station, although the entire installation also includes the computer command console, and AVCS and HRIR ground station.

Figure 9 shows the two vans that house mobile ground-station equipment, which will be transported to the Pacific Missile Range for launch support.

Figure 10 shows some of the handling equipment specially built to ensure no damage to the spacecraft during handling maneuvers. This equipment has been thoroughly qualified.

The master program schedule for accomplishment of spacecraft integration and tests, Figure 11, is shown in elapsed time rather than in calendar dates, but should begin essentially in the month of January; 38 weeks will be required, from receipt of the last qualified prototype sensory ring subsystem to the delivery of flight model 1.

To help carry out the remaining work, the NIMIT (Nimbus integration and test) organization shown in Figure 12 has been set up at GE under the direction of Edward Pelling.

A quality control and test organization is responsible for providing the test facilities and test procedures, and for controlling the test documentation to ensure the validity of the results and the integrity of the equipment.

The manager of systems design and evaluation is responsible for overall systems engineering and for planning tests which culminate in issuance of the pretest report. He is also responsible for overall direction of the systems tests.

The manager of spacecraft and design engineering is responsible for the design, construction, and qualification of GE-furnished equipment.

The manager of NIMIT programming is responsible for control of the funds, scheduling, and production of flight hardware for the Nimbus integration and test portion of the program.

The manager of operational systems is responsible for planning computer programs, programming computers, and integrating all the ground-station equipment.

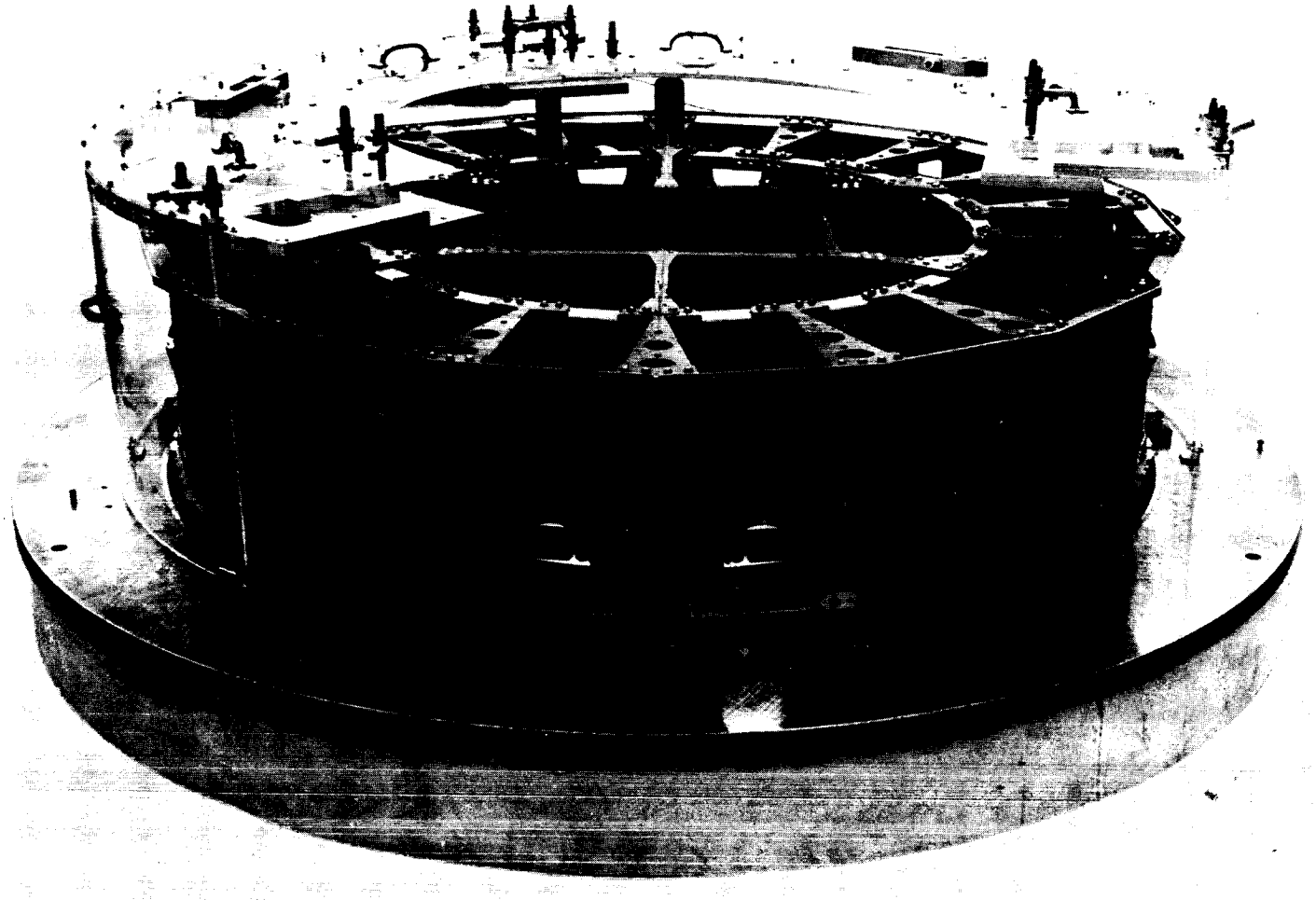

Figure 1 – Empty Prototype Sensory Ring

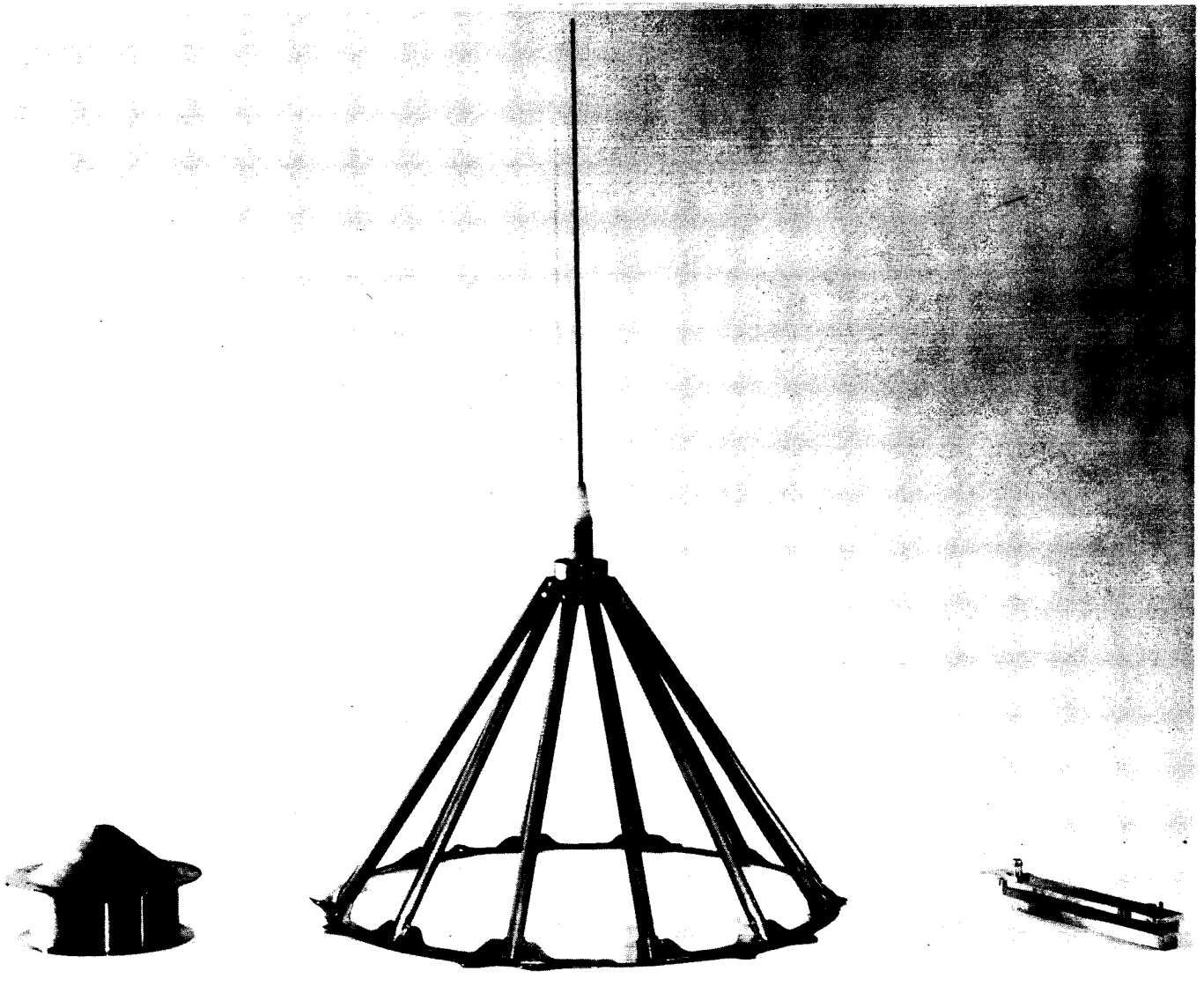

Figure 2 – Nimbus Spacecraft Antennas

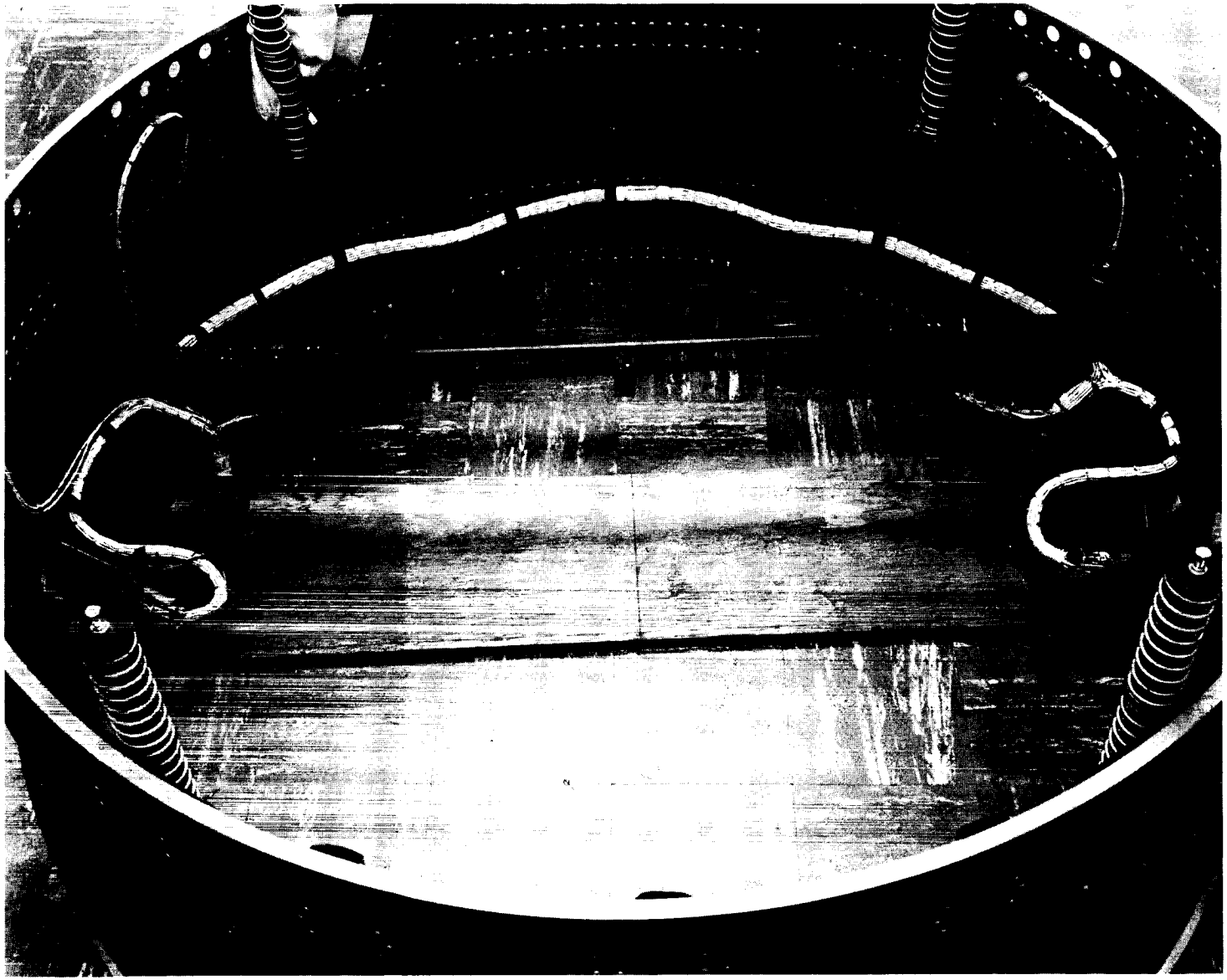

Figure 3 – Spacecraft Adapter Interior

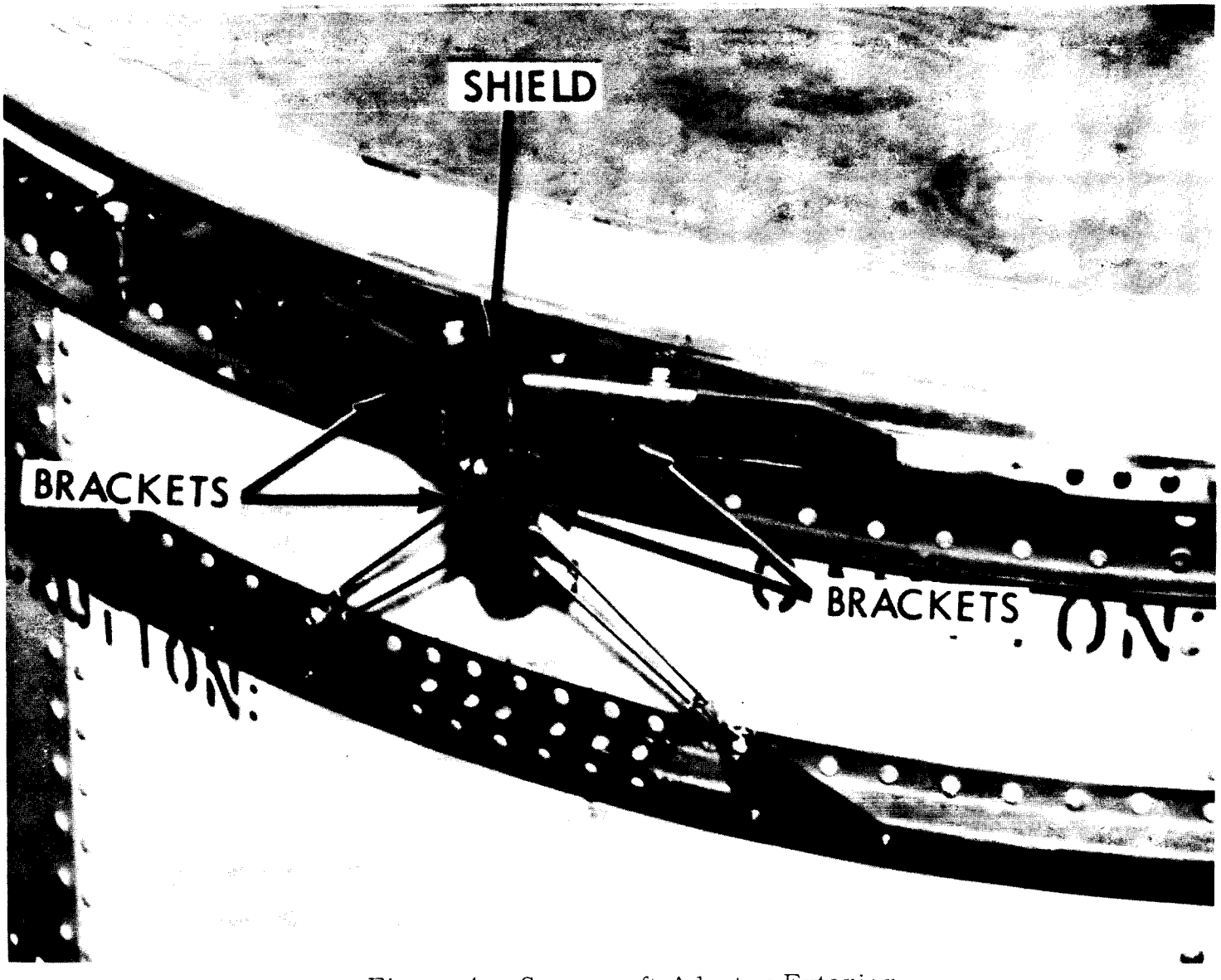

Figure 4 – Spacecraft Adapter Exterior

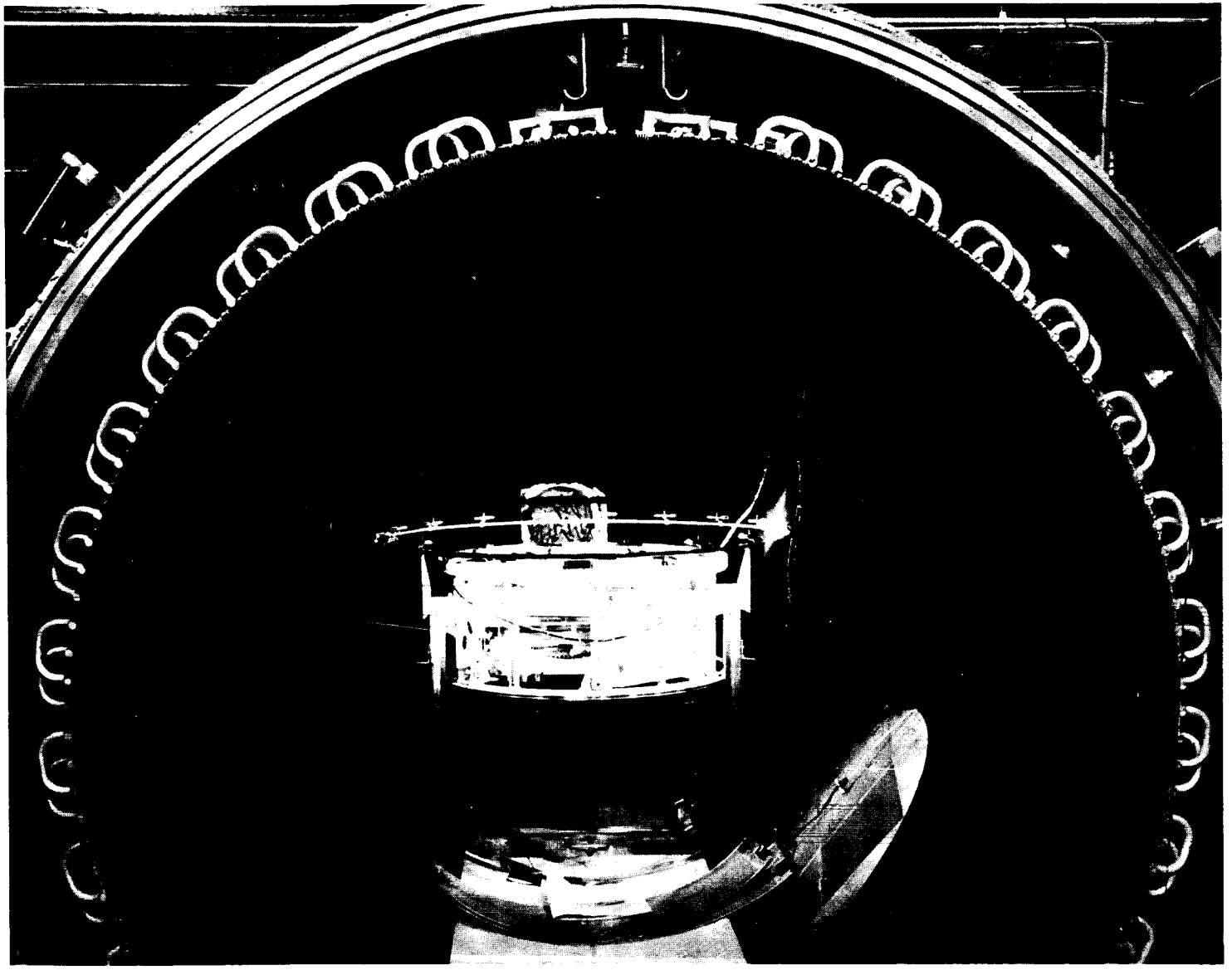

Figure 5 - Interior of 10-by 24-Foot Vacuum Chamber, Showing Check and Calibration Adapter

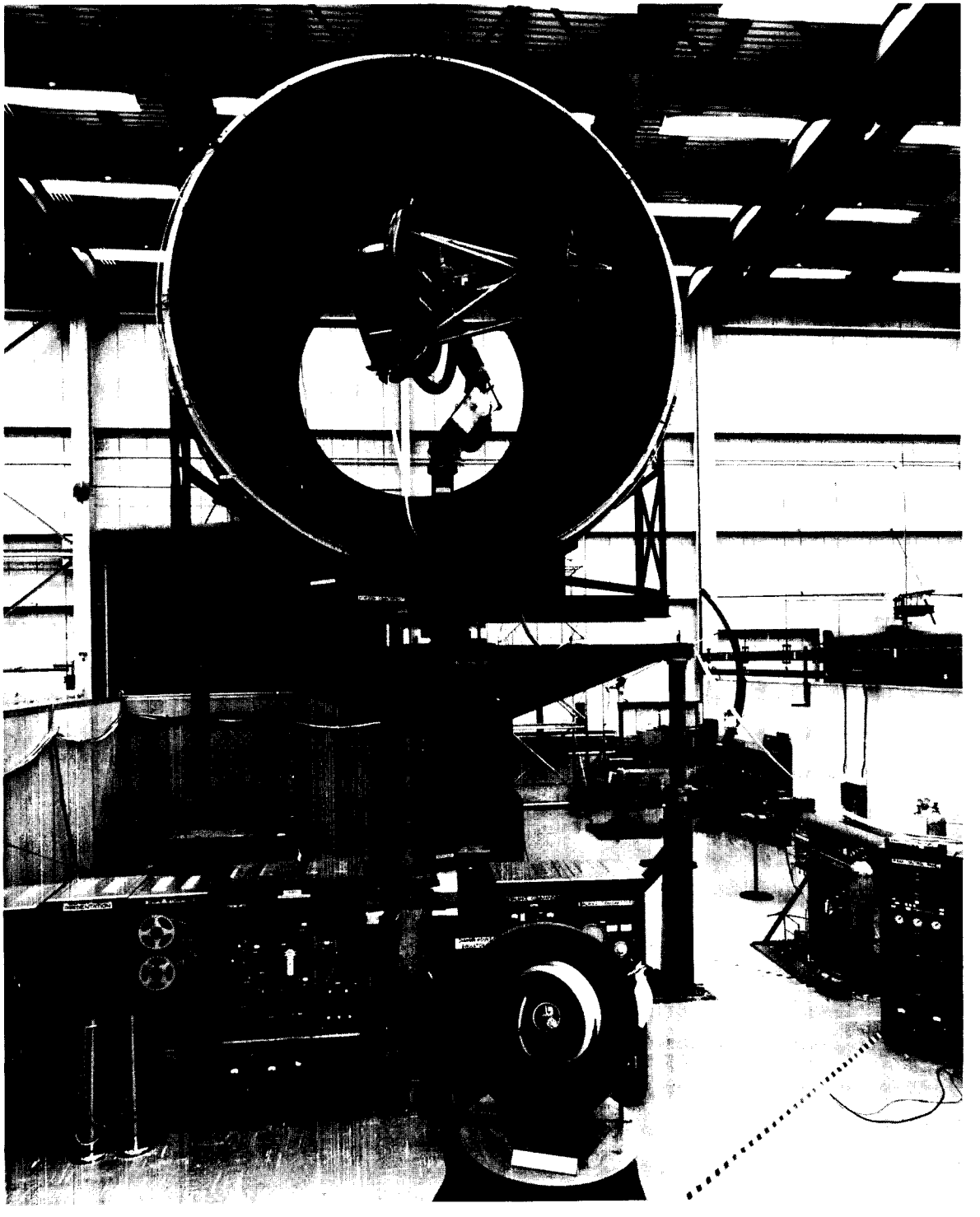

Figure 6 – Motion-Simulation System for 39-Foot Vacuum Chamber

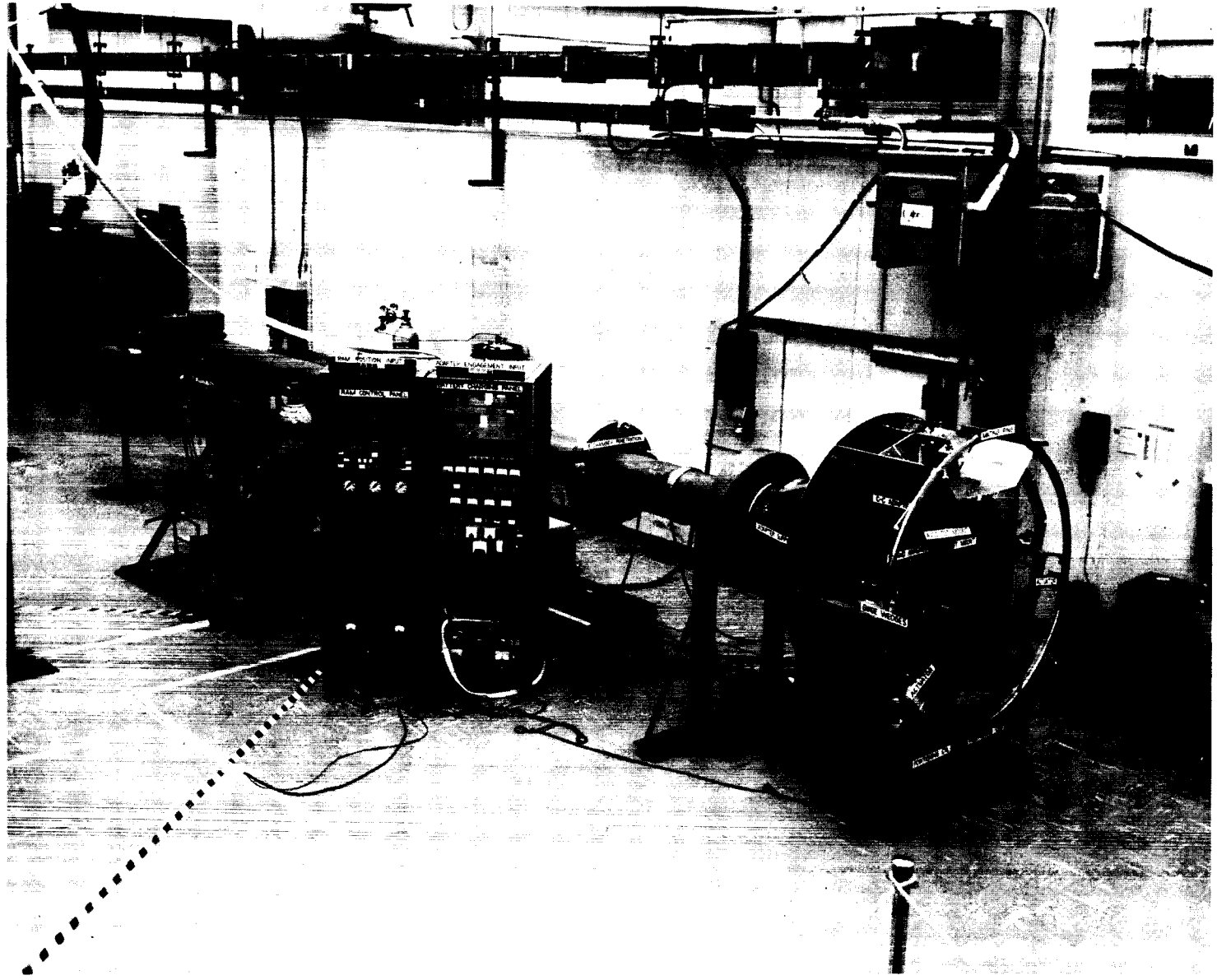

Figure 7 – Ram Assembly and Check-of-Calibration Adapter

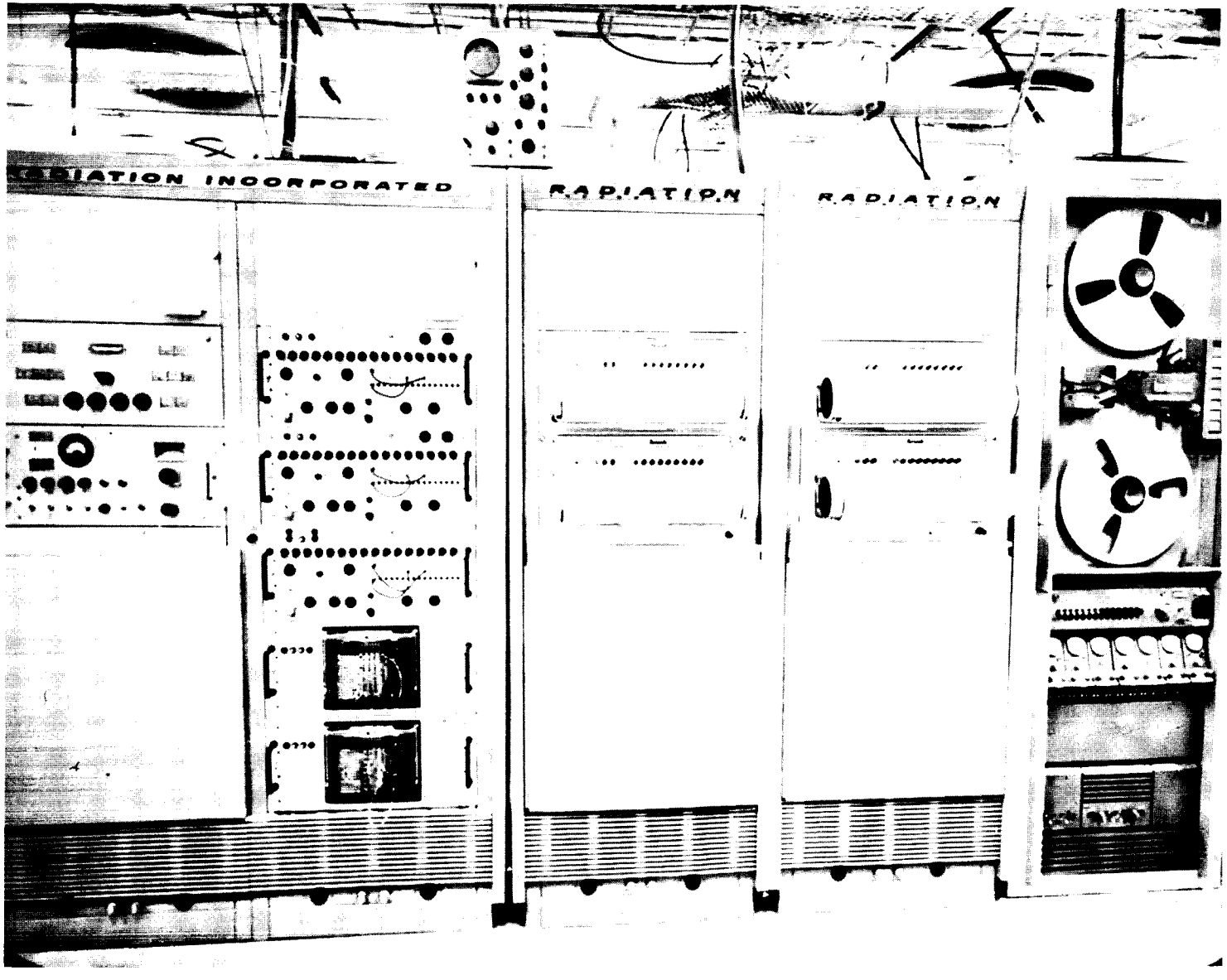

Figure 8 – Pulse-Code-Modulation Ground Station

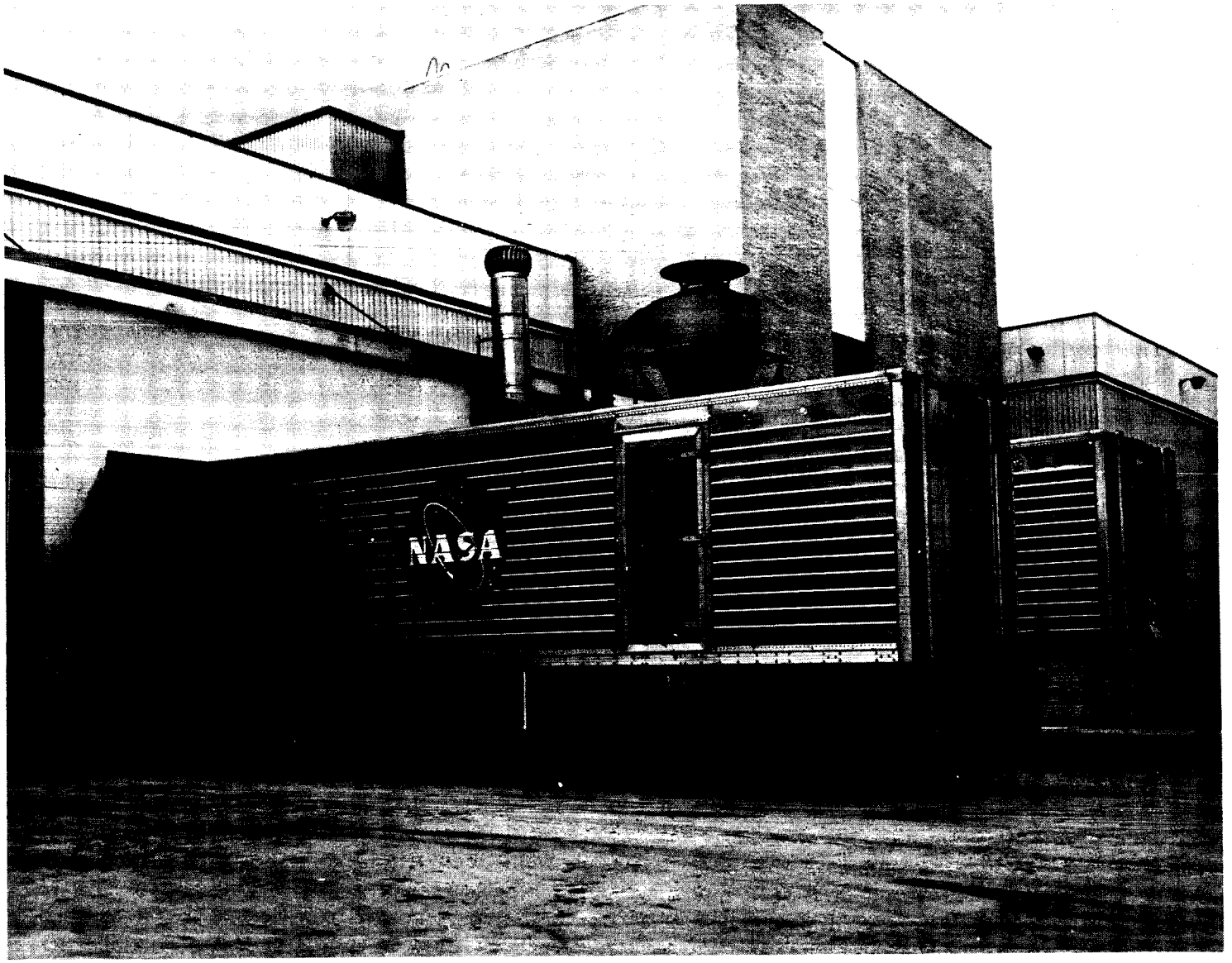

Figure 9 – Pacific Missile Range Vans

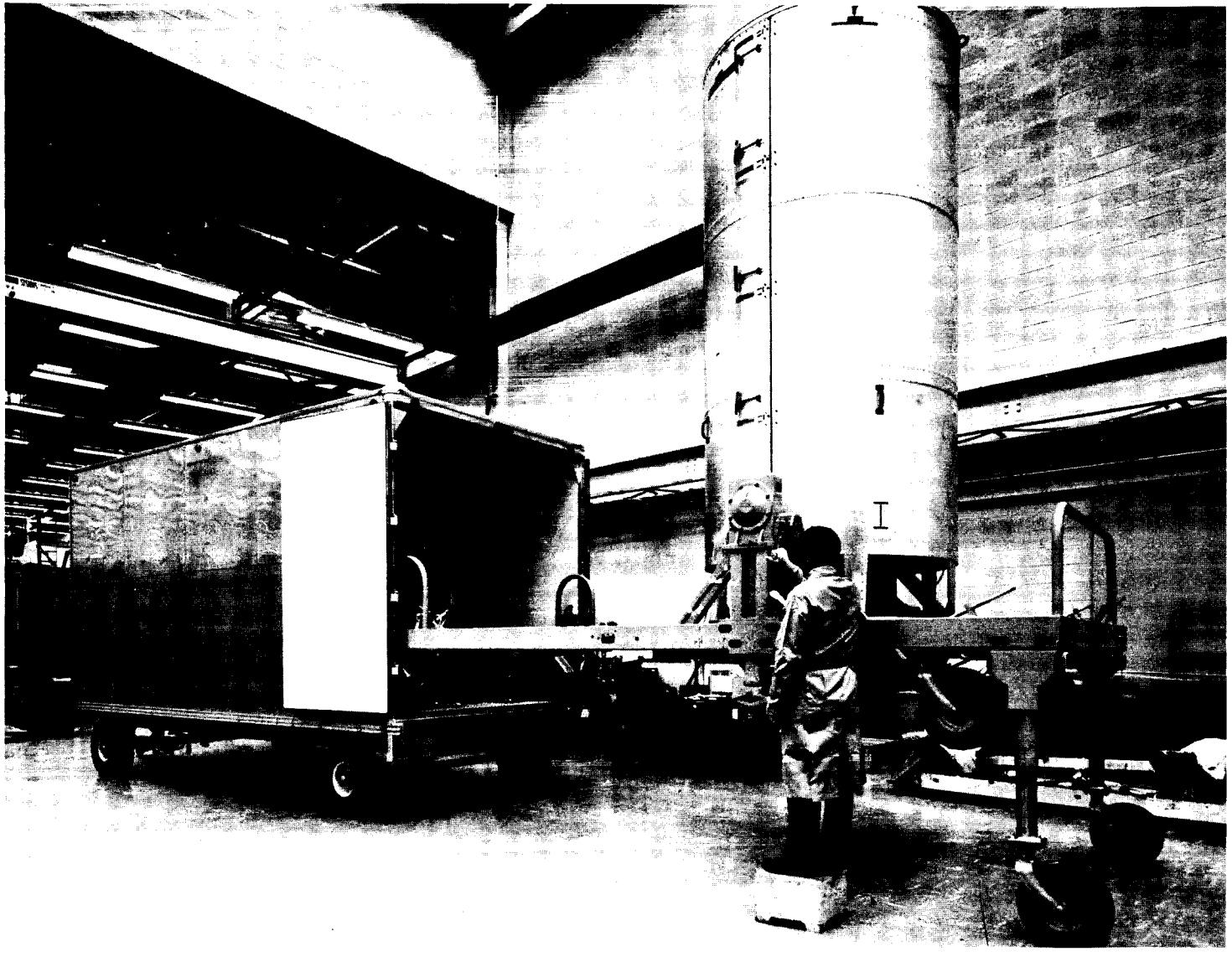

Figure 10 – Nimbus Transportation Equipment

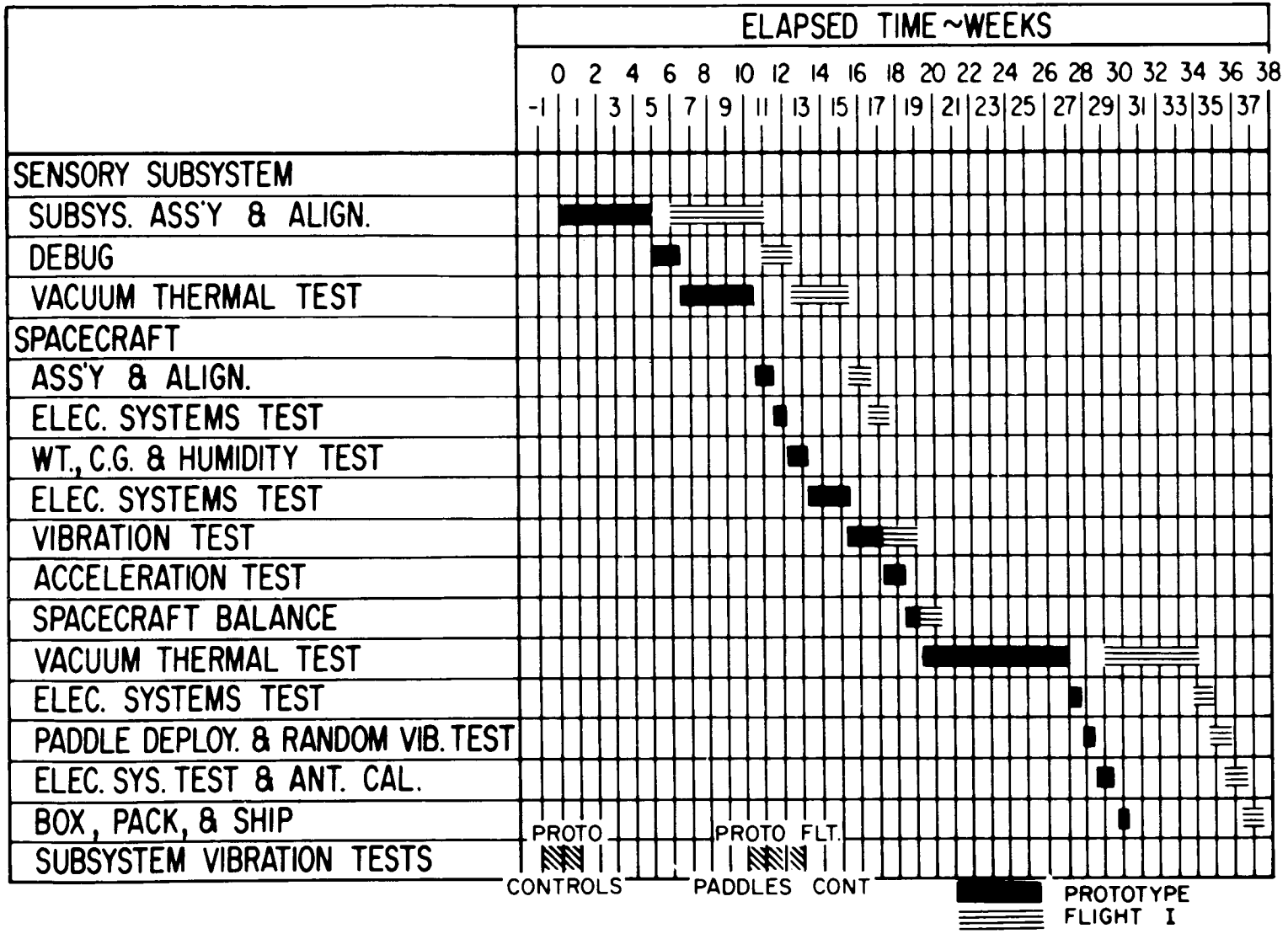

Figure 11 - Prototype and Flight 1 Master Program Schedule

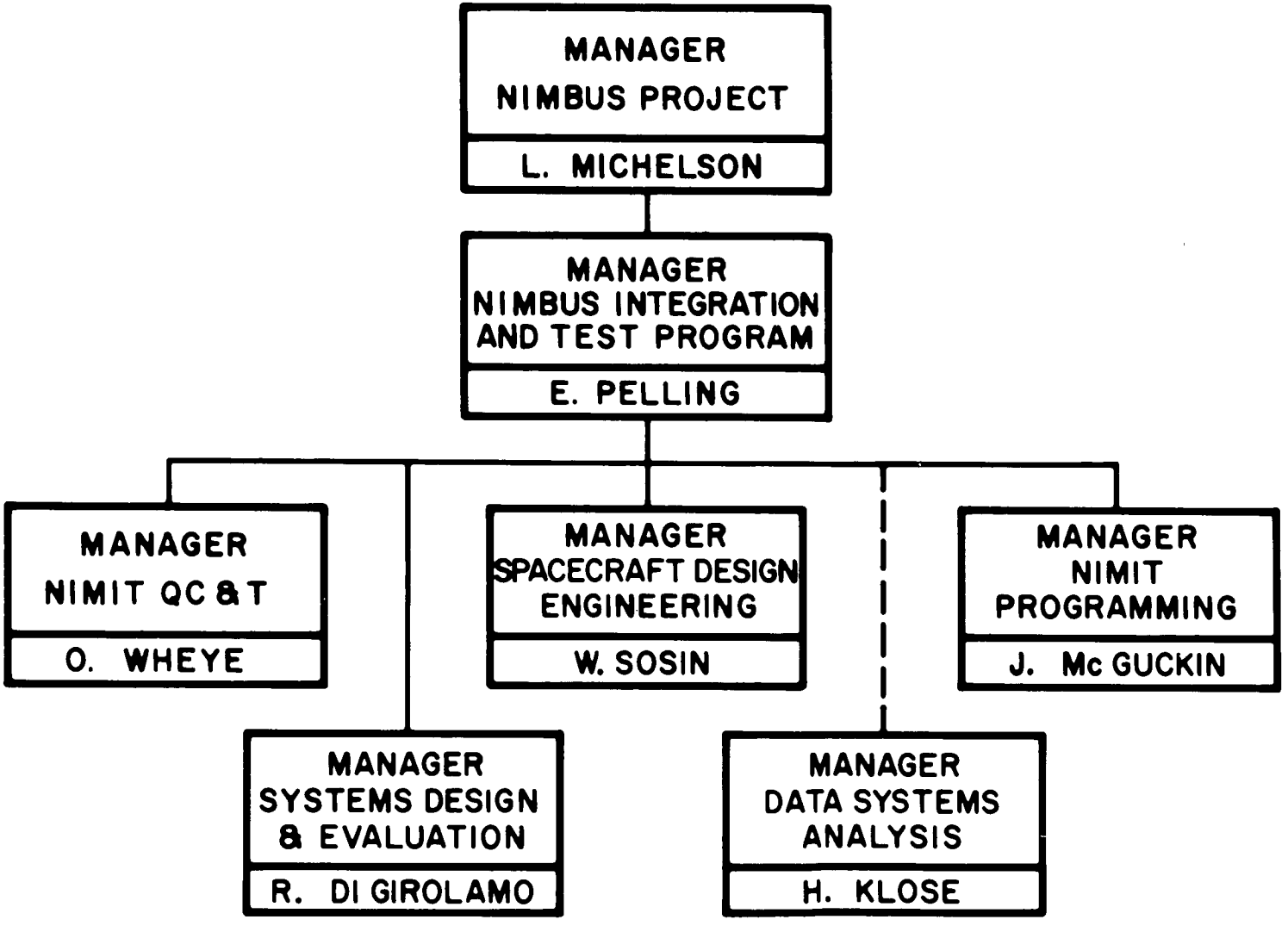

Figure 12 – Nimbus Integration and Test Organization Chart

7. NIMBUS GROUND SYSTEM

By L. Stelter, GSFC

7. NIMBUS GROUND SYSTEM

ILLUSTRATIONS

Figure		Page
1	Nimbus Ground System	8
2	Orbital Coverage from Fairbanks, Alaska	9
3	Command and Data-Acquisition Station at Gilmore Creek near Fairbanks, Alaska	10
4	Command and Data-Acquisition Station: Antenna System	11
5	Command and Data-Acquisition Station: Pulse-Code-Modulation "A" and "B" Subsystem	12
6	Advanced Vidicon Camera System/High-Resolution Infrared Radiometer Subsystem	13
7	Command and Data-Acquisition Station: Command Subsystem	14
8	Ground Communications System	15
9	Functions of Nimbus Technical Control Center	16
10	Proposed Nimbus Technical Control Center	17
11	Gilmore Creek Nimbus Operational System Command and Data-Acquisition Station	18

7. NIMBUS GROUND SYSTEM

By L. Stelter, GSFC

INTRODUCTION

The Nimbus ground system consists of two command and data-acquisition (CDA) stations, one being established in Alaska and the other in eastern Canada. Each of these stations contains two major elements, the antenna system and the Nimbus unique equipments (Figure 1). The antenna system includes an 85-foot-diameter parabolic antenna, its tracking and pointing systems, telemetry receivers, command transmitters, and command antenna.

The Nimbus unique equipments are so called because they represent the ground subsystems which complement the Nimbus spacecraft subsystems. They include a clock/command subsystem, equipment required for processing PCM telemetry data received from the spacecraft, equipment for processing the TV and IR data received from the spacecraft, and computers for additional data processing.

Wideband communication circuits are required to transmit the data received at the CDA stations to the Nimbus Technical Control Center (NTCC) and the National Weather Satellite Center (NWSC) in as near real time as possible, since the meteorological data are perishable.

NTCC exercises operational control over the ground system, and is equipped with the displays shown in Figure 1 so that the operators may perform the control functions.

NWSC receives all Nimbus operational meteorological data and in turn disseminates it to forecasters and various other users of the data.

LOCATION OF CDA STATIONS

Figure 2 shows a subsatellite track of the Nimbus satellite at 500 nautical miles. The circles on the left are the 5-degree and 10-degree antenna-elevation visibility curves, or range circles, for a CDA station located at Fairbanks, Alaska. If a single CDA station were located at the North Pole, the range circles would extend in such a way that every

single orbit of the Nimbus spacecraft would be visible from that station. However, in view of the logistic problems associated with building and maintaining a station at the North Pole, it was decided instead to build one station near Fairbanks, Alaska (called Gilmore Creek), and another in eastern Canada in the vicinity of Hiland, Nova Scotia. These two stations will provide coverage for almost every orbit of a Nimbus spacecraft for a 600-nautical-mile orbit, missing only two or three orbits per week. For a 750-nautical-mile altitude, the two stations will miss less than one orbit per week. The first Nimbus (A-4) will be launched into a 500-nautical-mile orbit and, of the 14.7 orbits per 24-hour day that this spacecraft will make, the Gilmore Creek CDA station alone will see an average of 9.7. It is not likely that the Hiland CDA station will be operational by the time of the Nimbus A-4 launch; therefore, use of the 85-foot antenna now under construction at Rosman, North Carolina, is being considered to provide interim supplemental and backup coverage.

ELEMENTS OF THE NIMBUS GROUND SYSTEM

Figure 3 is a photograph of an existing CDA station at Gilmore Creek near Fairbanks, Alaska. Three thousand feet up the valley from this station, another station is being built expressly for the Nimbus operational system (NOS). Because the NOS antenna will probably not be operational by the time the first Nimbus is launched, the existing antenna shown in Figure 3 will be used for this spacecraft. However, the Nimbus unique equipment will be located up the valley in the NOS operations building. When the NOS antenna becomes operational, it will be used for Nimbus coverage, and the existing antenna will be used as a backup for Nimbus and for other satellite projects. Figure 3 shows the operations building (measuring approximately 120 by 60 feet), a power building, and the antenna itself. The station is located in a valley so that the natural terrain will shield it from manmade radio-frequency interference (RFI). The station, designed to be completely self-sustaining, has its own power-generation sources and limited facilities to house personnel in the event of snowstorms. It also is equipped with a snowplow. The NOS station 3000 feet up the valley will be similar to the one shown in Figure 3, except that it will not have a separate power building. Diesel-electric generators in the existing power building will supply power to the NOS station.

ANTENNA SYSTEM

The first major element in the CDA station is the antenna system (Figure 4). The antenna proper is an 85-foot-diameter parabola constructed of solid aluminum panels which can be individually adjusted to achieve a parabolic shape. The supporting structure is made of a special nickel-alloy steel designed to maintain its strength at extremely low temperatures; this is required because temperatures as low as 60 degrees below zero are experienced at the Gilmore Creek CDA site.

The antenna is on an X-Y mount especially designed for satellite tracking. There are no gimbal-lock positions above the horizon and excessive shaft velocities are not required. This type of mount permits maximum tracking rates of 3 degrees/sec for both X and Y axes. Hydraulic motors are used for the antenna-drive system.

A feedbox mounted at the focal point of the antenna contains the dipole feeds, hybrids required for monopulse tracking, and preamplifiers. The 136-Mc signals received by the antenna are amplified by conventional preamplifiers and fed through Styroflex cable to the tracking and telemetry receivers located in the operations building. Special parametric preamplifiers are used on the 1700-Mc signals received from the Nimbus spacecraft. Because of the high cable loss at 1700 Mc, a converter in the feed box beats the 1700-1710-Mc band to 132-142 Mc, which is transmitted through Styroflex cable to tracking and telemetry receivers in the operations building.

A 3-kw command transmitter transmits commands through an auxiliary antenna which is collimated with the large antenna.

An optical system consisting of TV cameras and 35-mm cameras is used to calibrate the antenna. Remote collimation towers are also used for calibration, tracking, and antenna-gain checks.

There are four tracking modes for the antenna:

(1) Manual positioning
(2) Automatic tracking on 136-Mc signals transmitted from Nimbus spacecraft
(3) Automatic tracking on 1700-Mc signals transmitted from Nimbus spacecraft
(4) Programmed tracking based on pointing vectors produced by the Goddard Space Flight Center Computing Center

The antenna has a gain of about 50 db at 1700 Mc with a 0.6-degree beamwidth, and a gain of about 28 db at 136 Mc with a 6-degree beamwidth.

NIMBUS UNIQUE EQUIPMENT

The first major subsystem associated with the Nimbus unique equipment is the PCM telemetry, including both subsystems "A" and "B" (Figure 5). PCM "A" data are those which can be stored in the spacecraft; PCM "B" data are those which are sampled in real time from the spacecraft on ground command. PCM "A" data are read out of the spacecraft on command at the rate of 15 kilobits/sec and received by means of 136-Mc telemetry receivers, then recorded on a tape recorder or processed in real time as read out of the spacecraft. The subsystem includes appropriate sync and decommutation equipment. The amount of PCM "A" data read out of the spacecraft can be as large as 385,000 7-bit words. Obviously, this is far beyond the capacity of a human being to analyze and comprehend. Consequently, a Control Data Corporation (CDC) 924 computer will be used to detect out-of-limit telemetered items, and to select certain key telemetry items of interest from orbit to orbit. These will be transmitted to NTCC and a portion of them to NWSC.

Separate analog displays of up to 32 channels can show data from a complete orbit for a time-correlation of events in the spacecraft.

PCM "B" data are read out of the spacecraft from the same spacecraft transmitter as PCM "A" data, but not simultaneously. They can be recorded on the tape recorder or processed directly in real time. PCM "B" data transmissions use separate demodulators, sync, and decommutation equipment and, because of the low data rate (10 bits/sec), can be printed out directly on an ordinary teletypewriter.

AVCS/HRIR SUBSYSTEM

While the PCM telemetry subsystem is mainly concerned with obtaining information on the internal operation of the spacecraft, the AVCS/HRIR subsystem (Figure 6) represents the main reason for conducting the Nimbus project; i.e., to collect meteorological data. This subsystem operates as follows:

On command from the ground, TV and IR data are transmitted from the spacecraft at 1700 Mc. It takes about 3.8 minutes to receive and record 32 sets of TV pictures on a tape recorder operating at a tape speed of 60 in/sec. It takes about 8 minutes to record all the HRIR data from one orbit on the same tape recorder. After all data are received, the tape recorder is played back at 1/8 record speed, or 7.5 in/sec. Thus, it takes about 30 minutes to play back 32 sets of TV pictures. During playback, the pictures can be gridded (latitude-longitude lines electronically superimposed) or not, as desired. The computer used for gridding will be the same CDC 924 used for reduction of the PCM telemetry data. The main reason for using the slowed-down tape-recorder playback is to effect bandwidth conservation in the wideband data links between the CDA stations and Washington, D. C. The 1/8 playback speed results in reducing the wideband link bandwidth by 1/8.

The three TV displays in the DCA stations are capable of producing pictures at the same rate as they are read out of the spacecraft. Associated with the TV displays are index computers which display the actual time a TV picture was taken, the orbit number, and other information.

Because the information bandwidth of the HRIR data is considerably smaller than that of the AVCS data, the wideband links are capable of transmitting the data at the same rate as it is transmitted from the spacecraft. Consequently, HRIR data can be transmitted to Washington, D. C. in about 8 minutes.

CLOCK/COMMAND SUBSYSTEM

The next major subsystem associated with the Nimbus unique equipment in the CDA station is the clock/command subsystem (Figure 7). This subsystem permits transmission to the spacecraft of up to 125 separate commands. The command encoder permits the pre-preparation of a paper tape which can be transmitted automatically once the spacecraft has been acquired. Provision is also made for manual transmission, so that punching the appropriate pushbuttons can transmit a command in real time while the spacecraft is within acquisition range. Facilities are also provided for transmitting four unencoded commands. The output of the command transmitter is sampled and checked to determine if the desired command was in fact transmitted.

During those intervals when PCM "A" and "B" data are not being read from the spacecraft, the same 136-Mc transmitter continually transmits the time as produced by the clock in the spacecraft. The clock/command subsystem also includes the real-time display of the spacecraft clock time.

WIDEBAND COMMUNICATIONS LINK

Another major element in the ground system is the wideband communications link. Figure 8 pertains to the Gilmore Creek, Alaska, CDA station, but exactly the same system will be used at the Hiland, Nova Scotia, CDA station.

Two 48-kc bandwidth circuits or groups will be used. The transmission medium is microwave, and the link is about 4000 miles long. The two groups will be channelized as shown in Figure 8; in Mode 1 position, Group 1 will accommodate HRIR and its timing channel. Since HRIR can be transmitted in about 8 minutes, the tape recorder in the CDA station need not be slowed down for playback. Six voice-frequency bandwidths are obtained in Group 2; these will be used for teletype, order wire, or service channels, for digital-data transmission of select items of PCM telemetry, and for transmission of AVCS timing data. In the Mode 1 position the 17-kc slot will probably not be used.

In the Mode 2 position, Group 1 is channelized to accommodate the left and right TV cameras. There is no change in the channelizing of Group 2 when switching from Mode 1 to Mode 2; the center camera is accommodated in Group 2, and the six voice-frequency bandwidths are used as described above. As stated previously, it takes about 30 minutes to transmit 32 sets of pictures through these links.

NIMBUS TECHNICAL CONTROL CENTER

NTCC, located in Building 3 at the Goddard Space Flight Center, will be the control point for the entire Nimbus ground system. Figure 9 shows some of the functions of this center.

To aid the operators in carrying out these functions, a number of displays will be provided (Figure 10). These include:

(1) Subsatellite track showing picture swaths and CDA station range or visibility circles

(2) Subsystem status both in the spacecraft and at the ground stations

(3) Key spacecraft telemetry items

(4) Meteorological data, including AVCS pictures, HRIR and weather maps

CURRENT STATUS OF NIMBUS GROUND SYSTEM

Figure 11 shows the Nimbus operation system (NOS) at the Gilmore Creek CDA. The apparent discrepancy in the operational dates for the NOS antenna and the Nimbus unique equipment is explained by the fact that the existing antenna at Gilmore Creek will be used until the NOS antenna is operational. Completion dates for the Nova Scotia CDA station are indefinite at this time, because the formal government-to-government agreements between the United States and Canada have not yet been signed. Formal agreement is expected soon. Because of the efforts of the Department of Transport of the Canadian government, surveys, test borings, and preliminary clearing at the site are now in progress. It is expected that the Hiland station will be operational in mid-1964.

COST AND PERSONNEL

A single CDA station represents an installed cost of about $8 million. This includes site improvements, buildings, the antenna system, and Nimbus unique equipment. Operation costs are expected to be $1.5 to $2 million per year, the largest single item being personnel costs. It is estimated that more than 100 employees will be required at each station.

The annual recurring or lease costs for the two 48-kc microwave circuits from Alaska and Hiland to Washington, D. C., are about $1 million per year.

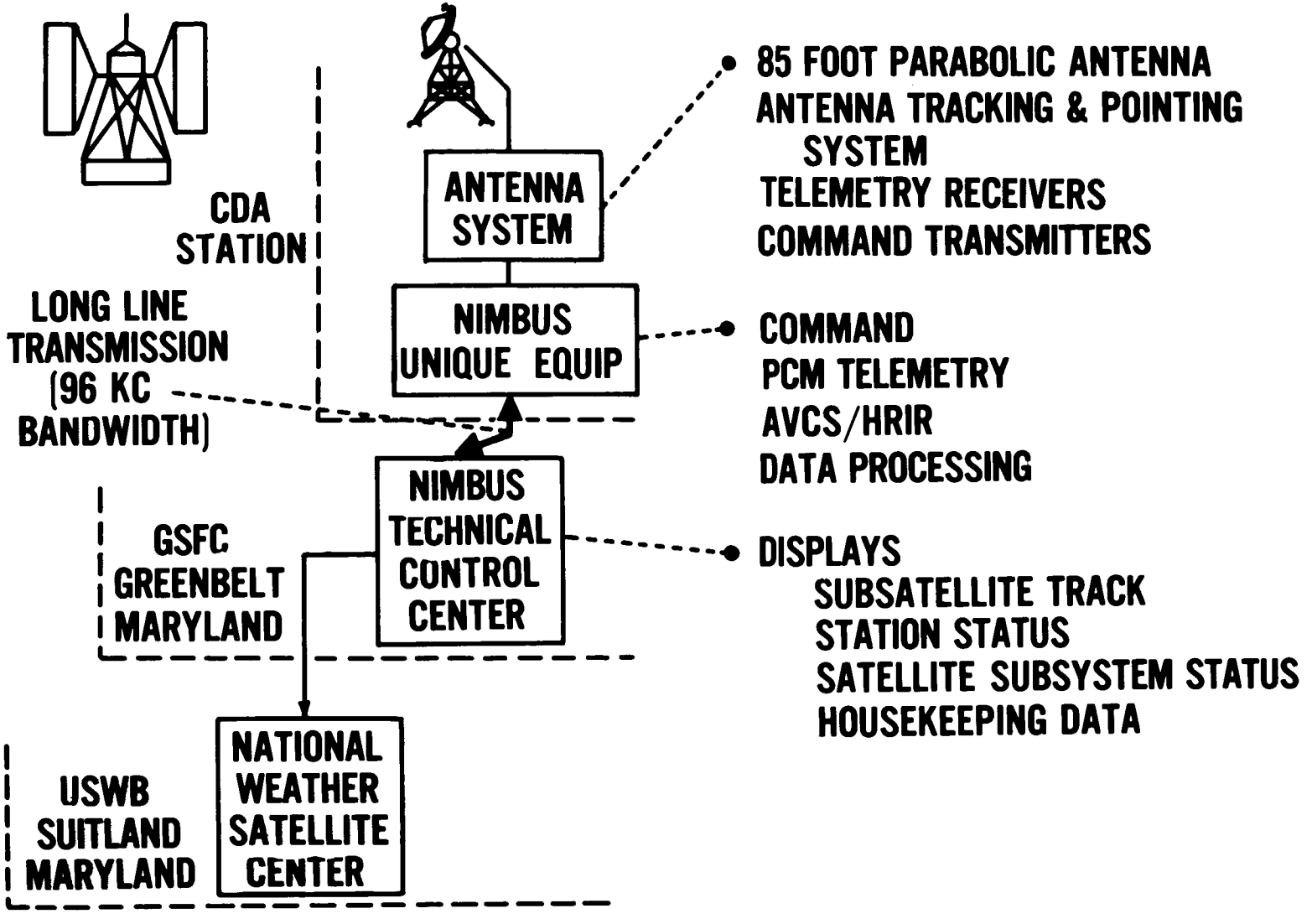

Figure 1 – Nimbus Ground System

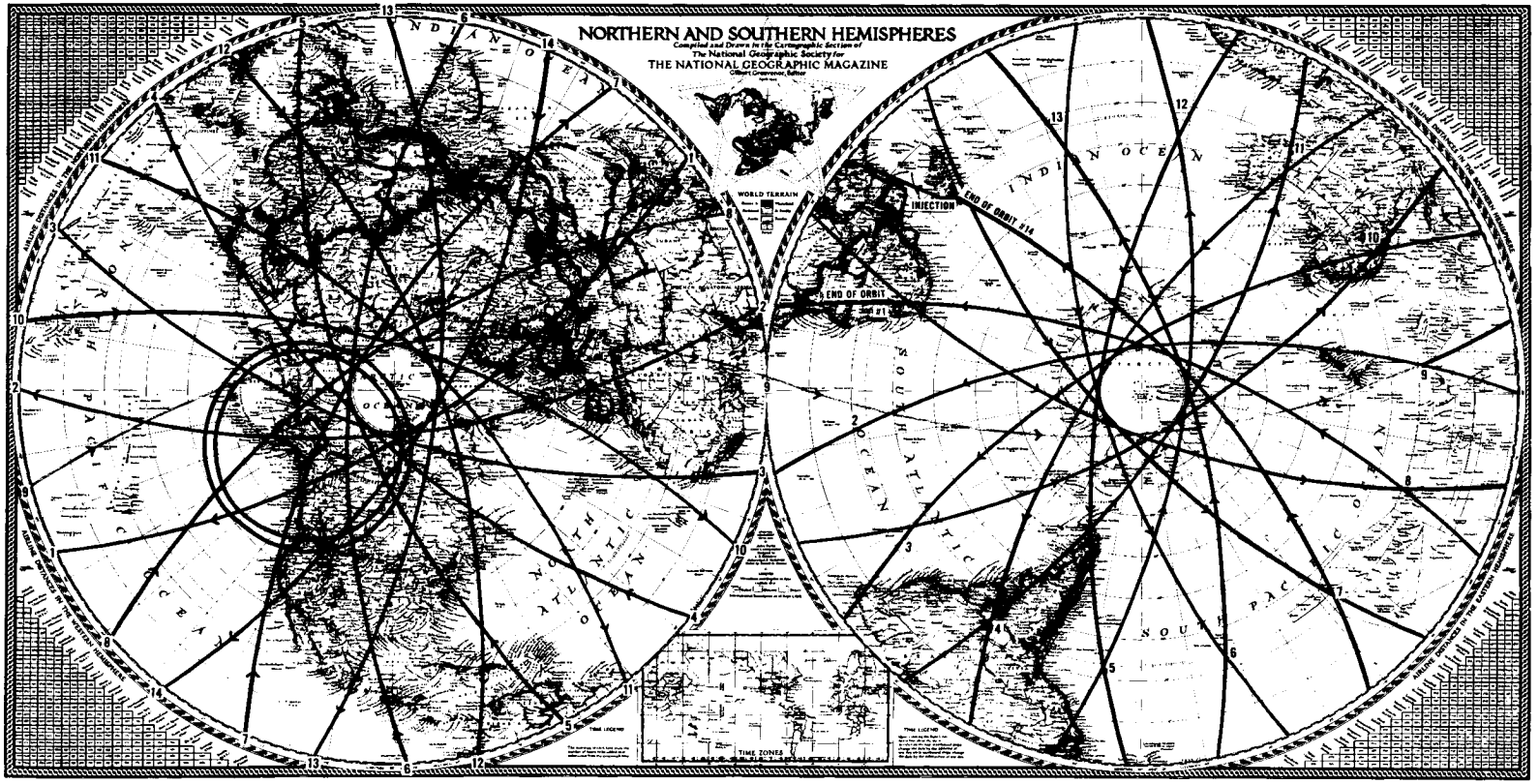

Figure 2 - Orbital Coverage from Fairbanks, Alaska

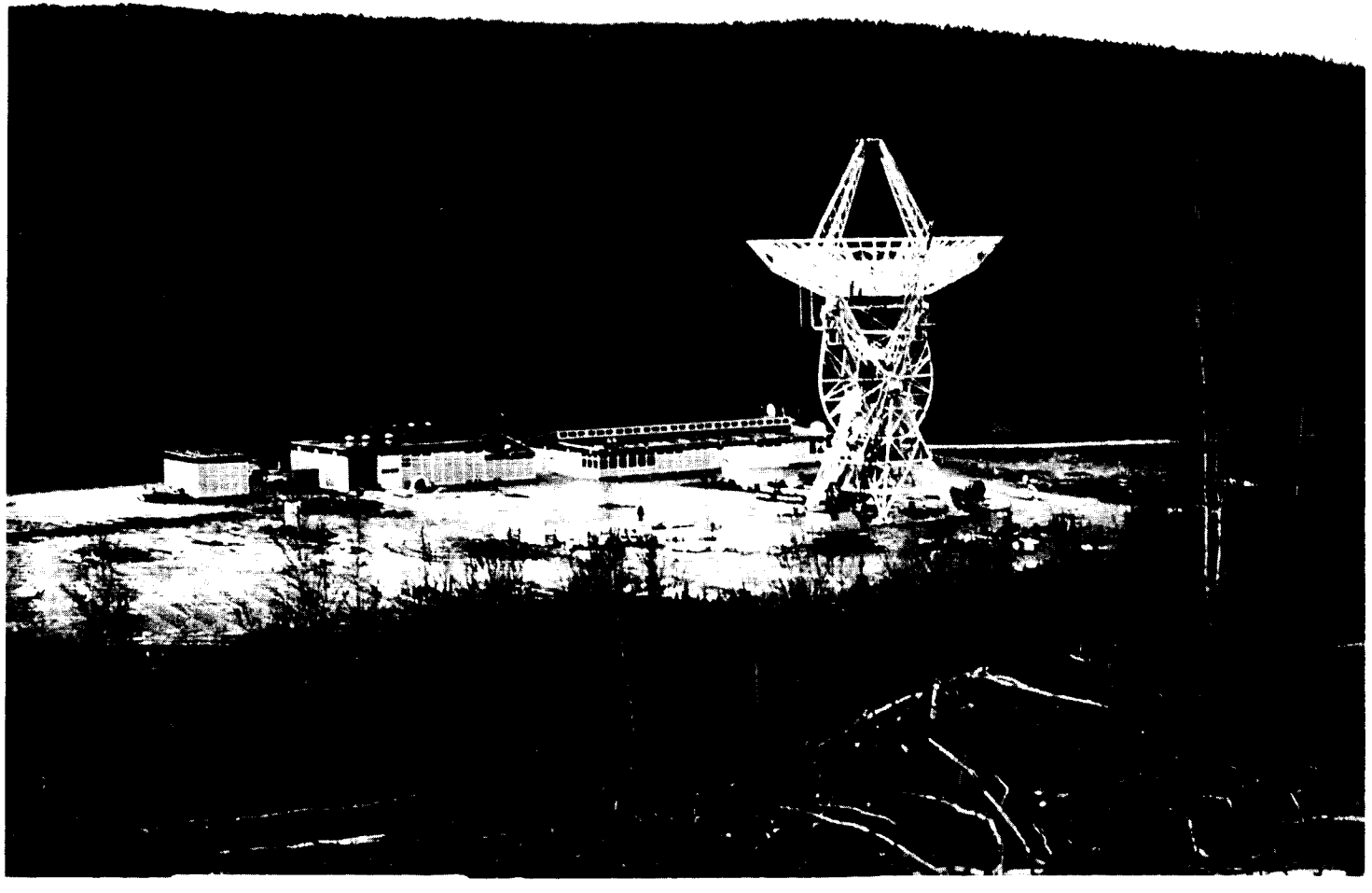

Figure 3 – Command and Data-Acquisition Station at Gilmore Creek near Fairbanks, Alaska

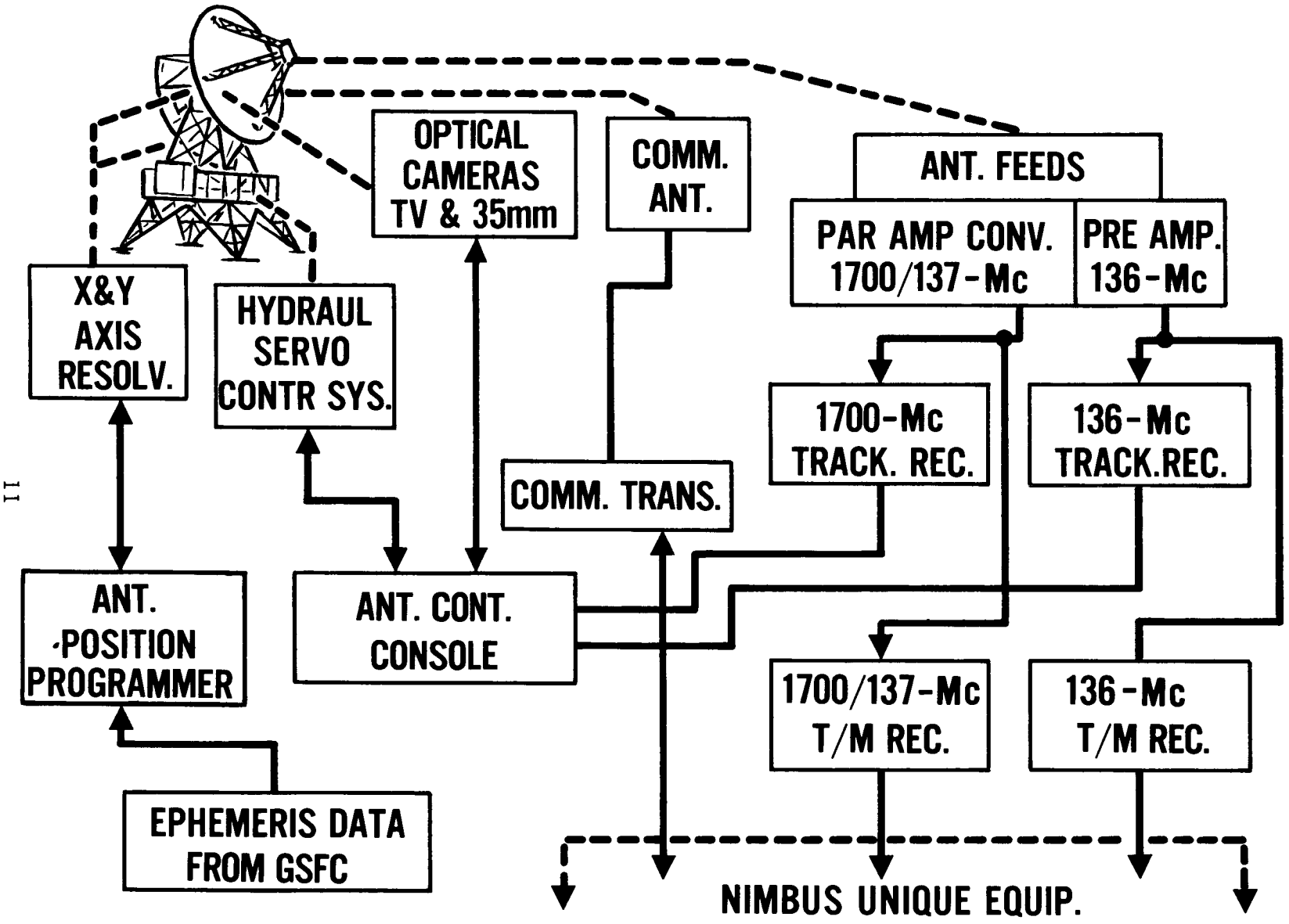

Figure 4 - Command and Data-Acquisition Station: Antenna System

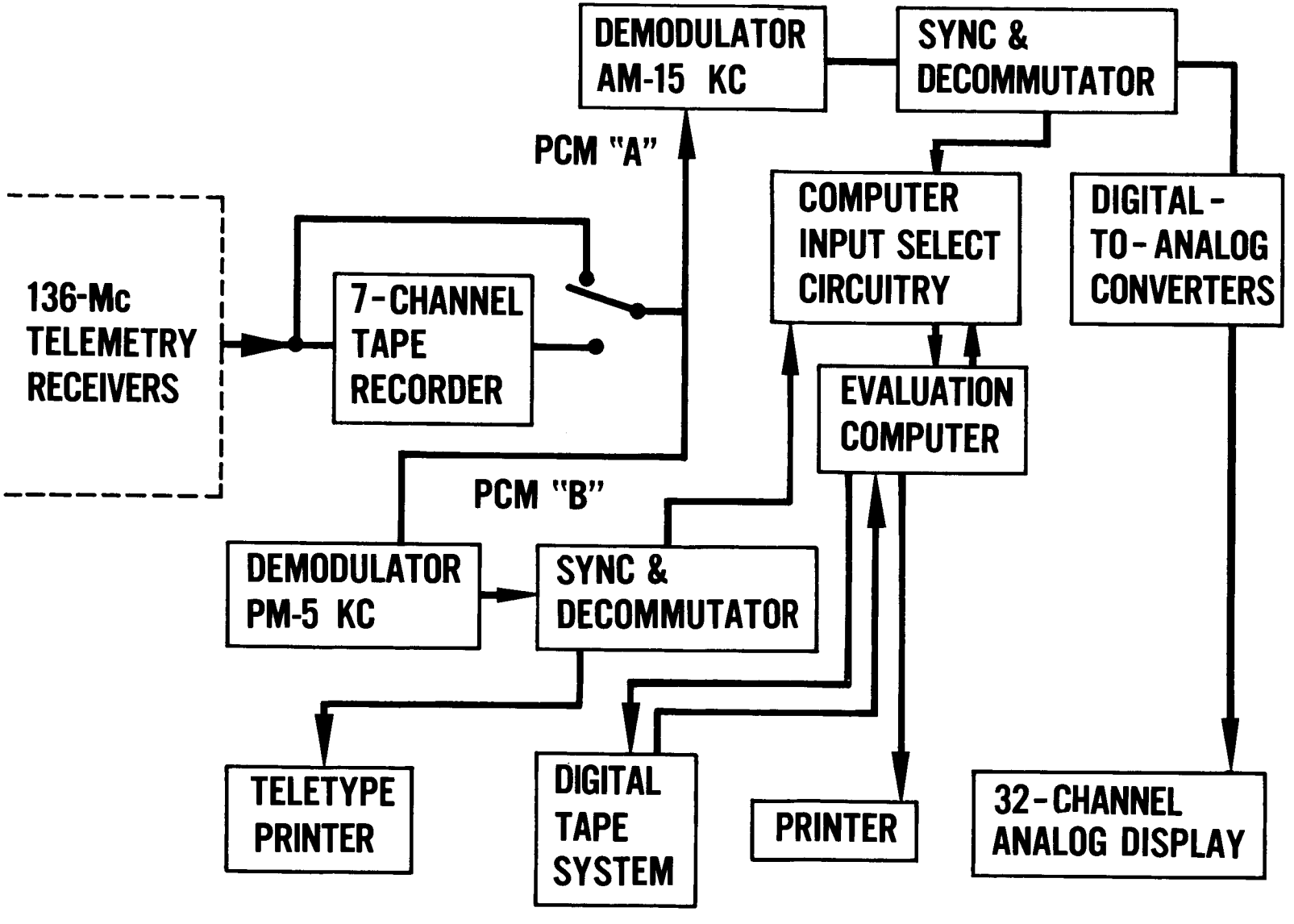

Figure 5 - Command and Data-Acquisition Station: Pulse-Code-Modulation "A" and "B" Subsystem

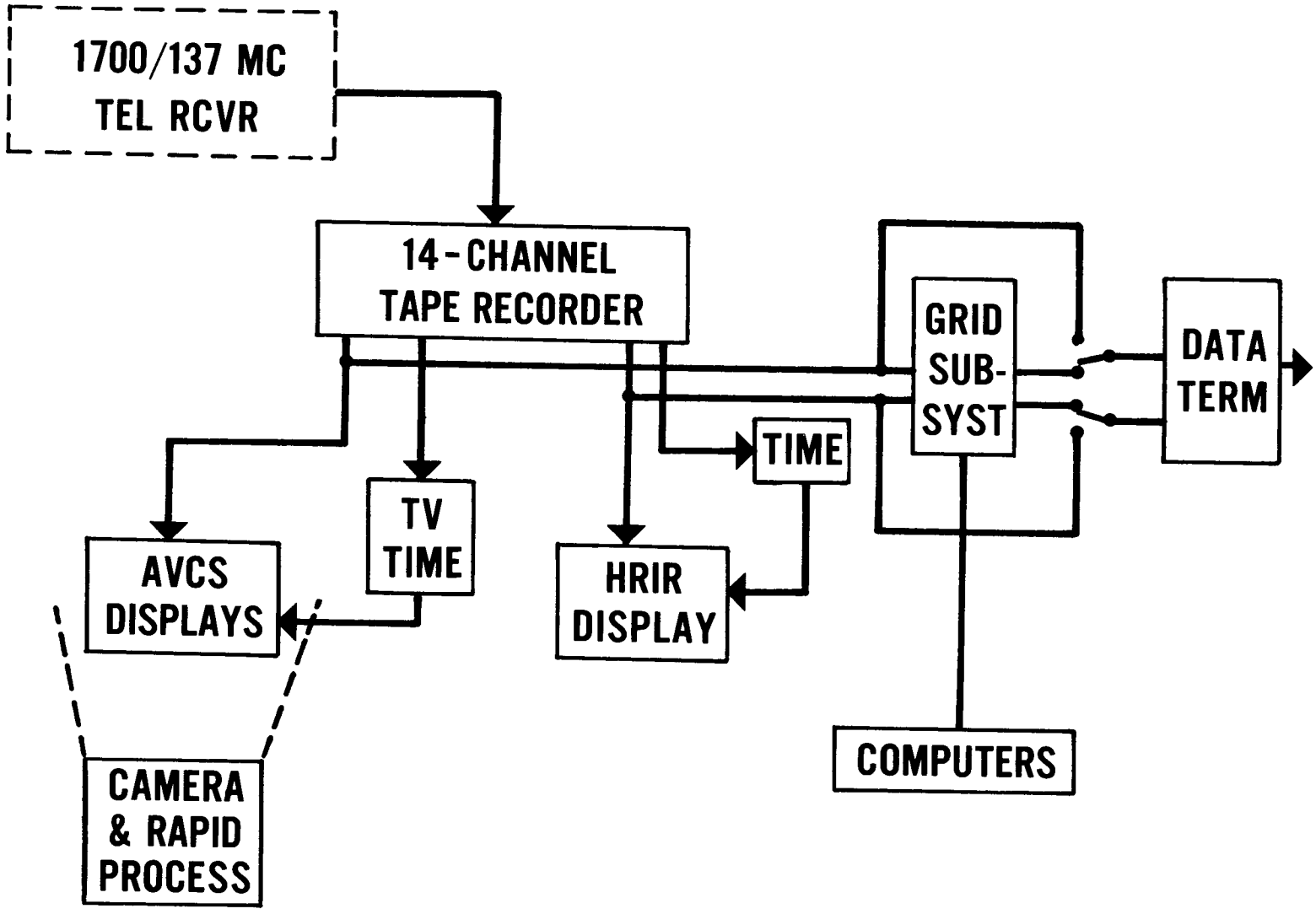

Figure 6 - Advanced Vidicon Camera System/High-Resolution Infrared Radiometer Subsystem

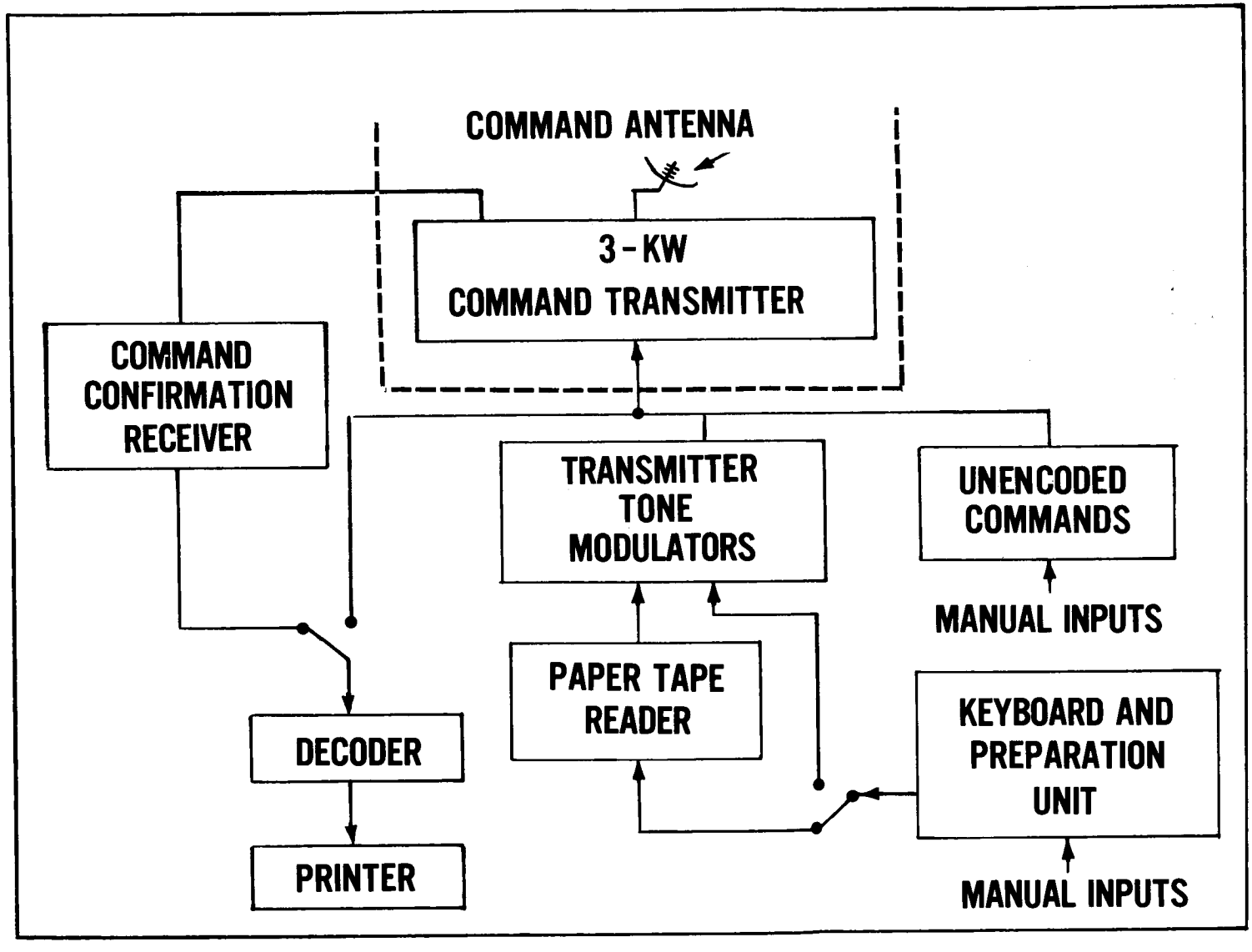

Figure 7 - Command and Data-Acquisition Station: Command Subsystem

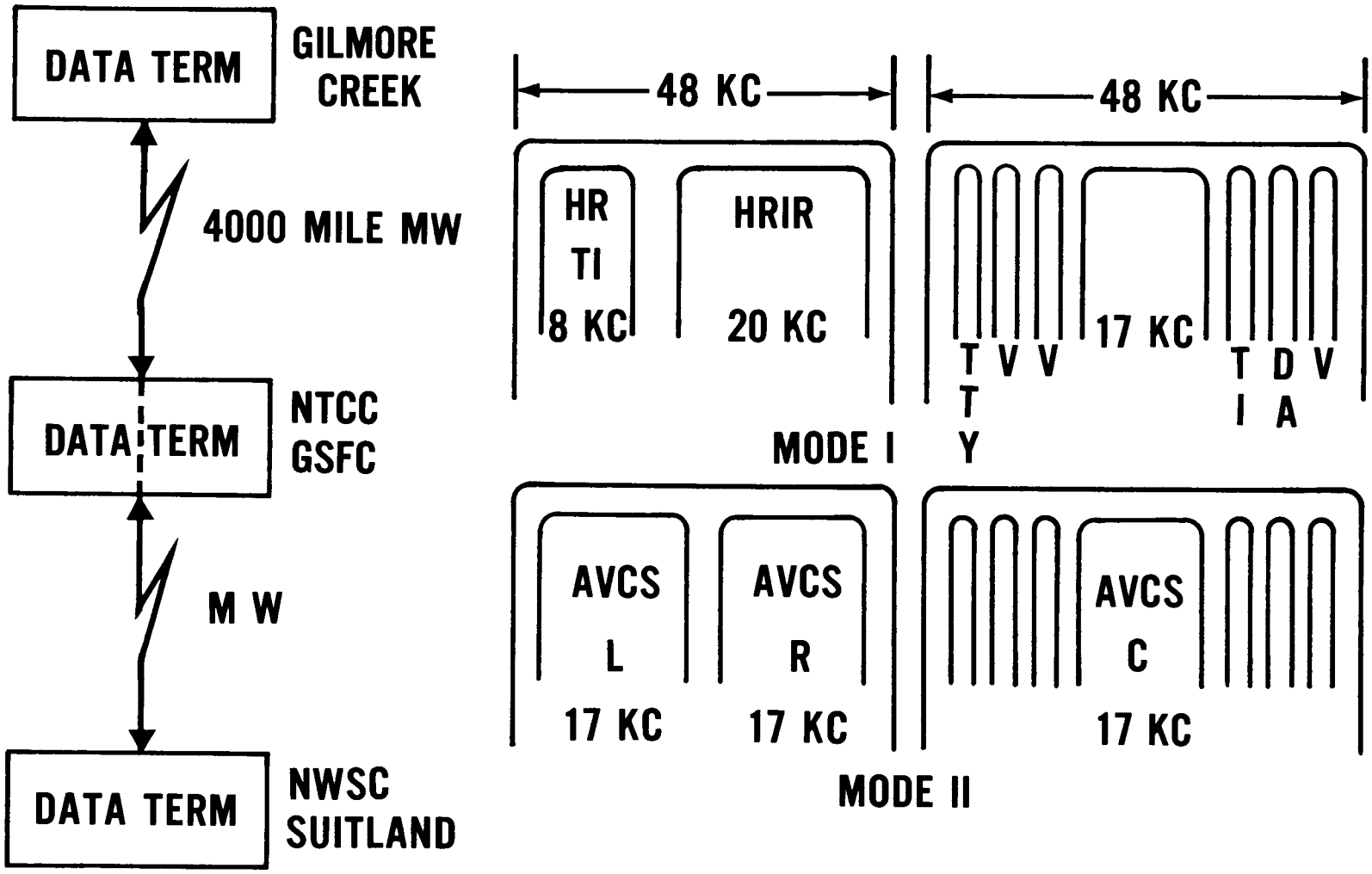

Figure 8 – Ground Communications System

- PREPARE SPACECRAFT COMMAND PROGRAM
- PERFORM CONTINUING ANALYSIS OF KEY TELEMETRY PARAMETERS
- EVALUATE SYSTEM PERFORMANCE BY STUDY OF QUALITY OF RECEIVED DATA
- DETERMINE CORRECTIVE ACTION TO BE TAKEN IN CASE OF SPACECRAFT SUBSYSTEM MALFUNCTIONS
- SCHEDULE AND DETERMINE SEQUENCE OF TRANSMISSION THROUGH WIDEBAND GROUND COMMUNICATIONS SYSTEM
- IN CONJUNCTION WITH NWSC, DETERMINE PICTURE COVERAGE WHEN CHOICE IS REQUIRED

Figure 9 – Functions of Nimbus Technical Control Center

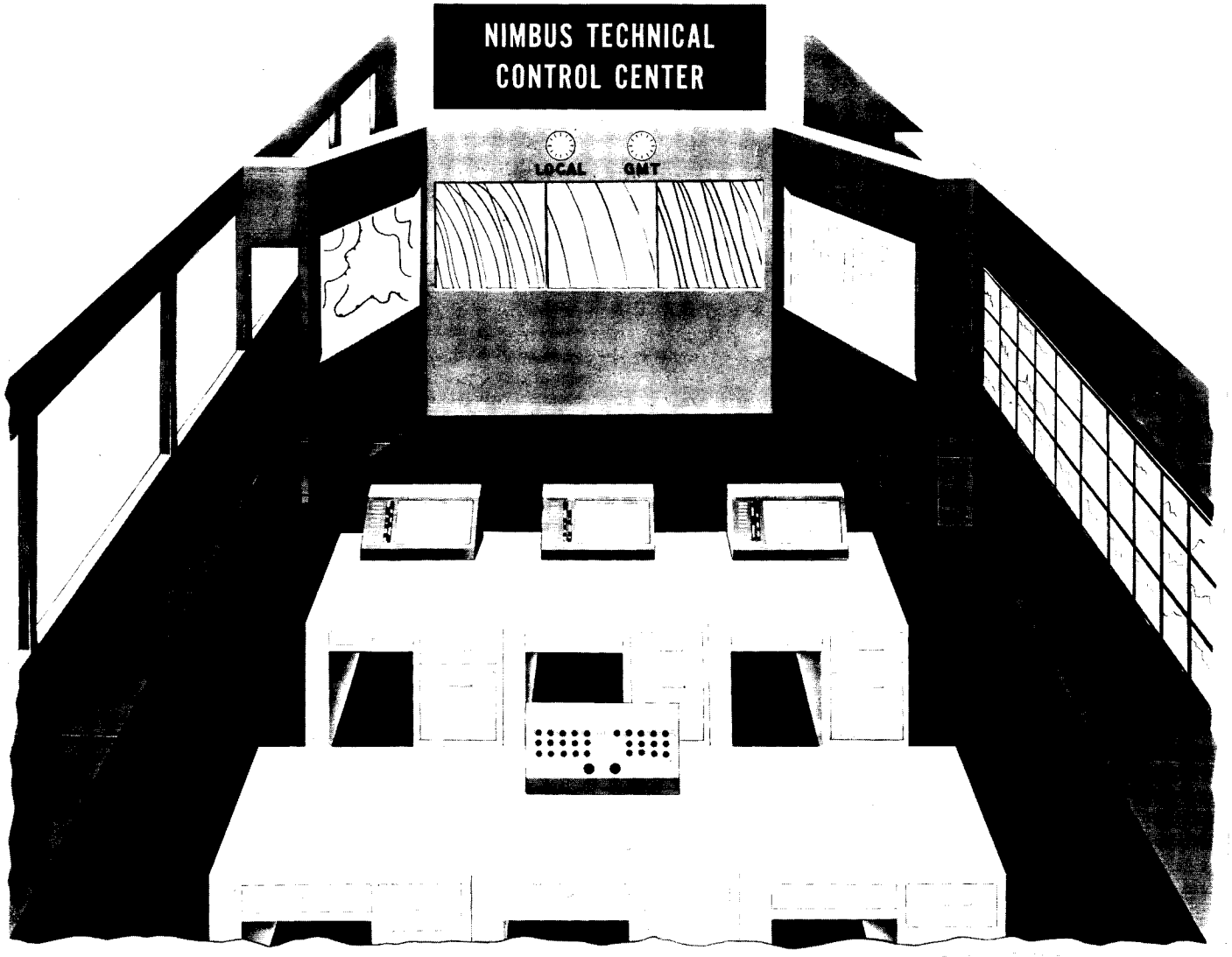

Figure 10 - Proposed Nimbus Technical Control Center

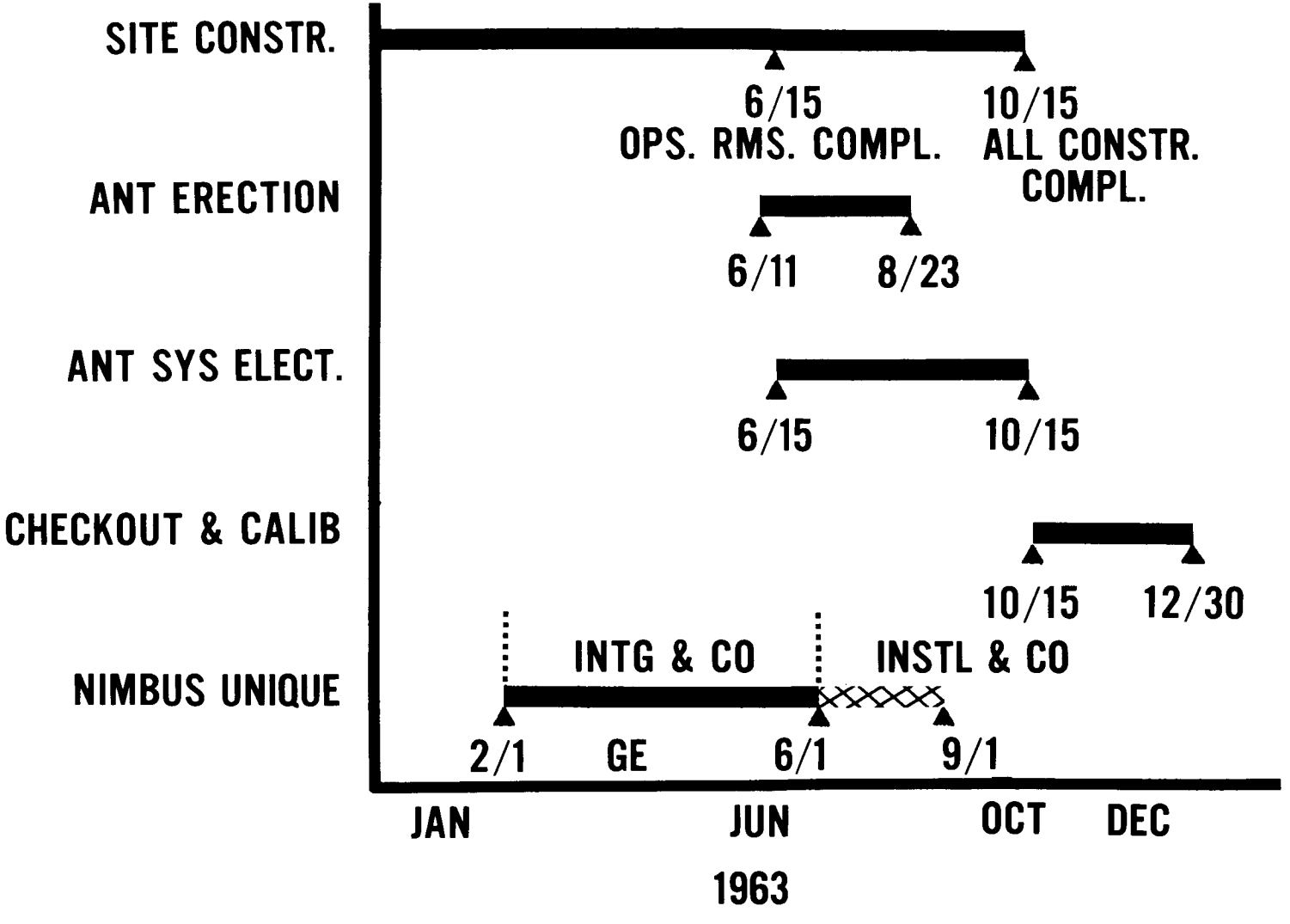

Figure 11 - Gilmore Creek Nimbus Operational System
Command and Data-Acquisition Station

8. STABILIZATION AND CONTROL SUBSYSTEM

By K. Hoepfner, GSFC; J. F. Turtil,
GE/Missiles and Space Division

8. STABILIZATION AND CONTROL SUBSYSTEM

ILLUSTRATIONS

Figure		Page
1	Nimbus Configuration	14
2	Nimbus Spacecraft Body Axes	15
3	Definition of Nimbus Orbit Axes	16
4	Nimbus Stabilization Sequence	17
5	Nimbus Control Subsystem, Block Diagram	18
6	Earth as Seen by Scanners in Stabilized Nimbus	19
7	Roll and Pitch Error Computation from Front and Rear Scanners	20
8	Nimbus Control Prototype	21
9	Model of Three-Axis Test Facility	22

8. STABILIZATION AND CONTROL SUBSYSTEM

By K. Hoepfner, GSFC; J. F. Turtil,
GE/Missiles and Space Division

GENERAL

One of the significant features of the Nimbus meteorological satellite is the provision for stabilization and control by means of an attitude-control subsystem. The purpose of this control subsystem is to keep the Nimbus satellite accurately oriented relative to the earth so that the Nimbus can effectively carry out its mission of gathering meteorological data. To maintain operational flexibility of the Nimbus satellite, the control subsystem has been conceived and developed as a separate and complete unit, constituting one of the masses of the so-called dumbbell configuration of Nimbus. Figure 1 shows the arrangement of the main components in the Nimbus configuration.

The use of control systems for stabilization and attitude control of satellites is a new art in some respects, even though the basic control techniques are well known and are being used in one form or another. The first closed-loop control for a satellite was that used on the Discoverer II in April 1959; control in this case was established for one axis only, with inertial methods serving to stabilize and control the other two axes. The Nimbus control subsystem will be one of the first using a closed-loop control in all three axes.

Test and evaluation of an attitude-control subsystem involve some interesting considerations. One reason for choosing a dumbbell configuration for the spacecraft is to permit access to the center of mass. An air bearing, supporting the center of mass, facilitates three-axis dynamic tests of the control subsystem as well as the actual Nimbus spacecraft. An appreciable amount of three-axis testing of the controls subsystem has emphasized the importance of careful instrumentation and conduct of the testing in order to obtain meaningful results. Normal operation of the control subsystem in space involves primarily the so-called fine-control function of the system, calling for very small torques. Because of these low control torques and other considerations, the three-axis simulation requires close

mechanical tolerances for the air bearing, high rigidity of all structural parts, methods of fine balance, and close control of the testing environment.

CONTROL AXES

In discussing the components of the control subsystem, as well as its operation in space, it will be useful to begin by defining the body axes of the spacecraft and the orbital axes. The body axes are a set of orthogonal axes as indicated in Figure 2. The yaw axis coincides with the longitudinal axis of the Nimbus satellite, and the pitch axis is parallel to the paddle shaft; the roll axis is at right angles to these two axes. The orbital axes are a set of right-hand orthogonal axes which hold for each point of the orbit:

- The yaw axis is the local vertical and is positive from orbital position to the center of the earth.
- The roll axis is positive in the direction of the velocity vector and lies in the orbit plane, perpendicular to the yaw axis.
- The pitch axis is the third member of the orthogonal set that includes the roll and yaw axes. The positive direction is to the right when facing along the velocity vector. These axes are indicated in Figure 3.

LAUNCH SEQUENCE

General aspects of the launch and stabilization sequence are shown in Figure 4. Stabilization of the Nimbus satellite begins when separation from the Agena second booster stage closes a switch, which places the system programmer in operation. Initially, the yaw axis will be approximately horizontal. To align the spacecraft yaw axis with the desired orbital axes, a blind pitchup maneuver is executed 2 seconds after separation. This 2-second delay is provided to allow the Nimbus to clear the Agena B vehicle. The pitchup maneuver lasts for 20 seconds; at the end of this time, pitch and roll control loops are activated. If separation is designated as t=0 seconds, then pitchup lasts from t=2 seconds to t=22 seconds. Thereafter the pitch and roll pneumatics are closed-loop-controlled in the control subsystem; during the interval t=22 seconds to t=180 seconds, pitch and roll stabilization should be

completed. The yaw pneumatics and solar-paddle drives are made closed-loop-operative at t=180 seconds. Beginning at this time, the yaw loop is operated in a control loop with the coarse sun sensor. Coarse yaw stabilization and solar array orientation should be completed by the time the Nimbus enters the umbra. When the Nimbus passes into the earth's shadow, yaw control is switched from the coarse sun sensor to the gyroscope; yaw stabilization is then maintained in the gyro mode for the remainder of the spacecraft's life.

SUBSYSTEM CONTROL LOOPS

The stabilization sequence indicates the use of the four control loops: pitch, roll, and yaw for control of system attitude, and the solar-array position loop for control of the solar paddles. These four control loops appear in simple block diagram in Figure 5. It may be observed that the pitch and roll control loops have common elements, and the block diagram therefore represents them as partially combined. As these loops are similar in their operation, they will be described together. Error-sensing for the pitch and roll loops is performed by two horizon scanners. One scans forward in the direction of the velocity vector, and one scans rearward. Each horizon scanner generates a voltage pulse as it scans across the interface of cold sky and warm earth. The scanner viewing cone and the Nimbus/earth space geometry for stabilized pitch-roll axes are shown in Figure 6.

As indicated in Figure 6, the field-of-view of the horizon scanners is approximately 3 by 10 degrees; this scanning aperture is rotated at 16.2 cps about an apex angle of 90 degrees. Scanning is accomplished by a rotating prism; energy transmitted through the prism and associated scanner optics is focused on a bolometer. The passband for the optics is 12 to 18 microns, with peak response at 14 microns, corresponding to the CO_2 absorption band of the earth's atmosphere. The scanning action generates a voltage pulse once per scan, and this pulse processed through the computer serves to establish the pitch and roll position error. Figure 7 is a diagram of the processing of scanner pulses in the computer to obtain pitch and roll errors. Pitch error is measured by the difference in pulsewidth of the front and rear scanners. Roll error is determined by measuring the position of the pulse with respect to a body-aligned reference; a magnetic pickup positioned in the scanner housing generates a reference pulse which

will in effect bisect the scan pulse when the roll-position error is zero. A pulse from either front or rear scanner is thus sufficient to establish roll error. The logic of the computer will select the pulse from the front scanner when the pitch error is less than 8 degrees, or from the rear scanner when the pitch error is greater than 8 degrees. This logic serves to optimize the roll-error accuracy for given magnitudes of error; for instance, in the case of pitch errors greater than 8 degrees, the pulse seen by the front scanner becomes quite small, disappearing completely for large pitch errors. Conversely, the pulse seen by the rear scanner will be large and can be used when the front scanner does not scan the earth.

Operation of the pitch and roll loops is similar in that portion of the loop used for processing the error signal. The error signal is passed through a lead network which generates rate information for stabilization purposes. A combination of position and rate error signal is fed to the pneumatic and flywheel control loops. For large error signals, the control torques are provided by firing the pneumatic jets; for small error signals, fine-control torques are provided by the flywheels. These flywheels, of which there are three (one each for pitch, roll, and yaw), are motors whose speed is a function of the input voltage and generated torque. Torques which accelerate the flywheel also accelerate the vehicle. In summary, the pneumatic system serves for coarse control and the flywheels for fine control; the pneumatics also serves to unload the flywheel momentum which is used for momentum removal when flywheel speeds approach saturation. The flywheel speed information and telemetry is obtained from tachometers built into the flywheel structure.

As Figure 5 indicates, the yaw loop has two modes of control: The first is the coarse sun-sensor mode, normally used only during initial stabilization. Briefly, in this mode, the yaw position error is determined by the yaw coarse sun sensor with a 360-degree field-of-view in yaw and a +70- to -40-degree field-of-view in pitch. The response-characteristic of the coarse sun sensor is such that by means of the control loop it will attempt to drive the negative roll axis to point toward the sun; this is the desired orientation for yaw. As shown in the yaw-control loop in Figure 4, the error sensed by the coarse sun is processed as an error signal through electronics, pneumatics, and flywheel similar to those used in the pitch and roll loop.

The second mode of control for the yaw loop is an integrating gyroscope used in the rate mode to sense yaw error. An error signal is generated when the gyro's input axis is rotated. The input axis of the gyro is aligned in the roll-yaw plane so that it senses the component of orbital pitch rate due to a yaw error. Although the gyro senses any roll rate, roll rates are nearly zero after initial stabilization. The actual alignment of the gyro input axis also results in a signal proportional to negative yaw rate which serves to stabilize the closed yaw loop.

The three control loops (the pitch, roll, and yaw loops) serve to control the attitude of the body axes of the satellite. The fourth control loop, also shown in Figure 4, maintains the position of the solar array perpendicular to the sun for maximum interception of solar energy. When the vehicle is in a high-noon orbit with the earth-sun axis in the orbital plane, only one axis control is necessary to drive the solar array about its axis. (In case of poor orbit conditions, ground commands yaw the vehicle for optimum solar energy collection.) Two solar-array sun sensors, similar to the yaw coarse sun sensors, generate an error signal proportional to the paddle misalignment with the sun; the amplified error signal energizes a two-phase motor, which through a gear reduction drives the solar drive shaft. The rotational rate for the solar array corresponds to the orbital pitch rate and only low shaft speeds are involved. Included in the solar-array position loop are provisions to drive the array while the satellite is in the earth's umbra. This is accomplished by means of a signal from a feedback potentiometer which is summed with the signal from the sun sensor to generate an input signal to the motor drive. In the absence of the signal from the sun sensor, the potentiometer signal will drive the array at larger than orbital rate until the potentiometer reaches the null position, the potentiometer null being the desired position for the array as it emerges from the earth's shadow. Additionally, the feedback potentiometer includes a cosine function winding to provide a signal for the camera-iris control.

COMPONENT CHARACTERISTICS

The four loops thus far discussed compose the essential control aspects of the control subsystem. Some other considerations pertinent to the control subsystem should be mentioned briefly. Among the design goals established by NASA are low weight, modular packaging,

and 6-month orbital life; these goals entail considerations of structural and thermal design, which in turn involve selection of materials and improvement of component packaging. Figure 8 affords an idea of the basic control subsystem structure and general arrangement of components.

The system housing is a hexagonal structure of 0.032-gauge magnesium sheet metal with an internal supporting Y configuration; electronic components are mounted on six panels which constitute the six faces of the structure. The electronics include the programmer, which performs the initial stabilization and command functions of the controls; the IR amplifiers, which process the IR horizon-scanner pulse; the horizon-attitude computer, which generates the pitch and roll error signals; and the attitude-control amplifiers, solar-array drive amplifiers, dc power converters, and other network and amplifier circuitry to provide the required control signals. These electronics, packaged in potted modules, use welded connections and printed board bases. Thermal control of the control subsystem is accomplished in part by passive means using thermal paints. Additionally, two of the panels have thermostatically operated adjustable shutters for active control; one of the two panels with active controls is shown in Figure 8.

Some of the various components which are part of the control subsystem are shown externally mounted or in cutaway view in Figure 8. Functions of most of these components have been described in connection with the control loops. To summarize basic characteristics of the components:

- Infrared horizon scanners

  Two identical scanners for each control subsystem are used to control the pitch and roll axes. The scanners use bolometer detectors and germanium optics to provide an instantaneous field-of-view measuring 3 by 10 degrees.

- Sun sensors

  The control subsystem incorporates two sun sensors: a coarse yaw sun sensor, and a solar-array sun sensor. The sun sensors are individual silicon p-on-n cells arranged and electrically connected to provide a linear error voltage versus angular position transfer function. The sensors operate in a null-sensing loop.

- Gyroscope

  The yaw gyro is an integrating gyro used in the rate mode. The input axis is aligned so that the gyro senses yaw error angle and negative yaw rate by sensing a component of orbital pitch rate in the absence of roll rates.

- Flywheels

  The control subsystem uses three momentum generators for fine attitude control, one for each axis. Total momentum capacity of the flywheels from zero speed to full speed is 0.4 ft-lb-seconds with a stall torque of 2 oz-in. The maximum no-load speed is 1250 rpm. Unloading of the flywheel speed is accomplished by means of pneumatic gating which will unload 0.1 ft-lb-seconds of momentum.

- Solar-array drive

  The solar-array drive positions the solar array shaft as a function of the error signal provided by the solar-array sun sensor and a feedback-potentiometer bias voltage in the light portion of the orbit, and by the feedback potentiometer in the umbra. The drive incorporates a two-phase servomotor and operates through a gear ratio of 84,000 to 1. The drive contains a springball slip clutch designed to slip above 250 oz-in of torque, protecting the drive.

- Slip rings

  A slip-ring assembly is mounted on the solar-array drive shaft to deliver power from the solar array to the spacecraft. The slip rings include four power rings capable of handling 20 amperes each, and twenty rings for electrical signals.

- Pneumatic subsystem

  A pneumatic subsystem provides the primary control torques for coarse stabilization and for unloading the flywheels as they approach saturation speeds. Approximately 6 pounds of nitrogen at 2500 psig is stored in a spherical titanium tank

located directly under the control subsystem housing. The gas is delivered to the solenoids and nozzles for each axis through a pressure regulator which provides a reduction to 35 psig.

- Electronics

  The electronic components mentioned previously in connection with the thermal control of the subsystem include a programmer, IR amplifiers, a horizon-attitude computer, and circuitry for processing control signals.

TELEMETRY AND COMMAND CHANNELS

Two additional functional aspects of the control subsystem pertain to telemetry outputs and to provisions for implementing ground commands which are received by the Nimbus spacecraft and then passed on to the control subsystem. Telemetry data is provided for 50 measured variables, plus two video signals of the control subsystem; these output variables require conversion circuitry in order to be compatible with the telemetry equipment in the sensory ring. Parameters monitored in the subsystem are listed in Table 1.

(The purpose of the telemetry data is to permit assessment of control subsystem performance. Most of the measured quantities listed in Table 1 pertain to temperatures of the various parts of the subsystem, and the others refer to parameters of the vital components of the control loop: the pneumatics, the gyroscope, the flywheels, the scanners, etc.)

TABLE I

Panel #1 temperature	N_2 tank temperature
Panel #2 temperature	N_2 tank pressure
Panel #3 temperature	N_2 manifold pressure
Panel #4 temperature	Gyro fluid temperature
Panel #5 temperature	Coarse gyro output
Panel #6 temperature	Fine gyro output
Top surface temperature	Fine roll signal (-)
Bottom surface temperature	Fine roll signal (+)
Shutter #1 position	Coarse roll signal
Shutter #2 position	Scanner "A" temperature

TABLE I (CONT.)

T/M ground (-24v ret)
Scanner amplifier "A" output
Coarse sun sensor amp. output
Yaw valve solenoid
Yaw flywheel temperature
Yaw flywheel speed
Yaw flywheel direction
Yaw flywheel amplifier output
400-cps Ø 1 signal
400-cps Ø 2 signal
+10 vdc signal
+24.5 vdc signal
-10 vdc signal
Array drive amplifier output
Roll flywheel speed
Roll flywheel direction
Roll flywheel temperature
Roll valve solenoid
Roll flywheel amplifier output
Gyro transfer signal
Scanner "B" temperature
Scanner amplifier "B" output
Scanner amplifier "A" output
Pitch flywheel speed
Pitch flywheel direction
Pitch valve solenoid
Pitch valve amplifier output
Coarse pitch signal
Fine pitch signal (-)
Fine pitch signal (+)

The ground commands previously mentioned permit corrections in the yaw-control loop that can be accomplished by commands from the ground. They are described below:

- Yaw Fine Correction

  The yaw attitude can be corrected in 1-degree steps from -3 to +3 degrees to compensate for gyro drifts and misalignment. These commands provide a bias signal into the yaw summing amplifier. The yaw position will then be moved by the action of the flywheels to null out this bias voltage with the gyro signal

- Yaw Bias

  The control subsystem can be commanded to move large angles in yaw to compensate for orbits which differ considerably from the nominal. Yaw bias commands in 6-degree increments from -18 to +18 degrees can be provided to the control system. The bias voltage is then supplied to the yaw summing amplifier from the output of the yaw bias potentiometer, which is designed to provide a varying bias voltage

throughout the orbit in order to maximize solar-paddle energy during the light portion of the orbit. As in the case of fine yaw correction, the vehicle position is moved by the action of the flywheel to null out the bias voltage in the yaw summing amplifier.

An additional command capability permits command of the pitchup maneuver previously described under launch sequence.

PROBLEM AREAS

During the development of the Nimbus control subsystem, difficulties typical of most development programs were encountered. Two examples are cited that required special consideration.

For three-axis tests of the control subsystem, the test facility shown in Figure 9 was constructed after earlier three-axis tests revealed that undesired input signals, emanating from visually hidden IR sources, were disturbing system performance. The walls of the new test facility provide for more uniform sky representation. In the fine balance of the test vehicle, it was observed that the balance changed with time and position. To make the balance more stable, all components were anchored to the test vehicle as securely as possible and anisolastic springs were used to compensate for elastic variations.

Another area of difficulty pertained to the IR horizon scanners. The essential requirement is to receive a spectrum of the earth's radiated energy that will permit unambiguous recognition of the earth's horizon as the scanner scans from cold sky across the warm earth. The ideal waveform in this case would be a square wave pulse with steep leading and trailing edges, and with flat response during the pulse. Such a waveform can be only approximated. The original scanner spectrum covered a band of 8-12 microns. Based on data obtained from TIROS flights and other sources, it was realized that this spectrum could involve waveforms with considerable amplitude variations and poorly defined leading and trailing edges. To make the scanners less sensitive to the variable-temperature water-vapor energy bands and more sensitive to the nearly constant CO_2 energy bands, the IR horizon scanner was redesigned to cover a spectrum of 12-18 microns; tests of the redesigned scanner indicate satisfactory performance.

THREE-AXIS TESTS

Three-axis testing of the control subsystem is carried on in a test facility with equipment necessary to simulate orbital conditions. A cutaway model of the test facility is shown in Figure 9. Essential elements of the test facility are:

- A gas bearing, to support the simulated spacecraft and to provide freedom of motion of the spacecraft similar to that under orbital conditions
- An earth simulator, to provide a proper stimulus for the IR horizon scanners
- A sky simulator, to provide a cold background for earth-horizon recognition
- A solar simulator, to provide the proper stimulus for the coarse yaw sun sensor
- An orbit-motion simulation, achieved by rotating the simulated earth at orbital rates, to provide the required stimulus for gyroscopic control of the yaw axis

The walls of the test facility are shaped into a truncated cone 25 feet high with a 40-foot base diameter. The walls of this cone are cooled with refrigerated water at 45° to 50°F which, during test, flows continuously down the outside of the walls. This arrangement simulates the cold sky. In the center of the conical test facility is the air bearing support. A 10-inch ball is anchored securely to the test vehicle, the center of the ball being located at the center of mass of the test vehicle. When the vehicle is in position for three-axis test, the 10-inch ball rests in a cup provided with vents through which gas can be expelled. Gas expansion creates an upward thrust capable of balancing the weight of the test vehicle, floating the vehicle on a frictionless cushion of air; when the vehicle is floated, it rests on a 0.001-inch film of air at 95 psig. By means of this air bearing, freedom of motion of 360 degrees in pitch and +40 degrees in roll can be achieved. The earth simulator is a 13-foot-diameter cylinder, closed at one end and similar in shape to a tunafish can. During the test, the "earth" is maintained at 120°F by means of electrical surface

heaters mounted on the "earth." This "earth" is placed in appropriate position relative to the floated vehicle to permit simulation of the desired Nimbus/earth space relationship. The geometrical relationship between the earth simulator, air bearing, and test-vehicle horizon scanners generates correct scan pulses as the scans cross the earth-sky interface for proper system testing. The earth simulator is hung from the ceiling of the test facility and has provisions for being driven at orbital rate. This arrangement provides the proper simulation for gyro control of the yaw axis. To null out the effect of the real earth's rotation, earth-rate compensation is incorporated in the instrumentation during system testing.

The prototype control subsystem has been fabricated, using "certified" components (the term "certified" signifies that the components have passed environmental tests in excess of those expected during launch and orbit, and that they function properly). Three-axis test of prototype subsystem is being initiated. Performance of the control subsystem is evaluated on the basis of design goals established by NASA at the outset of the program, such as:

- The control subsystem shall be capable of maintaining the alignment of the body axes within ± 1 degree of the orbit axes. (This requirement will provide information on the direction in which the satellite cameras and other instruments are pointed, so that resulting data can be related to earth coordinates.)

- The instantaneous angular rate of satellite-body axes relative to the orbit axes shall be limited to less than 0.05 degree/sec. (This requirement is consistent with the parameters of the video camera system.)

- After passing the launch environment, the lifetime of the control subsystem shall exceed 6 months in orbit without degradation.

Three-axis tests have thus far been performed on the preprototype system; the preprototype is functionally identical to the prototype system but consists of "breadboard" packaged components. Because of this packaging, the preprototype does not permit as fine a balance as desired on the air bearing, which limits the nature and duration of test runs. More satisfactory three-axis tests probably will be obtained

with the prototype subsystem. Despite the limitations of the pre-prototype control subsystem, a number of successful three-axis tests were completed for limited periods of time. In general, it can be concluded from these tests that the control subsystem can maintain stable control, and that the design goals previously cited will be approximated.

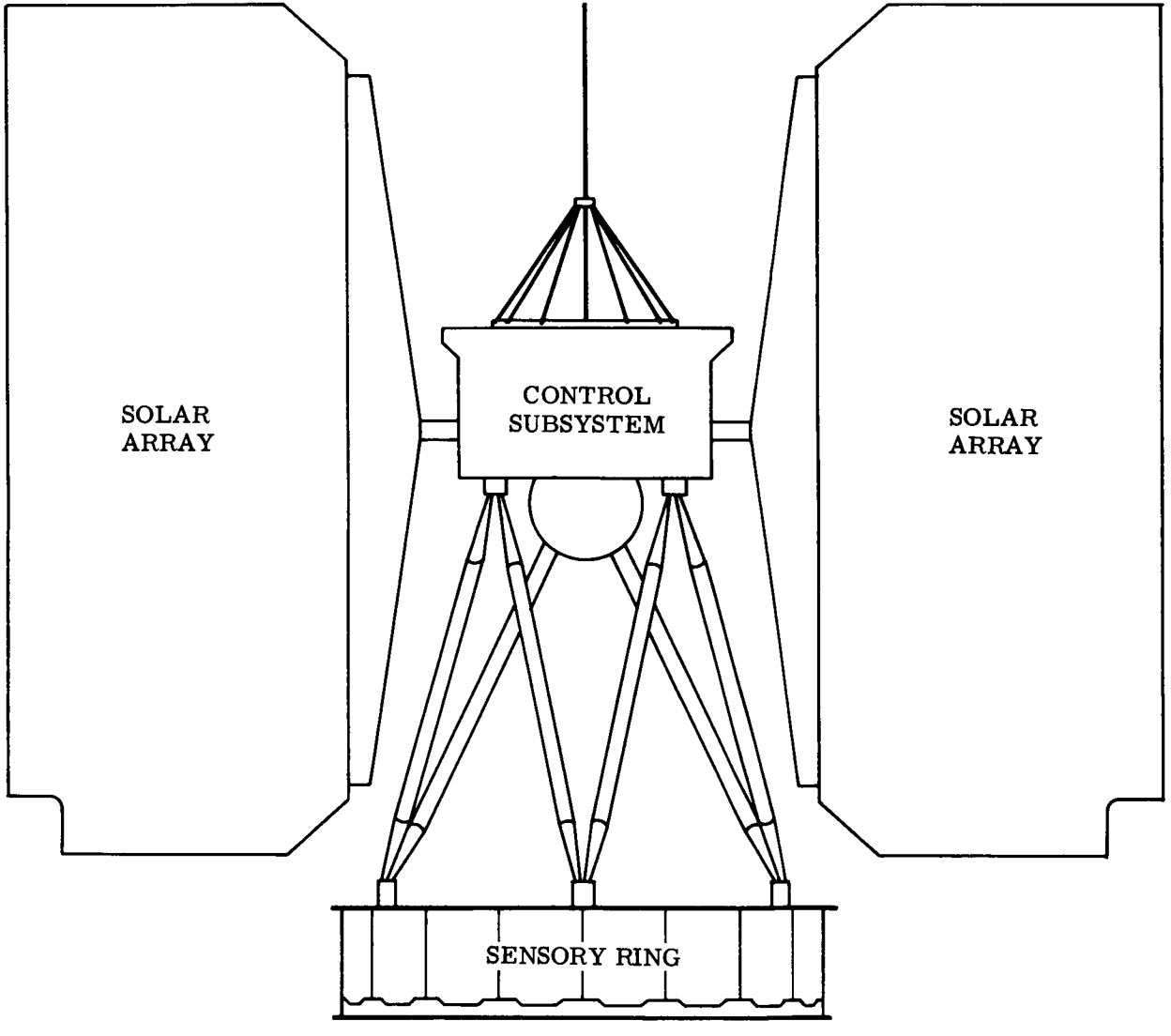

Figure 1 – Nimbus Configuration

9. STRUCTURAL CONCEPTS IN NIMBUS SPACECRAFT DESIGN

By A. F. White, Jr. and M. B. Weinreb, GSFC

9. STRUCTURAL CONCEPTS IN NIMBUS SPACECRAFT DESIGN

ILLUSTRATIONS

Figure		Page
1	Nimbus Breakaway.	6
2	Empty Prototype Sensory Ring	7
3	Nimbus Modules	8
4	Nimbus Modules	9

9. STRUCTURAL CONCEPTS IN NIMBUS SPACECRAFT DESIGN

By A. F. White, Jr. and M. B. Weinreb, GSFC

INTRODUCTION

A first glance at the structural design of the Nimbus spacecraft may raise the following questions: "What are the concepts behind the design?" and "How were these concepts translated into a mechanical configuration?"

As the answers to these questions may not be immediately apparent, this report discusses the concepts and design objectives of the Nimbus program as initiated in 1959.

CONCEPT AND OBJECTIVES

System flexibility — the planning of various missions over an extended period of time — was the prime concept in the mechanical design of the Nimbus spacecraft. Therefore, the objective was to make each system as independent as possible in the mechanical design, and to have the design itself contribute to the desired thermal and electrical independence.

Thus, the design, depicted in Figure 1, treats the spacecraft as three major elements: controls, solar array, and sensory section. Each element is mechanically and thermally independent, with the exception of structural interfaces. The design had to be sufficiently flexible to permit many tradeoffs, in order to obtain optimum conditions for the entire spacecraft system.

For such a complex system, the concept and objectives of the design are by no means pessimistic. The mechanical configuration which has evolved demonstrates the attainment of many of the objectives.

In the control system and solar array and in their interfaces to the sensory section, for example, the following elements were desired:

(1) Mechanical and thermal independent structures

(2) A long torque arm for controls relative to a low center of gravity

(3) A solar array of extremely lightweight construction

(4) An array which would provide the necessary power, and yet could be contained within the vehicle shroud during launch (to take full advantage of the high-noon retrograde orbit, the array was designed for a 1-degree of freedom movement)

(5) An interface rigid between the controls and sensory section, enabling the spacecraft to be tested on a gas bearing in a thermal-vacuum chamber

The control system is considered primarily as an independent structure, attached to the sensory section through truss members. A bearing-supported shaft extends through, and protrudes from, the control housing; this shaft incorporates slip rings and an interface design for attachment of the solar paddles. It is driven by a motor-gear reducer drive assembly in the control housing.

The solar power system consists of batteries located in the sensory section, charged by solar cells on the paddles which are attached to the control-solar driveshaft. The paddles, approximately 8 by 3 feet, are designed with a triangular transition section, incorporating the shaft interface which attaches to the solar array by hinge mechanisms. The paddles, folded on the hinge line in order to fall within the shroud envelope in the launch configuration, are fastened together and to the sensory structure by a paddle-lock mechanism; after separation, the paddles unlock and are driven open by means of a mechanical drive system on the transition section.

The controls and sensory section are joined through a 48-inch-high truss network. The truss, traded off with solar-paddle configuration, structure weights, etc., provides a nearly equal moment-of-inertia distribution for the entire system. The primary design consideration in the truss is rigidity rather than structural strength; accurate alignment must be maintained between controls and sensors in the sensory section, and the dynamic envelope of the spacecraft relative to the vehicle shroud must not be exceeded during the vibration and steady static loads of the launch phase. Each interface accommodates a mono-ball joint which results in pure axial loads being induced in the truss members. In addition, the truss interface area supports an air-bearing assembly used to test the controls.

In the sensory section, Figure 2, a modular concept allows for interchangeability of the subsystems located in the sensory section. A

design was desired that would permit the addition, elimination, or substitution of subsystems without redesign of the primary structure. To achieve this "black box" feature, the following characteristics were sought:

(1) A thermally homogeneous and well-damped system, in which mechanical tolerances are closely held, and in which temperatures of the subsystems can be accurately controlled

(2) A high ratio of component-packing density to structure weight, allowing the standardization of sizes on many subsystems and the accommodation of odd configurations when practical

(3) Ease in arranging modules to obtain optimum center-of-gravity location and thermal balance

(4) Simple fastening methods, retaining the ability to incorporate thermal isolation or vibration isolation when necessary

(5) An interface design which would ensure reliable, clean separation

(6) A connector-to-connector principle for electronic integration

The sensory section is a toroid with a 57-inch outside diameter, 40-inch inside diameter, and 13-inch depth. The assembly is composed of four machined rings and 18 machined V-shaped ring separators.

The lower outside-diameter ring forms one side of a large V-band clamp separation joint. The spacecraft is clamped to a 24-inch-long truncated adapter section which, in turn, fastens to the forward end of the Agena B. The adapter contains flight checkout equipment and matched separation springs. Upon release of the separation clamp, the separation springs impart the desired separation velocity to the spacecraft.

The assembled structure forms 18 module cavities measuring 8 by 6 by 13 inches. Magnesium module boxes, providing for close tolerances in the cavities, were designed to house the electronics. Excessive clearances are reduced with lightweight shims where necessary.

The design permits the structure to accommodate eight different sizes of modules which can be top- or bottom-loaded. All modules have a common 6-inch dimension (tangential to rings), but may be 2, 4, 6, or 8 inches wide (radial from center) and 6.5 or 13 inches deep. Figures 3 and 4 illustrate the modules and their arrangement.

The V-shaped separators between sets of modules in the sensory ring have tapped holes on top and bottom. The modules have mounting tabs with elongated clearance holes to accommodate screws for attaching them to the ring separators, and to permit the modules to be clamped toward the outer rings for better thermal conductivity.

The close tolerances and improved clamping procedures result in a sound mechanical structure and isothermal mass. A simplified fastening allows the modules to be isolated thermally or mechanically when necessary.

The modules have external connectors, and all electrical integration is accomplished by means of an external wiring harness using a connector-to-connector principle.

The inside volume of the toroidal section is used for mounting odd-shaped equipment which cannot feasibly be packaged in a module; the equipment is mounted on a network of lightweight crossbeam structures (see Figure 2). However, the basic toroid is designed to survive vibration and static load forces without relying on the crossbeams as necessary structural members; this feature enhances the flexible nature of the spacecraft in planning future missions. Equipment in the center may also be thermally or mechanically isolated if alignment factors are not paramount.

Because the sensory structure is designed with 18 flat sides, each face if necessary could readily accommodate a thermal-control assembly consisting of a plane of shutters, each system acting independently and primarily sensitive to those modules in each particular cavity.

In summary, the concept provides for a growth or shrinkage in any direction or parameter of any subsystem. The sensory ring, for instance, could be enlarged or decreased in diameter or height, as could the truss; it is not inconceivable that an even greater packing density and weight might be attained simply by interfacing two such entire sensory sections

by means of the separation-joint design. Thus, many system aspects can be adjusted to maintain the use of existing components or to perpetuate experience gained on earlier spacecraft, and the original concept of system flexibility has been achieved.

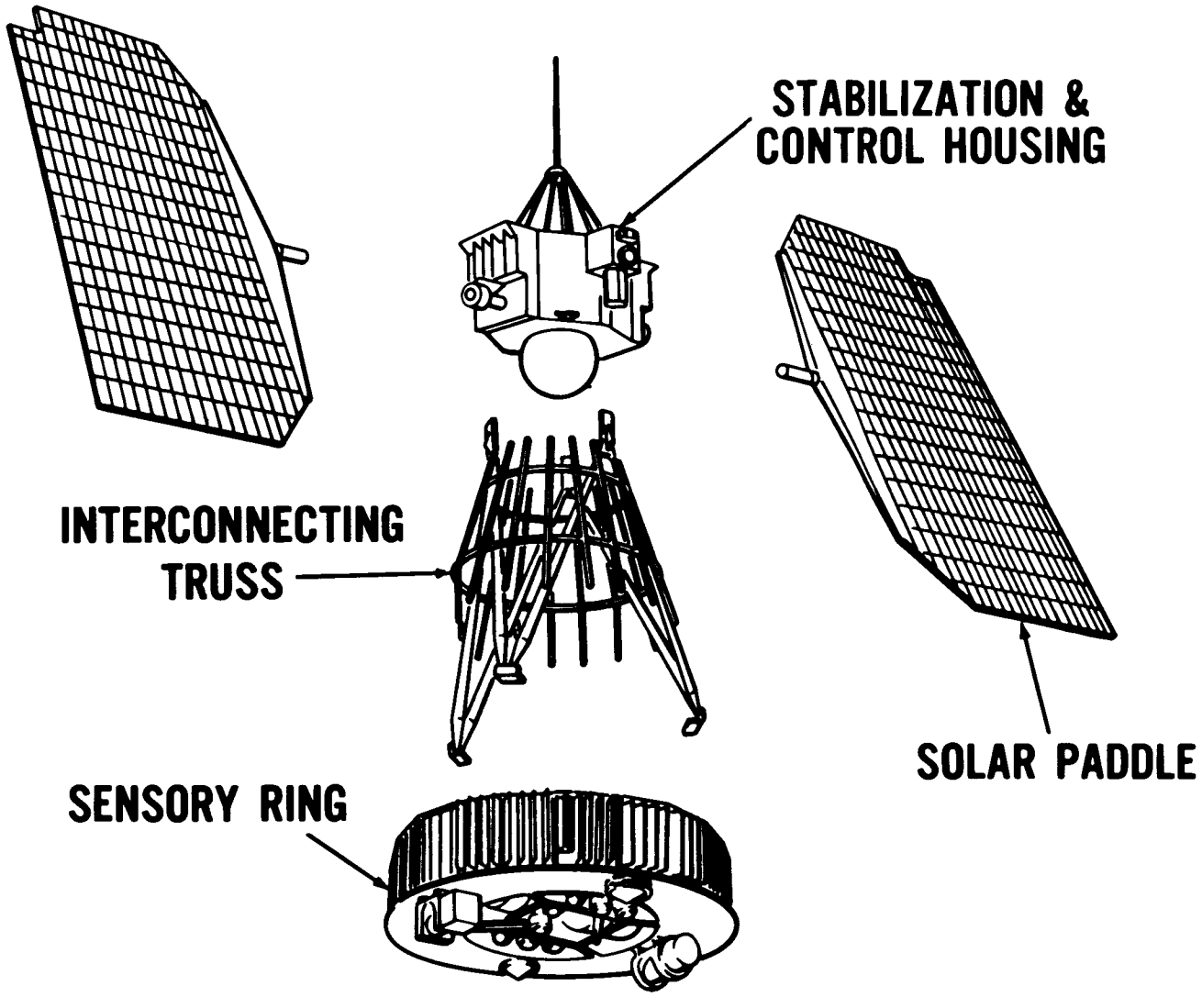

Figure 1 - Nimbus Breakaway

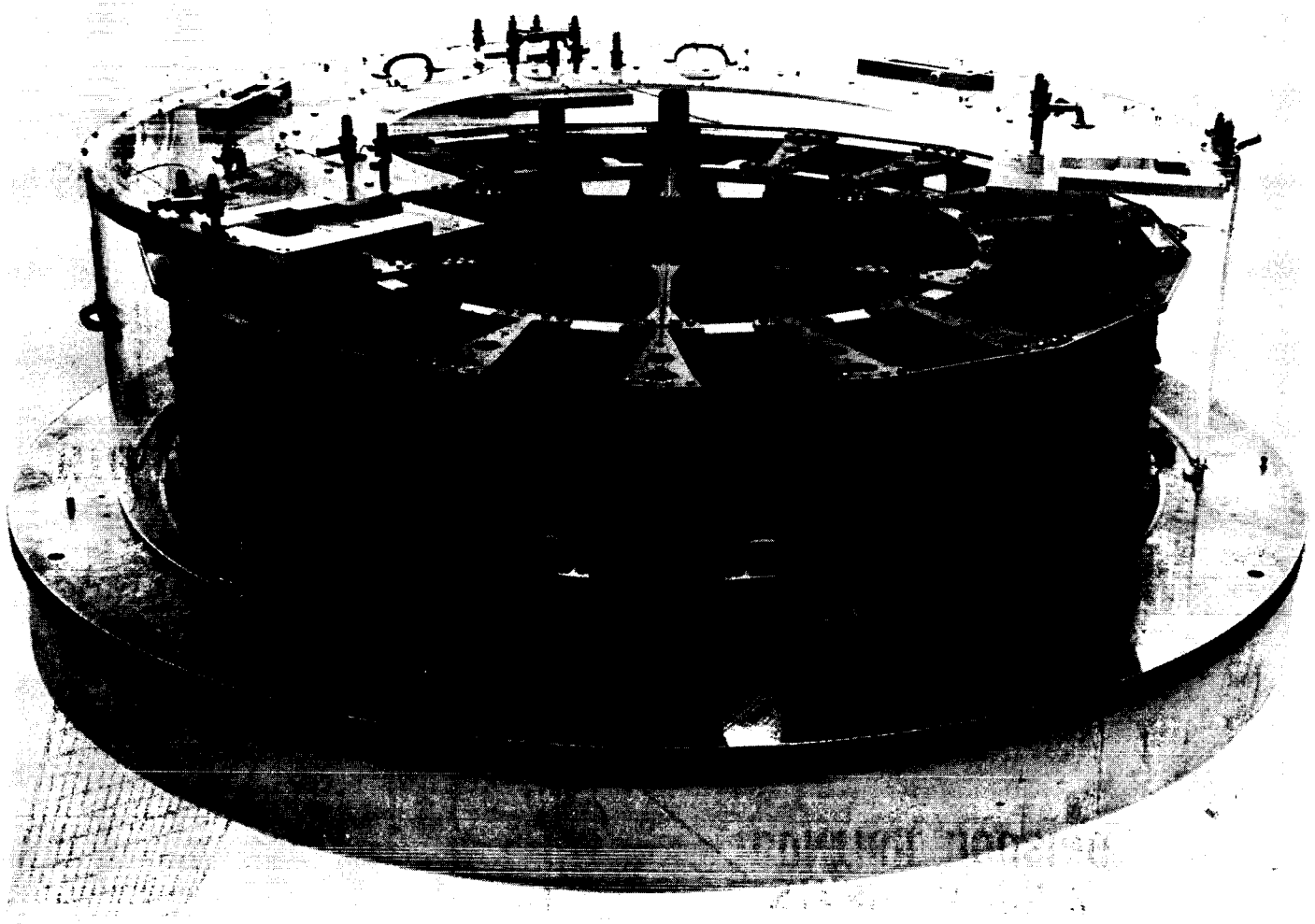

Figure 2 - Empty Prototype Sensory Ring

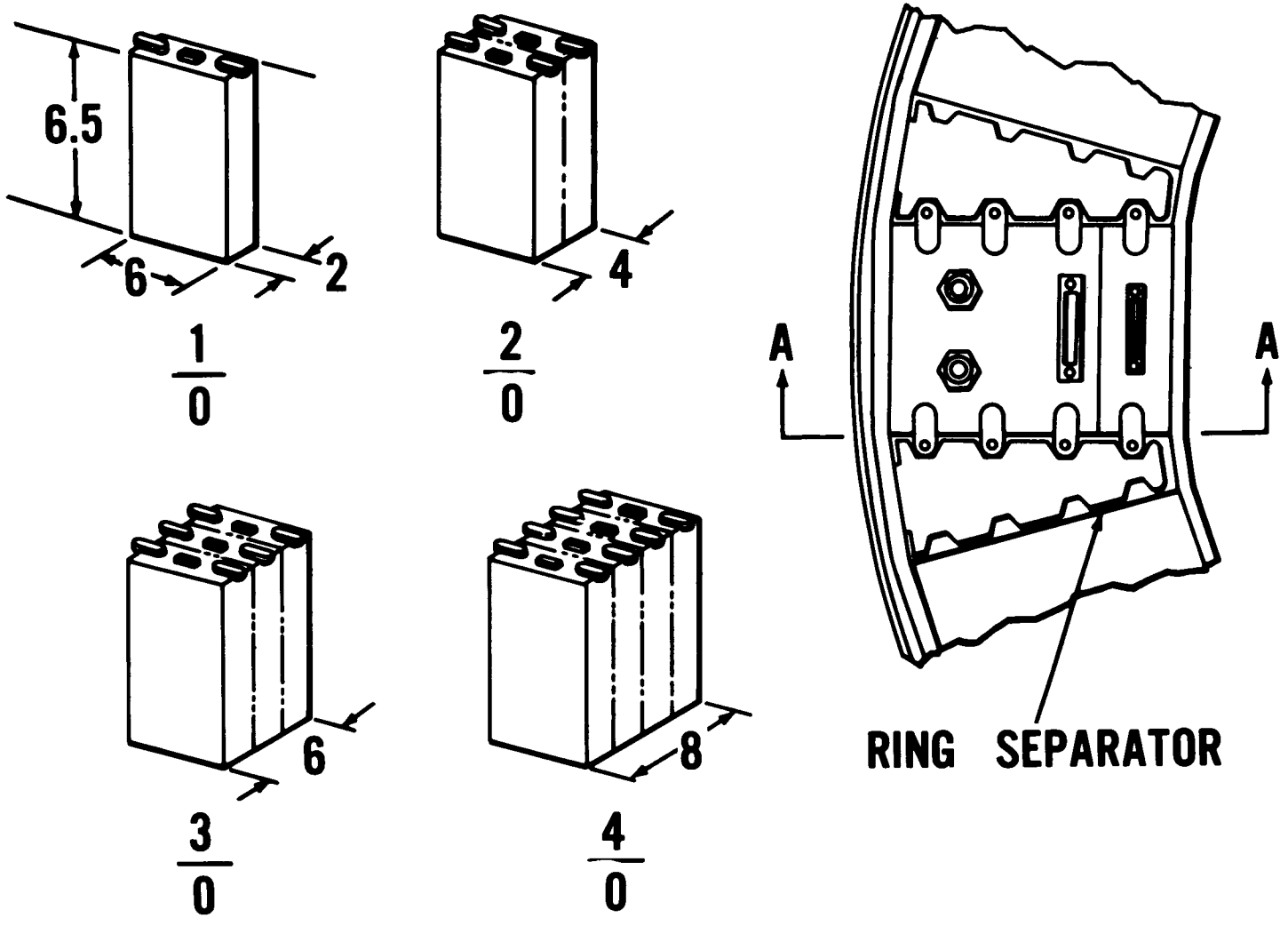

Figure 3 - Nimbus Modules

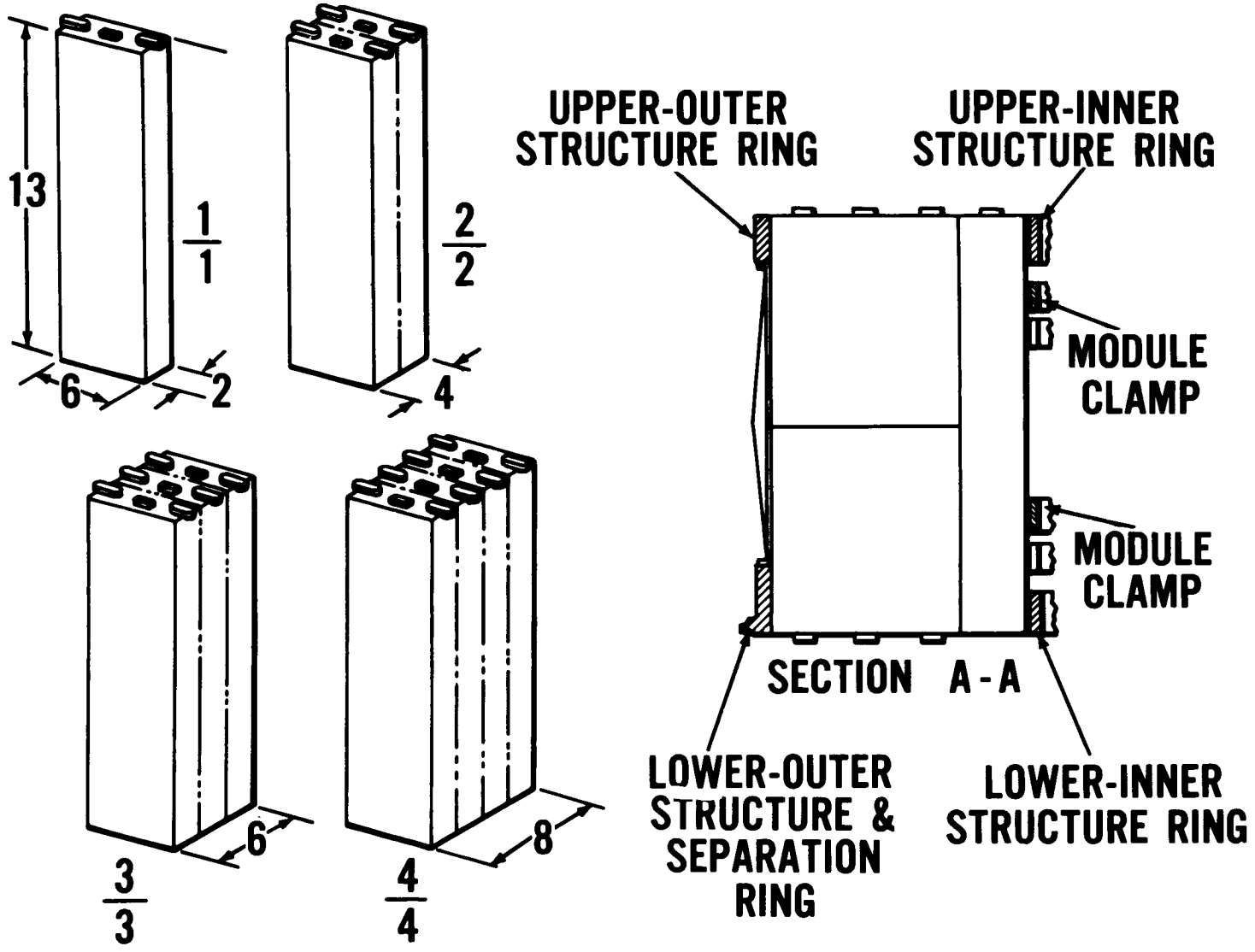

Figure 4 - Nimbus Modules

10. DEVELOPMENT OF THE NIMBUS STRUCTURE

By E. O. Stengard, GSFC

10. DEVELOPMENT OF THE NIMBUS STRUCTURE

ILLUSTRATIONS

Figure		Page
1	Nimbus Spacecraft	8
2	Solar Platform Support	9
3	Solar Platform Hub-to-Control Shaft Joint	10
4	Solar Platform Stiffening	11
5	Solar Platform Support Dashpots	12
6	Separator Casting Failure	13

10. DEVELOPMENT OF THE NIMBUS STRUCTURE

By E. O. Stengard, GSFC

The initial concept of the Nimbus structural design was given in a previous report. This paper describes the differences between the initial concept and the present Nimbus structural design, as well as major problems arising during its development.

The solar paddles are the same size as originally specified; however, a small rectangular cutout had to be made on each paddle to accommodate the method of supporting the paddles on the toroidal sensory ring. Because connectors, a wire harness, and insulation were added on top of the sensory ring, the solar paddles were raised to allow a 5-inch rather than a 3-inch clearance between the bottom of the paddles and the top of the sensory-ring structure with the paddles folded.

No structural changes have been made in the controls system configuration or its support. The truss supporting the controls package has the same geometry as in the original concept, but the height has been shortened from 48 to 47.75 inches. It has remained a stiff structure as originally conceived.

Some detail design changes have been made in the sensory ring, but it is close to the original concept. Shear webs were added inboard and outboard of the sensory ring, and some added along the sides of the separators where the truss members are supported. Originally, the modules were to be in close-fitting compartments, but the addition of shear webs to some compartments left others with large clearances. Manufacturing tolerances on the cast V-shaped separators and the assembly procedure also contributed to the larger clearances in the compartments. The use of shims to take up the clearance is being considered.

In the original concept, the center beam was to be cross-shaped; however, studies of mounting the sensors on the beam led to the choice of the H-shaped beam. The H-beam has an aluminum honeycomb core with aluminum skin; the caps, webs, and gussets are made of magnesium.

The adapter which fastens the spacecraft to the launch vehicle has not changed in size or geometry.

A variety of materials is used for the spacecraft and adapter structure. The control box is made of magnesium, with magnesium side plates and a fiberglass cover. The solar paddles are of 1-mil aluminum honeycomb, the paddle covers are of 3-mil aluminum, and aluminum internal structural members are used along the edges and at other load-carrying locations.

The truss struts are made of aluminum tubing. Aluminum is used for the following parts of the sensory ring: separation ring, top outboard ring, separator side plates, inboard webs, separator thermal panel, and inboard ring channels. The outboard webs in the sensory ring are magnesium, and the V-shaped separators are magnesium castings.

Aluminum, magnesium, and steel are used for the adapter structure. The following parts of the riveted shell assembly are made of aluminum: flanges, longitudinal stiffeners, circumferential flanged channels, and spring brackets. The skin and access doors are magnesium. In the spring cartridges, the springs and guideshaft are made of steel, and the end fittings are made of magnesium. In the band assembly, the band is stainless steel, ten clamp segments are aluminum, and two clamp segments at the explosive bolts are made of steel.

The Nimbus A spacecraft has no redundant systems; this eliminates equipment from both the sensory ring and the H-beam. Present Nimbus A spacecraft weight is 707.9 pounds, while the original concept called for a complete spacecraft weight of 650 pounds. The center of gravity in the original concept was 24 inches forward of the adapter/spacecraft interface; presently it is 24.5 inches forward of the adapter/spacecraft interface. A comparison of the moments-of-inertia shows that they average 10 percent higher now than in the initial concept.

The spacecraft's unique design permits significant changes, such as eliminating redundant systems, while maintaining the center of gravity within the specified 2.5-inch radial distance from the vertical geometric axes. The center of gravity presently is 0.23 inch from the geometric axis with the solar paddles folded, and 0.59 inch with the

paddles unfolded. The design also permits such changes without upsetting the specified isothermal temperature balance of $25^{\circ} \pm 10^{\circ}$ C throughout the sensory ring.

Vibration studies conducted with the sensory ring mounted on the adapter showed an average amplification factor of 3.25 obtained in the yaw, or thrust, direction. This is the direction of greatest input. This factor, obtained without any change from the original concept, falls well within the original requirement that the amplification factor should not exceed 4.

To explore vibration problems, a vibration model of the Nimbus was built and tested on the adapter. Vibration problem areas on the spacecraft (Figure 1) have been excursions and failures of the solar paddles; failure of the solar paddle-to-sensory ring support; clearance between the hub of the solar paddle and the solar-array drive shaft; and failure of the V-shaped separator. All the problems have been solved, and the structure now will survive the vibration environment.

During a sine test of the vibration model with a 3g input, the preload cable at the solar-platform support failed. A heavier cable was installed and the test continued. During the 4g-level sine test, the compression strut failed and a new one was installed. A 5g-level sine sweep was attempted, and the new compression strut failed. At this point, it was decided to completely redesign the solar-platform support.

The first compression-strut failure at a 4g input was believed to be a secondary failure incurred as a result of inadequate preload, allowing the strut to bounce free of the detent; the strut failed by bending through the threads of the adjustment screw located at the bottom of the strut. The second compression-strut failure at 5g input was a column failure at midlength. These failures indicated that the preload on the cable holding the paddles down should be increased, in order to eliminate the bounce; this, in turn, would make it necessary to have a heavier compression strut. Regardless of the increased preload, however, the preload cable would elongate in accordance with Hook's Law and, possibly, would not alleviate the bounce problem.

The new solar-platform support design is shown on the right in Figure 2. The preload cable is appreciably shortened, and the compression strut eliminated along with its eccentric loading. This design

also eliminates the high concentrated bearing load at the upper end of the strut by taking up the bearing load in the paddle fitting.

The solar-paddle latch cable, which has latch pins spaced intermittently for paddle deployment, stretched sufficiently during the vibration test to allow the top latch to be released at 21 cps with 5g input. This cable was test-preloaded to 100 pounds and stretched 0.25 inch. This in itself would not cause failure, but the cable was laid in one direction only, allowing the cable to unwind. To correct the latch-cable problem, three changes were made: (1) the cable was double-laid; (2) it was prestressed; and (3) it was restrained from unwinding by a slot-key arrangement.

The redesigned solar platform was vibration-tested, but the monoball fittings at the ends of the links were galled and binding. Rotation of the links allowed the monoball joints to overtravel and gall. Bars were placed between the links to prevent rotation, and since that time there has been no trouble with the redesigned solar-platform support.

While the 5g yaw-axis test was being conducted, one of the solar paddles and its transition piece cracked through the skin and honeycomb. Repairs were made to the cracks by potting the honeycomb cores in the cracked areas and bonding on doubler skins. When the repairs were completed, an attempt was made to vibrate the spacecraft model in the lateral axis. Tests with 1g input, one-half the prototype level, resulted in solar-paddle excursions that exceeded the allowable spacecraft envelope at low frequencies. During these tests, considerable movement was noted between the hub of the solar-paddle transition piece and the shaft extending from the controls box. This movement was due to excess clearance. To save time and money, since the transition sections were all made, the joint was tightened by adding a two-piece clamp as shown in Figure 3. The relatively soft solar-paddle hub was slotted, allowing the clearance to close and transmitting the load from the clamp to two structural channels on either side of the hub. Rotation of the hub on the shaft is prevented by three taper pins, one of which can be seen in Figure 3. Originally, there were three small straight pins that elongated the relatively soft hub material during vibration. From the figure it can be seen that the taper pin picks up the harder clamp material, the hub, the shaft, and the electrical plug spacer. The clamp and taper pins solved the clearance problem. The tight fit at the joint does not reduce the excursions appreciably, but it eliminates rotation between the hub and the shaft.

To control the solar-paddle excursions, damped channel sections were placed across the top and bottom of each paddle, as shown in Figure 4. The early damped channel sections had transverse slots on each side, spaced about 1 inch apart; the strips failed in several locations as a result of these slots. The strips reduced the excursions appreciably before they failed, and analysis of the vibration and static deflection tests indicated that solid flanged channels would reduce the excursions by approximately the same amount. In addition, the slotless stiffeners would be less likely to fail. The stiffeners are bonded to the back side skin of the solar paddles, with the ends bolted to structural members in the solar paddles. Vibration surveys indicated that the solar-paddle excursions were considerably reduced, but additional reduction was required.

Engineering model constant-volume hydraulic dashpots were placed between the solar platform and the two truss members (Figure 5), and the resulting excursions were acceptable for the specified 59-inch spacecraft dynamic envelope. Flight model dashpots, which will have the same operating characteristics, are being designed and manufactured. Preliminary data indicates that the dynamic internal envelope of the shroud, which covers the spacecraft, intrudes into the allowable envelope for the spacecraft. This is one problem area that remains to be resolved.

After all the changes were made on the spacecraft structure, the vibration structure was tested again. The spacecraft survived the yaw direction test, but at 1.5g roll-axis input, the separator casting supporting the solar-platform support failed as shown in Figure 6.

The failure consisted of a complete fracture of the upper portion of the two forward posts of the separator casting. Shear webs were cracked in the vicinity of the post fractures. The fracture on the right post was through a fastener hole. Microscopic examination of the fracture area has revealed that:

(1) Failure of the casting originated at the "as cast" inside edge of the left front post, where a corroded surface pit was found. Failure of the right front post, as well as shear web cracks, occurred as secondary effects.

(2) Pitting corrosion, coupled with alternating stress, led to the failure.

(3) Another contributing factor was segregation in the failure area.

A stress analysis from strain-gage information in the failed area indicated the stress level was below that allowable for the magnesium casting alloy ZH62A-T5, even at 10^8 cycles. As a result, the following decisions were made:

(1) Select only grade 1-B or better castings for the highly stressed areas that support the trusses and solar platforms.

(2) Change X-ray techniques to improve readability of pictures taken in the critical areas.

(3) Face the "as cast" inside edges of the castings, and break sharp corners.

(4) Remove scribe marks.

(5) Move fastener holes away from the tangency points of inner radii.

(6) Improve control of the application of protective coating.

New castings, based on the above criteria, survived the prototype-level sinusoidal vibration in all three axes. No other failures occurred; the structure now will survive the prototype-level vibration tests.

Originally, the controls box was treated like any other subsystem in the sensory ring, which meant that the controls system would be vibration-tested independently of the spacecraft. An attempt was made to vibrate the controls system as a separate subsystem while trying to simulate the effects of the solar paddles. Review of the data showed that the components in the box encountered higher g's than they did in the tests conducted with the controls box on the spacecraft; this is because the spacecraft structure attenuates the transmission of higher frequencies to the controls box. The controls subsystem contractor was then directed to make the following changes to lower the g forces to which some of the components were subjected: stiffen the regulator bracket, and add stiffener brackets to support the horizon scanners; redesign the top cover, stiffen it, and make it of fiberglass.

Prototype-level tests of the modified vibration-model controls package on the spacecraft resulted in lower g levels on the components. The

highest g level, 15g, was recorded on a momentum or flywheel package. Above 100 cps, the structure starts to attenuate and maximum g force is 6. All controls system components are qualified to 10g from 5 to 2000 cps.

Requalifying the components to the higher g forces in the low-frequency band appears feasible, since the actual components have survived levels approximately 33 percent above the present prototype levels in vibration model tests.

The Nimbus spacecraft is attached to the adapter by a V-clamp, and the adapter section is bolted to the Agena B. The spacecraft is separated from the adapter and the Agena B by firing two explosive boltcutters to release the V-clamp. Four carefully calibrated springs in the adapter then impart a forward separation velocity to the Nimbus. Specifications require that the Nimbus separate at a velocity of 4.0 to 4.5 ft/sec, with a tumble rate not to exceed 0.5 deg/sec.

Six drop tests have been made, using an adapter and a dummy spacecraft. Separation velocities have varied from 4.16 to 4.18 ft/sec, all within the requirement. Tumble rates ranged from 0.067 to 0.605 deg/sec. Two one-boltcutter drops exceeded the requirement. Statistically, to have a 95-percent probability of success at a 90-percent confidence level, all six drops should have a tumble rate not greater than 0.20 deg/sec. Flat surfaces are required between the spacecraft and the adapter, and between the adapter and the Agena B, if the springs are to function within the requirements. An epoxy shim is being used between the spacecraft and the adapter to achieve the required flatness, but the Agena-to-adapter interface remains to be resolved.

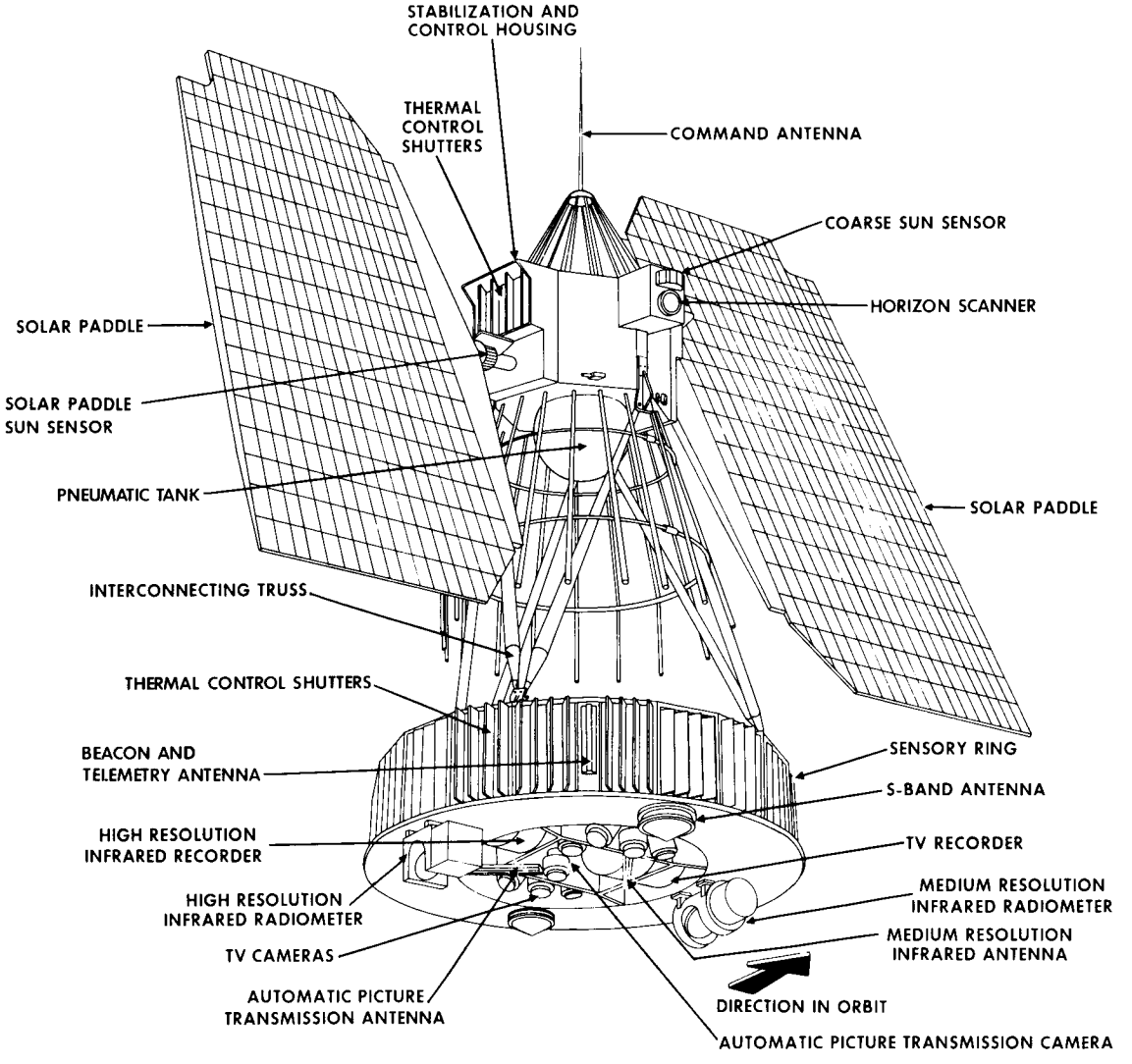

Figure 1 – Nimbus Spacecraft

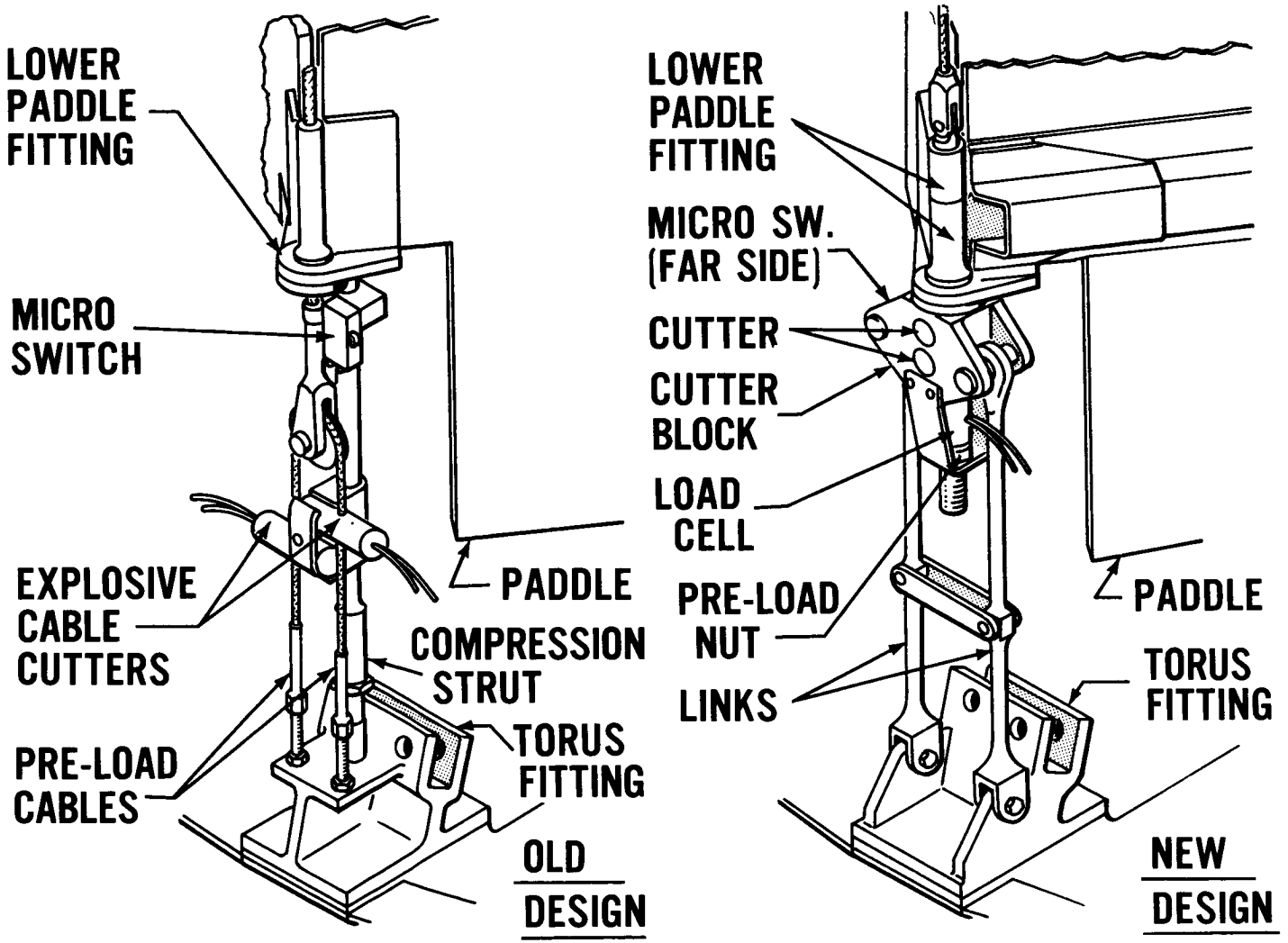

Figure 2 – Solar Platform Support

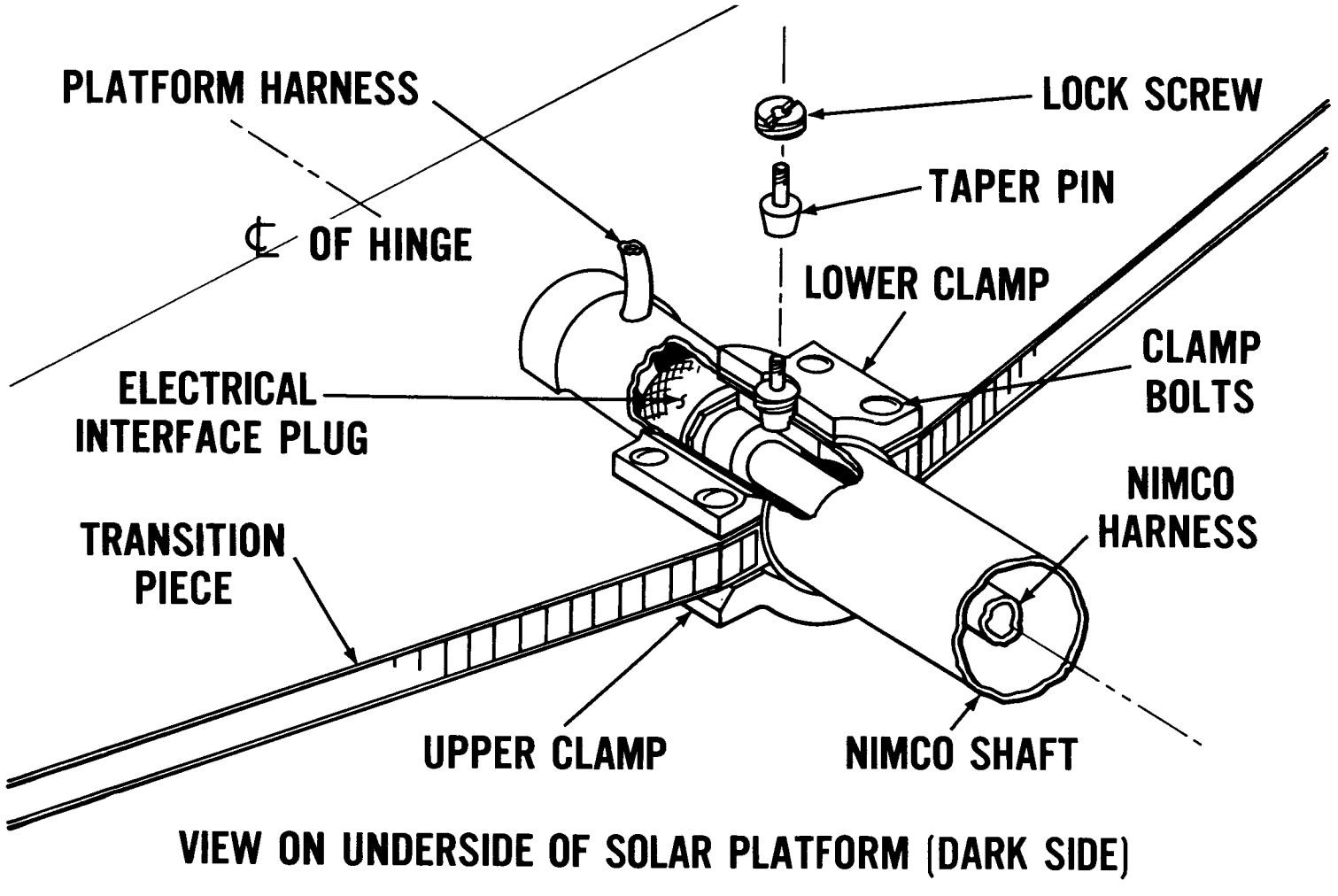

Figure 3 – Solar Platform Hub-to-Control Shaft Joint

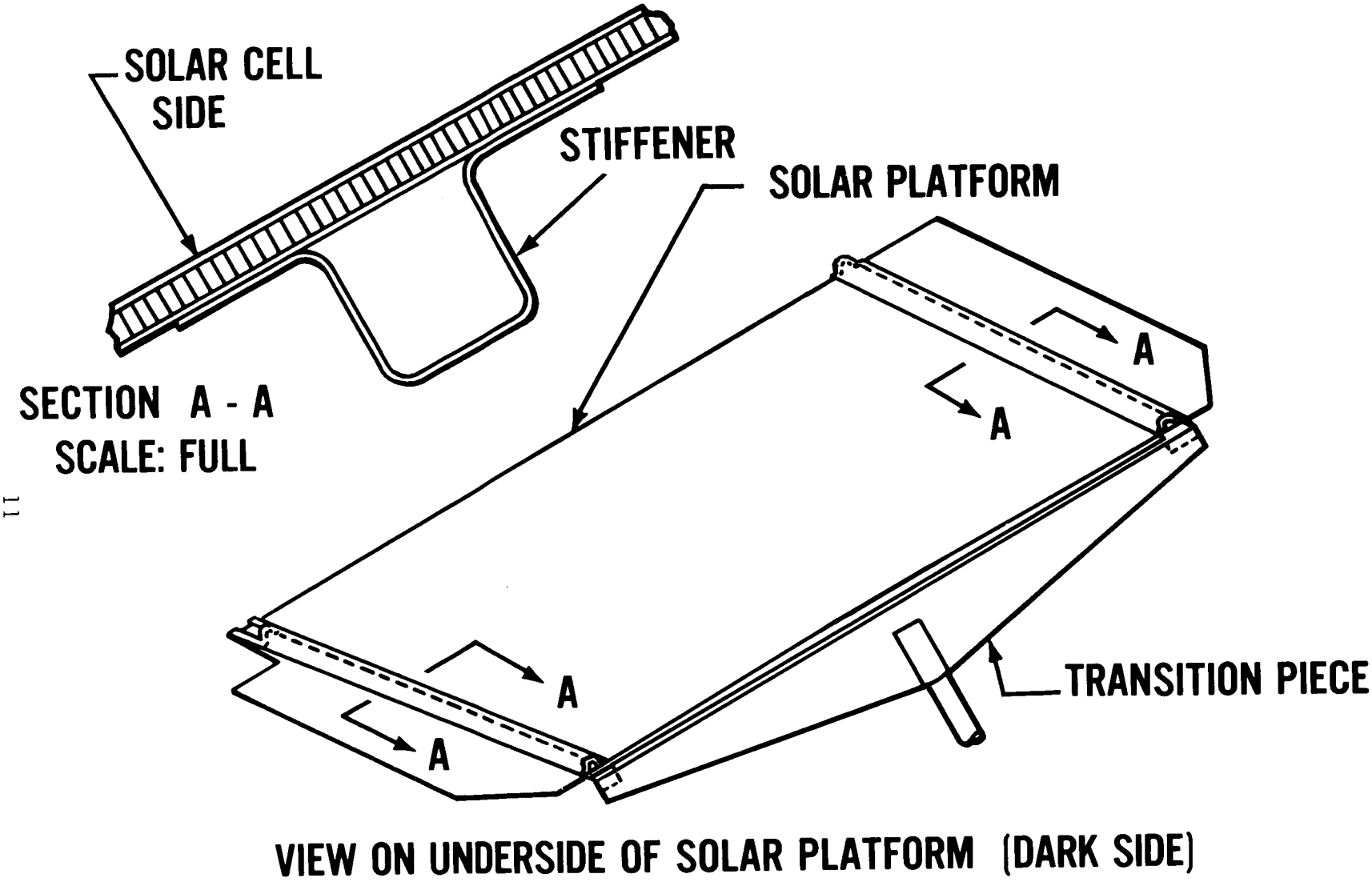

Figure 4 – Solar Platform Stiffening

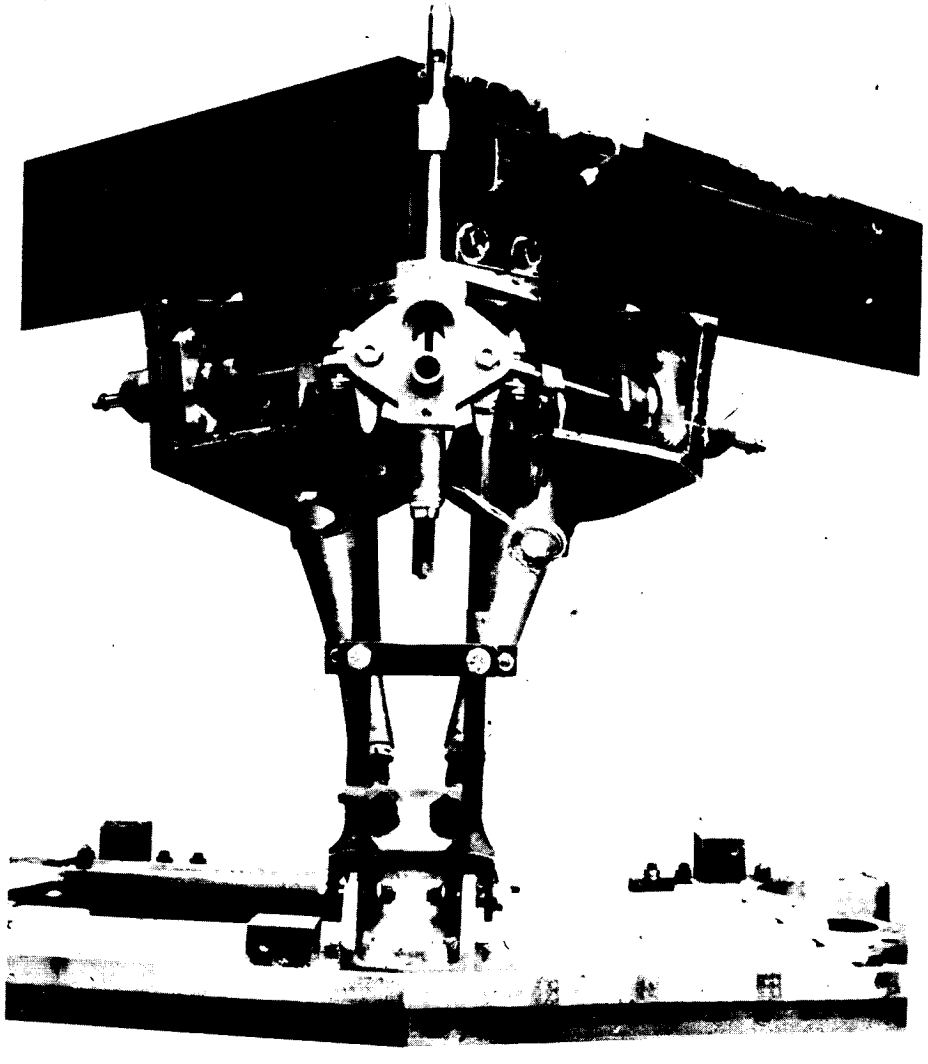

Figure 5 – Solar Platform Support Dashpots

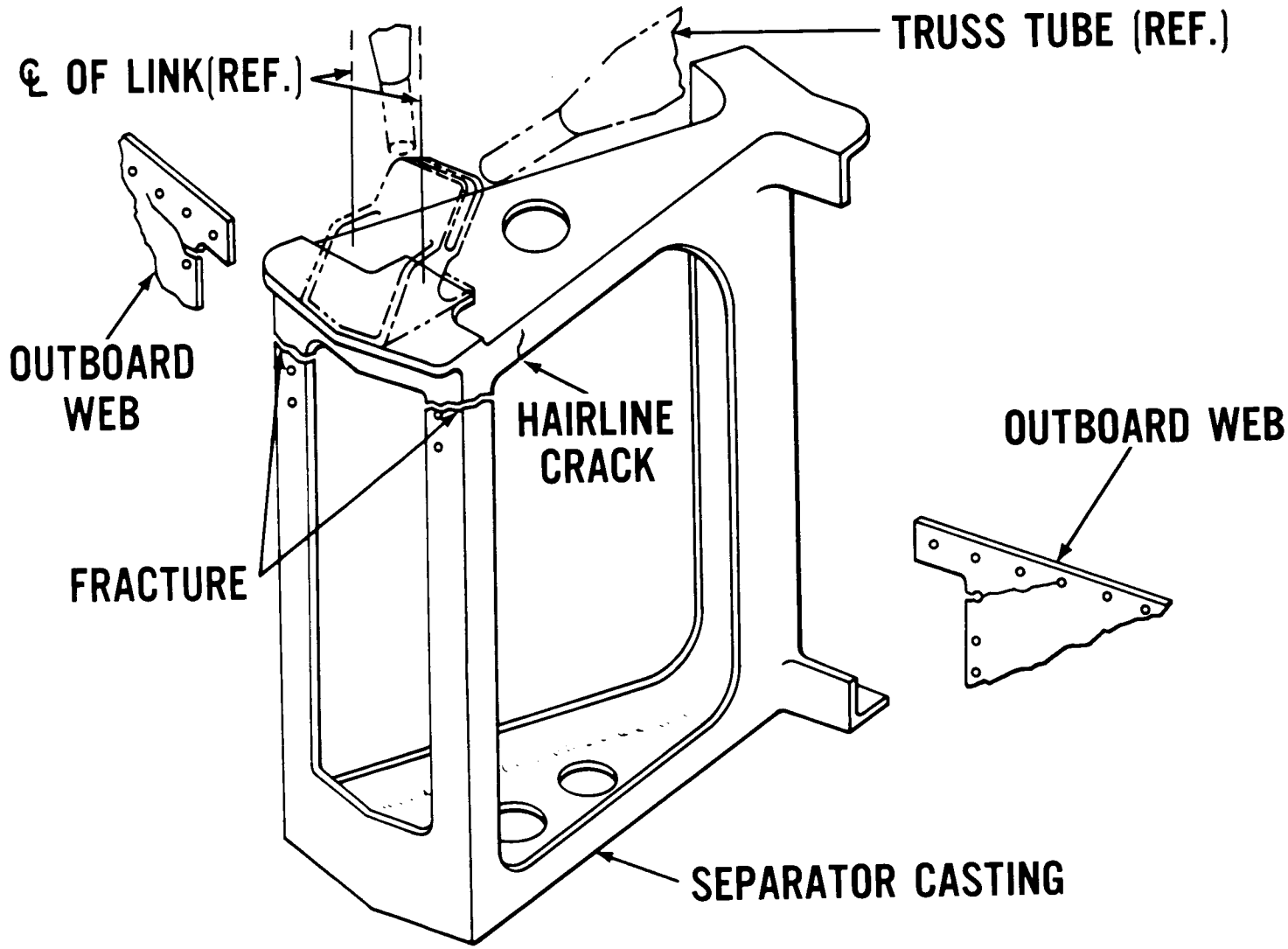

Figure 6 – Separator Casting Failure

11. THERMAL CONTROL OF THE NIMBUS SPACECRAFT

By P. Crossfield, GSFC; F. Drummond,
GE/Missiles and Space Division

11. THERMAL CONTROL OF THE NIMBUS SPACECRAFT

ILLUSTRATIONS

Figure		Page
1	Basic Thermal Design Specifications for the Nimbus Sensory Assembly	9
2	Nimbus Spacecraft Solar Illumination	10
3	Typical Nimbus Orbit Heat-Flux Patterns	11
4	Nimbus Spacecraft Orbital Power Demand	12
5	Nimbus Thermal Model	13
6	Thermal Radiation Characteristics	14
7	Temperature Controller, Schematic Diagram . .	15
8	Nimbus Thermal Model Performance	16
9	Nimbus Shroud Configuration	17

11. THERMAL CONTROL OF THE NIMBUS SPACECRAFT

By P. Crossfield, GSFC; F. Drummond,
GE/Missiles and Space Division

Nimbus, in common with all contemporary spacecraft, contains an array of components and materials -- mechanical, electrical, and chemical -- which will operate effectively and reliably only when maintained in a hospitable thermal environment. Pressing existing hardware into use for space exploration, subjecting it to the rigors of outer space and possibly to uses for which it was not designed, necessitates careful thermal design to provide the proper environment.

The Nimbus design uses both active and passive control to achieve a thermal environment in which the sensors and experiments will perform, with a minimum of degradation, for the 6-month spacecraft life. The sensory assembly, the controls assembly, and the solar platforms, the three main subassemblies of the spacecraft, have thermal control.

The four basic requirements governing the thermal design, shown in Figure 1, are:

1. The sensory subsystem temperature shall be stable to $25^{\circ} \pm 10^{\circ}$ C.

2. The day-to-night temperature fluctuations shall not exceed 10° C.

3. The highest possible heat conduction shall be achieved; i.e. max instantaneous dT equals 10° C.

4. The surface temperatures of individual components and subsystems shall not vary from frame temperatures by more than 5° C.

The effective temperature-versus-time constant of the sensory assembly should be long, compared to the time required for one orbit, and should be consistent with the permissible 10° C variation of day-to-night temperature. Fail-safe provisions are provided to increase reliability.

Temperatures of all major subsystems and structures are monitored and telemetered to a ground station. There are 60 thermistors which sense and report temperatures to the PCM telemetry system. Each shutter of the active-control system is instrumented for continually monitoring and telemetering its angle of attitude.

Specifications require that thermal control remain effective with a 10-percent change in the absorptivity-emissivity (α - ϵ) ratio due to degradation of surface finish. Thermal control also must remain effective throughout variations of internal power dissipation from minimum to maximum values. The thermal control was to be effective with 500- to 700-nautical-mile orbits.

In summary, the temperature of the sensory structure is defined as that of an isothermal ring, the temperature measured being the average of the temperature sensors located around the ring. The temperature gradients of these sensors must remain between 10^{o} and 40^{o} C; however, when the shutters of the active control are not working, the limits may be widened to between 5^{o} and 45^{o} C.

The program which General Electric, the spacecraft integrator, followed in developing the thermal design, and in proving the design through test, consisted of:

1. Radiative-coating development effort to evaluate the absorptivity-emissivity relationship for aluminum, gold, black lacquer, etc.

2. Joint-conduction tests to define the efficiency of joint fillers

3. Heat-transfer network analysis

4. Computer programming of orbital heat-flux on various surfaces

5. Development of a thermal model for test and evaluation

6. Temperature controller and shutter design, development, test, and evaluation

7. Analysis and evaluation of the overall power profile (a continuing task)

Figure 2, representing one quarter of the orbit, considers the orbital heat flux (OHF) on the spacecraft from solar, earth, and albedo sources. Significant heat-flux change occurs during the orbit at satellite sunrise, earth sunrise, satellite noon, earth sunset, and satellite sunset.

Before a thermal analysis of the spacecraft in orbit can be made, the magnitude and extent of the heat fluxes on the various surfaces must be known for each instant of time. The level of heat flux from solar, earth, and albedo sources was calculated by the 7090 digital computer. To prepare the program, it was necessary to know the orbital path, the altitude, and the angular relationship of the various surfaces under consideration with respect to the earth and earth-sun axis.

To translate the OHF into absorbed-heat rate, the value of the flux is multiplied by the area of the surface in question, the cosine of its angle to the source energy, and the α of the surface.

In preparing the analysis of the effectiveness of the sensory insulation, four limiting flux locations were chosen: the front or leading edge, a point on the side of the sensory ring 90 degrees from the velocity vector, and one point each on the top and bottom of the spacecraft. The OHF on all other surfaces will fall within the limiting values for these areas.

Figure 3 illustrates the variation during the orbit cycle of the incident energy from solar, earth, and albedo sources, using typical spacecraft locations such as a point on the bottom, a leading edge, and a trailing edge as examples. On these surfaces, the angle of attack of the incident flux varies with orbit time. The curves for the leading and trailing edges are similar but are out of phase. In these curves, 128 watts can be attributed to solar energy; albedo, a measure of the solar energy reflected by the atmosphere, reaches a peak of 15 watts. Energy radiated from the earth on these points is relatively minor.

The curves for a point on the bottom of the spacecraft show that the earth OHF is constant at 17 watts/ft^2, and the value of the albedo plots as a parabolic curve with a maximum value of 46.4 watts/ft^2 just before spacecraft noon. The incident solar OHF also plots as a

parabolic curve, with the top surface receiving a maximum of 129 watts/ft^2 at noon; the bottom receives a maximum of 63 watts/ft^2 during the periods, spacecraft sunrise to earth sunrise and earth sunset to spacecraft sunset.

Figure 4, the power profile, shows how the energy generated by the solar power system is utilized or dissipated during a typical orbital period.

For the purpose of thermal analysis, the average output of the solar power system is assumed to be 402 watts. Maximum power to the load from the solar array is 285 watts at 24.5 volts and 11.62 amperes.

The minimum power, identified by the dot-dash line at the 98-watt level, includes power for spacecraft "housekeeping." This is made up of controls-assembly power at 80 watts, PCM telemetry-system power at 9 watts, clock-system power at 9 watts, and minor power required for standby use of the sensor systems.

The 162-watt earth day level provides approximately 62 watts for the advanced vidicon camera system (AVCS) and the automatic picture transmission subsystem (APTS). The 113-watt earth night limit includes the requirements for HRIR operation.

The duration of interrogation per orbit varies, as does its place in the orbit cycle. Duration for the 1st, 2nd, 3rd, 6th, 7th, and 8th passes varies between 10.37 and 11.88 minutes; for the 4th and 5th passes, it is just under 9 minutes; for the 9th pass it is 4.56 minutes; the 10th through 13th passes have no interrogation; and the duration for the 14th pass is 3.6 minutes. Principal interrogation-power demands are 145 watts for the S-band transmitter, approximately 21 watts for the tape-recorder playback, and approximately 8 watts for telemetry.

The cameras and tape recorders in the center of the torus of the sensory structure consume about 10.5 watts. The high-resolution infrared radiometer below the sensory ring uses 2.5 watts during earth night. The remaining power is distributed among the components in the sensory ring.

Figure 5, a photograph of the Nimbus spacecraft, will help to show how the thermal control is provided. As mentioned earlier, there is both active and passive thermal control. Passive temperature control is established by selecting a particular surface coating and using it either over an insulation barrier or directly on a spacecraft component. All surfaces have passive control except for 15 of the 18 modular cavities, which have an active shutter system at the peripheral surface, and the two sides of the controls system which normally encounter a minimum of solar energy.

The solar-power paddles will be surface-coated (solar cells with α of 0.773 and ϵ of 0.942; back side, PV 100 or white epoxy with α of 0.2 and ϵ of 0.88) to hold a mean 25° C temperature. However, temperature limits of the paddles will vary from +60° C to -81° C as the spacecraft passes into and out of earth umbra.

The controls and system thermal design provides a blanket of insulation (30 layers of aluminum foil and tissue glass) across the top surface. Passive surface-coating protects the four sides (exclusive of the two with shutters) and the bottom surfaces. Internal equipment and components have been located to provide optimum heat transfer. The electronic module panels will be striped to achieve the necessary absorptivity-to-emissivity surface relationship. Faying surfaces of components and panels will be coated with Eccobond 56C (Emerson and Cummings product) for efficient conduction.

The sensory assembly crossbeam structure on which camera-system components are mounted is located in the center of the torus shown in the figure. It is painted with absorptive flat black paint, to achieve an adiabatic structure.

An insulation blanket of 30 layers of aluminized Mylar will be used to cover the top of the sensory ring, and a formed fiberglass insulating blanket will be fitted around the cameras and radiometer at the bottom of the ring. The bottom insulation is cut away under each of the seven battery modules.

A joint conduction test program, using a single bay test vehicle, resulted in the use of Eccbond 56C noncatalyzed as a means of increasing the efficiency of conduction. Current developments indicate that a

change to silicone grease (O.S. 4073) filled with silver powder for thermal and electrical contact may be desirable. Thermal conduction of the filled joints is increased by a factor of 10 or better over that experienced with metal-to-metal joints. Interface joints using one of the above fillers provide conduction in the order of 0.5 watts/in^2/°C.

Thermal radiation characteristics of the materials used as surface coatings on the spacecraft are shown in Figure 6.

PV 100 (Vitavar, titanium oxide with silicon alkyd base) is used on the outboard faces of compartments and on the bottom surfaces of batteries.

D4D (aluminum-pigmented silicon alkyd paint) is used on the quadraloop antenna, separation ring, struts, lower section of command antenna, outer surface of insulation on compartments 4, 9, and 14, and on the insulation blanket shell.

Amfab (TV 20-60, a Teflon-impregnated glass fabric manufactured by AM&F) is used as the outer coating of the top insulation, and on the control-system surfaces.

Active temperature control is provided by the mechanism shown schematically as Figure 7. All but three of the 18 modular cavities (4, 9, and 14) have one of these controller assemblies. Tests verified that these three modules did not need active control.

The sensory tube is spring-loaded to firmly engage the side of the module package. The tube-and-bellows system is charged with Freon 21 refrigerant. The primary bellows reacts to refrigerant pressure changes to open or close the shutters through a mechanical linkage system (or a pinion-and-rack mechanism for the controls system). The selected temperature range of the controller is from 19° to 32° C.

As the shutters open, the effective emissivity may range from 0.15 effective ϵ at a 10° shutter opening to 0.65 effective ϵ at 90° shutter angle. The curve formed by plotting ϵ versus shutter angle has a "knee" which assures that an angle of 65° or greater will yield 93 percent or better of the maximum value. The radiation area per module is 693 cm^2.

If the system becomes inoperative due to a fluid leak, the fail-safe bellows functions to open the shutters to the position giving the most effective ϵ. A failure mode is sensed when the fluid-system pressure drops to below 6.6 psia, which corresponds to -10° C.

The shutters are made up of four vane assemblies, except at either side of the quadraloop antennas, where five vanes are most effective. The vanes are hinged to provide shade from the sun. They are sleeve-bearing mounted with Nylotron (2-1/2 percent moly-disulphide in nylon) which has good lubricity and stability in a vacuum environment. The shutter fabric consists of 30 layers of 0.25-mil aluminized Mylar, the outside surface being coated with D4D.

Figure 8 shows typical results of testing the thermal model in a vacuum-thermal environment.

The test gave maximum normal spacecraft-component temperature of 34.5° C in module 5, and a minimum temperature of 19.5° C; the maximum structure temperature was 26.5° C, and the minimum temperature was 19.5° C.

With a Nimbus A configuration, the maximum component temperature was 30° C in module 3 and a minimum of 15° C in module 1. Structure temperature ranged from a maximum of 25.5° C to a minimum of 18° C (adjusted for radiometer location).

Effective emissivities shown are a function of shutter opening.

Modules 1 and 5 contain the S-band and television-system transmitters, respectively. Modules 3, 6, 8, 11, 13, 15, and 17 carry the batteries in the lower half of the modules.

Figure 9 shows the spacecraft and shroud configuration as it will appear when delivered and ready for launching. Temperature control can be maintained on the launch pad by free convection cooling, if 300 CFM of air at 4.4° C is available. As an upper limit, it has been calculated that air at 15.6° C could maintain the spacecraft components just below the maximum allowable temperature of 55° C.

In conclusion, it should be noted that the Nimbus, as presently designed,

carries about 30 pounds of thermal-control material and equipment. Conversion of any of this weight to productive sensor or experiment capacity, by maximizing component subsystem and spacecraft design, can serve to increase the effectiveness of the Nimbus program. This should present a definite challenge to program integrators and to the suppliers of components or systems.

1. OVERALL TEMP. STABILITY TO 25°C ± 10°C

2. DAY TO NIGHT TEMP. FLUCTUATION SHALL NOT EXCEED 10°C

3. MAX. HEAT CONDUCTION BETWEEN PARTS REQUIRED

4. COMPONENT SURFACE TEMP. SHALL NOT VARY FROM FRAME TEMP. MORE THAN 5°C

Figure 1 - Basic Thermal Design Specifications for the Nimbus Sensory Assembly

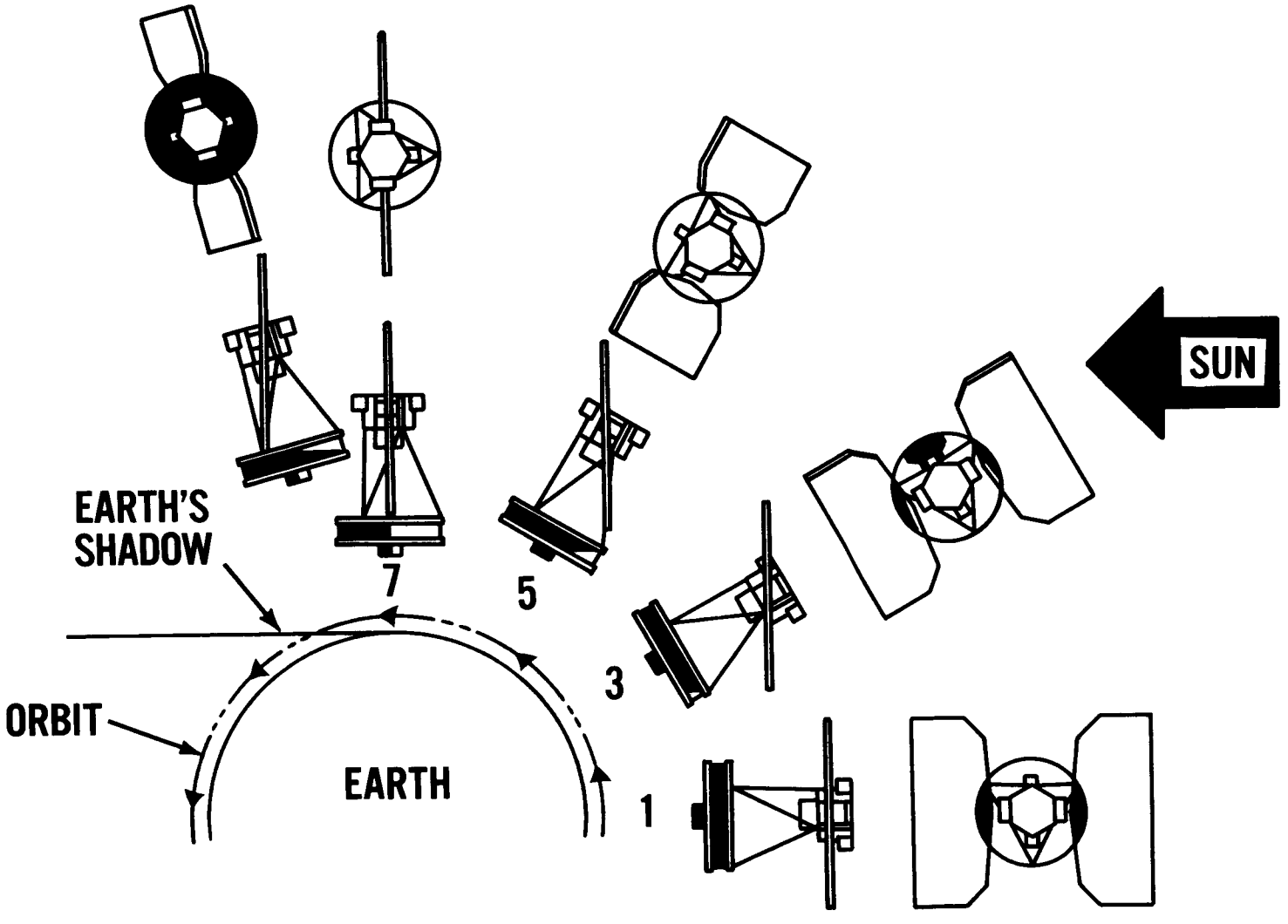

Figure 2 - Nimbus Spacecraft Solar Illumination

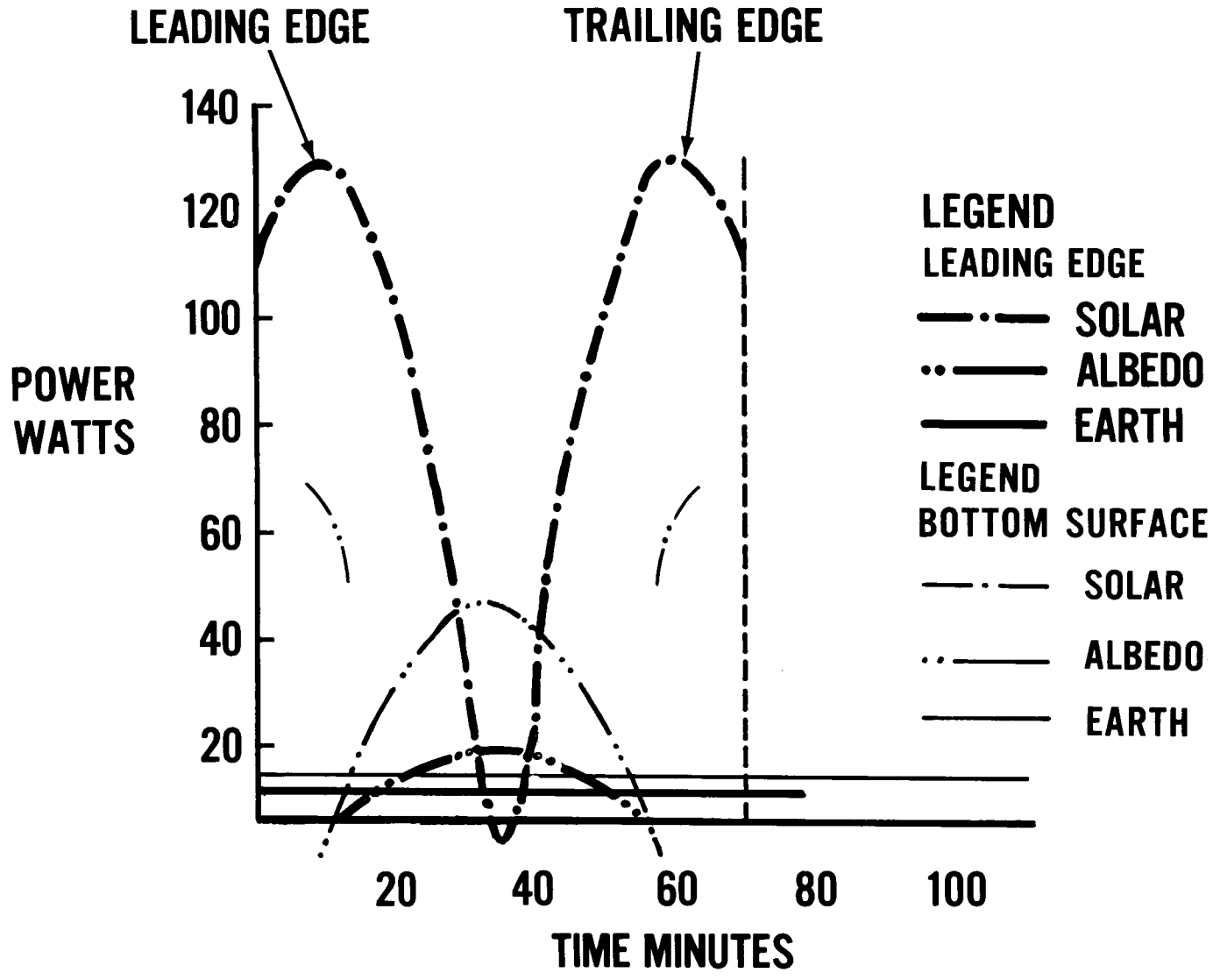

Figure 3 - Typical Nimbus Orbit Heat-Flux Patterns

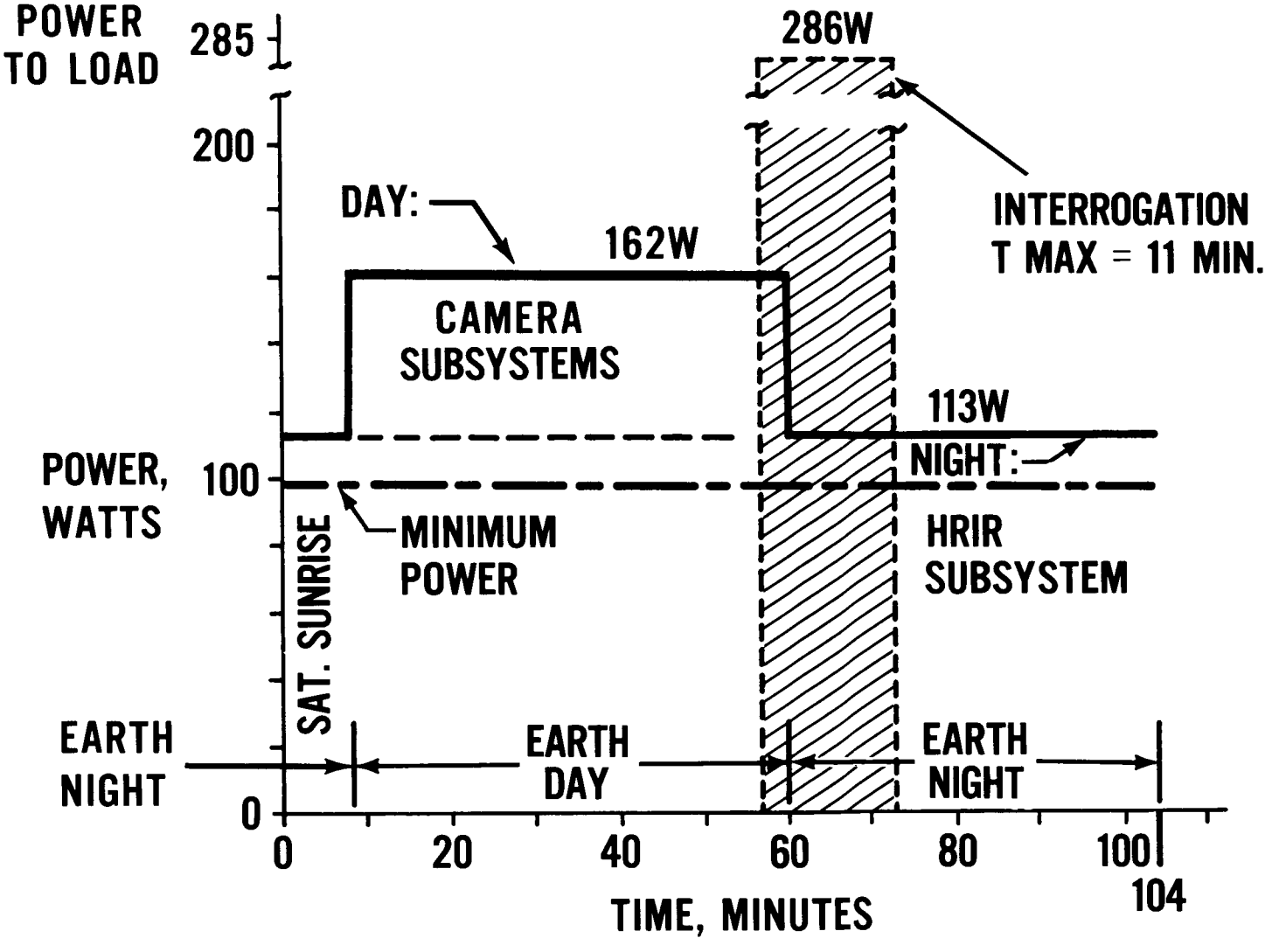

Figure 4 - Nimbus Spacecraft Orbital Power Demand

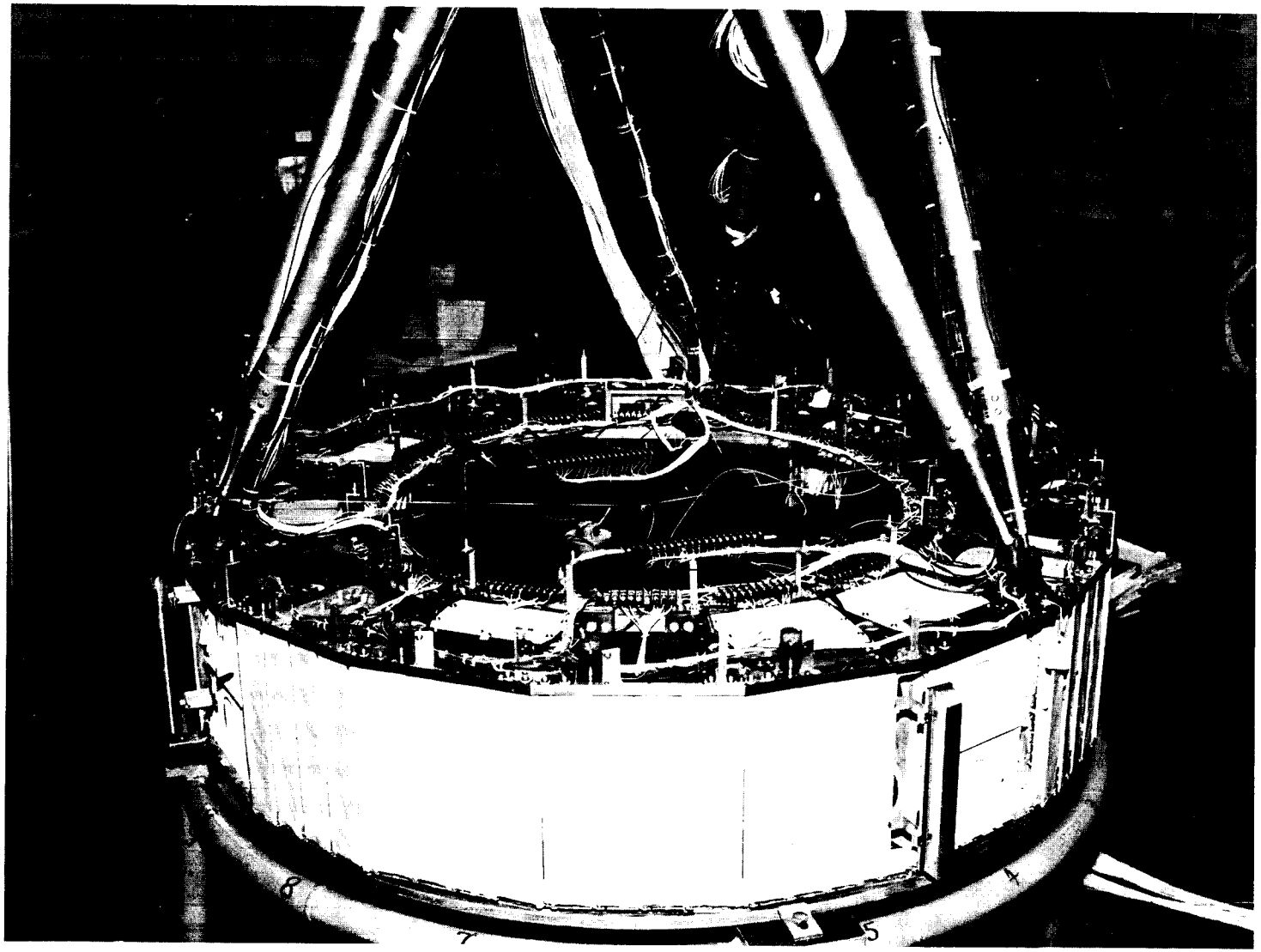

Figure 5 - Nimbus Thermal Model

ALL EXPOSED SURFACES HAVE SPECIFIC RADIATION PROPERTIES-ONE OF THREE BELOW:

PV100	$\alpha = .25$	$\epsilon = .9$	**HEAT REJECTION**
D4D	$\alpha = .33$	$\epsilon = .30$	**PASSIVE SURFACES**
AMFAB	$\alpha = .3$	$\epsilon = .6$	**PASSIVE BUT DIRECT EXPOSURE TO AERO-HEATING DURING LAUNCH**

Figure 6 - Thermal Radiation Characteristics

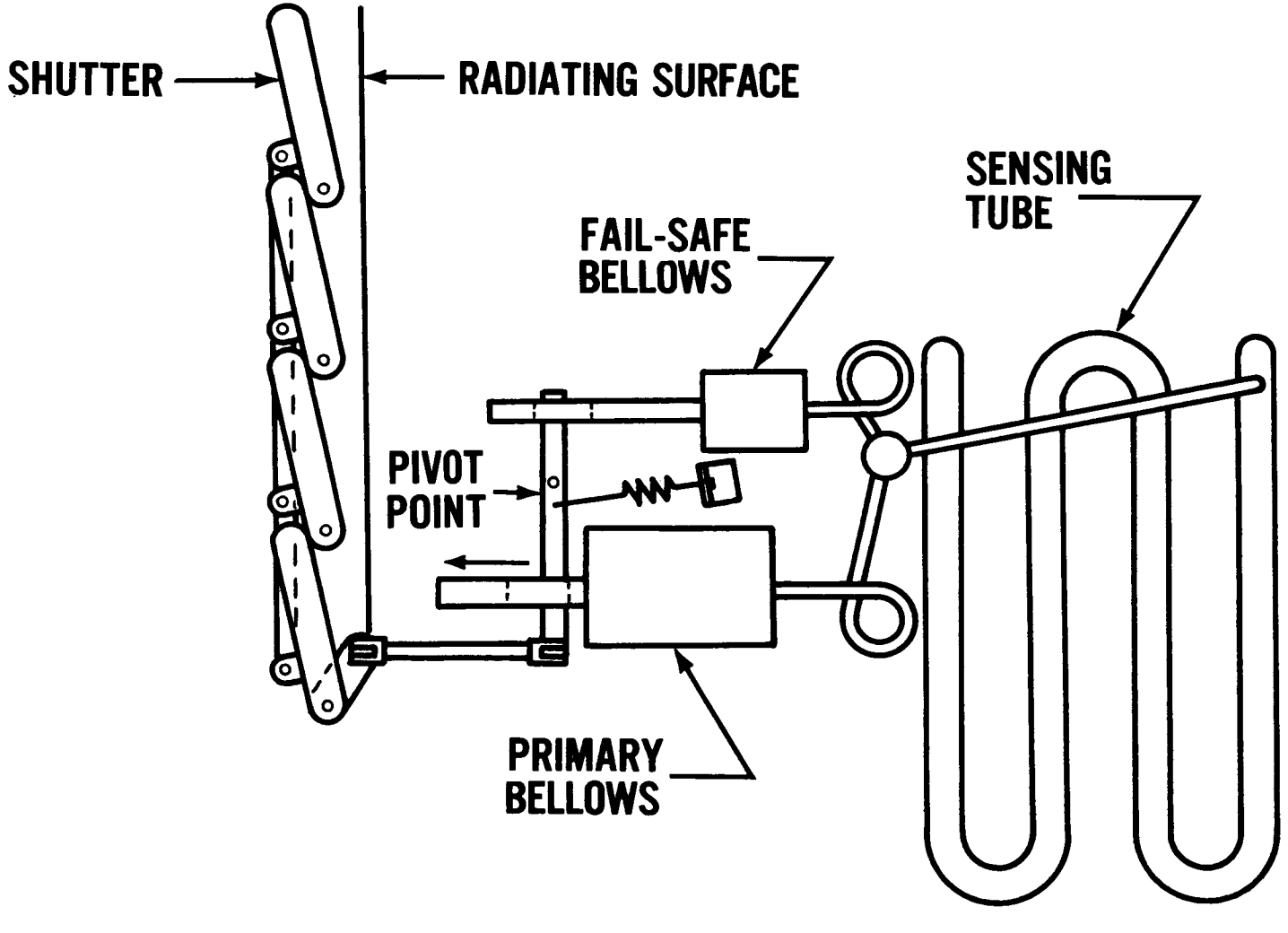

Figure 7 - Temperature Controller, Schematic Diagram

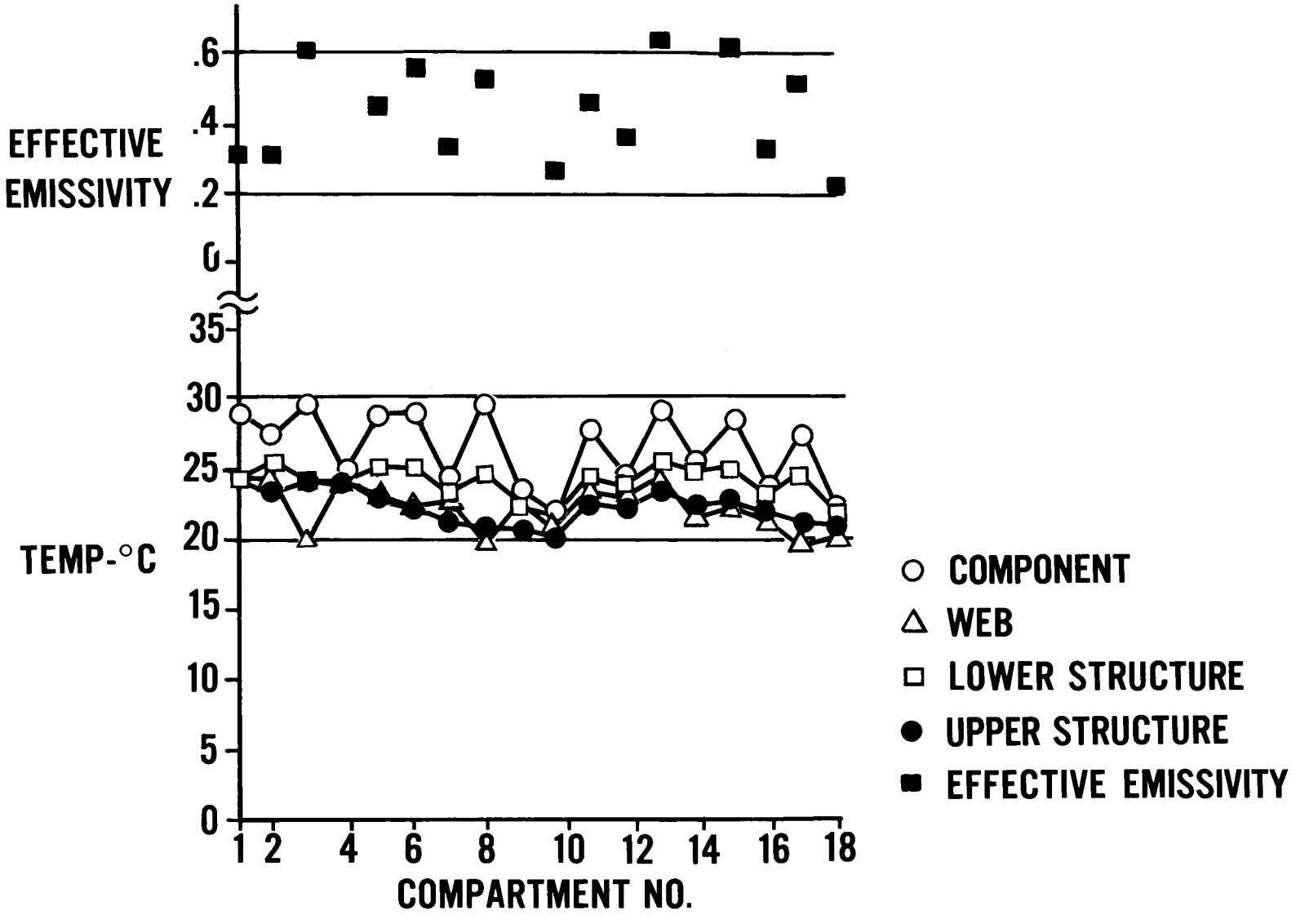

Figure 8 - Nimbus Thermal Model Performance

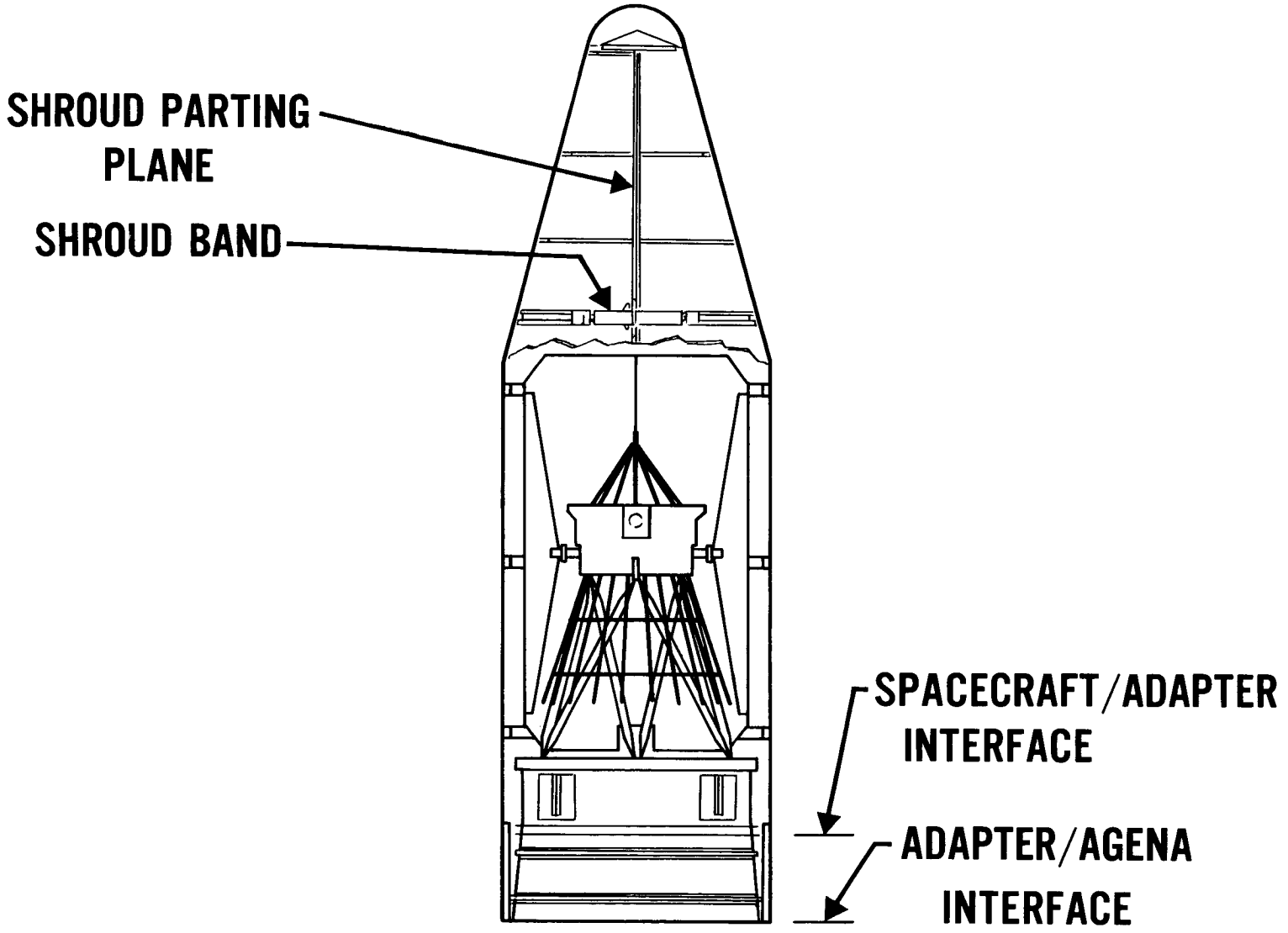

Figure 9 - Nimbus Shroud Configuration

12. SPECIAL ASPECTS OF NIMBUS SPACECRAFT INTEGRATION

By J. P. Strong, Jr., GSFC; R. DiGirolamo,
GE/Missiles and Space Division

12. SPECIAL ASPECTS OF NIMBUS SPACECRAFT INTEGRATION

ILLUSTRATIONS

Figure		Page
1	Nimbus A Component Locations	8
2	Sensory Ring Wiring Harness	9
3	Command Antenna (122-124 Mc)	10
4	S-Band Antenna (1700-1710 Mc)	11
5	Nimbus Telemetry and Tracking Antenna	12
6	Nimbus Command Antenna Pattern	13
7	Nimbus S-Band Antenna and Pattern	14
8	Nimbus Telemetry Antenna Linear Polarization Components	15
9	Ram Assembly and Check-of-Calibration Adapter	16

12. SPECIAL ASPECTS OF NIMBUS SPACECRAFT INTEGRATION

By J. P. Strong, Jr., GSFC; R. DiGirolamo,
GE/Missiles and Space Division

INTRODUCTION

The purpose of this report is to describe some of the efforts involved in integrating a group of electrical and mechanical Nimbus subsystems into a unified, operational spacecraft. Major tasks to be covered are the module location in the sensory ring, wiring assemblies, vibration requirements, operational commands, antenna design, unfolding of the solar paddles, electrical load simulation, telemetry conversion, the beacon killer, and test programming.

SENSORY RING

Many preliminary designs were discarded before the present sensory ring configuration was approved. One unique problem was the location of many modules and sensors which compose the Nimbus spacecraft. Figure 1 shows the present location of these units for Nimbus A; its very density gives an idea of the number of black boxes involved.

The three major factors governing location of the units are (1) dissipation of the heat generated within the units; (2) distribution of weight to produce an optimum weight balance of the spacecraft; and (3) the requirements for the wiring harness. Another report describes the exhaustive tests necessary to perfect a sensory ring which would operate in the required temperature range under all orbital flight conditions. The weight balance was maintained to provide moments-of-inertia that conform to the capabilities of the stabilization subsystem. The center of gravity is on the vertical axis of the spacecraft, within 0.5 inch vertically of the original specification requirement.

WIRING ASSEMBLIES

The greatest problem encountered in developing a wiring installation was the changes which occurred as a result of tests and redesign; numerous "hold" and "go" orders were given to the integration contractor as the development and qualification tests of the various sub-

systems proceeded. The result has been a wiring harness which will permit changes with a minimum of reworking and at minimum cost.

As far as possible, separate harnesses are provided for individual subsystems, with interconnections between subsystems kept to the minimum required for actual operation of the spacecraft. Figure 2 shows the harness developed for the advanced vidicon camera subsystem (AVCS). Although wiring changes are still expected, they can be accommodated readily.

VIBRATION

Typical of the special studies required was the one involving spacecraft/booster vibration. This study related the vibration criteria established for Nimbus with those of other programs using the same class of launch vehicle. Flight data were correlated with analytical definitions to determine realistic vibration requirements.

Vibration tests led to a further study of the spacecraft-shroud clearance. Dynamic and static deflections of the shroud and spacecraft are being evaluated, along with allowable manufacturing tolerances. The effect on spacecraft flight of the action of uncompensated internal and external torque is also being studied. One of these torques is observed during separation of the spacecraft from the adapter; the turning effect transmitted to the spacecraft, if not held within specified limits, could make the initial stabilization of the spacecraft very difficult.

OPERATIONAL COMMANDS

A study was made of the operational commanding of the spacecraft subsystems. In developing controls for flight operation of the Nimbus subsystems, reliability was of prime importance. Automatic changing from one mode of operation to another was kept to a minimum because of the complexity of such devices, and every effort was made to use direct ground commands to actuate the various functions of the spacecraft. Where automatic sequencing proved more practical, it was backed up by a direct ground command.

An example of this policy is the control of the S-band transmitter which sends AVCS pictures to the ground station; this transmitter uses power from the spacecraft batteries at the rate of 145w and, if left on unnecessarily, could easily drain power from the batteries down to the danger point. Ground commands sent to the spacecraft will energize the transmitter and start the playback of pictures stored in the tape recorder. To minimize transmitter drain on the power, a relay controlled by a switch indicating the end of the tape will turn off power to the transmitter. This automatic action will, however, be followed by a ground command which will also turn off the transmitter power.

ANTENNA DESIGN

Important links in the Nimbus communication chain are the spacecraft's transmitting and receiving antennas, which were designed under a NASA contract with New Mexico State University and were manufactured by General Electric.

The command receiving antenna, in the 120-Mc range, is a short dipole mounted on top of the spacecraft, with a conical ground plane formed by a tubular skeleton above and below the stabilization unit (Figure 3).

The AVCS and the high-resolution infrared radiometer (HRIR) subsystem use a conical spiral antenna for transmission in the 1700-Mc range (Figure 4).

Quadraloop antennas are used in the 136-Mc range for transmitting the beacon signal and telemetry data; the ground plane is a flat rectangular grid on a transparent surface, which will not interfere with heat radiation from the thermal shutters (Figure 5).

Four quadraloop antennas are mounted on the periphery of the sensory ring. Antenna-pattern tests conducted on ranges in New Mexico and at Valley Forge show all patterns within specifications, and no trouble is expected from this source. Figure 6 represents the pattern of the command antenna and the effect on this pattern of different solar-paddle positions. Figure 7 shows the pattern obtained from the S-band antenna; solar-paddle position has little or no effect on radiation from

this antenna because of its location on the underside of the spacecraft. Figure 8 shows the patterns obtained from the beacon antenna at several positions of the solar paddles.

One problem in the development of the quadraloop antenna was to obtain a suitable dielectric material. The Fluorosint material specified, a mica-bearing teflon, has moisture-absorbing characteristics which tend to detune the antenna with changes in moisture content. Thus, if the antenna is tuned in the humidity of earth's atmosphere, launching into the vacuum conditions of outer space will cause the dielectric material to expel its moisture, detuning the antenna to a point which prevents satisfactory operation. Waterproof coatings over the Fluorosint did not remedy this defect, and new materials were investigated to avoid a complete redesign of the antenna. Those materials which were not hygroscopic usually did not have the optimum dielectric constant. A polyethylene material called Tellite now under test gives indication of a satisfactory solution to this problem.

UNFOLDING OF THE SOLAR PADDLES

The spacecraft integration contractor has developed the electrical and mechanical equipment for unfolding the solar-cell paddles. Upon receiving the signal that the spacecraft has separated from the adapter, two explosive wirecutters are fired at delays of 2.5 and 5.0 seconds respectively. The wirecutters release the paddle-latching mechanism which, in turn, actuates a switch to energize the unfolding motors. When the paddles are in the fully open position and latched, another switch turns off the power to the motors. This is a relatively simple device composed of solid-state components with several relays for transmitting the separation signal to the stabilization subsystem. This signal starts the "pitch up" positioning of the spacecraft for its orbital flight.

ELECTRICAL LOAD SIMULATORS

Subsystem electrical-load simulation capability has been added to the spacecraft. Load simulation (defined as the dissipation, by auxiliary means, of the power normally used by the individual subsystems) is accomplished physically by dissipating power in electric strip heaters mounted on the sensor or module.

System design requirements call for several uses of the simulators. The initial use may come during the first few orbits of the spacecraft when the subsystems will be turned on one at a time; the load simulators will be turned on to keep non-operating units within the normal temperature limits. By drawing power from the spacecraft power supply, the simulators will prevent overheating of the battery-charge regulators while the regulators are preventing battery over-charge.

The simulators may also be used if subsystem failure occurs, or if subsystems are turned off for troubleshooting.

TELEMETRY CONVERSION

A telemetry conversion unit was devised as a central electronic interface between temperature-monitoring instrumentation and the telemetry subsystem. There are sixty thermistor temperature sensors located on the spacecraft; in addition, there are six resistance thermometers for sensing wider temperature ranges. Thermal shutters are provided on the outboard faces of the sensory ring compartments to control heat radiation from the compartments.

The telemetry conversion circuit consists basically of a fixed resistor in series with a thermistor. This voltage-divider network provides a voltage to the telemetry subsystem which is proportional to temperature.

The thermal shutter position indicator consists of switches and a voltage-divider network which provides the telemetry subsystem with a signal indicating shutter fully open, fully closed, or any of four intermediate positions.

BEACON KILLER

After the spacecraft has been in orbit for its expected life cycle and a replacement has been launched, it is no longer desirable to transmit tracking beacon signals. A beacon "killer" device has been added which is independent of any other spacecraft subsystem. It is controlled by a Bulova Accutron clock movement energized by self-contained mercury batteries. Battery life is estimated to be 2 years. To improve reliability, the spacecraft carries a redundant clock movement.

The clock movement will actuate switches to turn off power to the beacon transmitters at a predetermined time after the spacecraft has passed its anticipated life. This turnoff time has nominally been set at 12 months. The telemetry subsystem will transmit additional indications from the clock movement to show that the beacon killer is functioning properly.

TESTING

The proof of performance for any mechanical or electrical device lies in a comprehensive program of testing. The Nimbus test program, based on past experience with similar spacecraft, is designed to qualify a spacecraft for 6 months of satisfactory performance under anticipated Nimbus-orbit conditions. Every effort has been made to anticipate and reproduce actual conditions which will be encountered by the spacecraft on the ground, during launch, and in orbit. Much of the special testing equipment and apparatus required to attain test objectives has been described and discussed in other reports.

Typical of this equipment is the check-of-calibration adapter. Several of these adapters have been made for testing during the assembly process, in the vacuum chambers, and, if necessary, at the launching site. Figure 9 shows the adapter to be used in the 39-foot-high vacuum chamber. Mounted on the end of a ram which goes through the side of the chamber, it provides the spacecraft with electrical, mechanical, and pneumatic connections required during calibration. The adapter contains the calibration targets for the spacecraft cameras and radiometers.

Of extreme importance to the spacecraft as a system is the debugging test, in which every subsystem is operated simultaneously with the other subsystems as in a normal orbit. Primary concerns are malfunctions indicative of wiring trouble or component failure, as well as interferences between the integrated subsystems. This test has already been performed, using preprototype subsystems, and has resulted in many design changes.

After the debugging test, the sensory ring will be given a thermal-vacuum test; following this, the complete spacecraft will be subjected to a humidity test, a vibration test, an acceleration test, a weight

and balance test, and finally a complete series of operational tests in vacuum chamber.

The integration contractor has prepared the overall test plans and scheduled the tests according to the availability of the subsystems. The details of these tests, the philosophy behind them, and governing regulations are explained in other reports in this series.

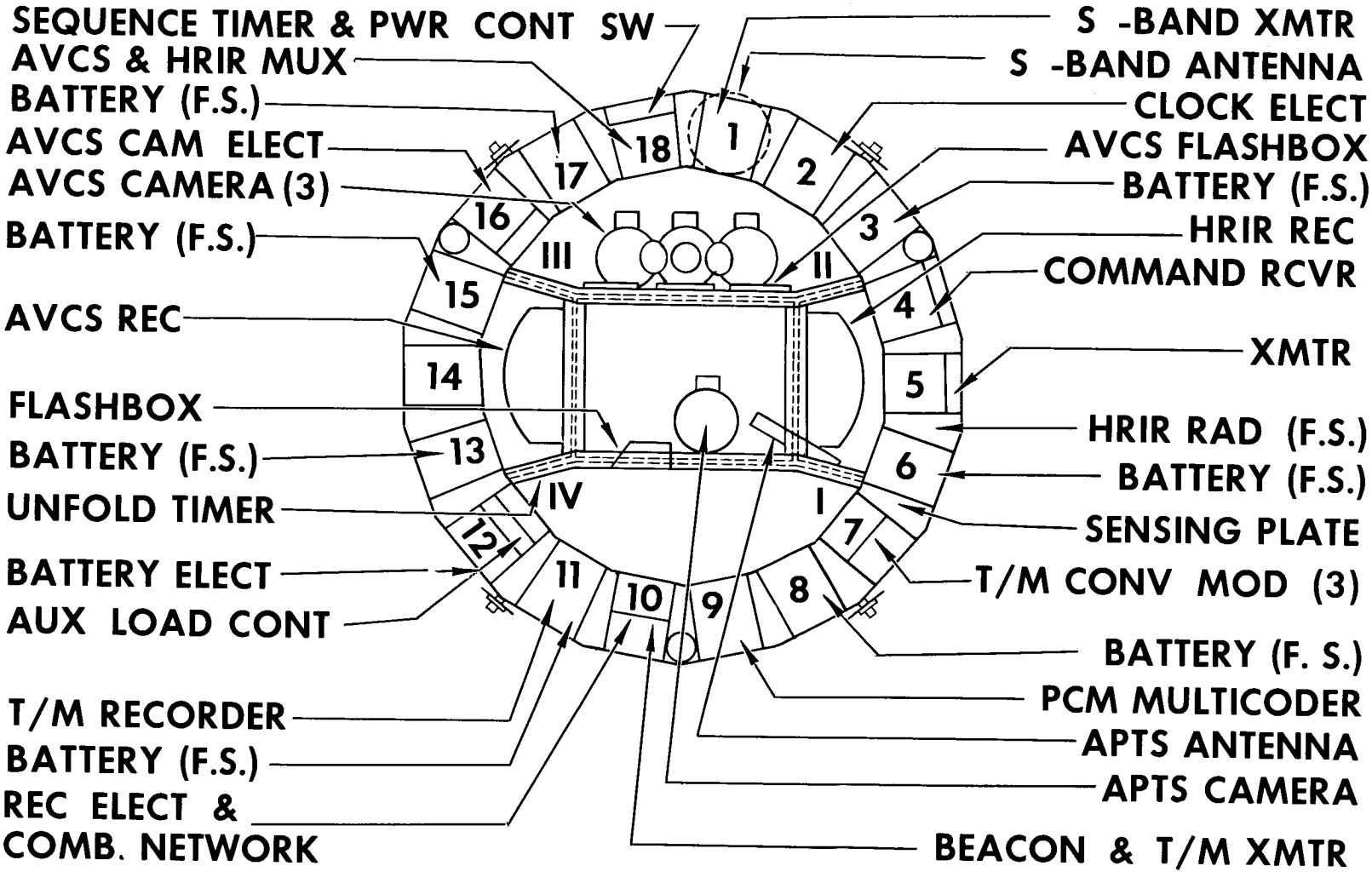

Figure 1 - Nimbus A Component Locations

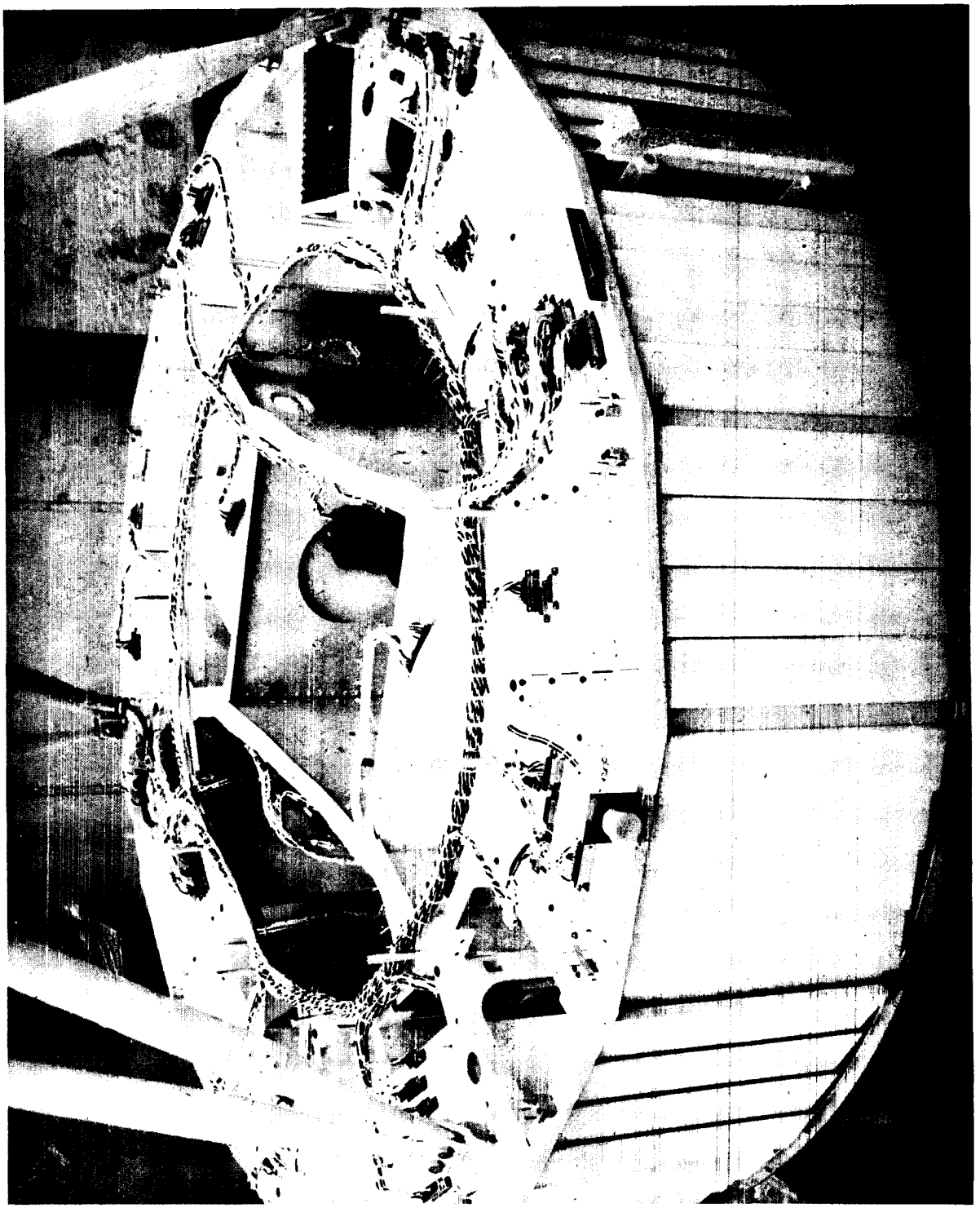

Figure 2 - Sensory Ring Wiring Harness

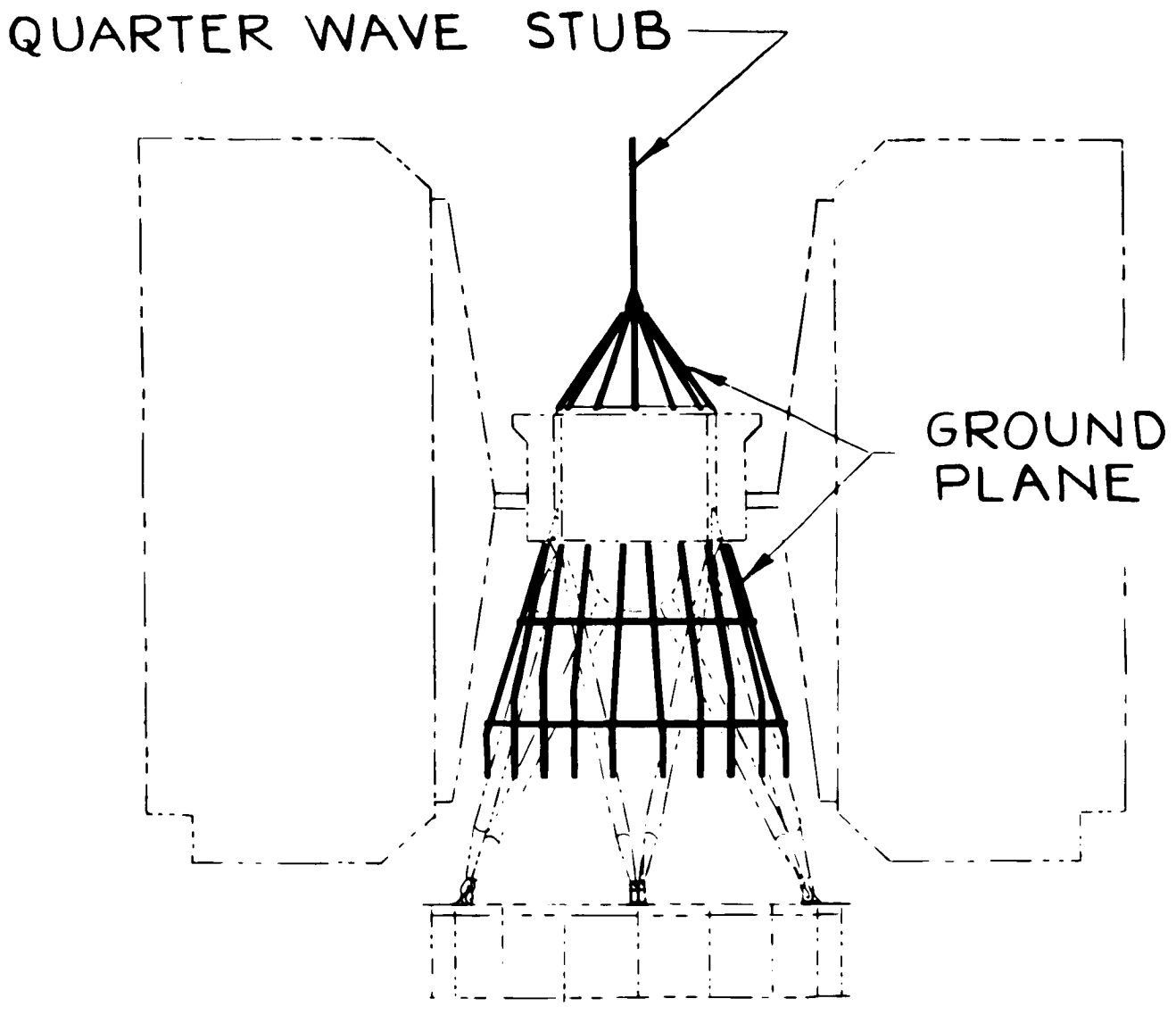

Figure 3 - Command Antenna (122-124 Mc)

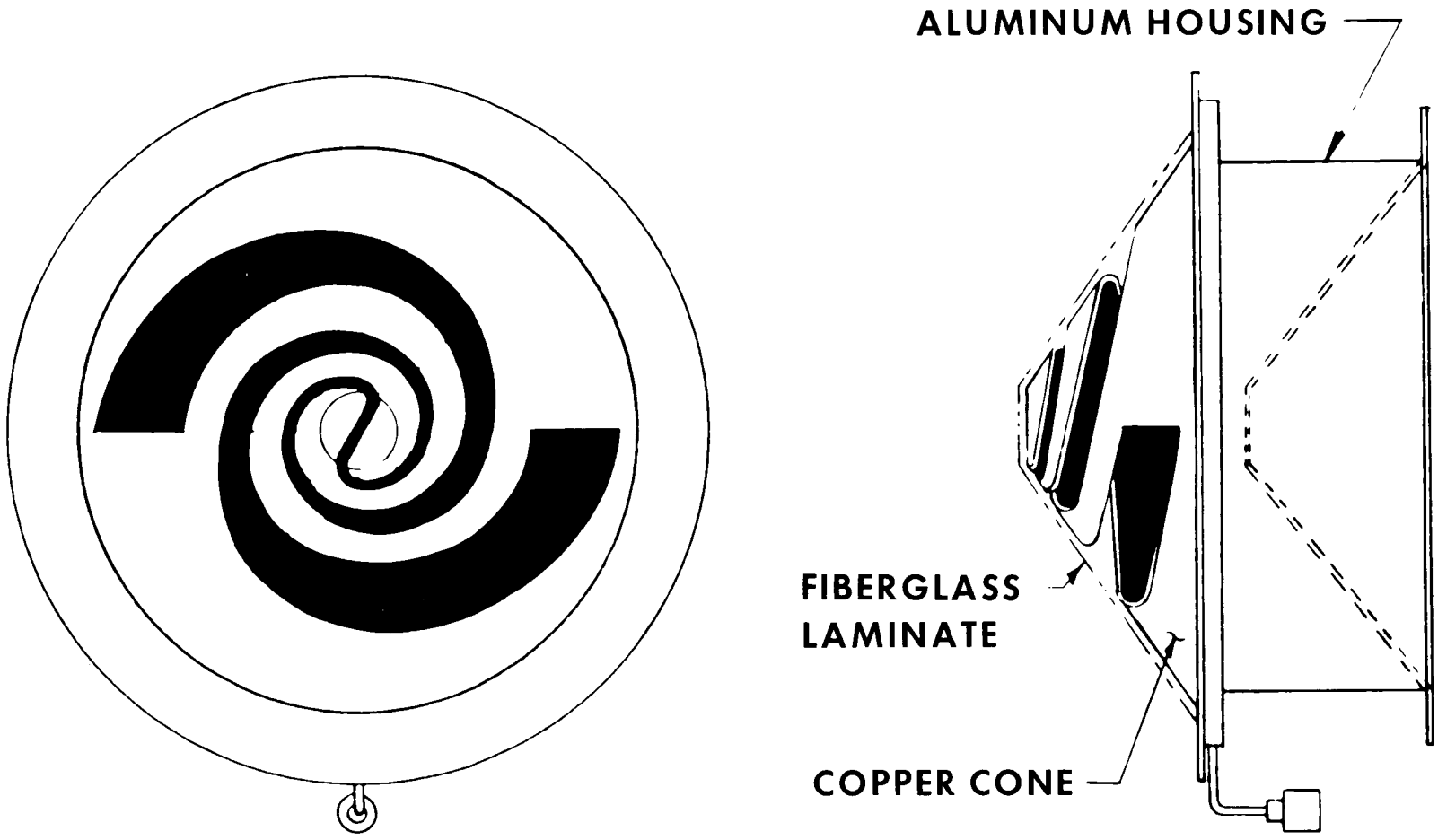

Figure 4 - S-Band Antenna (1700-1710 Mc)

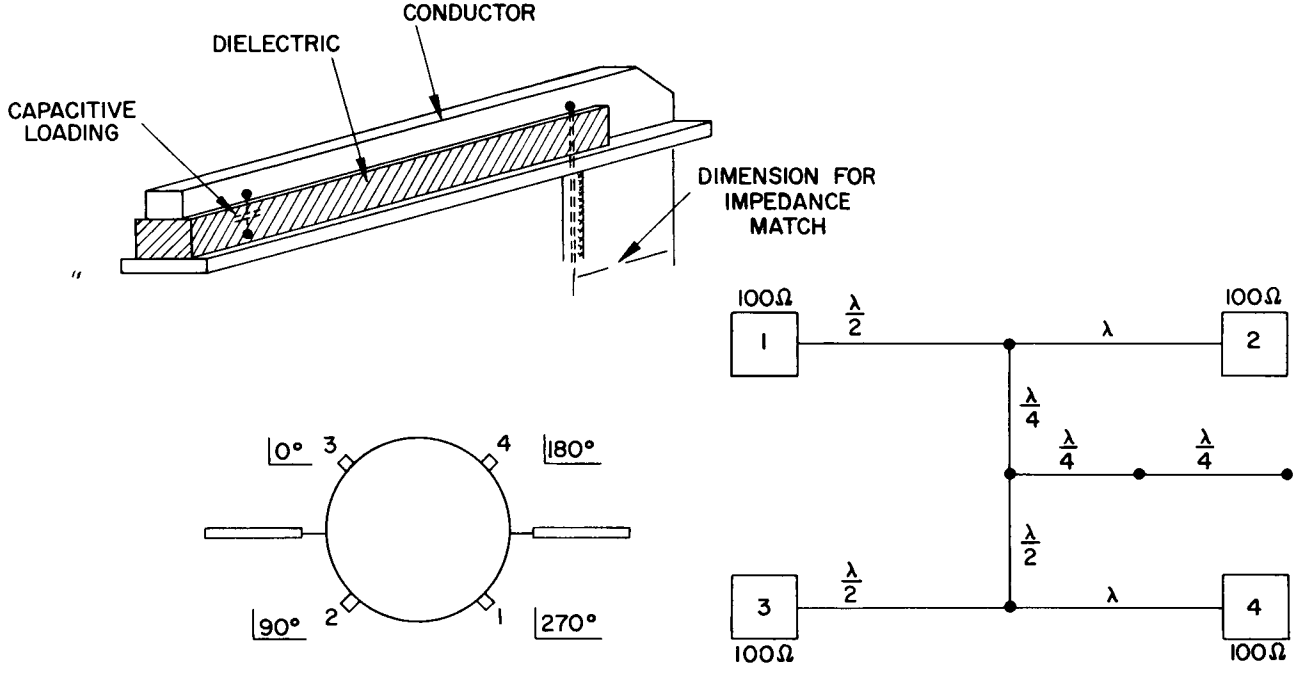

Figure 5 - Nimbus Telemetry and Tracking Antenna

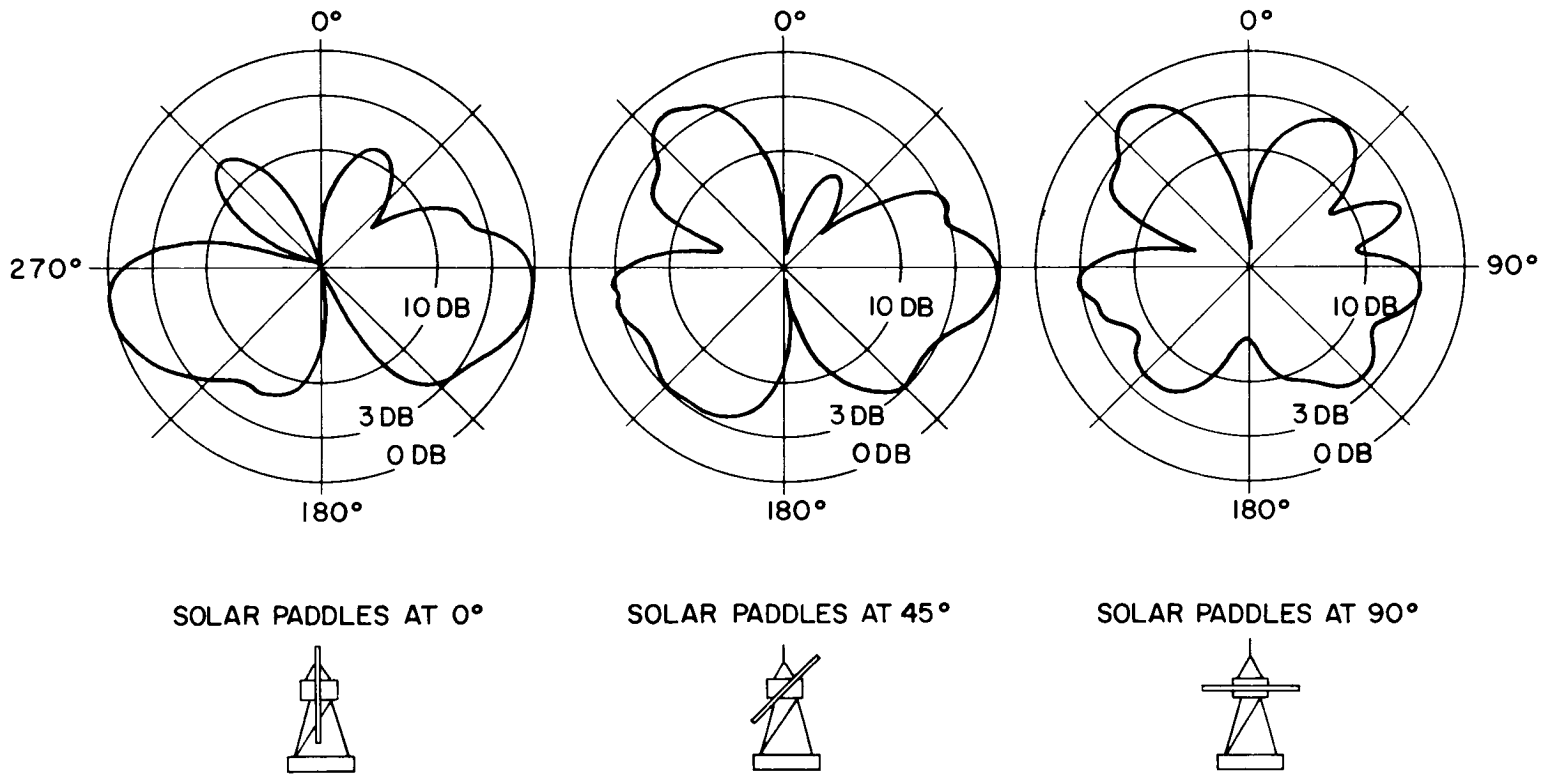

Figure 6 - Nimbus Command Antenna Pattern

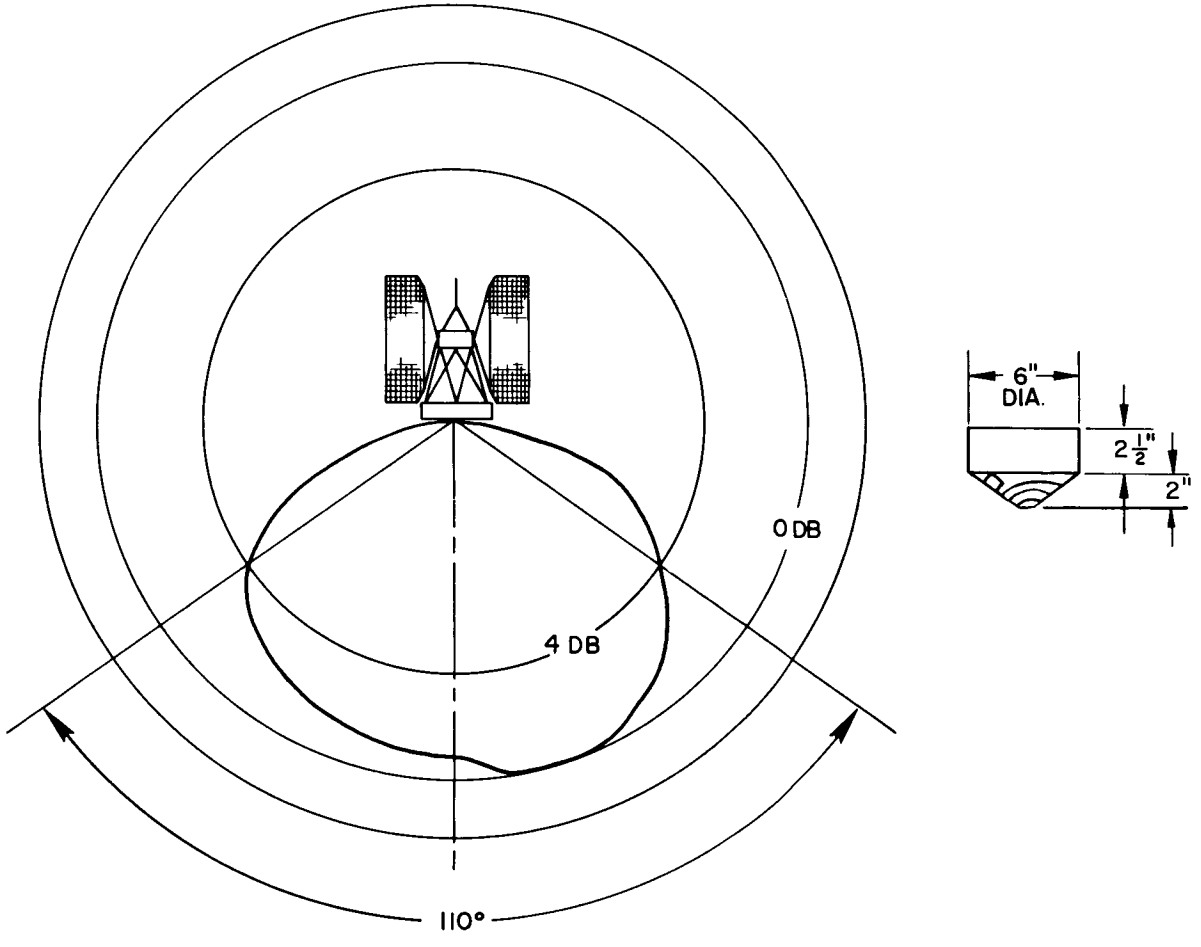

Figure 7 - Nimbus S-Band Antenna and Pattern

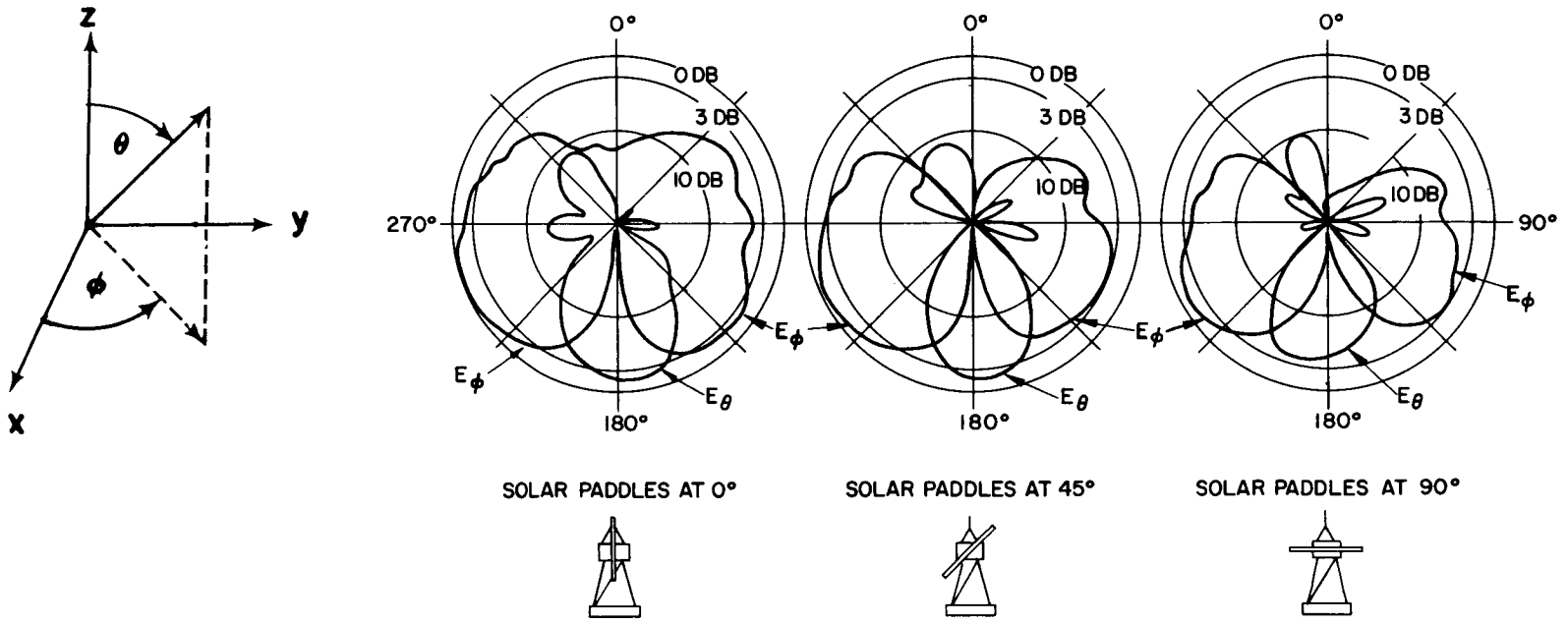

Figure 8 - Nimbus Telemetry Antenna Linear Polarization Components

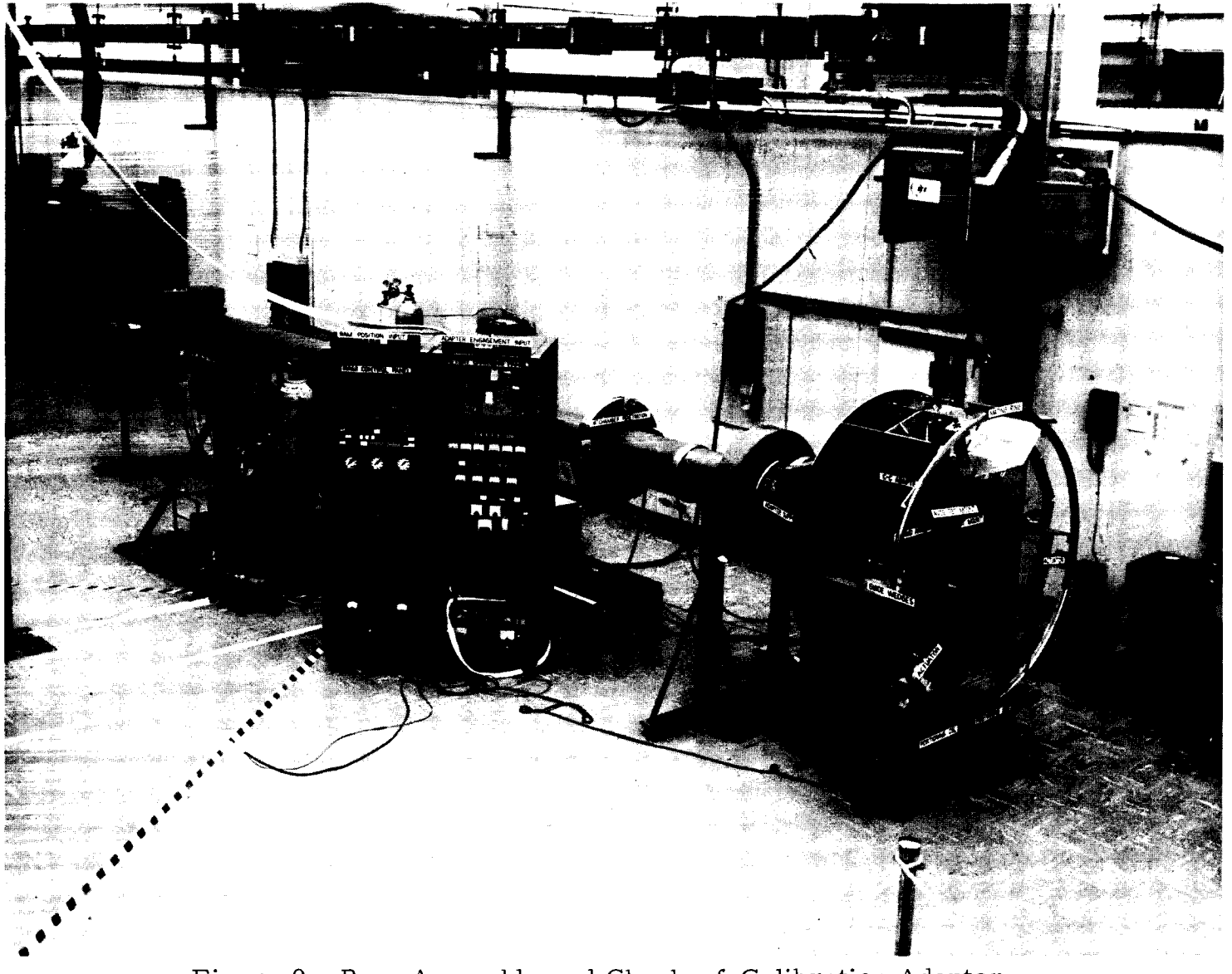

Figure 9 - Ram Assembly and Check-of-Calibration Adapter

13. NIMBUS SOLAR POWER SUPPLY

By M. B. Weinreb and C. MacKenzie, GSFC

13. NIMBUS SOLAR POWER SUPPLY

ILLUSTRATIONS

Figure		Page
1	Nimbus Spacecraft, Artist's Conception	7
2	Battery Modules	8
3	Preprototype Solar Platforms	9
4	Solar-Cell Interconnection	10
5	Solar-Cell Module	11
6	Solar-Cell Component Board	12
7	Battery Module, Showing the Two Major Subassemblies	13
8	Nimbus Storage Cell	14
9	Electronic Module, Showing Unregulated Bus and Regulated Bus Current Telemetry Circuits	15
10	Power Supply, Block Diagram	16
11	Solar Illuminator	17
12	Nimbus Ground Support Equipment	18
13	Power-Supply Subsystem Function Analyzer	19

13. NIMBUS SOLAR POWER SUPPLY

By M. B. Weinreb and C. MacKenzie, GSFC

INTRODUCTION

The solar-conversion power supply is one of the major service subsystems of the Nimbus spacecraft (Figure 1). It consists of a solar array, used to convert the sun's energy into electrical power, and the electronics equipment required to store and convert the power into the form needed by the other Nimbus subsystems. The power supply, although closely associated with the design of the spacecraft structure and control subsystem, was designed as a separate unit to allow for flexibility and interchangeability.

This paper describes the complete Nimbus solar power-supply subsystem, problems encountered in its development, and its current status.

SUBSYSTEM DESCRIPTION

Figure 2 is a picture of the preprototype storage and regulating assembly, consisting of an electronic control module and seven battery or power modules. These modules provide the electrical power while the satellite is in the earth's umbra. The system is designed so that the entire spacecraft electrical load can be supported by six battery modules. Up to two additional battery modules are used to provide for reserve capacity and a certain degree of redundancy.

Some of the major system characteristics are:

(1) Regulated bus voltage of -24.5v, regulated within ± 2 percent of nominal voltage

(2) Transient response of 25 microseconds to a 4-amp changing load

(3) Total system weight of 173 pounds

SOLAR ARRAY

Figure 3 is a picture of the preprototype solar platforms. The solar array consists of two honeycomb platforms and transition sections clamped to the shaft of the spacecraft control system. The platforms and transition sections are designed with a high strength-to-weight ratio, utilizing a 1-mil (. 001-inch) aluminum honeycomb core material covered with a 3-mil (. 003-inch) aluminum foil skin. The platform has one flat face for mounting solar cells; the reverse side tapers from a 1-inch thickness in the center to 1/4-inch thickness at the tip. Total weight of the solar array is 58 pounds.

The platforms, hinged at the transition section, are folded to form a triangular column during the launch phase. As the spacecraft is launched, the paddle-latch mechanism is released and the solar platforms are unfolded by motors located on the transition section. When the platforms are in the deployed position, the control system orients the platforms perpendicularly to the sun's rays. Each platform measures approximately 3 by 8 feet, giving about 45 ft^2 of mounting space; this space is covered with 10, 500 2x2 cm silicon solar cells to gather the sun's energy and convert it into electrical power. The cells are wired in parallel and series combinations to form an array with an average power output of 400w during the sunlit portion of the orbit.

Figure 4 shows details of the interwiring of the cells. The basic building block is a module, consisting of ten cells connected in parallel, with an output of about 1 amp at . 46v. Eighty-two of these modules are wired in series to increase the voltage to about 36v. This is called a solar board, and there are seven solar boards on each platform. The boards are connected in parallel to yield a total current of about 12 amperes.

Figure 5 is a picture of the solar module, ten cells connected in parallel by means of beryllium-copper interconnecting strips. A 6-mil (. 006-inch) microsheet glass cover coated with suitable filters is mounted on each cell to reduce the heating effects of those wavelengths of solar radiation outside the response region of the solar cell.

Temperature extremes of the Nimbus orbit are -80° to 60°C. Because no data were available on the operation of solar cells over this temperature range, especially with regard to life as a function of repeated cycling, a test was conducted to verify the adequacy of the design. The first solar modules received were mounted on a honeycomb test board in exactly the same way as they would be mounted on the solar platform; Figure 6 is a picture of the test board with 32 mounted modules. The test, consisting of 1000 thermal cycles in a vacuum, resulted in fatigue failures of the interconnecting strips. Redesign of the interconnecting strips to incorporate stress relief resulted in no further strip failure; however, new cycling tests revealed a degradation of solar-cell efficiency as a function of the number of cycles. Analysis of this degradation led to the conclusion that the cause is related to a deterioration of the cell contact.

The p-on-n solar cells used for the power supply are made by standard industry techniques; the contacts are formed by a nickel film deposited by an electrolysis nickel-plating process. It was concluded that the degradation could not be appreciably reduced without using solar cells whose contacts are made by the more reliable sintering technique. It was therefore decided to measure the expected thermal cycling degradation and factor it into the design for the Nimbus A spacecraft. All future spacecraft will use solar cells made with the more reliable sintered contacts.

The solar-cell problem was further complicated by the creation of the artificial radiation belt, since considerable degradation results when solar cells are exposed to radiation. To alleviate this problem, the more radiation-resistant n-on-p solar cells will be used instead of the p-on-n type. Schedule demands may preclude making this change in time for Nimbus A.

STORAGE AND REGULATING MODULES

The storage and regulating assembly previously mentioned consists of seven battery modules and an electronic control module. As the seven battery modules are identical, a description of one will suffice. Figure 7 is a picture of a battery module, consisting of hermetically sealed nickel-cadmium storage cells, supporting electronic protection circuitry, and an output-voltage regulator. Figure 8 is a picture of one nickel-cadmium cell. Two problems were presented by this cell

during vibration-testing of the module: internal mechanical failure due to core movement, and leakage of electrolyte through the ceramic-to-metal seals. Experience gained on the TIROS program was used to solve both these problems. The core movement is restrained by use of a crimping technique, as shown in Figure 8; the electrolyte is contained by applying a potting compound over the seal area.

Twenty-three of these cells connected in series form the battery, whose capacity is 3.2 ampere-hours at a nominal output voltage of -28v. A protective charge-current regulator is provided to limit the maximum amount of current supplied to the battery. The electronics module, shown in Figure 9, serves all the battery modules and contains the spacecraft fuses, the regulated and unregulated busses, and the control circuitry for the power systems. Its principal function is to maintain the regulated bus voltage by use of a common feedback amplifier for all of the modules.

SYSTEM OPERATION

Referring to the block diagram shown in Figure 10, the system operates as follows: (As the seven battery modules are identical, only one is shown in detail; the others are represented on the block diagram by dashed lines. Blocking diode protection of each module is also shown in Figure 10.) Power generated by the array, transferred to the storage and regulating system through a set of slip rings, is transmitted to the unregulated bus. The unregulated bus supplies the shunt losses of the power-supply regulating circuitry, and is used to charge the batteries and to establish the regulated bus.

The voltage regulator drops the voltage of the unregulated bus to that of the regulated bus, -24.5v. Regulation of this output voltage is maintained within ±2 percent of nominal by means of a feedback circuit. The voltage level of the regulated bus is sensed by the feedback amplifier which, in turn, supplies drive current for the voltage-regulator control circuits. Thus, fluctuations caused by load changes in the regulated bus voltage are minimized by compensating changes in the output of the voltage regulators.

As the feedback amplifier is critically important in maintaining the regulated bus, a redundant feedback amplifier has been provided to increase reliability. A relay operated by a voltage-comparator circuit is used to switch on the redundant amplifier when necessary. The

voltage comparator senses the regulated bus voltage for high or low limits; if the bus exceeds these limits, a signal is sent to the relay, which performs the switch. A ground override command is also provided to switch to the redundant amplifier if the reference locks in the wrong position.

The charge current to the nickel-cadmium battery is supplied through a limiter which prevents the current from exceeding 1.5 amp; this protective measure is necessary because the variations in array output can produce charge currents greatly in excess of 1.5 amp, which would damage the storage batteries.

Other protective circuits are provided in the battery module. One cell is monitored for pressure; if the pressure is in excess of 500 psi, the charge current is reduced to a trickle of approximately 100 milliamps. Three battery cells are monitored for temperature, and if the temperature of any one exceeds 65°C the charge current is similarly reduced. When normal pressure and temperature again prevail, the full charging rate is resumed. These precautions are necessary to protect the battery from becoming permanently damaged.

Each battery module is also provided with overvoltage protection to protect the circuitry against excessive voltage output from the solar array. This is necessary because solar-cell output is dependent on temperature, and large thermal extremes are encountered in the Nimbus orbit. As the solar array emerges from the earth's shadow, its temperature is about -80°C; at this temperature, the array-output voltage is considerably higher than at the normal operating temperature of 60°C, which is reached after 20 minutes of daylight. The surge limiter protects against this overvoltage condition by dissipating the excess power from the array, thus reducing the unregulated bus voltage.

GROUND SUPPORT EQUIPMENT

Necessary ground support equipment, developed concurrently with the power supply subsystem, consists of:

(1) Solar source illuminator (Figure 11) -- a 36- by 20-inch light source that utilizes xenon and tungsten lamps with appropriate filters and mirrors. The intensity of the light source is 140

milliwatts/cm^2. The spectrum closely simulates the Johnson spectrum. Initial tests of the illuminator indicate that intensity and temperature can be maintained within 4 percent. Figure 11 is a view directly into the light source.

(2) Bench test equipment (Figure 12) -- two 6-foot racks containing a solar-array simulator, load and control circuits, an oscilloscope, a two-channel Sanborn recorder, a differential voltmeter, and a function analyzer shown in Figure 13. This equipment is capable of checking out individual modules or the complete power-supply system. In particular, the function analyzer is able to test the power-supply storage and regulating system when installed and operating in the sensory ring of the spacecraft.

PROGRAM STATUS

A set of preprototype solar platforms has been delivered to the integration contractor and tested on the vibration model. These tests have been successfully completed and are described by Stengard in his report. A complete set of preprototype storage and regulating modules has also been delivered to the integration contractor and used in preprototype sensory ring integration. Operation and compatibility of these modules with all other major subsystems were considered excellent. The prototype modules have now successfully passed prototype vibration testing and are presently undergoing a final qualification test in the vacuum thermal chamber. Technical problems with the solar cells have delayed completion of the solar platforms, but it is estimated that they will be completed by April 1963.

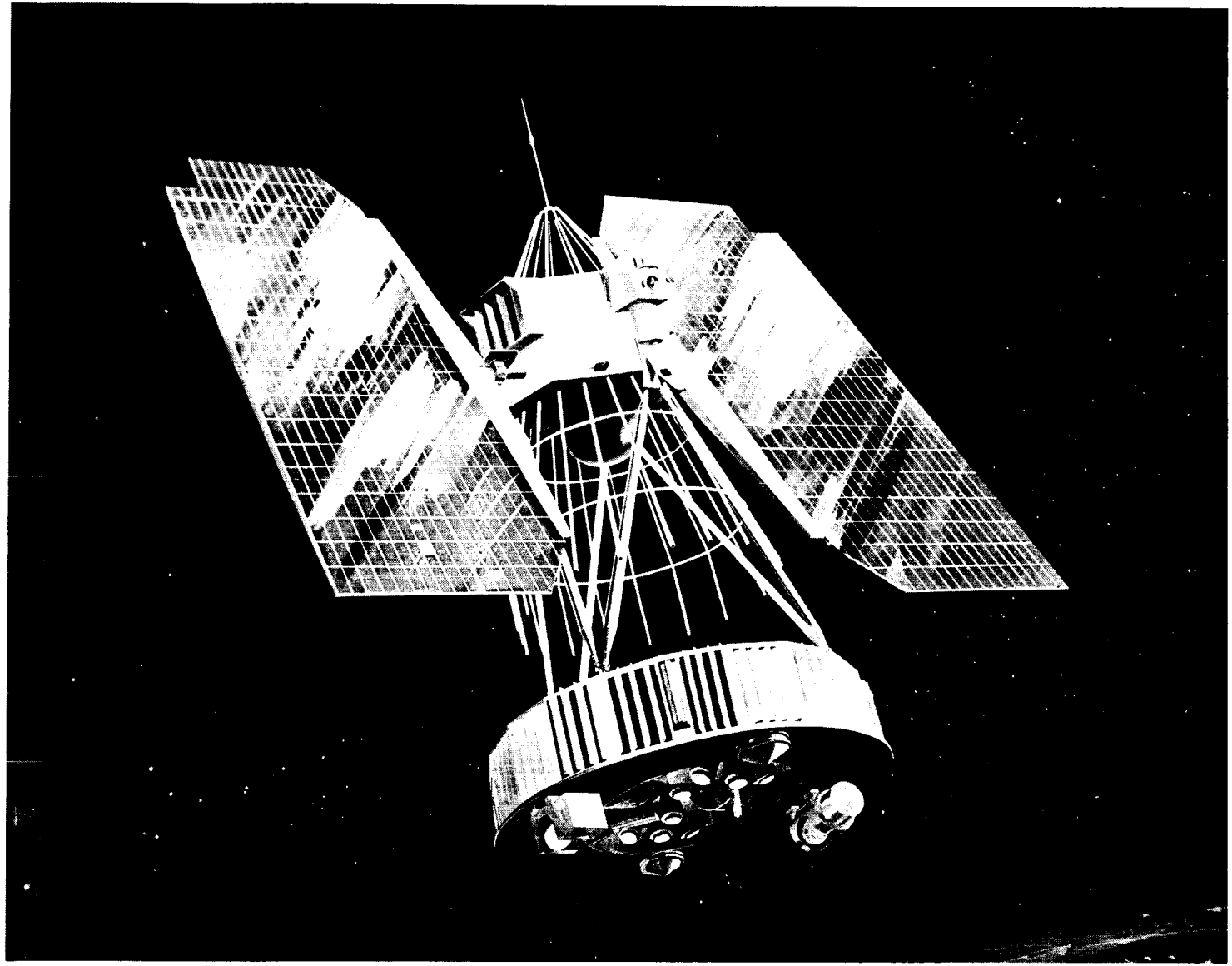

Figure 1 - Nimbus Spacecraft, Artist's Conception

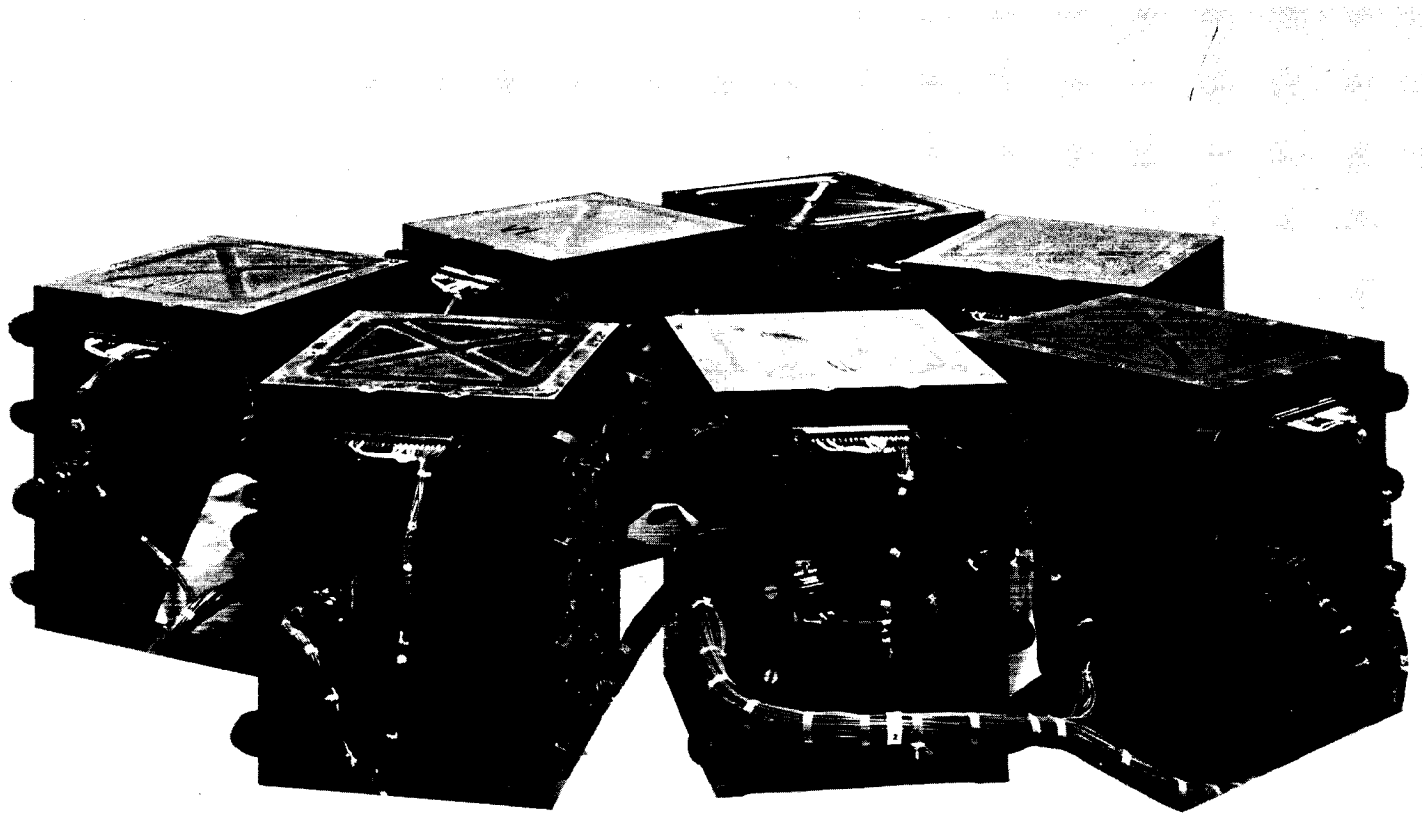

Figure 2 - Battery Modules

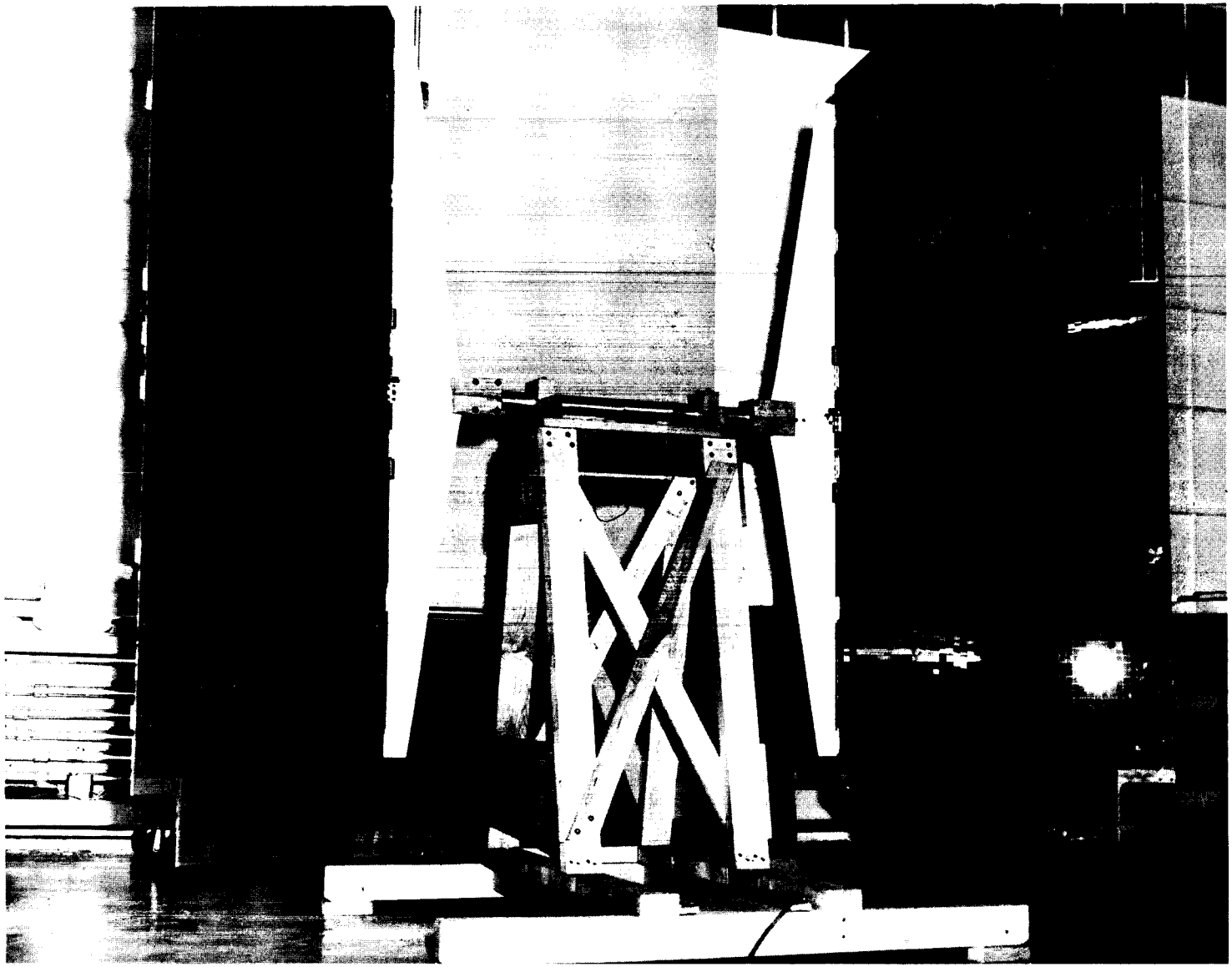

Figure 3 - Preprototype Solar Platforms

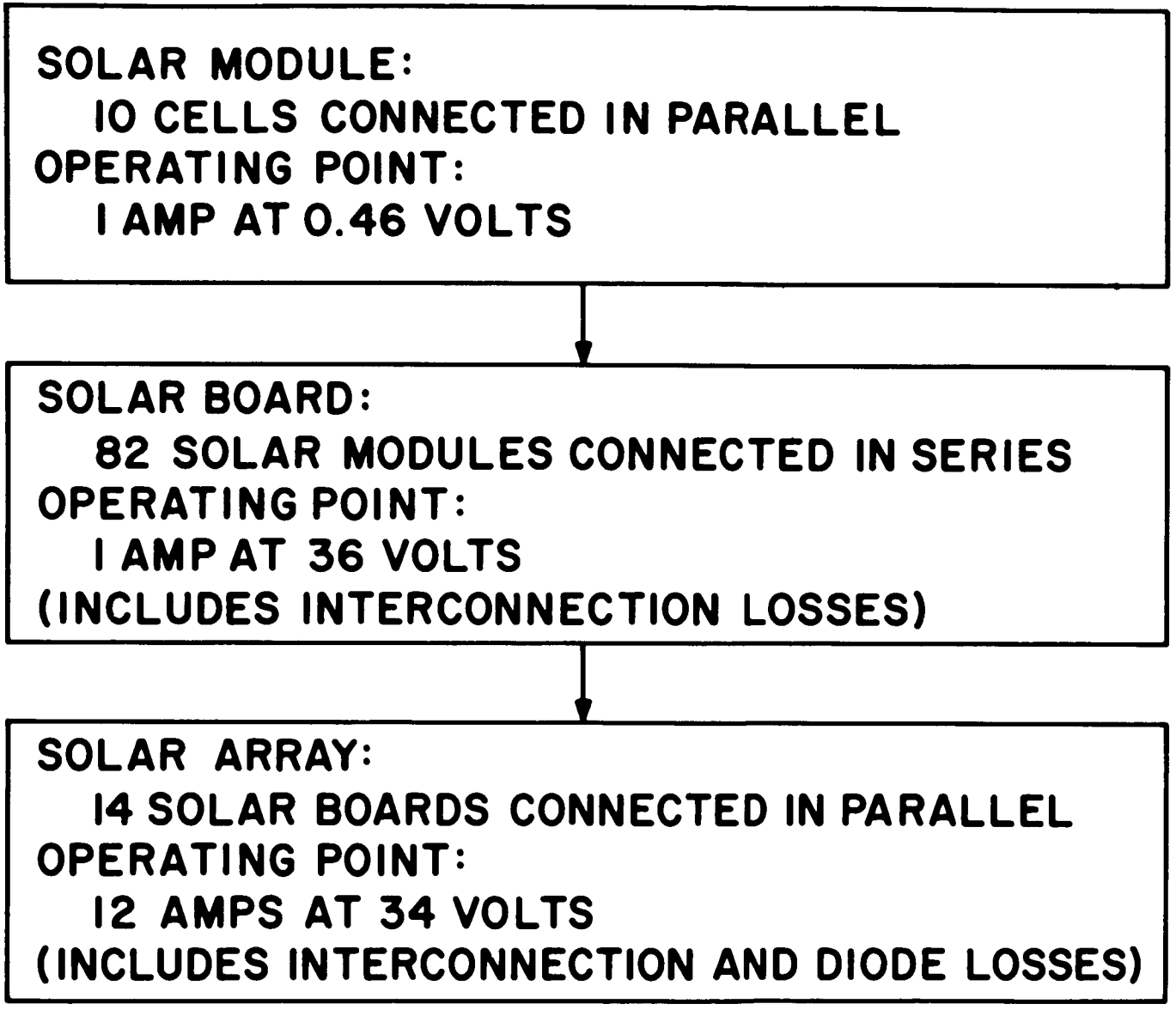

Figure 4 - Solar-Cell Interconnection

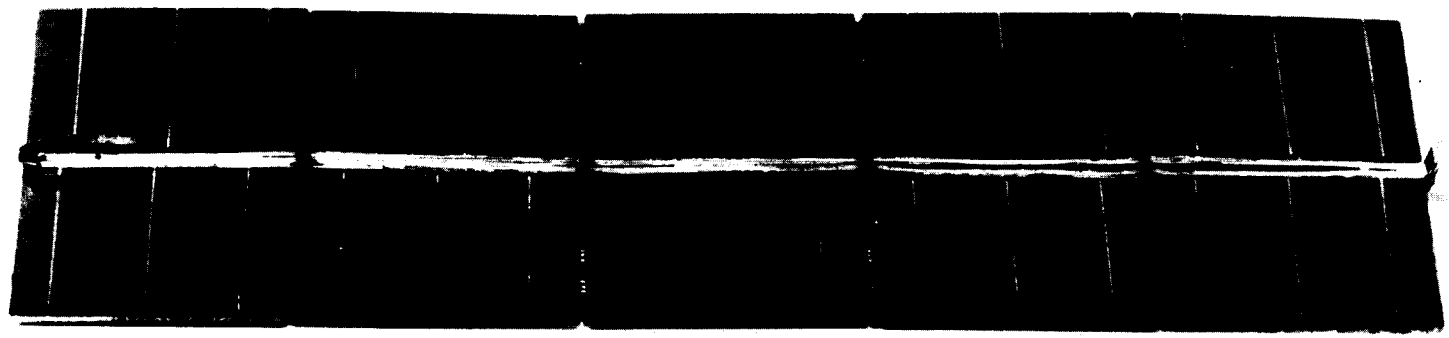

Figure 5 - Solar-Cell Module

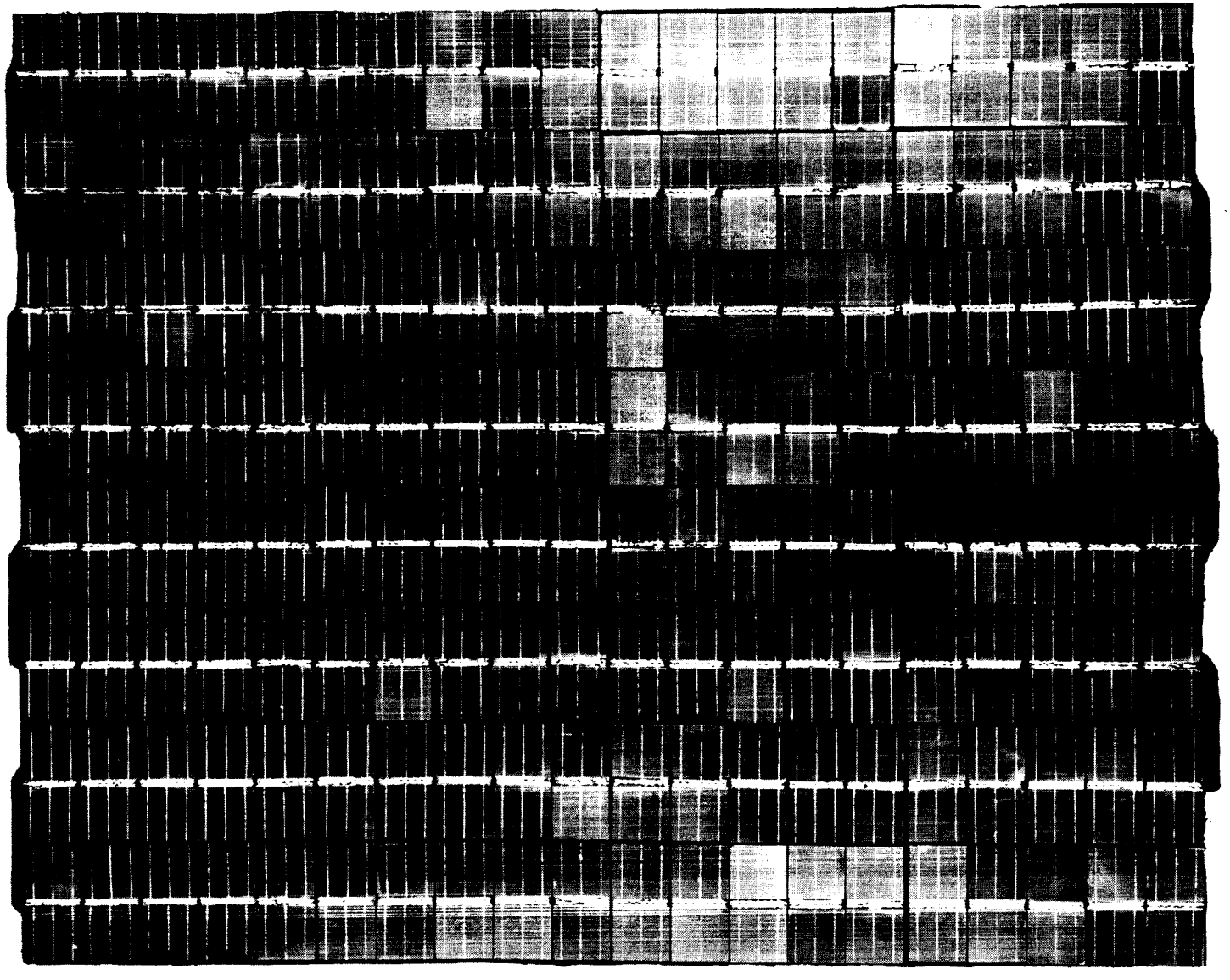

Figure 6 - Solar-Cell Component Board

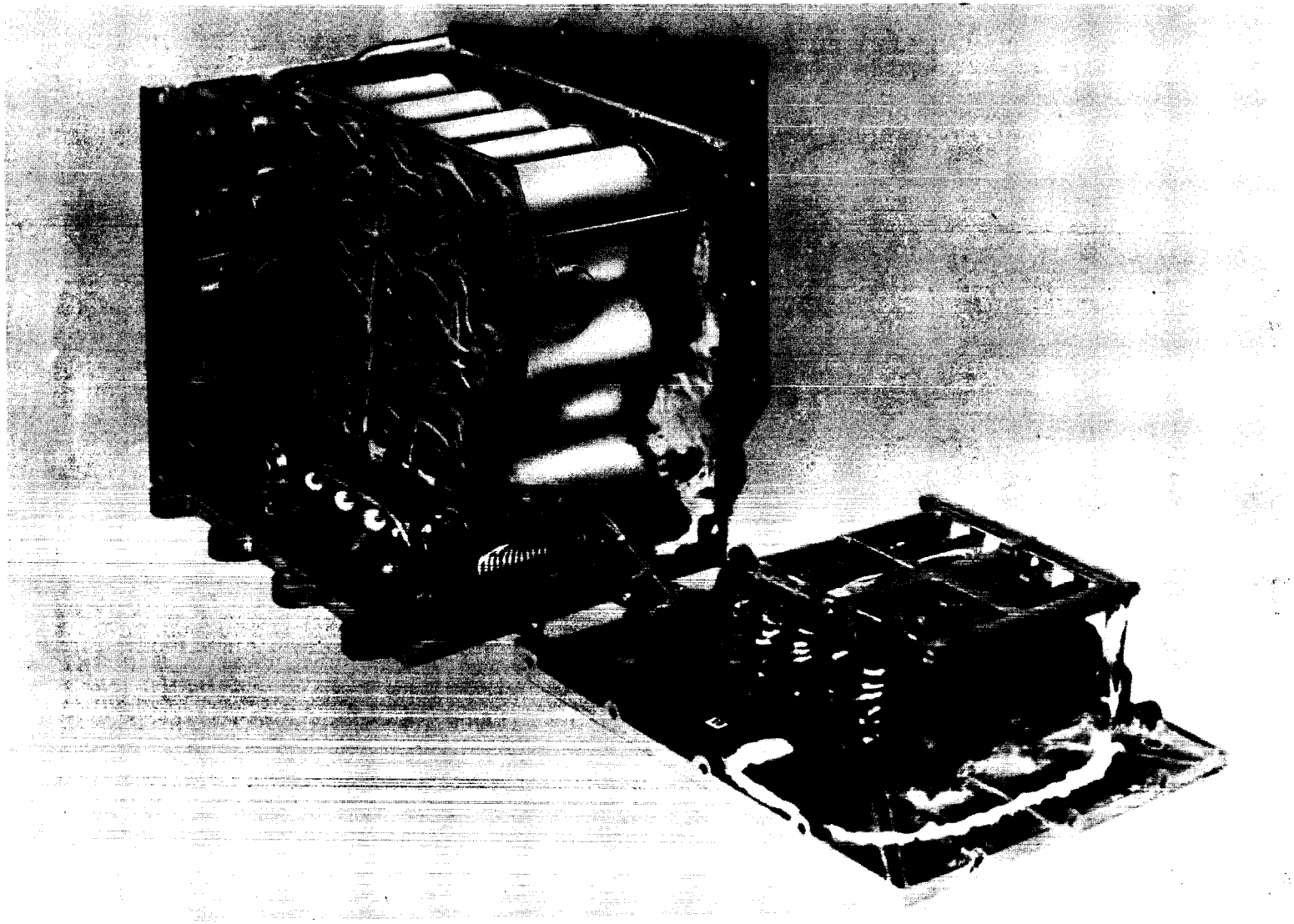

Figure 7 - Battery Module, Showing the Two Major Subassemblies

Figure 8 - Nimbus Storage Cell

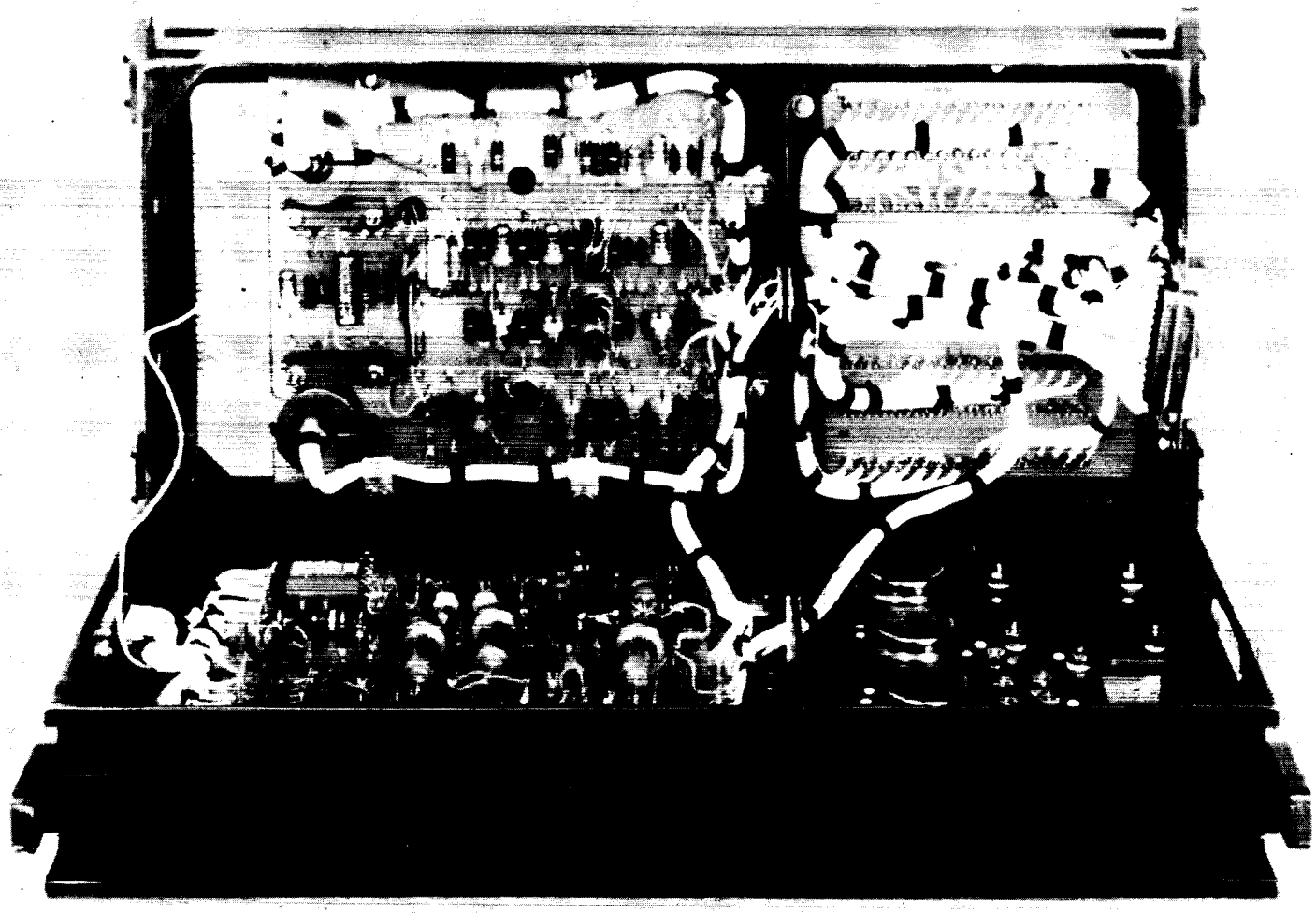

Figure 9 - Electronic Module, Showing Unregulated Bus and Regulated Bus Current Telemetry Circuits

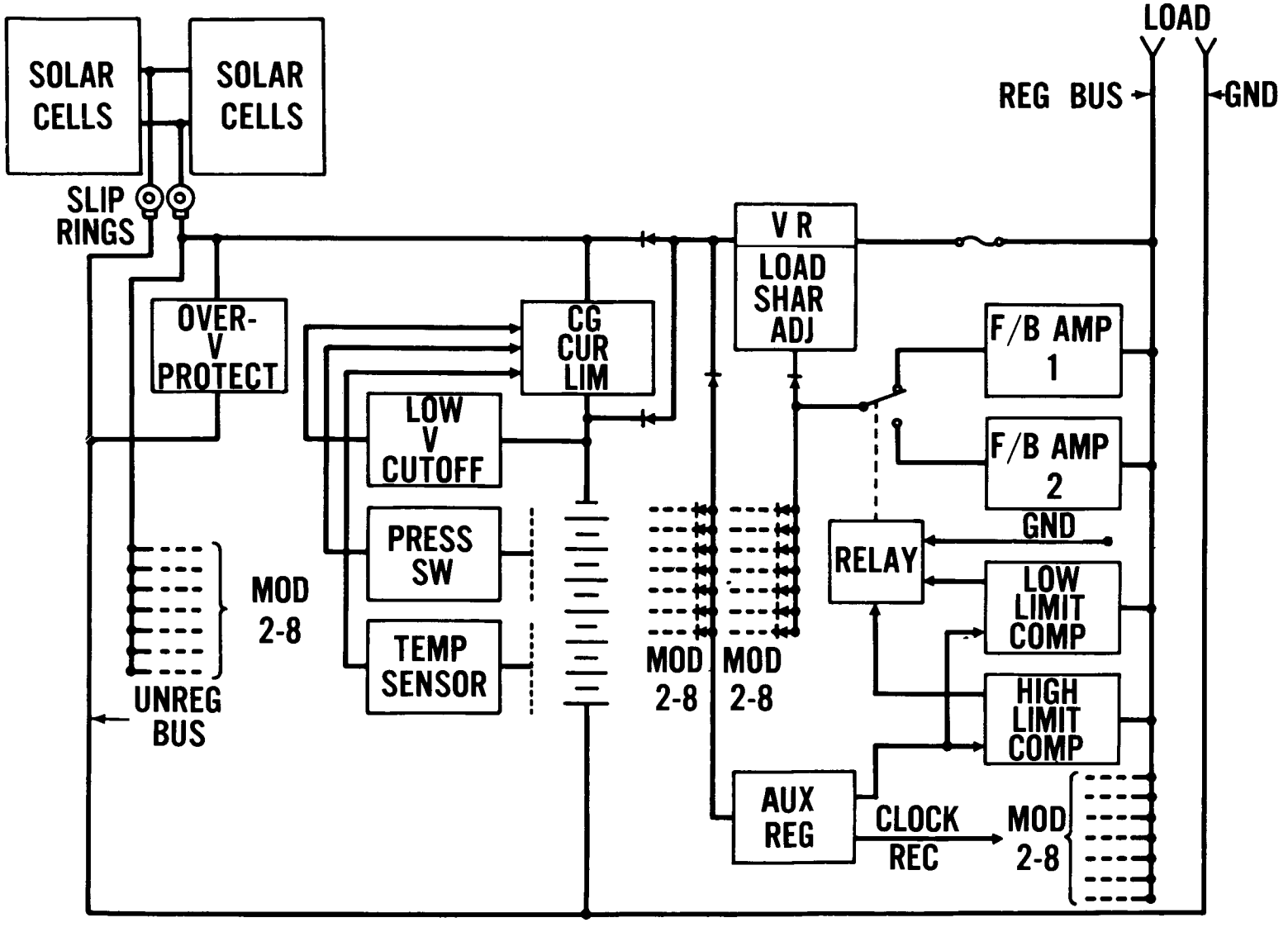

Figure 10 - Power Supply, Block Diagram

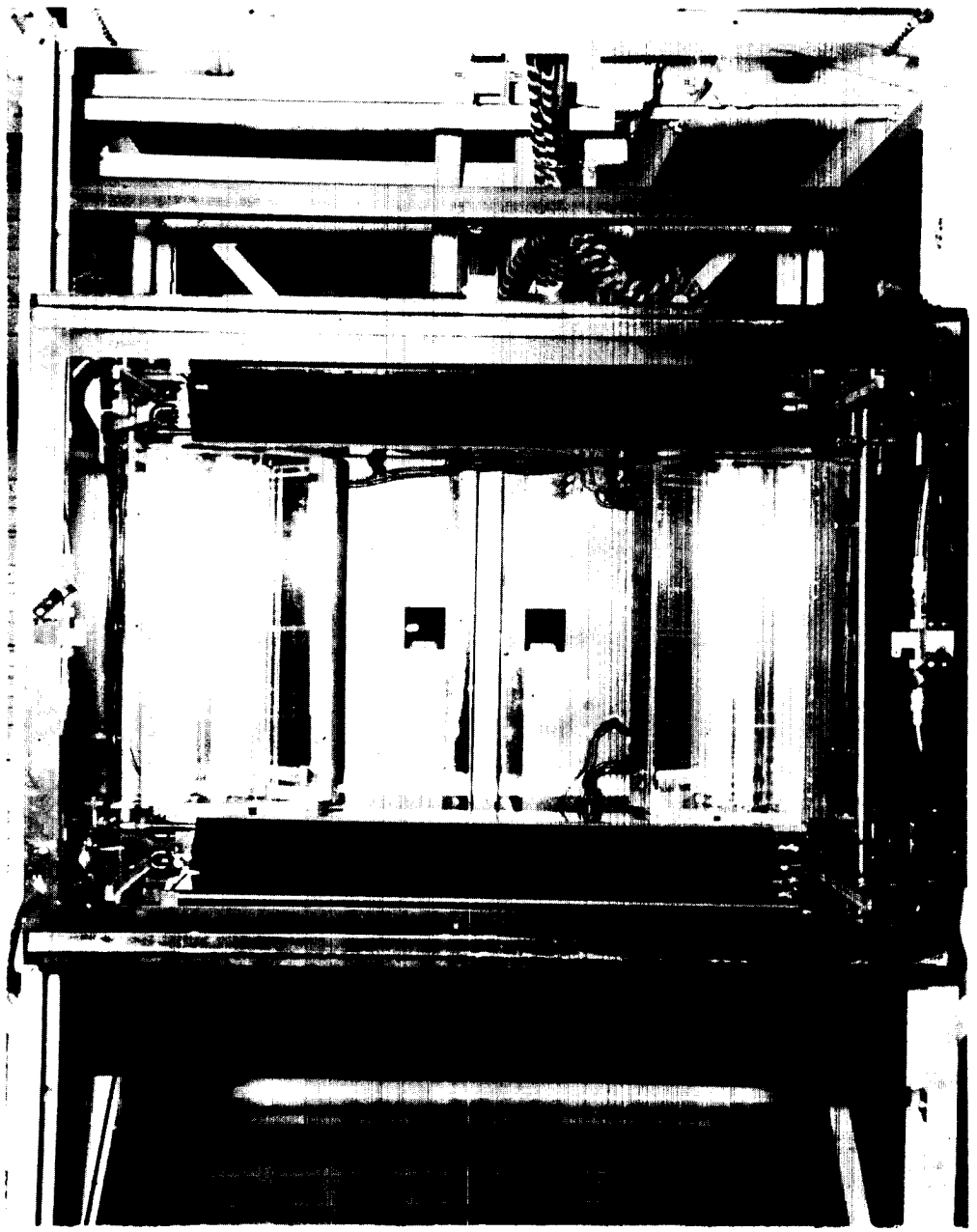

Figure 11 - Solar Illuminator

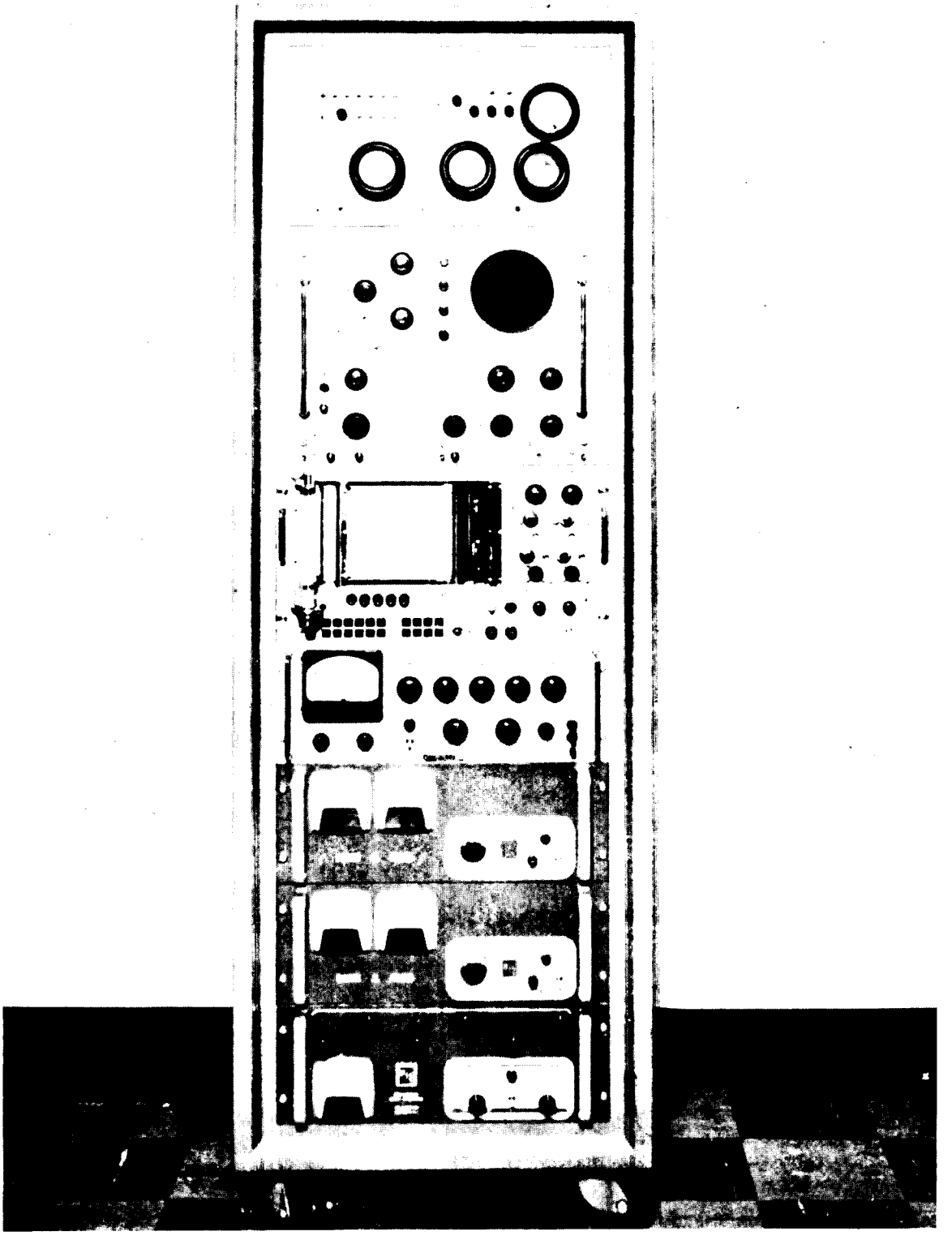

Figure 12 - Nimbus Ground Support Equipment

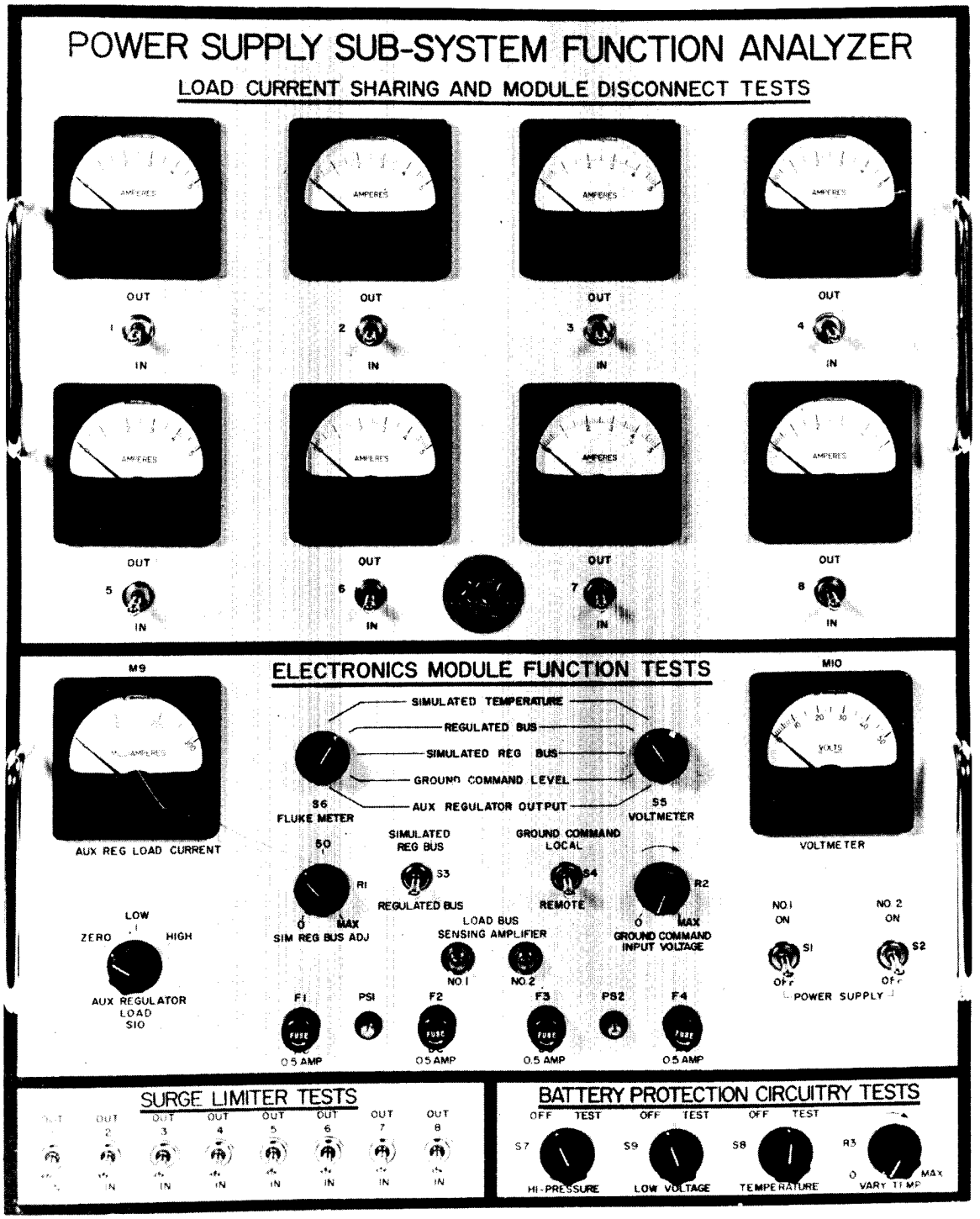

Figure 13 - Power-Supply Subsystem Function Analyzer

14. NIMBUS COMMAND SUBSYSTEM

By J. J. Over, GSFC; D. W. Gade,
R. E. Trousdale, and F. Wiley,
California Computer Products, Inc.;
J. Bunn, RCA/Astro Electronics Division

14. NIMBUS COMMAND SUBSYSTEM

ILLUSTRATIONS

Figure		Page
1	Exploded View of Command Clock	8
2	Typical Logic Mechanization	9
3	Timing Section, Block Diagram	10
4	Command Section, Block Diagram	11
5	Reliability Program Equipment	12
6	Rear View, Etched Board	13
7	Command Clock, Flip-Flop Circuit.	14
8	Clock Receiver Module	15
9	Nimbus Clock Receiver, Functional Blcok Diagram.	16
10	Command Clock, Ground Station Equipment	17

14. NIMBUS COMMAND SUBSYSTEM

By J. J. Over, GSFC; D. W. Gade
R. E. Trousdale, and F. Wiley,
California Computer Products, Inc.;
J. Bunn, RCA/Astro Electronics Division

INTRODUCTION

All satellites have one common requirement, known as the command facility. This is usually a real-time direct RF link from a ground transmitter through the satellite receiver and decoder to a relay or controlled circuit. The more sophisticated research and operational satellites require a command facility which will permit storing of commands to activate systems at predetermined future times when the satellite is beyond the range of the command ground station. These satellites require an accurate clock and a source of precision frequencies.

In the Nimbus spacecraft, all these functions are performed by an integrated command and clock subsystem, which includes the command-clock and clock-receiver modules in the spacecraft, plus the associated command ground station. This paper will describe the functions and features of these various equipments.

SPACECRAFT PORTIONS OF COMMAND SYSTEM

COMMAND-CLOCK SUBSYSTEM

The Nimbus command clock, developed and fabricated by California Computer Products, Inc. (CALCOMP), functions in the spacecraft as the final stage in the command link. It also provides precision frequency outputs and serves as the satellite clock. To maintain a minimum component usage, mutual dependence of logic circuitry is maximized in the command clock to provide these independent functions.

Figure 1 is an exploded view of the command-clock module, a 4/4 Nimbus module weighing 18 pounds and dissipating a maximum of 7 watts. The package is a magnesium casting into which are mounted conventional etched circuit boards, a chopper power-supply submodule, a precision oscillator submodule, and the two magnetostrictive delay lines used for the recirculating store-memory functions.

Figure 2 is a diagram of the command clock, a digital subsystem using precision synchronous-logic techniques. The logic mechanization is accomplished by germanium transistor flip-flops and silicon diode gates together with germanium transistor logic drivers and inverters. In this phase of the project, the CALCOMP designers drew on their previous experience in the Minuteman project. This mechanization is typical of much of the circuitry in both the command clock and the ground station.

The input and output interfaces of the command clock are handled primarily with germanium and silicon transistor switching amplifiers. Wherever possible, the -24.5 vdc spacecraft regulated-bus voltage is used directly; however, to conserve power, lower dc voltages are provided by the chopper power supply.

The command clock has two major functions: timing and command. The timing section provides the precision frequencies and the spacecraft clock. The precision frequencies are mutually coherent square-wave outputs which are free-running, and in no way connected with the ground control.

In the timing section, shown in Figure 3, signal frequencies above 100 cps are generated by flip-flop counting chains which count down from the precision oscillator. The precision oscillator is a conventional quartz-crystal type with proportional oven control. Long-term oscillator stability of better than one part per million is expected.

Signal frequencies below 100 cps are generated by using the T-loop (Time Loop) delay line to count pulses and report overflows. The T-loop with its associated logic circuitry also provides the command-input buffer register, plus time storage and time-code generation. The time used to initiate commands is stored in a portion of the T-loop, and is constantly updated with an accuracy determined by the precision of the oscillator.

The command section reciprocates by supplying the timing section with the capability to reset the time to within 0.5 second of ground time upon orders from the ground station. The time is stored in the T-loop in standard time nomenclature, from 1 second to 999 days, and is made available in a special coded form to the command-clock interface. For these interface outputs, the code is transformed to a pulsewidth-

modulated format at 100 pps. It appears as a direct output, or on carriers of 10 and 50 kc modulated 50 percent with the code.

A second major function of the command clock is the command facility, Figure 4. Command signals are transmitted to the command clock on three separate input lines which transmit simultaneously to provide command data as well as bit and parity synchronization.

A command message contains the command number, time of execution up to 24 hours after transmission, and memory location for storage, plus flag and identity codes. For example, a command message might be as follows: "Execute command number 120 at 18 hours 32 minutes and 16 seconds ground time, and store in memory location two." Thus, when orbital parameters are accurately known, a satellite system can be activated at any desired point in the orbit.

As shown in Figure 4, the three command signals pass into an input amplifier and sequencer section which inserts the data into the input buffer register, which is a portion of the T-loop. While being inserted into the register, the data is checked for proper format and parity. If at any time an illegal code is received, or parity does not check, the register is dumped and the entire message must be repeated. Command messages are transmitted at a rate of two per second, and each message is transmitted twice, in sequence, to assure reception. At the conclusion of each satisfactory command message, the information is inserted into the memory location in accordance with the address given in the message. A maximum of five commands can be stored in the memory, or M-loop, delay line.

When the satellite-clock time carried in the T-loop agrees with the instruction time, the associated command is executed. Execution may involve up to 128 individual command operations in the satellite. The command clock communicates these instructions to the other satellite subsystems through an 8 by 16 matrix. The matrix drivers have sufficient capacity to drive conventional latching relays. Satellite functions such as AVCS, record, playback, direct picture, camera selection, and iris opening may be controlled through the coded command system. On-off control of experiments, interrogation for stored data, and beacon-transmitter selection are provided. In the telemetry subsystem, the mode of telemetry is chosen through the command link, as is the interrogation for data stored in the PCM tape recorder.

Because of the expected high count of components in the command clock, a special in-house component-reliability program was initiated by CALCOMP at the beginning of the development to select component types; specify production lots; age components; measure parameters, and process parameter data. Silicon components were aged at 100°C and germanium components at 55°C for periods up to 2000 hours. Parameters were measured by electronic test equipment built specifically for this purpose, shown in Figure 5. The test equipment automatically sequences from component to component, measures up to eight parameters, and simultaneously prints out the measurements on IBM punched cards. The resulting data is then processed by digital computers which supply data on parameter shifts as well as parameter distributions.

The command clock incorporates an unusual and very effective thermal design, shown in Figure 6. Semisolid copper planes are permitted to remain on the etched circuit boards after the etching operation; these planes, in close proximity to component leads, serve as effective heat sinks to all components. The copper planes are terminated at the top of each etched board to aluminum straps which, in turn, are terminated directly to the casting. Using this design, the temperature difference between the hottest transistor junction and the coldest mounting bracket of the casting is less than 13°C.

The command-clock flip-flop, Figure 7, is a good example of the circuitry developed specifically for this job. The flip-flop uses six micro-energy germanium transistors and dissipates 15 milliwatts. The input buffers save additional gate power, and the output buffers eliminate false triggering due to noise. In all, the command clock uses only 42 flip-flops, at a maximum speed of 800 kc, to perform all of the functions described previously.

COMMAND-CLOCK RECEIVER

Command messages in coded form come to the command clock from the ground by way of the clock receiver. These coded signals are transmitted to the satellite by FM/AM transmissions in which three frequency-shift-keyed subcarriers are multiplexed to amplitude-modulate a radio-frequency carrier. The clock receiver amplifies, demodulates, and processes these signals for subsequent input to the command-clock subsystem.

The clock receiver, shown in Figure 8 with dust covers removed, was developed and fabricated by the Astro-Electronics Division of the Radio Corporation of America. The receiver, contained in a module, weighs approximately 5.6 pounds and consumes less than 1 watt of power. This module also contains the redundant, ultrasensitive, highly selective AM receivers, the two redundant FM-subcarrier demodulators, and the AM tone demodulator.

Figure 9 is a block diagram of the RCA clock receiver. When encoded commands are being transmitted to the command clock, the three FM subcarriers are used; the subcarriers are demultiplexed with filters and are amplified, limited, and fed to the discriminators. The discriminator outputs are coupled to Schmitt triggers which square up the binary signals.

The audio outputs of the parallel, continuously operating receivers are also resistively added and fed to the AM subcarrier-demodulator section, where four single-tone emergency backup commands are produced. The normal command receiver and FM subcarrier-demodulator are used unless failure occurs. Should either the normal receiver or FM demodulator fail, redundant equipment contained in the module can be made operative by switching on the power with one of the single-tone commands. The FM demodulator outputs are "or" gated into the code output lines. Power for the auxiliary receiver and AM demodulator is supplied by special auxiliary regulators, so that these portions will operate even if the main regulators should fail. The other single-tone commands provide emergency telemetry readout, activation of backup power-supply feedback amplifier, and turn-off of the S-band transmitter. Satisfactory commands can be received with less than a 3-microvolt RF signal at the clock receiver RF input terminal.

Reliability was the principal design criterion for the clock receiver. This receiver, which provides the command link with the satellite, must operate at all times if the satellite is to fulfill its mission. To obtain the necessary reliability, the clock-receiver design specified maximum use of extremely high-reliability components, and selection of components on the basis of proven performance. As an example, the AM receivers are similar to those used on TIROS. Redundant receivers and demodulators were included when studies indicated that they were required to achieve the desired reliability goal. Subsystem simplicity was emphasized throughout to obtain inherent reliability, and all components were baked and checked carefully.

All prototype and flight models of the clock receivers and the command-clock subsystems have been subjected to, and have successfully survived, the severe environmental testing specified for all Nimbus spacecraft equipment. Bench checkout equipment, specifically designed for the purpose, is provided for both the command-clock and clock-receiver subsystems. This equipment contains all items necessary to rapidly determine the operating condition of the spacecraft subsystems. Test procedures have been developed to assure consistency of test methods.

EARTH-BASED COMMAND GROUND STATION

The command-clock ground station, Figure 10, was designed and fabricated by California Computer Products, Inc., concurrently with the development of the spacecraft command-clock subsystem.

Reading from the left in the figure, the command ground station contains a tape-preparation and readout bay, a control console, a modulator-verification bay, a clock-computer bay, and a transmitter bay.

Normally, the encoded command programs are prepared and stored on punched paper tape. If desired, operation of the ground station can begin automatically when the satellite comes into view of the command antenna; however, commands can also be generated immediately by the operator at the control console. The encoded command messages are transformed into frequency-shift-keyed signals on the three FM subcarriers in the modulator bay, for transmission to the satellite by means of the command transmitter. The four single-tone commands are also generated in this ground station.

In addition to the above capabilities, the command ground station can independently verify the transmitted messages and provide a permanent record of all transmissions. It also accepts the satellite time code from the beacon, compares the satellite time to ground time, and prints out the difference as a permanent record. Simultaneously, the ground-station clock is synchronized with the satellite clock so that present-time commands can be easily generated. The ground station facilitates the present-time command operation by automatically inserting satellite or ground time plus 3 seconds into the command message, when so directed. This results in the execution of the command 3 seconds after transmission to the satellite. (All commands are future commands;

present-time commands are just in the very near future.) Accurate time is maintained at all command sites by time-code generators, designed and fabricated by NASA, and by associated WWV receiving equipment.

PRESENT STATUS OF NIMBUS COMMAND SUBSYSTEM

The entire command system has been in a "go" status since early in 1962.

CALCOMP delivered the first qualified prototype command-clock subsystem and bench test equipment in late December of 1961. Another qualified prototype, and five qualified flight-model, command-clock subsystems followed in rapid succession thereafter.

In addition, CALCOMP has delivered three command ground stations: one for the launch van in February 1962, one for integration in April 1962, and the Alaska CDA station in May 1962.

RCA delivered the first qualified prototype clock receiver and bench test equipment in March, 1962, followed in rapid succession by a second qualified prototype, and two qualified flight-model, clock receivers.

Complete operation and maintenance documentation has been delivered for all of this equipment.

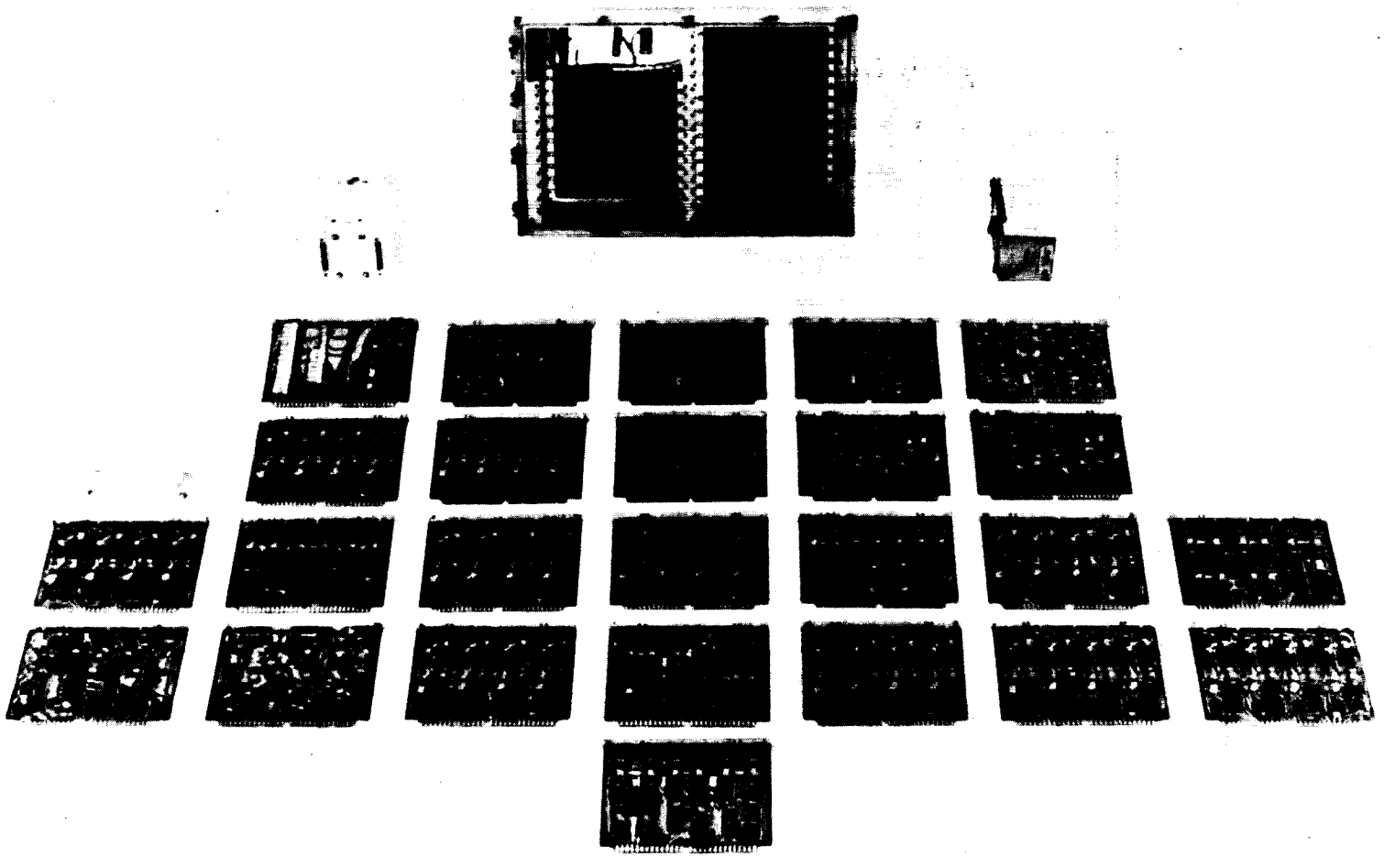

Figure 1 - Exploded View of Command Clock

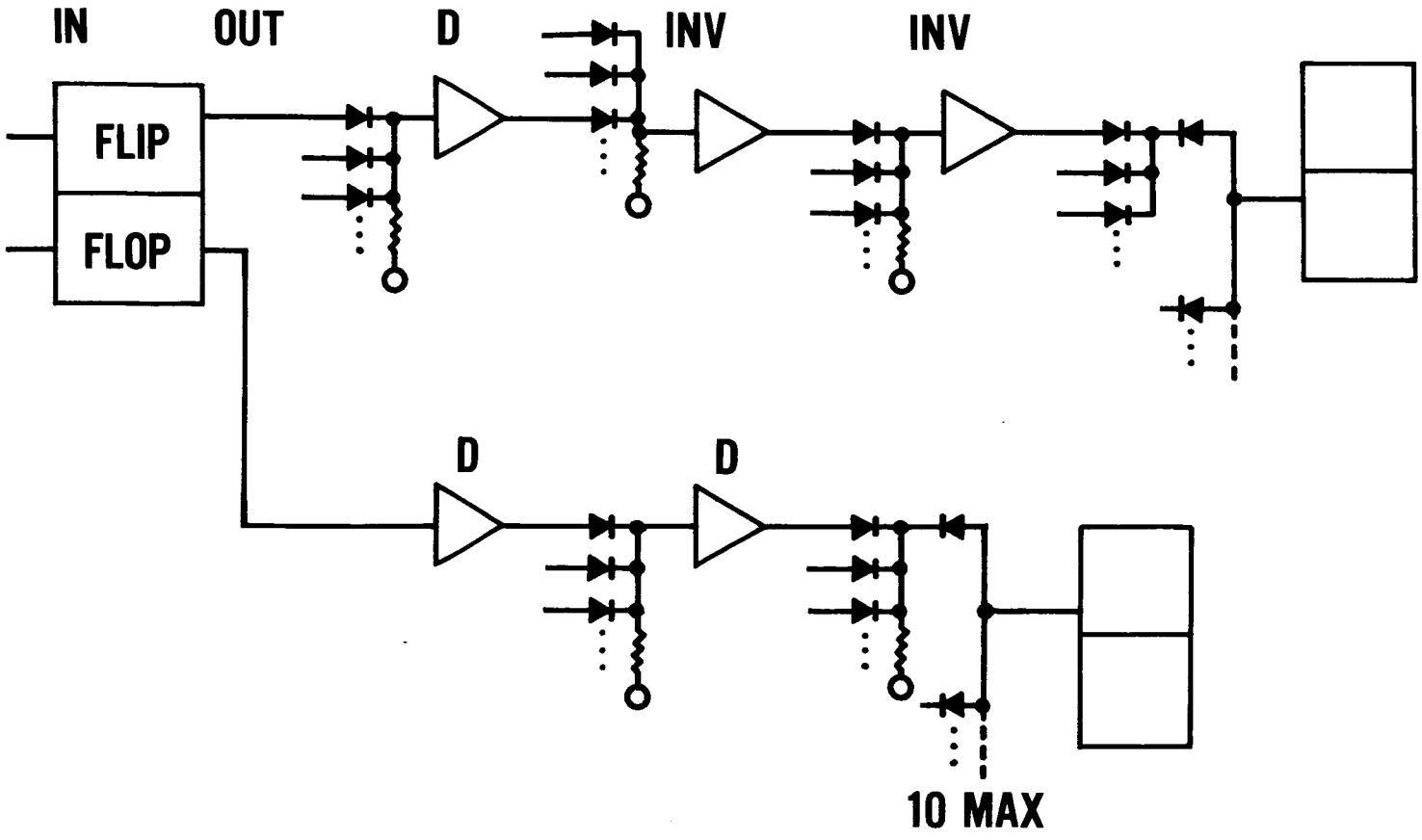

Figure 2 - Typical Logic Mechanization

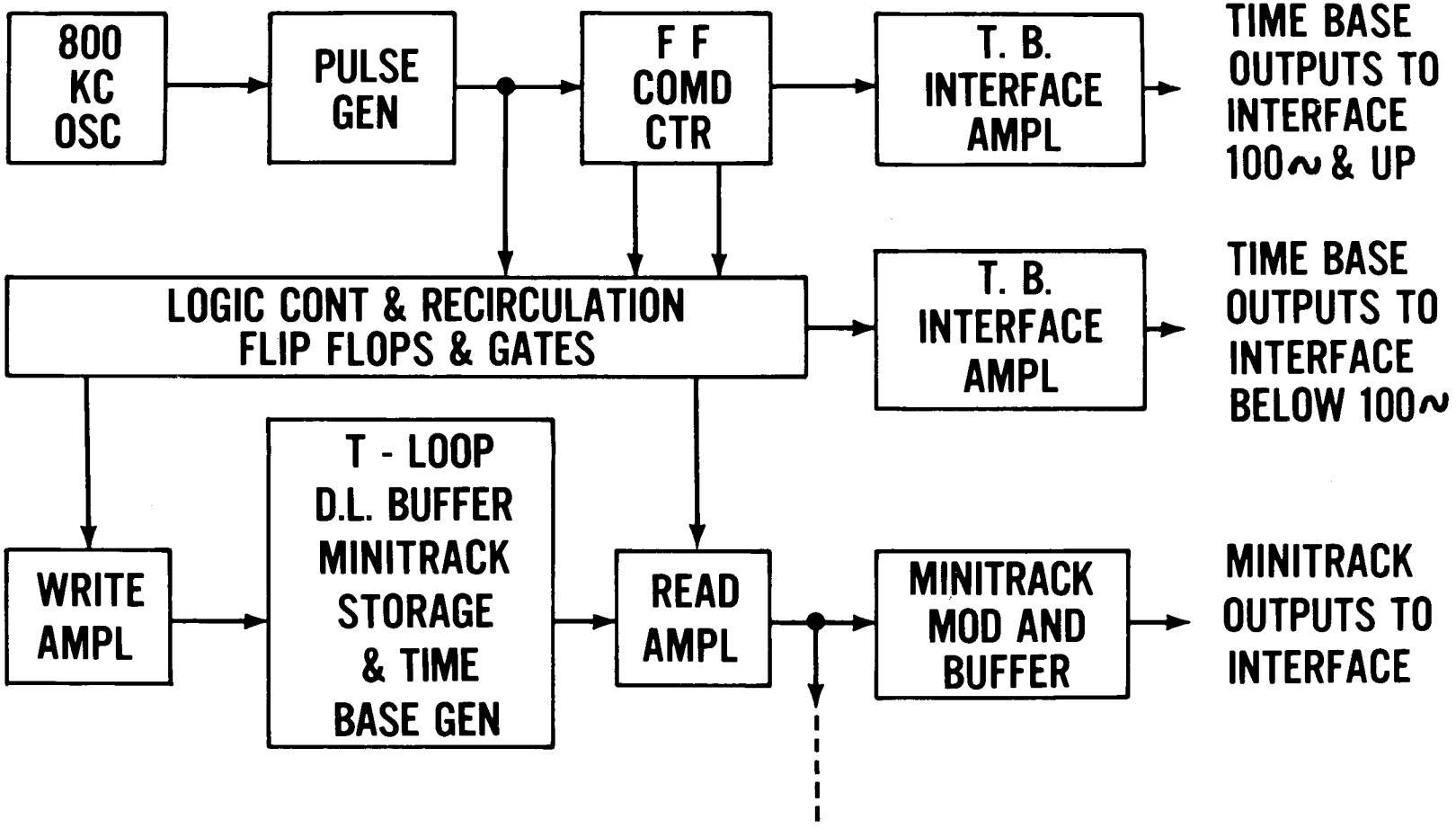

Figure 3 - Timing Section, Block Diagram

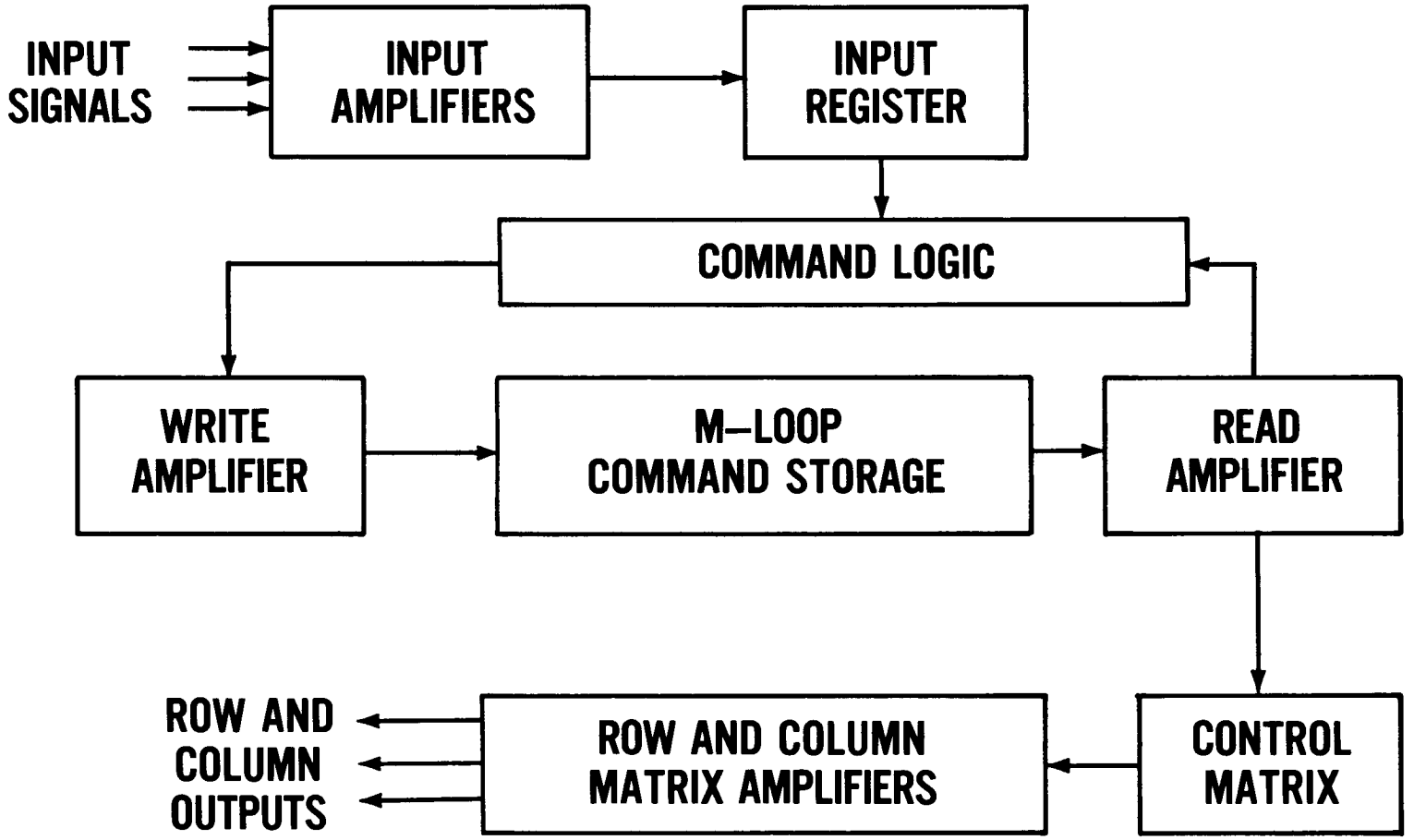

Figure 4 - Command Section, Block Diagram

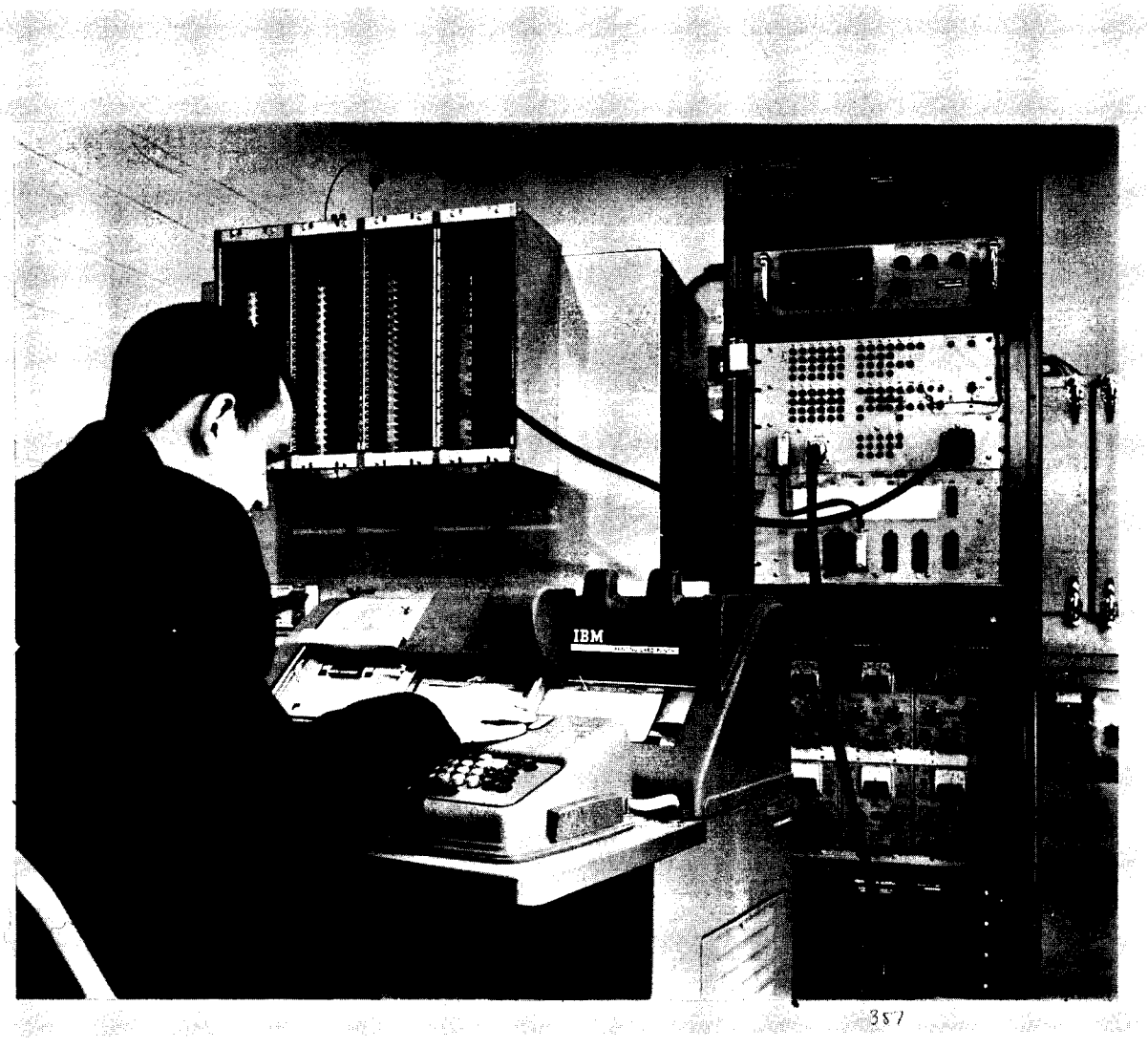

Figure 5 - Reliability Program Equipment

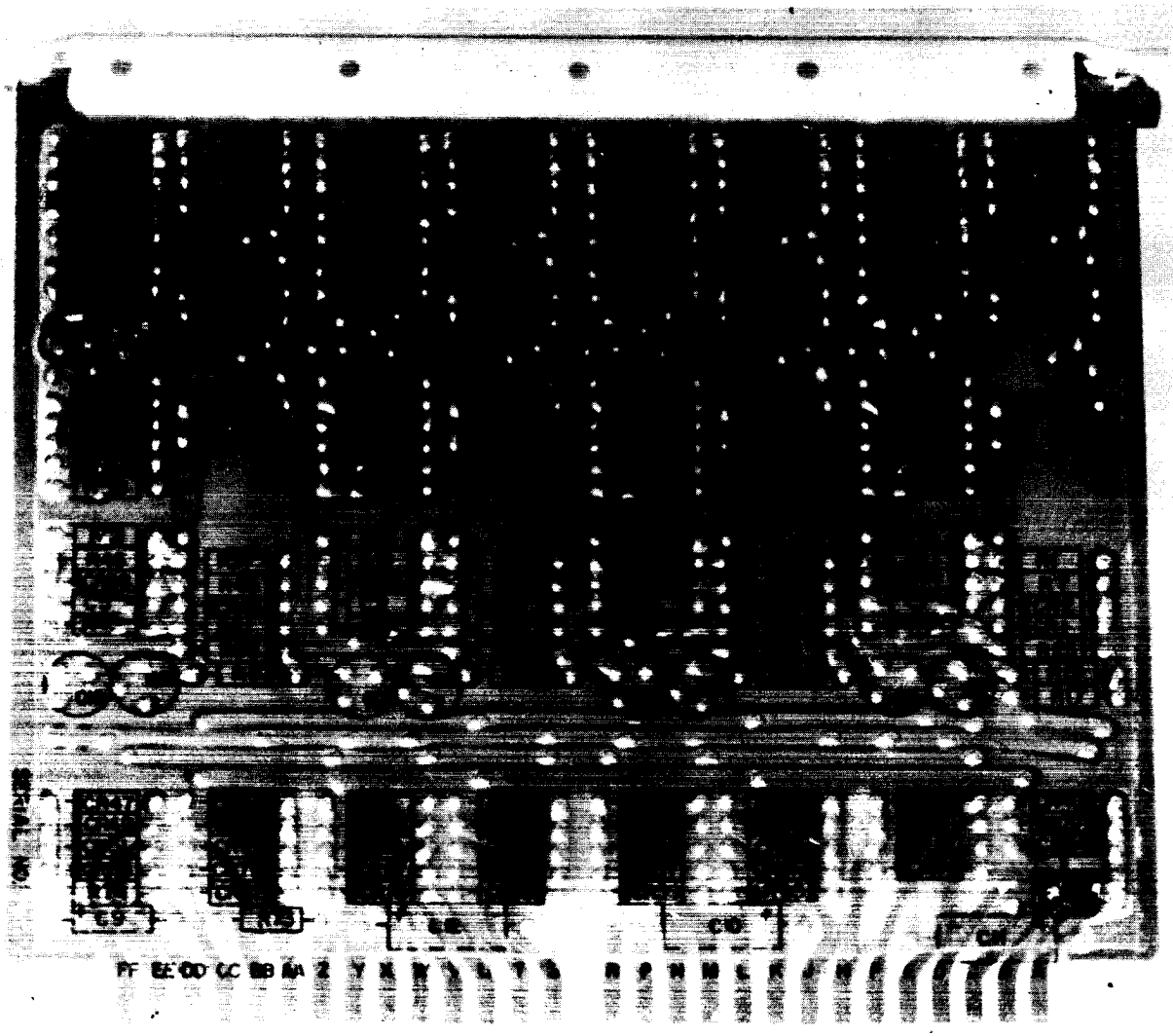

Figure 6 - Rear View, Etched Board

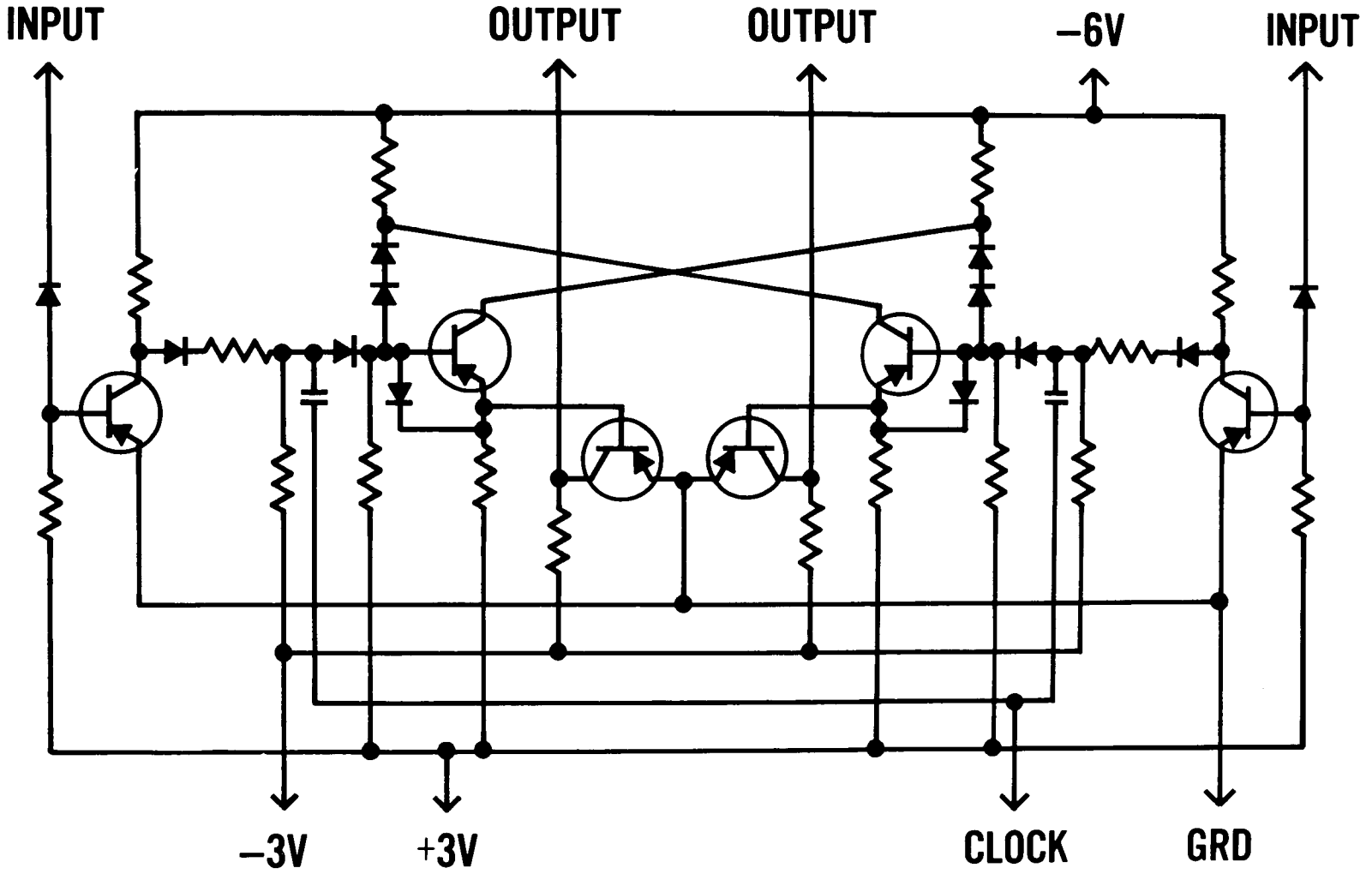

Figure 7 - Command Clock, Flip-Flop Circuit

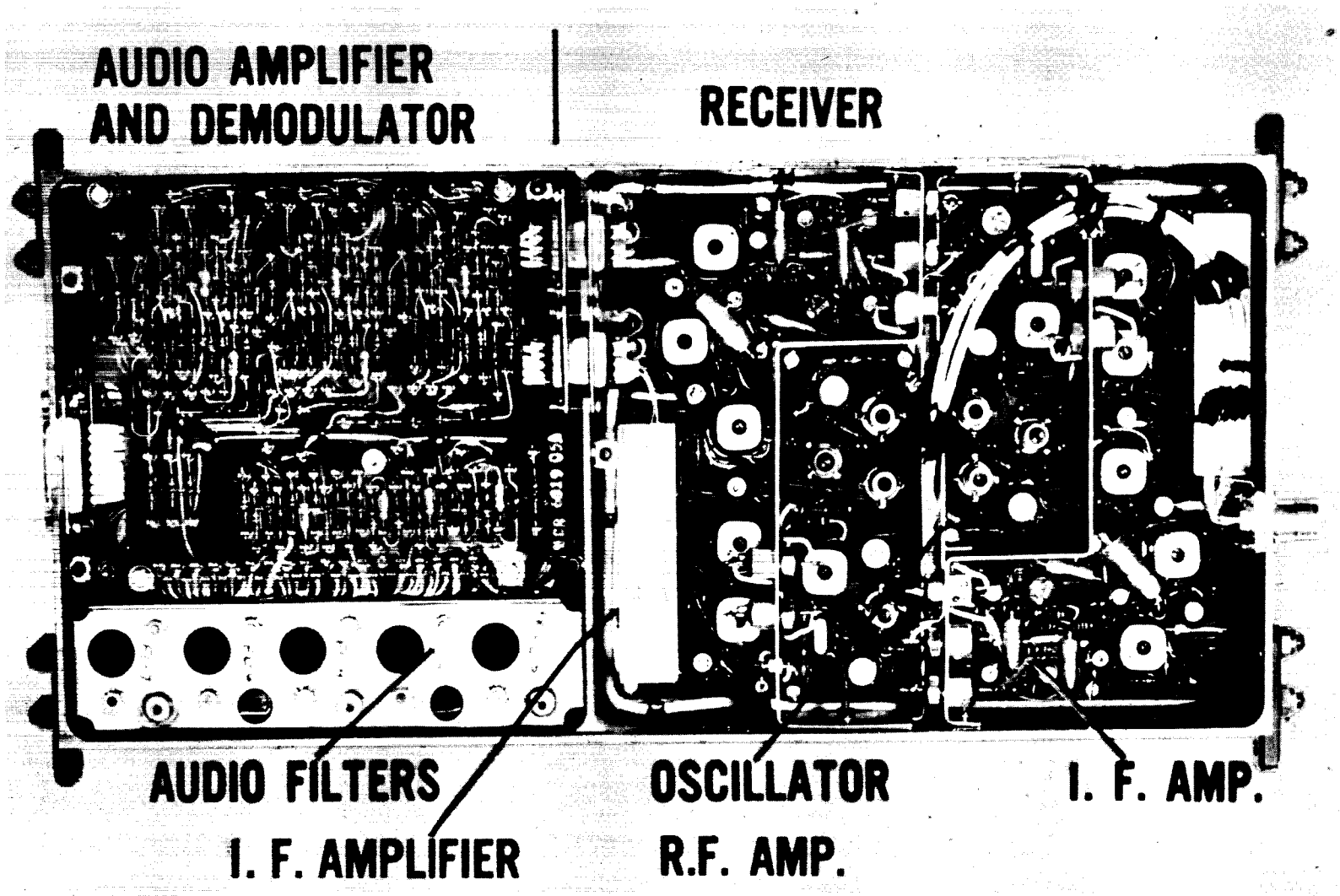

Figure 8 - Clock Receiver Module

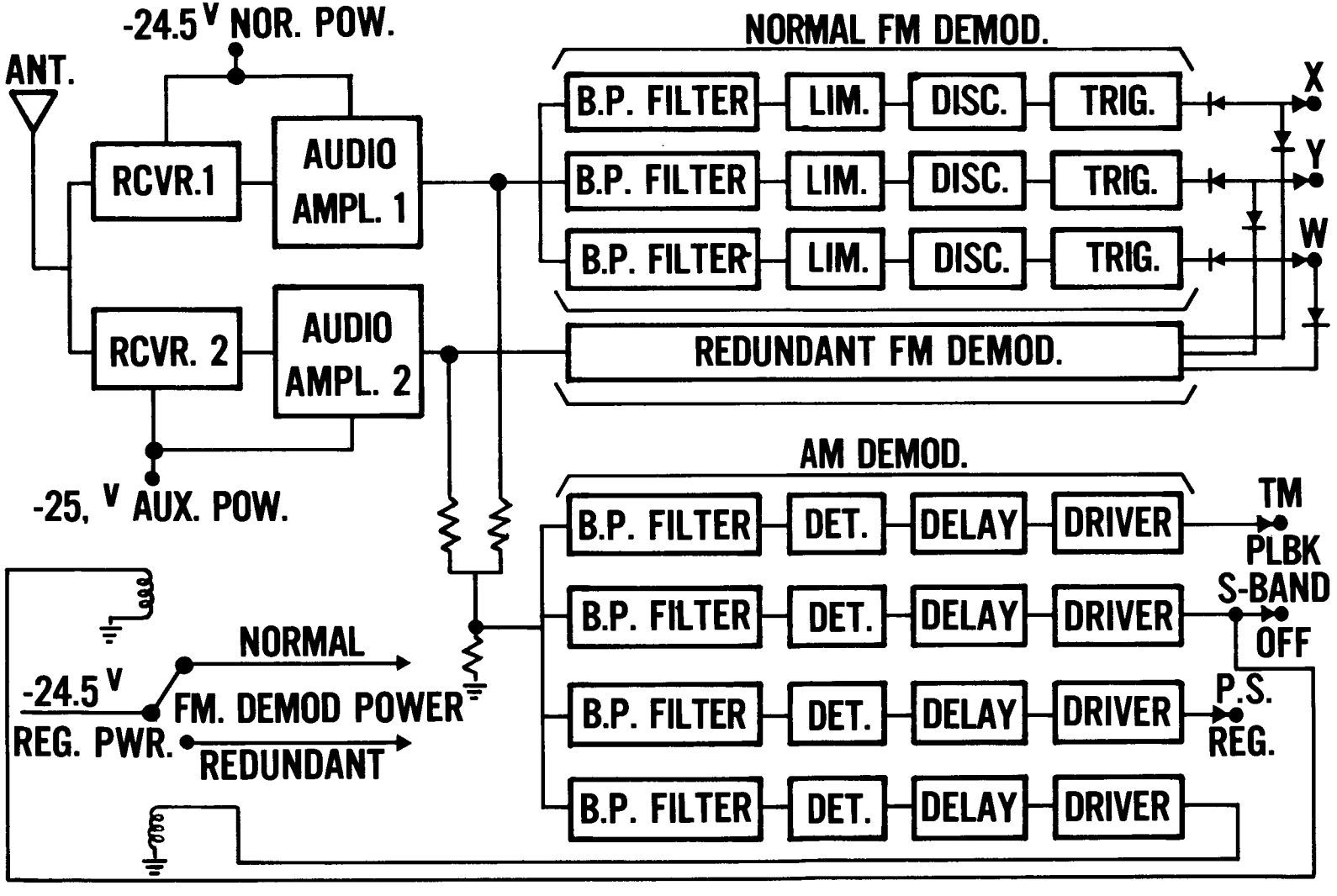

Figure 9 - Nimbus Clock Receiver, Functional Block Diagram

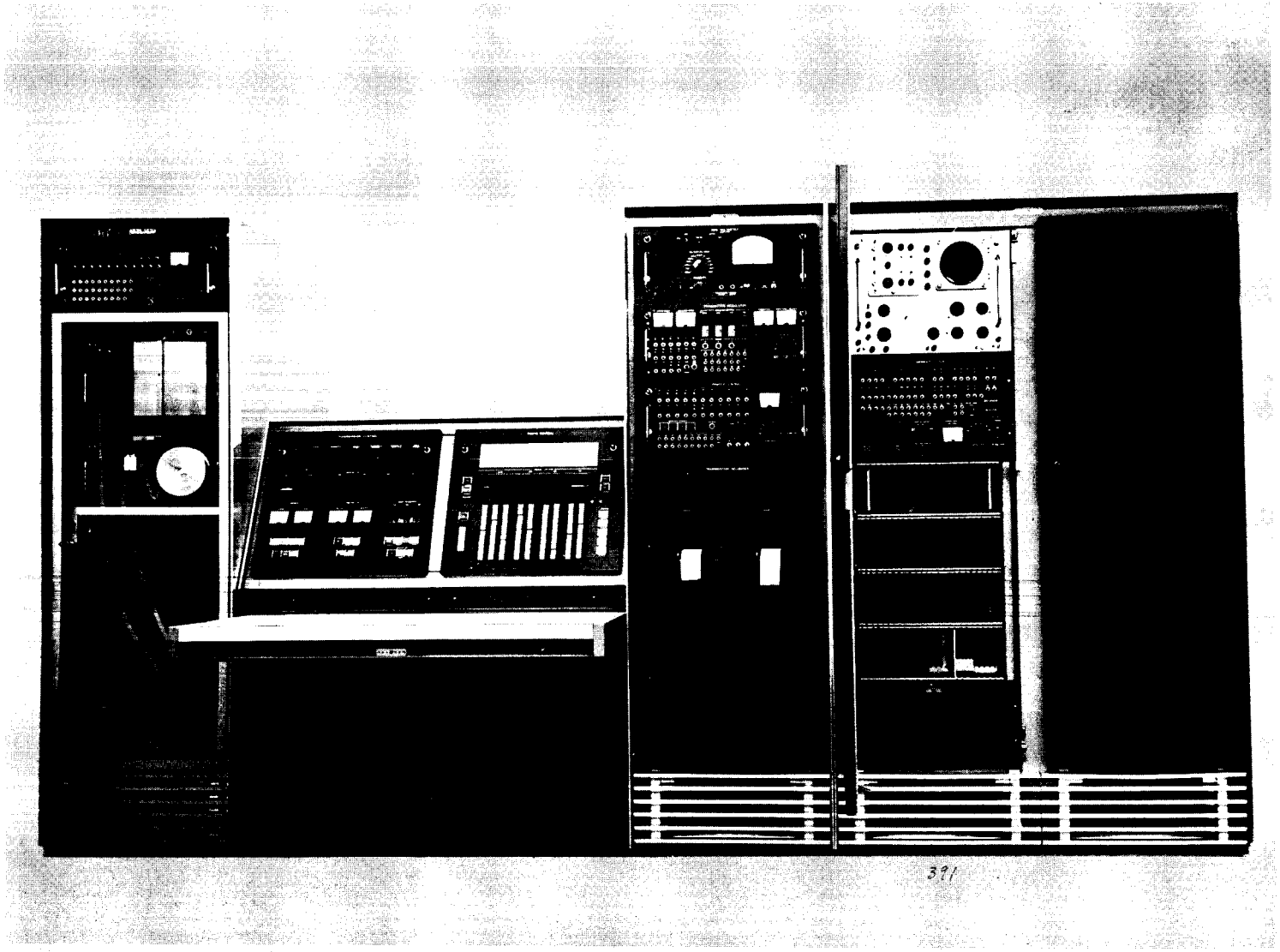

Figure 10 - Command Clock, Ground Station Equipment

15. NIMBUS TELEMETRY

By R. Golden, GSFC; F. L. Adkins
and C. E. Griffin, Radiation, Inc.

15. NIMBUS TELEMETRY

ILLUSTRATIONS

Figure		Page
1	Pulse-Code-Modulation Subsystem - Unit A, Block Diagram	8
2	Pulse-Code-Modulation Subsystem - Unit B, Block Diagram	9
3	Telemetry Electronics Subsystem	10
4	Pulse-Code-Modulation Subsystem Module	11
5	Module Board and Tray	12
6	Module Board and Tray	13
7	Video Input From Telemetry Receiver, Nimbus PCM Ground Station	14
8	Bits Without Error vs. Signal-to-Noise, in DB, Nimbus PCM Ground Station	15
9	Nimbus PCM Ground Station Equipment	16
10	Nimbus PCM Ground Station, Block Diagram	17

15. NIMBUS TELEMETRY

By R. Golden, GSFC; F. L. Adkins
and C. E. Griffin, Radiation, Inc.

The purpose of the Nimbus pulse-code-modulated (PCM) telemetry subsystem is to gather, store (if required), and transmit to ground stations, the engineering information needed to evaluate the detailed performance, environmental conditions, and general function of all spacecraft subsystems. In addition, the Nimbus PCM telemetry subsystem provides all attitude information needed to determine the exact location of meteorological pictures.

The choice of pulse-code modulation over other types of telemetry was made because of its accurate and reliable data-transmission capability, and the ease with which the data can be reduced.

The Nimbus spacecraft will carry two electrically independent PCM units. Unit A handles 544 channels, which it continually records on tape for readout on command; unit B delivers 128 channels by direct transmission.

The PCM telemetry subsystem will accept information from all the spacecraft subsystems for "housekeeping" purposes and will also acquire control-subsystem attitude data. Information can be of the yes-no type or in analog form, stored by the unit A recorder for command readout, or for direct transmission by unit B upon interrogation.

Unit A consists of a 7-bit analog-to-digital converter, 544-channel multiplexer, subcommutation, gates and registers (Figure 1). It uses less than 0. 75w of continuous power to monitor 542 data channels for information such as voltages, current, and temperatures, and to continuously check the performance of other spacecraft subsystems. These channels are time-multiplexed and serially recorded on tape at a bit rate of 500 cps for playback at 15, 000 cps, a 30-to-1 ratio of time compression.

Frame composition is 64 words, including a synchronization word composed of all "ones". Maximum number of bits per word is eight,

including word synchronization. Subcommutation is used with the 8-bit synchronization word following the frame sync. Subcommutated groups 49 to 64 may be expanded to a total of 32 subframes simply by adding the necessary gate modules and timing circuits.

Unit A coder, similar to that used in unit B for redundance, accepts asymmetric inputs from zero to -6. 4v; channel input impedance is in excess of 100, 000 ohms.

Unit B operates only upon ground command, using less than 0. 25w operating power to scan the 128 channels for a 1. 75-minute reporting period (Figure 2). This unit employs a bit rate of 10 bits/sec, with a maximum of 128 words, including synchronization with three words in the form of all "ones" followed by all "zeros", followed by all "ones". After completion of one frame, the unit is deenergized.

Unit B consists of an analog-to-digital converter similar to that of unit A, a multiplexer, gates, and a phase-shift modulator. Output of unit B phase-shift-modulates a 5000-cps coherent subcarrier. Modulator output is a 5000-cps sine wave. A 180-degree phase relation exists between a "one" and a "zero" when compared to a reference signal.

Units A and B both are controlled by signals from the Nimbus clock subsystem which furnishes 500-cps and 10-cps square waves, respectively, to the units.

For test purposes, telemetry data at 500 cps (not stored) can be read out from the PCM subsystem.

The non-return-to-zero (NRZ) output of unit A is converted in the "A" modulator, located in the telemetry electronics (TME) package (Figure 3). One cycle of a 500-cps sine wave is generated for each "zero" bit of information. The modulator output is stored on tape and may be read out directly. The TME unit also contains record amplifiers which furnish the record signal and the 8000-cps erase and bias signals to the tape recorder heads. Playback amplifiers, also located in this unit, provide an output to amplitude-modulate the beacon transmitter 80 percent. Dual record and playback amplifiers are available for a redundant tape recorder.

The TME unit includes a tuning-fork oscillator to provide 500-cps signals for the PCM unit A bit rate and "A" modulator, as well as a two-phase 100-cps signal for one tape recorder, in case the clock signals should be interrupted.

Command switches for the PCM, TME tape-recorder amplifiers, standby clock, tape-recorder functions, and transmitter input are located in the TME package. Clock signals and unit B signals are also routed through the TME for control and output to the beacon transmitter. Special test equipment is provided to check out all units of the PCM telemetry system.

The PCM and TME subsystems employ a unique packaging concept known as the "solid mass" approach to electronic packaging, which means that all portions of the system, including the components themselves, contribute to the rigidity of the package. By holding the internal parts in compression, the side panels need be only thin lightweight sections since they experience only tension forces. This results in a very high "electronics weight" to "box weight" ratio, as compared with other types of satellite electronic packaging. The PCM module (Figure 4) weighs less than 23 pounds; the TME (Figure 3), 5 pounds.

The printed circuit cards and module layout are very important as integral parts of the package. A novel concept is the face-to-face interlocking of module-card assemblies, not only resulting in structural rigidity, but also doubling the surface area of the available printed circuit boards, thus providing more room for module interconnections.

The interlocked module-card assemblies (Figure 5), or trays, are insulated from each other by a layer of cast polyurethane foam. The trays are interconnected through a special high-density lightweight connector developed for this special application by Radiation, Inc. and U. S. Components, Inc.

The modules are welded assemblies, potted with rigid polyurethane foam (Figure 6).

System testing begins with a module test. Following this initial test, the module is potted, X-rayed, and vibrated. The second test is performed with modules temporarily connected together as a system;

the first temperature cycling is done under this condition. Upon completion of these module-level tests, the system is assembled and the system test is also conducted over the temperature range. Not until the system has passed these tests is it put into the package and the acceptance tests started.

Environmental tests consist of the Nimbus subsystem sinusoidal and random vibrations, and thermal vacuum tests. The thermal vacuum tests are conducted with the entire telemetry system, including the Hughes beacon transmitter and the Raymond Engineering tape recorder. To date, a qualified prototype and flight-model PCM and TME have been delivered.

Two units, the Nimbus PCM tape recorder and the beacon transmitter, which complete the telemetry subsystem are extremely important in data transmission.

The Nimbus PCM tape recorder is a 4/0 pressurized module, weighing 10 pounds; power input is 1.6 watts during the record cycle, and 10 watts in the playback mode. A 216-foot, 1/4-inch-wide lubricated mylar endless-loop tape is used as the storage medium for the PCM "A" data. The tape unit records at a speed of 0.4 inches/sec and plays back at 12 inches/sec to give the 30-to-1 time compression. The 100-cps rate signal required for the drive mechanism is provided by the clock subsystem or the PCM emergency oscillator. The recorder module also contains motor-drive amplifiers for record, playback, and momentum compensation.

An internal automatic-turnoff device assures that the tape unit will return to its "record" mode after a playback of slightly more than the full length of tape, or approximately 3.6 minutes. The recorder utilizes a single head for record and playback, with switching of the respective amplifiers.

The physical distance between the erase and record heads provides a blank area on this magnetic tape at the moment the tape unit is interrogated. Knowing the exact time of the tape "gap" from command time, all data on the tape may be correlated to time with the known PCM bit rate.

The beacon transmitter continuously transmits Minitrack time except when PCM interrogation is commanded; during this period, PCM data are telemetered to a ground station. The transmitter, a solid-state device using a pre-aged crystal which assures a frequency stability of 0.005 percent, has a minumum CW output of 250 mw. The AM modulator's frequency response is flat within 3 db from 100 cps to 60 kc, and within 1 db from 200 cps to 30 kc. Distortion is less than 2 percent at 50-percent modulation. The transmitter output excites four quadraloop antennas located on the periphery of the Nimbus spacecraft.

To date, three beacon transmitters have performed successfully with PCM subsystems.

The Nimbus PCM ground station has been designed to accept all video outputs of the PCM telemetry receiver, and to process, record, and display the PCM telemetry data received from the satellite. The equipment will accept and speedily process the data, allowing an immediate review of information gathered during the satellite orbit. The station is designed to display the information visually and to prepare it for relay to remote facilities; it also can present visual displays of selected data on oscillographs for a quick look at the information as it is being received. In addition, it contains a computer complex for real-time and delayed editing and processing of the information.

The ground station will, while completely unattended, acquire data from the satellite with no commands from external equipment. It will recognize, program, acquire, and process any of the three PCM data formats in any sequence.

Figure 7 presents characteristic video waveforms of the data formats. The "B" PCM signal is 10-cps bit rate, non-return-to-zero-inverted (NRZI) on a 5-kc coherent subcarrier, phase-modulated 180 degrees. Each frame of "B" data consists of 128 data words. The "B" as well as both "A" formats contain word and frame synchronization groups.

Both "A" PCM signals contain 64 channels in a primary or minor frame. Thirty-two of the 64 channels are subcommutated to 16 minor frames. As shown in Figure 7, both "A" signals are NRZ signals amplitude-modulated on a coherent subcarrier. The real-time "A" data is received at a 500-cps bit rate, the tape-playback "A" data at a 15-kc bit rate.

System performance in the presence of noise is indicated in Figure 8, which presents measured versus theoretical signal-to-noise ratio versus bits without error plots for a 15-kc "A" data. The actual curve is approximately 3 db away from the theoretical, and predicts one bit error out of one million with a signal-to-noise ratio of 17 db.

Figure 9, a photograph of the ground station, indicates the major system components. From left to right, the picture shows a teletype send-receive set; a MinCom G107 magnetic-tape recorder-reproducer; two racks containing digital-to-analog converters and oscillographs; a two-rack acquisition station; and the computer subsystem, comprising a high-speed printer, digital magnetic-tape recorder-reproducer, and the computer console. Functions of each of these components are shown in the block diagram of the station (Figure 10).

The video output from the telemetry receiver is routed to the demodulators, which remove the subcarrier from the incoming signal and put out regenerated serial data. The video output is also routed to the MinCom tape recorder where a record of the incoming signal is made for delayed processing and for backup.

The regenerated serial PCM from the three demodulators is also recorded on the MinCom. Outputs of the demodulators are also routed to the synchronizers, where the word and frame sync patterns are recognized and the data is converted from a serial to a parallel form. Therefore, the output of the synchronizers is 7-bit parallel binary data, as well as the synchronization pulses and data-status signals required to process and display the data.

As shown in Figure 10, all "B" data are routed to the teletype where the raw data are printed out in decimal form in real time.

The output of the "A" data synchronizers is routed to two decommutators which, by means of a patchboard program, can select any 32 channels from the real-time or tape-playback "A" data required to be converted to analog information and plotted on the four- to eight-channel oscillographs.

All the incoming PCM data are routed through the computer-input circuitry to the CDC-160A computer console for processing, recording, and displaying under control of the program in the computer.

An outstanding feature of the ground station is its simplicity; there are no buttons or controls to be manipulated during a satellite pass, regardless of the sequence in which the PCM data are transmitted. Also, it is complete in that all the equipment required to process, record, and display the data is an integral part of the station.

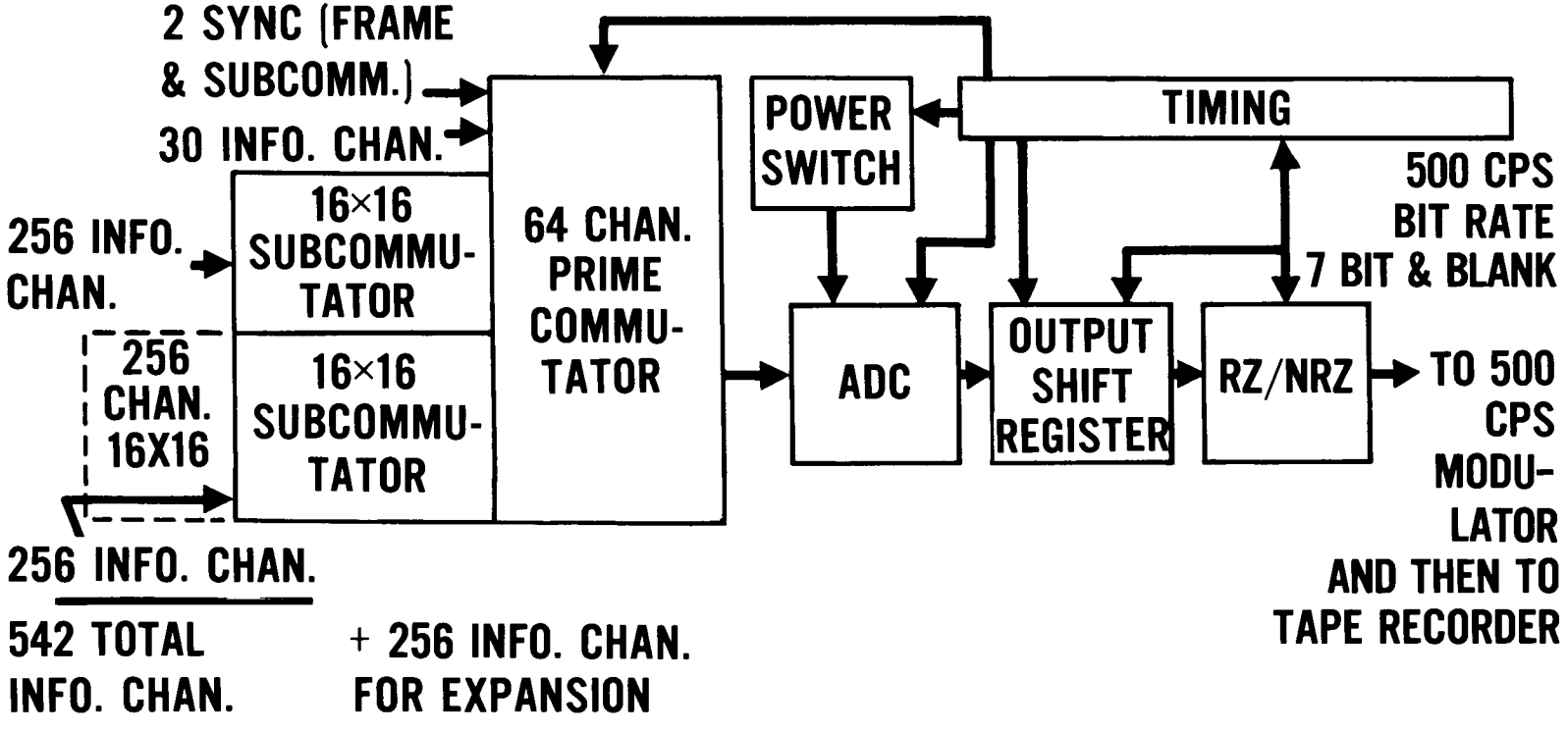

Figure 1 - Pulse-Code-Modulation Subsystem - Unit A, Block Diagram

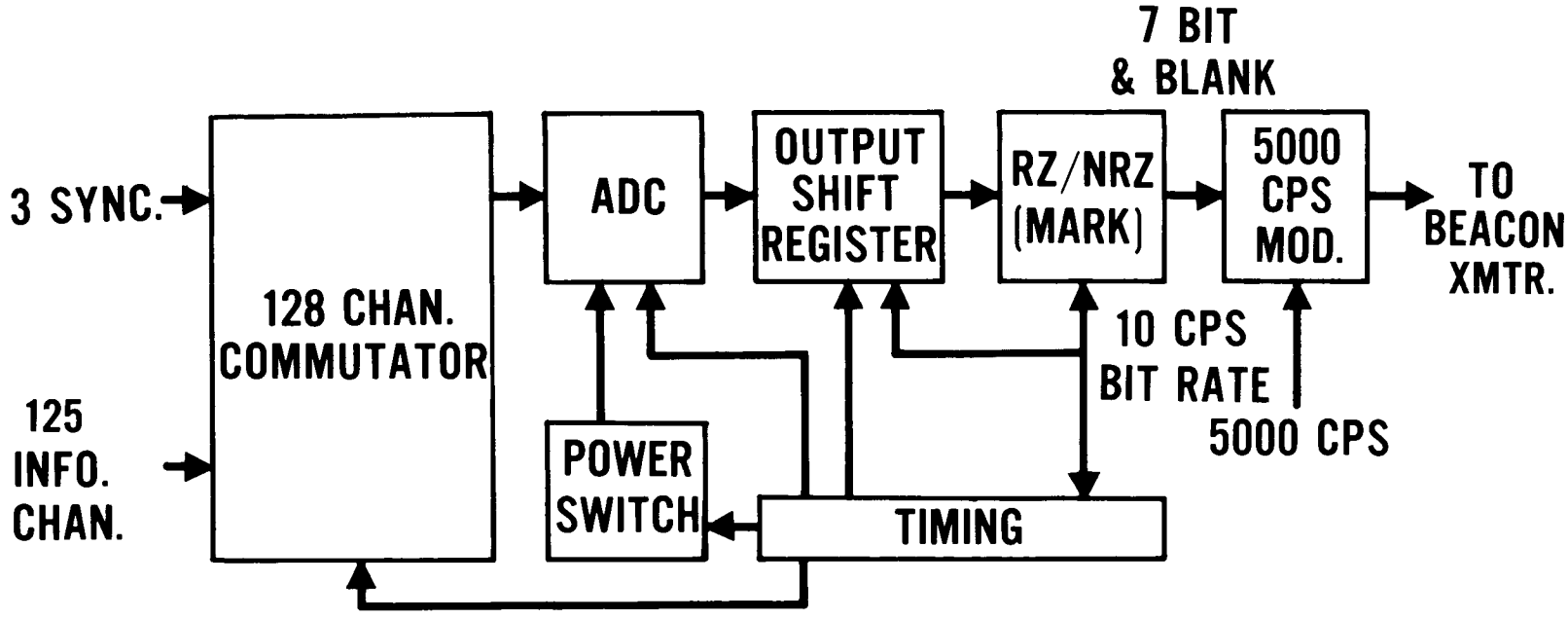

Figure 2 - Pulse-Code-Modulation Subsystem - Unit B, Block Diagram

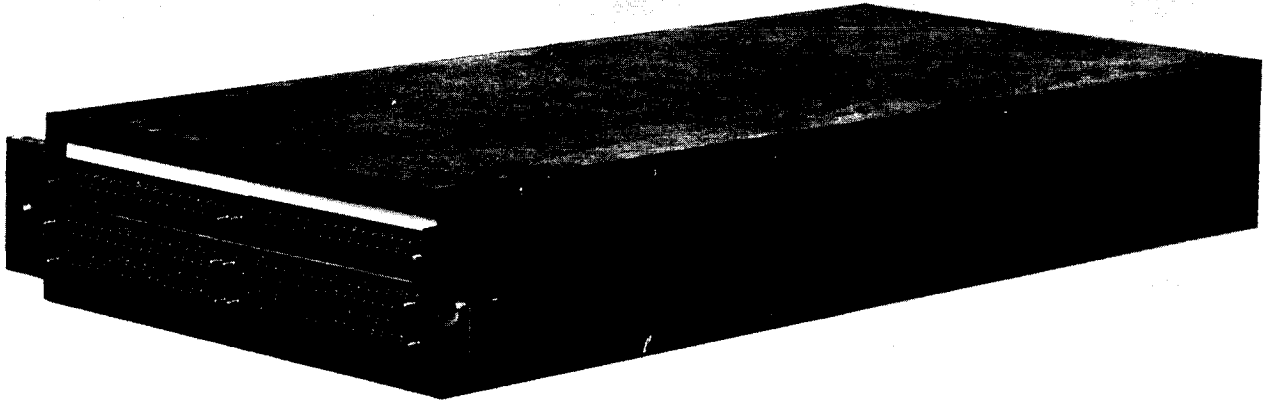

Figure 3 - Telemetry Electronics Subsystem

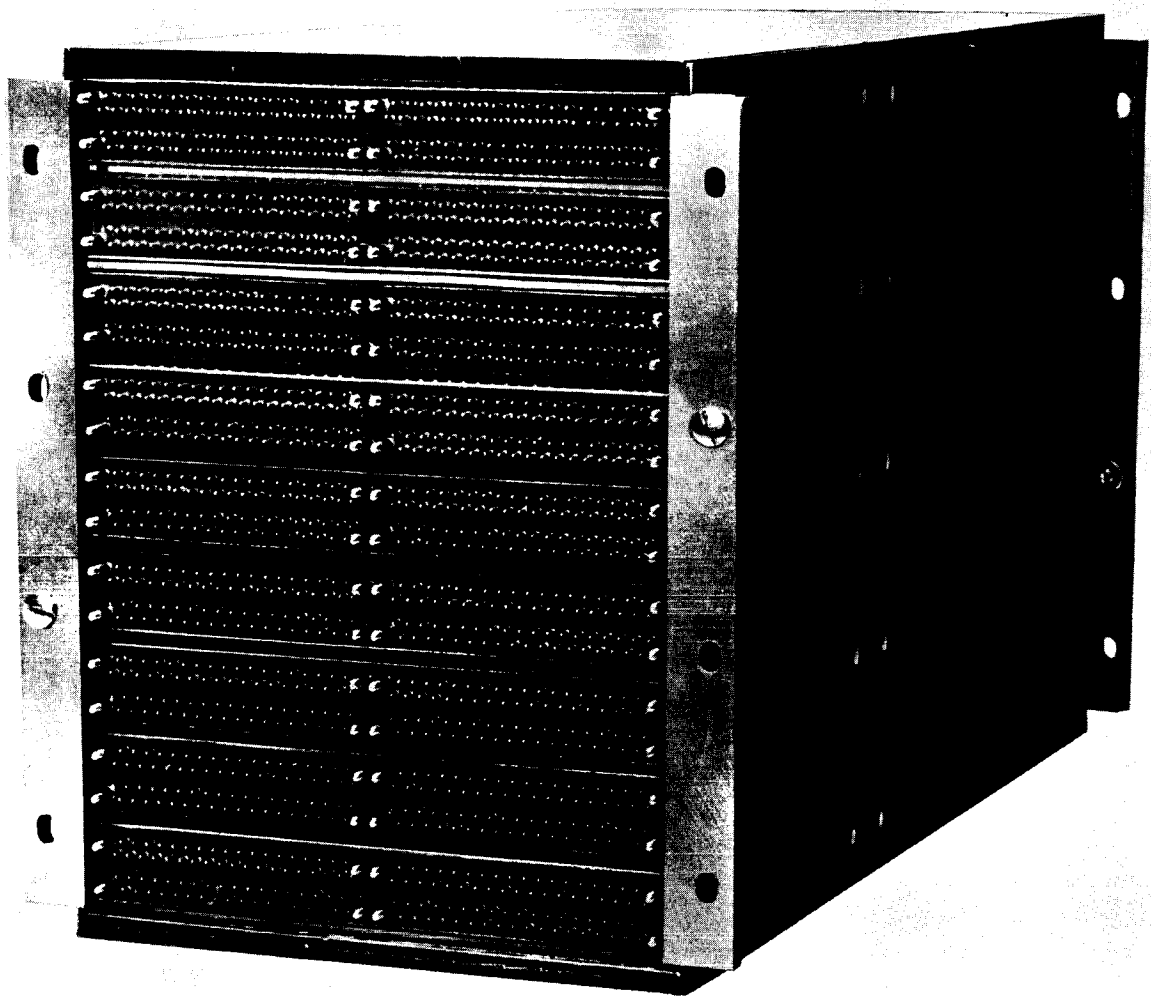

Figure 4 - Pulse-Code-Modulation Subsystem Module

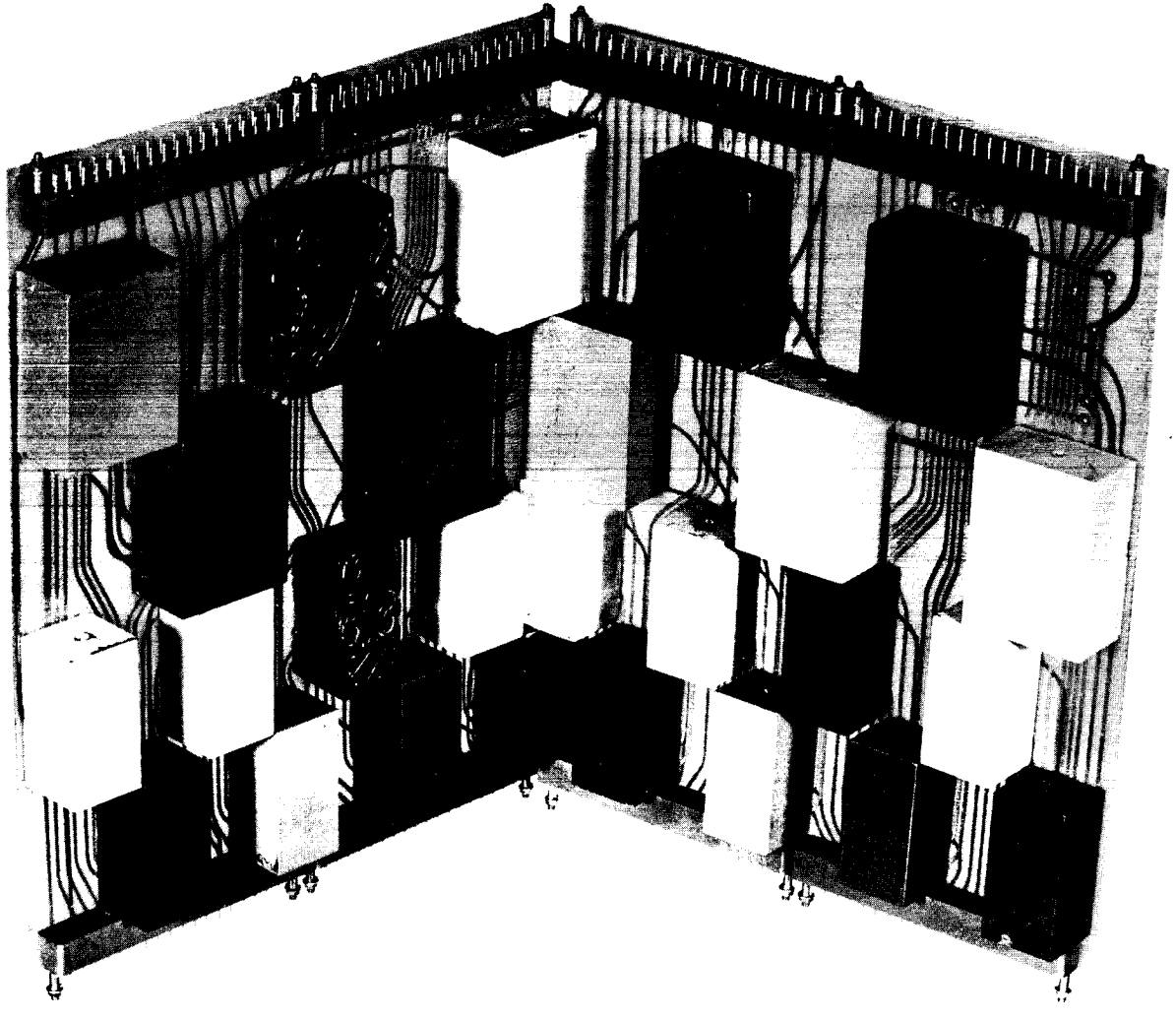

Figure 5 - Module Board and Tray

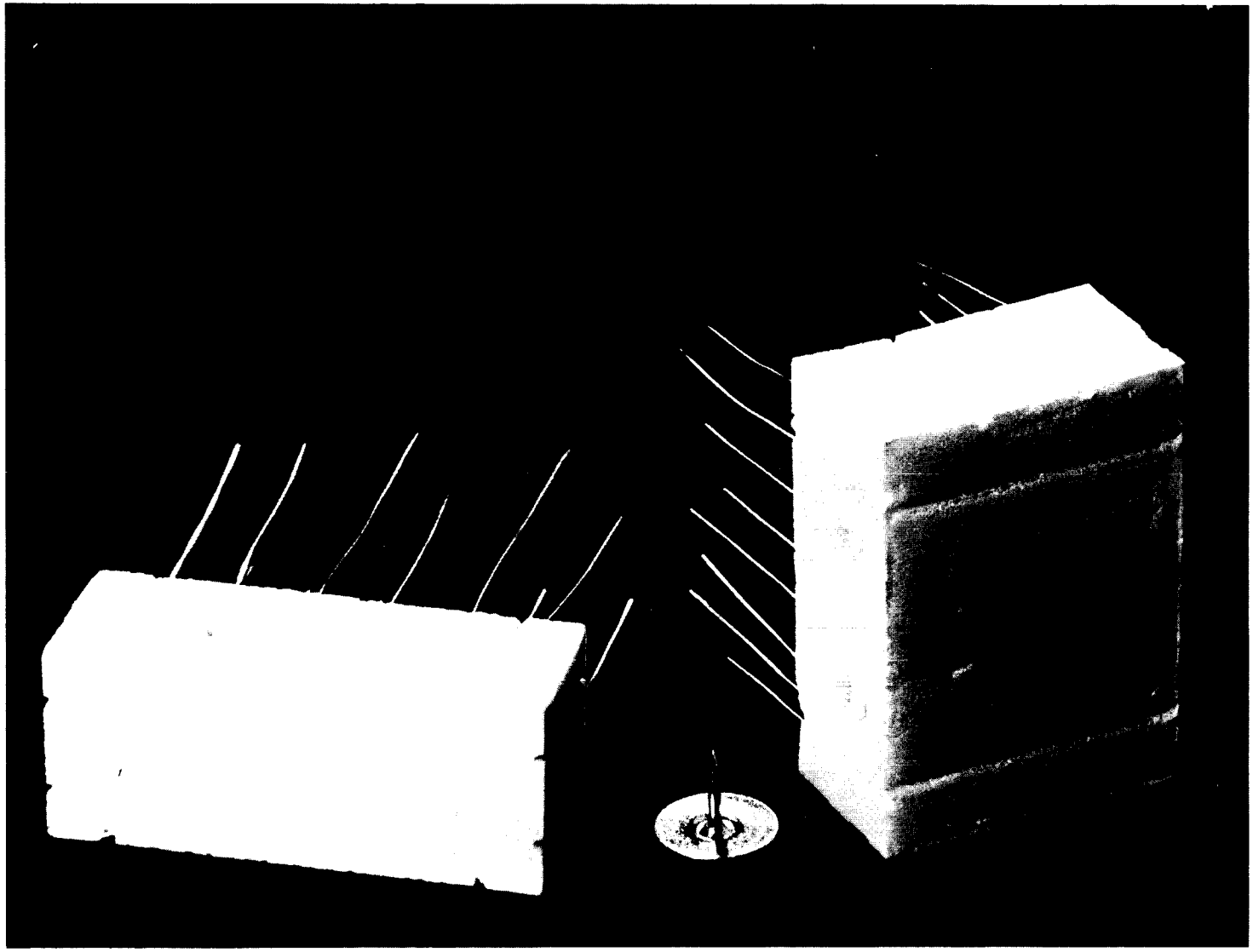

Figure 6 - Typical Modules

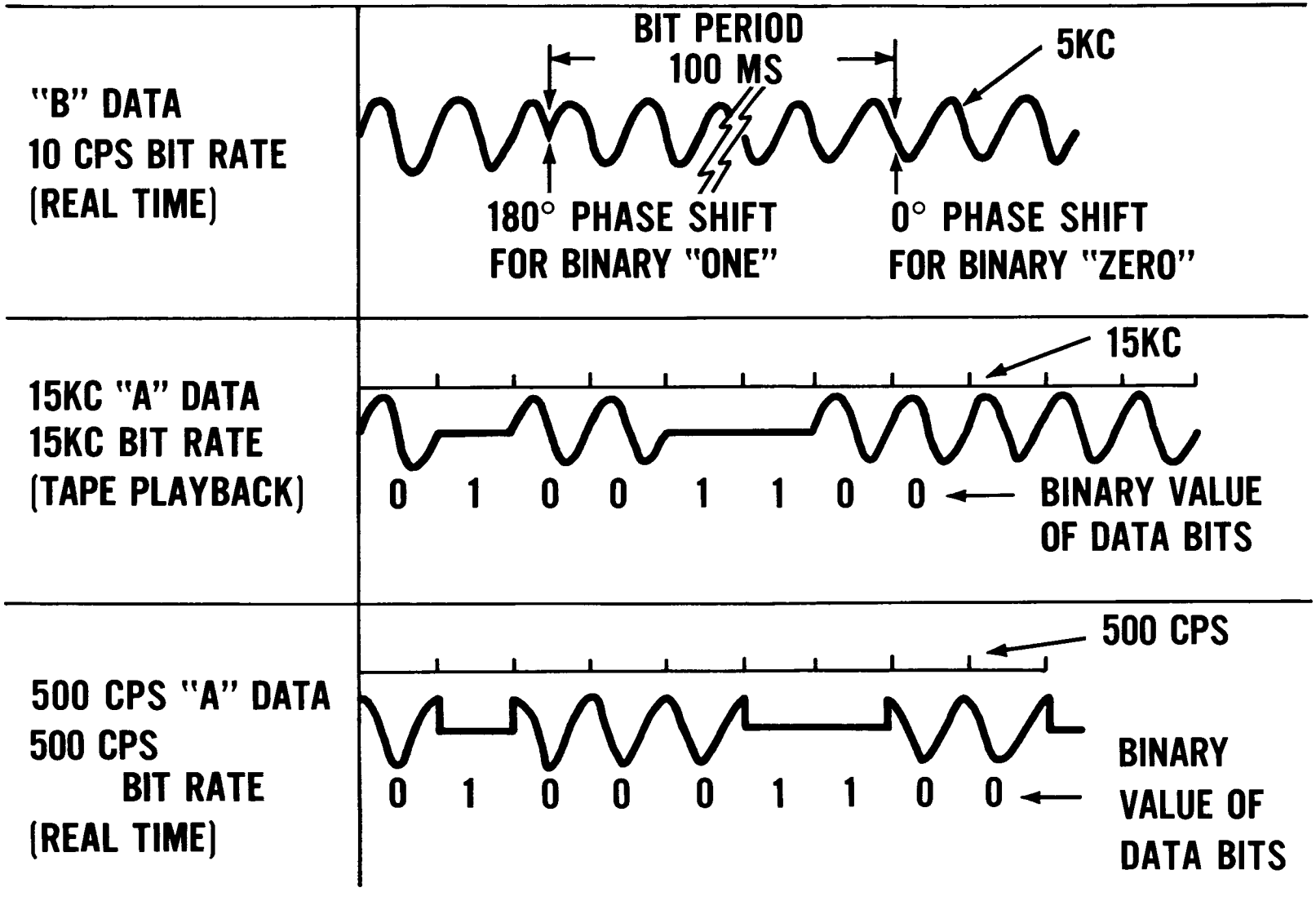

Figure 7 - Video Input From Telemetry Receiver,
Nimbus PCM Ground Station

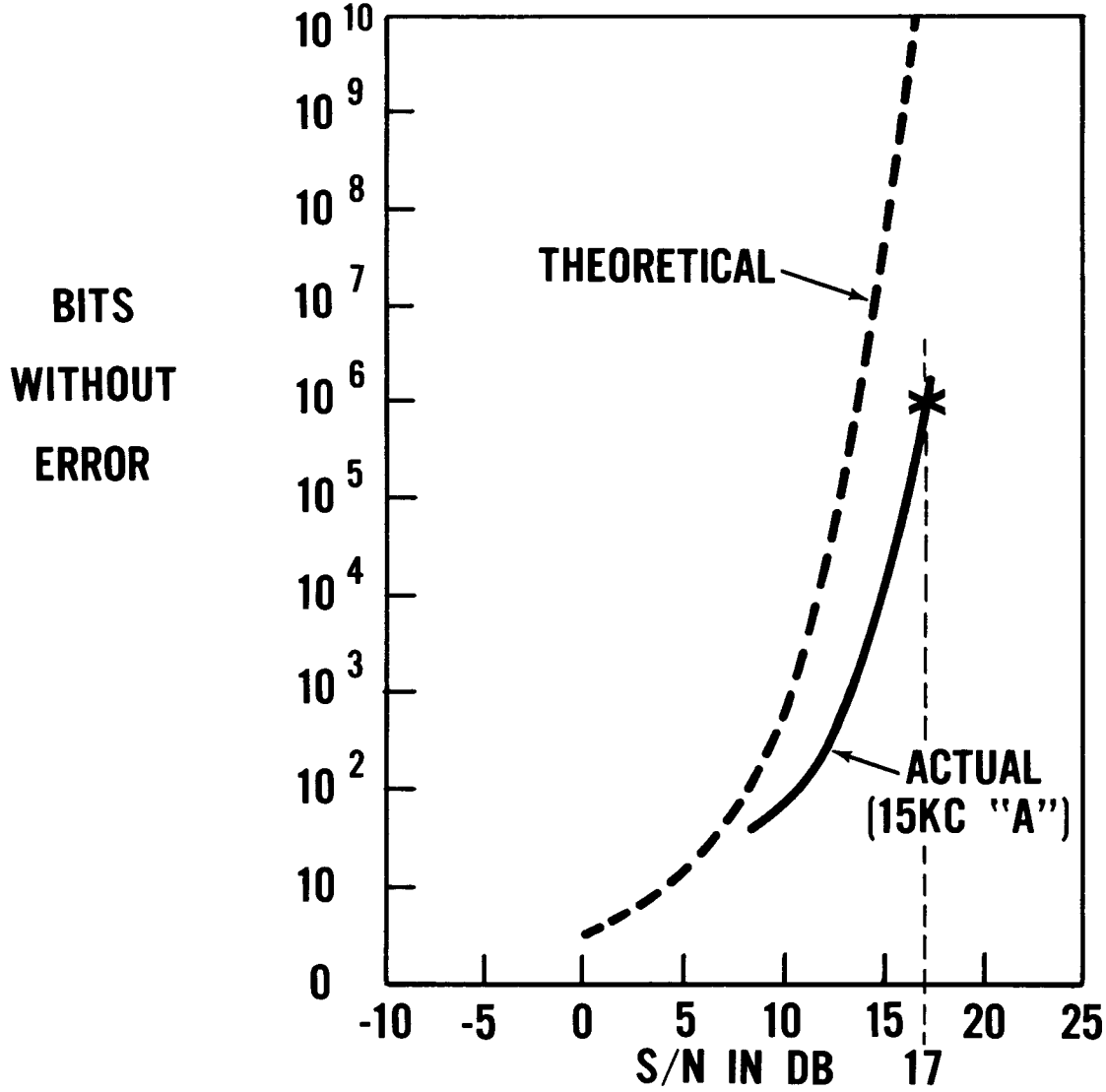

Figure 8 - Bits Without Error vs. Signal-to-Noise, in DB, Nimbus PCM Ground Station

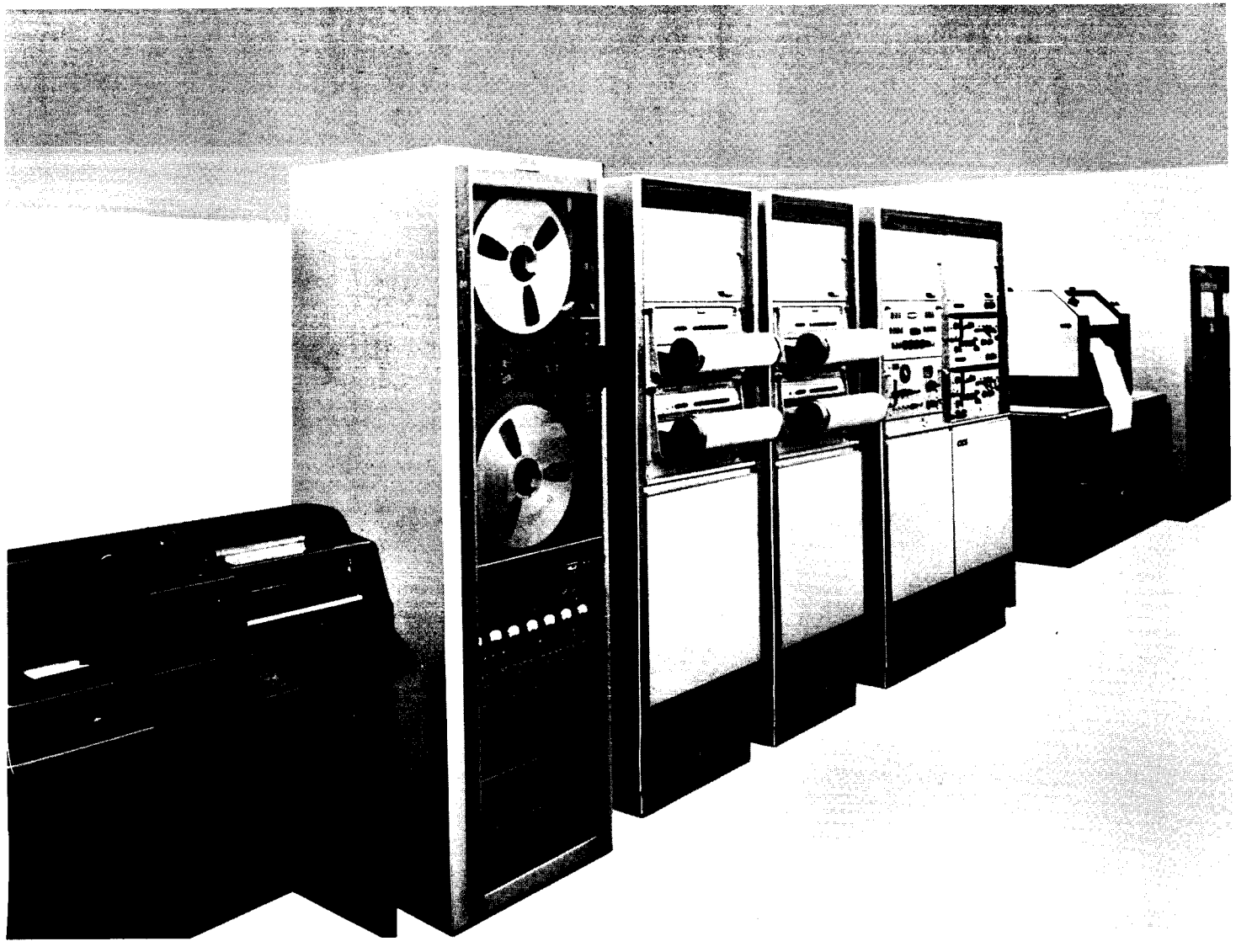

Figure 9 - Nimbus PCM Ground Station Equipment

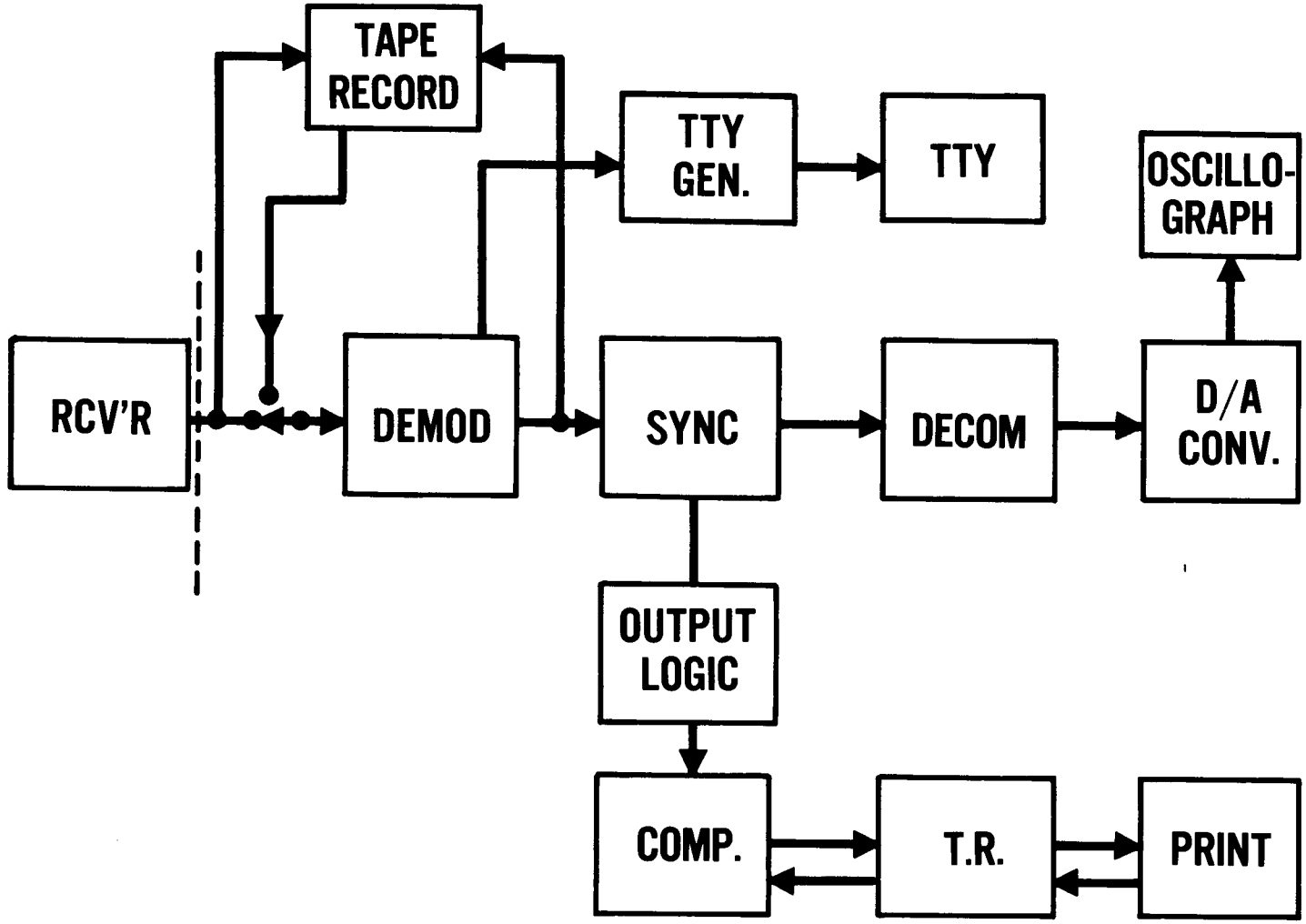

Figure 10 - Nimbus PCM Ground Station, Block Diagram

16. NIMBUS RADIOMETRY

By I. L. Goldberg, GSFC

16. NIMBUS RADIOMETRY

ILLUSTRATIONS

Figure		Page
1	Nimbus 5-Channel Medium-Resolution Infrared Radiometer	7
2	MRIR Spectral Regions	8
3	MRIR Components	9
4	Nimbus MRIR Subsystem, Block Diagram	10
5	Nimbus High-Resolution Infrared Radiometer . . .	11
6	HRIR Optical System	12
7	Nimbus HRIR Subsystem, Block Diagram	13

16. NIMBUS RADIOMETRY

By I. L. Goldberg, GSFC

Two scanning radiometers have been designed for Nimbus, the medium-resolution infrared radiometer (MRIR) and the high-resolution infrared radiometer (HRIR).

The MRIR being fabricated by Santa Barbara Research Center is shown in Figure 1. The scan-mirror drive motor, the scan mirror, the reflection of three of the five telescopes, the preamplifiers, and the chopper motor are visible; the electronics module is not shown.

This radiometer measures emitted infrared and reflected solar radiation in five spectral regions, using thermistor bolometer detectors. The spectral regions, and the reasons for selecting them, are listed in Figure 2. The spectral regions are similar to those measured by the TIROS five-channel radiometer. The 6.6-7.0-micron channel, covering an intense water-vapor absorption band, is intended to give a measure of the amount of water vapor or temperature distribution above the cloud tops. The 10-11-micron region lies within an atmospheric window and is well suited for determining surface and cloud-top temperatures, or cloud-top heights. The 7.5-30-micron channel will be used to determine the total radiant emission of the earth. Two visible-light channels are also included. The 0.6-0.75-micron region is the most transparent portion of the visible spectrum; this red end of the visible spectrum is less scattered by the atmosphere than the blue portion. This channel can be used to measure cloud cover during daylight, and can serve as a comparison to the television measurements. The 0.2-4.0-micron channel spectrally encompasses about 99 percent of solar radiation and is intended to measure the earth's albedo (reflected solar radiation).

Scanning is accomplished similarly in both radiometers; they scan the surface of the earth in strips perpendicular to the orbital track. The optical axis is in the direction of the subsatellite point, and the scanning rates and fields of view are chosen so that subsequent scan paths overlap reasonably well at the subsatellite point. The width of an individual scan path, as well as the amount of overlap, increases considerably toward the horizon.

The MRIR scanner (Figure 3) consists essentially of a scanning plane mirror oriented at 45 degrees with the axis of rotation, a Cassegrainian telescope for each channel, a chopper to modulate the incoming radiation, and one detector per channel. The detector "sees" the difference between the radiation from the target and that from the chopper disc, whose temperature must be measured and telemetered. Four of the channels have light pipes between the chopper and detectors to converge the beam onto the tiny bolometer. There is no light pipe for the 6.6-7.0-micron channel which, for greater optical gain, uses an immersed bolometer.

Both the MRIR and HRIR will have a calibration check in orbit. This is a significant improvement over the TIROS system. For both radiometers, the space scan will serve as the zero reference, and during each scan a housing target of known temperature is seen which will serve as a second calibration point for the infrared channels. The temperature of this target must be telemetered. The sun will be used as the target for the second calibration point for the two solar-radiation channels. This point will be measured once during each orbit, when the lower portion of the spacecraft is exposed to direct sunlight.

The MRIR instantaneous field-of-view is about 2.8 degrees which, at 600 miles, corresponds to a 30-mile linear resolution directly below the vertical. It scans at 7.9 rpm and has an information bandwidth of 8 cps. Total power consumption is 7.2 watts and the total weight, including the electronics module, is 11 pounds.

During vibration tests, the scan drive motor failed due to the 60g amplification experienced at the motor mount. Two major steps were attempted to alleviate this condition:

1. The casting was remade of KIA magnesium. This material has a greater specific damping capacity than the AZ91C magnesium used originally; however, a comparison of vibration amplitudes between the two types of castings showed only a small improvement. This improvement was not considered sufficient to warrant the time and expense of remaking the castings.

2. Bearings of the scan drive motor were redesigned to withstand the higher loads. Indications are that this approach will lead to the successful qualification of the prototype.

Many of the optical materials used in the Nimbus MRIR are the same as those in the TIROS five-channel radiometer. As some of these materials were found to deteriorate in the TIROS space environment, the Santa Barbara Research Center conducted tests to determine the effects of ultraviolet radiation and high vacuum (10^{-9}mm/Hg) on the MRIR filters. The tests showed that KRS-5, an important material used in the filter of the 7.5-30-micron channel, deteriorated in this environment. Steps have been taken to prevent ultraviolet radiation from entering this channel.

Figure 4, a block diagram of the MRIR subsystem, shows that the radiometer output is fed into a voltage-controlled oscillator (VCO), the output of which is put on tape along with a 500-cps time-reference signal from the master clock. The frequency range of each of the five VCO channels is given in Figure 4. On playback (at a speedup ratio of 1:30) the stored information is transmitted via an FM transmitter to the ground station, where it is stored on tape. Real-time application of the "window channel" data may be possible in plotting cloud maps with associated cloud-top heights. Full data processing will be performed in Washington, D.C., using equipment similar to that used for TIROS. A breadboard unit of the MRIR was accepted in January 1962, and a prototype unit is undergoing qualification tests.

The single-channel HRIR, fabricated by the International Telephone and Telegraph Co. (ITT), is shown in Figure 5. This equipment will be used to map nighttime cloud cover and cloud-top temperatures or heights. The cylindrical projection shown at the right holds the motor which drives both the scan mirror and the chopper. The white collars are sunshields; the scan mirror is visible between them. At the bottom left is the rectangular pyramid used to cool the detector by radiation. Cooling by liquid nitrogen or cryogenics is not feasible on Nimbus. The radiometer electronic items are located around this pyramid. This radiometer uses a photoconductive lead selenide detector (PbSe) operating in the 3.4-4.2-micron region, which is considered reasonably free of atmospheric absorption. The HRIR has an instantaneous field-of-view of 8.6 milliradians, which at 600 miles corresponds to a linear

resolution of 5 miles below the vertical. The field-of-view, originally 2.8 mr, was changed when tests showed that the radiometer was not sufficiently sensitive. TIROS measurements indicate that the equivalent blackbody temperature of a cloud can frequently be as low as 200°K, and the field-of-view was opened up to permit detection of these cold clouds.

Figure 6 illustrates the HRIR optical system. The scan mirror is inclined 45 degrees to the axis of rotation and the radiation is chopped at the focus of a 4-inch f/1 Cassegrainian telescope. It is then refocused at the detector by means of a reflective relay which contains the filter. Radiation cooling is accomplished by means of a highly reflective gold-coated rectangular pyramid containing a black cooling patch at the bottom. The pyramid is oriented to view cold space during the entire orbit, and the patch is suspended by thin wires to reduce heat conduction from the housing. The detector is connected to the cooling patch by a high thermal-conductance transfer bar. The radiation cooling system requires no electrical power.

After tests indicated that the wires suspending the cooling patch were not strong enough to withstand the vibration forces encountered, their diameter was increased by 40 percent. This change permitted the HRIR prototype to pass vibration tests with little loss in cooling capability. The detector which was formerly stabilized at -80°C is now kept at -74°C. This difference has little effect on detector sensitivity.

Figure 7 is a block diagram of the HRIR subsystem. The radiometer output is fed to an FM modulator, and then to a tape recorder which is similar to the TV recorder. At the same time, a 10-kc time signal from the clock is placed on the tape. The recorder accepts data at a tape speed of 3.75 inches per second and plays it back at 30 inches per second, which is eight times the recording tape speed. Both the MRIR and the HRIR recorders carry momentum compensation motors to reduce spacecraft disturbances. The recorder information is fed to a multiplexer, added as part of the AVCS composite television signal, and then transmitted by the S-band transmitter. At the ground station, the HRIR information goes to a demultiplexer and then both to a MinCom tape recorder and (after demodulation) to a facsimile recorder. The facsimile recorder converts the electrical signals into a continuous strip picture, line by line. The scanning rate of 44.7 rpm was chosen so that the radiometer would make one complete scan during the time

required for the satellite to advance the width of one line on the ground directly below the vertical, at a 600-mile altitude.

A breadboard model of the HRIR was accepted in April 1962, and a qualified prototype is due in December 1962. The multiplexer and recorder used in this radiometer have recently been qualified.

The total weight of the HRIR is 11.3 pounds, and it draws approximately 4 watts of power. The radiometer motor, which consumes about 1 watt of power, will be on continuously; however, the electronics equipment will be turned off during the daylight hours by means of a day/night switch.

Weight considerations necessitated the removal of one of the radiometers from the first Nimbus. The choice was made to fly the HRIR, because it will photographically display nighttime cloud cover with comparatively high resolution, which was felt to be of great immediate need. This radiometer also contains some unique features, such as a radiation-cooled detector, which it was desired to test in orbit.

The precise calibration of the sensors, and a continuous check of the stability of this calibration during integration and prelaunch procedures, is of the utmost importance. Both the relative spectral response and the absolute total-intensity response of each sensor channel are measured. In the primary calibration, the total response of the thermal channels is measured by exposing each channel to a blackbody target whose temperature can be varied, and precisely measured, over a temperature range of 80°K to 320°K. In the spectral calibration, the response of the sensors is compared to the response of special "standard" detectors. A Nernst glower is usually employed as a source for the thermal channels; for the visible channels, well-calibrated tungsten sources are used. Precise knowledge of the spectral response of the radiometer is especially necessary because the tungsten calibration, with a filament temperature of 2900°K, must be converted to solar energy with an equivalent blackbody temperature of 5800°K to obtain a valid total-energy calibration. To check calibration, blackbody and visible light sources must be used throughout the preflight period to ensure that the predetermined total-energy calibration is maintained. Only a few points on the calibration curve are checked, but the emphasis is still on high precision.

Thorough tests of both the MRIR and the HRIR will be made during the next several months, both in balloon and in aircraft flights, in order to evaluate the performance of the instruments and to aid in the interpretation of the data.

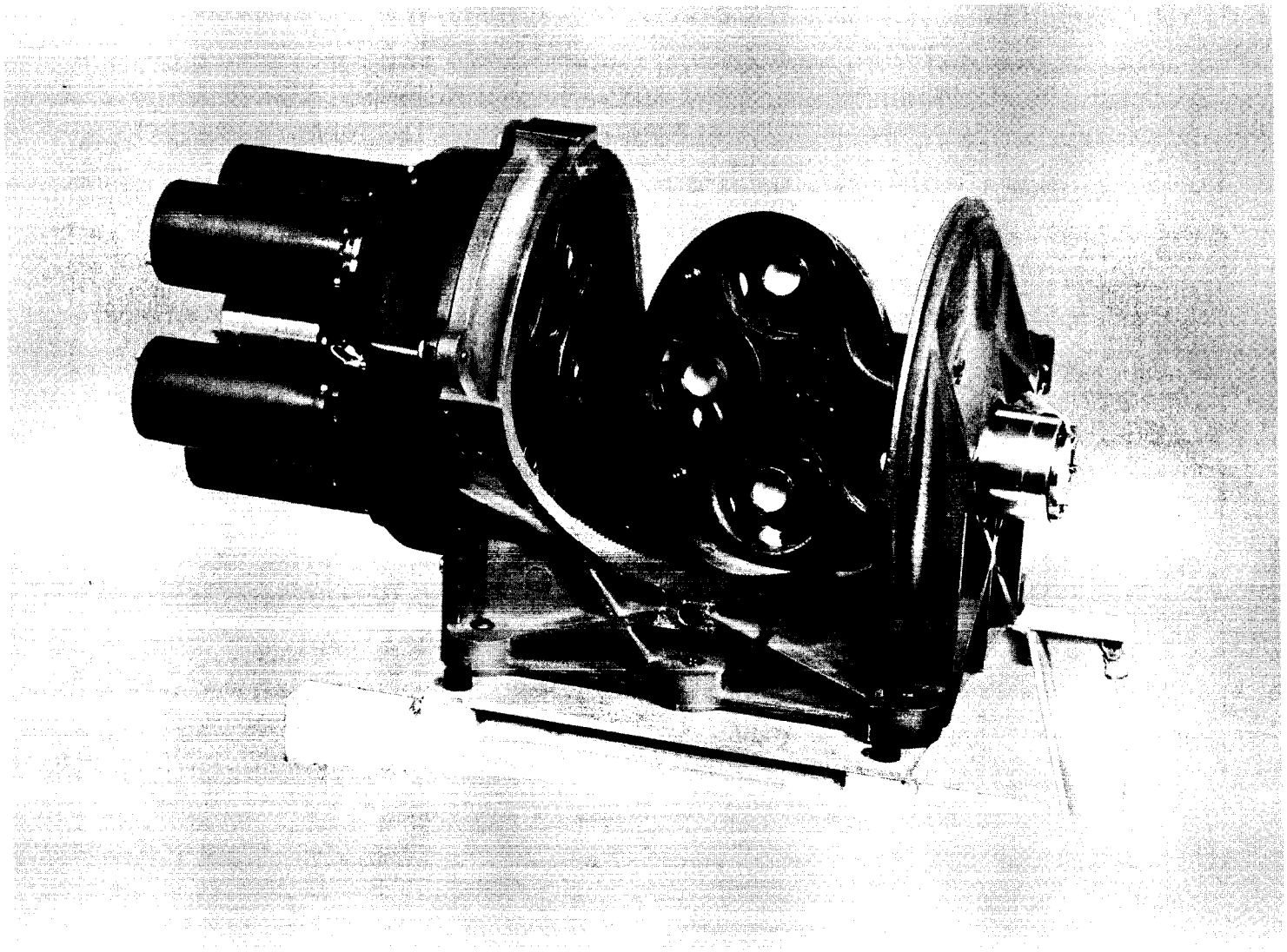

Figure 1 - Nimbus 5-Channel Medium-Resolution Infrared Radiometer

WAVELENGTH (MICRONS)	FUNCTION
6.6 – 7.0	WATER VAPOR ABSORPTION
10.0 – 11.0	SURFACE AND CLOUD RADIATION
0.6 – 0.75	CLOUD COVER
7.5 – 30	TOTAL EARTH EMISSION
0.2 – 4.0	ALBEDO (REFLECTED SOLAR RADIATION)

Figure 2 - MRIR Spectral Regions

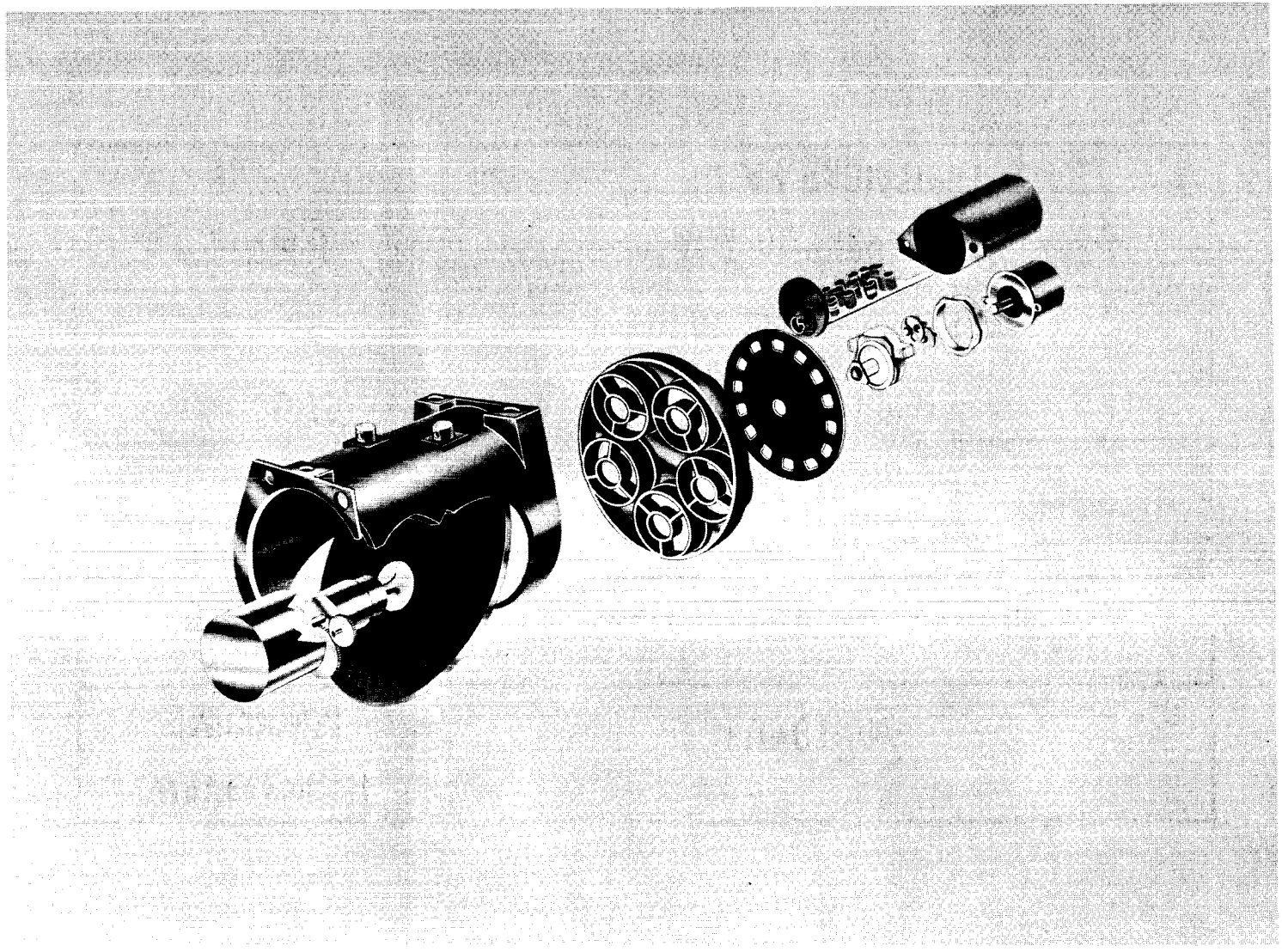

Figure 3 - MRIR Components

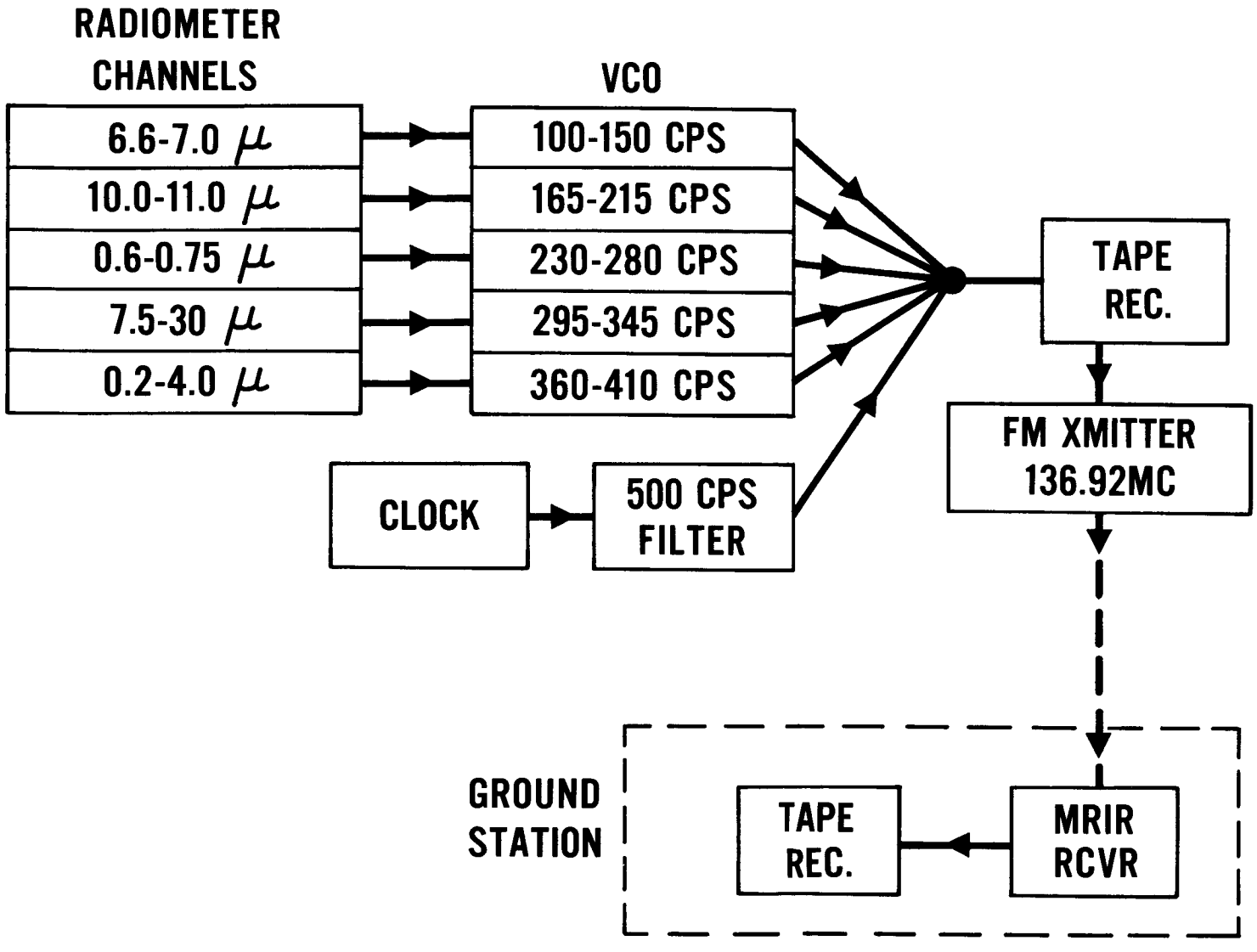

Figure 4 - Nimbus MRIR Subsystem, Block Diagram

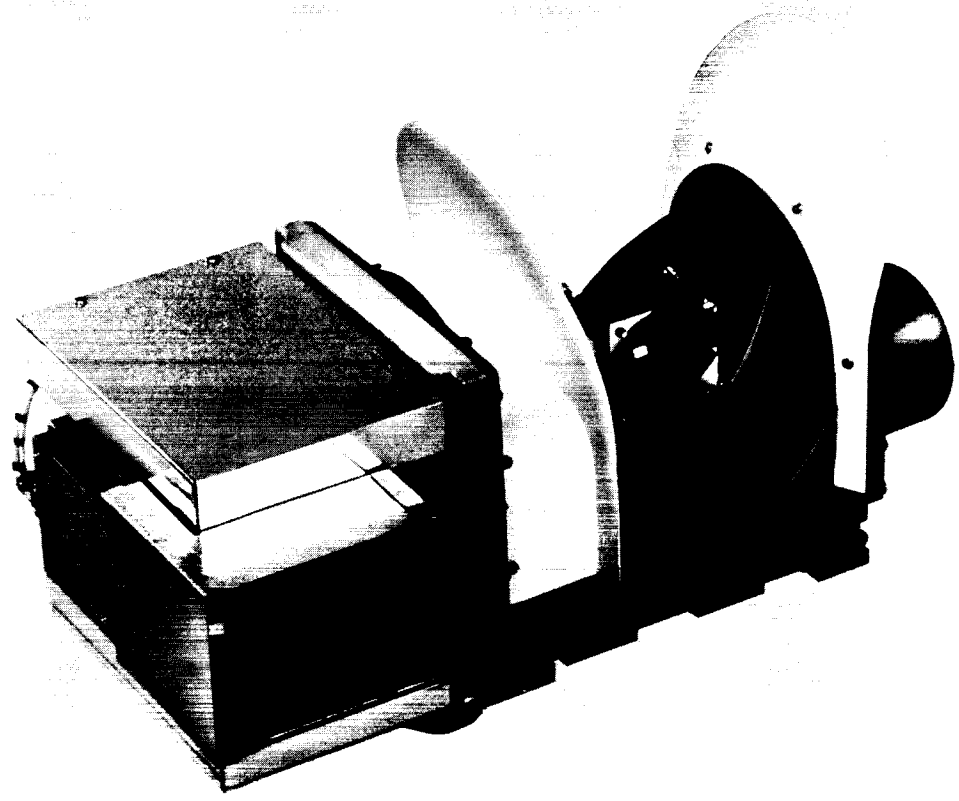

Figure 5 - Nimbus High-Resolution Infrared Radiometer

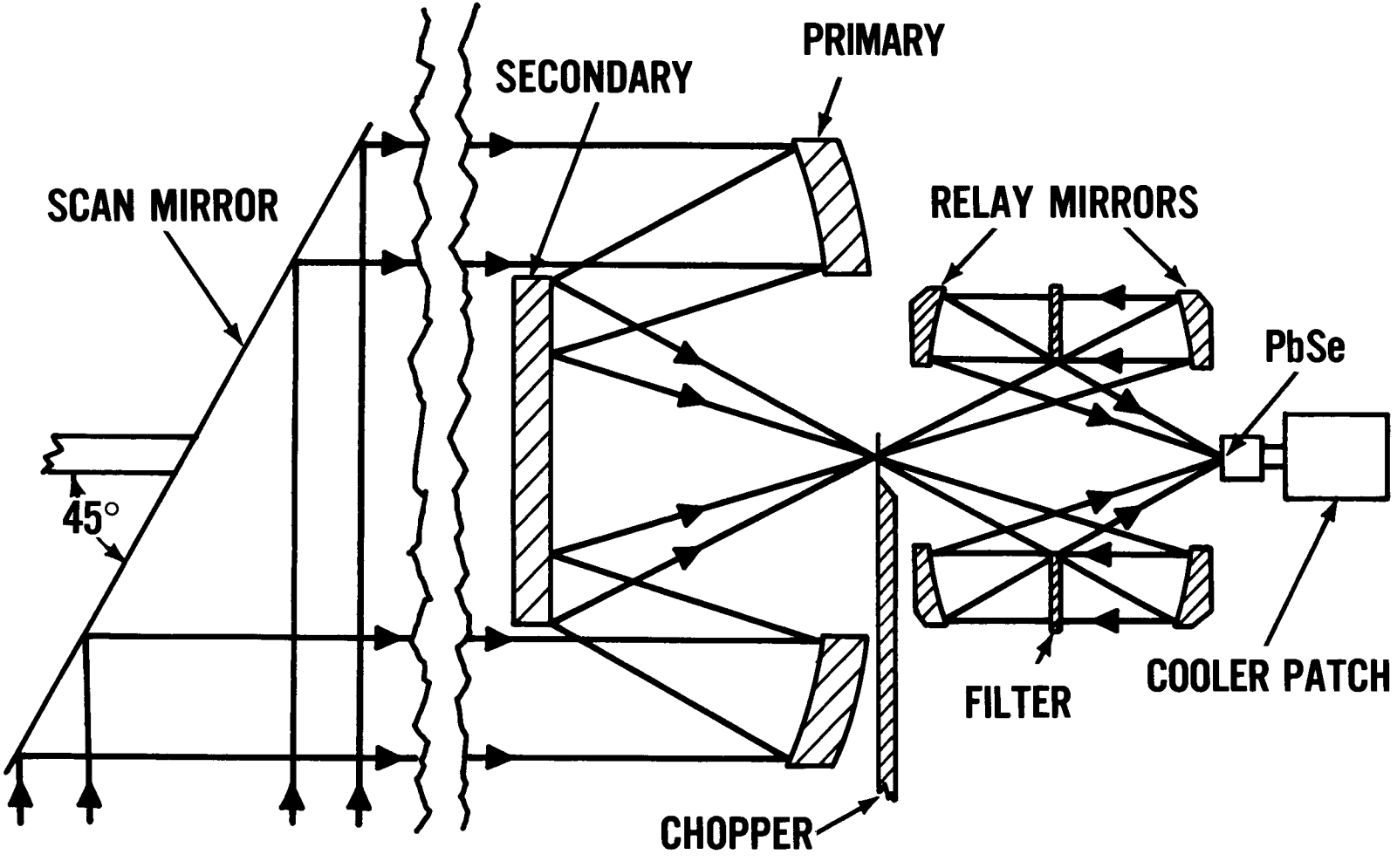

Figure 6 - HRIR Optical System

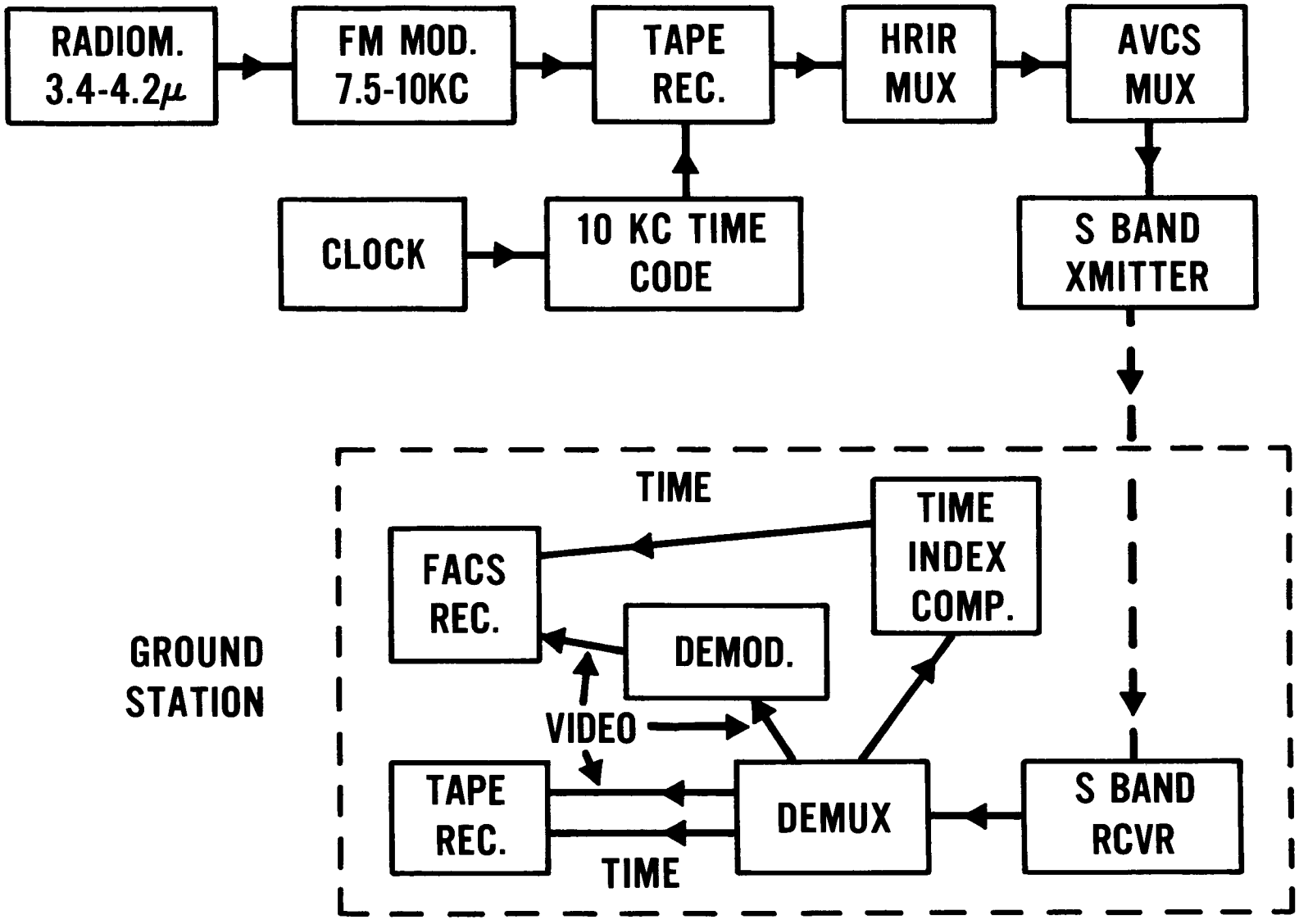

Figure 7 - Nimbus HRIR Subsystem, Block Diagram

17. NIMBUS ADVANCED VIDICON CAMERA SUBSYSTEM

By G. L. Burdett and R. Shapiro,
GSFC; Dr. J. E. Keigler, RCA/Astro
Electronics Division

17. NIMBUS ADVANCED VIDICON CAMERA SUBSYSTEM

ILLUSTRATIONS

Figure		Page
1	Nimbus AVCS Characteristics	7
2	Nimbus AVCS Vidicon Characteristics	8
3	Nimbus AVCS Prototype Characteristics	9
4	Nimbus AVCS Coverage	10
5	Nimbus AVCS Prototype #2	11
6	Nimbus AVCS Spaceborne Equipment, Block Diagram	12
7	Nimbus AVCS Cameras	13
8	Vidicon Tube, Diagram	14
9	Nimbus AVCS Tape Transport	15
10	Nimbus Spacecraft, Artist's Conception	16
11	Nimbus AVCS and HRIR Ground Support Equipment, Block Diagram	17
12	Nimbus AVCS and HRIR Ground Station Equipment	18
13	Nimbus AVCS Kinescope	19
14	Nimbus AVCS Ground Station Equipment	20
15	Nimbus AVCS Resolution Test	21
16	Test Photograph Taken by Nimbus AVCS Prototype #2, Camera #1	21

17. NIMBUS ADVANCED VIDICON CAMERA SUBSYSTEM

By G. L. Burdett and R. Shapiro,
GSFC; Dr. J. E. Keigler, RCA/Astro
Electronics Division

The Nimbus advanced vidicon camera subsystem, commonly referred to as the AVCS, will provide cloud pictures during the daylight portions of the Nimbus orbit. It is so named because of its improvement over previous TV systems.

Figure 1 lists the detailed characteristics of the AVCS camera. The field-of-view shown here represents that of three adjacent cameras. The variable iris, an important advance in the AVCS, gives the camera a greater dynamic range.

Figure 2 lists the characteristics of the AVCS vidicon. The resolution of the overall system was greatly improved by doubling the diameter of the vidicon, and increasing the number of scan lines from 500 to 800 per frame.

Figure 3 shows the demonstrated characteristics of the prototype AVCS. A comparison of this system with previous ones shows that the dynamic range has been doubled, the limiting resolution improved by a ratio of approximately 2 to 1, and the linearity improved by an order of magnitude.

Figure 4 shows how the arrangement of three identical AVCS cameras can provide instantaneous television coverage of an area measuring 420 nautical miles in a north-south direction, and 1,575 nautical miles in an east-west direction. These cameras cover a path which, at the equator, provides adjacent picture coverage for successive orbits. A new set of three pictures is taken automatically at 91-second intervals, providing an approximate 5-percent overlap between successive exposures during daylight portions of the orbit. The AVCS is automatically turned on at daybreak and off at nightfall by a sensing circuit which senses the position of the solar paddles.

Figure 5 is a photograph of AVCS prototype #2 now in the final stages of environmental testing. This photograph shows the three television

cameras set up for calibration with the collimators attached. The sequence timer and power-control module, a 2/2 configuration, is visible just behind the cameras. Next to this module is the camera-electronics module, a 3/3 configuration, with the frequency multiplexer, a 1/1 configuration, directly behind it. The cylindrical can at the upper right contains the four-track magnetic tape recorder. Future AVCS flight models will be completely redundant, consisting of six cameras, two tape recorders, two multiplexers, and two sequence timers. All equipment will be remotely controlled by commands from the CDA ground station.

Figure 6 is a block diagram of the spaceborne AVCS. The television video signals and the time signal are stored in the tape recorder. On playback, these stored signals, together with the HRIR data and the associated time code, are multiplexed and transmitted to the Nimbus ground station by means of the S-band transmitters.

The three television cameras are arranged in a trimetrogon array, as shown in Figure 7. This arrangement provides maximum coverage and adequate resolution, and eliminates the distortion which is characteristic of wide-angle lenses. A 17-mm focal-length lens, used with a 1-inch vidicon tube, gives a ground resolution of approximately 1/2 mile per television line.

The gear mechanism is the variable iris with which each camera is equipped to ensure consistently high picture quality through the orbit. Normally, this iris is adjusted automatically by a servo cosine pot attached to the solar platforms. The opening can vary from f/16 at the solar zenith to f/4 near the poles. The iris also may be set at either of two preset openings (f/8 or f/16) by command from the ground. For each picture, the vidicon is exposed for 40 milliseconds by a 2-bladed solenoid-operated focal-plane shutter. This exposure results in a smear of less than 1/2 a TV line in a 500-nautical-mile orbit.

Figure 8 sketches an end view and a side view of the vidicon. A unique addition to each camera is a self-contained 16-step gray-scale calibrator, a small prism attached to the faceplate of the vidicon. The calibrator wedge is illuminated by means of a Xenon flash tube fired simultaneously with each opening of the camera shutter. The gray-scale image appearing at the edge of each picture serves as a

reference for the information given in the picture. Also, each camera has a self-contained sweep calibration, consisting of a precision reticle pattern etched directly on the nonconductive side of the vidicon face. This pattern becomes an inherent part of each picture and provides a reference for the measurement of geometrical distortion. Vertical shading of the picture, a serious problem in slow-scan TV, is reduced in this system by clamping the video signal to a fixed voltage at the beginning of each TV line. This fixed voltage, often referred to as black-reference voltage, is generated in the vidicon by means of a light mask on its face.

The tape recorder used in this system has four tracks, one for each of the three TV cameras and one for the timing signal. Thirty-two frames of three pictures each are taken during each orbit, and the 1200 feet of 1/2-inch mylar-base tape contained in the recorder are sufficient to record two full orbits of data. FM, with a subcarrier deviating between 70 kc and 120 kc (including sync tips), is used to record the video signals. The tape recorder operates only during the readout of the picture from the cameras. A tape speed of 30 in/sec gives a maximum tape-packing factor of 4, 000 cycles/in. The Nimbus clock time code is recorded on channel 1 as the amplitude modulation on a 50-kc carrier. Besides providing exposure time for the video data on the other three tracks, the 50-kc carrier is used as a pilot tone for wow and flutter compensation in the ground-station monitoring equipment. The tape recorder can be bypassed on command from the ground station to permit the transmission of direct pictures.

Figure 9 illustrates the unique tape-transport design used in the Nimbus system. The entire transport mechanism, with associated electronics, is mounted in a single pressurized enclosure. The tape is stored on two 8-inch coaxial reels, and the path of the tape between the two reels is regulated by a driving capstan and three rollers. The tape wraps 180 degrees around the capstan immediately after leaving one reel and again immediately before entering the other reel. Thus, the tape is wrapped twice around the capstan, in opposite directions, to form a closed loop about the recording heads. Transient changes in tape speed oppose and cancel torque transients at the capstan, reducing recorder flutter to less than 0. 2 percent rms. As there is only one drive motor, negator springs, located on the under side of the base casting, are required to torque the reels against each other and thus to maintain constant tape tension. A flywheel is used to cancel the mean

angular momentum of the tape transport and to maintain the uncompensated angular momentum at less than 0.004 lb-in/sec. This reduction in angular momentum of the tape transport helps to minimize the demands on the Nimbus stabilization system.

Figure 10 is an artist's conception of the Nimbus spacecraft in orbit. When the craft comes within range of the CDA station, the AVCS tape recorder is instructed, through the command system, to play back the recorded pictures. During playback, the signals from the four channels of the recorder, plus another four from a separate multiplexer associated with HRIR, are frequency-multiplexed into a 700-kc composite signal. The resulting signal is used subsequently to modulate the S-band transmitter. Frequency translation to the proper subcarrier slot in the 700-kc composite baseband is performed by balanced mixers and bandpass filters. The filters provide high attenuation outside the passband to prevent crosstalk, and linear phase response inside the passband to prevent distortion of the video image. The composite signal is transmitted to the ground station by a General Electronics Laboratory transmitter. This transmitter, with a power output of 5 watts, is designed for FM telemetry applications in the 1700-Mc region.

Figure 11 is a block diagram of the AVCS and HRIR ground support equipment. The S-band signal received from the spacecraft is demodulated by the S-band receiver, and the composite signal is separated into eight subcarrier channels and translated into frequencies which can be recorded. All eight of these channels are recorded on the MinCom G-114 tape recorder. Simultaneously, the three video signals are demodulated and displayed on three kinescopes which reproduce the pictures on 70-mm film. The timing channel is also demodulated, and the exposure time of the pictures is sorted out by the index computer and displayed on each picture.

Figure 12 is a photograph of a portion of the AVCS and HRIR ground station which is intended to be used during the interrogation and debugging of the spacecraft, and also during the thermal-vacuum test. The CDA ground station will be very similar, but will contain a central control console for operational use.

The first two racks shown at the right of the figure contain the power supplies and the S-band receiver used by the integration ground station and the van at the Pacific Missile Range. This receiver is a UHF

telemetry receiver with a noise figure of 13 db, and demodulation linearity of 1 percent over a ±1. 5-Mc band.

The next three racks shown in the figure contain the demultiplexer, the FM demodulator, the jack panel which allows maximum flexibility, and the kinescope with its deflection circuitry, camera, and film processor.

The last rack shown in the figure contains the HRIR index computer for computing HRIR exposure time, and an A-scope for line-by-line monitoring of the AVCS video signal.

In the CDA ground station, the three video signals from the three TV cameras in the spacecraft are demodulated and displayed on three kinescopes identical to the one shown in Figure 13. A 70-mm camera, in conjunction with a rapid film processor, photographs the kinescope display and develops the film. This kinescope system was especially developed for the AVCS ground station. On playback, the recorder signal generates a new picture on each kinescope every 8 seconds. Each kinescope picture is photographed, processed, and made available 1 minute after it is received. Therefore, the 96 pictures accumulated during one orbit can be available for analysis approximately 5 minutes after transmitting the playback command.

Figure 14 shows the MinCom G-114 tape recorder/reproducer which records the four AVCS channels and the four HRIR channels during interrogation of the spacecraft. The MinCom is played back at one-eighth the recording speed, and the AVCS and HRIR data are subsequently retransmitted to Washington, D. C. for use by the U. S. Weather Bureau. The center rack in the figure contains the tape-speed control unit, which uses the 50-kc time signal from the Nimbus clock (recorded in the spacecraft) to control the MinCom playback speed; the rack shown on the left contains the AVCS index computer, which computes the exposure of each set of three pictures in real time and displays this information on each picture. The HRIR video and time code are displayed in real time on a 70-mm 13-inch film strip similar to that used for the AVCS pictures.

Figures 15 and 16 are pictures taken with a prototype AVCS system. Figure 15 is a test pattern photographed during an AVCS resolution test, and Figure 16 is a photograph by camera 1 of prototype 2. Both

pictures show the identifying camera, orbit, and frame numbers, together with the time code and reticle pattern described previously.

With the exception of the satellite transmitter and the ground receiver, the entire AVCS system was developed by the Radio Corporation of America's Astro-Electronics Division at Princeton, New Jersey.

I CAMERA CHARACTERISTIC

a. LENS- FOCAL LENGTH- 17MM

b. FIELD OF VIEW-37°

c. TRIMETROGON FIELD OF VIEW-107°

d. SHUTTER-DOUBLE BLADED FOCAL PLAIN

e. SHUTTER SPEED 40 MS

f. CONTINUOUSLY VARIABLE IRIS f/4 TO f/16

g. DYNAMIC RANGE- MIN BRIGHTNESS 14 FOOT LAMBERT AT f/4

- MAX 11,400 FOOT LAMBERT AT f/16

Figure 1 - Nimbus AVCS Characteristics

a. 1" DIAMETER (0.625" USEFUL DIAGONAL)

b. 800 SCAN LINES PER FRAME

c. VIDICON SENSITIVITY 0.004 FT CANDLE SEC. TO 0.4 FT CANDLE SEC

Figure 2 - Nimbus AVCS Vidicon Characteristics

a. BRIGHTNESS RATIO OF 32:1 (10 GRAY SCALES)

b. 60KC VIDEO BAND WIDTH

c. 6.5 SEC READOUT

d. 91 SEC BETWEEN FRAMES

e. LIMITING RESOLUTION 725 TV LINES

f. LINEARITY 0.5%

g. STORES 32 PICTURES PER ORBIT

h. GROUND RESOLUTION ½ MILE PER TV LINE

Figure 3 - Nimbus AVCS Prototype Characteristics

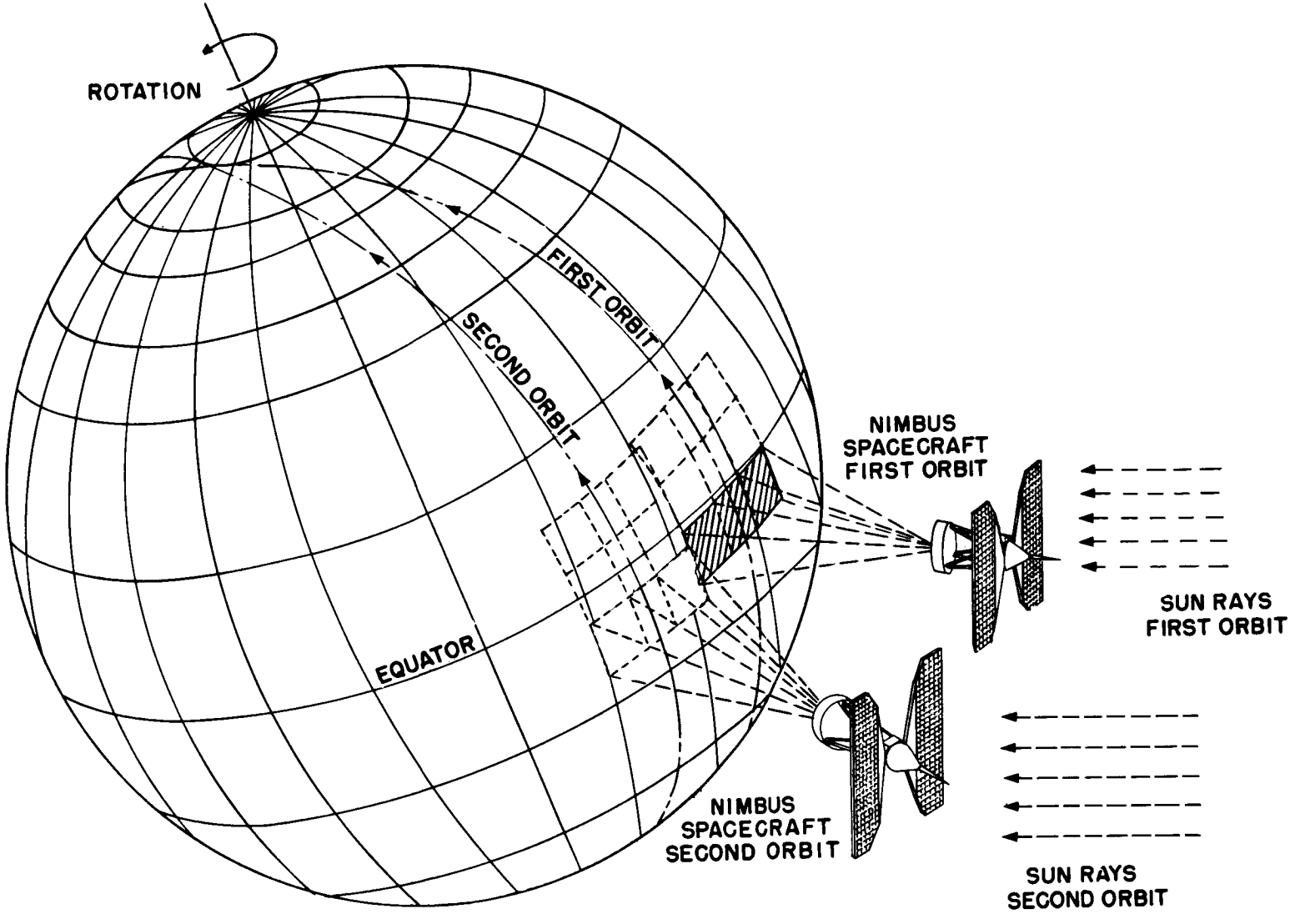

Figure 4 - Nimbus AVCS Coverage

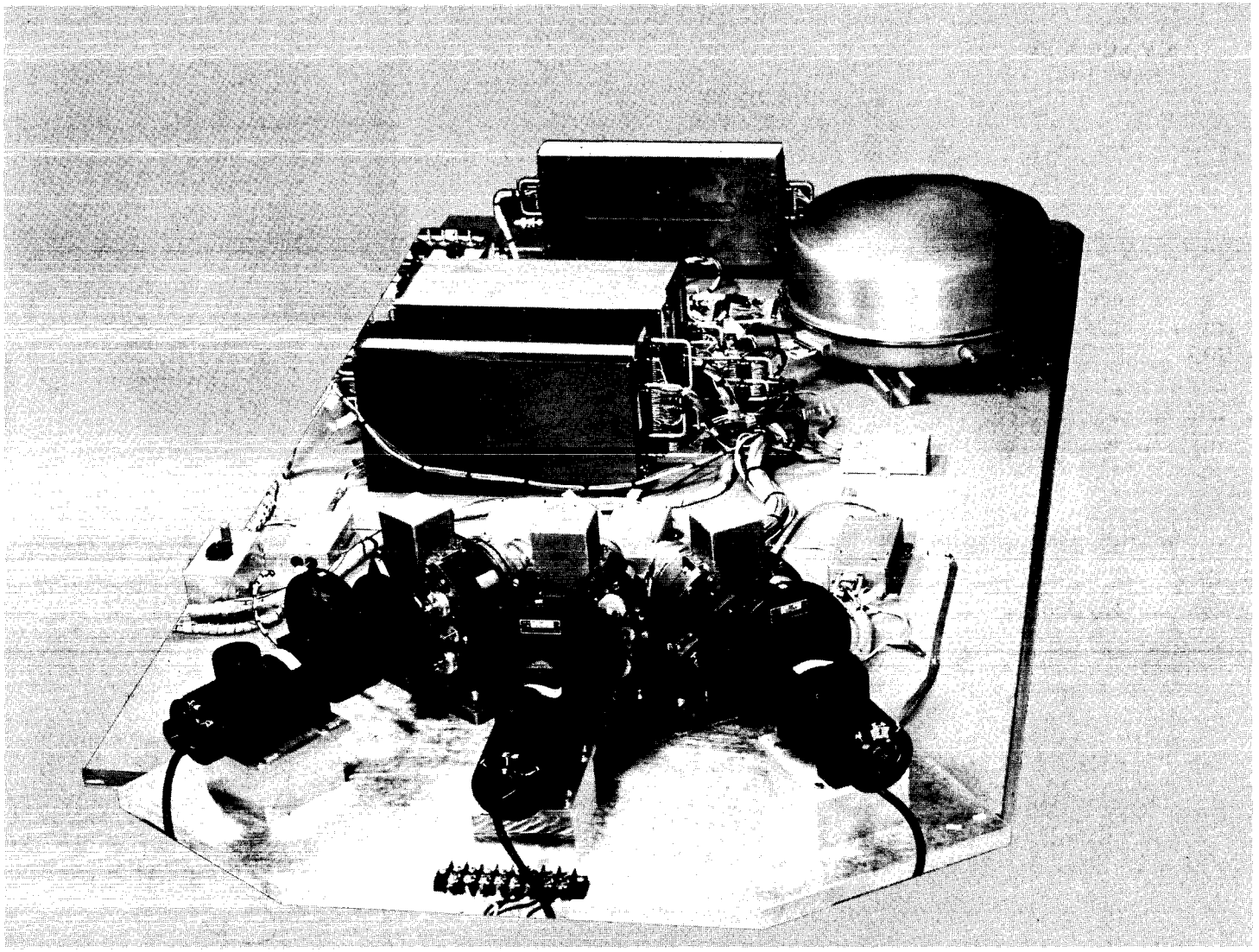

Figure 5 - Nimbus AVCS Prototype #2

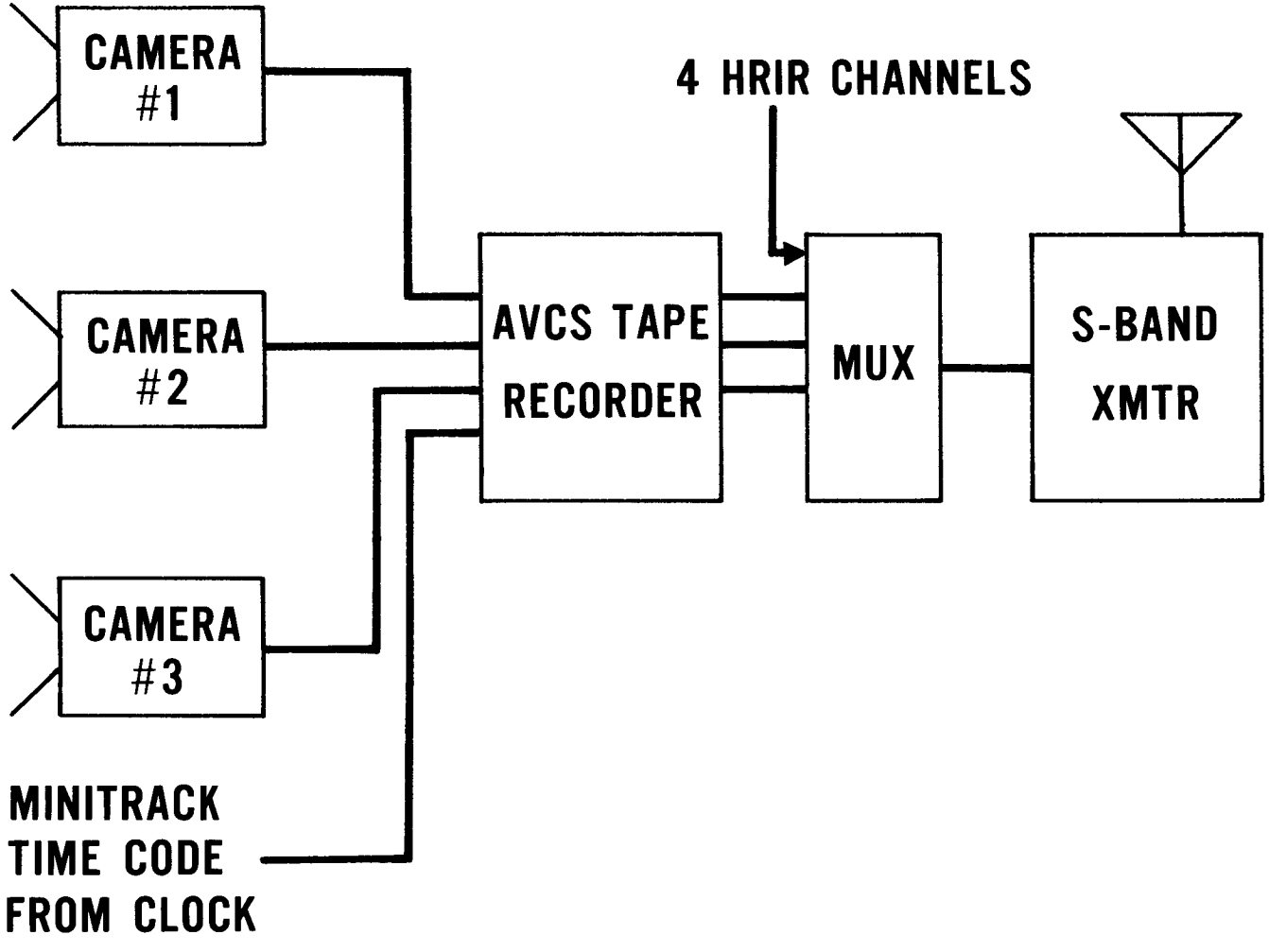

Figure 6 - Nimbus AVCS Spaceborne Equipment, Block Diagram

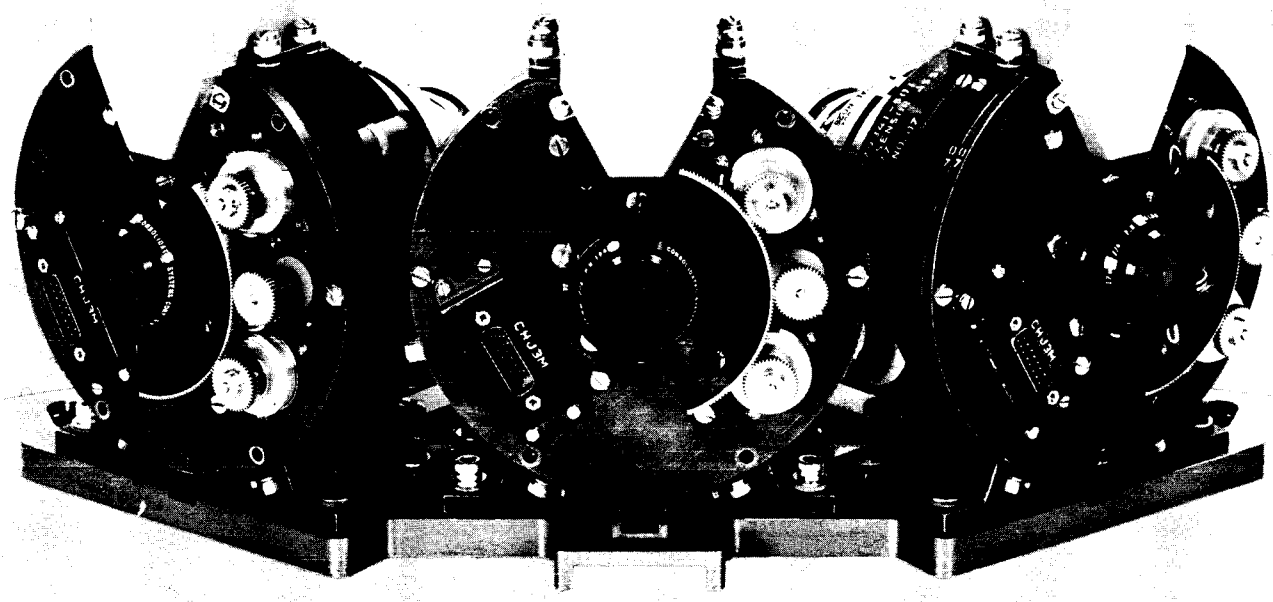

Figure 7 - Nimbus AVCS Cameras

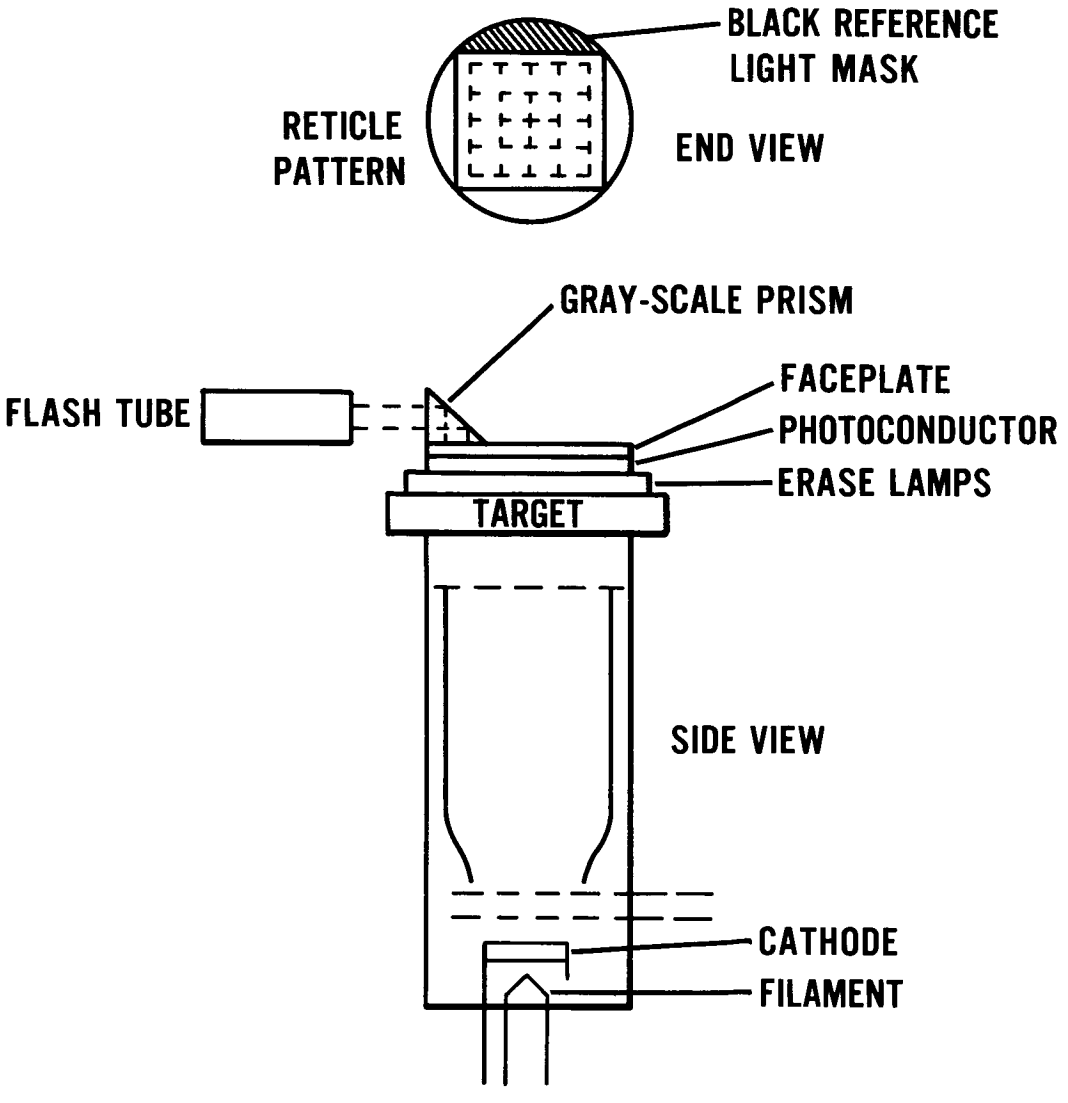

Figure 8 - Vidicon Tube, Diagram

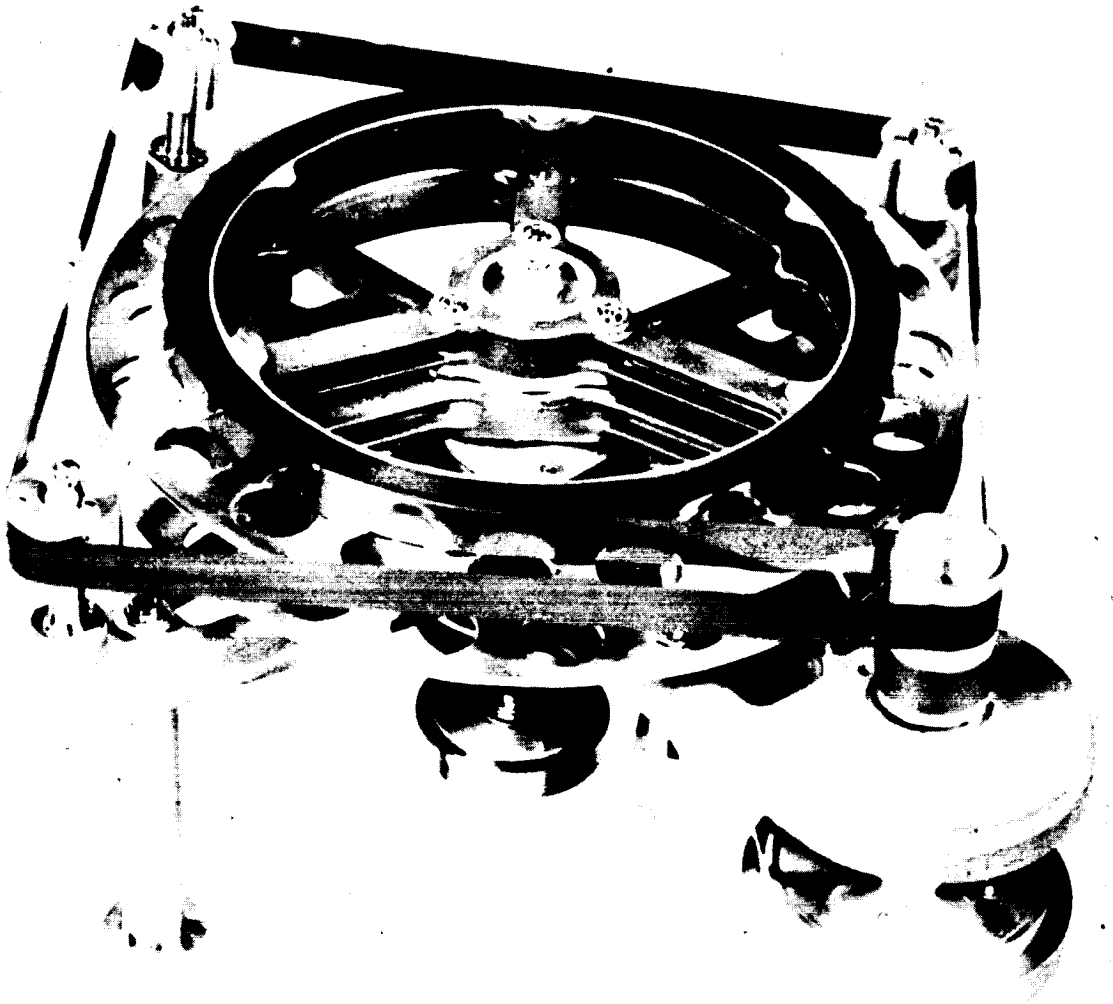

Figure 9 - Nimbus AVCS Tape Transport

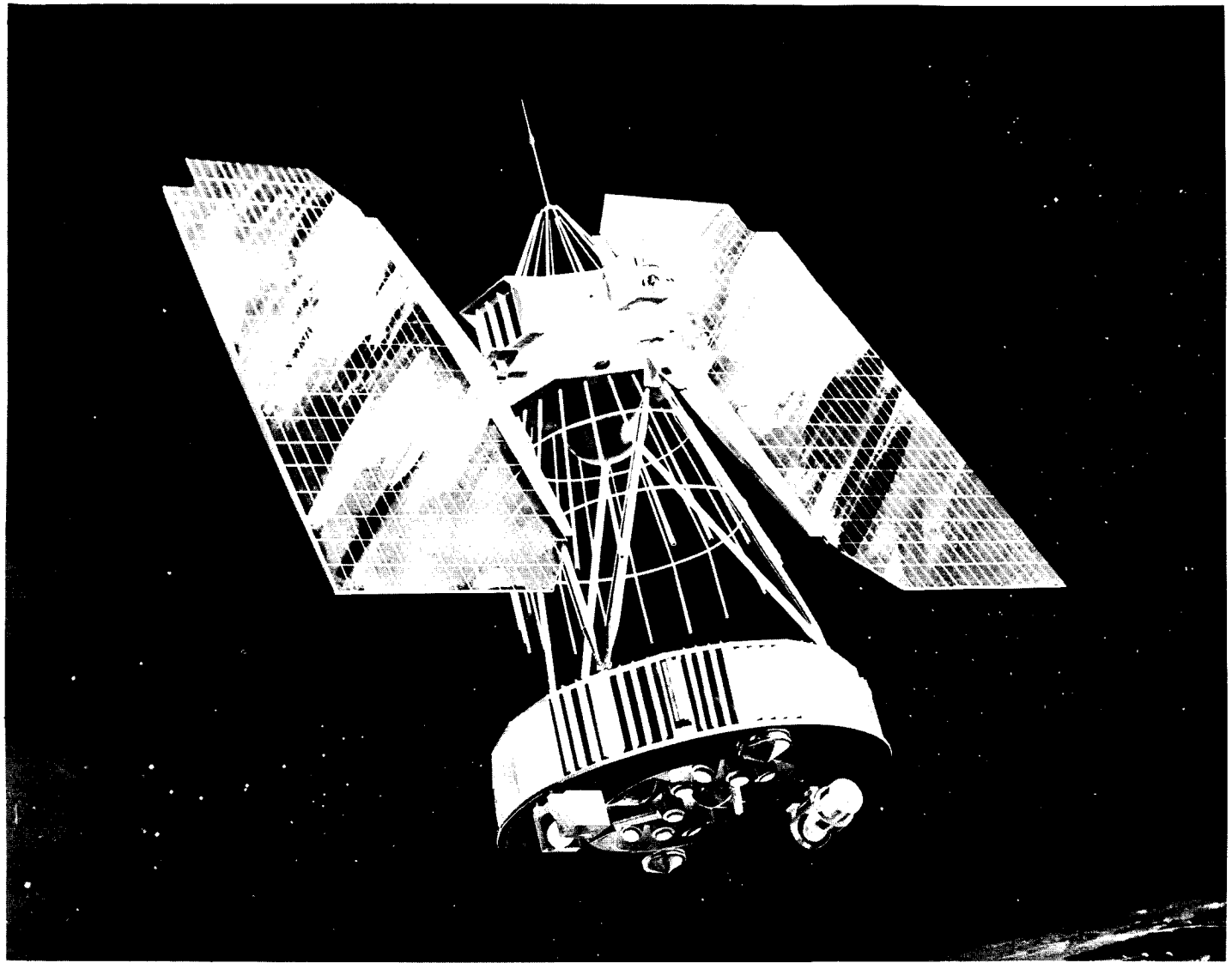

Figure 10 - Nimbus Spacecraft, Artist's Conception

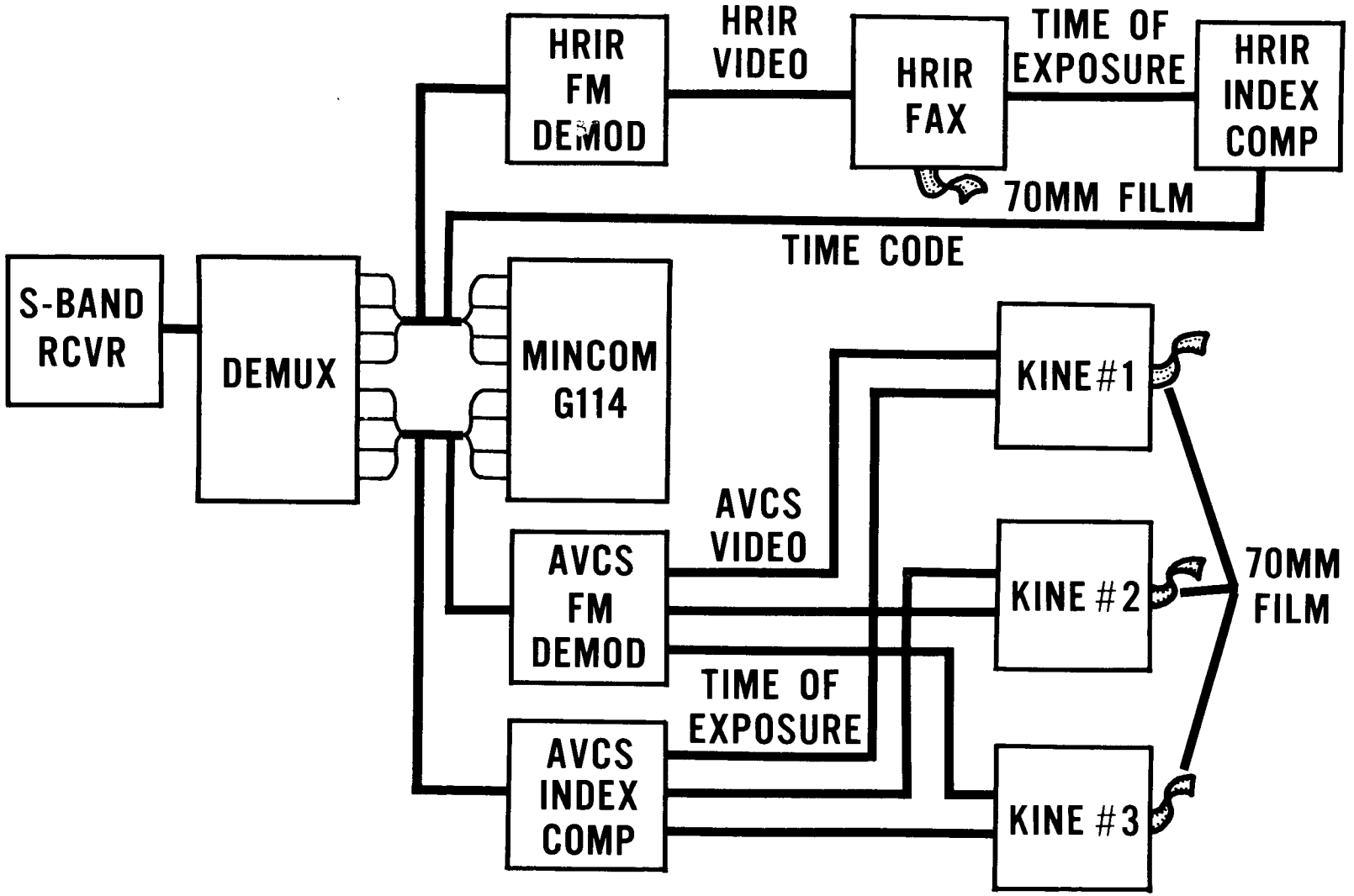

Figure 11 - Nimbus AVCS and HRIR Ground Support Equipment, Block Diagram

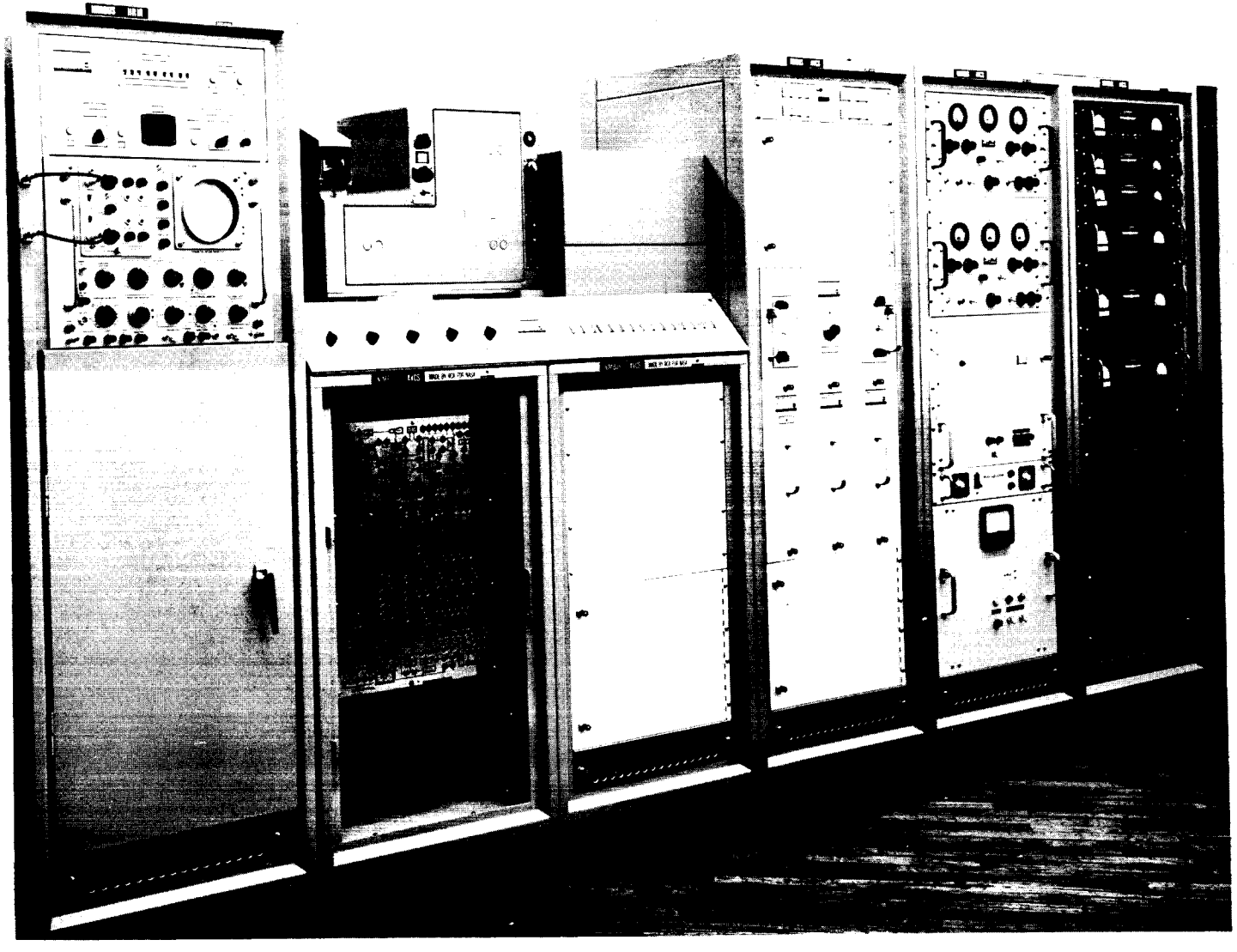

Figure 12 - Nimbus AVCS and HRIR Ground Station Equipment

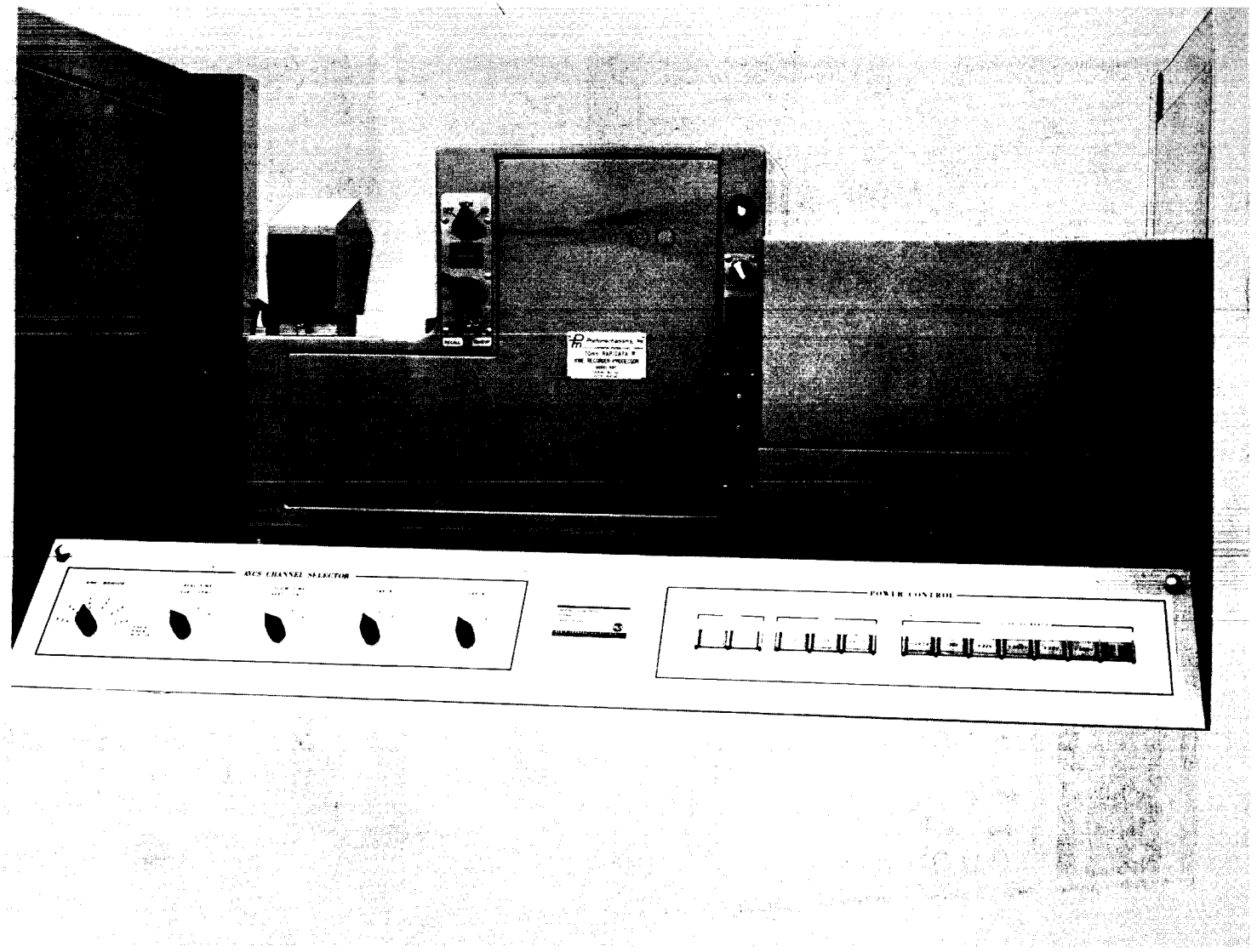

Figure 13 - Nimbus AVCS Kinescope

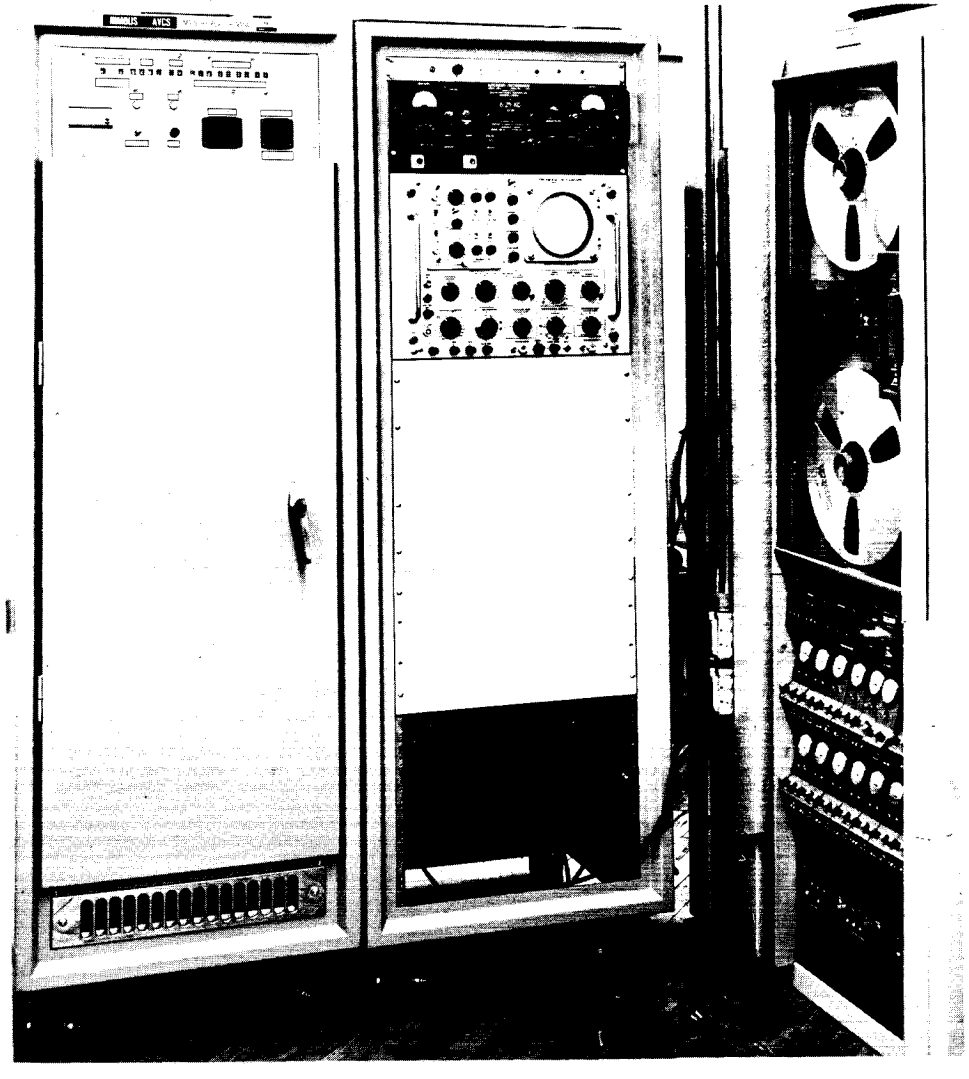

Figure 14 - Nimbus AVCS Ground Station Equipment

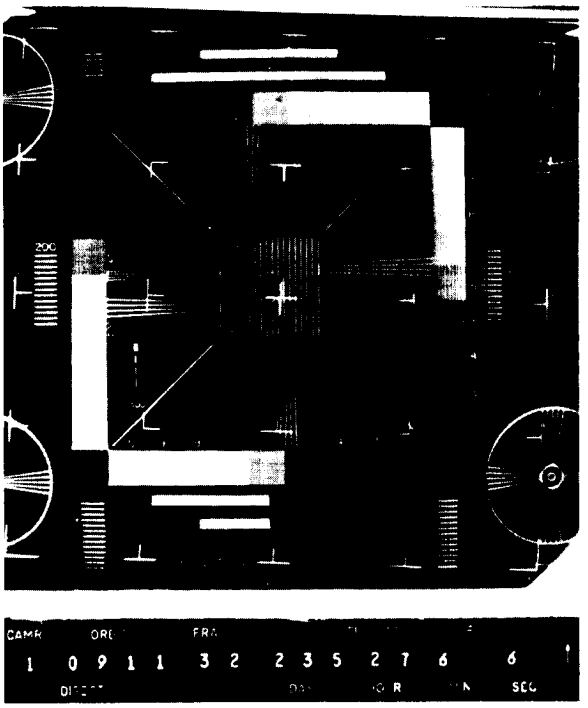

Figure 15 - Nimbus AVCS Resolution Test

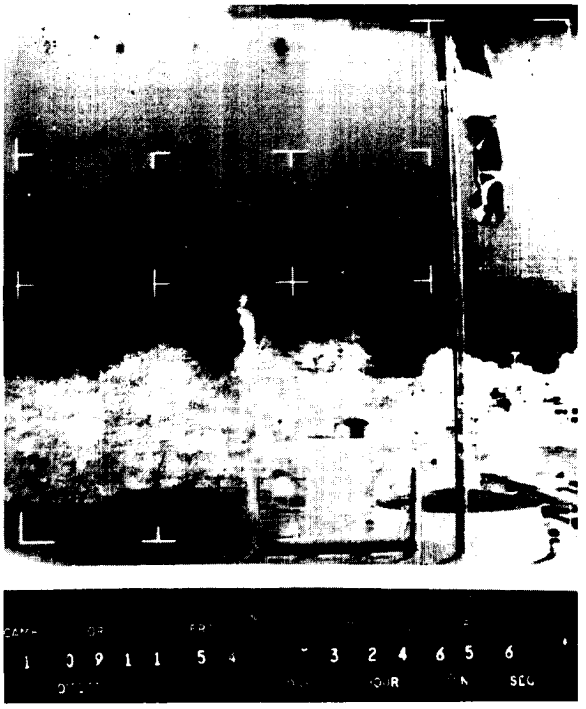

Figure 16 - Test Photograph Taken by Nimbus AVCS Prototype #2, Camera #1

18. AUTOMATIC PICTURE TRANSMISSION SYSTEM

By C. M. Hunter, GSFC; P. H. Werenfels, L. G. Saxton, and M. Shepetin, RCA/Astro Electronics Division; T. F. Maher and P. Metzner, Fairchild Stratos Electronic Systems Division

18. NIMBUS AUTOMATIC PICTURE TRANSMISSION SUBSYSTEM

ILLUSTRATIONS

Figure		Page
1	Polystyrene Vidicon Front End (Cutaway)	12
2	Automatic Picture Transmission Sensory Housing	13
3	Automatic Picture Transmission Space-borne Equipment, Block Diagram.	14
4	Automatic Picture Transmission Ground Station, Block Diagram	15
5	Automatic Picture Transmission Antenna and Pedestal	16
6	Automatic Picture Transmission Ground-Station Console.	17

AUTOMATIC PICTURE TRANSMISSION SYSTEM

By C. M. Hunter, GSFC; P. H. Werenfels, L. G. Saxton, and M. Shepetin, RCA/Astro Electronics Division; T. F. Maher and P. Metzner, Fairchild Stratos Electronic Systems Division

INTRODUCTION

The Automatic Picture Transmission System (APTS), developed under the technical direction of the Goddard Space Flight Center (GSFC), is composed of two subsystems: a satellite camera and transmission subsystem, and a ground-station receiving and recording subsystem.

The satellite camera and transmission subsystem was designed and fabricated by RCA/AED and is a storage vidicon system capable of long-duration storage and a very slow readout rate. It takes wide-angle pictures from a satellite and transmits them in real time on a very narrow information bandwidth to the ground station for recording on facsimile equipment.

The ground-station receiving and recording subsystem was designed and fabricated by Fairchild-Stratos/ESD and consists of an antenna, receiver, and facsimile equipment which is relatively simple, inexpensive, and appropriate for wide distribution. Thus, the flight-ground system is well suited for application to local weather observation and forecasting applications.

PRINCIPLE OF OPERATION

The spaceborne system consists of optics, including the shutter; a 1-inch electrostatic-storage vidicon camera; and a telemetry-type FM transmitter for relaying video signals to ground stations equipped with an FM receiver and facsimile-recording equipment.

The camera is programmed for continuous cycles of prepare, expose, and readout. The image is projected on the storage vidicon through a 108-degree lens; the exposed picture, stored electrically in the insulating layer of storage vidicon target, is then available for very slow

readout. During readout, the transmitted narrowband video signal is picked up by the ground-station antenna and fed to the receiver, which in turn feeds it to an automatically phased facsimile recorder.

The lens is a Tegea Kinoptic 108-degree f/1.8 lens with a focal length of 5.7 millimeters. Optical exposure is through a double-bladed shutter operated by two solenoids; exposure time is 40 milliseconds.

Figure 1 indicates the construction of the 1-inch ruggedized vidicon developed by RCA. This vidicon is identical to the vidicons used in the AVCS, except for the addition of a layer of polystyrene which provides the image-storage capability. The tube is operated by holding the target potential constant, and raising or lowering the mesh voltage with respect to the target during the prepare, expose, and readout sequences. As with the AVCS vidicon, this vidicon has a number of reticles evaporated on the faceplate to provide an accurate means for measuring linearity, and to help align the vidicon in the camera.

The electron-beam deflection is accomplished electromagnetically, using precision deflection yokes; focusing is also performed electromagnetically.

The subsystem consists of three major elements: The sensory housing (Figure 2) containing the optic lens, shutter, vidicon, deflection yokes, video preamp, and amplifier; a 2/2 module containing the video detector, power converters, sequence timer, switching circuits, and modulator; and a 1/1 module containing the FM transmitter. Figure 3 is a simplified block diagram of the entire subsystem.

Once this subsystem is turned on, it operates continuously throughout the daylight portion of each orbit, reading out one picture every 208 seconds. Signals from the day-night switch turn it off each orbital "night," and turn it on again at the beginning of each orbital "day."

When the shutter is triggered, the image is projected on the photoconductive layer, after which it is electronically "developed"; that is, it is transferred to the polystyrene storage layer. This occurs during the first 8 seconds of every picture sequence. During the remaining 200 seconds, the picture information is read out at a scanning rate of 4 lines per second.

The video information is sampled by a pulse technique rather than by a continuous readout; this pulse technique provides a better signal-to-noise ratio than do other techniques for the very slow readout which is characteristic of the APT subsystem. During readout, the vidicon-scanning beam is pulse-modulated by applying pulses to the vidicon cathode. The beam-sampling rate is 1200 times per horizontal line, using a 12-percent duty cycle. The readout, as seen at the output of the video amplifier, consists of amplitude-modulated pulses. A video detector then detects the information, giving a continuous analog readout. Detection takes place during the sampling pulse intervals, thereby disregarding any noise which might be present between the sampling pulses.

The detected signal is then used to amplitude-modulate the 2400-cps subcarrier, resulting in a double sideband-modulated subcarrier with sidebands extending across 1600 cycles. The modulated subcarrier in turn frequency-modulates the 136.950-Mc transmitter, an all-solid-state device designed and fabricated by United Aerospace Division of United Electrodynamics in Pasadena, California. The transmitter produces about 5.5 watts of RF power at its output while drawing less than 1 ampere of current at -24.5 volts dc.

The output of the transmitter is fed to the Nimbus APT antenna mounted on the surface of the spacecraft and facing the earth at all times. The antenna produces a linearily polarized radiation pattern, so that the satellite antenna-to-ground antenna relationship remains constant.

On the ground, the signal is received by a relatively simple antenna and is processed by the FM receiver and the facsimile recording equipment, producing a real-time cloud-cover picture for the locale of the particular ground station.

Because facsimile equipment is used on the ground to reproduce the cloud image, the equipment must be started and the facsimile printout synchronized with the scanning beam of the vidicon; this is done during the 8-second period while the camera sensor is going through its prepare, expose, and develop cycle. At the beginning of the 8-second period, a 300-cps start tone lasting 3 seconds is transmitted to the ground and automatically shifts the facsimile equipment from the standby to the operate mode. During the next 5 seconds, phasing pulses are transmitted which automatically synchronize the facsimile machine

with the vidicon scanning beam; picture printout follows, being built up line by line as it is scanned from the vidicon storage layer. When the satellite passes out of range of the ground station, the facsimile equipment reverts automatically to the standby condition.

The sequence just described assumes automatic receipt of a picture sequence from the beginning of the 208-second frame. It is more likely that the satellite will come into view of the ground station at some time after the first 8 seconds; however, as soon as the satellite signal is detected the facsimile machine can be started and phased manually so that the maximum amount of information may be obtained; this should result in at least three pictures during a pass over the ground station. At an orbital altitude of 500 nautical miles, each picture will cover a ground area of approximately 1050 by 1050 nautical miles, with a north-south overlap of 300 nautical miles between adjacent pictures.

All timing is controlled by the sequence timer which is part of the system, and which operates from the 2400-cps signal from the spacecraft clock. However, should this clock signal be lost for any reason, an internal 2400-cps oscillator is automatically switched in to operate the system, provided spacecraft power is available.

The system has a linearity of 0.5 percent and a resolution of approximately 700 lines, based on the picture printed out on the facsimile recorder. Sensitivity is 0.7 foot-candle-seconds for highlight brightness (whitest white). The cutoff point where noise is the influencing factor is 0.03 foot-candle-seconds. The signal-to-noise ratio is 26 db, and approximately 7 shades of gray are observed with a change in density of 0.12 per step.

A prototype unit of the APT subsystem has been successfully qualified and has been delivered to GE for integration in the sensory ring. The first flight model is well along the road to completion and will soon be entering the environmental test phase.

Besides minor development problems too numerous to mention here, a few more significant ones occurred during environmental testing. Humidity tests revealed a moisture sensitivity in the preamplifier which was overcome by improved potting. Difficulties which developed during vibration in the shutter and in one of the mounting feet were easily overcome; however, one problem arose which is still unsolved. Like the

AVCS, the APT subsystem had a calibration gray scale flashed on the vidicon at the bottom of each picture; the preprototype subsystem pointed up a deficiency in this area attributable to the basic operation of the vidicon, and considerable time was expended trying to improve the gray scale, with little success. Proceeding with vibration tests, the flash-tube electrodes were broken and no simple measures solved the problem. As a consequence, rather than delay work further, the calibration gray scale was removed entirely. Both the operating and mechanical problems will be studied further, and the gray scale will be made a part of the subsystem again as soon as possible, although not in time for Nimbus A.

There were no failures of the camera as a result of vacuum-thermal tests, although noise problems and false triggering of the logic gave trouble and resulted in a second vacuum-thermal test; the coherent noise, caused by sporadic high-frequency oscillations from the focus-current regulator, was eliminated by additional low-pass filtering. The false triggering, located in the harnessing between the checkout equipment and the vacuum-thermal chamber, was eliminated by shielding various wires and by relocating other wires in the harness.

OPERATIONAL GROUND STATIONS

Operational ground stations consist basically of a receiving antenna, preamplifier, FM receiver, and facsimile recording equipment. Auxiliary equipment for each station consists of a test signal source and a facsimile test set. Figure 4, the block diagram for the ground stations, shows signal flow for the video information and for the antenna control.

After several months of evaluation, the ground-station contract for two prototypes and 40 production units was let in July 1962 to the Electronic Systems Division of the Fairchild Stratos Corporation in Wyandanch, Long Island, New York. Since that time, other areas such as spare parts, training programs, and other functions in support of the ground stations themselves, have been added, and are in various stages of contractual negotiations, which are progressing smoothly.

Because it is intended that the ground stations will be employed by the military and the Weather Bureau, a users working group has been established with representatives from each of the services, the Weather Bureau, and NASA/GSFC. Since Goddard is the prime contractor, this arrangement provides the contact between the users and the con-

tractor and is the means of information exchanges and resolution of problems affecting all users.

To obtain the best equipment for the ground stations in a reasonable time without undertaking significant additional R & D effort, every effort was made to use off-the-shelf commercial items wherever possible, and modifications and development efforts have been kept to the minimum. As a result, the ground station contains the following commercial items:

Antenna and Pedestal (Figure 5)

The antenna, manufactured by "TACO," is an 8-turn helix, 14 feet long and 27 inches in diameter, with a ground plane 72 inches in diameter. It has a beamwidth of 34 degrees at the half-power points and a gain of 13 db.

The pedestal, manufactured by The Scientific Atlanta Company, contains the position motor drives, gearing, position synchro transmitter, and limit switches. It is capable of 720-degree rotation from stop to stop in azimuth, and 180-degree rotation (horizon to horizon) from stop to stop in elevation. Total weight including antenna counterbalances is approximately 850 pounds.

The position control and indicator units located in the ground station console, which are also supplied by Scientific Atlanta, provide independent rate control of both azimuth and elevation and continuous display of the antenna position.

Preamps and Receiver

The preamplifier, mounted on the antenna pedestal, and the receiver, located in the console (Figure 6), are both supplied by Vitro Electronics. The preamp is the Nems-Clarke PR203A, a two-stage RF amplifier with a 5-Mc passband and a gain of 22 db, the latter required to compensate for losses in the RF cable when the antenna and the receiver must be located some distance apart. Maximum separation can be 1000 feet with the present cable.

The FM receiver is the Nems-Clarke Model 1440-2, crystal-controlled from 130 to 140 Mc, with a second oscillator vernier control which

allows tuning across 150 kc on either side of the operating frequency. The receiver has a selectable bandwidth of 50 or 100 kc.

The presence and condition of the input signal can be determined both aurally and visually, as the unit has a speaker and four indicators: signal strength, tuning, video output, and deviation.

Facsimile Recorder

The facsimile recorder, a modified version of the Fairchild Camera and Instrument Co. Scan-a-Fax, is a helix and writing-blade-type machine, using electrosensitive (wet) paper and forming the picture by depositing ions on the paper. The machine operates at 240 rpm with a resolution of 100 lines per inch, has an aspect ratio of 1 on an 8 by 8-inch format, and will produce 10 shades of gray varying from black to white. The unit will start and phase automatically upon receipt of the 300-cps start tone and the 5 seconds of phasing pulses from the satellite equipment, or it can be started and phased manually.

Facsimile Test Set

The facsimile test set is a noncommercial item designed and fabricated by Fairchild Stratos to provide the necessary signals to the facsimile equipment for checking its proper operation. These signals include start tones, phasing, pulses, resolution patterns, and gray shades.

Test Signal Source

The test signal source is a small lightweight portable transmitter designed to test the RF portion of the ground-station system. The unit is battery-operated with a pullout antenna for field use.

The transmitter operates at the 136.950-Mc carrier, frequency-modulated with a 2400-cps signal, and has a power output of 5 milliwatts. When using this unit, one shade of gray will appear on the facsimile recorder. The unit is also provided with a connector so that its signal may be plugged directly into the preamp or the receiver.

Console

The console also has a pullout writing desk on the left side, and a thermostatically controlled storage drawer under the facsimile recorder

for the electrosensitive paper to prevent the paper from freezing if the ambient room temperature drops below 30°F.

Also included in the console is the power distribution panel, which contains the main power, heated-drawer power, and preamp power switches, the indicator lights, and the fuses.

Environmental Considerations

Although the equipment is basically off-the-shelf-type items, every effort has been made to ensure performance in the various environments expected at the ground-station locations. Environmental tests will be to a modified Mil-E-4970 specification. Environmental conditions are:

	Unsheltered Equipment	Sheltered Equipment
Temperature, operating	-65°F to +160°F	+32°F to +125°F
Temperature, storage	-65°F to +160°F	-65°F to +160°F
Humidity	95% at +160°F	95% at +160°F
Altitude, operating	10,000 feet	10,000 feet
Altitude, storage	50,000 feet	50,000 feet
Sand and dust	yes	no
Vibration in shipping container	Up to 5g	Up to 5g
Shock in shipping container	10g	10g
Wind, operate	60 mph	--
Wind, survive	120 mph	--
Ice, operate	1/2-inch radial	--

System Status

The first prototype ground station was scheduled for acceptance tests (including compatibility tests with satellite equipment) early in December, 1962.

The second prototype was scheduled for the environmental tests previously outlined and then for final acceptance tests, during the latter part of December or early January, 1963. Production units are expected to be on schedule.

System Application

The usefulness of the APT system is tied in with the narrow bandwidth of information which makes it possible to use extremely simple and inexpensive ground-station equipment. Coupled with the continuous picture-taking and transmission cycles, the APT system will enable meteorological groups anywhere in the world to receive local real-time cloud pictures at least once a day.

Summary of System Parameters and Characteristics of Satellite Equipment

Lens: Tegea Kinoptic
108^{o}
f/1.8
5.7 mm focal length

Shutter: Double-blade, operated by 2 solenoids with time delay between their operation

Shutter time: 40 millisec

Vidicon: 1-inch ruggedized storage type
0.44x0.44 inch useful raster area
Layers: Reticle
Transparent conductive layer
Photoconductor
Polystyrene

Operating Voltages: Target: Constant 475 volts with respect to cathode
Mesh: 500 volts-prepare
450 volts-expose
485 volts-readout

Scanning: Pulse technique rather than continuous scanning
Pulse-modulated by pulsing cathode

Sampling rate: 1200 pulses per horizontal line

Sampling frequency: 4800 cps

Subcarrier modulator frequency: 2400 cps

Modulation frequency: 0-1600 cps

Degree of modulation: 50%

Timing: 2400-cps input from spacecraft clock, or internal 2400-cps oscillator

Start time for facsimile recorder: 300 cps for 3 sec (100% modulates 2400-cps subcarrier)

Phasing pulses: 5 seconds of white level interrupted by 12.5 milliseconds of black level at the beginning of each of the 20 lines

Transmitter: Solid-state FM
Frequency: 136.950 Mc
Transmitted bandwidth: 800-4000 cps
Deviation: ±10 maximum kc
Output power: 5.5 watts (approximate)
Input power: 22 watts (approximate) @ -24.5 volts

Subsystem Characteristics
Weight: 25.5 pounds
Power requirements: 40.1 watts
Linearity: 0.5%
Sensitivity: 0.7 ft. candle-sec (whitest white)
0.03 ft. candle-sec (lowest light sensitivity)
Signal-to-noise: 26 db (peak signal-to-RMS noise)
Resolution: 700 lines
Gray scale: 7 steps with change in density of 0.12 between steps
Readout time: 200 seconds
Ground coverage per picture: Approximately 1050 x 1050 nautical miles for 500-nautical-mile altitude
Picture overlap per frame, 300 nautical miles

Operational Ground Stations

Power: 5 kw, 105-130 volts, 50-60 cps, single-phase

Antenna: 8-turn helix
- Beamwidth: 34° @ 3 db points
- Gain: 13 db

Pedestal: Azimuth rotation: 720°
- Elevation rotation: 180°

Preamplifier: 2 stage RF amplifier
- Gain: 22 db
- Passband: 5 Mc

Receiver: Tuning range: 130 to 140 Mc - crystal-controlled
- Vernier control: ±150 kc
- Bandwidth: 50 to 100 kc, selectable
- Indicators: Signal strength
  - Tuning
  - Video output
  - Deviation

Facsimile recorder: Helix and writing blade
- Continuous tone (10 gray steps)
- Automatic and manual start and phasing
- Electrosensitive paper (wet)
- 240 rpm
- Resolution: 100 lines per inch
- Subcarrier: 2400 cps
- Modulation: AM
- Aspect ratio: 1 (8- by 8-inch format)

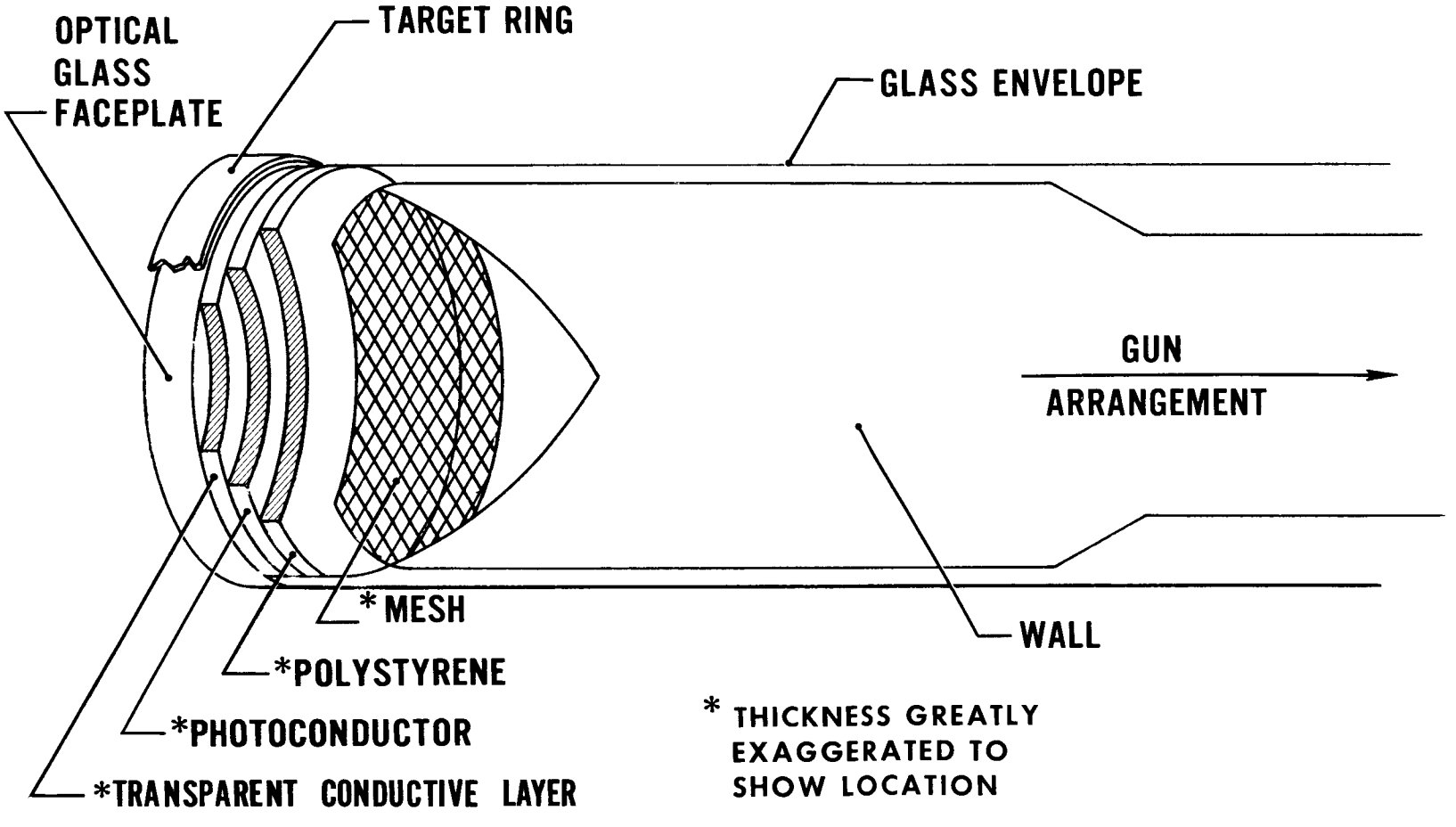

Figure 1 - Polystyrene Vidicon, Front End (Cutaway)

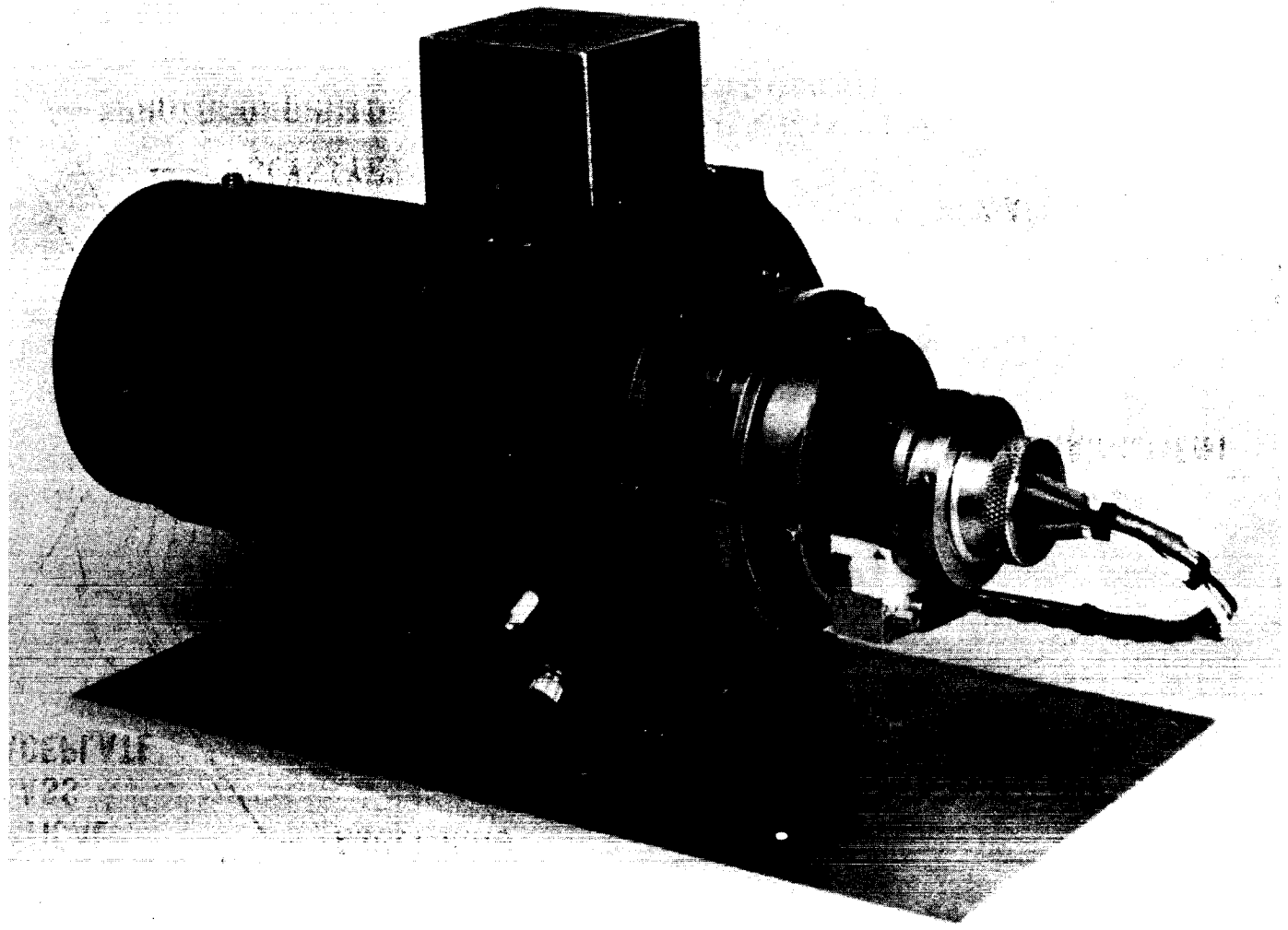

Figure 2 - Automatic Picture Transmission Sensory Housing

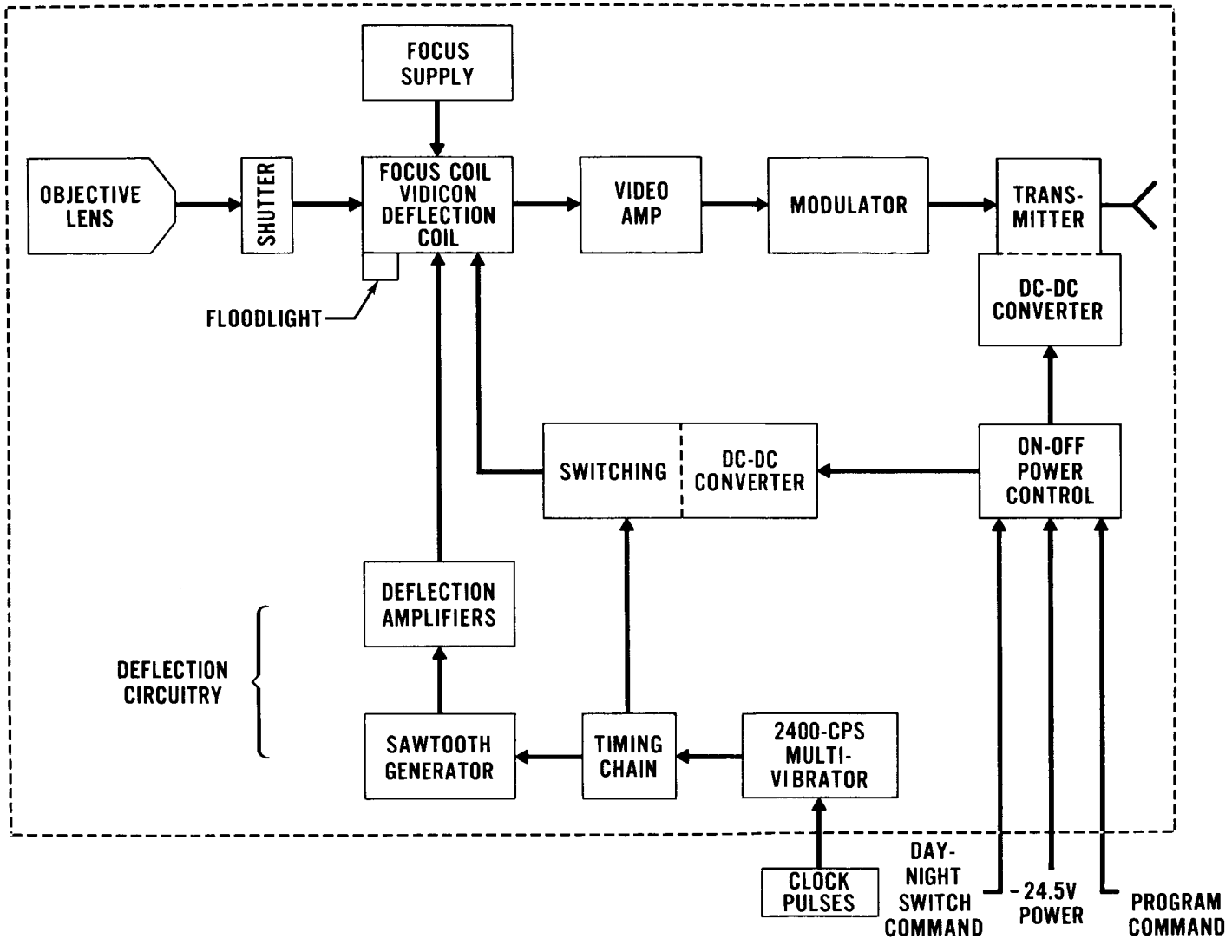

Figure 3 - Automatic Picture Transmission Spaceborne Equipment, Block Diagram

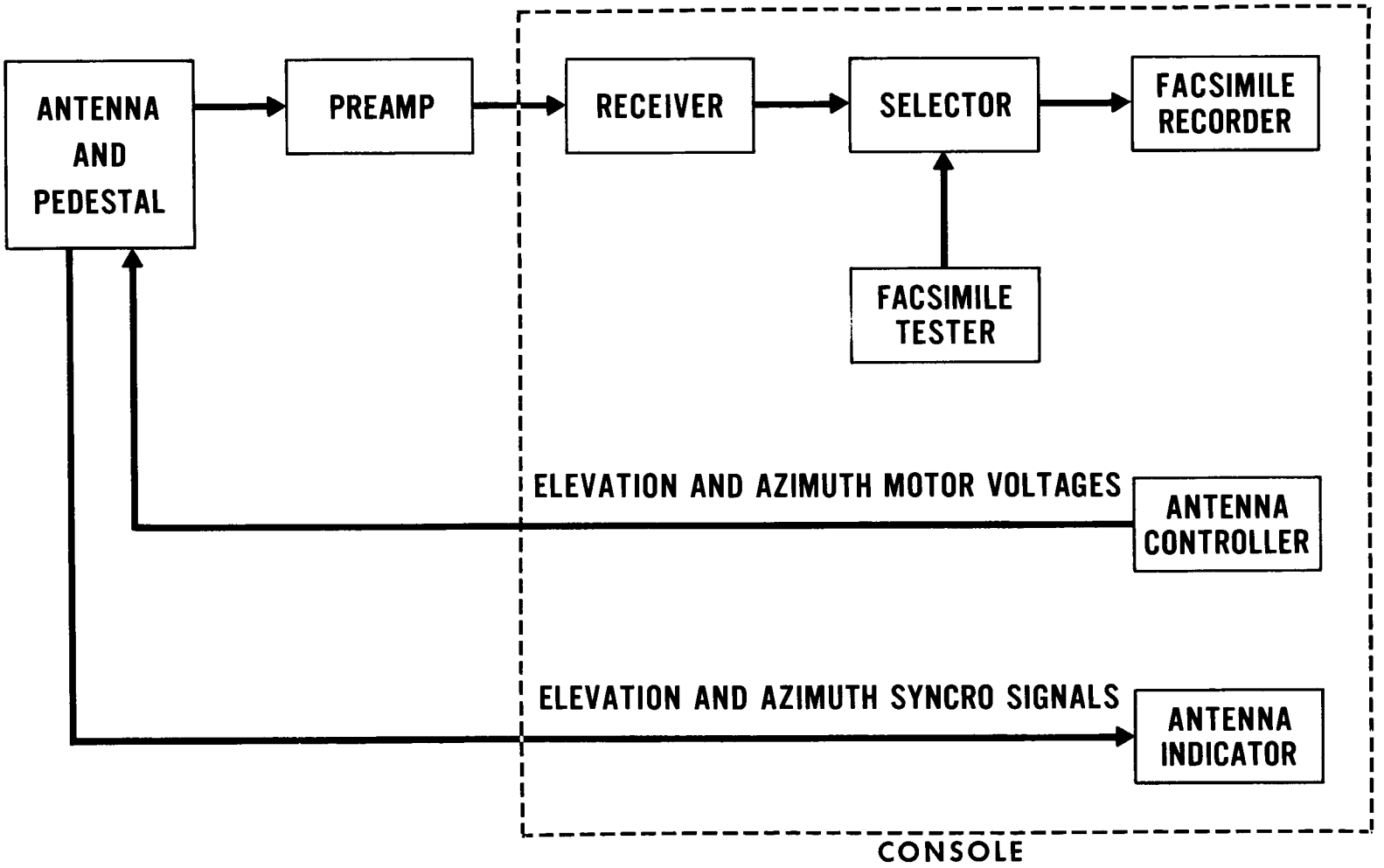

Figure 4 - Automatic Picture Transmission Ground Station, Block Diagram

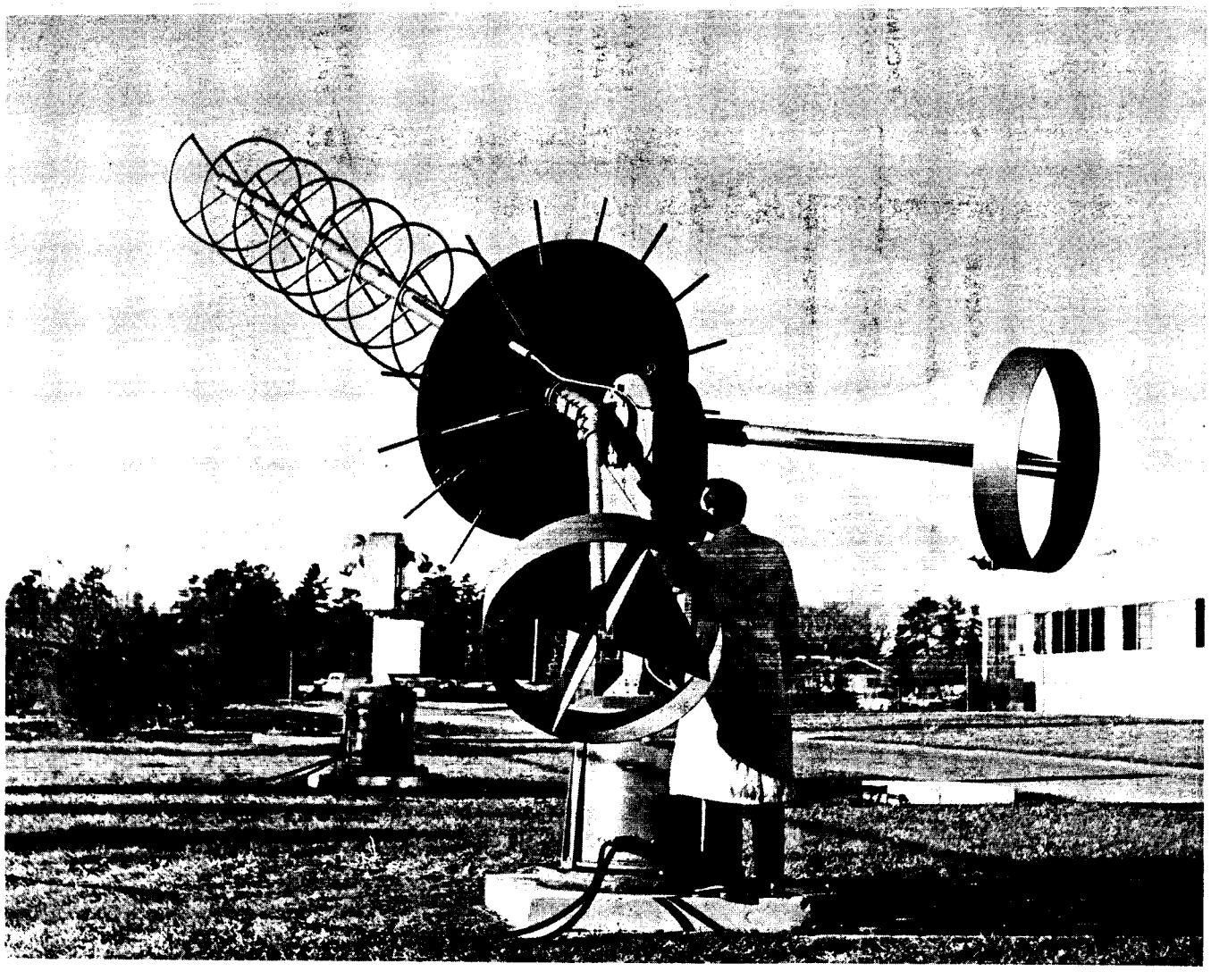

Figure 5 - Automatic Picture Transmission Antenna and Pedestal

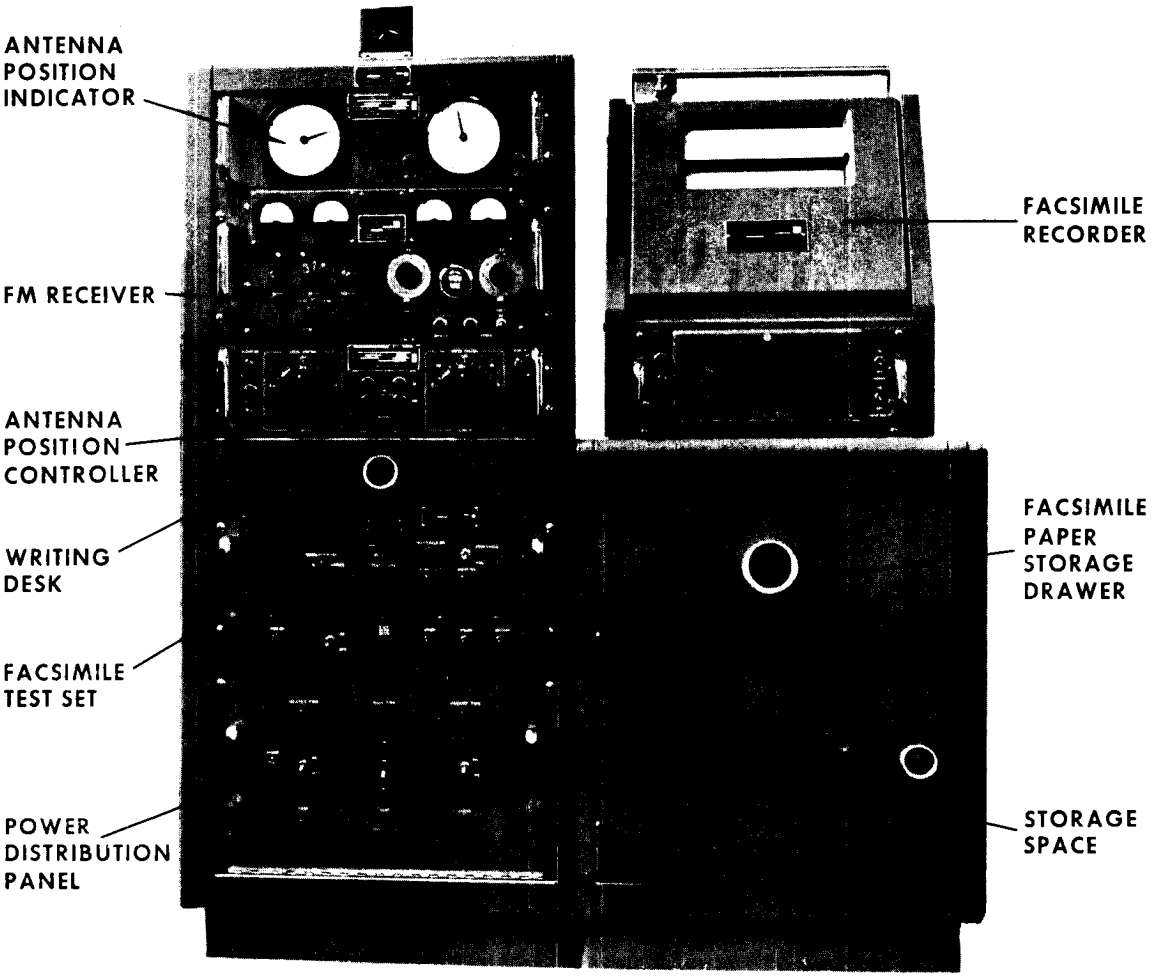

Figure 6 - Automatic Picture Transmission Ground-Station Console

19. ENGINEERING APPLICATIONS OF THE NIMBUS TELEMETRY

By D. Beiber, GSFC; M. Schmitt and
R. Cox, GE/Missiles and Space Division

19. ENGINEERING APPLICATIONS OF THE NIMBUS TELEMETRY

ILLUSTRATIONS

Figure		Page
1	Frame Times	6
2	"B" Directory (Real Time)	7
3	"A" Directory	8
4	Valve-Solenoid Sampling	9
5	Vacuum-Chamber Testing	10
6	Solar-Power Telemetry	11
7	Temperature Study	12
8	Attitude Calculation	13
9	S-Band Transmitter, Grid Drive	14
10	Telemetry Logic	15

19. ENGINEERING APPLICATIONS OF THE NIMBUS TELEMETRY

By D. Beiber, GSFC; M. Schmitt and
R. Cox, GE/Missiles and Space Division

This report describes the role of telemetry in the overall Nimbus spacecraft design, evaluation, and operational effort.

A previous report described the PCM telemetry subsystem, indicating the three data forms transmitted from the spacecraft on ground command. As shown in Figure 1, "B" data is real-time data containing 128 eight-bid words occurring at a bit rate of 10 cps, requiring 102.4 seconds for a single frame. "A" stored data contains frames of 1024 words sampled in 16.4 seconds, recorded and played back at 30 times the recording speed; this data will provide previous-orbit history during acquisition. The "A" real-time data contains the same 1024-word frame directly transmitted in 16.4 seconds; this data will be used during environmental testing of the spacecraft.

The various subsystems in the Nimbus spacecraft telemeter 338 measured functions. To logically document all of these functions, the "B" and the "A" directories were established.

The "B" directory lists data which reflect the general overall status of all Nimbus subsystems, and which can be used as backup in case of "A" data-transmission failure. Sixty-two of the 338 functions were selected as best meeting these requirements. Figure 2 shows typical "B" directory functions. The 62 functions were placed in 124 time slots, providing a redundancy factor of 2 for higher reliability. Time slots 1 through 3 are reserved for sync words.

The "A" directory is a complete listing of all 338 functions, showing: (1) the connector where the data is developed on each subsystem; (2) whether the data is also included in the "B" directory; (3) the number of the time slot (including the matrix and the matrix bus number); (4) whether a function has been given a redundant time slot; and (5) the sampling rate. Figure 3 is a presentation of typical "A" directory functions.

The sampling rate for each function was determined by analyzing the nature of the function. Steady-state functions, such as dc voltages, can

be sampled at the minimum sampling rate of once every 16 seconds. Non-steady-state functions require more frequent sampling. Take for example a valve solenoid opening which is not cyclic in operation but is evidenced by a 1/2-second pulse; this function will have to be sampled at least twice per second for detection. Figure 4 shows the effects of different sampling rates on reproducing the function; for low sampling rates, the possibility exists that the function will never be detected. Other factors involved in the sampling rate were times of earth day and night; on-off operations; times of satellite day and night; expected high rate of change functions; and special test considerations, such as the timing of a collimator turn on-turn off sequence for the AVCS cameras.

With the directories established, the telemetry information will be used to assess spacecraft and subsystem performance during qualification, prelaunch, and the 6 months of orbital operation.

During vacuum-thermal qualification of the Nimbus, the spacecraft will be placed in the 39-foot vacuum chamber, as shown in Figure 5, and its operation checked by correlating telemetry information with ground-station video indications. A program has been developed in which the computer examines the real-time data for out-of-limits measurements and establishes a go-no-go condition for satellite operation. If both the telemetry and video indications are satisfactory, testing will continue for the prescribed vacuum-thermal test period.

If a no-go condition is detected by either the telemetry or the video, or both, a failure analysis will be made to determine the cause of the malfunction. The results of this analysis will determine whether testing should continue or should be interrupted for corrective action. Similar procedures will be adopted during prelaunch at the Pacific Missile Range to establish a go condition for the spacecraft.

During all phases of spacecraft checking, assessments will be made of specialized aspects of Nimbus performance. Included in this category are a study of the solar-power subsystem, a temperature analysis, the extraction of attitude data, and operation of the control subsystem.

In the solar-power subsystem, Figure 6, total spacecraft power versus time in orbit will be checked by referring to regulated bus current at any specific time. Power demands will increase during earth day when the camera systems are operative; a larger increase occurs during in-

terrogation, when S-band transmission takes place and play-back power is required by the AVCS, HRIR, and PCM recorders.

Telemetry will also be used to evaluate the performance of the power-supply subsystem; for example, unregulated bus current telemetry will give a direct indication of solar-array output. Abrupt changes in the values of unregulated bus current will indicate the presence of open or short circuits in individual solar-array matrices. Any gradual decline in unregulated bus current will indicate a cumulative decrease in solar-array output due, possibly, to radiation damage.

Regulated bus voltage should be -24.5 ± 0.5 v. Variation from this value may require switching the feedback amplifiers by unencoded command.

Perhaps the most important performance appraisal to be made by the power-supply telemetry will be to evaluate operating characteristics of the nickel-cadmium batteries. Since there is no direct way of measuring the state of charge of the batteries, a continuous record of the charge-discharge periods of the batteries will have to be made. During satellite day, the energy flow to the batteries can be determined directly since charge current is measured by telemetry; during satellite night or battery discharge, regulated bus current telemetry will give an indication of energy drawn from the batteries. No direct measurement is available, however, of the power dissipated by the power supply; the amount of this power will have to be established during test and factored into the power-supply energy balance during actual operation.

During interrogation periods, if the solar array and batteries share load requirements (satellite day), unregulated bus current must be subtracted from regulated bus current and the estimated internal power-supply requirement subtracted from this total, in order to compute energy withdrawn from the batteries. By integrating the current during each mode of operation (charge and discharge) over the time of operation for each orbit, two parameters will be established: the ratio of ampere-hours of charge to ampere-hours of discharge (which should be at least 1.25 for one day-night cycle), and the depth of discharge of the batteries (which should not exceed 15 percent, based upon the nominal ampere-hour capacity established by test).

As the foregoing procedure is rather involved, it is recognized that a programmed subroutine should be established for computer use so that these two parameters can be continuously established for each orbit.

Other telemetry data will give operating characteristics of batteries, solar paddles, and the regulation system, such as temperature and voltage of selected solar-paddle matrices; temperature of individual cells in a battery module; regulated and unregulated bus voltage. Individual battery voltages and feedback-amplifier voltage will be telemetered and evaluated diagnostically. The mode of operation of the pressure cutoff will also be indicated.

For an analysis of spacecraft thermal conditions, the telemetry includes temperature and shutter-position sensing devices to provide in-flight information about spacecraft performance, as well as to check sensory subsystem performance in the vacuum-thermal testing chamber.

As shown in Figure 7, the computer will be provided with three procedures for handling temperature data: (1) check all previous orbit-temperature points for out-of-limits conditions; (2) for out-of-limits sensors, read out all the adjacent sensors; and (3) assuming no out-of-limit operation, compute the maximum, minimum, and average value for each sensor during the previous orbit.

Procedure 1 will be used for a quick performance check to allow time for corrective action while the spacecraft is still in interrogation range. Procedure 2 will be used to provide a more detailed picture of local performance in order to appraise more accurately the performance indicated by the first readout. Correlation of spacecraft performance with predicted performance will be possible by the information derived from procedure 3.

The telemetry information will give an accurate measurement of satellite attitude, provided the assumption is made that the sky-earth signals received by the IR scanners truly reflect the earth's surfaces. As shown in Figure 8, attitude is computed from pitch and roll error signals and from measurements of the coarse gyro output. Arrangements will be made to correlate this attitude information with the time at which pictures were taken by the Nimbus camera systems. This information will be used to feed a computer for the gridding of picture information.

The large number of telemetry functions (49) for the controls subsystem will permit a fairly thorough analysis of the operation of this complex subsystem. The effectiveness of the controls subsystem in keeping the spacecraft properly earth-oriented will be evidenced by evaluation of valve-solenoid openings, error signals, flywheel speeds and directions, and gas-volume measurements. Other telemetry functions of the controls will be closely observed to determine causes of subsystem malfunctions and to permit prediction of a shortened satellite life.

To best perform the assessments and evaluations which have been described above, and to provide NASA and General Electric personnel with the logic for the preparation of an overall computer systems design, GE is preparing a performance and evaluation manual which will include calibration curves for all functions with appropriate limits of operation and special conditions, if applicable. Figure 9 is a typical curve representing the S-band transmitter RF-grid drive. The drive is off when the transmitter is being warmed up and will cause an alarm if the limits shown on the curve are exceeded. The manual will also contain a description of each function and its mode of operation. Figure 10 shows the operation of the AVCS camera high voltage, which goes on at time T=0 and stays on for 39 seconds. At time T=32.5 seconds, the shutter is snapped and a picture is taken for 6.5 seconds. The high voltage then goes off for 52 seconds and the process is repeated. There will be no high-voltage output during night operation. In addition, the manual will include a failure analysis containing every anticipated failure condition and possible remedies, an analog directory of functions to be read out on analog recorders, and evaluations to be conducted at the request of NASA with the means for accomplishing them.

1. B DATA

$$128\ \frac{\text{WORDS}}{\text{FRAME}} \times 8\ \frac{\text{BITS}}{\text{WORD}} \times \frac{\text{SEC}}{10\ \text{BITS}} = 102.4\ \frac{\text{SECONDS}}{\text{FRAME}}$$

2. A STORED DATA

$$1024\ \frac{\text{WORDS}}{\text{FRAME}} \times 8\ \frac{\text{BITS}}{\text{WORD}} \times \frac{\text{SEC}}{15000\ \text{BITS}} = .546\ \frac{\text{SECONDS}}{\text{FRAME}}$$

3. A REAL-TIME DATA

$$1024\ \frac{\text{WORDS}}{\text{FRAME}} \times 8\ \frac{\text{BITS}}{\text{WORD}} \times \frac{\text{SEC}}{500\ \text{BITS}} = 16.38\ \frac{\text{SECONDS}}{\text{FRAME}}$$

Figure 1 - Frame Times

FUNCTION	TIME SLOT	TIME SLOT
SOLAR POWER:		
REG. BUS VOLTS	4	66
UNREG. BUS I	5	67
⋮	⋮	⋮
CONTROLS:		
N_2 TANK TEMP.	26	88
N_2 TANK PRESS.	27	89
⋮	⋮	⋮
THERMAL:		
SHUTTER #1	61	123
SHUTTER #5	62	124
⋮	⋮	⋮
SPARE		128

Figure 2 - "B" Directory (Real Time)

CONN	FUNCTION	T/M	RATE	SLOT(P)	SLOT(R)
SOLAR POWER					
J1103-4	BATT.#1V.	A/B	1/16	83-7A	84-23B1
J1103-1	BATT.#1P.	A	1/16	75-5A	76-21B1
⋮					
CONTROLS					
J7903-GG	COARSE	A	1/1	10-2A	
	PITCH		1/16	615-12A	616-44B2
⋮					
AVCS					
J4310-7	VIDEO	A	1/4	7-4A	
	OUTPUT			263-4A	
	#1			519-4A	
				775-4A	

Figure 3 - "A" Directory

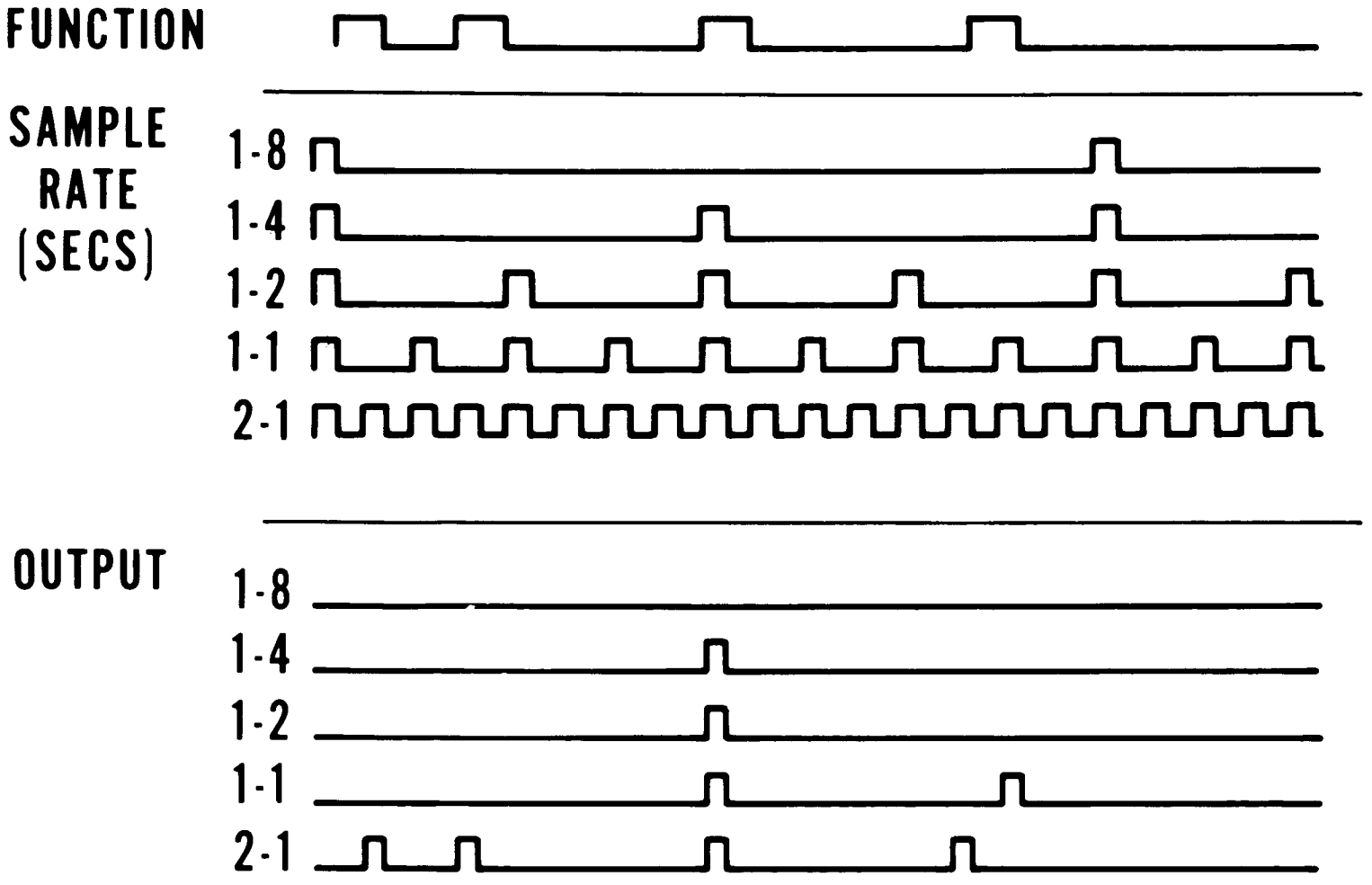

Figure 4 - Valve-Solenoid Sampling

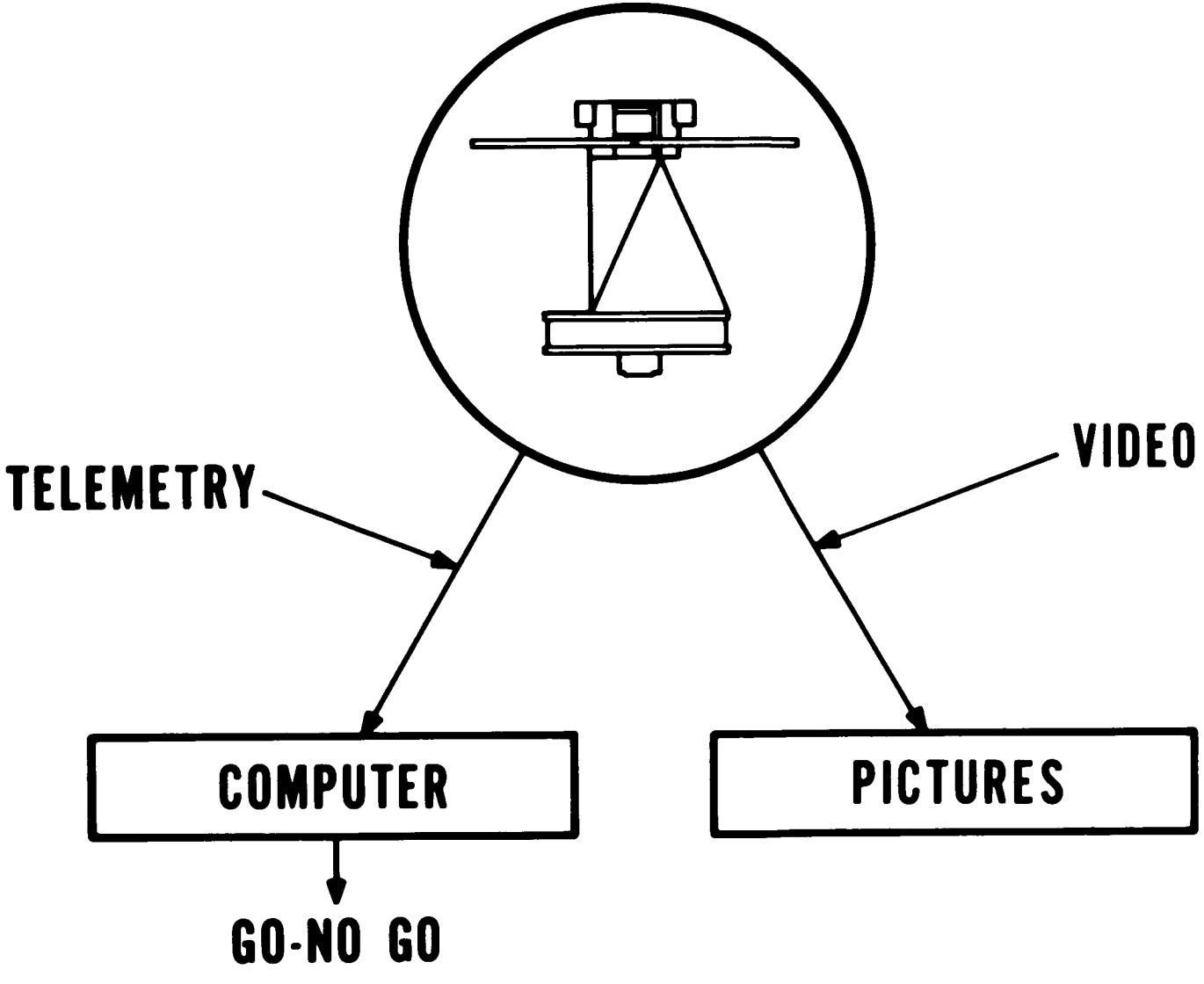

Figure 5 - Vacuum-Chamber Testing

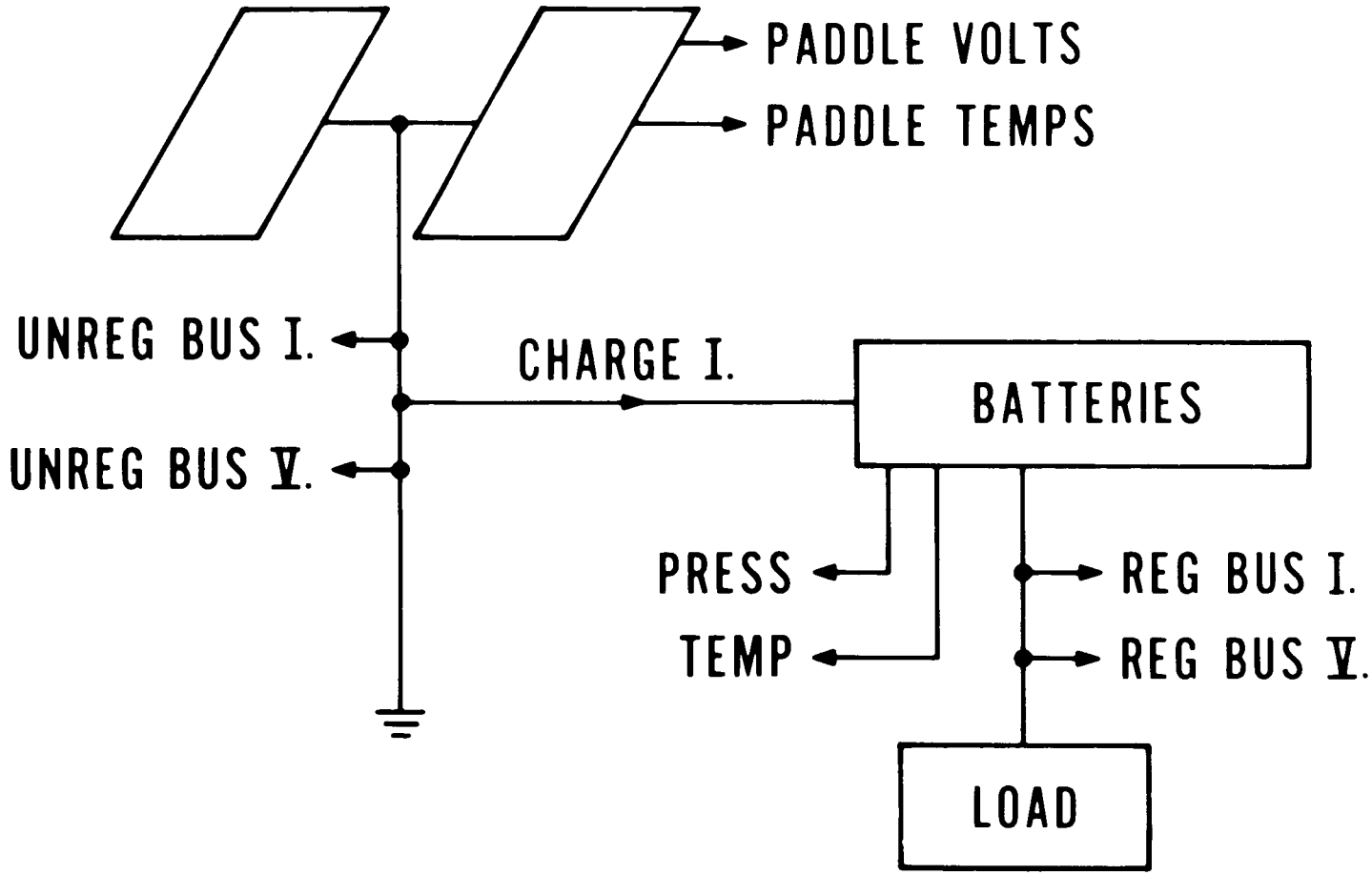

Figure 6 - Solar-Power Telemetry

PROCEDURE

1. TH18 42°C*
   TH46 44°C*
   TH23 41°C*

2. TH17 40°C
   TH19 39°C
   TH45 40°C
   TH47 40°C
   TH22 39°C
   TH24 38°C

3. TH1 MAX 35°C
   MIN 15°C
   AVER 25°C

   ⋮

   TH50 MAX 34°C
   MIN 16°C
   AVER 24°C

*OUT OF LIMITS

Figure 7 - Temperature Study

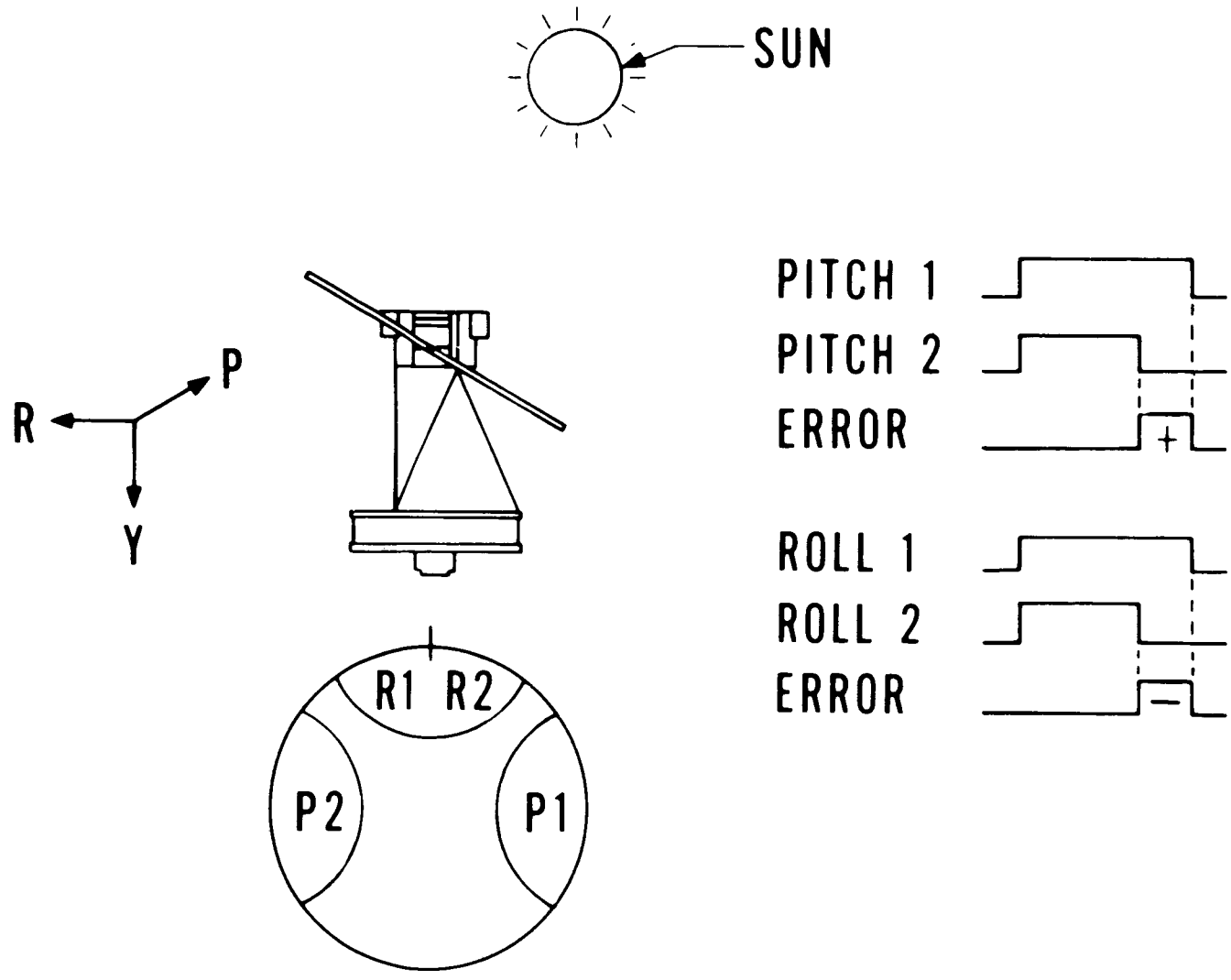

Figure 8 - Attitude Calculation

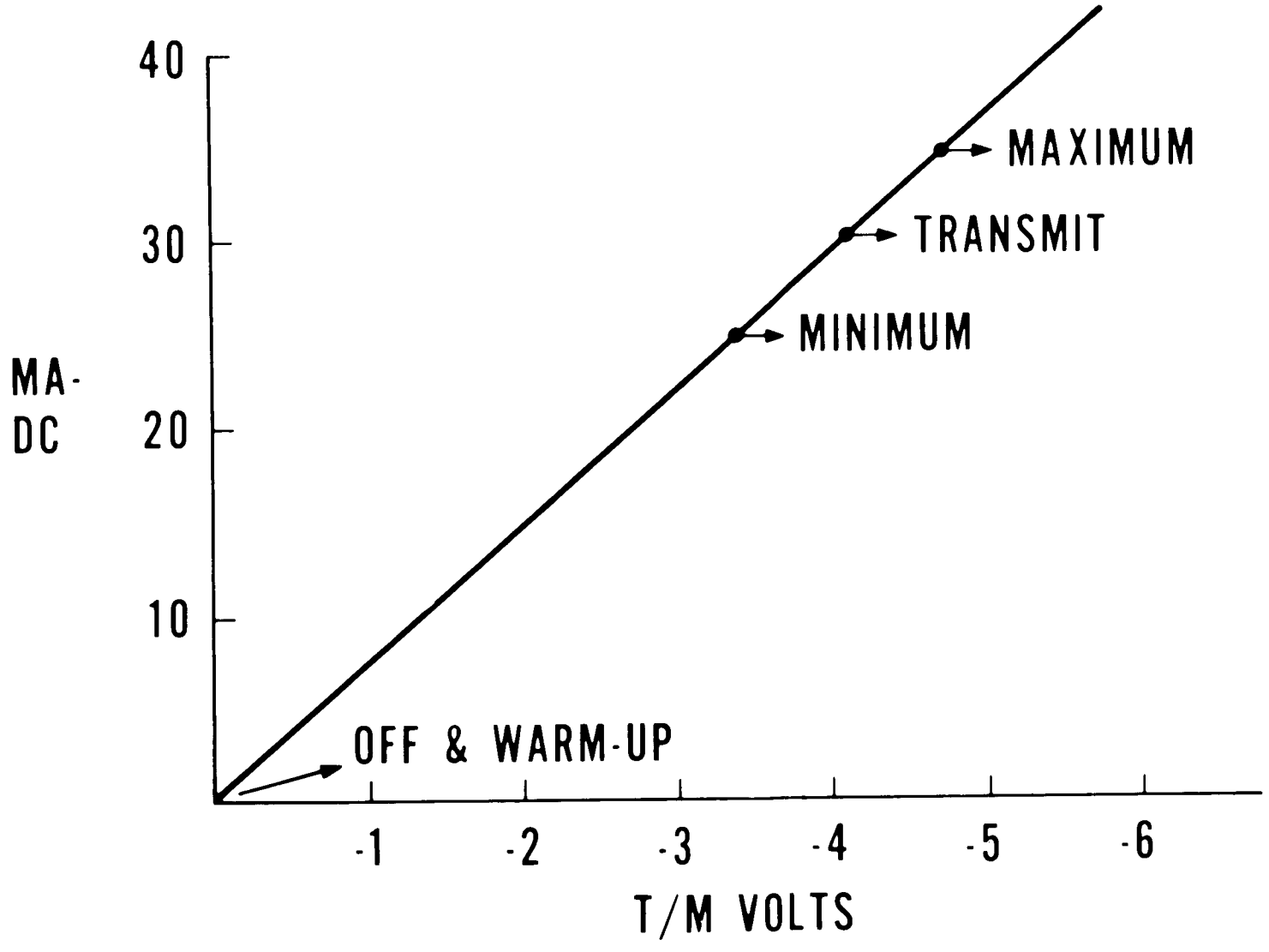

Figure 9 - S-Band Transmitter, Grid Drive

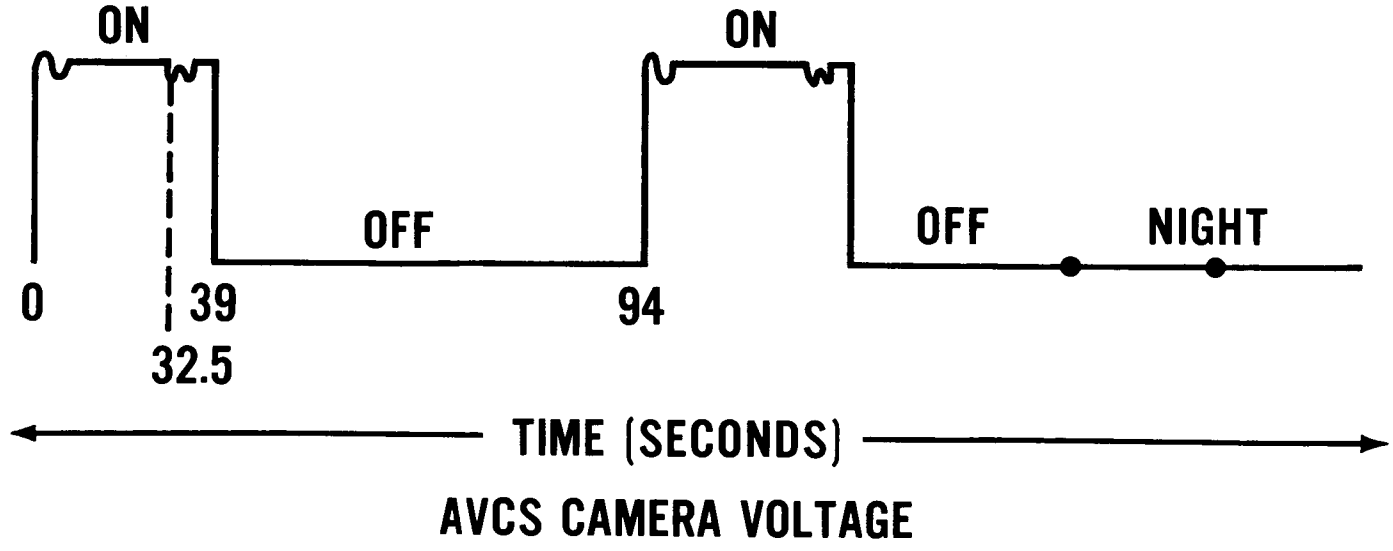

Figure 10 - Telemetry Logic

20. NIMBUS COMPUTER SYSTEM DESIGN

By L. H. Byrne, GSFC; H. G. Klose
and F. E. Lilley, GE/Missiles and
Space Division

20. NIMBUS COMPUTER SYSTEM DESIGN

ILLUSTRATIONS

Figure		Page
1	Why A Computer?	11
2	Data Monster.	12
3	Snowed Under!	13
4	CDC-160A System	14
5	Computer Input Circuitry, CDC-160A System	15
6	PCM Input to Computer	16
7	Real-Time "A" Routines	17
8	Real-Time "A" Program	18
9	Real-Time "A" Program (cont.)	19
10	Calibration Curve Fitting	20
11	Output Format	21

20. NIMBUS COMPUTER SYSTEM DESIGN

By L. H. Byrne, GSFC; H. G. Klose
and F. E. Lilley, GE/Missiles and
Space Division

INTRODUCTION

The purpose of this report is to explain in general terms the function of the Control Data Corporation (CDC) 160A computer as part of the fixed ground-station system for Nimbus spacecraft integration and test procedures.

Why is a computer needed at all for the Nimbus integration effort (Figure 1)? The answer is that the computer is an engineering tool made necessary by the large quantities of data which must be reduced to usable form in near-real time. The function of the computer is to perform the required computations, logic, formating, routing, and display of reduced results, so that Nimbus project personnel may know the "state vector" of the satellite and all of its subsystems during environmental tests. This computer processing will be used in addition to, and in conjunction with, the analog Brush recordings.

The quantity of data from Nimbus is enormous. Figure 2 shows some of the data quantities and rates: the 542 telemetry channels acquire data in the spacecraft at a rate of 500 bits/second or 30,000 bits/minute, equivalent to 3,210,000 bits for a 107-minute orbit, or 43,200,000 bits per day of recorded PCM "A" data. The 8-bit data words from the spacecraft are expanded in the ground-station equipment to 12-bit words for input to the computer, so that the computer must handle over 60 million bits per day of the recorded "A" data alone. Furthermore, because the playback rate is 30 times the record speed, resulting in a ground-station acquisition rate of 15,000 bits/second, one 12-bit word is sent to the computer every 533 microseconds. In addition, the "B" data, a real-time subset of the "A" data, must be accepted by the computer during acquisition periods; these data are transmitted at a much slower rate, 10 bits/second, resulting in 125 words per major frame.

The principal mode of operation during spacecraft integration and test will depend on the processing of real-time "A" data; for these operations, the computer must process 1024 words of data every 16 seconds.

Why not merely print a list of the raw "A" data on an on-line printer? Approximately 1000 sheets of paper would be required to print out, in octal format, the 401,250 words of data acquired from one orbit; for one day of testing, this would amount to more than 13,000 sheets of printed computer output! Who could read and interpret this vast amount of data in a reasonable amount of time?

The computer must be prepared to accept data in any of the three telemetered modes and process them into reduced, meaningful output (Figure 3). Obviously, certain subsets must be processed as quickly as possible and in as near real time as possible. Because of the high rate of acquisition of recorded "A" data, the computer can do little more than accept the data, perform some formating, correlate the data with time*, and write a master record to magnetic tape. Any further processing of the data will be done "off-line." The "B" data are used to validate the corresponding results obtained from processing the real-time "A" data, and to provide a backup capability (for example, in the event of the failure of a tape recorder).

For purposes of discussion, and since the real-time "A" will be the principal operational mode for Nimbus spacecraft integration, the rest of this report will concern the processing of real-time "A" data, although some aspects may be common to all of the modes of processing.

COMPUTER SYSTEM CONFIGURATION

The central processor is a CDC Model 160A with 8,192 12-bit words of magnetic-core memory (Figure 4). The instruction cycle time of the computer is 6.4 microseconds, and up to 4 cycles are required per

---

* It should be noted that the correlation of time is one of the major differences between real-time "A" and recorded "A" data; no time annotation is necessary for real-time "A" data. In processing recorded "A" data, however, relative time must be counted backward from the end-of-tape pulse and then correlated with absolute time.

instruction. Average instruction execution time is about 15 microseconds. Six-bit characters or 12-bit words are transferred in parallel at speeds up to 150,000 characters per second. Buffered input/output provides for simultaneous read/write-while-compute capability. Internal and external interrupts make it possible to interrupt internal processing and to communicate with associated peripheral equipment.

The computer is equipped with a 350-character/second paper-tape reader and a 110-character/second paper-tape punch. There are two Model 164 magnetic tape units, each with the ability to transfer data at the rate of 15,000 characters/second. The on-line printer is a Model 1612 Annalex which has a printing rate of up to 1000 lines/minute.

COMPUTER INPUT CIRCUITRY/CDC-160A INTERFACE

The interface between the computer input circuitry (CIC) and the CDC-160A computer, shown in Figure 5, is highly simplified in order to illustrate the functions of the various wires between these two pieces of equipment. Operations start when the receiver picks up the telemetry signal; when the signal becomes strong enough, the tuned squelch circuit closes the data path through the demodulator to the data synchronizer. The latter unit converts the data from serial to parallel format. The synchronizer also puts out a number of signals to CIC that are lumped together and can be interpreted as a "new word ready" signal to the CIC.

Each data word is entered separately into the computer from the synchronizer via the CIC by the following process:

(1) The CIC sends an "INTERRUPT 30" signal to the computer.

(2) The computer recognizes the interrupt, and exits from its main program to its "INTERRUPT 30" routine. This routine contains the instruction EXC 7000 (or the binary number 111 000 000 000) on the 12 external function lines in addition to the FUNCTION READY signal.

(3) The CIC "ANDS" the signals of (2) and returns an OUTPUT-RESUME signal to the computer.

(4) The "INTERRUPT 30" routine also contains the instruction INA (INPUT TO A), which, upon receipt of signal (3) above, sends an INPUT REQUEST to the CIC; if signal (3) were not received for any reason, the program would be delayed indefinitely.

(5) The CIC sends the 12-bit data word and INPUT READY signal to the computer.

(6) The computer receives the new data word in its "A" register and transfers it to memory.

(7) The computer program also contains the instruction CIL (CLEAR INTERRUPT LOCKOUT), which makes it possible for the computer to receive another interrupt signal. This is required because interrupts will be locked out both by acknowledgement of receipt of an interrupt and by execution of any EXC instruction.

This process repeats for each new data word. The computer is notified in the following manner when the vehicle has terminated its transmission: Loss of signal input to the demodulator-tuned squelch circuit will result, 60 milliseconds later, in an appropriate signal to the CIC which then activates the "INTERRUPT 40" line. This causes the computer to exit from its main program to the interrupt routine at location (r) 0041. When the computer finds itself there, it knows that receipt of the data has ended.

REAL-TIME "A" DATA INPUT FORMAT

The real-time "A" data input format is shown in Figure 6. The information bits are denoted by the A_i, $B_i, \ldots, N_i$ (where $i = 1, 2, \ldots, 7$). These information bits are the first seven least significant bits of every word, except the first two words, of each minor frame. The minor frame identification is indicated here by the binary count S_1, S_2, S_3, S_4, in bit positions 0-3 of the second word of each minor frame.

All other bits of this word are zeros. The small letter "n" denotes the minor frame (or subframe) number. The major frame identification is denoted by R_1, R_2, R_3, in bit positions 9-11. R_1, R_2, R_3 are always all ones for n = o (that is, for the first minor frame of every major frame) and are 0, 1, 0, respectively, for the other 15 minor frames of a given major frame. Thus, R_1, R_2, R_3, identify only the beginning of a major frame and do not constitute a frame count as do the minor frame identifications, S_1, S_2, S_3, S_4.

PROGRAM DESCRIPTION

GENERAL

The general reason for providing a computer program of the type described here is to afford the test director a means of monitoring the performance of the test vehicle in near real time, over and above the capability provided by the analog recorders. Taking into account the restrictions imposed by the size and speed of the CDC-160A computer in relation to the amount and rate of the data, along with the requirement that the data be displayed in an easily discernible format, it was decided to display a reasonable number of telemetry functions, calibrated in engineering units, with flags attached to signify the relationships of the data samples to their expected operating limits. Other out-of-limit quantities are identified as they are detected, although their actual calibrated values are not printed. Moreover, the choice of those quantities which are to be calibrated and displayed is left to the test director. Before actually processing data, the test director may choose whatever quantities he desires to see displayed, within the restrictions imposed by the printout format; during processing, the selection may be changed at any time. No attempt is made to preserve any data on tape, since these same data become available later from other sources.

REAL-TIME "A" ROUTINES

The computer program consists of three separate modules, the first being the setup routine (Figure 7), whose function is to bring into computer core memory those tables which are on magnetic tape and which will be used by the display routine. After the tables have been read into memory, and before processing begins, modifications may be made to the tables via paper-tape input. The second module is the modify

routine; it is used to change the output display after processing has begun. The third module is the display routine, which performs the real-time processing and transmits the selected data to the on-line printer for display.

Description of Flow Chart 1, Real-time "A" Program

These functional concepts are more easily illustrated by the simple flow chart shown in Figure 8. Necessary initialization and housekeeping functions are performed in these operations, and the setup routine is loaded into core memory. The setup routine then reads from magnetic tape into core memory the tables required to process and display information according to a nominal, predetermined, and fixed format; that is, the display format is fixed until these tables are placed in core memory.

At this point, the computer stops and asks the question, "Do you want to change the display format for this run?" If the answer is "Yes," changes may be made to the tables located in core memory by reading into the computer a paper tape selected from a library of previously prepared paper tapes. After necessary table changes have been made, or if no changes at all are required, the computer will list out the functions and their format, which it is now prepared to display.

The computer then reads the instructions of the modify and display routines from magnetic tape into core memory. These routines overlay the instructions of the setup routine; however, the tables to be used by the display routine are still in core memory. The modification instructions are split into two parts because of memory restrictions, since there is insufficient core memory to hold the display routine and all of the modification instructions simultaneously. This is why the initial modifications are incorporated with the setup routine.

Processing is then begun. If it is desired to change the display during the course of processing, this is done by stopping the run and modifying the tables by means of one of the paper tapes in the tape library. During this time, the computer cannot accept and process data. However, the modifications can be made rapidly and processing can continue until an "end of data" signal is received, or until further display changes are required.

Description of Flow Chart 2, Real-time "A" Program

Some of the things that the display routine must perform during processing are shown in the flow chart, Figure 9.

The computer must bring a word into core memory when the computer input circuitry signals that it has a word ready. This involves sending an external interrupt to the computer, causing it to interrupt its current processing and accept the PCM word. The program must make certain that it is synchronous with the incoming data word, whenever the word permits this type of test. It must be determined if the data word is to be limit-checked, and if so, which set of limits to use; the limit check is then performed. If this is a function which is to be displayed, the data must be placed in the proper output block, after they are calibrated and converted to engineering units. If the function is not to be displayed, but has gone out of limits, its flagged identity must be placed in another output block. (Note that the capability exists to modify limits or calibrations, as well as to select any function, during the course of a processing run.)

Whenever the program has a spare moment, it finds itself in the print routine, setting up lines of print as fast as it can with no attempt to synchronize the printing with the incoming data rate; this is necessary to accomplish the printout in real time. However, since only one data word comes in at a time, part of the program is synchronized; that is, each time the computer receives a signal of a new data word via an interrupt, it must do a certain number of things with this word before it can return to what it was doing when interrupted.

Calibration Curve Fitting

The method of curve fitting used in the calibration process is approximation by straight-line segments. Depicted in Figure 10 is a slightly exaggerated, "worst-case" curve -- a typical thermistor curve. This is referred to as a "worst-case" curve because the majority of the calibration curves are more nearly linear than this one. Each curve is approximated by whatever number of straight-line segments are required (up to a maximum of six) to give the desired accuracy. The sampled points representing the curve are carried in the form of tables, as stated above, and the capability exists to modify these tables at any time.

OUTPUT FORMAT AND INTERPRETATION OF OUTPUT

The primary purpose of the display module is to present sufficient information on the status of the spacecraft for the test director to make a preliminary evaluation of its operation. This information must be supplied almost as fast as it is monitored in the spacecraft (i.e., within a few seconds) and in a format easily interpreted by the test director.

The first line of the output format (Figure 11) contains a frame number or counter, which is actually generated by the computer and is not part of the incoming data. It is used merely to keep the pages in order. All the data appearing on a single page of output are associated with the same major frame, and there is exactly one page of output per major frame. Following this, a list of twelve columns of data appears, with sixteen data samples in each column. Any function sampled at 1/1, 1/4 or 1/8 (samples/seconds) can be listed here. In the case of a sampling rate of 1/1, a sample will be listed for each of the sixteen subframes of the major frame. If the sampling rate is 1/4 or 1/8, the appropriate number of samples will appear with blanks separating them uniformly. At the top of the column, fifteen alphabetic characters give the name of each function, in cryptic form if necessary, and three alphabetic characters give the units. The numerical values consist of four decimal digits with the proper sign and decimal point location. The letter "F" to the right of each sample signifies that that sample is outside the operating limits for that particular variable; the letter "F" stands for "flag", which would actually be a "U" if the quantity were above the operating limits and an "L" if below the operating limits. Any 1/1, 1/4, or 1/8 function may be placed in any of the twelve columns by informing the computer via paper tape at the beginning of the run. At any time during the run, the computer can be requested to insert any appropriate quantity in these columns in place of another. Any or all of these columns may be blanked at any time if such a request is made via paper tape.

Following the twelve columns of data are forty-eight 1/16 quantities, to which the same remarks also apply.

If the test director makes no request for specific data at the beginning of a run, a nominal set of functions is printed out, probably consisting of those quantities which appear in the "B" telemetry matrix.

Following the forty-eight 1/16 quantities is a history of the sampling of the condition of the yaw-valve solenoid, the roll-valve solenoid, the pitch-valve solenoid, and the nitrogen-valve solenoid. A zero indicates "off," a one (in the case of the N_2 solenoid) indicates "on," and + or - indicates "on plus" and "on minus." The grouping of four or two digits indicates data for a given subframe. There are sixteen such groupings.

At the bottom of the page, the functions which are out of limits but which are not displayed above are identified by a three-digit number (decimal) assigned to them; also, a flag tells which way they are out. This information is grouped according to subsystems. The definition of "out of limits" is that the function has either exceeded its upper limit a specified number of consecutive times, or has been below its lower limit a specified number of consecutive times. These specified numbers can be changed either at the beginning of a run or during a run, and may be different for upper and lower limits and for different functions. Also, a modification is being made to the output format to display the total number of times that a given function has exceeded its limits.

EXTENSION OF INTEGRATION PROGRAMS TO OPERATIONAL PROGRAM FOR ALASKAN CDA STATION

These routines which have been described tax the CDC-160A computer almost to its limits in terms of both time and memory. In contrast to this program for Nimbus spacecraft test and checkout, the principal mode of operation at the Alaskan command and data-acquisition (CDA) station will utilize recorded "A" data, with real-time "A" and "B" data used for backup, correlation, and verification. Processing requirements will be more severe for the Alaskan CDA station; consequently, that computer subsystem will consist of CDC-924 computers and associated peripheral equipment. The CDC-924 is completely hardware-compatible with the CDC-160A, and will be able to perform the complete assessment of the spacecraft and to handle the meteorological data as required.

PROGRAM STATUS

Computer program analysis for the CDC-924 is now under way. Much of the detailed analysis already completed for the CDC-160A program

can be transferred to the CDC-924 application. The CDC-924 computer system has been ordered and will be delivered in February 1963.

Analysis and program logic design for the program just described for Nimbus spacecraft integration and test have been completed, and a detailed program specifications document exists. Coding on the CDC-160A is now proceeding. This program will be completed, debugged, tested, and fully documented by the last week in January 1963--on schedule, without a single slip in schedule, and ready for the first Nimbus spacecraft thermal-vacuum chamber tests.

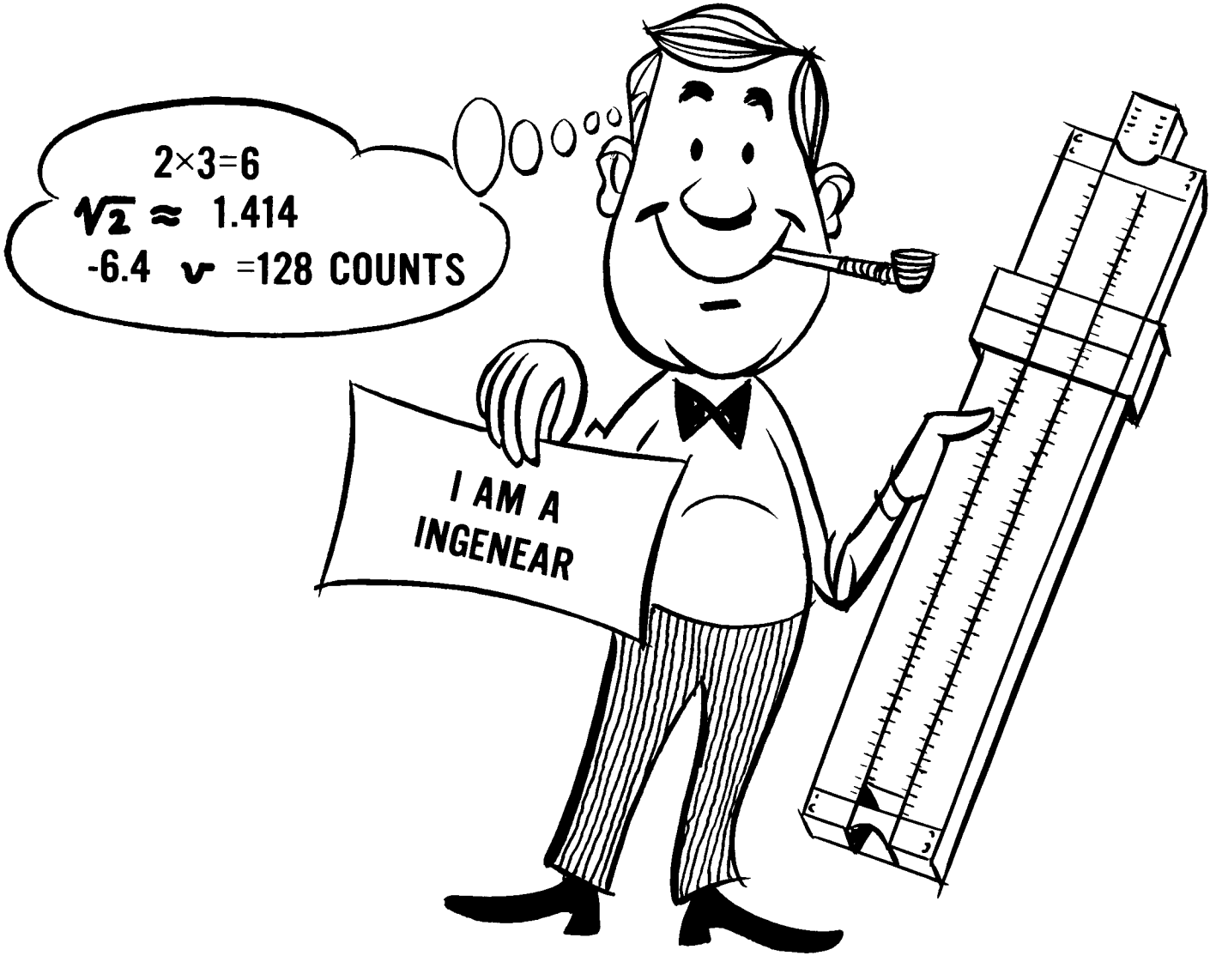

Figure 1 - Why a Computer?

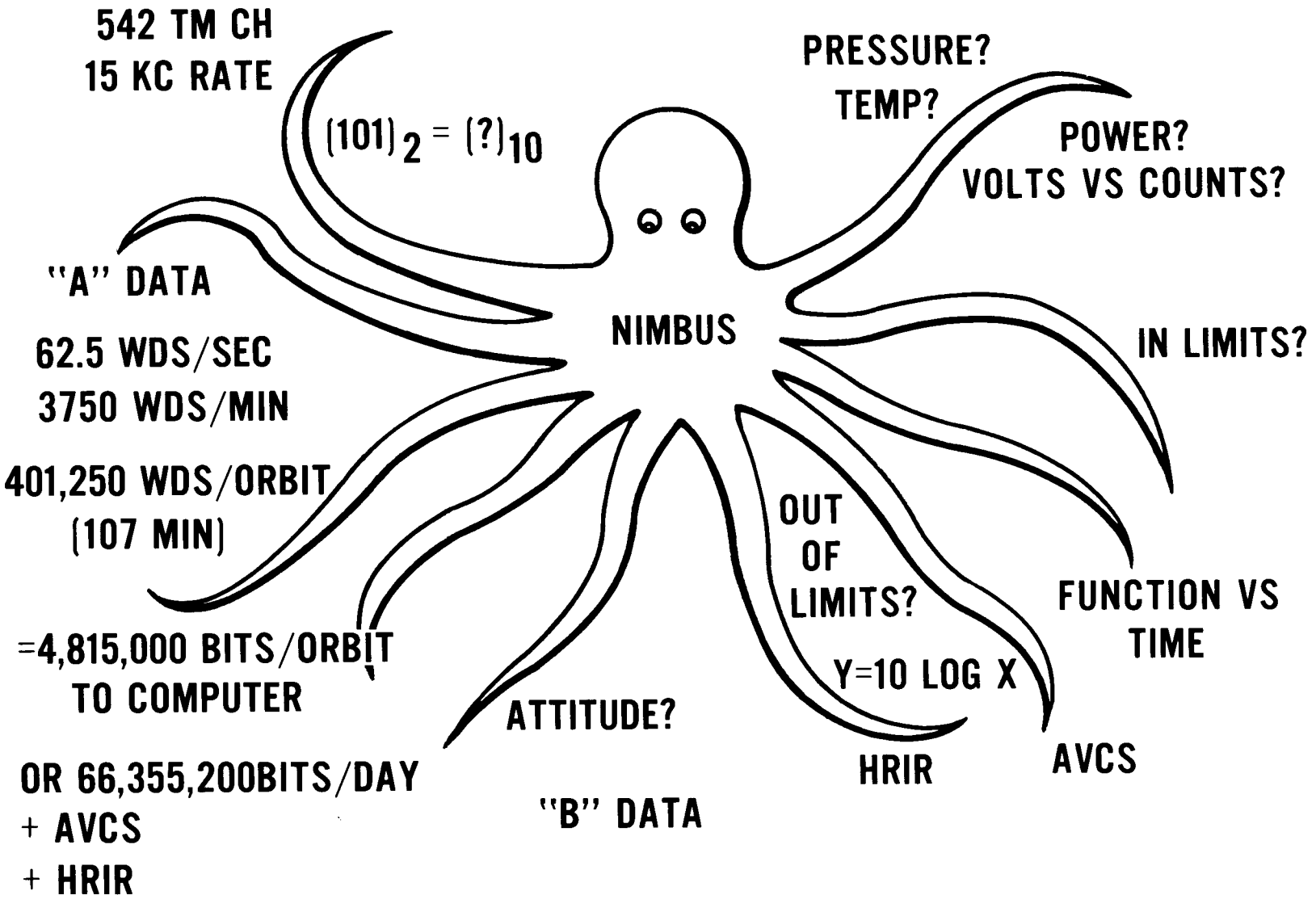

Figure 2 - Data Monster

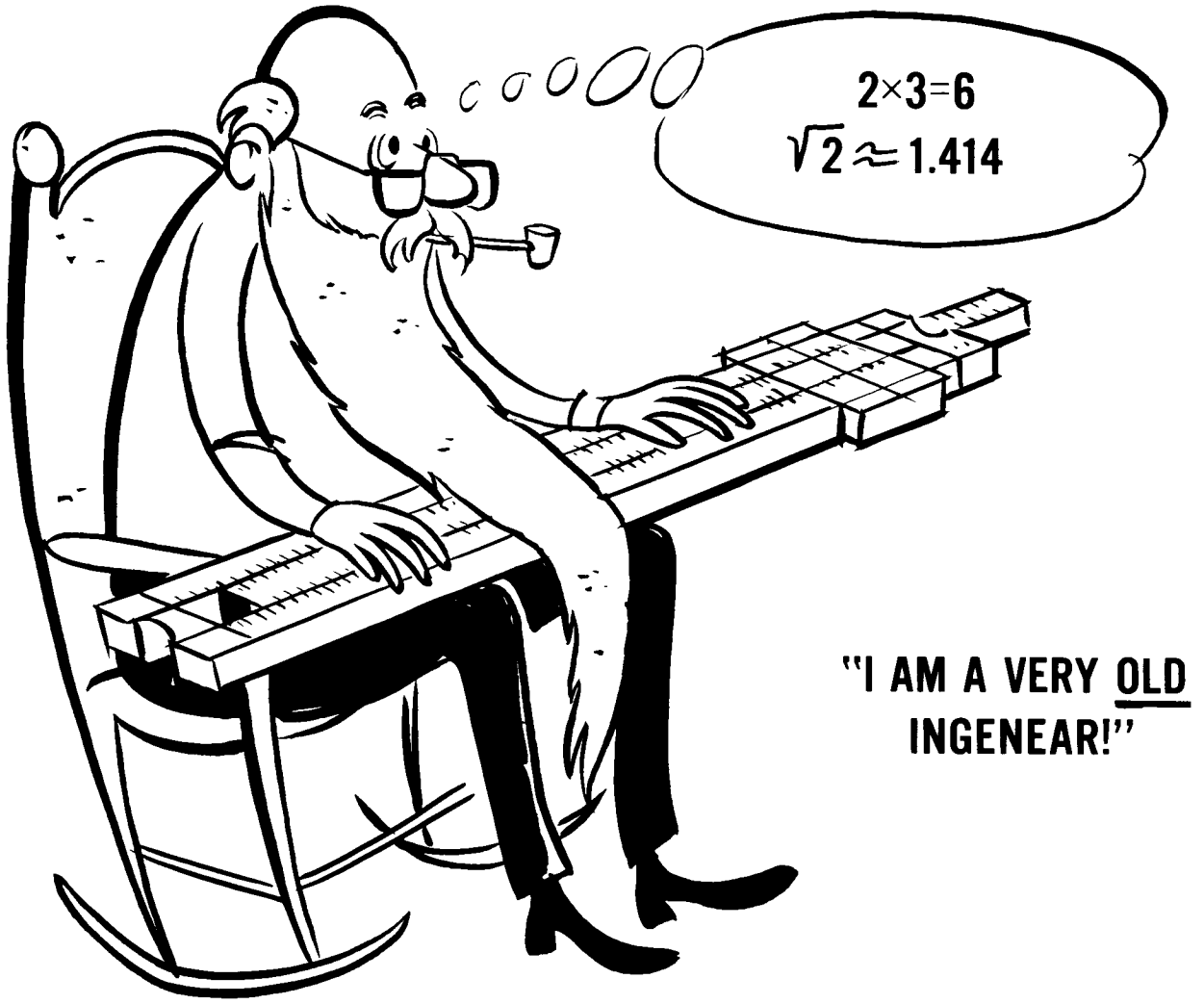

Figure 3 - Snowed Under!

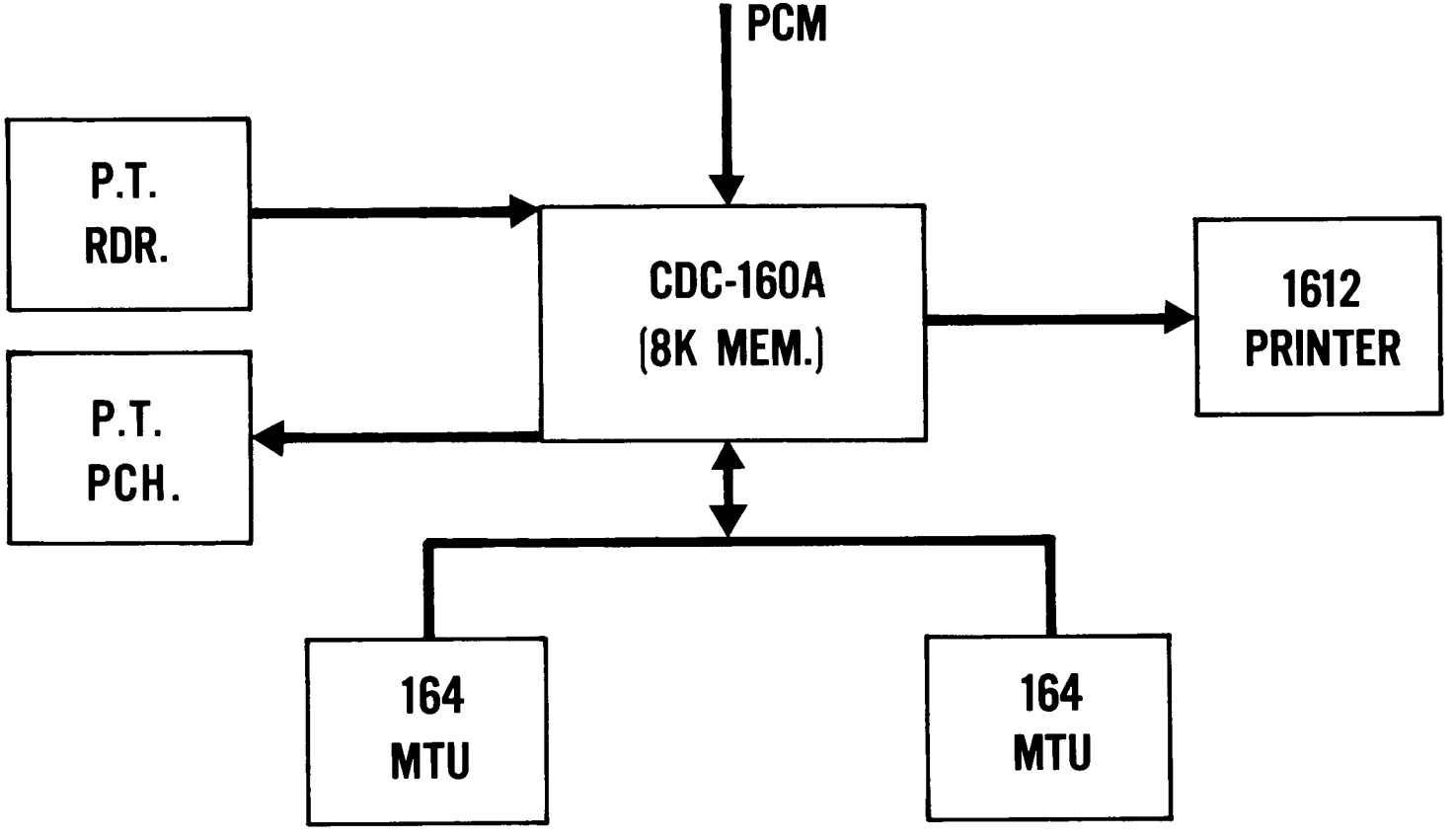

Figure 4 - CDC-160A System

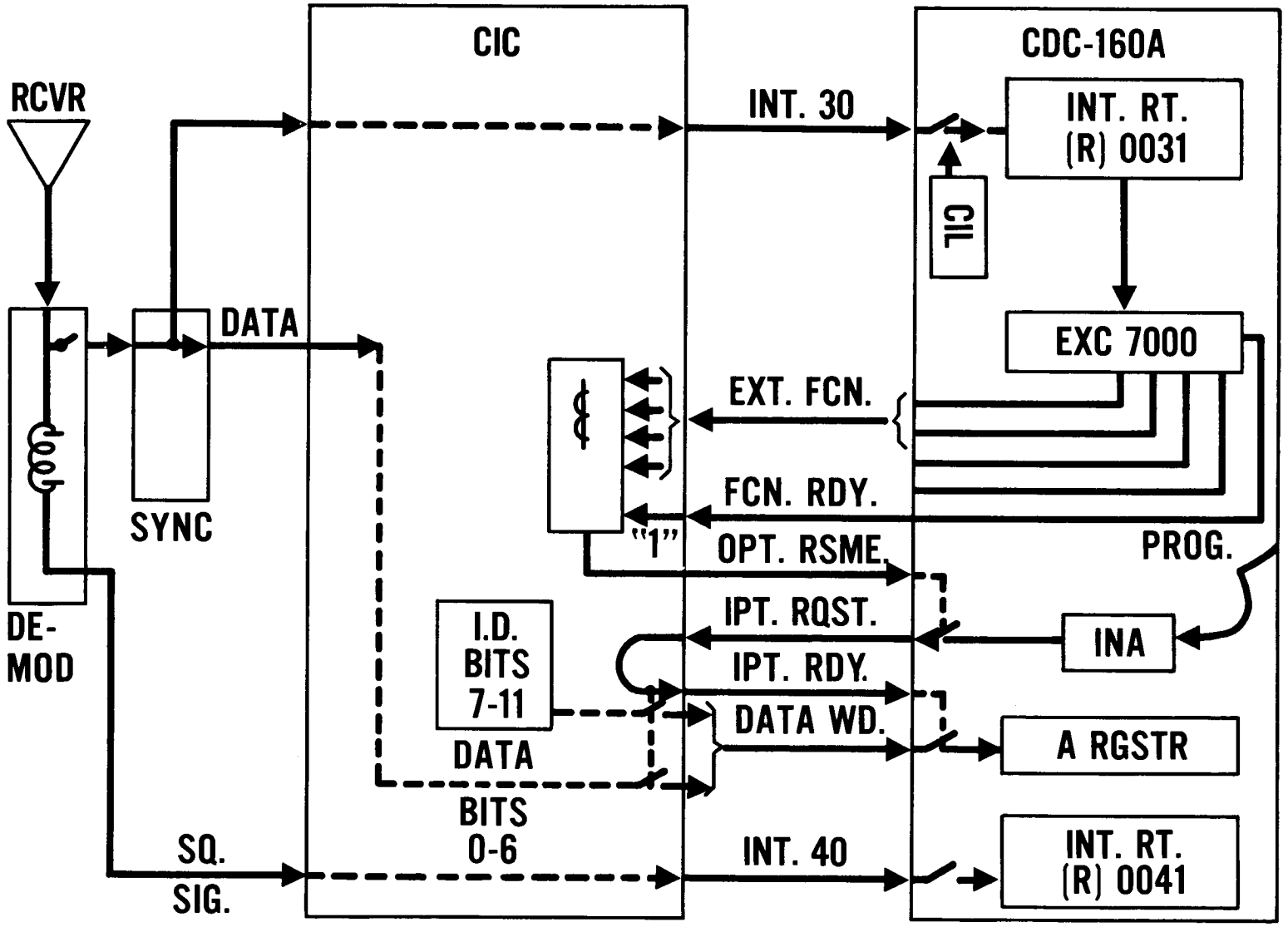

Figure 5 - Computer Input Circuitry, CDC-160A System

	BIT NO.											
WORD NO.	11	10	9	8	7	6	5	4	3	2	1	0
1+64 n	R_1	R_2	R_3	0	1	1	1	1	1	1	1	1
2+64 n	0	0	0	0	0	0	0	0	S_1	S_2	S_3	S_4
3+64 n	0	0	0	0	0	A_1	A_2	A_3	A_4	A_5	A_6	A_7
4+64 n	0	0	0	0	0	B_1	B_2	B_3	B_4	B_5	B_6	B_7
•	•											
•	•											
•	•											
64+64 n	0	0	0	0	0	N_1	N_2	N_3	N_4	N_5	N_6	N_7

SUBFRAME NO., $n = 0, 1, 2, \bullet\ \bullet\ \bullet, 15$

SUBFRAME I.D. : $(S_1\ S_2\ S_3\ S_4)_2$

MAJ. FRAME I.D., $R_1\ R_2\ R_3 =$ { 111 FOR $n = 0$; 010 FOR $n = 1, 2, \bullet\ \bullet\ \bullet, 15$ }

$A_i, B_i, \bullet\ \bullet\ \bullet, N_i \longrightarrow$ INFO. DATA

Figure 6 - PCM Input to Computer

I SETUP MODULE

- LOAD PREDETERMINED TABLES REQUIRED BY DISPLAY MODULE
- CHANGE TABLES IN CORE MEMORY PRIOR TO RUN

II MODIFY MODULE

- MODIFY DISPLAY DURING RUN

III DISPLAY MODULE

- PRINT SELECTED DATA ACCORDING TO ESTABLISHED OUTPUT FORMAT

Figure 7 - Real-Time "A" Routines

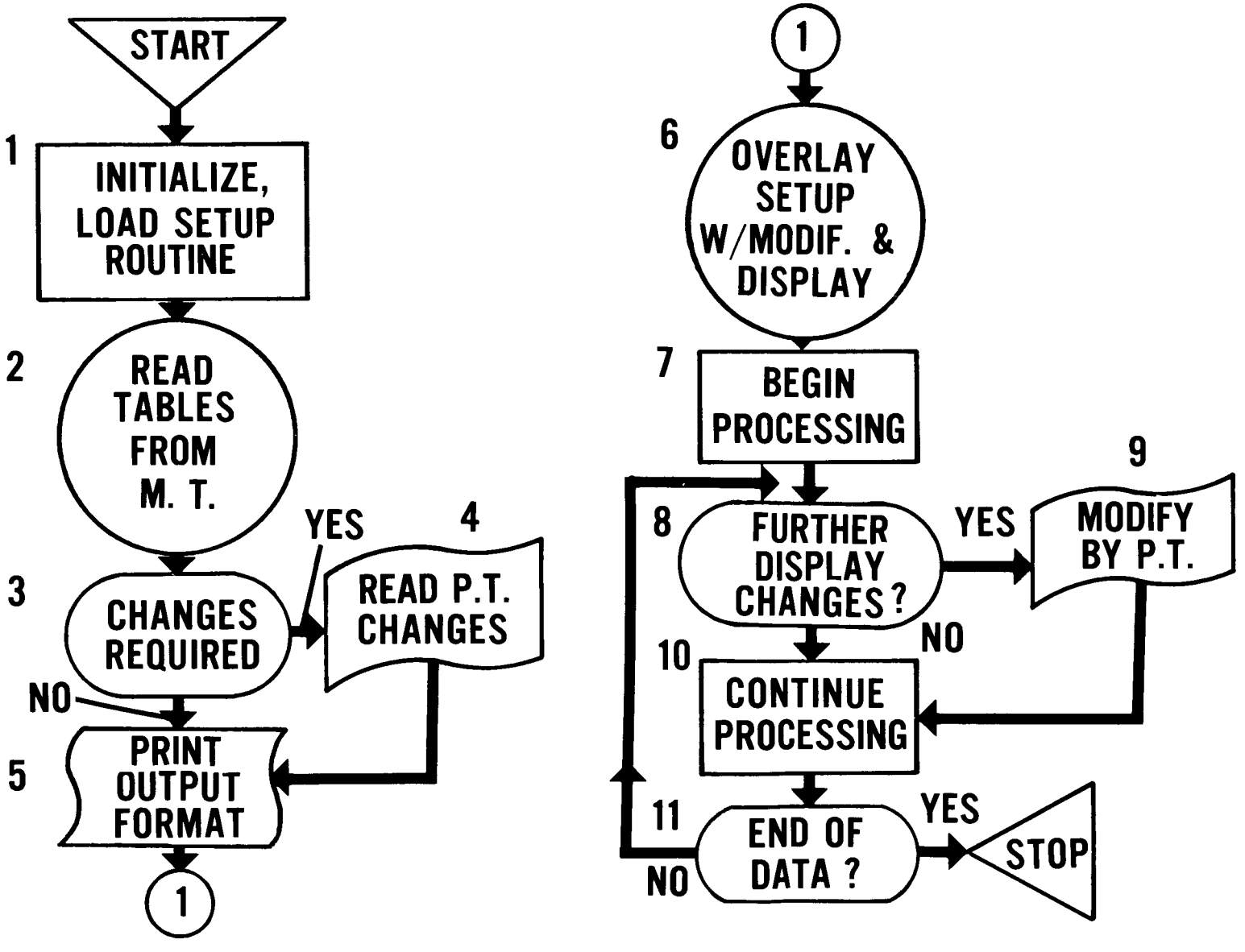

Figure 8 - Real-Time "A" Program

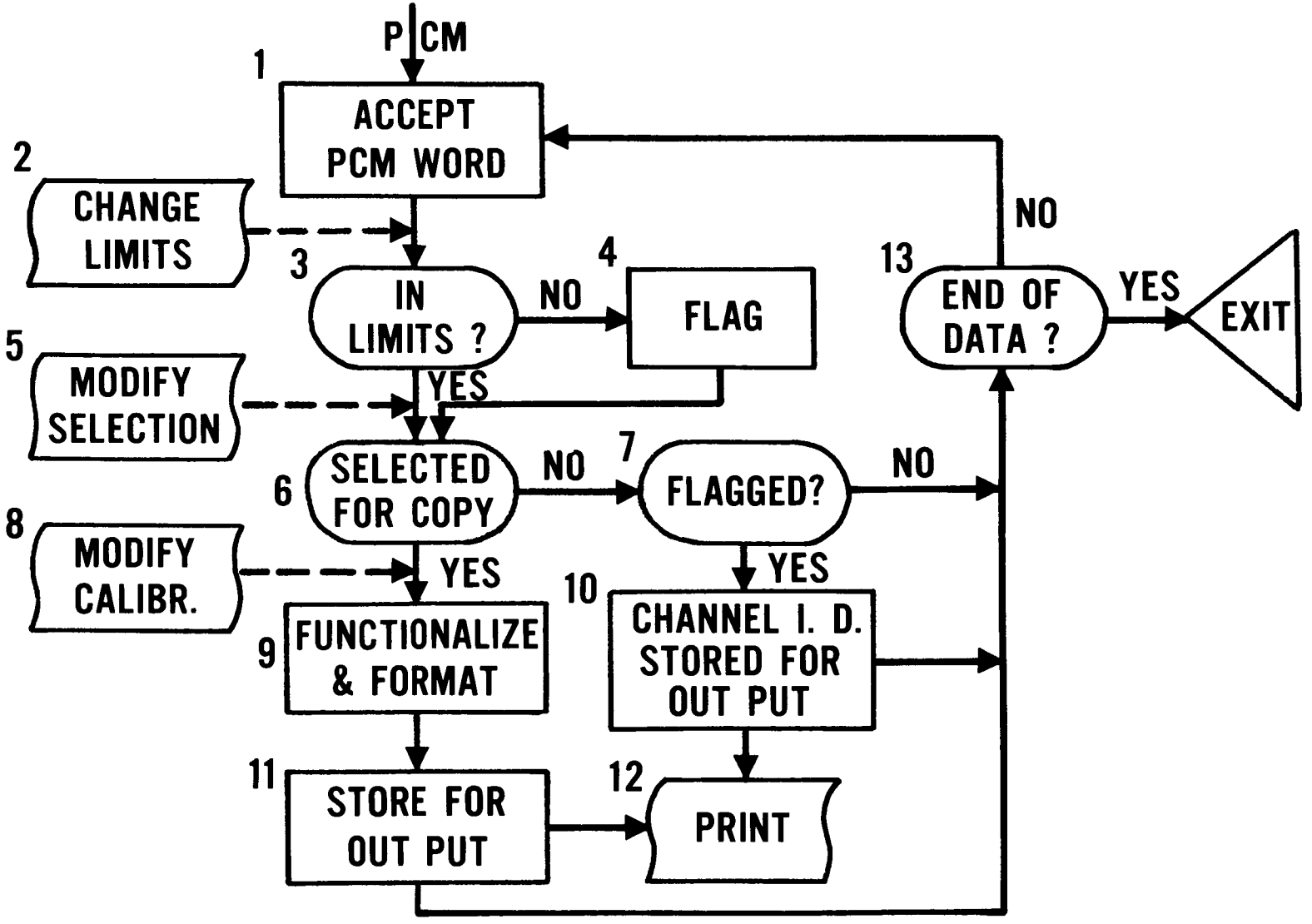

Figure 9 - Real-Time "A" Program (cont.)

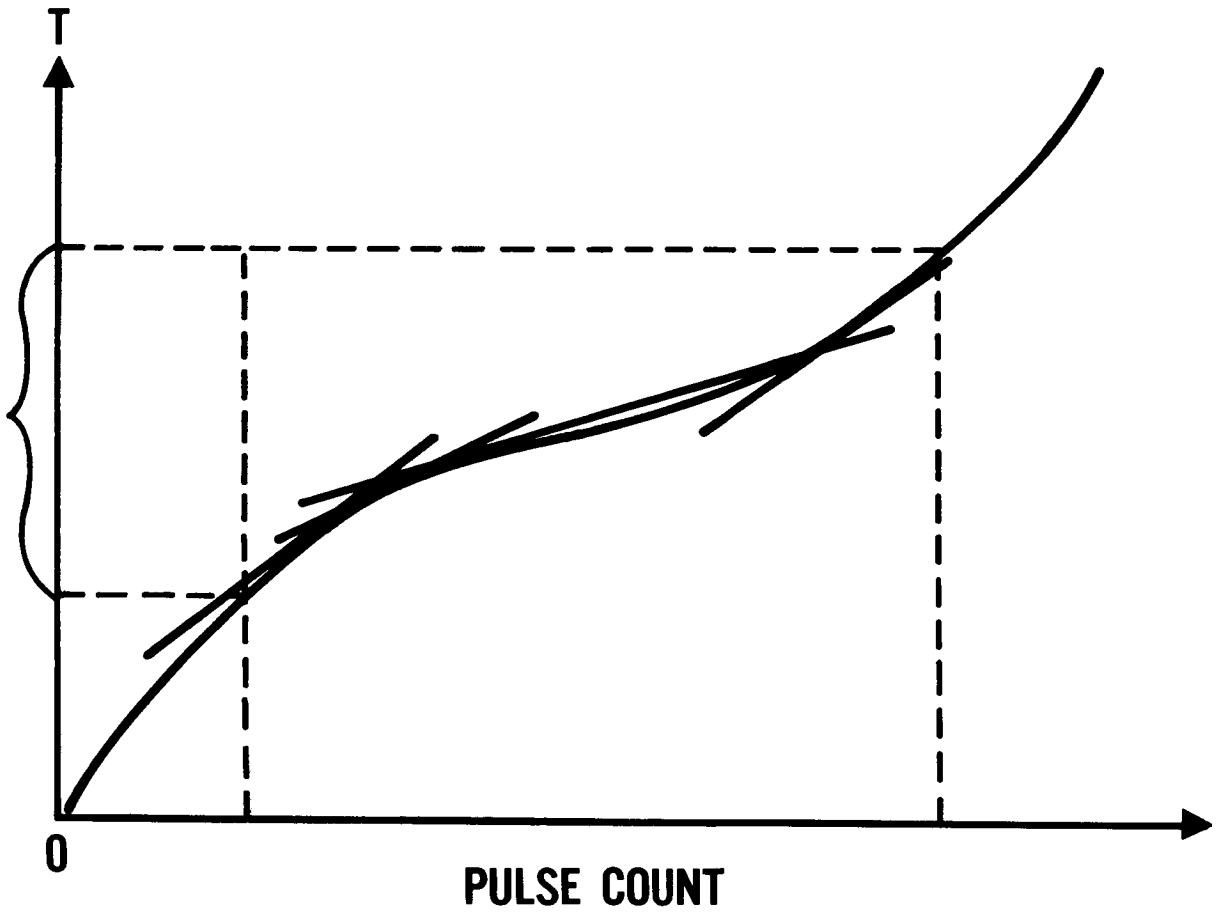

Figure 10 - Calibration Curve Fitting

FRAME NO. 0056

NAME OF FUNCTION UNT	NAME OF FUNCTION UNT	NAME OF FUNCTION UNT	NAME OF FUNCTION UNT	NAME OF FUNCTION UNT	NAME OF FUNCTION UNT	NAME OF FUNCTION UNT	NAME OF FUNCTION UNT	NAME OF FUNCTION UNT	NAME OF FUNCTION UNT	NAME OF FUNCTION UNT	NAME OF FUNCTION UNT
SXX.XF	SXX.XF	SXX.XF	SXX.XF	SXX.XF	SXX.XF	SXX.XF	SXX.XF	SXX.XF	SXX.XF	SXX.XF	SXX.XF
SXX.XF	SXX.XF	SXX.XF	SXX.XF	SXX.XF	SXX.XF	SXX.XF	SXX.XF	SXX.XF	SXX.XF	SXX.XF	SXX.XF
SXX.XF	SXX.XF	SXX.XF	SXX.XF	SXX.XF	SXX.XF	SXX.XF	SXX.XF	SXX.XF	SXX.XF	SXX.XF	SXX.XF
SXX.XF	SXX.XF	SXX.XF	SXX.XF	SXX.XF	SXX.XF	SXX.XF	SXX.XF	SXX.XF	SXX.XF	SXX.XF	SXX.XF
SXX.XF	SXX.XF	SXX.XF	SXX.XF	SXX.XF	SXX.XF	SXX.XF	SXX.XF	SXX.XF	SXX.XF	SXX.XF	SXX.XF
SXX.XF	SXX.XF	SXX.XF	SXX.XF	SXX.XF	SXX.XF	SXX.XF	SXX.XF	SXX.XF	SXX.XF	SXX.XF	SXX.XF
SXX.XF	SXX.XF	SXX.XF	SXX.XF	SXX.XF	SXX.XF	SXX.XF	SXX.XF	SXX.XF	SXX.XF	SXX.XF	SXX.XF
SXX.XF	SXX.XF	SXX.XF	SXX.XF	SXX.XF	SXX.XF	SXX.XF	SXX.XF	SXX.XF	SXX.XF	SXX.XF	SXX.XF
SXX.XF	SXX.XF	SXX.XF	SXX.XF	SXX.XF	SXX.XF	SXX.XF	SXX.XF	SXX.XF	SXX.XF	SXX.XF	SXX.XF
SXX.XF	SXX.XF	SXX.XF	SXX.XF	SXX.XF	SXX.XF	SXX.XF	SXX.XF	SXX.XF	SXX.XF	SXX.XF	SXX.XF
SXX.XF	SXX.XF	SXX.XF	SXX.XF	SXX.XF	SXX.XF	SXX.XF	SXX.XF	SXX.XF	SXX.XF	SXX.XF	SXX.XF
SXX.XF	SXX.XF	SXX.XF	SXX.XF	SXX.XF	SXX.XF	SXX.XF	SXX.XF	SXX.XF	SXX.XF	SXX.XF	SXX.XF
SXX.XF	SXX.XF	SXX.XF	SXX.XF	SXX.XF	SXX.XF	SXX.XF	SXX.XF	SXX.XF	SXX.XF	SXX.XF	SXX.XF
SXX.XF	SXX.XF	SXX.XF	SXX.XF	SXX.XF	SXX.XF	SXX.XF	SXX.XF	SXX.XF	SXX.XF	SXX.XF	SXX.XF
SXX.XF	SXX.XF	SXX.XF	SXX.XF	SXX.XF	SXX.XF	SXX.XF	SXX.XF	SXX.XF	SXX.XF	SXX.XF	SXX.XF

NAME OF FUNCTION UNT	NAME OF FUNCTION UNT	NAME OF FUNCTION UNT	NAME OF FUNCTION UNT	NAME OF FUNCTION UNT	NAME OF FUNCTION UNT	NAME OF FUNCTION UNT	NAME OF FUNCTION UNT	NAME OF FUNCTION UNT	NAME OF FUNCTION UNT	NAME OF FUNCTION UNT	NAME OF FUNCTION UNT
SXX.XF	SXX.XF	SXX.XF	SXX.XF	SXX.XF	SXX.XF	SXX.XF	SXX.XF	SXX.XF	SXX.XF	SXX.XF	SXX.XF

NAME OF FUNCTION UNT	NAME OF FUNCTION UNT	NAME OF FUNCTION UNT	NAME OF FUNCTION UNT	NAME OF FUNCTION UNT	NAME OF FUNCTION UNT	NAME OF FUNCTION UNT	NAME OF FUNCTION UNT	NAME OF FUNCTION UNT	NAME OF FUNCTION UNT	NAME OF FUNCTION UNT	NAME OF FUNCTION UNT
SXX.XF	SXX.XF	SXX.XF	SXX.XF	SXX.XF	SXX.XF	SXX.XF	SXX.XF	SXX.XF	SXX.XF	SXX.XF	SXX.XF

NAME OF FUNCTION UNT	NAME OF FUNCTION UNT	NAME OF FUNCTION UNT	NAME OF FUNCTION UNT	NAME OF FUNCTION UNT	NAME OF FUNCTION UNT	NAME OF FUNCTION UNT	NAME OF FUNCTION UNT	NAME OF FUNCTION UNT	NAME OF FUNCTION UNT	NAME OF FUNCTION UNT	NAME OF FUNCTION UNT
SXX.XF	SXX.XF	SXX.XF	SXX.XF	SXX.XF	SXX.XF	SXX.XF	SXX.XF	SXX.XF	SXX.XF	SXX.XF	SXX.XF

NAME OF FUNCTION UNT	NAME OF FUNCTION UNT	NAME OF FUNCTION UNT	NAME OF FUNCTION UNT	NAME OF FUNCTION UNT	NAME OF FUNCTION UNT	NAME OF FUNCTION UNT	NAME OF FUNCTION UNT	NAME OF FUNCTION UNT	NAME OF FUNCTION UNT	NAME OF FUNCTION UNT	NAME OF FUNCTION UNT
SXX.XF	SXX.XF	SXX.XF	SXX.XF	SXX.XF	SXX.XF	SXX.XF	SXX.XF	SXX.XF	SXX.XF	SXX.XF	SXX.XF

YAW SQL	0000	0000	0000	0100	0000	0000	0000	0000	0000	0000	0000	0000	0000	0000	0000	0000
ROLL SQL	00	00	00	00	00	10	00	00	00	00	00	00	00	00	00	00
PTCH SQL	01	00	00	00	00	00	00	00	00	00	00	00	00	00	00	00
N2 SQL	00	00	00	00	00	00	00	00	00	00	00	00	00	00	00	01

POWR	COMD	CLOK	CONT	HRIR	PCM	AVC	TVC	THRM
XXXU XXXL	XXXU XXXL		XXXL			XXXU XXXL	XXXU	
XXXL XXXL								
XXXL XXXL								
XXXL XXXL								
XXXL XXXL								
XXXL XXXL								
XXXL XXXL								

Figure 11 - Output Format

21. NIMBUS INTEGRATION AND TEST PROGRAM PLAN

By J. V. Michaels, GSFC; J. F. McGuckin,
GE/Missiles and Space Division

21. NIMBUS INTEGRATION AND TEST PROGRAM PLAN

ILLUSTRATIONS

Figure		Page
1	General Electric Test Program Schedule	8
2	Prevacuum-Thermal Test Profile	9
3	Vacuum-Thermal Sensory Subsystem Test Profile, Prototype	10
4	Vacuum-Thermal Sensory Subsystem Test Profile, Flight Model	11
5	Humidity Test Profile, Prototype	12
6	Sinusoidal Vibration Test, Prototype	13
7	Sinusoidal Vibration Test, Flight Model	14
8	Random Vibration Test	15
9	Acceleration Test, Prototype	16
10	Vacuum-Thermal Spacecraft Test Profile, Prototype	17
11	Vacuum-Thermal Spacecraft Test Profile, Flight Model	18

21. NIMBUS INTEGRATION AND TEST PROGRAM PLAN

By J. V. Michaels, GSFC; J. F. McGuckin,
GE/Missiles and Space Division

This report describes the program plan for the integration and test portion of the Nimbus program at General Electric Company.

Environmental test facilities provided by the General Electric Company consist of a 39-foot spherical vacuum-thermal chamber, a 10- by 24-foot vacuum chamber, a dual C-210 vibration facility, a humidity walk-in chamber, RFI screen room, and weight and balance facilities. Often overlooked in the glamor associated with the Nimbus spacecraft is the challenging design work associated with the equipment required to support vacuum-thermal tests in the 39-foot chamber. This consists of the motion simulator (gas-bearing), artificial horizon, simulated sun, and position and rate instrumentation.

The philosophy developed in NASA's test program is intended to provide a high level of confidence in the reliability of the spacecraft and the success of the mission.

The prototype test program is set up to demonstrate a sufficiently conservative margin of design safety in the complete spacecraft and all its subsystems. Therefore, all tests and test levels are more severe for the prototype than are anticipated in flight.

The flight acceptance test program is designed to demonstrate the successful reproduction of the complete spacecraft and all its subsystems. Test levels are the best possible simulations of those anticipated in flight. In accordance with NASA's basic philosophy, a series of environmental and functional tests has been established to determine that the design objectives have been met and the spacecraft is ready for launch. Figure 1 shows the duration of each test and whether it is applicable to the prototype and/or the flight models.

The first step is to conduct a debugging test on the payload in the torus structure, to determine electrical and mechanical compatibility of each of the subsystems when tested as an assembly. This is an operational test performed on the prototype and all flight units and requires ground-

station operation from the subsystem contractors.

Debugging will be followed by a step 1 check of calibration. This consists of a one-point calibration of each subsystem at room ambient and will be conducted both before and after environmental exposure of the sensory subsystem and spacecraft. The purpose of this test is to determine that the subsystem calibration has been maintained. It also is an operational test performed on the prototype and flight spacecrafts and will require ground-station operation.

Next, the sensory subsystem will be placed in the 10- by 24-foot chamber and undergo a prevacuum-thermal and vacuum-thermal test cycle. Prevacuum thermal is a functional test (Figure 2) simulating orbital conditions at ambient pressure. The purpose of the prevacuum-thermal test is to determine if deficiencies exist in the thermal design of the sensory subsystem structure, sensing devices, or payload equipment.

In the vacuum-thermal test (Figures 3 and 4), the excursions for the prototype appear greater than those for flight. The test profile includes pretest, temperature, cycling, step 2 calibration, and post-test cycles. Step 2 check of calibration of the subsystems is conducted at many temperature levels. After the step 2 check of calibration, the torus structure with the experiments is exposed to several temperature cycles, and the test is concluded with a final step 2 check of calibration at 25°C. The results of the final step 2 check of calibration will be compared with the initial calibration data to determine any degradation or drifts in performance characteristics.

Bi-hourly interrogations will be made via the telemetry system, to simulate spacecraft activation and interrogation during actual orbits. Monitoring of spacecraft housekeeping data will be conducted throughout on a real-time or near real-time condition. Data will be reduced using the full ground station. This test, conducted at 10^{-5}mm/Hg, will eliminate many of the problems before the total spacecraft is exposed to the full environmental test cycle. Upon completion of the sensory subsystem vacuum-thermal test, the solar paddles and controls package will be assembled and aligned to the torus structure.

Now, for the first time, a complete spacecraft will be ready for the full environmental test cycle. The first check will be an electrical system test, consisting of a step 1 check of calibration of each of the

subsystems installed in the torus structure, in addition to a test of the controls subsystem and a measurement of the solar-array output. Initial tests will be conducted by direct hardwire to the transmitters as well as air transmission by means of spacecraft antennas. Subsequent postenvironment tests will be by means of air transmission only.

Conditions at the Pacific Missile Range are known to be severe with regard to humidity. The humidity test (Figure 5) is a nonoperating test on the prototype spacecraft only. The spacecraft will be subjected to an environment of 40°C with a relative humidity of 95 percent for 50 hours. The temperature will then be lowered to 25°C with the relative humidity maintained at 95 percent. The objective of this test is to ensure that severe dewpoint condensation does not occur when the temperature is lowered, and to determine if a change in weight and subsequent shift in the center of gravity occurs as a result of water-vapor absorption. Both weight and center of gravity will therefore be measured before and after the humidity test.

The post-humidity test will be an electrical system test, followed by an RFI test to establish RF susceptibility, emission characteristics, and mutual compatibility of the subsystems integrated within the spacecraft. This test, requiring ground-station operation, is conducted only on the prototype.

In the sinusoidal vibration test (Figures 6 and 7), levels for the flight units are reduced from the prototype levels. Operating conditions of the spacecraft will be the same as those exhibited during normal powered flight. This test will be conducted on the dual C-210 shaker. Data from the spacecraft antennas will be picked up by test antennas feeding the ground-station equipment.

In the random vibration test (Figure 8), as for sinusoidal, the levels are reduced for flight units. The spacecraft will be in the same operating condition as during normal powered flight. To assure that the spacecraft is ready for further testing, or to pinpoint any problems, a go-no-go test will be made between each axis. The post-vibration test will consist of an electrical system test.

The acceleration test at the Allegany Ballistics Laboratory (Figure 9) will be conducted only on the prototype spacecraft. Again, this is an operational test, conducted at 15g in one direction along the thrust axis

and at 3g in both directions along each of the transverse axes.

In the weight and balance test, measurements of spacecraft total weight, location of center of gravity, and moments and products of inertia are experimentally determined and used to analytically compute the location of the principal-moment axes. This is a nonoperating test. The solar paddles are removed from the spacecraft before the dynamic portions of the measurements and remain off for the spacecraft vacuum-thermal test in the 39-foot chamber.

The spacecraft vacuum-thermal test (Figures 10 and 11) is an operational test conducted at 10^{-5}mm/Hg at the levels shown. Both excursions and duration are reduced for flight units. The test profile includes step 2 calibration, flight simulation, and temperature cycling.

The step 2 check-of-calibration phase will be performed on the various payload units to stimulate the cameras and radiometers and to measure the performance of the units at various spacecraft temperature conditions as well as sensor target conditions. During changes of temperature, bi-hourly interrogations will be made as in orbit. Spacecraft housekeeping data will be monitored throughout by means of an RF link on a real-time or near real-time basis.

The flight-simulation phase is to demonstrate the control subsystem's ability to control the attitude and maintain the pointing accuracy of the spacecraft in free space. Maneuvers will be repeated at various temperatures.

The thermal cycling phase is conducted to determine whether the spacecraft and payload can withstand a thermal cycling operation. After an initial high-low cycle, a series of cycles will be run as indicated. Note the excursion difference between the prototype and flight levels. Bi-hourly interrogation will be conducted with ground-station operation.

After the vacuum-thermal test, the solar paddles will be remated to the spacecraft and an electrical system test will be performed, followed by paddle deployment and a final confidence low-level random vibration test of both prototype and flight units.

The last check before shipment ot the Pacific Missile Range consists of an electrical system test, antenna calibration, mechanical inspection,

and check of alignment.

In addition to the tests described, a magnetic field test on the prototype may be included to determine the effects on spacecraft imbalance of magnetic field torques created by turning on the various subsystems. The test will provide data on the amount of attitude correction required to maintain stabilization and pointing accuracy.

The Nimbus spacecraft will be subjected to an extensive test program: 177 days of continuous testing with the prototype, and 110 days for each flight model. When the testing starts it will go round-the-clock, 7 days a week.

The overall test program will be under the direct supervision of NASA/GSFC. All test plans, joint operating plans, hardware acceptance, and test results will be approved by NASA.

The General Electric systems test engineer will be responsible for technical direction of each test, and for analysis and reporting of test results. Changes in test procedures will be made only by the systems test engineer.

The test conductor will implement and supervise the test operation. He will integrate and supervise the efforts of subsystem contractors, test engineers, and technicians during test operation for the various areas shown. He provides a centralized channel of communications for control of test operation and reporting.

Further responsibilities are defined as follows:

> The subsystem contractor will provide hardware, component bench-test equipment, suitable system calibration equipment, controls, and respective operating procedures for use at the integration contractor's plant. The integration contractor will review and approve government-furnished equipment component and subsystem bench-test procedures, system calibration test equipment, and hardware operating procedures. GE will review and integrate various system test procedures, and will develop the test planning in a completely detailed procedure, embracing all operating functions of the spacecraft and test equipment, and will submit it to NASA/GSFC for approval.

Each of the subsystem contractors will provide primary calibration data for the spacecraft hardware to be used as standards during the system test sequence at the integration contractor's facility. The integration contractor will review and integrate primary calibration data into system test specifications and detailed test procedures.

The subsystem contractor will conduct bench tests on its spacecraft hardware at the integration contractor's facility, according to approved bench test procedures. GE will witness bench tests performed by the subsystem contractors in accordance with bench-test procedures which have been reviewed and approved by GE and NASA. When the subsystem has successfully passed the bench test, it will be placed in bonded stock until required for assembly.

Each of the subsystem contractors will check out his system test equipment here at Valley Forge for the fixed ground station and vans in accordance with approved procedures. General Electric will receive, visually inspect, install, and monitor checkout of the fixed ground-station and van-mounted test equipment; it will also provide standard calibration services as required on all test equipment.

The subsystem contractors will operate the fixed ground-station and van-mounted equipment, including system calibration equipment, during the system test sequence. GE will provide two test engineers to assist in the monitoring operation of the fixed and van-mounted ground stations during the system test sequence.

The subsystem contractors, together with the NASA technical officers, will review and analyze system test data resulting from the spacecraft system test for the respective spacecraft subsystems. The integration contractor will conduct the test, and will monitor, review, and analyze system test data, solicit individual reports from subsystem contractors, and prepare final test reports at the conclusion of each major test phase.

The subsystem contractors will each provide experts for the respective spacecraft subsystems to assist in alignment and debugging exercises and to conduct troubleshooting activities on the space-

craft subsystems as problems arise. General Electric will be assisted by the subsystem contractor during assembly, alignment, and test activities.

Complete sets of co-contractor-supplied subsystems, with the exception of the paddles and control subsystems, are required at about the midpoint of the sensory subsystem assembly cycle. In addition, for a logical assembly of the sensory subsystem and to prevent excessive loading in bench testing, subsystems should be received at General Electric at intervals of about two per week.

As previously mentioned, this schedule has been phased to conform to in-plant facility limitations. The limiting facility item of this schedule, the 39-foot vacuum chamber, is the reason for the approximate 6-week interruption of the test cycle of the flight units. Spacecraft vacuum-thermal testing is delayed until completion of vacuum testing of the preceding unit.

Fixed ground-station availability is almost as limiting as the 39-foot chamber because there is a utilization factor of about 83 percent during the entire test program. It is planned to use the vans for in-plant testing until they are shipped to the Pacific Missile Range. Other facilities appear to present no particular problem at this time.

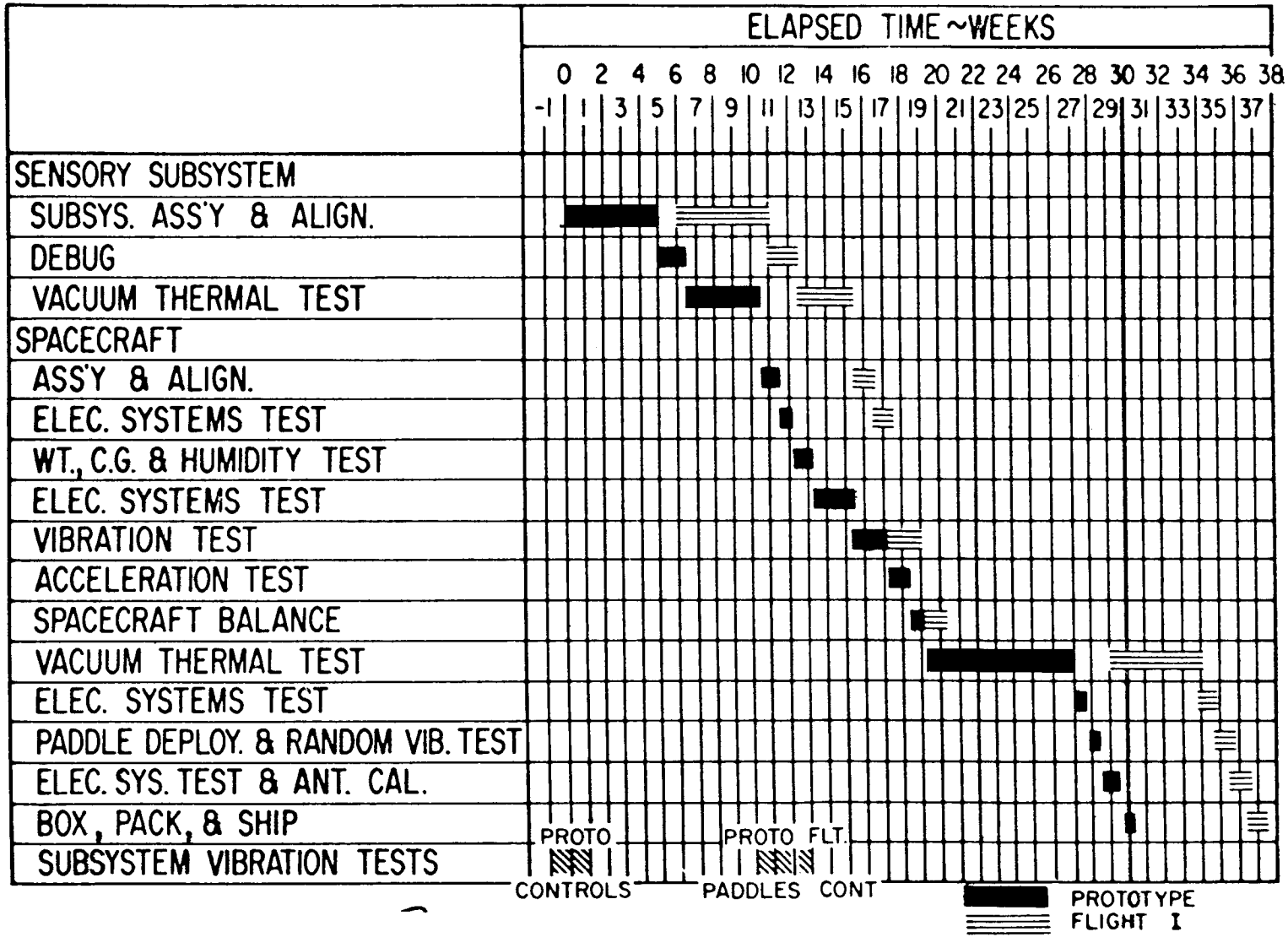

Figure 1 - General Electric Test Program Schedule

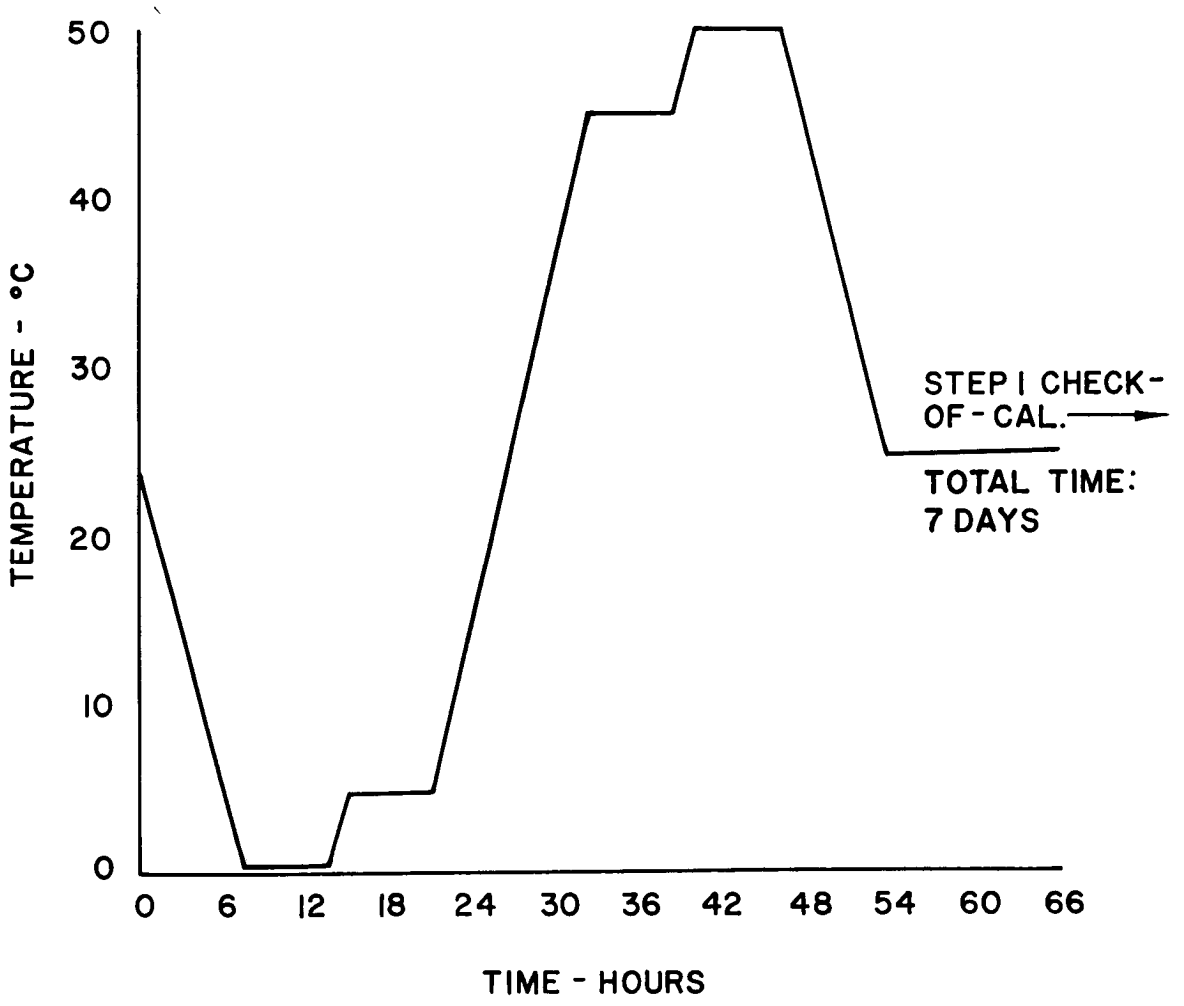

Figure 2 - Prevacuum-Thermal Test Profile

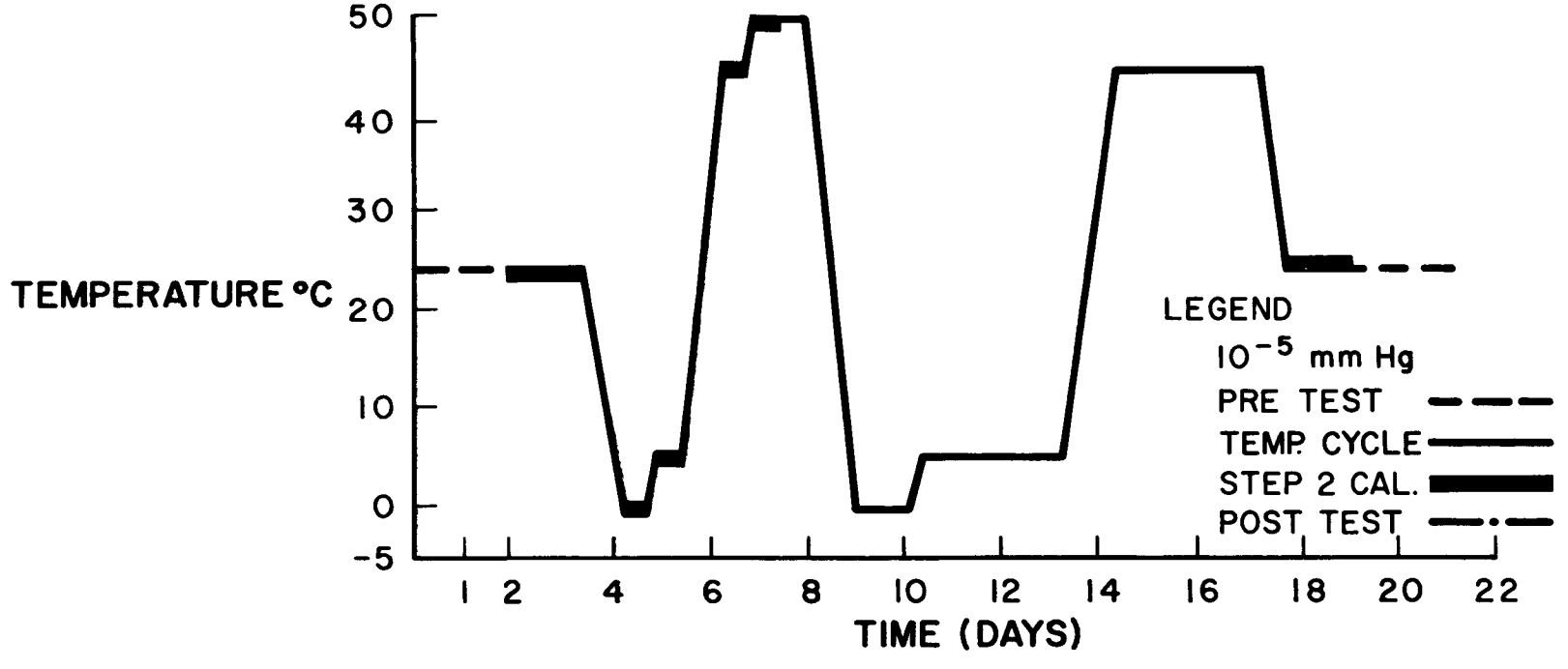

Figure 3 - Vacuum-Thermal Sensory Subsystem Test Profile, Prototype

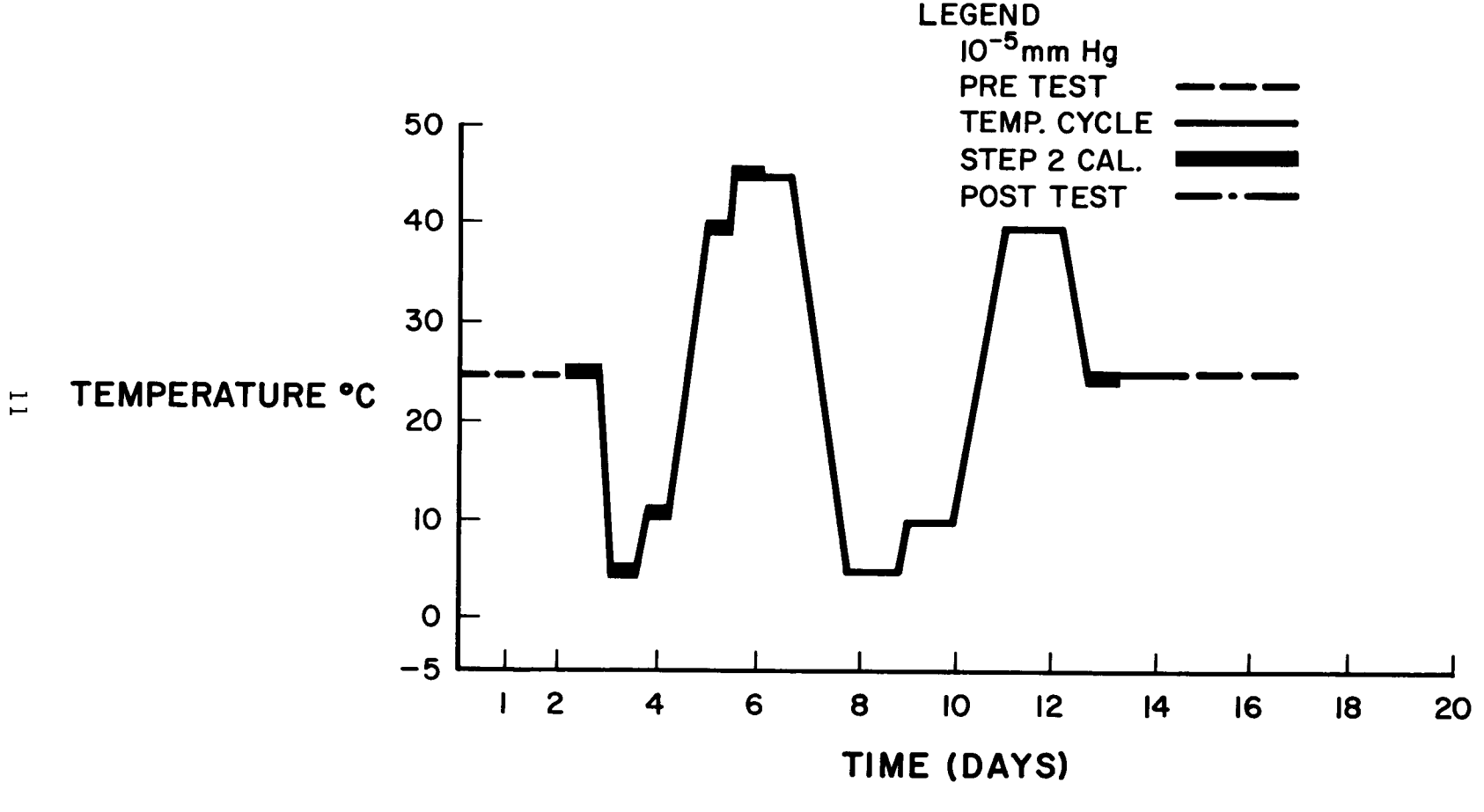

Figure 4 - Vacuum-Thermal Sensory Subsystem Test Profile, Flight Model

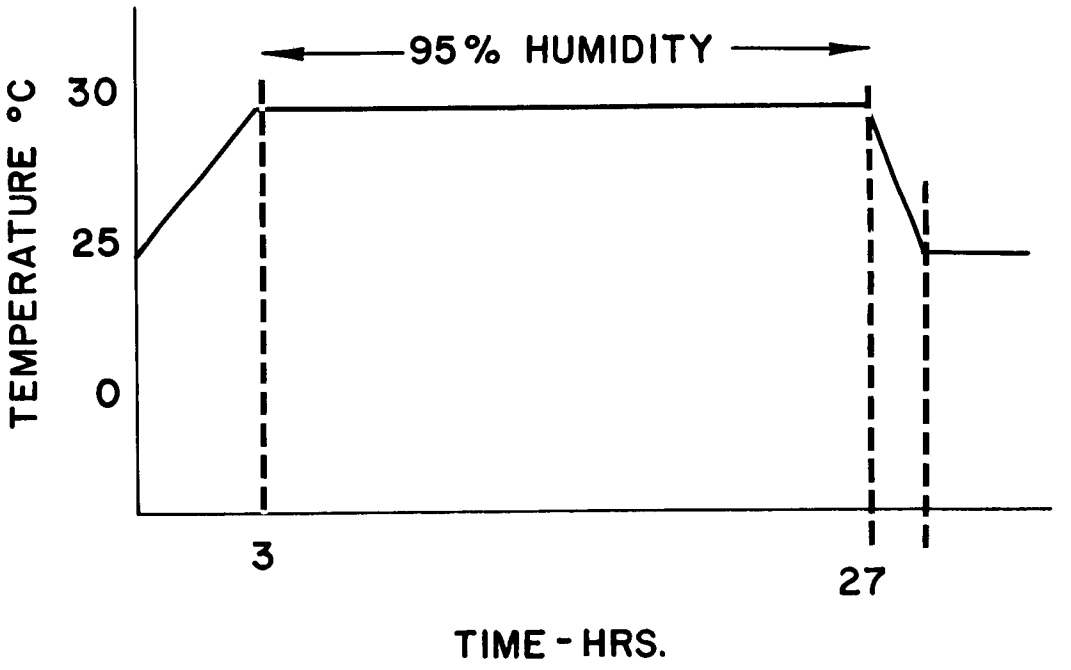

Figure 5 - Humidity Test Profile, Prototyp

AMPLITUDE- g - "0" TO PEAK			
FREQUENCY CPS	THRUST AXIS	TRANSVERSE AXIS	SWEEP DURATION
5 - 16	1.0 *	0.75	2 MIN./OCTAVE
16 - 22	4.5	0.75	
22 - 150	1.5	0.75	
150 - 400	3.0	-	
400 - 2000	7.5	-	

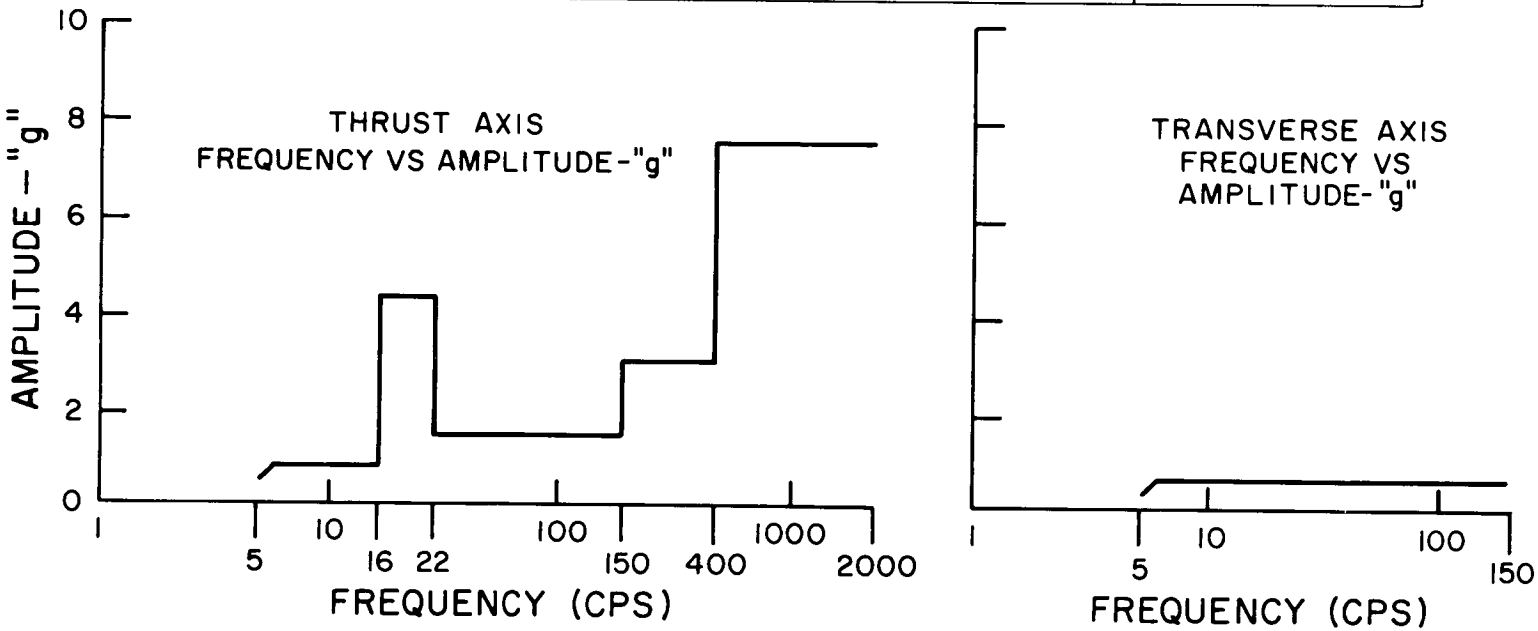

*LIMITED TO SHAKER AMPLITUDE OF 0.25 IN.

NOTE:

OPERATION - NORMAL POWERED FLIGHT MODE DURING ENVIRONMENT

GO - NO-GO TEST BETWEEN AXES.

Figure 6 - Sinusoidal Vibration Test, Prototype

AMPLITUDE – g – "0" TO PEAK			
FREQUENCY CPS	THRUST AXIS	TRANSVERSE AXIS	SWEEP DURATION
5 – 16	0.7	0.5	1 MIN./OCTAVE
16 – 22	3.0	0.5	
22 – 150	1.0	0.5	
150 – 400	2.0	–	
400 – 2000	5.0	–	

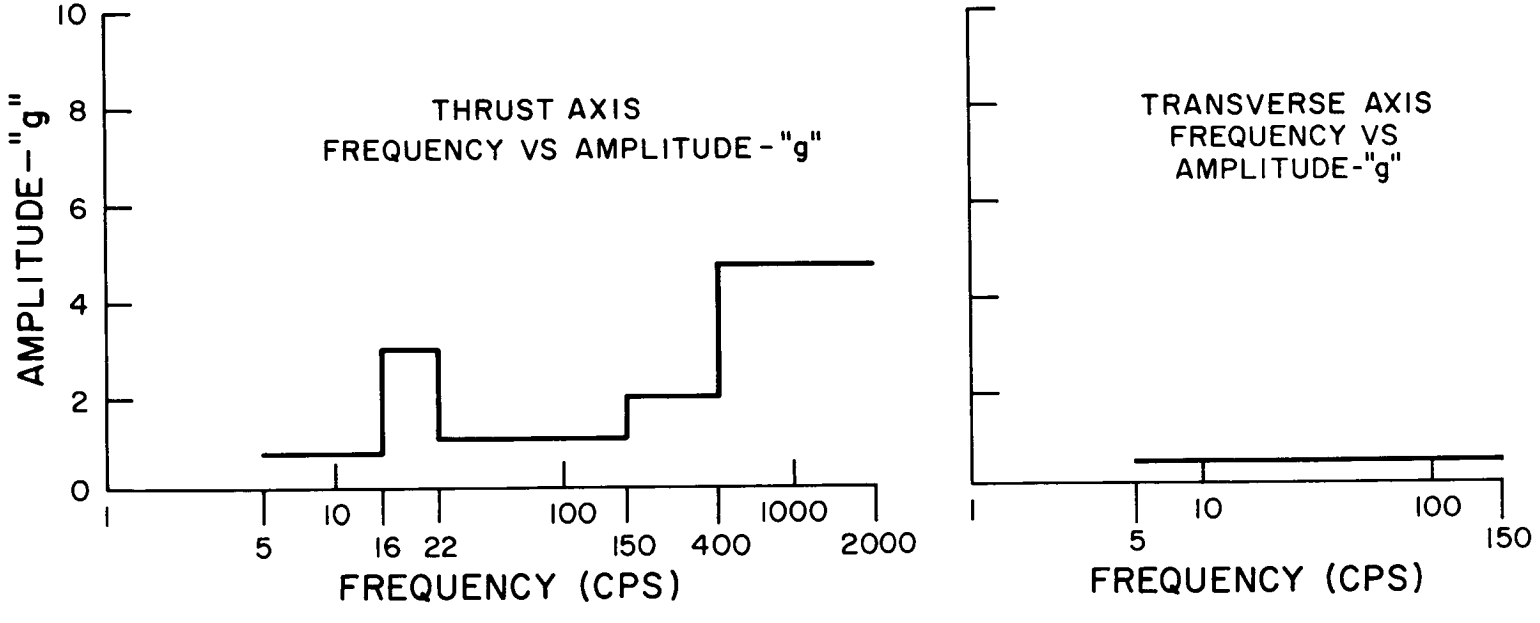

NOTE:

OPERATION – NORMAL POWERED FLIGHT MODE DURING ENVIRONMENT

GO – NO-GO TEST BETWEEN AXES.

Figure 7 - Sinusoidal Vibration Test, Flight Model

PROTOTYPE SPACECRAFT
EACH AXIS

FREQUENCY-cps	SPECTRAL DENSITY g^2/cps AMPLITUDE-g-RMS			SWEEP DURATION
20-110	0.045			4 MIN./AXIS
110-1275	0.6	db/OCTAVE INCREASE	11.2	↓
1275-2000	0.07			

FLIGHT SPACECRAFT

FREQUENCY-cps	SPECTRAL DENSITY g^2/cps AMPLITUDE-g-RMS			SWEEP DURATION
20-80	0.02			2 MIN./AXIS
80-1200	0.45	db/OCTAVE INCREASE	7.5	↓
1200-2000	0.03			

OPERATION-NORMAL POWERED FLIGHT MODE DURING ENVIRONMENT
-GO-NO-GO TEST BETWEEN AXES

Figure 8 - Random Vibration Test

DIRECTION	ACCEL. - g's	DURATION
THRUST AXIS (I DIRECTION)	15	5 MIN.
TRANSVERSE AXES (2 DIRECTIONS)	3	5 MIN.

OPERATION - NORMAL POWERED FLIGHT MODE DURING ENVIRONMENT

FLIGHT SPACECRAFT

NOT REQUIRED ON FLIGHT SPACECRAFT

Figure 9 - Acceleration Test, Prototype

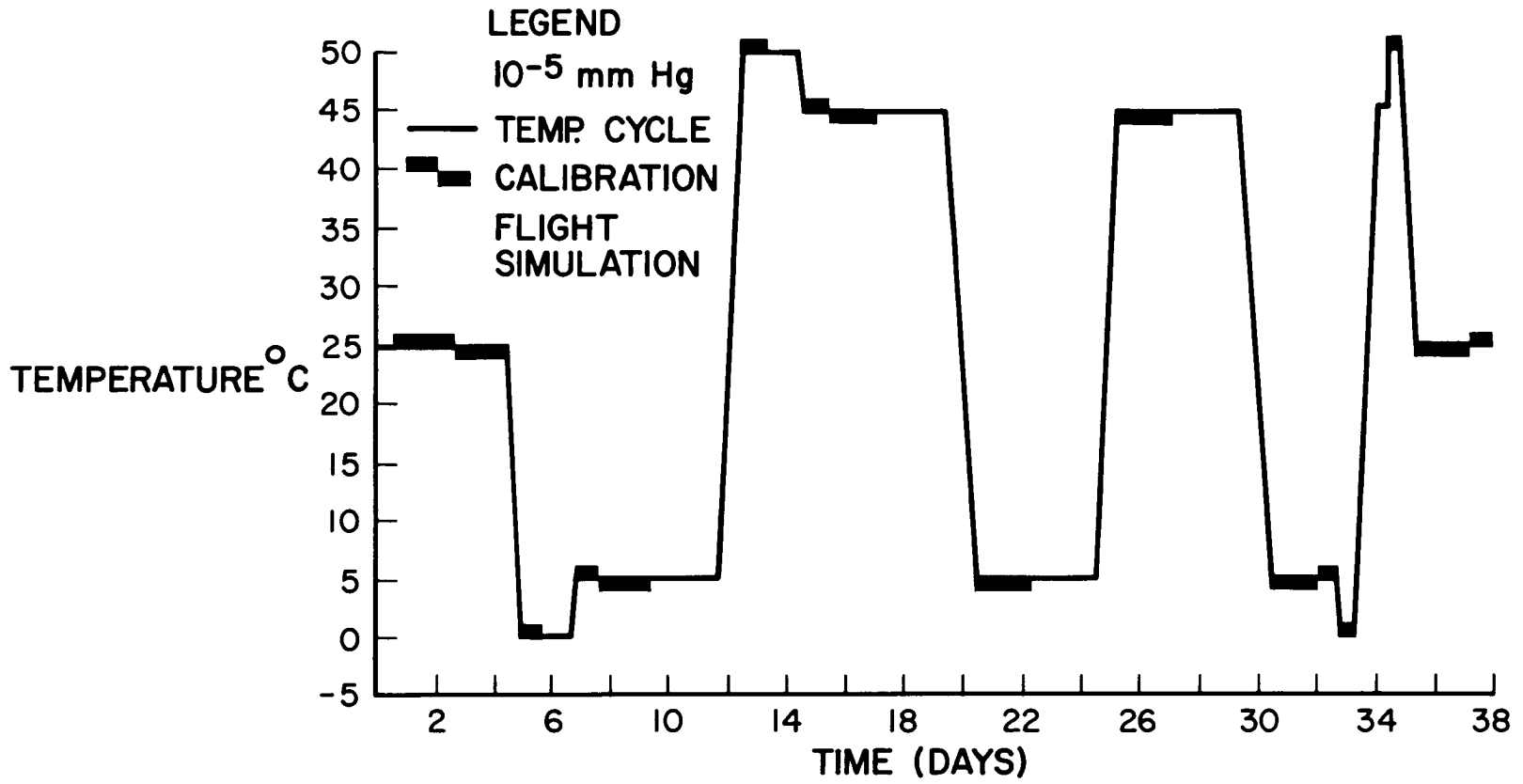

Figure 10 - Vacuum-Thermal Spacecraft Test Profile, Prototype

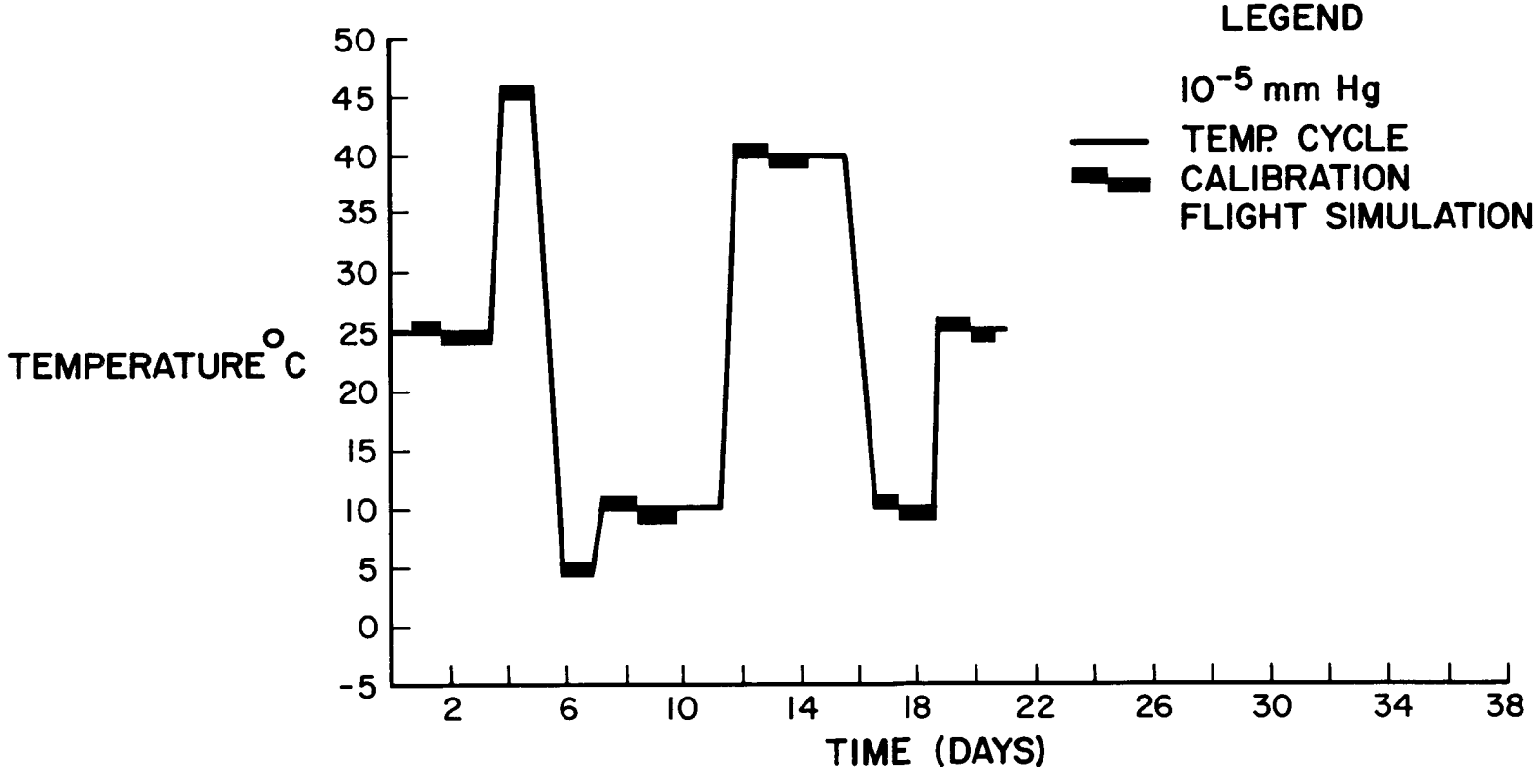

Figure 11 - Vacuum-Thermal Spacecraft Test Profile, Flight Model

NIMBUS PROGRAM REVIEW

November 14, 15, and 16, 1962

Attendance List

Name	Affiliation
C. Abbate	General Electric
G. E. Abid	NASA/GSFC
F.L. Adkins, Jr.	Radiation, Inc.
E. G. Albert	U.S. Weather Bureau
E. J. Almquist	Raymond Engineering Lab., Inc.
A.C. Andersen	General Electric
S. Andersen	University of Alaska
J. Arlauskas	NASA/GSFC
R.D. Ashby	Control Data Corporation
C.D.Ashworth	NASA/Headquarters
D. Atkinson	General Electric
N. W. Atkinson	U.S. Army - Ft. Monmouth
J. Bailey	General Electric
G. M. K. Baker	RCA
R. Barcus	General Electric
M. Bardonaro	Raymond Engineering Lab., Inc.
G. Barna, Jr.	RCA
U.R.Barnett, Jr.	Radiation, Inc.
D.T. Barry	General Electric
F. Bartko	NASA/GSFC
F. Bartman	University of Michigan
F. E. Beaumont	RCA
J. Bebris	NASA/GSFC
R.E. Becker	RCA
D. Beiber	NASA/GSFC
F.L. Bentley	Dept. of Transport - Canada
W. T. Bernard	RCA
D. Berry	General Electric
W.C. Boccius	Lockheed Missiles and Space Co.
Prof. W. Bollay	Massachusetts Institute of Technology

Name	Affiliation
R.G. Bounds	Air Force Systems Command
P. Bowen	General Electric
H.E. Bowers	U.S. Air Force
J. A. Boyd	Radiation, Inc.
G. Branchflower	RCA
C. Bristor	U.S. Weather Bureau
A.D. Brown	NASA/Western Operations Office
G. Brush	NASA/GSFC
G.L. Burdett	NASA/GSFC
L. H. Byrne	NASA/GSFC
T. Caldwell	General Electric
E. Cameron	General Electric
C. F. Catlett	Fairchild Stratos Corp.
C. E. Catoe	NASA/GSFC
W.C. Chambliss	California Computer Products, Inc.
S. Charp	General Electric
G. T. Cherrix	NASA/GSFC
A.T. Christensen	General Electric
F. Christensen	U.S. Weather Bureau
L.H. Clem	Travelers Research Center, Inc.
D. Clyman	General Electric
J. Cohen	RCA
S.G. Cohen	Ess Gee, Inc.
S. O. Cohen	NASA/GSFC
K. Collins	National Computer Analysts
B.L. Compton	RCA
T. Cooney	NASA/GSFC
Lt. Col. L. Cowen	U.S. Air Force
R. Cox	General Electric
J. Cressey	NASA/GSFC
P. Crossfield	NASA/GSFC
Cmdr. J. J. Crowder	U.S. Dept. of the Navy
L. H. Cutler	RCA
E. E. Dangle	NASA/Headquarters
J. T. Daniel	RCA

Name	Affiliation
E. M. Darling, Jr.	NASA/GSFC
J. Davis	NASA/GSFC
M. L. Davis	NASA/GSFC
R. M. Davis	NASA/GSFC
R. F. Decker	Federal Aviation Agency
E. DeGraff	NASA/GSFC
G. J. Delio	NASA/GSFC
R. Devlin	NASA/GSFC
J. Diaz	Radiation, Inc.
R. DiGirolamo	General Electric
W. R. Donsbach	Westinghouse
J. Dowling	NASA/GSFC
S. Drabeck	General Electric
E. Dresio	RCA
F. Drummond	General Electric
R. R. Drummond	NASA/GSFC
R. Fenn	U.S. Navy
L. L. Foshee	NASA/GSFC
W. B. Foster	Dept. of Defense
C. Freedman	NASA/Headquarters
C. L. Frey	U.S. Weather Bureau
D. W. Gade	California Computer Products, Inc.
G. Gemunder	NASA/GSFC
R. Gibson	NASA/GSFC
D. Giovacchino	General Electric
S. V. Giovannetti	NASA/GSFC
R. Girard	Department of Commerce
M. Gisser	NASA/GSFC
A. H. Glaser	Allied Research Associates, Inc.
T. Gleiter	U.S. Weather Bureau
H. J. Goett	NASA/GSFC
R. R. Golden	NASA/GSFC
G. I. Goldberg	NASA/GSFC
I. L. Goldberg	NASA/GSFC
H. Grenard	Allied Research Associates, Inc.
C. E. Griffin	Radiation, Inc.
L. J. Grills	Aero-Geo-Astro

Name	Affiliation
F. Hall	U.S. Weather Bureau
R. A. Hanel	NASA/GSFC
D. Harris	U.S. Weather Bureau
Capt. A. Hayes	Air Force
J. D. Heinzmann	Raymond Engineering Lab., Inc.
H. Hermann	General Electronics
G. M. Hieber	RCA
E. Hilsenrath	NASA/GSFC
J. N. Hines	NASA/GSFC
R. Hirsch	National Aeronautics & Space Council
K. Hoepfner	NASA/GSFC
G.D. Hogan	NASA/GSFC
R.E. Hogan	RCA
A. Holl	General Electric
D. Holmes	U.S. Weather Bureau
G. B. Holmes	Lockheed Missiles & Space Co.
K. Howard	Aero-Geo-Astro
L. Huband	RCA
P. Hui	NASA/GSFC
C.M.Hunter	NASA/GSFC
W. B. Huston	NASA/GSFC
E. J. Isbister	Radiation, Inc.
Lt.Cmdr. M.J. Jenkins	U.S.Navy
H.O. Jensen	Roters Motors
A.W. Johnson	U.S. Weather Bureau
R.W. Johnson	Hughes Aircraft
Lt. Col. J. A. Jones	Joint Meteorological Satellite Advisory Committee
W. W. Jones	NASA/GSFC
H. Kahl	Bell Telephone Labs.
T.J. Keegan	Air Force Cambridge Research Labs.
J. E.Keigler	RCA
L. J. Kiefer	RCA
J. C. Kilpatrick	General Electric
A.S. Kirpich	General Electric

Name	Affiliation
H.G. Klose	General Electric
G.S.S. Kranz	Fairchild Stratos Corp.
A. Krasnick	NASA/GSFC
B. Kreuzer	RCA
P. H. Kutschenreuter	U.S. Weather Bureau
C. R. Laughlin	NASA/GSFC
J. Leary	NASA/GSFC
Major R. B. Lefstad	U.S. Air Force
S. Leibowitz	NASA/GSFC
J. F. Lenmon	General Electric
F. E. Lilley	General Electric
C. Loeper	General Electric
J. W. Lovelace	NASA/GSFC
R. Luck	General Electric
R. Ludwig	General Electric
C. V. Lundstedt	NASA/Wallops
F. Luteran	RCA
B. Lyman	NASA/GSFC
D. MacCandless	RCA
C. M. MacKenzie	NASA/GSFC
R. Madvig	Stanford Research Institute
D. J. Mager	RCA
T. F. Maher	Fairchild Stratos Corp.
F. R. Malinowski	Santa Barbara Research Center
P. Marchetta	General Electric
J. Martis	RCA
J. Mathers	NASA/GSFC
M.S. Maxwell	NASA/GSFC
H.R. McBirney	U.S. Weather Bureau
J.B.McClung	RCA
K. R. McConnel	Westrex Corporation
R. McCrea	General Electric
J.C.McGee	Fairchild Stratos Corp.
J. F. McGuckin	General Electric
J. McRoberts	NASA/Headquarters
J. E. Meehan	NASA/GSFC

Name	Affiliation
K. R. Mercy	NASA/GSFC
J. V. Michaels	NASA/GSFC
L. Michelson	General Electric
B. W. Miller	NASA/GSFC
R. Miller	General Electric
R. F. Mize	NASA/Headquarters
J. C. Moody	NASA/GSFC
M. Morgan	RCA
A. I. Moskovitz	NASA/Headquarters
E. A. Neil	NASA/GSFC
J. J. Neilon	NASA/GSFC
H. E. Nichols	NASA/GSFC
W. Nordberg	NASA/GSFC
J. O'Connell	RCA
J. J. Over	NASA/GSFC
H. W. Paige	General Electric
J. W. Peddicord	NASA/GSFC
A. J. Pehta	RCA
E. S. Pelling	General Electric
P. L. Perez	General Electric
A. Petty	General Electric
J. D. Platt	General Electric
L. Podrasky	General Electric
W. K. Powell	RCA
H. Press	NASA/GSFC
R. L. Pyle	U.S. Weather Bureau
R. M. Rados	NASA/GSFC
S. Ranner	RCA
F. W. Reichelderfer	U.S. Weather Bureau
F. Reynolds	General Electric
W. Risley	NASA/GSFC
A. G. Robison	General Electric
D. Rodgers	General Electric
S. Rodkin	General Electric
J. H. Roe	RCA
E. L. Rosette	NASA/GSFC

Name	Affiliation
I. J. Ross	NASA/GSFC
H. C. Roters	Roters Motors
L. G. Saxton	RCA
I. Schechtman	National Computer Analysts
B. Schlachman	NASA/GSFC
J. Schell	General Electric
M. J. Schmitt	General Electric
M. I. Schneebaum	NASA/GSFC
N. J. Schruefer	NASA/GSFC
J. M. Schulman	General Electric
L. M. Schwartz	NASA/GSFC
H. L. Schwartzberg	RCA
K. P. Senstad	NASA/GSFC
R. Shapiro	NASA/GSFC
M. Shepetin	RCA
T. M. Sherlock	RCA
R. Sigismonti	General Electric
J. R. Silverman	NASA/GSFC
Col. A. Smith	Joint Meteorological Satellite Advisory Committee
D. S. Smith	NASA/GSFC
G. Smith	General Electric
H. R. Smith	NASA/Headquarters
R. D. Smith	NASA/GSFC
W. Sosin	General Electric
N. W. Spencer	NASA/GSFC
C. Spillane	NASA/GSFC
F. J. Spollen	General Electric
R. A. Stampfl	NASA/GSFC
I. Stein	RCA
L. R. Stelter	NASA/GSFC
E. O. Stengard	NASA/GSFC
J. Sternberg	RCA
S. Sternberg	RCA
M. J. Stoller	NASA/Headquarters
H. Street	NASA/GSFC
J. Strong	NASA/GSFC

Name	Affiliation
W. G. Stroud	NASA/GSFC
M. V. Sullivan	RCA
W. J. Swiacki	General Electric
C. A. Taylor	General Electric
M. Tepper	NASA/Headquarters
C. Thienel	NASA/GSFC
L. Thompson	Raymond Engineering Lab., Inc.
J. W. Townsend	NASA/GSFC
M. Townsend	NASA/GSFC
R. E. Trousdale	California Computer Products, Inc.
B. J. Trudell	NASA/GSFC
J. Turtil	General Electric
M. J. Vaccaro	NASA/GSFC
J. G. Vaeth	U.S. Weather Bureau
E. Vernon	U.S. Weather Bureau
A. Wachtel	Ess Gee, Inc.
G. W. Wagner	General Electric
A. Wallace	Ess Gee, Inc.
F. C. Warther	Control Data Corporation
E. W. Wasielewski	NASA/GSFC
H. Weber	General Electric
S. Weiland	NASA/GSFC
M. Weinreb	NASA/GSFC
P. H. Werenfels	RCA
F. Whedon	Joint Meteorological Satellite Advisory Committee
G. Wheeler	General Electric
O. Wheye	General Electric
A. White	NASA/GSFC
C. W. Whitmore	General Electric
W. K. Widger, Jr.	NASA/Headquarters
P. Wiener	RCA
E. T. Wiggins	Space Technology Lab., Inc.
F. L. Wiley	California Computer Products, Inc.
R. W. Wilkes	RCA

Name	Affiliation
A. T. Williams	RCA
W. W. Wolman	NASA/GSFC
R. Woodyard	NASA/GSFC
W. Wynne	General Electric
R. Ziller	Lockheed Missiles & Space Co.